Graduate Theses, Dissertations, and Problem Reports

2009

Chemical and physical properties of abandoned underground coal mine pools

Eric F. Perry
West Virginia University

Chemical and Physical Properties
of Abandoned Underground Coal Mine Pools
by

Eric F. Perry

Dissertation submitted to the Eberly College of Arts and Sciences
at West Virginia University
in partial fulfillment of the requirements
for the degree of

Doctor of Philosophy
in
Geology

Approved by

Henry Rauch, Ph.D.
John Renton Ph.D.
John Sencindiver Ph.D.
Jeffrey Skousen Ph.D.
Dorothy Vesper Ph.D.

Department of Geology and Geography

Morgantown, West Virginia
2009

Abstract

Chemical and Physical Properties
of Abandoned Underground Coal Mine Pools

by Eric F. Perry

Long term drainage quality of five closed underground coal mines in West Virginia and Pennsylvania was investigated for mineral reactions, chemical processes, and hydrogeologic controls. Three mines were flooded and had circumneutral water with dissolved iron and sulfate. Two unflooded mines had acidic water with high concentrations of iron, aluminum and sulfate. The monitoring record ranged from 12 to 35 years for the five mine-pools.

The two acidic mine-pools had large long term declines in chemical concentration and flux. Both mine-pools approached equilibrium for hydrous iron sulfate minerals of the jarosite series. One mine-pool also exhibited equilibrium for the hydrous aluminum sulfate mineral jurbanite.

Annual recharge rate for the unflooded mines was 0.28 and 0.36 gallon/A-min. About 75% of the total annual chemical flux is discharged in a six month period.

Flooding profoundly affected drainage quality of closed mines. Three mines had circumneutral pH after inundation and flushing. Extreme chemical stratification can occur in flooded mines. One mine-pool with two pumping rates had greater chemical concentrations at increased pumping rate.

Significant in-situ acid consumption occurred in all five mine-pools. The unflooded mine-pools consumed 50 to 70% of original mine acidity, and neutralization exceeded 100% in the flooded net alkaline mine-pools. Mineral weathering accounts for most in-situ acid consumption.

Chemical concentration time trends fit a first order decay function. Decay constants for total acidity, iron, sulfate, aluminum and total dissolved solids were on the order of 10^{-4}/day in all mine-pools. Decay times of 30 to 70 years were estimated to approach suitable water composition. Decay constants are useful for estimating long term trends.

Flushing model calculations suggest that chemical concentration change in mine-pools is largely a function of transport of reactants and products, not chemical kinetics.

.

ACKNOWLEDGMENTS

Table of Contents

List of Figures

List of Tables

List of Appendices

...

CHAPTER 1: INTRODUCTION AND SUMMARY FINDINGS

1.1 The Extent of Mine Drainage Pollution in Appalachia

Acid and metal rich water from closed underground coal mines has degraded many streams and aquifers in the Appalachian region. Over 80 years ago, polluted drainage from Appalachian coal mines was described as a "problem of long standing", a "public nuisance" and an expense to the mining industry (Crichton, 1927). The Appalachian Regional Commission (1969) published an assessment of coal mine drainage impacts in eight states. That study reported that water quality in more than 10,000 stream miles was affected by mine drainage. About 5,700 miles were reported to be acidic; and about 75% of the low pH streams were in the Susquehanna, Allegheny, Monongahela and Potomac River basins. The most severe acid drainage from bituminous coal mines was concentrated in southwestern Pennsylvania, northern West Virginia, and western Maryland. The Commission report also estimated that 80% of the drainage came from abandoned mines and that abatement would cost more than 6 billion dollars in 1969 values. At that time, there was no formal government funding mechanism for abatement.

The Clean Water Act (CWA), passed into federal statute in 1972, and the Surface Mining Control and Reclamation Act (SMCRA) in 1977, established national standards for water discharges from coal mines and environmental standards for reclamation. SMCRA established a fund for reclaiming abandoned mined lands with priority given to public safety, but a portion of the projects do address water pollution abatement as well. Although the incidence of "new" sources of mine drainage pollution has declined in Pennsylvania (Smith et al, 2000) and elsewhere, pollution from old or abandoned sites remains a widespread problem in the region.

Koryak et al. (2004) noted that total acidity levels have been gradually declining over a period of several decades in the Allegheny River basin, which they attribute in part to depletion of the source mineral pyrite within old mines. However, sulfate, a soluble product of pyrite oxidation, was leached from the Monongahela and Allegheny River basins at annual loading rates of 644 Kg per hectare and 368 Kg per hectare in the 1990s (Sams and Beer, 1999). Many individual drainage basins remain degraded. Figure 1-1 illustrates the condition of Muddy Creek, in Preston County, WV. This basin has multiple sources of acid drainage, including one of the mines examined in this study. The stream has a pH of about 3.2, iron and aluminum in the tens of mg/L and sulfate concentration of about 1000 mg/L. Most of the local mines have been closed for more than ten years and some are approaching 50 years in age. The stream has little value for biota, consumption or recreation in its current state.

The art and science of mine drainage prediction and mitigation is more advanced for surface mining effects than underground mine effects. The largest pollutant loads and impacts are however, usually associated with underground mine drainage, and observations suggest the effects can persist on the order of decades.

Figure 1-1. Muddy Creek, Preston County, WV, Degraded by Multiple Acid Discharges from Closed Underground Mines.

1.2 Objectives, Source Data and Methodology

In the work described in this study, the author examined the chemical and hydrogeologic processes and conditions in five underground mine-pools, with an overall objective of:

- identifying common variables, processes and "rules of thumb" that could improve the understanding, remediation and management of mine-pools.

These five mine-pools are a subset of the total population of closed mines, in that these discharge water of objectionable quality and require chemical treatment to comply with water quality standards. Some mine-pools not included in this study generate water of acceptable quality without intervention.

Some specific questions that were addressed in this work included:

- How long does the discharge of objectionable concentrations of metals, sulfate and acidity last in partly flooded and fully flooded mines?

- Are there identifiable mineral reactions controlling the concentrations of metals and sulfate in flooded and partially flooded mine-pools?

- What is the magnitude of seasonal variation in recharge/discharge in partly flooded mines?

- How much does recharge water and mineral weathering contribute to in-situ acid neutralization?

- What are the short term effects of in-situ treatment on mine pool quality?

- How should flooded or flooding mines be sampled for chemical characterization?

- What hydrologic conditions favor abatement or attenuation of mine drainage pollutants, and what hydrologic conditions favor continued mobilization of acid drainage?

- What are the likely sources/sinks for iron?

- How is water quality likely to change after flushing several mine pool volumes?

While the mine-pools in this study are pollution sources and liabilities to society at this time, they are also potential water resources. One of the subject mine-pools, Barnes and Tucker, is located in Cambria County, PA. The pumped and treated discharge releases about 22,700 liters per minute into the Ohio River basin. The mine-pool has been examined by the Commonwealth of Pennsylvania as a potential source for augmenting flow in the Susquehanna Basin, where water demand is approaching limits of the current supply. In West Virginia, Lessing and Hobba (1981) reported that several mine-pools in low sulfur underground coal mines have been developed as water supplies for consumptive use.

This work is an applied study, utilizing data collected by the author, and data acquired from other sources. Multiple source data introduced concerns about consistency, and these concerns were addressed by simple quality control methods including charge balance checks, acidity calculations, and examining expected relationships between parameters. Much of the data was originally collected for project monitoring purposes, and includes occasional missing values or apparent entry errors. These are real world data, with all of their imperfections. These data sets represent the type of information that companies, regulators or environmental groups base decisions on. The drawbacks to these data sets are that they lack an additional level of detailed analysis that could provide further understanding of the processes at work in mine-pools. For example, none of the five mine-pools were directly accessible for in-mine sampling of sediment and rocks for mineralogical characterization. Potential water-mineral interactions were inferred from geochemical calculations, water composition and literature reports for similar conditions, rather than by direct sampling.

Five mine-pools with reasonably complete long term (i.e. greater than ten years) water quality monitoring were selected for analysis. Two are partly flooded, and discharge acidic, metal rich drainage, while the other three have circumneutral water. The flooded mine-pools however, still discharge waters with objectionable concentrations of Fe and sulfate. General characteristics of the five mine-pools are summarized in table 1-1. Additional, more limited data, for three other flooded mine-pools, the "Fairmont mine-pool" located in Marion County, WV, the "Shannopin mine-pool" in Greene County, PA, and the "Uniontown mine-pool", in Fayette County, PA are also included in chapter four.

Each mine-pool has a unique associated history that could affect water composition. The two partly flooded mine-pools, Omega and T&T, both had in-situ treatment, including injection of flyash and cement, and impure limestone, respectively. These events were included in overall evaluation of

mine-pool behavior. The Omega and T&T mine-pools are managed by West Virginia Dept of Environmental Protection (WVDEP), which generously shared their data and insights with the author. The US Dept of Energy also provided a data set for part of the record at the Omega mine-pool. The Barnes and Tucker mine-pool receives leakage from an overlying mine-pool that flooded midway through the monitoring record. This mine-pool is managed by the Pennsylvania Dept of Environmental Protection (PADEP), which also shared data and observations with the author. Data for the Hahn and Arden-Westland mine-pools were originally reported by Donovan et al. (1999), and this dissertation does not repeat work already reported for these two sites.

Table 1-1
General Characteristics of Long Term Mine-pool Discharge Data Sets

Mine	Coal bed	Location	Period of Record	Sample Frequency	Water Quality Conditions	Flow/Pump Data	Remarks
T&T #2	Upper Freeport	Preston Co., WV	1994-2007	Weekly to quarterly	pH 2-3, high Fe, Al, SO_4	Daily flow since 1995	Mine flooding & blowout 1994
Omega	Upper Freeport	Monongalia Co., WV	1993-2007	Weekly to quarterly	pH 2-3, high Fe, Al, SO_4	Daily flow since 1997	Full suite chem. samples 1993-1999
Hahn	Pittsburgh	Washington Co., PA	1980-1999	Weekly to monthly	pH 6-7, high Fe, Na	Average 13,250 L/min	Full suite chem. samples 1984-1994
Arden-Westland	Pittsburgh	Washington Co., PA	1986-1999	~ Monthly	pH 6-7, high Fe, Na	Average 6800 L/min	Some full suite chem. samples
Barnes&Tucker	Lower Kittanning	Cambria Co., PA	1969-2005	Daily to quarterly	pH 6-6.5, high Fe	Average 22,700-26,500 L/min	Initially acidic, leakage from overlying mine-pool

Relatively few long term mine-pool data sets exist that include sampling at close intervals of days to a few months. Thus, the research could either concentrate on a small number of sites with more extensive information, or elect a larger number of sites having more sparse data sets. Mack and Skousen (2008), and work cited therein, followed the latter approach, examining more than 40 mines over multiple decades, but with limited sampling events. Their work produced some valuable general conclusions and observations on rate of change in chemical composition of mine waters. The current study focused on a few mines in an attempt to provide more detailed analysis and insight on mine-pool geochemistry and hydrogeology.

The chapters of the dissertation are organized as follows:

- Chapter one (this chapter), <u>Introduction and Summary Findings.</u> Provides an overview of the purpose of the research, principal findings and conclusions from chapters three, four and five, and assessment of additional research needs on mine-pools.

- Chapter two, <u>Mining, Stratigraphic and Hydrogeologic Conditions</u>, provides a short discussion of underground mining methods, stratigraphic and mineralogical considerations, conceptual discussion of ground-water recharge, storage and discharge in the Appalachian region, and general hydrologic properties of mine-pools.

- Chapter three, <u>Chemical and Hydrologic Properties of Partly Flooded Mines</u>, provides geochemical, mineralogical and flux calculations and recharge estimates for two acidic partly flooded mines.

- Chapter four, <u>Chemical and Hydrologic Properties of Flooded Mines,</u> provides geochemical, mineralogical and flux calculations for three mostly flooded underground mine-pools. Spatial variation in chemical composition, sampling considerations, and pumping effects on chemical composition are described.

- Chapter five, <u>Temporal Trends and Geochemical Behavior of Mine-pools,</u> provides calculations of in-situ acid neutralization by mineral weathering, recharge water and other mechanisms, estimating time dependent chemical composition using decay functions, metal solubility controls in aging mine-pools, and mineral weathering kinetics.

Appendices A, B, C, and D contain four published conference and journal papers by the author. Observations, conclusions and parts of those papers are incorporated into chapters three and four. The complete text of the four papers is included in the appendices as supplemental information.

- Appendix A includes a 2004 conference proceedings paper "Long-Term Water Quality Trends in a Partly Flooded Underground Coal Mine" presented at the National Meeting of the American Society of Mining and Reclamation and the 25th West Virginia Surface Mine Drainage Task Force.

- Appendix B contains the journal paper "Modelling Rock–Water Interactions in Flooded Underground Coal Mines, Northern Appalachian Basin" Geochemistry: Exploration, Environment, Analysis, Vol. 1 , 2001.

- Appendix C contains the 2004 conference proceedings paper "Ground-Water Flow and Quality in a Fully Flooded Underground Mine Complex", National Meeting of the American Society of Mining and Reclamation and the 25th West Virginia Surface Mine Drainage Task Force.

- Appendix D contains the 2005 conference proceedings paper "Water Quality Trends in a Flooded 35 Year Old Mine-Pool", National Meeting of the American Society of Mining and Reclamation.

Chapters three, four and five each contain a summary of findings for the respective section, and those findings are also incorporated into this chapter.

Chemical data from the five mine-pools are contained in appendices E, F, G, H and I. Input files for two geochemical models are in Appendix J. They were run in the software PHREEQCI.

1.3 Summary Findings of This Research
In chapter three geochemical processes are examined in two closed underground coal mines, Omega and T&T that are less than 30% flooded. Both mines discharged water with pH ranging from about 2.5 to 3.5, containing 10s to hundreds of mg/L of Fe and Al, and sulfate concentrations of 1,000 to nearly 5,000 mg/L. After more than 10 years, both mines still discharge acidic drainage, but chemical concentrations have declined. Chemical composition, mole ratios, solution complexes and chemical flux rates were examined as a function of time and from multiple discharge points. Potential solubility controls on Fe and Al activity were assessed from chemical equilibrium calculations. Recharge rate and seasonality were estimated in simple water budgets for both mines. The principal observations and findings from Chapter 3, Chemical and Hydrologic Properties of Partly Flooded Mines are:

- Conceptually, partly flooded mines can be viewed as large reactor and leaching chambers, that are regularly supplied with oxygen to oxidize pyrite, and water to rinse out soluble weathering products.

- Chemical concentrations and flux declined during the monitoring period, however overall water quality remains severely degraded. Significant short term (days to a few months) variations in concentration, flux and flow were common to both mine-pools, but long term (months to years) trends are also evident.

- Both mines had in-situ treatment consisting of grout injection in the Omega mine, and limestone injection in the T&T mine-pool. Chemical concentrations increased and water quality actually declined for 1 to 2 years after remediation, as stored weathering products were flushed from each mine. Each site has had some treatment sludge with excess alkalinity injected into the mine-works. The overall effect of treatment sludge return on mine-pool chemical composition is minimal or is masked by other processes.

- Chemical concentrations are inversely related to flow in the Omega mine-pool, increasing during low recharge periods of late summer and autumn. The distinct seasonal behavior in the Omega mine-pool suggests the complex has little additional ground-water storage capacity, beyond that in the mine-pool. The T&T mine-pool had little or indistinct seasonality in chemical concentrations.

- An estimated 60 to 80 % of the Fe associated with pyrite weathering is missing from aged mine-pool water. A large fraction of the Fe from pyrite weathering is therefore being attenuated within the mine-pool, even in very acidic conditions. The retention mechanisms could include hydrous sulfate minerals, oxyhydroxide minerals, cation exchange or adsorption.

- Mine-pool chemistry is very responsive to large imposed stresses. Both mine-pools had substantial increases in concentration and flux for several years after in–situ treatment. The T&T mine-pool also experienced a short term major "blowout" event in 2003 resulting in a large flux of pollutants. The T&T "blowout" was not associated with any anthropogenic activities. Rather it appears to have resulted from disruption of existing flow-paths, rapid head buildup, followed by failure of a barrier, pillars, or other subsidence that rapidly relieved the hydraulic pressure. Roof falls or partial collapse, and pillar failure are extremely difficult to predict on a temporal basis, but can affect chemical flux on short and long term bases by altering ground-water flow patterns.

- Sulfate, Al and Fe(III) form significant amounts of complexes in mine water. Complex formation, in general, increases the quantity of the element that can dissolve in solution and the solubility of the contributing mineral.

- Eh readings in acid mine waters can be used to estimate system redox conditions for iron. Fe^{2+}/Fe^{3+} activities are sufficiently large that both species can be sensed by the electrode and the couple is readily reversible. Measured Eh and Eh calculated from Fe^{2+}/Fe^{3+} activities had a median difference of -32 millivolts. Eh measurements collected from 2002 to 2007 for both mine-pools were consistent, indicating reproducible results and/or stable redox conditions.

- There is little change in water composition with respect to Al minerals over more than ten years in the Omega mine-pool. Three springs in the Omega mine-pool are near apparent equilibrium for jurbanite $(AlOHSO_4)$ and approach stability for alunite $(KAl_3(SO_4)_2(OH)_6)$. The T&T mine-pool is apparently under-saturated for Al-SO$_4$ minerals.

- Both partly flooded mine-pools approach apparent saturation for H-Jarosite $(H_3OFe_3(SO_4)_2(OH)_6)$. With the exception of one spring (Marshall) in the Omega mine-pool, both mine-pools show little change in composition with respect to Fe minerals over time.

- Annual chemical flux has declined in both partly flooded mine-pools. The Omega mine-pool flux is irregular from year to year, and after 14 years has declined to about 1/3 of its initial load. The T&T mine-pool has a consistent rate of change in annual chemical flux and has declined more rapidly than the Omega mine-pool.

- Flux has a strong seasonal component. About 75% of annual chemical flux is discharged in a six month peak recharge period from January to June in both partly flooded mine-pools.

- Average long term flux rates, normalized to mine area, are within about one order of magnitude for Fe and sulfate in both partly flooded mine-pools, and sulfate flux rate is greater than for Fe flux. Normalized flux rates are likely over-estimated since total rock surface area in caved and fractured rock exceeds plan view mine area. Flux rates normalized to mine area do provide a consistent basis for comparison among mines, however.

- Median annual recharge is 0.28 and 0.36 gal/A-min for the two partly flooded mines. Median recharge in spring is from 0.5 to 0.8 gal/A-min for the two partly flooded mine-pools. Both partly flooded mine-pools approach base-flow conditions of about 0.1 gal/A-min recharge in the autumn.

These findings are discussed in more detail in chapter three.

In Chapter four, <u>Chemical and Hydrologic Properties of Flooded Mines</u>, geochemical processes were examined in three closed underground coal mines, Barnes&Tucker, Hahn, and Arden-Westland, supplemented with more limited data from three other flooded mine-pools. The Barnes&Tucker and Hahn mine-pools initially produced acidic water, but both mine-pools developed circumneutral pH after flooding. Initial flooding data for the Arden-Westland mine-pool were not in the record, and this mine produced circumneutral pH water after flooding. Two other flooded mine-pools, Uniontown and Shannopin, also produced acid water during initial flooding, but later evolved into circumneutral pools. Fully or mostly flooded mines can transition from acid to neutral drainage within a decade. The principal findings and observations in flooded mine-pools are:

- Flooding profoundly affects aqueous chemistry of flooded mine-pools. Each mine-pool, initially contained or discharged low pH waters, or discharges acid water from small unflooded sections. After flooding, mine water shifted to circumneutral, net alkaline conditions, although Fe, sulfate and TDS remained elevated. The typical pH shift was three to four S.U.

- Extreme vertical stratification of chemical conditions can occur in mine-pool wells and shafts. Transitions can be abrupt, and include one to two order of magnitude changes in parameter concentrations. Samples collected at the beginning of a pumping cycle may not represent long term conditions, as turbulent flow and mixing occur over time.

- Varying stress on the mine-pool, in the form of changing pumping rates, may affect discharge quality. Flushing within the mine-pool is not uniform, and includes preferred flow-paths and short circuiting. Some sections of the mine-pool may have limited fluid exchange.

- Mine-pool water quality exhibits spatial variability. Water in recharge zones, at the beginning of the mine-pool flow-path are the least mineralized. Water becomes more mineralized as it migrates through the mine-pool flow system.

- Flooded mine-pools are deficient in Fe with respect to sulfate; indicating most iron originally liberated by pyrite oxidation has been retained in the mine-pool. About 60 to 80% of the Fe is "missing" from the discharge waters.

- Flooded mine-pools consume large amounts of acidity in-situ. Two moles of H^+, generated per mole of sulfide to sulfate oxidation, are consumed within the flow system. Net alkaline waters are discharged from each flooded mine-pool.

- Cation exchange of Na for Ca and Mg is a prominent feature in flooded mine-pools.

- Flooded mine-pools contain little or no detectable oxygen, a condition that favors inhibition of pyrite oxidation.

- Flooded mine-pools may approach saturation for one or more minerals especially during early flooding. Gypsum, calcite, dolomite and Fe oxyhydroxides were near apparent equilibrium in several mine-pools. The waters tend become under-saturated for carbonate minerals and gypsum as the mine-pool ages.

- Computed pCO_2 values are up to several hundred times atmospheric conditions, suggesting the mine-pools do not readily exchange gases with the above-ground atmosphere and that chemical weathering of carbonates is ongoing.

- Eh/pH plots based on field measured values show mine-pool waters near equilibrium with respect to poorly crystalline $Fe(OH)_3$.

- Sulfate reduction may occur in flooded mine-pools. Computed Eh for the S(-II)/S(VI) couple approaches conditions of FeS formation in one mine-pool.

- Long term flux rates of Fe and sulfate, normalized to area of mine-works, varied about one order of magnitude for each parameter. There was no discernible difference in flux rate between flooded and partly flooded mines. Normalized flux rates are likely over-estimated since total rock surface area in caved and fractured rock exceeds plan view mine area. Flux rates normalized to mine area do provide a consistent basis for comparison among mine-pools, however.

- Flooded mine-pools that are subdivided by barrier pillars can be visualized as a series of compartments, each with large internal hydraulic conductivity, and small hydraulic gradient and specific storage. Flooded mine-pools behave as confined or leaky confined aquifers.

- Head in confined mine-pools responds to pumping over distances of tens of km. This behavior has practical significance, in that large mine-pools can be controlled by a single pumping facility.

These findings are discussed in more detail in chapter four.

Chapter five, <u>Temporal Trends and Geochemical Behavior of Mine-pools,</u> addresses in-situ neutralization, longevity of pollutant discharges from flooded and unflooded mines and metal solubility controls in aging mine-pools. The principal observations and findings are:

- A large fraction of the acidity attributable to pyrite oxidation was missing from all five mine-pools. The missing acidity is described as in-situ neutralization and exceeds 100% in the flooded net alkaline mine-pools. Significantly, the two acid mine-pools had neutralization ratios on the order of 60 to 70%. In-situ neutralization mechanisms include carbonates, alumino-silicates and oxyhydroxides, and alkaline recharge from ground-water infiltration.

- Mineral weathering constituted about 60 to 95% of the in-situ neutralization, depending on mine-pool age and flooding state. Mineralogy of the residual coal, floor and roof rock is the principal control for in-situ weathering. Mineral weathering was reflected by increased concentrations of Ca, Mg and in acidic mine-pools, Al.

- Two methods for estimating neutralization ratio, cation summation and neutralization by difference produced similar estimates. Either can provide a useful estimate of in-situ weathering. A third method for estimating neutralization based on speciated solutions, was also useful for acidic waters containing appreciable Fe(III).

- Long term chemical concentration data often fit a first order type reaction plot. Decay constants are on the order of 10^{-4}/d are with few exceptions, and range over an order of magnitude, for total acidity, Fe, Al, sulfate and TDS.

- Chemical "decay" or rate of change with time can be divided into early flushing and late or long term leaching phases. The early phase includes the flushing of accumulated salts and acid weathering products and rapid concentration declines. The late phase includes the continued weathering of pyrite and other minerals and removal of "juvenile acidity". Separate decay values should be used to model early and late phase water quality conditions.

- Time periods to reach specified water quality concentrations, ranged in general, from about 30 to 70 years duration. Aluminum was predicted to have the longest decay period, in some instances exceeding 100 years. The range of statistical uncertainty can span one to two decades.

- Decay rates are useful for long term trend estimates. They are less useful for estimating concentration at specific points in time.

- The decay constant is a lumped variable that includes both chemical reaction and transport elements. A simple model of slow flushing of the mine-pool relative to mineral dissolution rates produced reasonable results. A model assuming rapid flushing relative to mineral

dissolution produced results deemed unreasonable. This analysis implies that transport controls observed decay more than chemical kinetics.

- Pyrite oxidation rates estimated from published rate data were about an order of magnitude faster in unflooded mines compared to flooded mines. The rates are sensitive to oxygen content.

- Advective transport of oxygen and weathering products in flooded mines could influence decay rates, and airflow driven by barometric changes may be important for oxygen transport in partly flooded mines.

- The decay constant has no provision for complying with mineral solubility constraints as the mine-pool ages. Samples of aged mine-pools seem to retain dissolved metals such as Fe and Al in the range of a few to a few tens of mg/L. Simulations of aged mine-pools, including acid water with dissolved Fe and Al, and a circumneutral water with dissolved Fe, showed that metals will not be removed by precipitation of common mine-pool minerals.

These findings are discussed in more detail in chapter five.

1.4 Additional Research Needs

The work conducted in this dissertation left some questions unanswered and raised new ones. The understanding of both physical and chemical mine-pool processes is still incomplete. Future mine-pool research should consider the following:

- For mine-pools exhibiting seasonal behavior, a predictive expression is needed that honors the underlying long term trend, while modeling seasonal or cyclic change. Time dependent prediction of chemical concentration or flux can be estimated using first order decay equations. The constant does not account for seasonality and estimates become less certain as the rate of change (dc/dt) slows.

- What is the long term (i.e. multiple decades) chemical composition of mine-pools? A chemical "decay" curve has a long tail, where the rate of change (dc/dt) in concentration or flux approaches zero. The slope and length of the tail becomes sensitive to small changes in chemical weathering and transport rates. Estimates derived from first order decay implicitly assume that constant hydrogeologic and geochemical conditions persist in the mine-pool, and that solubility or kinetic constraints do not affect behavior at low concentration or flux rate. Observations of several mine discharges for mine-pools 50 or more years old suggests that metal concentrations of a few mg/L can persist, and concentration or flux decay becomes asymptotic. This implies that chemical weathering and transport have reached a steady state condition that could be maintained indefinitely.

- Estimation of ground-water flow and transport in a dual porosity mine-pool system is needed. An improved understanding of dual porosity flow, beginning with simulations, could yield improved understanding of how rapidly chemical pollutants are transported

in and removed from mine-pools. A related question is: how rapidly will chemical concentration and flux reach values considered acceptable for some prescribed use? Mine-pools include a wide range in pore size that allows both true porous media and "pipeline" or turbulent flow to occur. The two flow systems may generate different flushing rates and efficiencies.

- How does one estimate the initial water chemistry composition of a mine-pool that is beginning to flood? At present, estimates of expected mine water composition are based in part on the analogue approach of examining existing underground mines that are believed to have similar hydrologic and geochemical conditions. A reliable predictive model that incorporates site specific geology, stratigraphy, and geochemical composition of the rocks and recharge water is needed to estimate the "starting point" for mine-pools.

- Simple flushing models should be pursued for estimating leaching efficiency in mine-pools.

- Improved characterization is needed for the composition and solubility of hydrous sulfate minerals associated with mine-pools. Some common mine-pool minerals, such as gypsum are well characterized. Others such as copiapite do not have published reproducible thermodynamic data. Others such as schwertmannite have variable composition.

- Could mine-pool pumping scenarios be developed that would accelerate flushing of pollutants from the system?

- Can pH and redox conditions be manipulated in-situ to induce pollutant removal within the mine-pool? Flooding is a primary example of redox management in mine-pools. Completely flooded or mostly flooded mines in this study evolved from acidic to circumneutral pH within about a decade, apparently by stopping or limiting further pyrite oxidation. Mine-pool pH adjustment has been attempted in a few mines, usually by injection of soluble bases. The two partly flooded mine-pools in this study had flyash and limestone injection. Post injection water quality showed little or modest improvement. The concept has merit, but alkaline sediment injection methods and rates, and water chemistry/base interactions need further development.

- Could passive treatment technology be modified to work in-situ in mine-pools?

Solutions to these issues could improve the understanding and management of mine-pools, reduce adverse effects on water resources and biota, and turn environmental liabilities into resources.

Chapter 2 Mining, Stratigraphic and Hydrogeologic Conditions

The quantity and quality of water discharging from closed underground mines is a function of three principal components: mining methods and conditions, stratigraphy and mineral composition, and hydrogeologic properties of the overburden and mine aquifer. This chapter provides a brief summary of mining methods, stratigraphy and mineralogy, and finally a short summary of ground-water recharge storage and discharge concepts for mine-pools in the Appalachian region. These concepts underlie the more detailed analyses in chapters three, four and five.

2.1 Underground Coal Mining Methods
Underground coal mines studied in this work had coal extracted using the room and pillar techniques. Figure 2-1 is a schematic representation of room and pillar development. Rooms ranging from about 18 to 30 feet wide are developed in parallel, separated by intact pillars left for roof support. Cross cuts are driven at right angles, resulting in a rectangular patter of rooms and pillars. There are several variations in pattern of development, but each follows the basic concepts shown in figure 2-1.
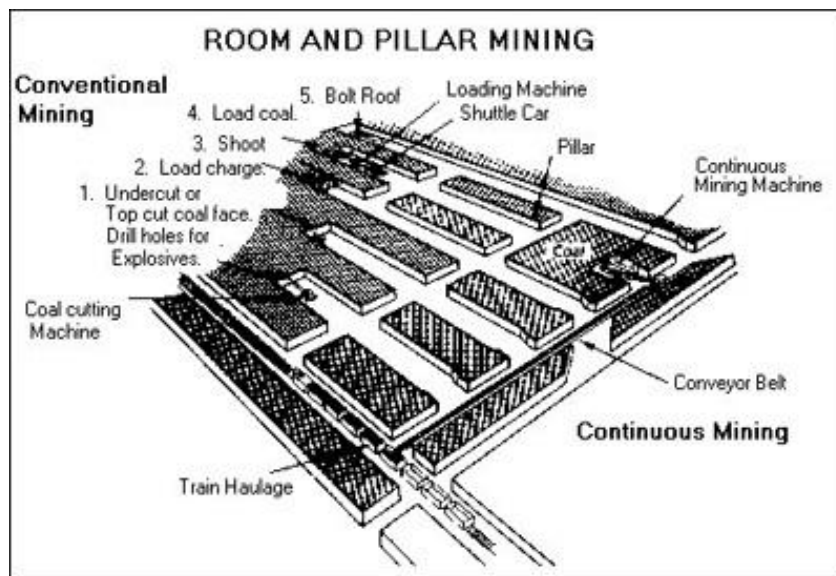
Figure 2-1. Schematic of Room and Pillar Development in Underground Coal Mines.
Adapted from United Mine Workers of America (http://www.umwa.org/)

After initial development, more coal may be extracted by retreat mining; where additional coal is removed from the existing pillars. Retreat mining (or second mining) removes a portion of the roof support, and increases the likelihood of subsidence. A retreat mined section can consist of a mixture of standing pillars with open void, partially subsided rooms, and fully subsided areas that are filled with a mixture of caved, broken rock from the overlying strata. The mine-pool matrix material may, therefore, vary in lithology, particle size and mineral composition. Extraction rates in room and pillar mining range from around 50 to as much as 80%, depending on mining conditions (Peng, 1986). The size of the pillars is based on overburden load, mining height and rock strength. Prior to about 1970, nearly all underground coal mining in the United

States utilized room and pillar methods. Figure 2-2 shows part of the underground mine-map for the T&T mine complex. The mine was developed using room and pillar methods, but the final geometry of the mine is complicated by topography, geologic structure, geologic variability, mineral ownership and other factors. The other room and pillar mines studied in this project also have irregular dimensions.
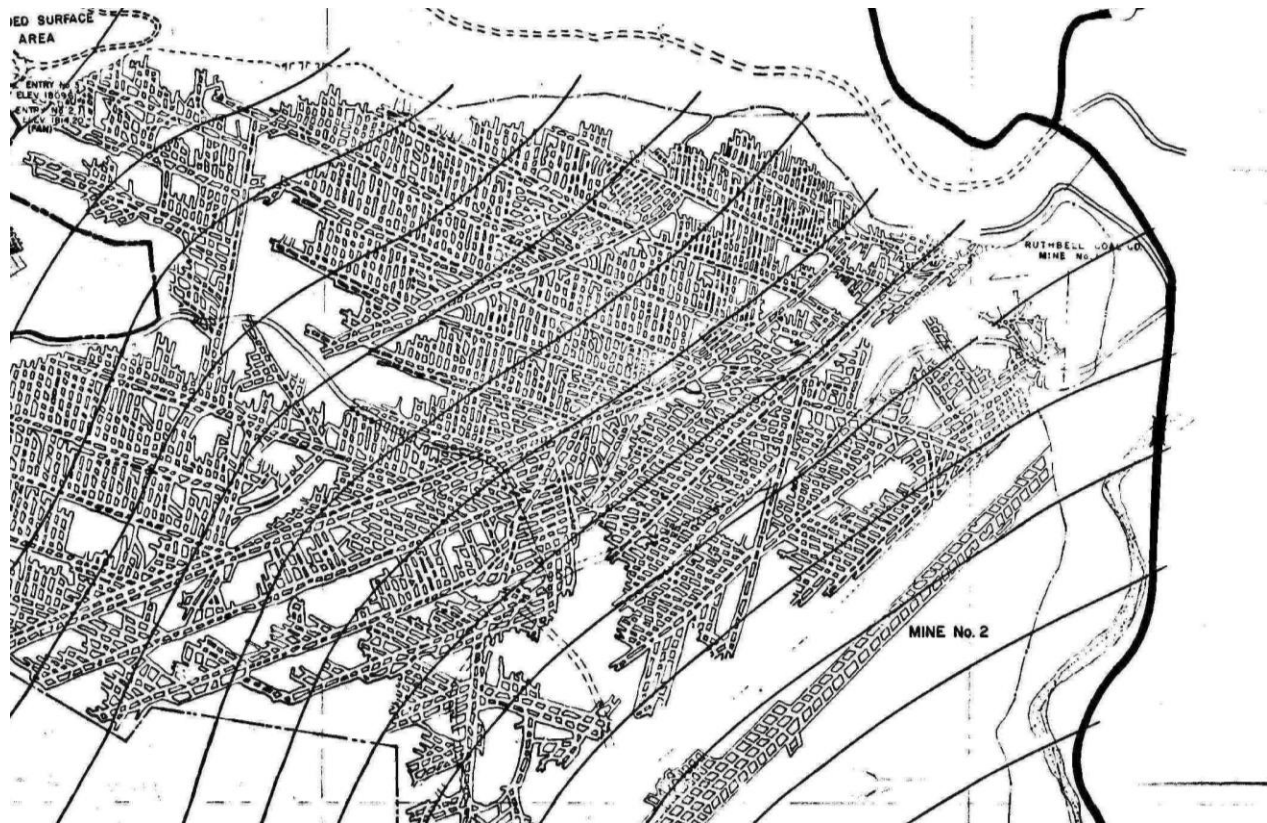
Figure 2-2. Portion of Underground Minemap for T&T Mine-pool, Illustrating Room and Pillar Mining Method and Variable Dimensions of Mine Development. Approximate Scale 1"= 1000 feet.

Longwall extraction is the second principal underground coal mining method used in the US. Although none of the mines in this study used longwall mining, much of the literature on subsidence and ground control focuses on longwall extraction. Figure 2-3 is a schematic of longwall mining. Rectangular panels are laid out in widths ranging up to 1200 feet, and lengths extending to 10,000 feet. Coal is extracted using a shear or "plow" that passes back and forth along the active face, with the immediate working area supported by moveable hydraulic shields. As mining and the shields advance, the unsupported roof collapses into the mined out area. Adjacent rectangular panels are separated by chain pillars which provide access and ventilation. The final mine geometry is generally more regular than room and pillar, and the entire panel area is subsided. The "gob" or subsided material is a mixture of caved and broken material overlying the coal bed. Mining effects on mine-pool hydrology are further developed in section 2.3.

14
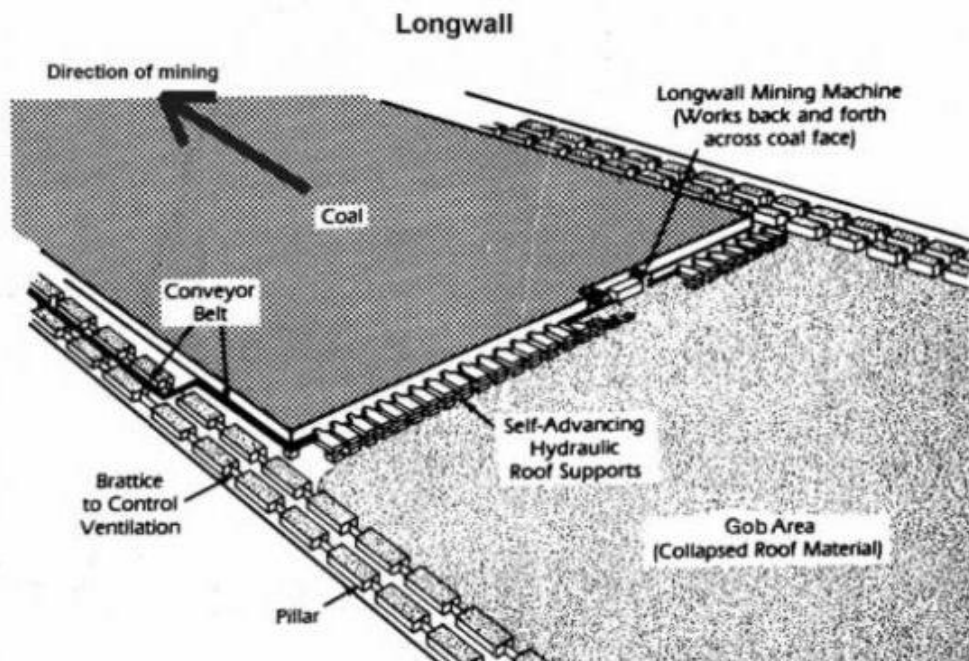
Figure 2-3. Schematic of Longwall Mining.
Adapted from United Mine Workers of America (http://www.umwa.org/)

2.2 Stratigraphy and Mineral Composition.

Stratigraphy and mineralogy of Pennsylvanian system rocks have been described both in terms of classical geology (see for example Arkle et al., 1979 for discussion of West Virginia, and Edmunds et al., 1979 for Pennsylvania), coal geology (see Donaldson et al.,1979) and in the context of mine drainage (see Brady et al., 1998). The mines in this study are developed in Upper Pennsylvanian rocks in the Allegheny and Monongahela groups in northern West Virginia (Preston, Monongalia and Marion Counties) and western Pennsylvania(Washington, Cambria and Fayette Counties). Figure 2-4 shows the general location, stratigraphic group and coal bed of mine-pools in this study.

The rocks in the study area were deposited in a foreland basin extending along a north-northeast axis across West Virginia into Pennsylvania. Basin subsidence created characteristic cyclothems, or repetitive sequences of coal, shale, mudstone, limestone and sandstone (Arkle et al., 1979; Edmunds et al., 1979). Stratigraphic relationships are complicated by repeated transgressions and regressions of inland seas, varying basin subsidence and shifting depositional environments including marine, lacustrine swamps, coastal plains and upper and lower delta plains. As a result, rock layers are frequently lenticular or discontinuous and vary in chemical and mineralogical composition over distances of kilometers or less. The basin also includes a series of low angle folds, with anticlines and synclines whose axes are generally oriented north-northeast along strike. These folds and regional dip influence the extent of flooding and flow direction in mine-pools.

Brady et al. (1998) made the following observations about these rocks in the context of mine drainage predictions in Pennsylvania:

15

- Acid drainage problems are more prevalent in the lower Allegheny group than in stratigraphically higher rocks.

- Pyrite and carbonate content are influenced by paleoclimate and depositional environment. Rocks formed in brackish waters were supplied with both Fe and sulfate and therefore have pyrite, but often contain few carbonates. Hence their tendency is to produce acid drainage. Marine rocks may contain abundant carbonates and pyrite and produce waters of high dissolved solids content. Fresh water limestones may be important alkalinity sources.

Mine-pool Locations, Group and Coal Bed
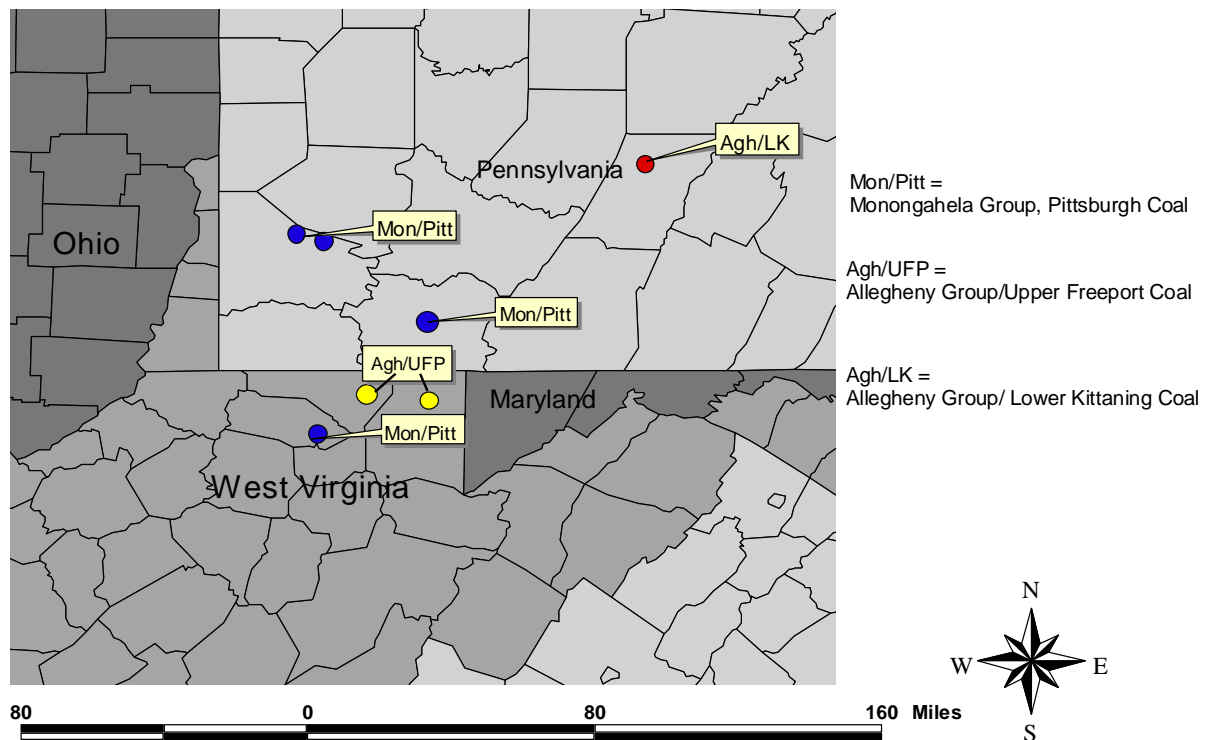
Figure 2-4. General Location Map of Mine-pools Studied in West Virginia and Pennsylvania.
Four are in the Monongahela Group, Pittsburgh coal bed; two are in the Allegheny Group,
Upper Freeport coal bed, and one is located in the Allegheny Group, Lower Kittanning coal bed.

Dulong et al. (2002) characterized the mineralogy and chemical composition of Upper Pennsylvanian rocks in several deep rocks cores. Their data support the regional observations of Brady et al. (1998). A generalized stratigraphic column for northern Appalachia is shown in figure 2-5. The Monongahela group, which includes the Pittsburgh coal at its base, contains limestones, abundant limy shales and mudstones, and high sulfur rocks. The Allegheny group (figure 2-5) which includes the Kittanning and Freeport coal beds contains few carbonates and some pyritic

zones, hence the tendency to produce acidic drainage. Local stratigraphy is described in more detail in county level geologic survey reports in West Virginia and Pennsylvania.

END OF THE LATE PALEOZOIC	
Dunkard Group 335 m + (1100 ft)	Proctor sandstone Windy Gap limestone Nineveh coal Nineveh limestone Jollytown sandstone Jollytown coal Hundred sandstone Upper Washington limestone Lower Marietta sandstone Washington coal Waynesburg sandstone Cassville shale—Elm Grove limestone
Monongahela Group 70–122 m + (230–400 ft)	Waynesburg coal Gilboy sandstone Uniontown coal Benwood limestone Sewickley coal Redstone coal Redstone limestone Upper Pittsburgh sandstone Pittsburgh coal
Conemaugh Group 137–259 m (450–850 ft)	Lower Pittsburgh sandstone Elk Lick coal Ames limestone[1] Harlem coal Saltsburg sandstone Woods Run limestone[1] Bakerstown coal Pine Creek limestone[1] Buffalo sandstone Brush Creek limestone[1] Brush Creek coal Mahoning sandstone { Mahoning coal / Thornton fire clay Uffington shale
Allegheny Formation 30–91 m (100–300 ft)	Upper Freeport coal Bolivar fire clay Upper Freeport sandstone Lower Freeport coal Upper Kittanning coal Washingtonville limestone[1] Middle Kittanning coal Hamden (Columbiana) limestone[1] Lower Kittanning coal Lower Kittanning clay Vanport (Ferriferous) limestone[1] Clarion fire clay
Pottsville Group 15(?)–61 m (50–200 ft)	Homewood sandstone Mercer coal Connoquenessing sandstone Sharon sandstone(?)
MISSISSIPPIAN SYSTEM	

Figure 2-5. Generalized Stratigraphic Column of Upper Pennsylvanian System Rocks in Northern West Virginia Showing Principal Coals, Limestones, Sandstones and Fireclays. The mines in this study are in the Pittsburgh coal (base of Monongahela Group) and Upper Freeport and Middle Kittanning coals (Allegheny Formation). Adapted from Arkle et al., 1979.

2.3 Hydrogeology of Unmined and Mined Rocks in the Appalachian Plateau

Chemical attributes of mine-pools are influenced by the quantity and quality of recharge water entering the pool, and water storage and transmission properties of the new mine-pool aquifer. This section provides a conceptual overview of ground-water flow and storage in unmined rocks, and the similarities and differences compared to aquifers developed in underground mine-works.

Callaghan et al. (1998) provide a summary review of ground flow water systems in the Appalachian plateau. They distinguish three types of flow systems; a shallow system in fractured and weathered regolith, a second system at intermediate depth, and deep regional flow systems, generally located below base level drainage. The shallow flow system is characterized by short residence times and rapid ground-water movement. Fracture flow dominates and the openings may be regular joints or stress relief fractures. Wyrick and Borchers (1981) noted that stress relief fractures were the most transmissive part of the aquifer. Callaghan et al. (1998) estimate that permeability increases due to joints and fractures may extend as deep as 500 feet. The Omega and T&T mine-pools are at depths generally less than 250 feet and contain thick sandstones in the overburden. Figure 2-6 shows the face-up area for the mine entries at the Omega mine. There are

Figure 2-6. Omega Mine Face-up Area Showing Vertical Fractures in Sandstone Overburden. Partially Open Mine Entry at Right.

several prominent vertical fractures exposed in the highwall, which would promote rapid infiltration and mine-pool response to recharge events. Stoner et al. (1987) estimate that as much as 99% of ground-water recharge, circulation and discharge occurs in the shallow ground-water zone.

Sames and Moebs (1989) indicate that the effects of stress relief fractures in underground coal mines are not significant under more than about 300 feet of cover. Bruhn (1985) found that hydraulic conductivity decreased as depth increased from about 150 to 300 feet at a West Virginia mine site. In Greene County, PA, Stoner et al. (1987) report that hydraulic conductivity decreased by about one order of magnitude per 100 feet of depth to a depth of about 500 feet. McCoy (2002)

found that at depths greater than about 500 feet, mine inflow rate and overburden thickness are unrelated. Thus it appears that at depth, fractures are less frequent with fewer interconnections and mine inflow rate is controlled more by primary porosity of the rocks.

Kozar and Mathes (2001) reported median aquifer transmissivity of 150 and 850 ft^2/day, in the Monongahela and Allegheny groups, respectively in West Virginia. Well depths were mostly between 100 and 200 feet. Hobba (1981) noted that transmissivity and hydraulic conductivity generally increased in rocks above underground coal mines.

The intermediate and deep flow systems have progressively longer residence times and slower ground-water circulation patterns. Fractures are less common, and primary, or intergranular hydraulic conductivity controls the movement of ground-water. The Barnes&Tucker, Hahn, Arden-Westland, and Fairmont mine-pools are located mainly in the intermediate and regional ground-water systems.

The development of underground mines, coal removal and dewatering during active operations generates stresses in the overburden rocks and aquifers. The immediate to short term effects can include subsidence and partial to complete dewatering (Cifelli and Rauch, 1986; Hobba, 1981; Kendorski, 1993). After closure and the onset of flooding, ground-waters may recover partially to completely (Booth, 1986; Booth, 2007; Liu et al., 1997), but the new mine-pool aquifer may have properties very different from the original bedrock aquifers.

Burby et al. (2000) for example, found that underground mine discharges had behavior similar to springs in karst aquifers. Adams and Younger (2001) found that ground-water flow in flooding mines in the UK could be adequately simulated by treating the mine as a series of ponds connected by pipes and applying pipe flow formulations. These findings and observations of subsidence and physical weathering suggest that mine-pools may have a dual flow (porosity) system consisting of large voids and rapid flow, and a slower Darcian component.

When mine-pools begin to form in abandoned workings, the new aquifer is recharged from ground-water infiltrating from overlying rocks, or in some instances, lateral flow and leakage from adjacent mines. Kendorski (1993) developed a five layer model which shows that large variation in aquifer properties is possible. He based his model on data from over 65 cases of high extraction mining (primarily longwall or room and pillar retreat mining) and extensive review of existing literature. Many of the case studies were in Appalachia and the Illinois basin. His generalized model identified five zones of differing hydrogeologic properties as illustrated in figure 2-7. They include:

- A zone of collapse and disaggregation (physical weathering) that extends six to ten times the mined thickness (height) above a panel (I, Caved Zone).

- A zone of continuous fracturing extending up to 24 times the mining height which allows for dewatering of intercepted aquifers or surface waters on at least a temporary basis (II, Fractured Zone).

- A dilated leaky zone extending 24 to 60 times mining height with increased ground-water storativity and low vertical transmissivity. (III, Dilated Zone).

- A constrained leaky zone above zone III, and below zone V, described below, where storativity and transmissivity are not affected (IV, Constrained Zone).

- Surface fracturing to depths of as much as 50 feet below ground surface (V, Surface Fracture Zone).

Kendorski (1993) comments that the caved zone height is in part a function of rock lithology, where more competent sandstones and limestones limit caving to six times mining height or less. Particle shape also influences caving as equidimensional blocks produce more rubble volume and void space. Kendorski's model is illustrated in figure 2-7, for a case of mines developed in two

Zone I -Collapsed Overburden, 6 to 10x mine height

Zone II- Zone of Fracturing, extending up to 24x mine height

Zone III-Dilated Zone, horizontal bedding plane seperations and fractures, extending about 24 to 60x mine height

Zone IV- Leaky Aquitard Zone

Zone V- Surface Fracture Zone
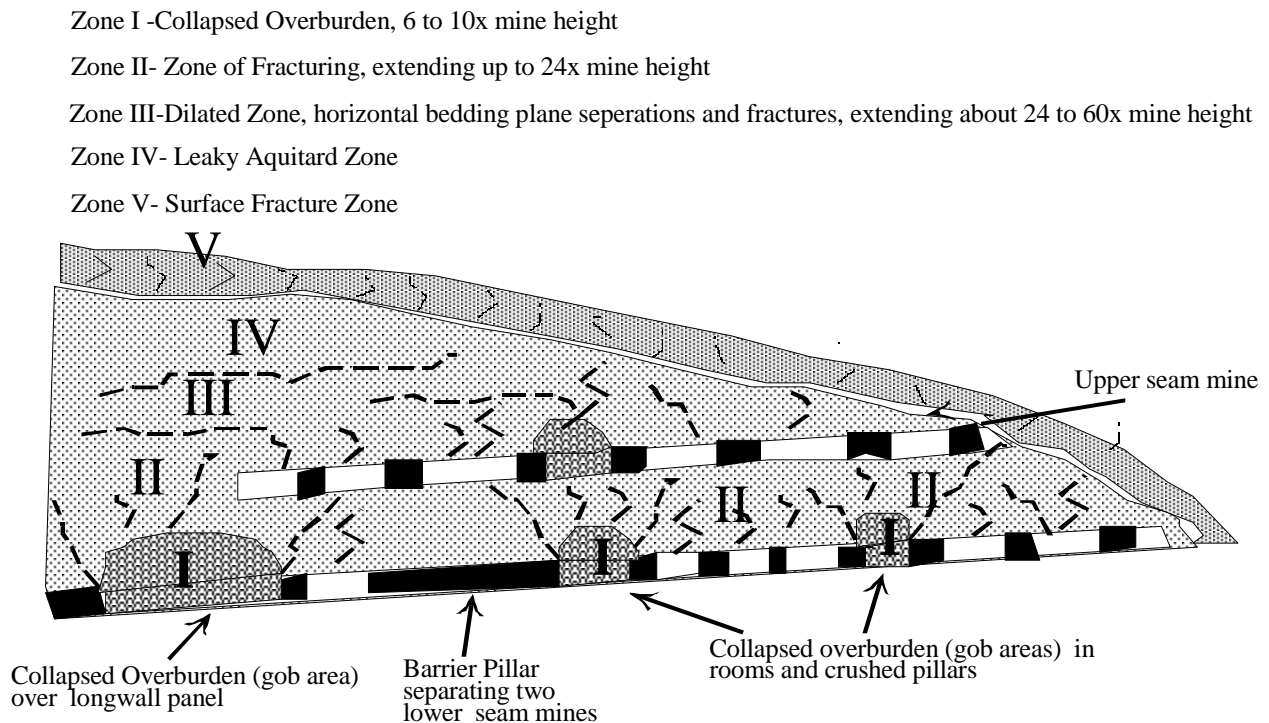
Figure 2-7. Simplified Cross Section of Barrier Pillars and Overburden Conditions after Mine Closure. (Modified from Kendorski, 1993).

coal beds. The propagation of zones I and II result in hydraulic connection between the mines. The Barnes&Tucker mine-pool, described in chapter four is an example of a mine-pool connected across two coal beds.

Krendorski's generalized model served as the basic concept on which mine-pools were evaluated in this study. Two significant implications of the model are:

- Mine-pool water quality is not determined solely by rocks at mine level. Caving deposits disaggregated rocks from the overburden into the mine-works. These materials are available to participate in chemical weathering reactions in the mine-pool, and influence chemical composition.

- Water storage and conductance may vary spatially. Mine-pool aquifer thickness is variable depending on extent of caving, and conductance can include both pipe flow and porous media components.

Chapters three and four examine partly flooded and mostly flooded mine-pools in more detail, while chapter five addresses long term trends in chemical composition.

Chapter 3: Chemical and Hydrologic Properties of Partly Flooded Mines

Partly flooded or "above drainage" underground mines are often continuing sources of acidic drainage after closure or abandonment. Skousen et al. (2006) reported on long term water quality of above drainage mines in northern West Virginia. Most mines had decreasing pollutant concentrations as they aged, but with few exceptions, they continued to discharge low pH water with Fe, Al, sulfate and other chemicals. Conceptually, partly flooded mines can be viewed as large reactor and leaching chambers, that are regularly supplied with oxygen to oxidize pyrite, and water to rinse soluble weathering products. Flooding mines, as discussed in chapters four and five, at some stage, become depleted in oxygen, and pyrite weathering is restricted or halted.

This chapter investigates some fundamental chemical and hydrogeologic processes in two partly flooded underground mines in northern West Virginia. Drainage from these and similar mines often degrade the receiving watershed, and few strategies, except chemical or passive treatment, are effective in reducing impacts. An improved understanding of the processes operating in closed partly flooded mines may provide insight into the duration and severity of pollution, and what reclamation schemes could be applied to these mine-pools.

3.1 Data Acquisition
Water quality analyses for the above-drainage mines were obtained from three sources including:

- samples collected by the author for the Omega and T&T mine-pools,

- samples collected by the West Virginia Dept of Environmental Protection (WVDEP) for the Omega and T&T mine-pools. Data were provided by the special reclamation unit and retrieved from a file search in the Philippi, WV office of WVDEP,

- samples collected by the US Dept of Energy (USDOE) office in Pittsburgh, PA from 1993 to 1999 for the Omega mine record. These data were made available to the author.

The author collected and preserved mine-pool samples following guidelines suggested by Cherceri et al. (1998). This included appropriate filtering, preservation and containers, and field measured pH, Eh, specific conductance, and dissolved oxygen.

Data obtained from WVDEP were analyzed at two different labs, with the change of service occurring in October 2001. Samples collected by the USDOE were analyzed at its' contract lab and the author's samples were analyzed at a fourth commercial lab. This introduced some uncertainty and limitations into the analyses. Where feasible, data were examined for quality control using charge balance, conductance/TDS relationships and similar techniques. A total of about 290 samples were compiled for the T&T mine-pool for the period 1994 to 2007. Multiple sample points exist at the Omega mine-pool and the number of samples varies. The main treatment inlet monitoring point includes about 230 samples from 1993 to 2007.

WVDEP data include standard mine drainage analyses for pH, Fe, Mn, Al, sulfate, total acidity, TDS and Specific Conductance. The USDOE data include mine drainage parameters plus major cations and anions, Fe(II) determinations, and selected trace elements. Fe(III) was determined as the difference between total dissolved Fe and dissolved Fe(II). Most samples from both sources also include an instantaneous flow measurement. Total acidity was calculated from metals in mg/L and pH as:

$$\text{Acidity}_{total} = 50[(2*\text{Fe(II)}/56) + (2*\text{Mn}/55) + (3*\text{Al}/27) + (1000*10^{\wedge -pH})] \qquad (3\text{-}1)$$

Kirby and Cravotta (2005), and Cravotta and Kirby (2005) discuss, in detail, theoretical and practical aspects of acidity measurements in mine waters. They concluded that Fe should be represented as Fe(II) in acidity calculations after examining Fe speciation in mine water. Unless otherwise noted, total acidity data are calculated values using equation 3-1.

Sampling has been conducted on monthly intervals, and at times more frequently for both the Omega and T&T mine-pools. Some monitoring points have periods of no discharge and hence no chemical analyses.

The WVDEP also provided daily flow and on-site precipitation data for part of the record at both mine-pools. This information was used for developing recharge and water budget estimates.

A large change in sulfate concentration occurred in October 2001 for both the Omega and T&T mine-pools, corresponding to the change in analytical lab service. No other chemical parameters exhibited similar change, nor were there any known changes in discharge, treatment etcetera that could reasonably account for the observed sulfate change. Sulfate concentrations were regressed against other chemical parameters to determine if a consistent estimator relationship could be identified. Potential predictors included Fe, Al, flow, total acidity and TDS. Dissolved solids provided the most consistent relationship among sample locations for the period 1993 to 1999. The computed regression for sulfate on TDS at three monitoring points; Marshall, DEF, and Treatment Inlet discharges, percentage of variation explained, and lower and upper bounds at 95% are shown in table 3-1.

Table 3-1
Regression Results Estimating Sulfate from TDS at Three Discharges, Omega Mine-pool

Site	Regression	R^2	95% Confidence Lower bound	95% Confidence Upper Bound
Marshall Discharge	SO$_4$ (mg/L) = 0.666 * TDS	96.9%,	0.645	0.686
DEF Discharge	SO$_4$ (mg/L) = 0.658 * TDS	95.1%	0.634	0.681
Treatment Inlet	SO$_4$ (mg/L) = 0.676 * TDS	96.8%	0.657	0.696

Slope for the three regressions are similar, with relatively narrow upper and lower bounds on 95% confidence limits. Samples collected by the author from 2002 to 2008, and analyzed at a different lab, had sulfate values comparable to those estimated for the WVDEP data, and sulfate/TDS ratios similar to the slopes in table 3-1. A similar analysis was conducted for the T&T mine-pool data. A slope of 0.58 was the "best fit" estimator for sulfate from TDS for the T&T data. The derived TDS-sulfate relationships were used to estimate sulfate data for WVDEP samples after October, 2001.

3.2 Mine Setting and Mining History

3.2.1 Omega Mine

The Omega mine is a small underground mine in the Upper Freeport coal bed at the top of the Allegheny Group (Hennen and Reger, 1913). The mine-works covers about 69 hectares and are located in Monongalia County, West Virginia. Coal thickness is commonly about 1.3 m, with a shale parting. The West Virginia Geological and Economic Survey (2002) reports an average total sulfur content of about 2.5 % and average pyritic sulfur content of about 1.7% for the Upper Freeport coal bed. The Bolivar fireclay, a hard siliceous mudrock, immediately underlies the coal bed. At this mine, the Uffington shale overlies the coal bed and is commonly less than 0.6 m thick based on observations of exposed strata in the face-up area. The Mahoning and Buffalo sandstones comprise most of the overburden above the Uffington shale. These rocks may reach a combined thickness exceeding 30 m, and where exposed at the mine face-up, they display prominent vertical fractures. The mine has a maximum overburden thickness of about 76 meters, and is located above the local base level drainage. The Omega mine is contained within a broad ridgetop on the western flank of the Chestnut Ridge anticline, and strata dip about 11 % to the northwest (Gray et al., 1998) The rocks in this section contain few carbonates (Hennen and Reger, 1913).

Coal was extracted by room and pillar methods from the Upper Freeport coal bed until mine closure in 1989. Recovery ranged from 50% in first mined areas, to over 70% in areas of second mining. Data presented by EPRI (2001) indicates that most of the mine-works had 60 to 70% extraction. Average mining height was about 1.3 m. In the early 1990s, acid drainage began seeping from several locations along the coal crop-line (figure 3-1). Further details of the Omega mine are provided by EPRI (2001) and by Perry and Rauch (2004, Appendix A). There are no adjacent underground mines and the Omega complex is surrounded by unmined coal.

The Omega mine discharge features are shown in figure 3-1. An estimated 30% or less of the mine-works are flooded, and the mine-pool drains by gravity discharges along the down-dip coal outcrop. The mine-pool is not pumped. After closure, the mine partially flooded, and the general ground-water flow pattern within the mine-works is inferred to be in the direction of dip.

Mine drainage was collected and treated after several lateral boreholes were drilled into the northern mine-works to divert mine-water away from a section adjoining a stream, Cobun Creek, with a public water supply (Morgantown reservoir). Treatment sludge was initially injected into the mine-works for disposal. The West Virginia Department of Environmental Protection (WVDEP) assumed control of the site in the mid 1990's and disposes of the material offsite.
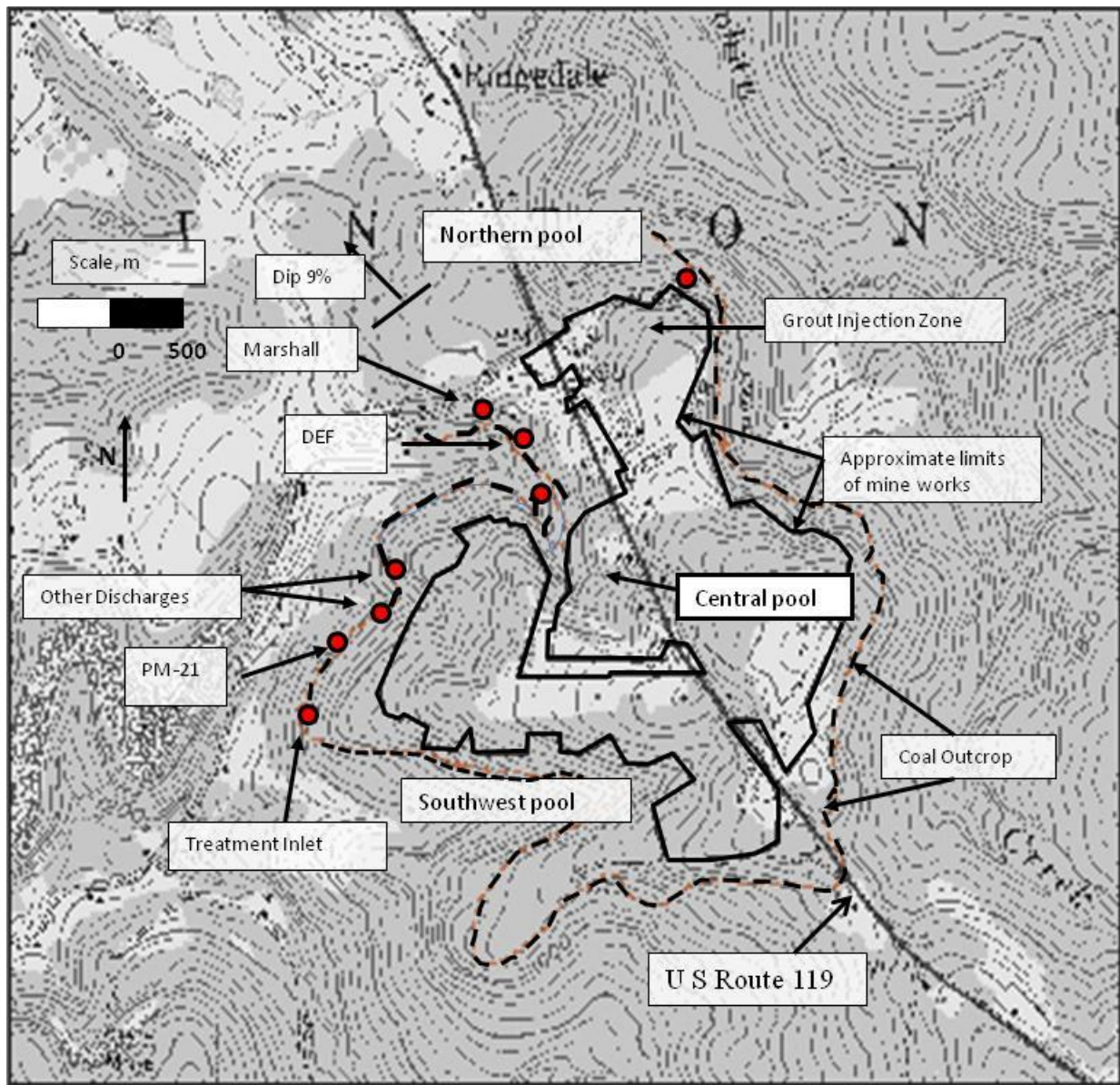
Figure 3-1. Extent of Omega Mineworks (black line), Coal Outcrop (dashed line) and Discharges (circles).

WVDEP also installed a series of pipelines and manholes to more easily and securely collect, sample, measure, and convey mine-water to the treatment facility. In some instances, several adjacent seeps were combined into a single monitoring point. In 1998, a cooperative state, federal and privately funded grouting project was initiated to reduce or abate acidic discharges in the north lobe (Figure 3-1) of the mine (Gray et al., 1998; EPRI, 2001). This area comprises about 10.5 hectares, or 15% of the mined area, but was estimated to be discharging about 55% of the acid load (EPRI, 2001). About 61,000 m^3 of grout mix containing fluidized-bed combustion ash, flyash and cement were injected in the North Lobe. Subsequent drilling and borehole camera observations confirmed that, in general, the grout mixture provided near complete filling of mine voids. Water

quality remained poor after grouting; however, flow, and consequently acid load, decreased (EPRI, 2001).

Summary data for four Omega mine discharges at two different time periods are shown in table 3-2. The 1993-1994 data represent conditions in the first few years after the mine closed, partly flooded and began to discharge. The 2001 data are indicative of long term conditions, after the grout injection and initial flushing occurred. Acidity and metal concentrations declined over the seven year period but overall water quality remains poor. Median values for one year periods illustrate the high concentrations of Al, Fe and sulfate. With the exception of the Marshall discharge in 2001, pH was less than three. Post-grouting, the Marshall discharge quality has shown a modest increase in pH to about 3.5, compared to less than 3.0 prior to grout treatment. The Marshall drainage has also been enriched in Ca, and approaches saturation for gypsum after grouting (Perry and Rauch, 2004). Some acid neutralization must be provided by dissolution of the grout material, based on increases in Ca, Mg, and Na from pre to post grouting. Except for PM-21 in 1993, total acidity exceeds 1000 mg/L $CaCO_3$ Eq.

Table 3-2
Omega Mine Summary Water Quality
for Three Discharges at Two Time Periods[1]

Site	Date	Grouting	pH	Total Acidity (mg/L)	Fe (mg/L)	Al (mg/L)	Sulfate (mg/L)
Treatment Inlet	2/93 to 1/94	Pregrout	2.94	2000	677	129	3316
Treatment Inlet	2001	Postgrout	2.8	1336	368	109	2300
Marshall	2/93 to 1/94	Pregrout	2.62	4550	1612	274	5975
Marshall	2001	Postgrout	3.3	1893	689	107	3275
PM-21	2/93 to1/94	Pregrout	2.99	464	119	41	2856
PM-21	2001	Postgrout	2.80	1300	214	139	2570
DEF	2/93 to1/94	Pregrout	2.71	2000	664	129	3141
DEF	2001	Postgrout	2.60	1261	313	103	2201

(1) Median values. pH in S.U. Acidity in $CaCO_3$ Eq.

3.2.2 T&T Mine-pool

The T&T mine-pool consists of about 588 hectares of mine-works in the Upper Freeport coal bed, the same coal mined at the Omega site. The T&T mine-pool, located in Preston county West Virginia, consists of three adjoining mines, as shown in figure 3-2. All three mines are located above the local base level drainage and dip to the southeast at about 8% southeast toward the axis of the nearby Kingwood syncline. The coal bed is about 1.2 m thick, and is overlain by several massive sandstones up to 18 m thick, interbedded with thinner shale units. The section contains few carbonates, and maximum overburden thickness is about 80 m. The author has observed subsidence cracks in land overlying the mine complex.

Barrier pillars of varying thickness separate the three mines, and the barrier is known to be breached in at least one location. The Ruthbelle mine, located in the northeast part of the complex, closed in the 1950s, while the T&T 2 and T&T 3 mine closed in the early and mid 1990s. The

three mines are hydrologically connected, and most of the mine-pool discharge occurs at the former portals of the T&T 2 mine. Leakage from the adjacent Ruthbelle and T&T 3 mines contributes part of the drainage that discharges from the T&T 2 mine (figure 3-2). All discharges are gravity drainage.

The T&T 2 mine is at the lowest elevation of the three workings and is the principal discharge point for the entire complex. The entries were developed along strike and mining proceeded up-dip from that location. This design allowed gravity drainage of the mine-works during operation. After closure, about 20% of the lower mine-works flooded to the elevation of the entries. The mine-pool contains about 300 million L of ground-water, as estimated from examining mine maps. A small pool may also be present up-dip of the coal barrier between the No. 3 and No. 2 mine-works.

A high volume discharge of acidic, poor quality water developed at the T&T No.2 portal area within six months of sealing the mine in 1994. The discharge volume subsequently declined but water quality remained poor. The drainage has been treated with conventional chemical methods since that time and treatment sludge is periodically reinjected into the up-dip end of the complex. About 72,000 metric tons of limestone byproduct (70 % $CaCO_3$ Eq.) was injected into the mine from late 1999 to 2001 in an attempt to treat acid water in-situ.
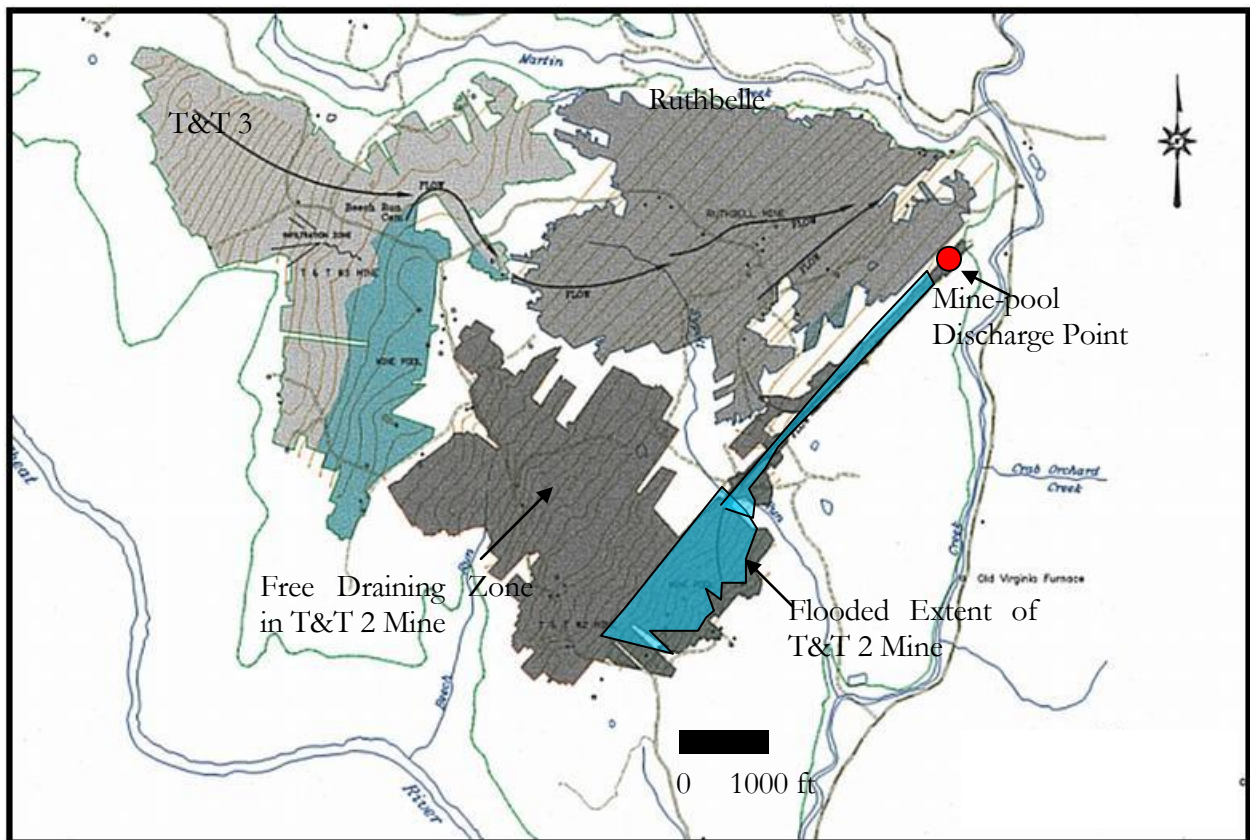
Figure 3-2. T&T Mine-pool. Dip is to Southeast at 8%. Main Discharge is from No. 2 Mine and represents draianage from T&T 2, T&T 3 and Ruthbelle mines. Scale in feet.

Table 3-3 provides summary water quality data for the T&T mine-pool in early flushing stage (1994), about two years after closure (1996); and about 10 years after closure (2006) and 5 years after limestone injection ceased. Water quality data immediately after closing are sporadic, and Al is not included in many of the analyses. The No.2 portal drainage was sampled by the author in 1994 about two months after the mine-pool began to discharge. This single event sample is included in table 3-3 to represent very early flushing water quality.

Table 3-3
Summary Water Quality Data T&T 2 Mine-pool,
Mostly Unflooded Upper Freeport Mine-Works [1]

Location	Date	pH	Total Acidity, mg/L	Fe, mg/L	Al, mg/L	SO$_4$, mg/L
No. 2 Portal	1994	2.8	1320	455	90	1910
No. 2 Portal	1996	2.6	728	216	40	1320
No. 2 Portal	2006	2.78	300	44	25.2	963
Ruthbelle	1996	2.6	238	36.3	14.7	382
Ruthbelle	2006	2.9	91	4.7	3.5	172

(1) Median values in 1996 and 2006. The 1994 data are a single event sample collected by the author. pH in S.U., Acidity in CaCO$_3$ Eq.

The Ruthbelle mine discharges some of the overflow but generally comprises only one to three percent of the total outflow from the mine-pool. The Ruthbelle overflow drains from an abandoned entry about 100 meters north of the main mine-pool discharge at the T&T 2 mine. Most of the Ruthbelle drainage flows into T&T 2 mine and exits the mine-pool through that point. It is included in table 3-3 because the mine-works are much older than other parts of the complex. Drainage quality of Ruthbelle may therefore indicate how the T&T mine water quality will evolve as it matures.

3.3 Water Quality in Partly Flooded Mines

3.3.1 Chemical Composition
The Omega and T&T mine-pools are characterized by high concentrations of dissolved metals, sulfate and total acidity. Tables 3-2 and 3-3 provide summary water quality information for both mine-pools soon after closure and after a period of flushing. Time series plots of cation composition (milliequivalent basis) of three individual discharges and the combined flow to the Omega treatment facility are shown in figures 3-3a-d. All four waters are composed of more than 98% sulfate in the anion fraction. The three individual discharges are located in different subsections of the mine-pool. PM-21 is located at the up-dip end of the mine and is near where treatment sludge was returned to the mine-works. Composition of the water has changed from Ca-Mg-SO$_4$ during early flushing to Fe-Al-SO4 as the mine-pool has aged (fig 3-3a).

Omega mine discharge DEF, located in the middle subsection of the mine-pool (fig 3-1), was initially an Fe-Al-SO$_4$ solution. The long term drainage contains a greater percentage of Al and

decreasing fraction of Fe. Calcium and Mg fractions remain constant. The third discharge, Marshall, is located at the down-dip end of the pool and receives drainage from the grouted north
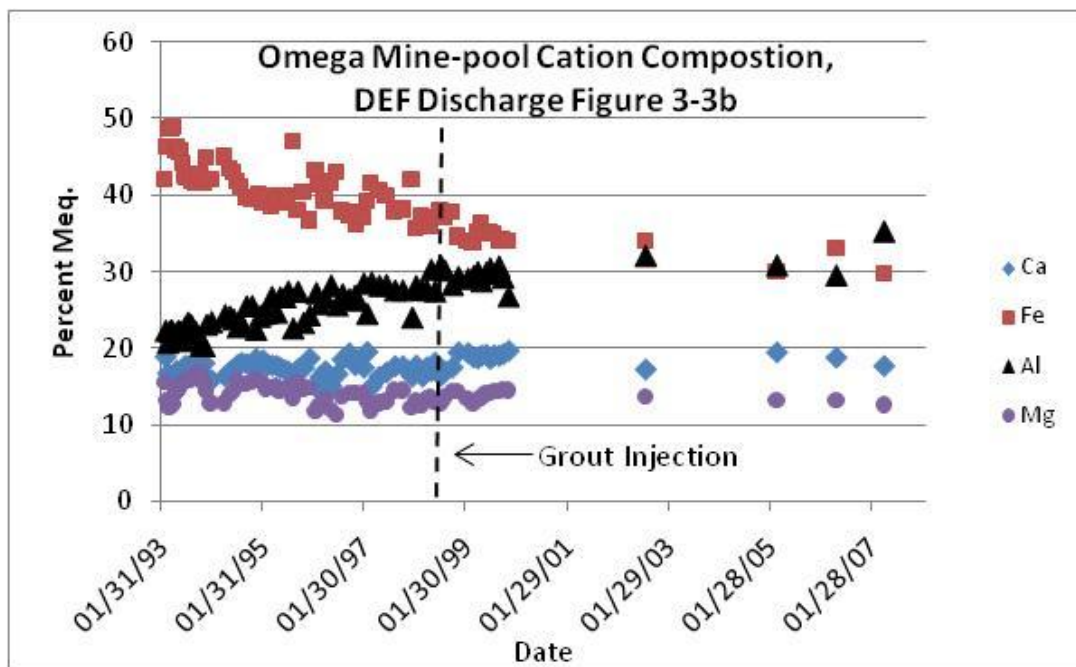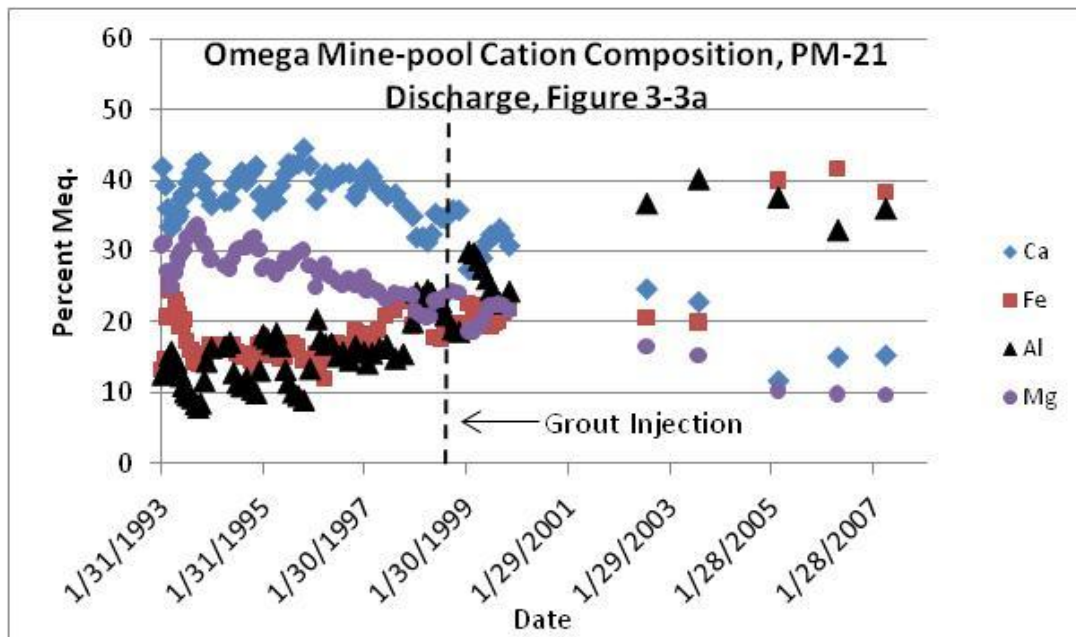
Figures 3-3a-b. Time Series Cation Milliequivalents Composition of Three Discharges and Combined Flow from the Omega Mine-pool. Calcium (diamond), Iron (square), Aluminum (triangle), and Magnesium (circle).
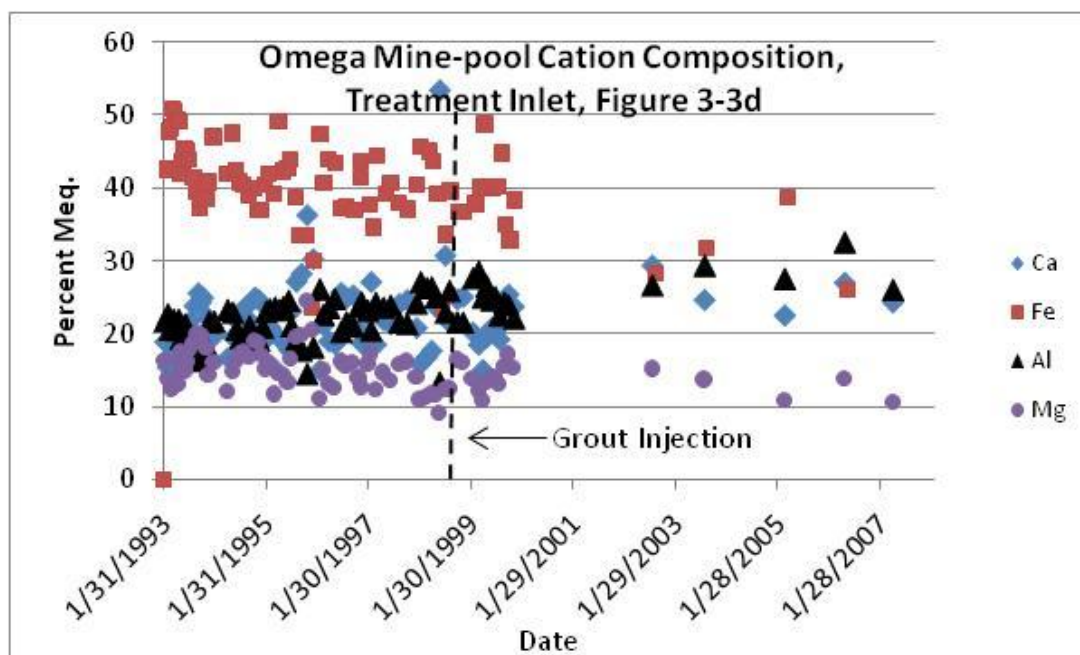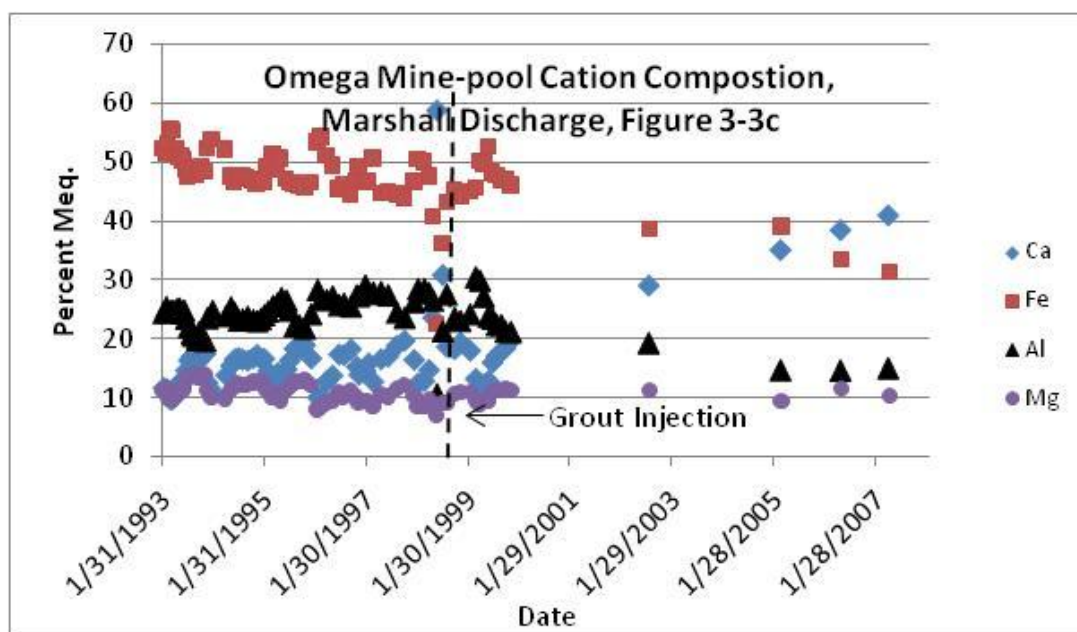
Figures 3-3c-d. Time Series Cation Milliequivalents Composition of Three Discharges and Combined Flow from the Omega Mine-pool. Calcium (diamond), Iron (square), Aluminum (triangle), and Magnesium (circle).

section. This water was also an Fe-Al-SO$_4$ solution initially, but shifted to a Ca-Fe-SO$_4$ composition after grout injection. The treatment inlet, which is the combined flow from all discharges, is an Fe-Al/Ca-SO$_4$ mixture. In two of three Omega mine discharges and the combined flow, Al comprises greater percentage of the cation charge as the mine-pool ages, and Fe declines with time. The Al decline post grouting at the Marshall discharge suggests that the flyash/cement injection is reducing Al mobility in this part of the mine-pool. The increasing Ca also indicates the

30

grout mixture is influencing solution chemistry in this part of the mine-pool. The decline in Ca and Mg at PM-21 with increasing age suggests the source mineral(s) are being depleted in this part of the pool. Both elements however comprise a relatively constant fraction of the combined mine-pool flow. These three plots (figures 3-3 a, b, and d) show a trend of increasing Al composition in the cation fraction as the mine-pool ages, and declining, though still significant proportion of Fe. Aluminum therefore may persist in the mine-pool for a prolonged period if geochemical conditions remain the same.

The T&T mine-pool does not have an extended time series record of major ion analysis. A single sample collected by the author in 1994 showed the water had an Fe-Ca-SO$_4$ composition (milliequivalent basis). Samples collected from 2002 to 2007 by the author are Ca-Mg-SO$_4$ type waters (milliequivalent basis).

The two mines, although located in the same stratigraphic interval, produced waters of somewhat different composition. Chemical weathering in the Omega mine-pool is sufficiently aggressive that Fe and Al, normally minor or trace constituents in ground-water, are the dominant cations on a milliequivalent basis. The T&T mine-pool while containing substantial dissolved Fe and Al, still has Ca and Mg as the dominant cations on a milliequivalent basis. Both mine-pools contain sulfate as the dominant anion. Site specific geochemical analyses of the coal, roof and floor rock could not be located for either mine. However, EPRI (2001) reports a zone of high pyrite content present in the Omega mine.

Figures 3-4a and b and 3-5a and b are time series plots of Fe, Al, and sulfate at the main discharge points for the Omega and T&T mine-pools for 14 and 12 years, respectively. Both figures show substantial declines in Fe and sulfate concentration of 50 to over 80% from initial conditions. Al concentration also declined but to lesser extent. Two other features are evident on figure 3-4a and 3-5a. First is a large short term variation, resulting in considerable scatter. Second are short term increases in chemical concentrations, corresponding to the grout and limestone injection in the two mine-pools.

The raw data scatter in figures 3-4a and 3-5a obscure more subtle trends and features that may be present in the data sets. Log and other types of transforms, nonparametric tests, and graphical methods can sometimes improve resolution of scattered data and detect trends and differences (Cleveland and Terpenning, 1982; Hirsch et al., 1982; Hirsch and Slack, 1984; Hirsch et al., 1991). A simple moving average or median, and locally weighted scatter plot smoothing (LOWESS), can be used to smooth time series data (Helsel and Hirsch, 1992; Cleveland and Devlin, 1988). The LOWESS procedure requires repetitive computations of least squares regression and application of weighting factors to the raw data.

The moving median or average method was attempted first as a simple, intuitive smoother. A five point moving average was computed on the raw data as follows:

$$\text{Smoothed n} = (n_{I-2} + n_{I-1} + n_i + n_{I+1} + n_{I+2})/5 \qquad (3\text{-}2)$$

Figures 3-4b and 3-5b show smoothed Fe, Al and sulfate data for the two mine-pools. The declining trends, and short term increases after grout and limestone injection become more obvious in the smoothed data sets. A cyclic, seasonal concentration trend is also visible in the smoothed
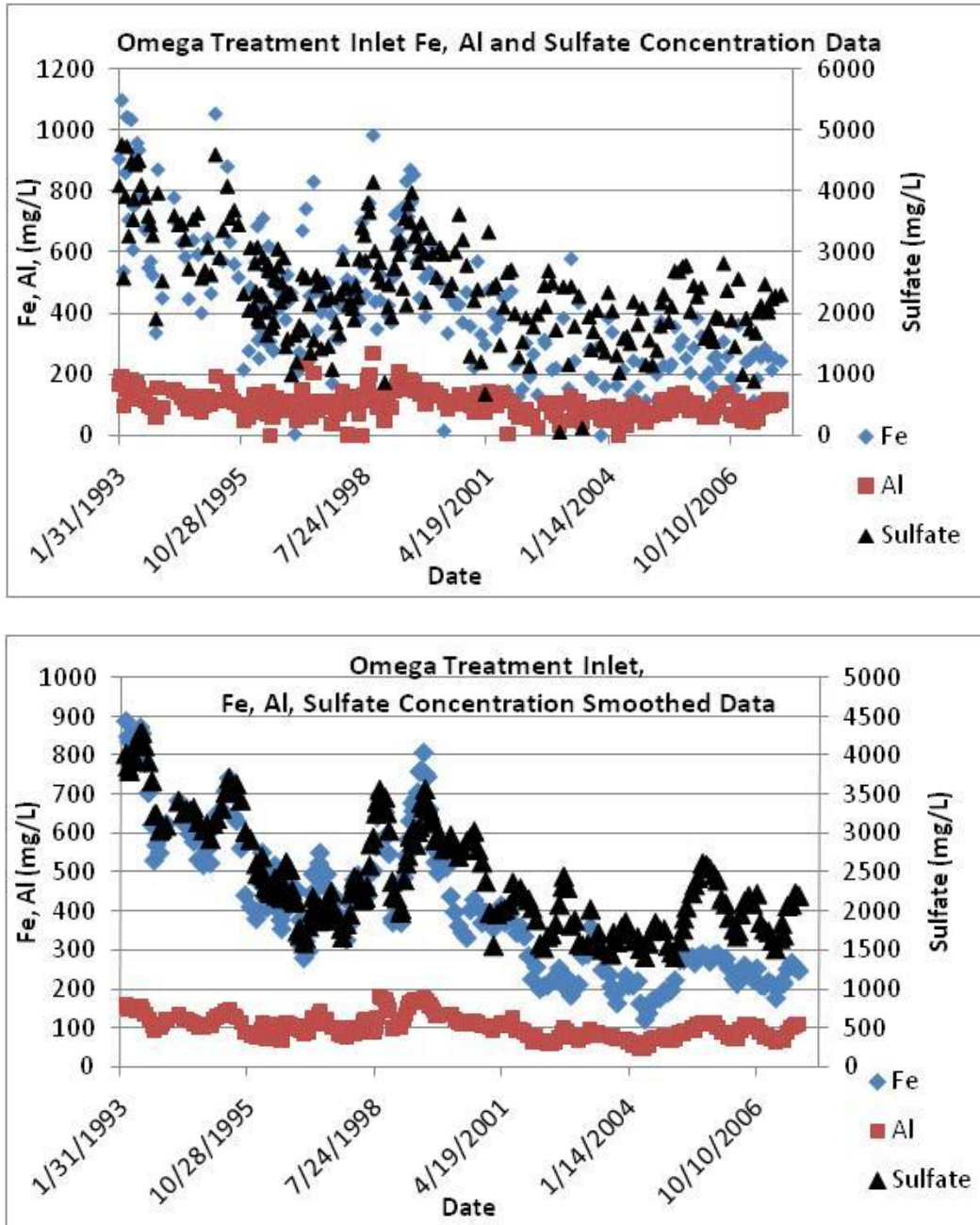
Figure 3-4 a and b. Time Series Plot of Chemical Concentrations, Omega Mine-pool Combined Discharge. Fe (diamond) and Al (square) on left axis, Sulfate (triangle) on right axis, in mg/L. Raw and smoothed data.

Omega data that would be difficult to detect in the raw scatter plot. The five point smoothing was adequate to delineate underlying trends and features. It was used to identify seasonality, which is

described in this section, and sections 3.3.3 and 3.3.4. In the Omega mine-pool, chemical concentrations were seasonal and inversely related to mine discharge rate. Maximum chemical concentrations occurred in late summer to autumn when flow rates were lowest. The observed time dependent trends and smoothing techniques are analyzed further in chapter five to establish trends and predictions in long term chemical composition of partly flooded and flooded mine-pools.
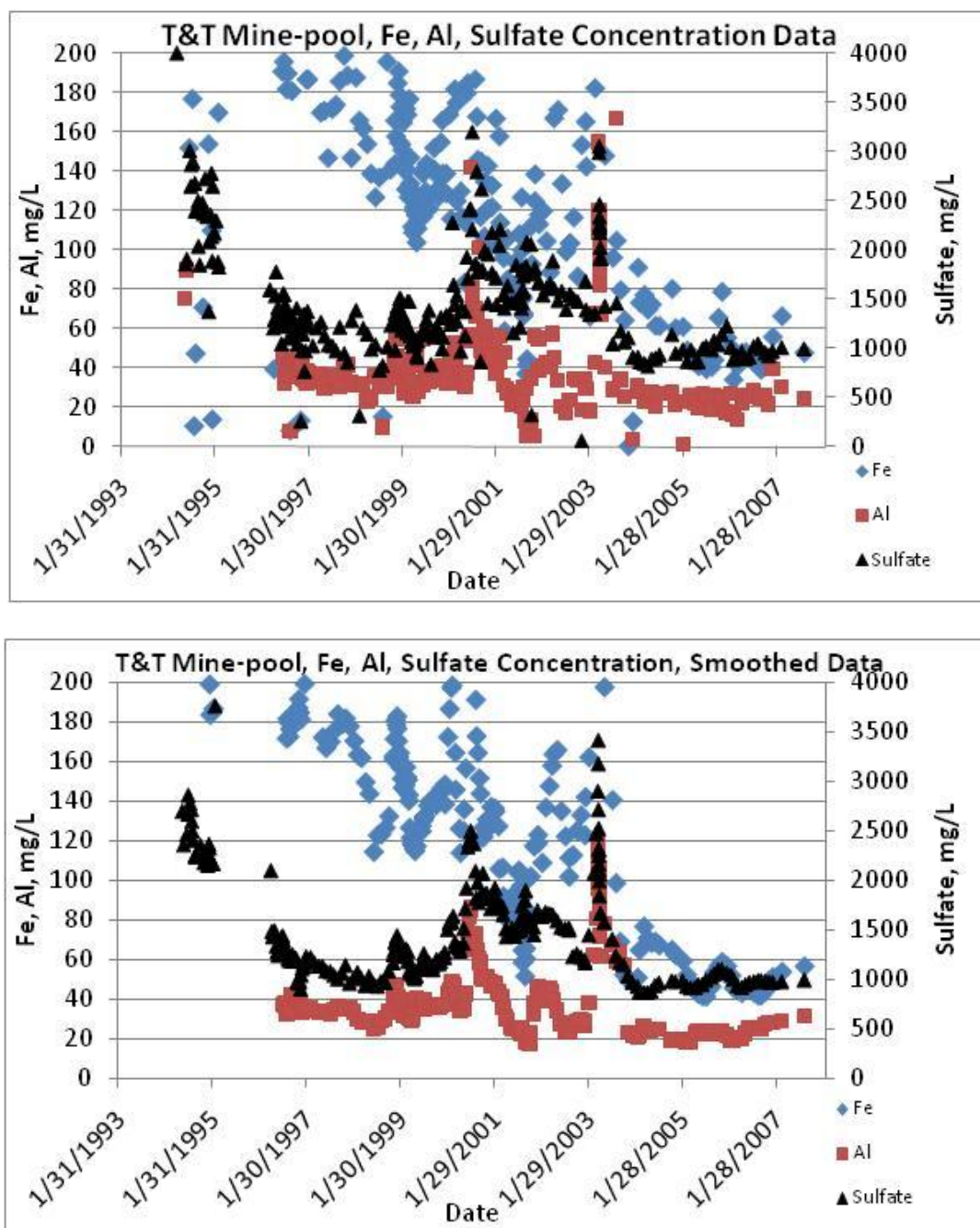
Figure 3-5 a and b. Time Series Plot of Chemical Concentrations, T&T Mine-pool Main Discharge. Fe (diamond) and Al (square) on left Axis, Sulfate (triangle) on right Axis, mg/L. Raw and smoothed data.

33

3.3.2 Mole Ratios

Oxidation of pyrite should yield a solution containing one mmole Fe to two mmoles sulfate, if pyrite weathers congruently, and soluble sulfate and Fe are retained in solution. Under these circumstances, a mole ratio plot can aid understanding of the mineral reactions and physical hydrology of the mine-pool. Figures 3-6 and 3-7 are smoothed time series plots of Fe to sulfate mole ratio for the Omega and T&T mine-pools, respectively. The heavy black line on both figures is the expected composition based on pyrite stoichiometry. Each mine-pool is deficient in iron with respect to sulfate. The largest ratios occur in the early phases of flushing. For early phase mine data the Omega mine has ratios of about 0.3 to 0.4, accounting for about 60 to 80% of Fe from pyrite, while the T&T mine-pool has Fe to sulfate mole ratios of 0.2 to 0.4, representing 40 to 80% of Fe from pyrite. The Omega mine-pool also exhibits a seasonal trend, with maximum ratios occurring in the spring at high recharge/discharge rates, and low ratios in the fall during low recharge/discharge rates. The seasonal trend in Omega mine-pool may reflect less conservative
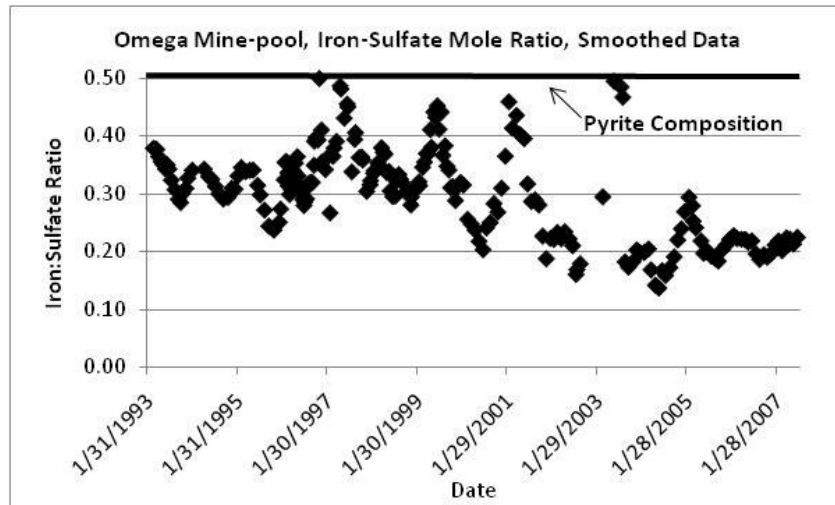
**Figure 3-6. Iron to Sulfate Mole Ratio, Omega Mine-pool
Combined Flow, Smoothed Data.**
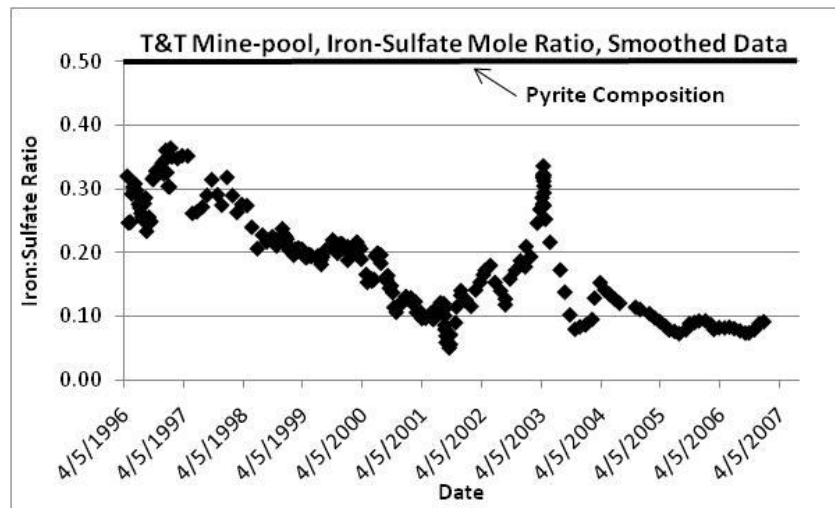
Figure 3-7. Iron to Sulfate Mole Ratio, T&T Mine-Pool, Smoothed Data.

behavior of Fe with respect to sulfate. The larger ratio during high flow conditions suggests more Fe is being flushed from the mine-pool at these times, and relatively more Fe is being retained in the mine during low discharge periods. Sulfate concentration is less affected by mine discharge rate than Fe. The T&T mine-pool shows no obvious seasonal trend.

Iron-sulfate mole ratio declines in both mine-pools as they age, and after injection of grout and limestone. The ratio declines to about 0.2 in the Omega mine-pool and about 0.1 in the T&T mine-pool, indicating respectively that 60 to 80% of iron from pyrite weathering in these mine-pools is not accounted for in the discharges. Both mine-pools approach a constant long term ratio.

These data yield the following interpretations and conclusions:

- Iron is being retained in the mine-pool both as short term storage and long term weathering products.

- The fraction of iron retained within the mine from pyrite weathering is significant, even in acid mine-pools, and may be more than half of the initial source.

- The fraction retained increases as the mine-pool ages and approaches a constant condition.

- Seasonal variation in the Omega mine-pool implies some Fe is in short term storage and is flushed during high recharge periods. Storage in soluble Fe salts could account for the observed behavior and enrichment of the discharge with iron during flushing.

- Iron to sulfate mole ratio could provide a means of distinguishing early flushing from long term weathering in mine-pools. This observation is used in chapter five to help differentiate short and long term leaching trends.

- Iron storage mechanisms within the mine could include formation of soluble salts, oxyhydroxides of varying solubility, adsorption, cation exchange or possibly other mechanisms.

Aluminum to sulfate mole ratio was calculated for the Omega combined flow and the T&T discharge. Most ratio values are from 0.1 to 0.15 in both mine-pools with a maximum of about 0.2. Both mine-pools are at or approach apparent saturation for the mineral jurbanite (section 3.4) which contains Al and sulfate in a one to one mole ratio. Thus, both mine-pools contain a large excess of sulfate relative to Al and jurbanite composition.

3.3.3 Solution Complexes
The speciation of elements in partly flooded mine-pools and the solid phase aquifer matrix partly controls the quantity of that element in solution. The sulfate ion can form aqueous complexes with various cations, and these complexes can comprise a significant percentage of the total element in

solution. The two partly flooded mine-pools contain substantial concentrations of sulfate, Fe Al, and other major and minor elements. Sample events that included major cation and anion analysis were speciated in PHREEQCI (Parkhurst and Appelo, 1999). In the Omega mine-pool, this included about 90 sampling events collected by the US Dept of Energy and the author. The T&T mine-pool includes seven sampling events collected by the author. Figures 3-8 and 3-9 show the distribution of sulfate complex species (mole/L) as a percentage of total S(VI) for the PM-21 spring in the Omega mine-pool, and the T&T main discharge.

The Omega sulfate species are shown in figure 3-8 for early flushing (1996) and long term conditions (2007), and at high and low discharge periods (respectively for April, May and September, October). Uncomplexed sulfate is the principal species, but significant amounts of S(VI) are complexed with Fe, Al, Ca and Mg. As the mine-pool aged, the amount of uncomplexed sulfate has declined to less than 50% of total S(VI), and Al and Fe sulfate complexes each comprise between 15 and 20 % of the total. During early flushing, $CaSO_4°$ was the second most abundant species but was replaced by Fe and Al sulfate complexes by 2007. The shift reflects the decline in soluble Ca, and relative persistence of Al and Fe. A small seasonal shift in percent amounts of Al-SO_4 and Fe-SO_4 species is also shown in figure 3-8. During initial flushing in April, 1996 (high discharge rate period), Al-SO_4 species were more abundant than Fe-SO_4. By May 2007, the trend was reversed and percent Fe-SO_4 species were more abundant than Al-SO_4. The seasonal and long term differences in sulfate speciation may reflect changes in chemical activity, and suggest individual elements may have characteristic leaching behavior influenced by source minerals and discharge conditions.
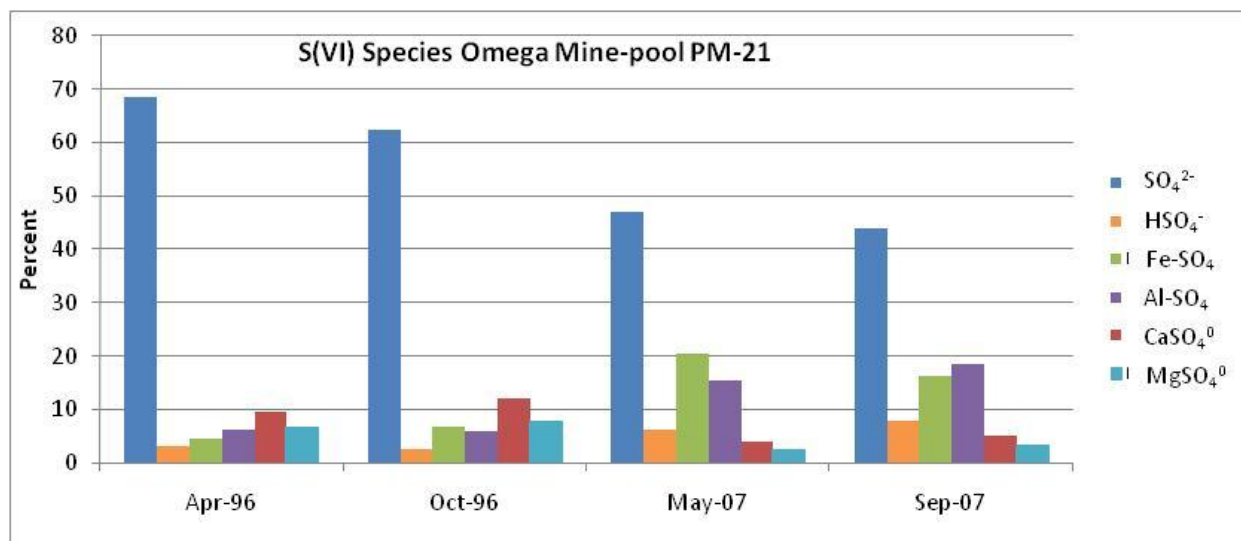
Figure 3-8. Distribution of Most Abundant Sulfate Complexes, Omega PM-21 Discharge, Initial Flush (1996) and Long Term Drainage (2007), and High (Apr, May) and Low (Oct, Sep) Discharge Periods. Fe-SO_4 includes Fe(II) and Fe(III) combined, Al-SO_4 includes $AlSO_4^+$ and $Al(SO_4)_2^-$.

Figure 3-9 shows sulfate species distribution for early and long term flushing, and seasonal low and high recharge periods in the T&T mine-pool. Unlike the Omega mine-pool, $CaSO_4°$ is the

second most abundant sulfate species after uncomplexed sulfate in long tern leaching (2003 and 2007) at the T&T site, and may result from the limestone addition. Iron and Al-SO$_4$ complexes were more abundant in 1994. The propensity for sulfate to complex with Fe, Al, Ca and Mg will, in general, increase the amount of source mineral that can dissolve, and contributes to the high concentrations of metals observed in these mine waters.
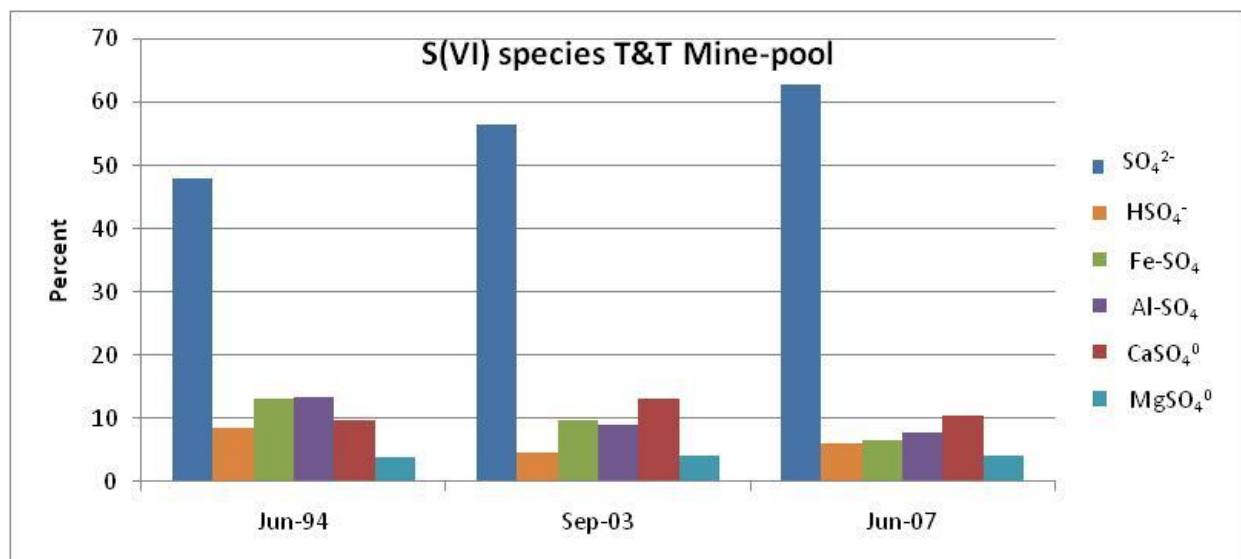
Figure 3-9. Distribution of Most Abundant Sulfate Complexes, T&T Main Discharge, Initial Flush (1994) and Long Term Drainage (2003, 2007), and High (Jun) and Low (Sep) Discharge Periods. Fe-SO$_4$ includes Fe(II) and Fe(III) combined. Al-SO$_4$ includes AlSO$_4^+$ and Al(SO$_4$)$_2^-$.

Figure 3-10a and b shows the abundance of principal species of Al, expressed as a fraction of total solution Al (mole/L basis) for the Omega and T&T mine-pools for the same sample dates and conditions as in figure 3-8 and 3-9. The distribution of species is consistent between sampling conditions and mines. About 70% of soluble Al is complexed with sulfate as AlSO$_4^+$, and Al^{3+} comprises 15 to 20% of total dissolved Al. This increases the amount of Al that can dissolve from source minerals including alumino-silicates, oxyhydroxides and sulfates.

The Al sulfate mineral jurbanite dissolves as follows:

$$AlOHSO_4 + H^+ \leftrightarrow Al^{3+} + SO_4^{2-} + H_2O \qquad (3\text{-}3)$$
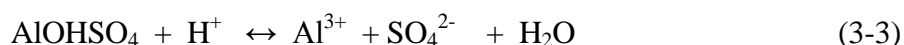
The log equilibrium constant in PHREEQCI for jurbanite is -3.23. Reaction 3-3 involves only Al^{3+} and does not include the formation of AlSO$_4^-$. Using data from the May, 2007 sample from the Omega mine-pool shown in figure 3-10, the water was equilibrated in PHREEQCI to saturation with jurbanite. The total dissolved Al, including complexes, is 6.16 x 10^{-3} mole/L. Solving the equilibrium expression for equation 3-3, and specifying Al^{3+} as the only aluminum species present, gives an estimated dissolved Al of 1.28 x 10^{-3} mole/L. Thus, the formation of the Al-SO$_4$ species increases the quantity of the mineral jurbanite that can dissolve by a factor of almost five, and the concentration of total soluble Al in the Omega mine-pool.
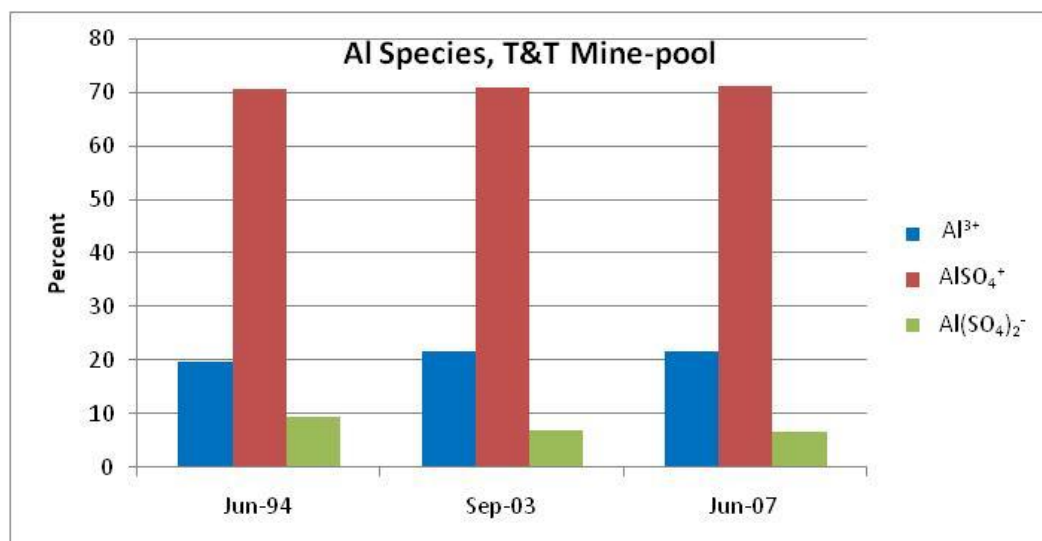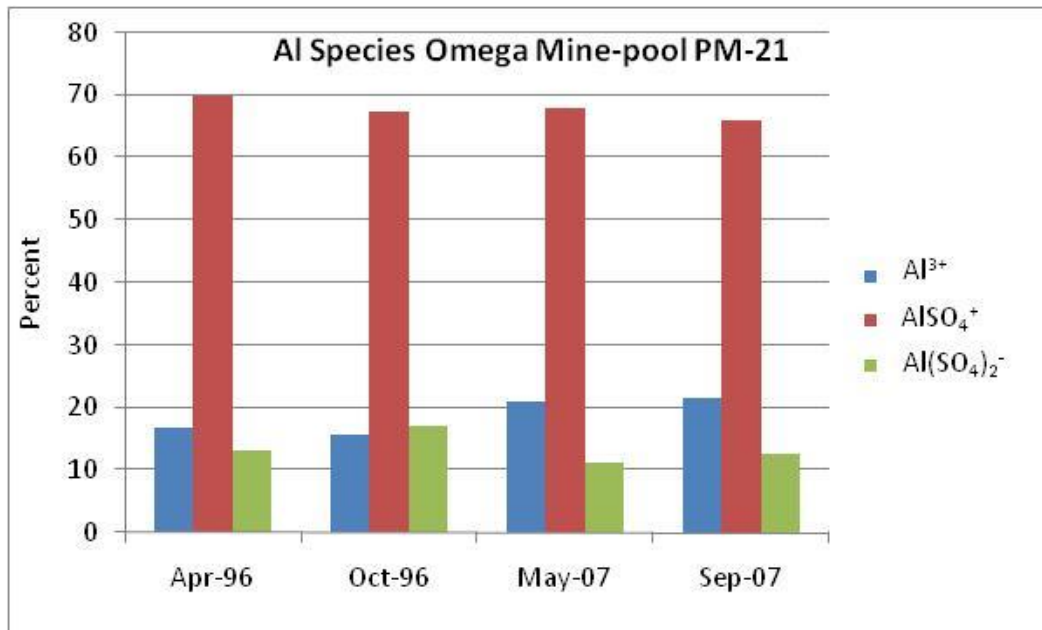
**Figure 3-10 a-b. Distribution of Most Abundant Aluminum Complexes,
Omega Mine-pool PM-21 and T&T Main Discharge.**

Figures 3-11a and b shows the distribution of the most abundant Fe II species for the same Omega and T&T mine-pool sampling events as described previously. Uncomplexed Fe^{2+} is most abundant species, and comprises about 70% of total dissolved Fe (II). There is little variation between mines or sampling conditions.
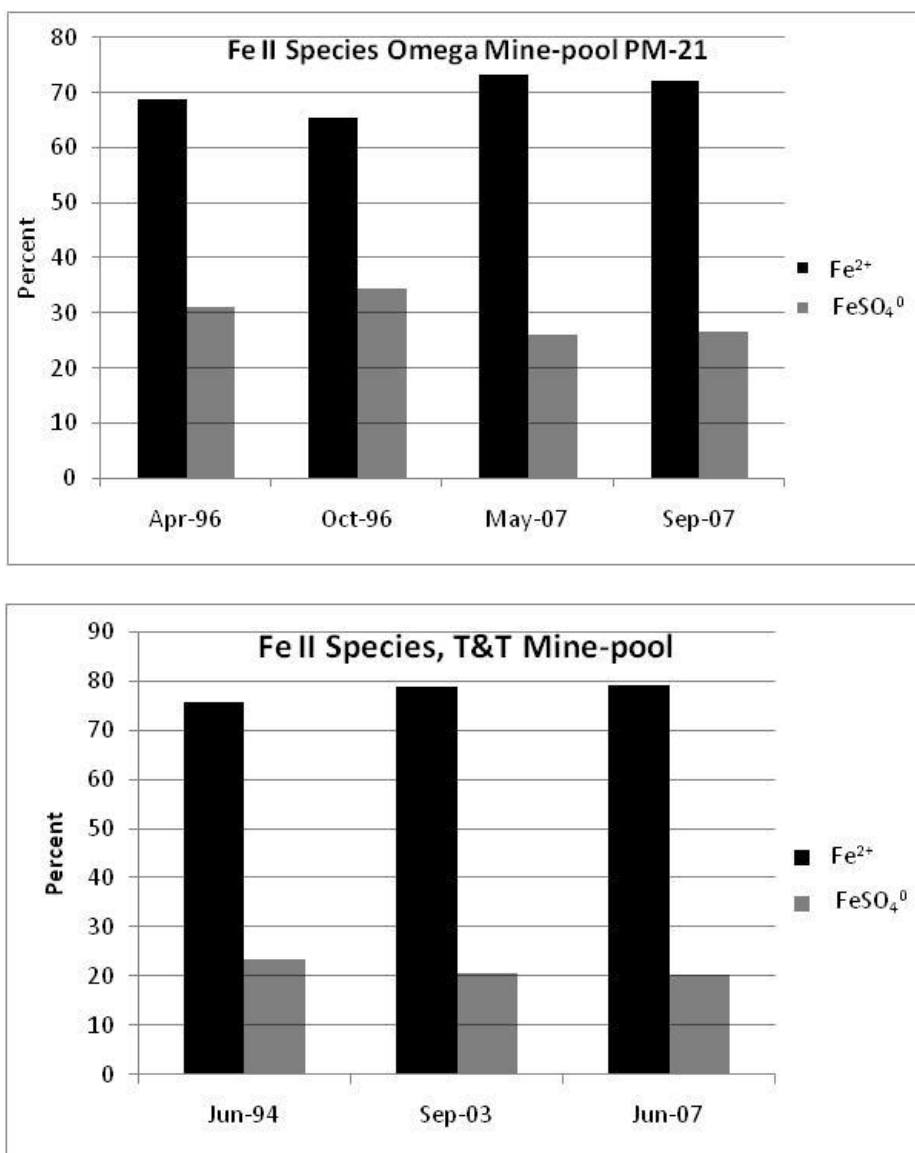
Figure 3-11a-b. Distribution of Most Abundant Fe II Complexes,
Omega Mine-pool PM-21 and T&T Main Discharge.

Figure 3-12a-b shows the distribution of the most abundant Fe (III) species for the Omega and T&T mine-pools under early and long term flushing and low and high discharge conditions. As with Al, about 70 to 80% of the dissolved Fe(III) is complexed with sulfate. The degree of Fe complexing is dependent on the charge state. For Fe(II) species, Fe^{2+} is the dominant species, while

for Fe(III); the $FeSO_4^+$ complex is the dominant species (figures 3-11 and 3-12). Like Al, the affinity for Fe to form complexes with sulfate increases the concentration of soluble Fe that can be maintained by mineral dissolution.
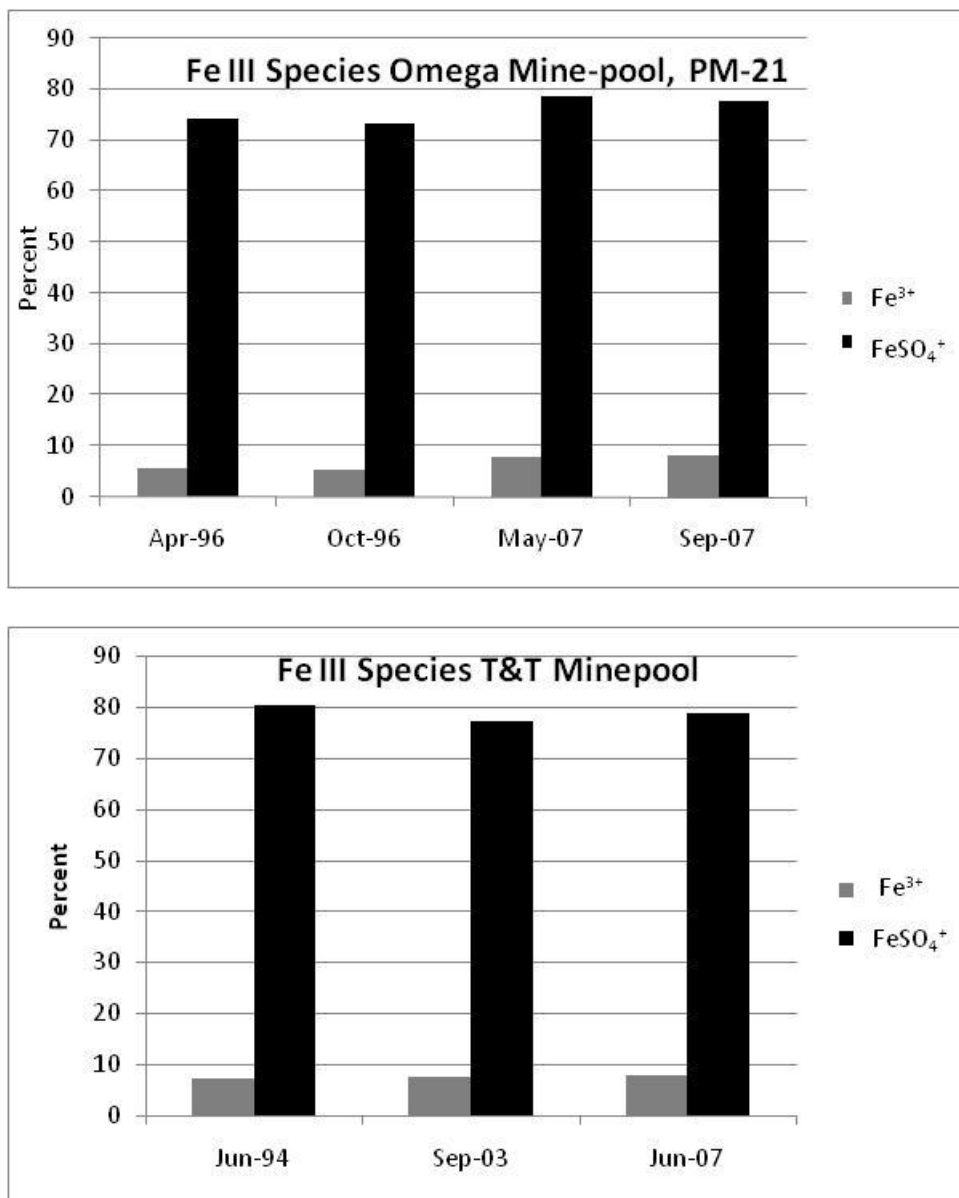
Figure 3-12a-b Distribution of Most Abundant Fe III Complexes,
Omega Mine-pool PM-21 and T&T Main Discharge.

Figure 3-13 shows the distribution of Ca species in solution for the same set of samples from the Omega mine-pool PM-21 discharge. Only two species are abundant, Ca^{2+} and $CaSO_4^{\,\circ}$, and there is little difference in distribution between early and late flushing or high and low discharge periods. Using data from the May, 2007 sample from the Omega mine-pool shown in figure 3-13, the

solution was equilibrated in PHREEQCI to saturation with gypsum.The total dissolved Ca including all complexes is 1.269×10^{-2} mole/L. Solving the equilibrium expression and specifying Ca^{2+} as the only calcium species yields a total dissolved Ca of 8.142×10^{-3} mole/L. The formation of $CaSO_4°$ increases total soluble Ca about 55% if gypsum dissolution is the controlling reaction. Sulfate complexes with Al, Fe and Ca substantially increase the dissolved concentrations of each of those elements that can be sustained in mine waters.
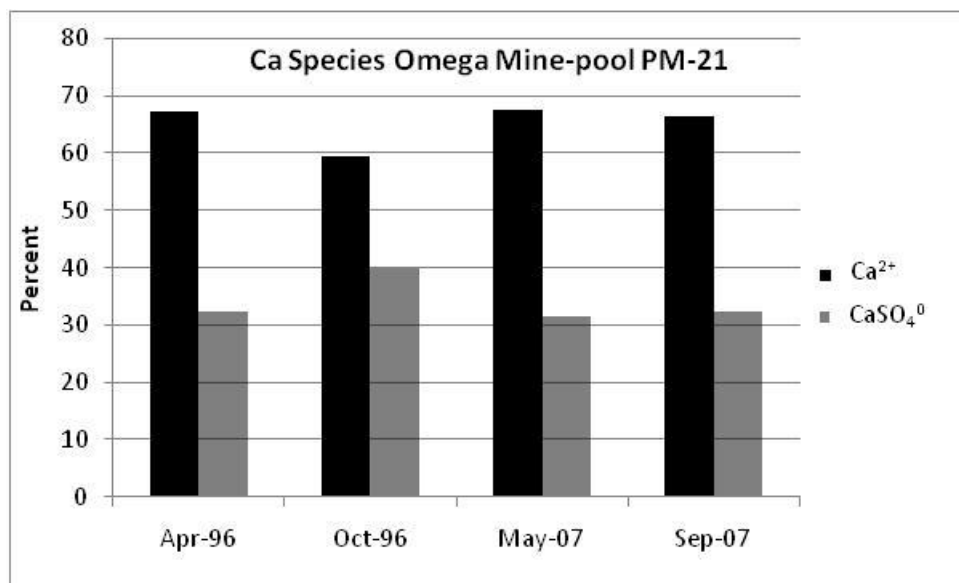
Figure 3-13. Distribution of Most Abundant Ca Complexes, Omega Mine-pool PM-21.

3.3.4 Redox State of Partly Flooded Mines

The reduction/oxidation (redox) state of waters in partly flooded mines has a large effect on sulfide oxidation; species distribution of elements with multiple valence states including Fe, Mn, As and others; and formation and dissolution of minerals containing those elements. In acid mine waters, good agreement between Fe(II)/Fe(III) distribution and measured (observed) Eh (Nordstrom et al.,1979; Auque et al.,2008; Nordstrom, 2009) has been found. This agreement can be attributed to the high concentrations of Fe often present in mines water, making it easier for the electrode to sense Fe^{2+} and Fe^{3+}. The iron couple is also readily reversible (Langmuir, 1997). Christensen et al. (2000), in a review of redox characterization techniques, also concluded that the Fe^{2+}/Fe^{3+} couple was reversible, and sufficiently rapid to be useful in ground-water studies. Studies of the Berkley pit in Montana, a large abandoned and partly flooded copper mine, have also shown good agreement between Fe^{2+}/Fe^{3+} equilibrium Eh and measured Eh (Davis and Ashenberg, 1989) if both species were present in readily detectable amounts, and the minor species was at least 5% of the total Fe.

Some ground-waters are at internal disequilibrium, and lack a single overall redox value (Lindberg and Runnells, 1984) resulting in a mixed potential. Acid mine waters are, however, systems where measured Eh may be a reliable index of the redox state for iron.

The author collected a set of measurements of Eh, dissolved oxygen and Fe(II) from the Omega and T&T mine-pools and several other locations with the objective of comparing field measured Eh values against equilibrium or system Eh calculated from various couples including:

- Fe^{2+}/Fe^{3+},
- $Fe^{2+}/Fe(OH)_3$,
- $Fe^{2+}/FeOOH$
- O_2/FeS_2

Goethite and $Fe(OH)_3$ were selected to represent end members of ferric oxyhydroxide minerals ranging from low solubility to poorly crystalline. Several studies (Macalady et al., 1990; Back and Barnes, 1965; Gang and Langmuir, 1974) have noted apparent equilibrium between Fe^{2+} and oxyhydroxide minerals in some waters. The pyrite/oxygen couple was selected to determine if dissolved oxygen is related to measured Eh.

Field Eh was measured with a portable meter and Pt electrode with Ag/AgCl solution that was calibrated against Zobell's solution before and after each field use. Readings were obtained by immersing the probe into the discharge at or near the point of emergence. Stable readings were usually obtained within ten seconds in acid, iron rich waters, suggesting the waters are well poised. The raw Eh reading was corrected to the standard hydrogen electrode scale using compiled tabular values of temperature correction factors and from equation 3-4 (Nordstrom and Wilde, 1998):

$$Ehsys. = Ehmeas. + Eref. \qquad (3-4)$$

For example, at 15° C, the correction factor for the Ag/AgCl probe is 212 millivolts. An instrument reading of 440 millivolts yields an equivalent Eh of 652 millivolts on the hydrogen electrode scale. The Pt electrode was rinsed periodically in an acid bath followed by distilled water to prevent fouling of the probe.

Dissolved oxygen was measured with a portable meter by immersing the probe in the discharge where Eh was measured. Both Eh and dissolved oxygen were measured prior to the discharge aerating as it flowed to the surface.

Samples were also collected for ferrous iron determination, filtered through a 0.45 micron filter for removing colloidal constituents, stored in opaque bottles, preserved with HCl and kept chilled until analysis. Ferrous iron determinations were run usually within 24 hours of collection using a colorimeter and 1,10 phenathroline. The instrument had a resolution of 0.01 mg/L but samples often had to be diluted by a factor of ten or sometimes 100 to read on scale. Ferric iron was determined as the difference between total dissolved Fe and ferrous iron. A method has been developed to measure Fe(III) directly using acetohydroxamic acid (To et al., 1999), but high concentrations of Fe(II) can interfere with the Fe (III) determination. To et al. compared Fe(III) data determined directly from the complexing technique with Fe(III) determined by difference for a set of acid mine water samples. They found that Fe(III) concentration by difference was

typically greater than Fe(III) by direct determination. A system Eh calculated on the basis of Fe(III) by difference would yield a greater apparent Eh value than one calculated from the direct determination.

Water samples were speciated in PHREEQCI using ferrous/ferric iron data as the basis for calculating system Eh in the first set of comparisons. Stipp (1990) compared calculated iron species concentrations to solutions of known composition for acid mine waters. She found good agreement between the two sets of values and concluded that that modeling of mine water solutions was a feasible approach to estimating solution composition. System Eh of the Fe^{2+}/Fe^{3+} couple was computed from the half-reaction and corresponding equilibrium expression:

$$Fe^{2+} \leftrightarrow Fe^{3+} + e^- \qquad \log K_{eq} = -13.02 @ 25°C \qquad (3-5)$$

$$Keq = \frac{(e^-)(Fe^{3+})}{Fe^{2+}}$$

in units of molar activity;

$$\log e- + \log Fe^{3+} - \log Fe^{2+} = \log K_{eq}$$
$$-pe + \log Fe^{3+} - \log Fe^{2+} = \log K_{eq}$$
$$pe = -\log K_{eq} + \log Fe^{3+} - \log Fe^{2+}$$

where pe is the negative log of e^- activity and $\log K_{eq}$ is the log equilibrium constant. Eh and pe are related by the expression:

$$pe = \frac{(nF)Eh}{2.303RT} \qquad (3-6)$$

derived from the Nernst equation, where Eh is in volts, n is the number of electron moles transferred, F is the Faraday constant, R is the gas constant and T is absolute temperature. For consistency, Eh values are expressed at 25°C. The equilibrium constants Keq, are obtained from the thermodynamic databases in PHREEQCI, so that Eh values are calculated consistently, whether done directly in PHREEQCI or in a spreadsheet.

The median difference between observed and calculated Eh is -32 millivolts for the half reaction described in 3-5 (see table 3-4). The largest differences are at the Omega Marshall discharge in 2005 and treatment inlet in 2008. Since the treatment inlet is a composite of all discharges at this mine, and has flowed several hundred meters through a partially full collection pipe, this water may not be at internal equilibrium. There is no obvious explanation for the difference for the 2005 Marshall sample. Lindberg and Runnells (1984) reported differences of several hundred millivolts for some redox couples. The differences in table 3-4 are biased towards calculated Eh exceeding measured Eh (median difference = -32 millivolts). This could result from Fe^{3+} being over-estimated when Fe(III) was determined by difference between total dissolved Fe and Fe(II). To et al. (1999) noted that Fe(III) determined by difference is a potential error source.

Table 3-4
Measured (Observed) and Calculated Eh values from Fe^{2+}/Fe^{3+} couple for Acid Mine Waters

Site	Date	Measured Eh (millivolts @25° C)	Fe^{2+}/Fe^{3+} Calculated Eh	Measured-Calculated
Omega Treatment Inlet	3/22/2005	622	696	-74
Omega PM-21	3/22/2005	661	661	0
Omega PM-24	3/22/2005	646	641	5
Omega PM-23	3/22/2005	619	685	-66
Omega Marshall	3/22/2005	497	662	-165
Omega DEF	3/22/2005	708	690	18
Omega DEF2	3/22/2005	626	648	-22
Omega 815 HI	3/22/2005	600	659	-59
Omega Seep E	3/22/2005	657	651	6
Omega Treatment Inlet	8/27/08	596	792	-196
Omega PM-21	8/27/08	646	723	-77
Omega PM-24	8/27/08	601	629	-28
Omega PM-23	8/27/08	No sample		
Omega Marshall	8/27/08	564	643	-79
Omega DEF	8/27/08	611	669	-58
Omega DEF2	8/27/08	608	629	-21
Omega 815 HI	8/27/08	No sample		
Omega Seep E	8/27/08	No sample		
T&T Main Discharge	5/15/2005	724	656	68
T&T Mine 3	5/15/2005	724	744	-20
Ruthbelle	5/15/2005	744	679	65
Rt 26 discharge	5/15/2005	652	703	-51
T&T Main Discharge	5/13/2008	695	736	-41
T&T Mine 3	5/13/2008	684	720	-36
Ruthbelle	5/13/2008	646	736	-90
Rt 26 discharge	5/13/2008	655	661	-6
Sterling 1	5/3/2005	797	797	0
Sterling 6	5/3/2005	770	795	-25
Commercial	5/3/2005	605	669	-64
			Median difference	-32 millivolts

Nordstrom et al. (1979) plotted measured versus calculated Eh from Fe^{2+}/Fe^{3+} for acid mine waters. The data plot included a band extending +/- 30 millivolts from the one to one plot of observed and calculated Eh. They viewed the +/- 30 millivolts as a type of confidence interval containing most of the data and constituting a degree of uncertainty in the comparison. Nordstrom et al.'s data are for Eh of about 600 to 800 millivolts. Table 3-4 data would require a slightly larger

grouping of spanning about 100 millivolts. The tenth and 90th percentiles of measured minus calculated values in table 3-4 are -85 and +11 millivolts, respectively. A later paper by Nordstrom (2000) was more cautious about the use of Eh. At more reduced conditions, approaching those measured in flooded mine-pools, Nordstrom found measured Eh was greater than calculated. The deviation was attributed in part to the decreasing Fe^{3+} concentration, and the difficulty of the electrode detecting small amounts of uncomplexed ferric iron. Nonetheless, used carefully, redox measurements based on Fe^{2+}/Fe^{3+} were deemed to have value in characterizing iron rich mine water.

Figure 3-14 is a plot similar to Nordstrom et al. (1979). The solid line represents an exact match of measured and computed Eh, with bands at +/- 30 and 50 millivolts. Most data fall within or near the 50 millivolts boundary, with the exception of the two outliers previously described.
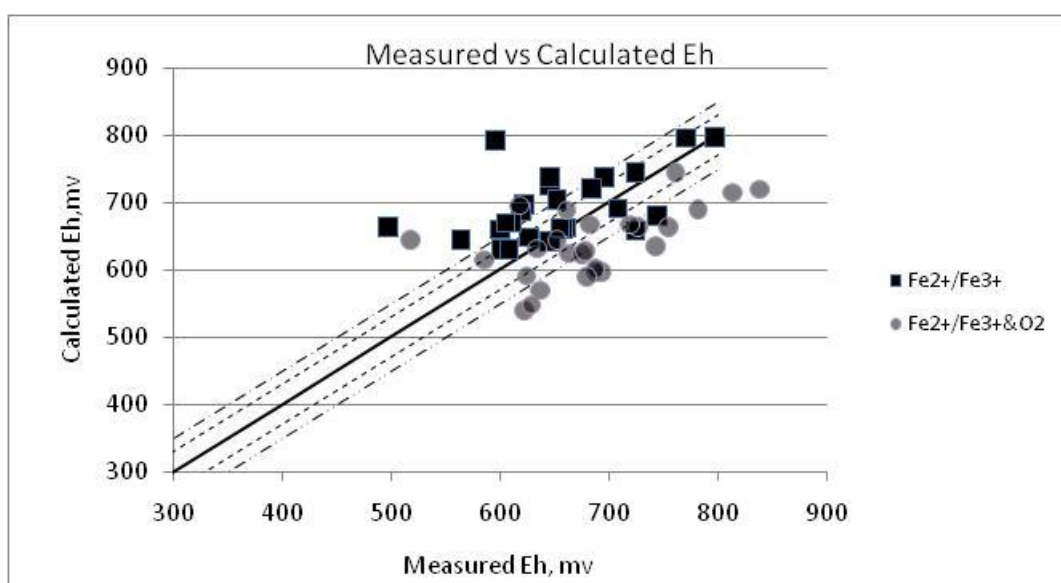
Figure 3-14. Plot of Eh Measured and Eh Calculated from Fe^{2+}/Fe^{3+} Half Reaction and Fe^{2+}/Fe^{3+} & O_2. Lines are at +/- 30 (fine dashes) and +/-50 (large dashes) millivolts from match between measured and calculated.

What effect does uncertainty in Eh measurement have on estimates of solubility for minerals containing redox sensitive elements? The analysis for the Omega PM-21 spring sampled in 2005 (table 3-4) was assigned Eh values of +50 millivolts and -50 millivolts from the measured value, while holding all other parameters constant. The water was speciated and saturation indices examined for poorly crystalline Fe (OH)$_3$ and goethite. Saturation index for Fe(OH)$_3$ was -0.84, -0.18 and +0.15 at Eh of 611 millivolts, 661 millivolts, and 711 millivolts, respectively. The water is either under-saturated or slightly super-saturated for poorly crystalline Fe(OH)$_3$, depending on the Eh value specified. Goethite saturation index was +4.52, +5.19 and +5.51 for the three specified redox states. Interpretation of goethite behavior is not affected by the choice of Eh value. For waters with redox sensitive minerals near saturation, Eh can be a critical variable for interpreting rock-water interactions.

The Fe^{2+}/Fe^{3+} couple was also examined by explicitly incorporating oxygen into the oxidation reaction by combining two half reactions as follows:

$$Fe^{2+} \leftrightarrow Fe^{3+} + e^- \qquad\qquad \log K_{eq} = -13.02 \text{ @ } 25°C \qquad\qquad (3\text{-}7a)$$

$$0.5\, H_2O \leftrightarrow 0.25\, O_2 + H^+ + e^- \qquad\qquad \log K_{eq} = -20.78 \text{ @ } 25°C \qquad\qquad (3\text{-}7b)$$

Rearranging and combining:

$$Fe^{2+} \leftrightarrow Fe^{3+} + e^- \qquad\qquad \log K_{eq} = -13.02 \text{@ } 25°C$$

$$\underline{H^+ + 0.25\, O_2 + e^- \leftrightarrow 0.5\, H_2O \qquad\qquad \log K_{eq} = +20.78 \text{@ } 25°C}$$

$$Fe^{2+} + H^+ + 0.25\, O_2 \leftrightarrow Fe^{3+} + 0.5\, H_2O \qquad\qquad \log K_{eq} = +7.76 \text{@ } 25°C$$
$$(3\text{-}7c)$$
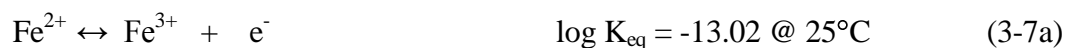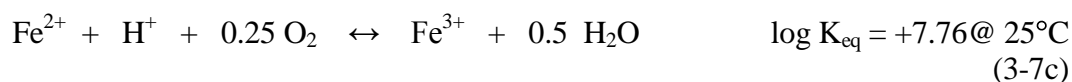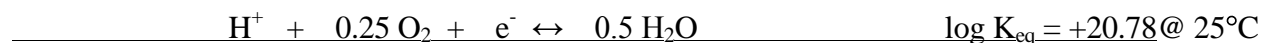
This ferrous to ferric oxidation reaction in 3-6c is the second step of the four step weathering sequence for pyrite. The corresponding equilibrium expression is:

$$(Fe^{3+})(H_2O)^{0.5}/[(Fe^{2+})(H^+)(O_2)^{0.25}] = K_{eq}, \text{ or if the activity of water is near 1,} \qquad (3\text{-}7d)$$

$$(Fe^{3+})/[(Fe^{2+})(H^+)(O_2)^{0.25}] = K_{eq} \text{ or}$$

$$\log(Fe^{3+}) - \log(Fe^{2+}) + pH - 0.25 \log(O_2) = \log K_{eq}$$

Find $\Delta G°_r$
$$\Delta G°_r = -1.364 \log K_{eq} \qquad\qquad (3\text{-}8)$$

$$\Delta G°_r = -1.364\,(+7.76)$$

$$\Delta G°_r = -10.58 \text{ kcal/mole}$$

Find $E°$
$$E° = -\Delta G_r/nF \qquad\qquad (3\text{-}9)$$
where n = number of electron moles transferred, F is Faraday constant, 23.061 kcal/V

$$E° = -\Delta G_r/nF$$

$$E° = -(-10.58)/(1)(23.061)$$

$$E° = 0.458 \text{ V}$$

Find Eh with the Nernst Equation
$$Eh = E° + (RT/nF)*2.303*\log((Fe^{3+})(H_2O)^{0.5}/(Fe^{2+})(H^+)(O_2)^{0.25}) \qquad\qquad (3\text{-}10)$$

Where $R = 1.987 \times 10^{-3}$ kcal/mole-deg; T is absolute temperature; n and F are as previously defined.

$Eh = 0.458 + 0.0592*(\log Fe^{3+} + 0.5 \log H_2O - \log Fe^{2+} - \log H^+ - 0.25 \log O_2)$
$Eh = 0.458 + 0.0592*(\log Fe^{3+} + 0.5 \log H_2O - \log Fe^{2+} + pH - 0.25 \log O_2)$

For most solutions, activity of H_2O is one or near one and the expression reduces to

$$Eh = 0.458 + 0.0592*(\log Fe^{3+} - \log Fe^{2+} + pH - 0.25 \log O_2) \tag{3-11}$$

Calculated and measured Eh results for the Fe^{2+}/Fe^{3+} and O_2 couple are shown in table 3-5 and plotted in figure 3-14. The tenth and 90th percentiles of measured minus calculated values in table

Table 3-5
Measured and Calculated Eh values from Fe^{2+}/Fe^{3+} and O_2 Couple for Acid Mine Waters

Site	Date	Measured Eh (mv @25°C)	Fe^{2+}/Fe^{3+} and O_2 Calculated Eh	Measured-Calculated
Omega Treatment Inlet	3/22/2005	653	643	10
Omega PM-21	3/22/2005	694	596	98
Omega PM-24	3/22/2005	688	596	92
Omega PM-23	3/22/2005	661	688	-27
Omega Marshall	3/22/2005	518	644	-126
Omega DEF	3/22/2005	743	633	110
Omega DEF2	3/22/2005	664	623	41
Omega 815 HI	3/22/2005	625	590	35
Omega Seep E	3/22/2005	688	600	88
Omega Treatment Inlet	8/27/08	618	695	-77
Omega PM-21	8/27/08	675	621	54
Omega PM-24	8/27/08	623	538	85
Omega PM-23	8/27/08	No sample		
Omega Marshall	8/27/08	586	614	-28
Omega DEF	8/27/08	637	568	69
Omega DEF2	8/27/08	629	547	82
Omega 815 HI	8/27/08	No sample		
Omega Seep E	8/27/08	No sample		
T&T Main Discharge	5/15/2005	754	663	91
T&T Mine 3	5/15/2005	761	745	16
Ruthbelle	5/15/2005	782	689	93
Rt 26 discharge	5/15/2005	683	666	17
T&T Main Discharge	5/13/2008	727	663	64
T&T Mine 3	5/13/2008	719	667	52
Ruthbelle	5/13/2008	678	627	51
Rt 26 discharge	5/13/2008	680	589	91
			Median difference	59

3-5 are -2 and +99 millivolts, respectively, and the median difference of measured minus calculated is +59 millivolts. Figure 3-14 shows that including oxygen in the Eh expression biases the data toward measured exceeding calculated. Fewer points fall within +/-50 millivolts of the match line than using the Fe^{2+}/Fe^{3+} couple only. The Fe^{2+}/Fe^{3+} couple provides slightly better agreement between observed and calculated Eh.

The second potential redox couple is poorly crystalline Fe hydroxide and ferrous iron.

$$Fe(OH)_3 \text{ (am)} + 3\,H^+ \leftrightarrow Fe^{3+} + 3\,H_2O \qquad \log K_{eq}@\ 25° = 4.891 \qquad (3\text{-}12a)$$

$$Fe^{2+} \leftrightarrow Fe^{3+} + e^- \qquad \log K_{eq}@\ 25° = \text{-}13.02 \quad (3\text{-}12b)$$

Rearranging and combining 3-12a and 3-12b:

$$Fe^{2+} \quad \leftrightarrow \quad Fe^{3+} + e^- \qquad \log K_{eq} = \text{-}13.02$$

$$\underline{\quad Fe^{3+} + 3\,H_2O \quad \leftrightarrow Fe(OH)_3 \text{ (am)} + 3\,H^+ \qquad \log K_{eq} = \text{-}4.891 \quad}$$
$$Fe^{2+} + 3\,H_2O \leftrightarrow Fe(OH)_3 \text{ (am)} + 3\,H^+ + e^- \qquad \log K_{eq} = \text{-}17.911$$
$$(3\text{-}12c)$$
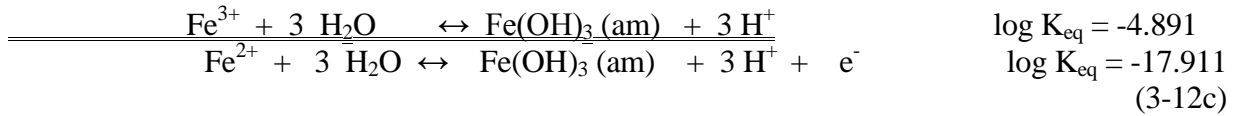
The corresponding equilibrium expression is:

$$3 \log H^+ + \log e^- - \log Fe^{2+} = \log K_{eq} \qquad\qquad (3\text{-}12d)$$

$$3 \log H^+ - pe - \log Fe^{2+} = \log K_{eq}$$

$$\text{-}pe = \log K_{eq} + 3\,pH + \log Fe^{2+}$$

$$pe = \text{-}\log K_{eq} - 3\,pH - \log Fe^{2+}$$

Results for the $Fe^{2+}/Fe(OH)_3$(am) data are shown in figure 3-15. There is no obvious relation
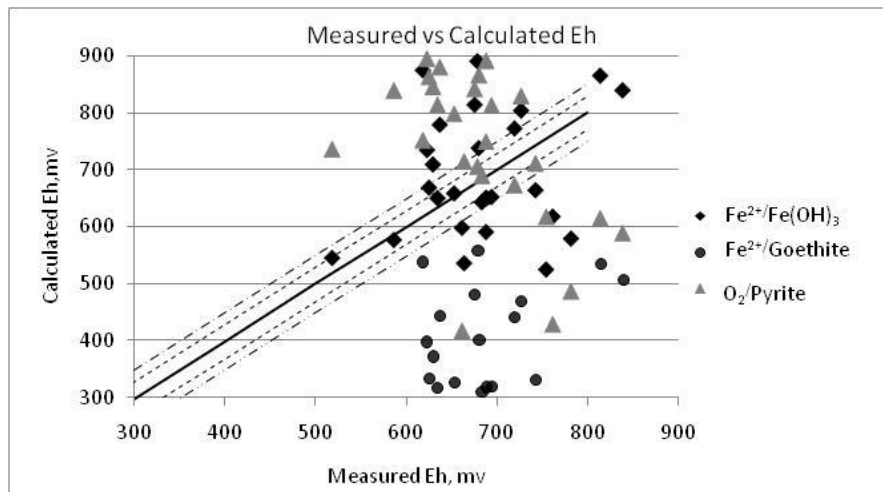
Figure 3-15. Plot of Eh Measured and Eh Calculated from $Fe^{2+}/Fe(OH)3$ am, $Fe^{2+}/Goethite$, and $O_2/Pyrite$. Lines are at +/- 30 (fine dashes) and +/-50 (large dashes) millivolts from match between measured and calculated.

between measured Eh, and Eh calculated based on equilibrium with $Fe(OH)_3$. Although the median difference is minus ten millivolts, there is considerable scatter among data pairs, and the tenth and 90th percentile differences are -139 and +135 millivolts, respectively.

The third potential redox couple is goethite and ferrous iron:

$$FeOOH + 3 H^+ \leftrightarrow Fe^{3+} + 2 H_2O \qquad \log K_{eq}@ 25° = -1.0 \qquad (3\text{-}13a)$$

$$Fe^{2+} \leftrightarrow Fe^{3+} + e^- \qquad \log K_{eq}@ 25° = -13.02 \qquad (3\text{-}13b)$$

Rearranging and combining:

$$Fe^{3+} + 2 H_2O \leftrightarrow FeOOH + 3 H^+ \qquad\qquad \log K_{eq}@ 25° = 1.0$$

$$\underline{Fe^{2+} \leftrightarrow Fe^{3+} + e^-} \qquad\qquad \log K_{eq}@ 25° = -13.02$$

$$Fe^{2+} + 2 H_2O \leftrightarrow FeOOH + 3 H^+ + e^- \qquad\qquad \log K_{eq}@ 25° = -12.02$$
$$(3\text{-}13c)$$
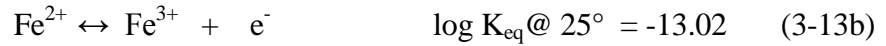
The corresponding equilibrium expression is:

$$3 \log H^+ + \log e^- - \log Fe^{2+} = \log K_{eq} \qquad\qquad (3\text{-}13d)$$

$$\log e^- = \log K_{eq} - 3 \log H^+ + \log Fe^{2+}$$

$$-pe = \log K_{eq} + 3 pH + \log Fe^{2+}$$

$$pe = -\log K_{eq} - 3 pH - \log Fe^{2+}$$

Eh results calculated from Fe^{2+}/goethite are plotted on figure 3-15. The median difference between measured and calculated values is 322 millivolts. The results are biased to measured exceeding calculated Eh. Measured Eh does not reflect Fe^{2+}/goethite equilibrium.

The final couple considered was pyrite and oxygen:

$$FeS_2 + H_2O + 3.5 O_2 \rightarrow 2 SO_4^{2-} + Fe^{2+} + 2 H^+ \qquad\qquad (3\text{-}14a)$$

The pyrite/oxygen reaction was compiled from the following four reactions:

$$SO_4^{2-} + 10 H^+ + 8 e^- \leftrightarrow H_2S + 4 H_2O \qquad \log K_{eq}@ 25° = 40.644 \qquad (3\text{-}14b)$$

$$FeS_2 + 2 H^+ + 2 e^- \leftrightarrow Fe^{2+} + 2 HS^- \qquad \log K_{eq}@25° = -18.479 \qquad (3\text{-}14c)$$

$$H_2S \leftrightarrow HS^- + H^+ \qquad \log K_{eq}@ 25° = -6.99 \qquad (3\text{-}14d)$$

$$2 \text{ H}_2\text{O} \leftrightarrow \text{O}_2 + 4 \text{ H}^+ + 4 \text{ e}^- \qquad\qquad \log \text{ K}_{eq}@ \ 25° \ = \ -86.08 \qquad (3\text{-}14\text{e})$$

The first step is to rearrange Equation 3-14b and combine and it with 3-14c as:

$$[\text{H}_2\text{S} \ + \ 4 \text{ H}_2\text{O} \leftrightarrow \ \text{SO}_4{}^{2-} \ + 10 \text{ H}^+ \ + 8 \text{ e}^- \quad \log \text{K}_{eq} = \ -40.644] \ \text{x 2} \qquad \log \text{ K}_{eq} = -40.644 \ \text{x 2}$$

$$\underline{\text{FeS}_2 + 2 \text{ H}^+ \ + \ 2 \text{ e}^- \ \leftrightarrow \ \text{Fe}^{2+} \ + 2 \text{ HS}^- \qquad\qquad\qquad\qquad \underline{\log \text{K}_{eq} = -18.479}}$$

$$\text{FeS}_2 + 8 \text{ H}_2\text{O} + \ 2 \text{ H}_2\text{S} \ \leftrightarrow \ \text{Fe}^{2+} + \ 2 \text{ SO}_4{}^{2-} \ +2 \text{ HS}^- + \ 18 \text{ H}^+ \ + 14 \text{ e}^- \qquad \log \text{K}_{eq} = -99.767$$
$$(3\text{-}14\text{f})$$
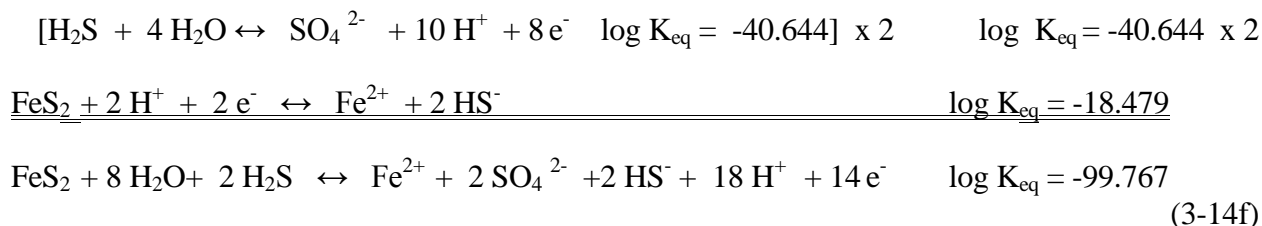
The second step is to rearrange and combine equation 3-14d and 3-14f as:

$$[\text{H}_2\text{S} \ \leftrightarrow \ \text{HS}^- \ + \ \text{H}^+] \ \ \text{x 2} \qquad\qquad \log \text{ K}_{eq} = \ -6.99 \ \text{x 2}$$

$$\underline{\text{FeS}_2 + 8 \text{ H}_2\text{O} + \ 2 \text{ H}_2\text{S} \ \leftrightarrow \ \text{Fe}^{2+} + \ 2 \text{ SO}_4{}^{2-} \ + \ 2 \text{ HS}^- \ +18 \text{ H}^+ \ + 14 \text{ e}^-} \qquad \log \text{K}_{eq} = -99.767$$

$$\text{FeS}_2 + 8 \text{ H}_2\text{O} \leftrightarrow \text{Fe}^{2+} + \ 2 \text{ SO}_4{}^{2-} \ +16 \text{ H}^+ \ + 14 \text{ e}^- \qquad\qquad \log \text{K}_{eq} = -113.75$$
$$(3\text{-}14\text{g})$$
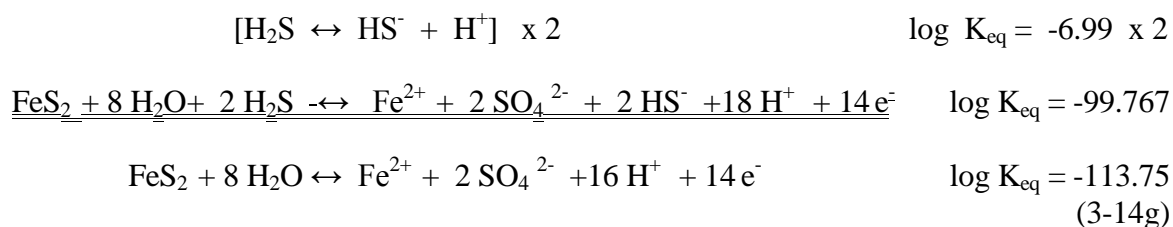
The third step is to rearrange equation 3-14e and combine with 3-14g as:

$$[\text{O}_2 \ + 4 \text{ H}^+ + 4 \text{ e}^- \ \leftrightarrow \ 2 \text{ H}_2\text{O}] \ \text{x 3.5} \qquad\qquad \log \text{ K}_{eq} = \ 86.08$$

$$\underline{\text{FeS}_2 + 8 \text{ H}_2\text{O} \leftrightarrow \text{Fe}^{2+} + \ 2 \text{ SO}_4{}^{2-} \ +16 \text{ H}^+ \ + 14 \text{ e}^-} \qquad\qquad \log \text{K}_{eq} = -113.75$$

$$\text{FeS}_2 + \ \text{H}_2\text{O} + 3.5 \text{ O}_2 \ \leftrightarrow \text{Fe}^{2+} + \ 2 \text{ SO}_4{}^{2-} + 2 \text{ H}^+ \qquad\qquad \log \text{K}_{eq} = \ 187.53$$
$$(3\text{-}14\text{h})$$
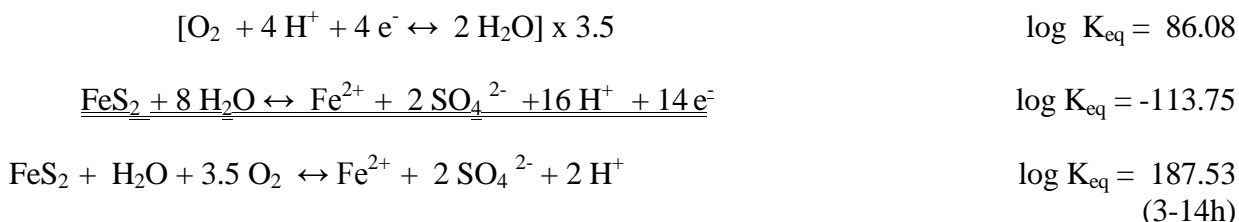
The corresponding equilibrium expression is:

$$\log (\text{Fe}^{2+}) + \ 2 \log (\text{SO}_4{}^{2-}) + \ 2 \log (\text{H}^+) \ -3.5 \log (\text{O}_2) \ = \ \log \text{K}_{eq} \qquad\qquad (3\text{-}14\text{i})$$

Find $\Delta G°_r$
$$\Delta G°_r = \ -1.364 \log \text{K} \qquad\qquad (3\text{-}15)$$

$$\Delta G°_r = \ -1.364 \ (+187.53)$$

$$\Delta G°_r = -255.79 \text{ kcal/mole}$$

Find E°

$$E° = -\Delta G_r/nF \tag{3-16}$$

$$E° = -\Delta G_r/nF$$

$$E° = -(-255.79)/(14)(23.061)$$

$$E° = 0.792 \text{ V}$$

$$Eh = E° + (RT/nF)*2.303*[\log((SO_4^{2-})^2(Fe^{2+})(H^+)^2/(O_2)^{0.25})] \tag{3-17}$$
$$Eh = 0.792 + 0.592*[(2*\log SO_4^{2-} + \log Fe^{2+} + 2 \log H^+ -0.25 \log O_2)]$$
$$Eh = 0.792 + 0.592*[(2*\log SO_4^{2-} + \log Fe^{2+} -2 \text{ pH} -0.25 \log O_2)]$$

Calculated values from the pyrite/oxygen couple are plotted in figure 3-15. There is considerable scatter and no obvious relationship between measured Eh and values calculated from pyrite and oxygen. The median difference between measured and calculated Eh is -110 millivolts with the tenth and 90th percentiles at -239 and +246 millivolts, respectively.

The Fe^{2+}/Fe^{3+} couple provided the closest agreement between measured and calculated Eh of the four equilibrium reactions considered. Some of the disparity may result from over-estimating Fe(III) by difference, rather than a direct measurement. To et al. (1999) suggests over-estimation of Fe(III) occurs when using the difference method. This would result in over estimating Eh, which is dominant error found in figure 3-15. The other couples displayed no consistent relation to measured Eh with differences up to several hundred millivolts. The Fe^{2+}/Fe^{3+} couple relationship with Eh in acid mine waters is consistent with the findings of Nordstrom et al. (1979) and Stipp (1990). Redox measurements and controls in flooded circumneutral mine-pools are examined in chapter four.

3.4 Mineral Controls on Metal Solubility

Iron and Al are major components of waters draining from the Omega and T&T mine-pools. Iron can be derived directly from pyrite oxidation or dissolution of other Fe bearing minerals including oxyhydroxides, sulfates, carbonates and silicates. The large number of potential sources and sinks makes reaction path identification difficult for Fe. Section 3.3.2 showed that waters from both mine-pools are deficient in Fe with respect to sulfate from pyrite weathering. Section 5.2 presents data suggesting that mineral weathering reactions are consuming much of the acidity in-situ. Soluble aluminum also has a variety of potential sources and sinks. This section examines some possible mineral and chemical controls on mobility of Fe and Al, since these two elements are principal pollutants in these mine-pools. Much of the analysis is based on assumption of local equilibrium and the application of thermodynamic calculations. A large body of literature on sulfate minerals has been summarized in review volumes "Sulfate Minerals, Crystallography, Geochemistry and Environmental Significance" (Alpers et al., 2000) and "Acid Sulfate Weathering" (Kittrick et al., 1982) These references and other citations provide considerable

background on the weathering, formation, solubility and stability of metal sulfates associated with pyrite weathering.

3.4.1   Aluminum Minerals

Aluminum is mobilized indirectly by sulfide weathering and dissolution reactions caused by the resulting low pH (acid waters), including dissolution of oxyhydroxides and silicates. The dissolution of poorly crystalline $Al(OH)_3$ is a function of pH and Al activity:

$$Al(OH)_{3\ (am)}\ +\ 3\ H^+\ \leftrightarrow\ Al^{3+}\ +\ 3\ H_2O \quad \log K_{eq} = 10.8 @ 25° \tag{3-18}$$
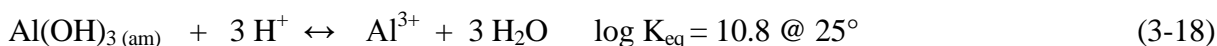
Complete feldspar dissolution is:

$$KAlSi_3O_8\ +\ 4\ H^+\ +\ 4\ H_2O \leftrightarrow K^+\ + Al^{3+}\ +\ 3\ H_4SiO_4{}^0 \tag{3-19}$$
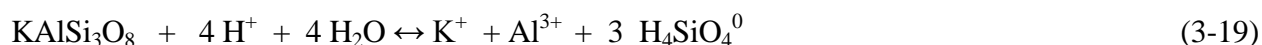
Kaolinite dissolution in strongly acidic conditions is:

$$Al_2Si_2O_5(OH)_4\ +\ 6\ H^+\ \leftrightarrow 2\ Al^{3+}\ + 2\ H_4SiO_4{}^0\ +\ H_2O \qquad \log K_{eq} = 7.435 @ 25° \tag{3-20}$$
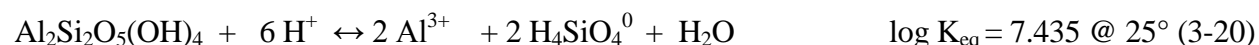
For each mineral, H^+ activity strongly influences the dissolution reactions.

Commonly recognized aluminum bearing minerals associated with acid drainage include $Al(OH)_3$, both as a poorly crystalline form, and as gibbsite; alunite, jurbanite, basaluminite, halotrichite, pickeringite, aluminocopiapite and others (Bigham and Nordstrom, 2000; Rose and Cravotta, 1998; Hammarstrom et al., 2005; Cravotta, 1994; Karathanasis et al. 1988). The minerals vary in crystallinity and composition. Many are poorly crystalline, hydrous sulfates and are moderately to highly soluble. These soluble minerals may precipitate during drier mine periods and redissolve during wet periods and recharge events, liberating Al, Fe, sulfate, H^+ and other metals.

Zodrow (1980), and Zodrow and McCandlish (1978) identified a series of hydrated sulfate minerals in underground coal mines in Nova Scotia including alunite, halotrichite, pickeringite, and aluminocopiapite. Brant and Foster (1959) identified halotrichite in underground mine entries in Ohio. The mine-works had similar conditions to the Omega and T&T mines. Bayless and Olyphant (1993) were able to relate ground-water chemistry and surface water runoff composition to the occurrence of acid generating sulfate salts at an abandoned coal mine in Indiana. Hammarstrom et al. (2005) also related water quality to the occurrence and dissolution of soluble mineral groups including halotrichite and copiapite at several metal mines in the eastern US. Highest metal loads occurred during spring runoff and intense summer storms. Leaching experiments showed the salts all produced acidic waters of pH two to three with Al and Fe concentrations in the 10s to 100s of mg/L.

Neither the Omega nor T&T mine-works were accessible for direct sampling of sediments and observation of minerals. Therefore, possible mineral controls on Al activity in these mine-pools were assessed indirectly by examining mineral saturation indices, and reviewing subject literature to identify minerals identified in similar settings, and graphical analysis.

Nordstrom (1982b) reviewed the aqueous chemistry of Al, in particular, behavior in acid waters. He estimated solubility of the mineral jurbanite $(Al(SO_4)OH* 5 H_2O)$ and concluded that it may control Al solubility in acid waters and soils. Jurbanite solubility data were subsequently incorporated into several common thermodynamic databases for minerals used in geochemical modeling. Based on apparent jurbanite solubility, acid waters from coal mines, metal mines and acid sulfate soils (van Breeman, 1973; Davis and Ashenberg, 1989; Eary, 1999; Perry and Rauch, 2004) have been variously reported to attain or approach equilibrium for the mineral. Bigham and Nordstrom (2000) however, concluded that the reported solubility of jurbanite was not reliable, and the ion activity product likely reflected a correlation between Al and sulfate activity at pH less than 4.5, rather than mineral control. They suggested that Al has few mineral solubility constraints at pH less than 4.5. Nonetheless, poorly crystalline hydrous Al sulfate compounds are present in acid mine water sediments (Kim and Kim, 2003), and apparent equilibrium with jurbanite has been noted in coal mine drainage (Cravotta, 2008b). Therefore, in this work, thermodynamic calculations refer to "apparent" equilibrium with respect to jurbanite.

Aluminum and other water quality parameters were compared to each other in a simple correlation to test Bigham and Nordstrom's observations of Al/sulfate/pH relationships in these data sets. Results are summarized in table 3-6 for three springs and the combined discharge from the Omega mine-pool, and the main discharge from the T&T mine-pool.

Table 3-6
Correlation coefficients among Aluminum, Iron, Calcium,
Sulfate and pH in Acid Mine Waters, Omega and T&T Mine-pools

	Omega PM-21	Omega DEF	Omega Marshall	Omega Main Inlet	T&T Main Discharge
Al vs. SO_4	0.15*	0.54	0.70	0.68	0.56
Ca vs. SO_4	0.94	0.97	0.39	0.65	0.42
Fe vs. SO_4	0.46	0.68	0.82	0.80	0.79
Al vs. pH	-0.52	0.07*	0.41	0.01*	0.18

(1) Values followed by * are not significant at $p = 0.05$

No relationship between Al concentration and pH is evident in three of five discharges. These waters span a narrow pH range of only a few tenths of a pH unit and all pH values are less than 4.5. Thus one chemical parameter, pH, is nearly invariant, while Al concentration has a wider range, resulting in low r values. Four of five correlation coefficients for Al versus pH are positive, and one is negative. An inverse relationship with negative correlation was expected if Al concentration increases as pH declines. Aluminum and sulfate have a moderate correlation for four discharges, and are unrelated in the fifth. The strongest overall correlations are between Fe and sulfate, with four discharges having an r value of 0.68 or greater. The Omega and T&T data sets do not follow the Al and sulfate correlation as closely as Bigham and Nordstrom (2000) suggest they might, and the mineral jurbanite was retained in the overall analysis as a potential source/sink for Al.

Jambor et al. (2000), and Bigham and Nordstrom (2000), reviewing a large set of literature summarized the formation of various aluminum sulfate mineral groups as a function of pH as follows:

Basaluminite ($Al_4(OH)_{10}SO_4$* 5 H_2O, monoclinic crystal system) forms at pH of about five to six;

Jurbanite ($Al(SO_4)OH$* 5 H_2O, monoclinic crystal system) forms at intermediate pH of about three to five, and;

Alunogen ($Al_2(SO_4)_3$*17H_2O, triclinic mineral system) forms at pH of about two to three.

The pH dependence is related to the Al to sulfate mole ratio, where the most acidic waters contain the highest sulfate concentrations, and consequently form the most sulfate rich minerals. Thermodynamic data are not available for all hydrous Al sulfate minerals, and calculations were performed for minerals with published equilibrium constants. The constant for alunogen was taken from Nordstrom (1982b).

Figure 3-16 is a plot of stability fields of several Al bearing minerals that could control Al activity in acid mine waters, and 77 sample analyses from discharge DEF in the Omega mine-pool from 1993 to 2008. The plot was constructed to include jurbanite, kaolinite, poorly crystalline $Al(OH)_3$, gibbsite, alunite, basaluminite and alunogen. Dissolution reactions used to construct figure 3-16 include equations 3-18 and 3-20 and the following:

$$Al(OH)_3 \text{ (gibbsite)} + 3 H^+ \leftrightarrow Al^{3+} + 3 H_2O \qquad \log K_{eq} = 8.11 @ 25° \qquad (3\text{-}21)$$

$$KAl_3(SO_4)_2(OH)_6 \text{ (alunite)} + 6 H^+ \leftrightarrow K^+ + 3 Al^{3+} + 2 SO_4^2 + 6 H_2O$$
$$\log K_{eq} = \text{-}1.4 @ 25° \qquad (3\text{-}22)$$

$$AlOHSO_4 + H^+ \text{ (jurbanite)} \leftrightarrow Al^{3+} + SO_4^{2-} + H_2O$$
$$\log K_{eq} = \text{-}3.23 @ 25° \qquad (3\text{-}23)$$

$$Al_4(OH)_{10}SO_4 \text{ (basaluminite)} + 10 H^+ \leftrightarrow 4 Al^{3+} + SO_4^{2-} + 10 H_2O$$
$$\log K_{eq} = 22.7 @ 25° \qquad (3\text{-}24)$$

$$Al_2(SO_4)_3 \text{*}17 H_2O \text{ (alunogen)} \leftrightarrow 2 Al^{3+} + 3 SO_4^{2-} + 17 H_2O$$
$$\log K_{eq} = \text{-}6.98 @ 25° \qquad (3\text{-}25)$$
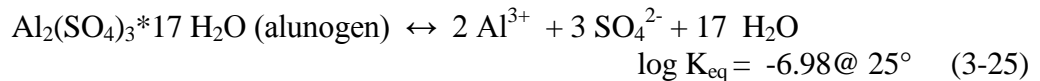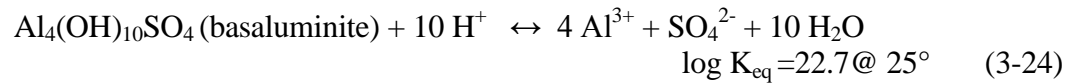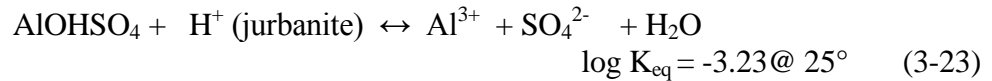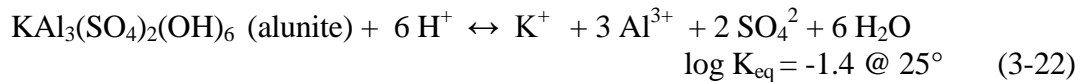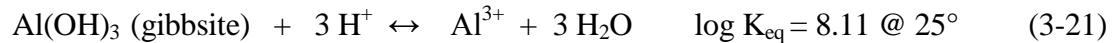
Each reaction was rewritten as an equilibrium expression and solved for Al^{3+} activity over a pH range of zero to 14. Log sulfate activity was fixed at -2.275, a typical value for the DEF spring. Kaolinite calculations required a value for Si, and total log Si activity was fixed at -3.47. That value was derived from water samples collected by the author that included Si analysis. Alunite calculations required a value for K^+ activity. The log activity was fixed at -4.0 as a representative value.

As an example, alunite dissolution (equation 3-22) when written as an equilibrium expression in log form is:

$$\log K^+ + 3 \log Al^{3+} + 2 \log SO_4^{2-} - 6 \log H^+ = \log K_{eq} \qquad (3\text{-}26a)$$

$$\log Al^{3+} = (\log K_{eq} - \log K^+ - 2 \log SO_4^{2-} -6\ pH)\ /3 \qquad (3\text{-}26b)$$

The calculated Al^{3+} activities were then substituted into the equilibrium expression for the following Al species using the appropriate constants:

- Al hydroxy species $AlOH^{2+}$, $AlOH_2^+$, $AlOH_3^0$, and $AlOH_4^-$
- Al sulfate species $AlSO_4^+$, $Al(SO_4)^{2-}$, HSO_4^- and $AlHSO_4^+$

The activity of Al^{3+} was plotted on the y axis of figure 3-16 as a function of pH. The 77 sample analyses are also plotted.

The plot shows that water composition, in terms of Al activity and pH has varied little over a 15 year period. DEF samples approach equilibrium for two minerals; jurbanite and alunite. Saturation indices were calculated for both minerals in PHREEQCI, and DEF waters approach apparent equilibrium for jurbanite. The median jurbanite saturation index for 77 samples is -0.15. Indices range from a minimum of -0.92 in 2008 to slight super-saturation at a maximum of 0.17. Alunite has a median saturation index of -4.6, and all others minerals shown on figure 3-16 are also under-saturated by multiple orders of magnitude.
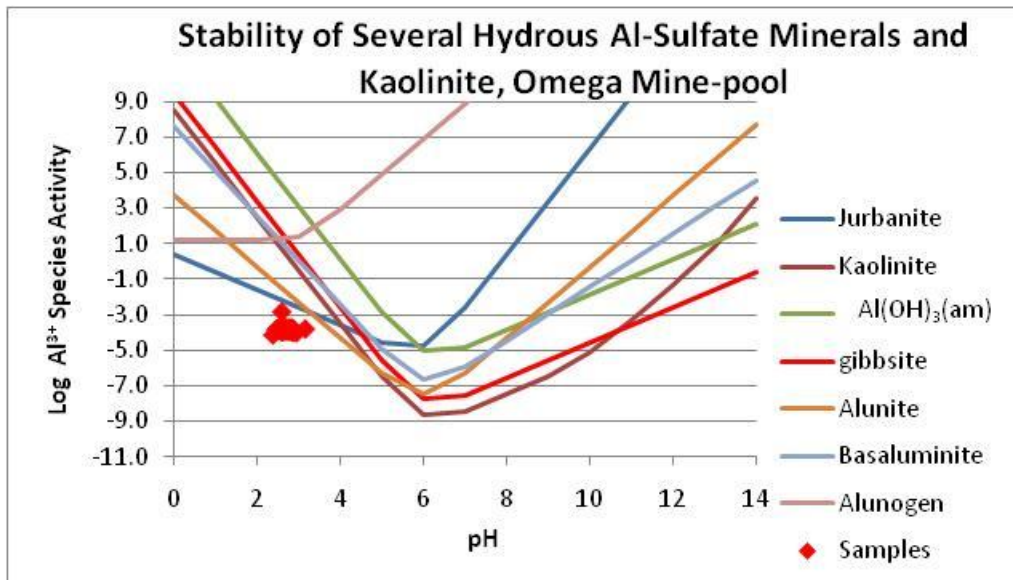
Figure 3-16. Stability of Hydrous Al-Sulfate Minerals as a Function of pH, Omega Mine-pool, Discharge DEF. Samples from 1993-2008. Total log molar activity of Al^{3+} on y axis.
Log sulfate activity fixed at -2.275; log silica activity fixed at -3.47; log potassium activity fixed at -4.0

Figure 3-17 shows a time series plot of jurbanite saturation index for the DEF discharge and two other springs in the Omega mine-pool, Marshall and PM-21. Waters in the DEF discharge approach the apparent equilibrium saturation index of 0, suggesting that jurbanite poses an upper limit to Al concentration at site DEF. Waters at the Marshall discharge are slightly oversaturated for jurbanite. Slight oversaturation suggests that within the mine, a slightly more soluble poorly crystalline phase of jurbanite is forming, jurbanite reaction rates are slow, the "dissolved" fraction on which the saturation index calculations were based contains colloidal Al, or jurbanite is not actually forming. Without direct sampling of mine sediments, it is difficult to determine which scenario is occurring. Beginning about 2006, saturation indices for the three springs show an irregular decline towards increasing under-saturation in DEF and PM-21 and near equilibrium in the Marshall spring.
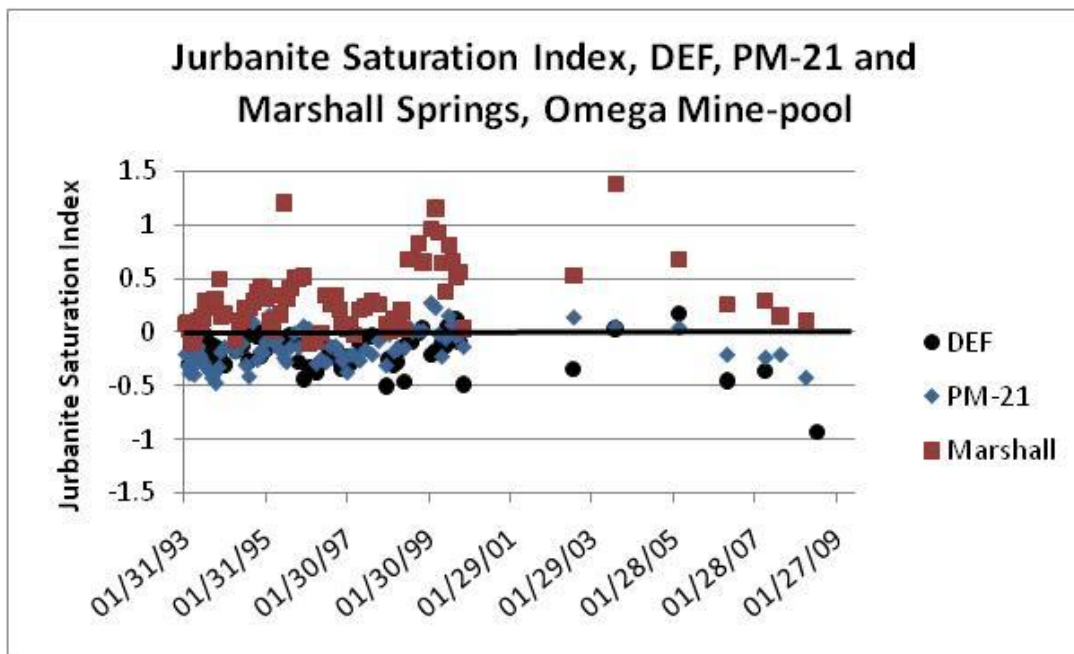
Figure 3-17. Time Series of Jurbanite Saturation Index, DEF, Marshall and PM-21 Springs, Omega Mine-pool.

If a jurbanite-like mineral is present, it could form as an alteration product of an alumino-silicate and sulfate. The alteration from kaolinite to jurbanite could occur as:

$$Al_2Si_2O_5(OH)_4 \;+\; 4\,H^+ + 2\,SO_4^{2-} \;+\; H_2O \leftrightarrow 2\,AlOHSO_4 \;+\; 2\,H_4SiO_4^0 \qquad (3\text{-}27)$$
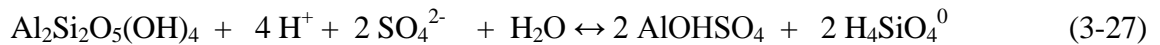
The equilibrium expression is:

$$K_{eq} = \; 2\log H_4SiO_4^0 - 4\log H^+ - 2\log SO_4^{2-} \qquad K_{eq} = 10.665\,@25° \qquad (3\text{-}28)$$

Substituting values for log sulfate activity of -2.275, and log Si activity of -3.47, as in figure 3-16, the equilibrium pH is 3.26 for jurbanite/kaolinite transformation. Actual pH values are about 0.5 to 0.8 units less, indicating that transformation from kaolinite to jurbanite is favored.

With various sulfate minerals present or potentially present in mine-pool sediments, common ion effects are possible. Figure 3-18 is a time series plot of the same three springs in the Omega mine-pool, but with gypsum saturation index plotted. With the exception of samples from the Marshall discharge in 1998-1999, the springs are slightly to moderately under-saturated with respect to gypsum. Super-saturation at Marshall was attained when cement grout and flyash, sources of Ca and sulfate, were injected in a section of the mine-works adjacent to the spring. Under-saturation with respect to gypsum could result from the dissolution of a more soluble sulfate bearing mineral, thereby suppressing dissolution of the less soluble gypsum. Gypsum saturation indices also show a time dependent trend, with waters becoming progressively more under-saturated as the mine-pool ages.
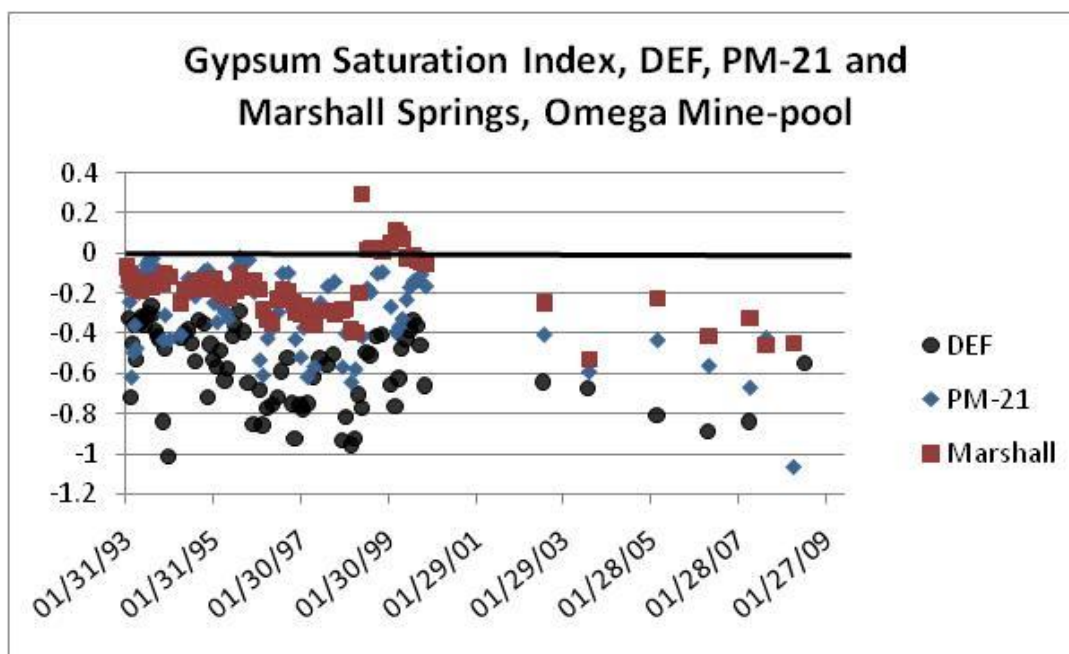
**Figure 3-18. Time Series of Gypsum Saturation Index, DEF, Marshall
and PM-21Springs, Omega Mine-pool.**

A limited number of complete suite samples were available to compute chemical activities and mineral saturation indices for the T&T mine-pool. Chemical activities were estimated by indirect methods as follows for samples that did not include all major cations and anions.

- Sulfate was assumed to approximate the total quantity of anion charge. Chloride was less than 5 mg/L in author collected samples and the acidic pH precludes significant bicarbonate or carbonate.

- The cation fraction was composed mainly of Ca, Mg, Al and Fe. Na and K were present at a few mg/L in author collected samples and were not included in charge calculations.

- Fe(II)/Fe(III) ratio was calculated from measured Eh and averaged about 0.8/0.2 in the main drainage.

- Sum cation charge was assumed to equal sum anion charge (electro-neutrality principle). Cation charge was estimated from reported Al and Fe data. "Missing" cation charge was distributed between Ca and Mg in a mole ratio of 0.76:0.24. This ratio was based on the complete suite samples.

- Ionic strength was calculated from:

$$I = \sum m_i z_i^2 \tag{3-29}$$

where I is ionic strength, m_i is molal concentration, and z is valence of the ith element. Ionic strength was then used to estimate log activity coefficients with the extended Debye Huckel equation:

$$\log \gamma_i = (-A z_i^2)(I)^{\wedge 0.5}/((1 + B_{a0}(I)^{\wedge 0.5}) \tag{3-30}$$

where $\log \gamma_I$ is log activity coefficient, A and B_{a0} are constants, and I is as previously defined.

Chemical activity was estimated from the activity coefficient derived as described above, total element concentration, and speciation data in section 3.3.3. The complexing information presented in section 3.3.3 was used to estimate the fractions of Al^{3+}, Ca^{2+} and SO_4^{2-} present in solution. Twenty percent of the dissolved Al is present as uncomplexed Al^{3+}, about 55% of dissolved sulfate is present as SO_4^{2-}, and about 70% of dissolved calcium is present as Ca^{2+}. These fractions were used to estimate chemical concentrations from total dissolved Al, sulfate and Ca data reported in the WVDEP date set. Chemical activities and mineral saturation indices computed with this indirect method were compared to values calculated in PHREEQCI for complete suite samples. The two methods agreed within about ten percent. Mineral saturation indices were computed for jurbanite and gypsum in the final step.

Jurbanite and gypsum saturation indices estimates for the T&T mine-pool are shown in figure 3-19 using smoothed data. Unlike the Omega mine-pool, T&T mine waters are under-saturated with respect to both minerals. Aluminum, sulfate and calcium activities in T&T mine-pool are apparently not limited by jurbanite and gypsum. After limestone injection, saturation indices increased for both minerals, especially gypsum. The gypsum increase likely results from additional Ca^{2+} activity. Both mineral indices also show short term scatter, and a small indistinct seasonal trend. Indices generally increase as much as 0.2 units during drier portions of the year, when mine waters should be more concentrated. Neither mineral appears to control Al or sulfate activity in the T&T mine-pool. The limestone injection process actually increased the degree of solution

58

saturation. That condition has persisted for more than 6 years after in-situ treatment, and shows no obvious declining trend.
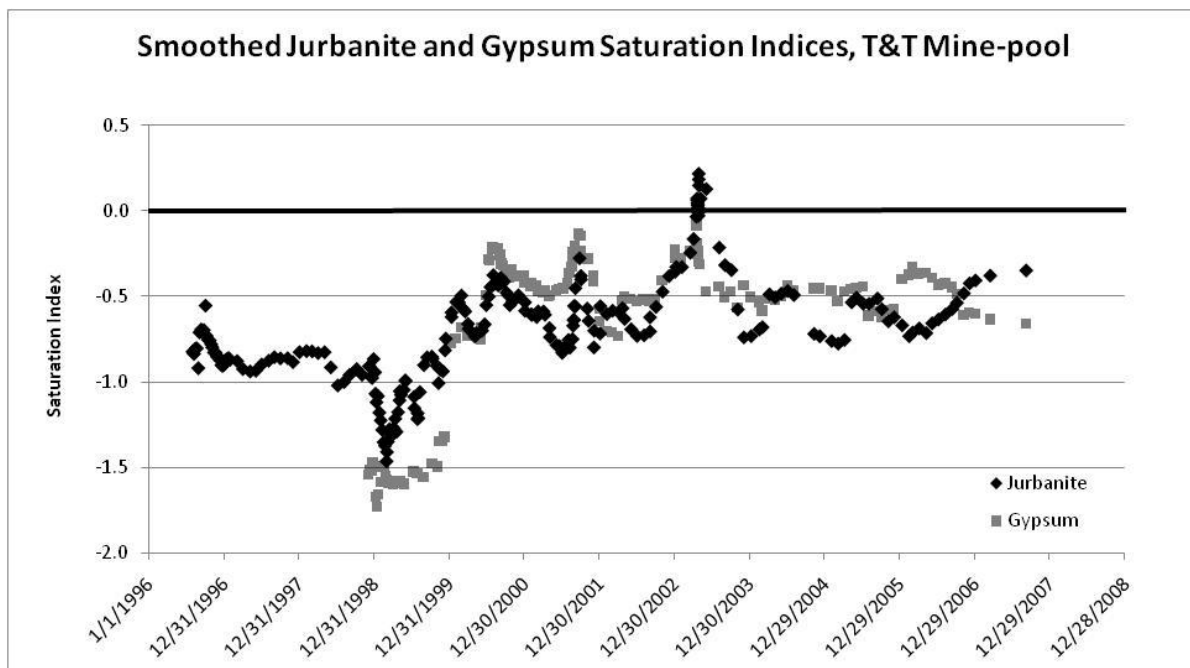
Figure 3-19. Time Series of Jurbanite and Gypsum Saturation Index, T&T Mine-pool.

What is the source of soluble Al in these mine-pools? The most obvious and abundant source is alumino-silicate minerals. Many weather slowly even under acid conditions. Kaolinite dissolution, for example, is about eight orders of magnitude slower than dolomite weathering under acid conditions (Palandri and Kharaka, 2004). The slow kinetics of most alumino-silicate weathering could result in waters under-saturated for these minerals, even if they are supplying soluble Al to the mine water. The Omega and T&T mine-pools are under-saturated with respect to kaolinite by three to seven orders of magnitude.

3.4.2 Iron Minerals
Like aluminum, iron can reside in a number of minerals associated with acid drainage, including sulfates and oxyhydroxides. Iron may be present as Fe(II) or Fe(III) and may occur in mixed valence states within the same mineral, such as copiapite. Iron minerals commonly identified as in mine drainage sediments include poorly crystalline $Fe(OH)_3$, ferrihydrite, goethite, melanterite, copiapite, halotrichite, schwertmannite, jarosite and others (Zodrow and McCandlish, 1978; Zodrow et al.,1979; Bowell and Bruce, 1995; Cravotta, 1994; Rose and Cravotta, 1998; Kaires et al., 2005; Jerz and Rimstidt, 2004; Hammarstrom et al., 2005; Bigham and Nordstrom, 2000; Alpers et al., 2000). The oxyhydroxide minerals can vary in solubility over six orders of magnitude (Langmuir and Whittemore, 1971) and may scavenge or sorb trace elements from mine waters (Smith, 1999; Bowell and Bruce 1995; Filipek et al., 1987; Bigham and Nordstrom, 2000).

In aerated, oxidized mine-pools like Omega and T&T, Fe(III) minerals may be present in abundance. The preferred mineral state will also be influenced by pH. In general, goethite is the most stable phase above a pH of about 3.5 to 4.0, schwertmannite, a hydrous hydroxysulfate, is stable at intermediate pH of about three to five, and jarosite is stable in oxidizing, acid environments (Bigham and Nordstrom, 2000, Bigham et al., 1996). Both jarosite and schwertmannite are considered metastable with respect to goethite. The conversion rate for schwertmannite to goethite is pH dependent. Jonsson et al. (2005) found that schwertmannite to goethite conversion was complete in 187 days at pH 9, while at pH 6, conversion was not complete at 514 days, and that higher sulfate concentration also slowed the conversion rate. A long term weathering experiment by Bigham et al. (1996) also confirmed conversion to goethite. Thus, a number of Fe minerals may form initially in acid mine-pools, but some may transform to more stable compounds like goethite as the mine-pool ages.

Schwertmannite was only recognized as a mineral in 1990 (Bigham et al., 1990). It has a formula of indefinite composition and its dissolution is given by Yu et al. (1999) as:

$$Fe_8O_8(OH)_{8-2x}(SO_4)_x * n\ H_2O\ + (8+2x)\ H_2O \leftrightarrow 8\ Fe^{3+} + 24\ OH^- + x\ SO_4^{2-} + 2\ x\ H^+ \quad (3\text{-}31)$$
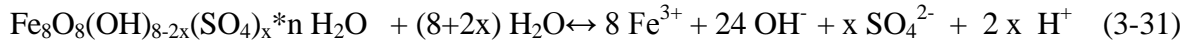
where $1.74 < x < 1.86$ and $8.17 < n < 8.62$. The estimated log K_{eq} is 10.5 ±2. Solubility data from Yu et al. (1999) were added to the PHREEQCI calculations using the keyword "Phases" to estimate schwertmannite saturation state in the Omega and T&T mine-pools. The composition parameter, x, was set at 1.80, corresponding to midpoint of the reported formula range, and log K_{eq} was set to 10.5. One set of calculations was conducted using the upper limit of log $K_{eq} = 12.5$.

Jarosite is the Fe bearing member of the jarosite-alunite group with the general composition $AB(SO_4)_2(OH)_6$, where B is Fe^{3+} (jarosite) or Al^{3+} (alunite) and A is usually K^+, Na^+ or H^+. Substitution for both the A cation and Fe^{3+} can occur (Baron and Palmer, 1996). The equilibrium expression for K jarosite is:

$$KFe_3(SO_4)_2(OH)_6\ +\ 6H^+ \leftrightarrow\ K^+ + 3\ Fe^{3+} + 2\ SO_4^{2-} + 6\ H_2O \qquad log\ K_{eq} = \text{-}9.21\ @\ 25°C \quad (3\text{-}32)$$
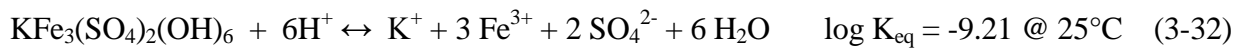
H-Jarosite and Na-Jarosite dissolve in analogous manner and have log equilibrium constants of -5.39 and -5.28, respectively. The low pHs of less than three and oxidizing conditions in both mine-pools are amenable to jarosite formation.

The reported solubility for K-jarosite varies significantly. The various thermodynamic databases available for use with PHREEQCI contain equilibrium constants over 5 orders of magnitude. The Wateq4F and PHREEQC databases both use a log Keq of -9.21, the Lnl data base compiled by Lawrence Livermore National Laboratory uses a log Keq of -9.34, while the MinteqV4 database, compiled for USEPA, uses a log K of -14.8. Baron and Palmer (1996) conducted jarosite solubility experiments and reported a log K of -11. They also reviewed other literature on jarosite solubility which they found ranged over 7 orders of magnitude. Finally, they noted that their experiments, conducted in the range of 5 to 35 ° C, took about 6 months to approach equilibrium. Thus, while jarosite is thermodynamically favored in acid, oxidizing mine-pools, the rate of formation may be constrained. After examining the data summarized by Baron and Palmer and discussions in Alpers

et al. (2000), the jarosite equilibrium constant in the Wateq4F and PHREEQC was selected for use in calculating solubility of K-Jarosite. A set of calculations using Baron and Palmer's value of log Keq = -11 was also conducted to examine effect on apparent solubility.

Mineral saturation indices were calculated in PHREEQCI for about 80 complete suite sample events at the DEF, PM-21 and Marshall springs in the Omega mine-pool and about six sample events collected by the author in the T&T mine-pool. The Omega sample events included analysis of all major cations and anions plus Fe(II)/Fe(III) analysis for data collected by the US Dept of Energy from 1993 to 1999. Samples collected by the author included Eh measurements, and Fe(II)/Fe(III) distributions were estimated from the redox data.

Figures 3-20 to 3-23 show the stability of selected Fe oxyhydroxide and hydrous sulfate minerals plotted with mine-pool composition. Lines on the graphs represent equilibrium for the mineral as a function of pH and log Fe^{3+} activity, and were computed from the equilibrium expression and constant, in the same manner as Al stability in figure 3-16. For mineral dissolution involving sulfate and K^+, representative log activity values were fixed as the median of all speciated samples for that sample point. Activity values on which the calculations are based are included in the caption material for figures 3-20 to 3-23, respectively. Chemical activities did not vary greatly over the monitoring record. The log sulfate activity for the Marshall spring, for example, ranged from -1.86 to -2.32 over more than 10 years and 80 samples. Median chemical activity values, therefore provide a reasonable approximation of entire data sets, and allow plotting of multiple samples on a single graph. The equilibrium constant was varied for schwertmannite and K-jarosite to examine effects on apparent solubility.
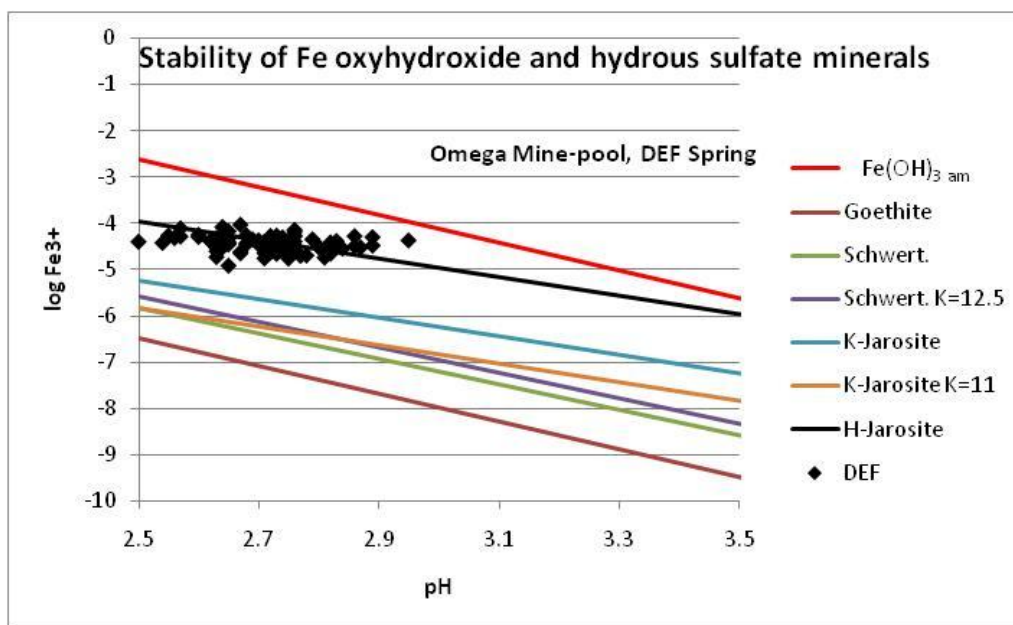
Figure 3-20. Stability of Selected Fe Oxyhydroxide and Hydrous Sulfate Minerals, Omega Mine-pool, and Composition of DEF Spring. Log activity of SO_4^{2-} fixed at -2.23, log activity of K^+ fixed at -4.71.

Equivalent solubility information for Fe and sulfate system minerals could be provided in an Eh-pH diagram, but figures 3-20 to 3-23 facilitate the display of several minerals concurrently. Three springs from the Omega mine-pool, DRF, PM-21 and Marshall are shown in figure 3-20, 3-21 and 3-22. Figure 3-23 shows samples from the T&T mine-pool. In figure 3-20, DEF spring, most samples cluster along the stability line for H-Jarosite, and fall within about one half pH unit. Mine-pool DEF composition is consistent with respect to these minerals over the 80 samples and approximately 13 years represented in figure 3-20.

Results for the PM-21 spring are in figure 3-21. As with the DEF spring, most samples cluster along the H-Jarosite stability line. However a few samples approach stability for poorly crystalline $Fe(OH)_3$ even under the strongly acid conditions. Three samples plot near stability for K-Jarosite, and one sample shows apparent near equilibrium with schwertmannite. Varying the schwertmannite equilibrium constant from ten to 12 has little effect on mineral stability interpretations for these waters.
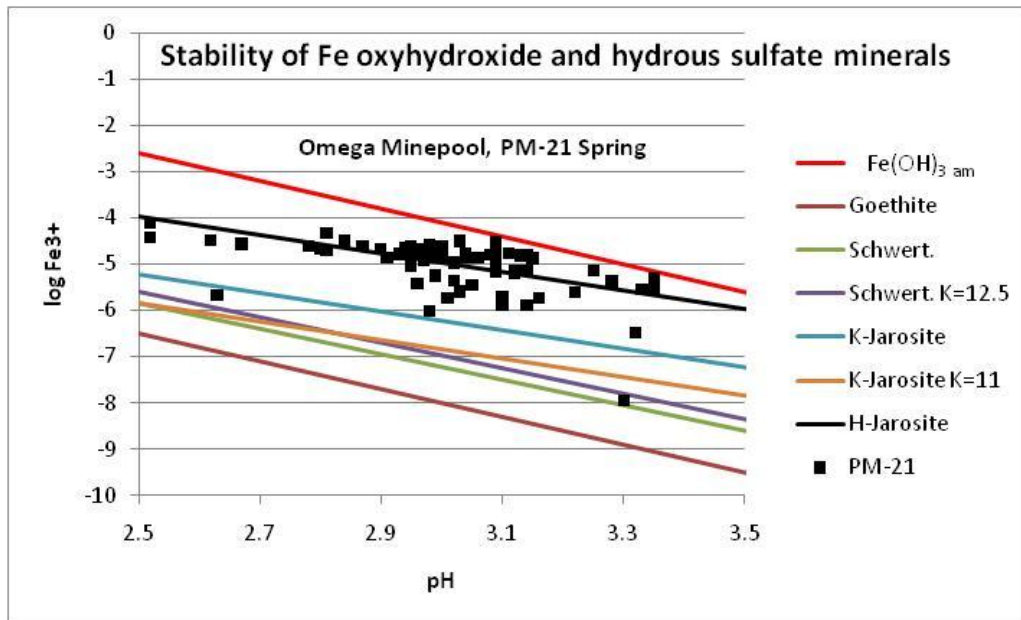
Figure 3-21. Stability of Selected Fe Oxyhydroxide and Hydrous Sulfate Minerals, Omega Mine-pool, and Composition of PM-21 Spring. Log activity of SO_4^{2-} fixed at -2.14, log activity of K^+ fixed at -3.81.

Results for the Omega mine-pool, Marshall spring, in figure 3-22 show two data groups, which correspond to pre- and post- grout injection in to the mine-pool. One group of samples with pH less than about 3.0, range from slight super-saturation for K-Jarosite to approaching equilibrium with H-Jarosite. After grout injection, Fe^{3+} activity is scattered over five orders of magnitude, and apparent equilibrium is displayed for several different iron minerals. Grout injection in 1999 changed the flow characteristics and chemical composition of this part of the mine-pool, and the discharge showed large short term variation for several years after (Perry and Rauch, 2004). By 2007, the latest sampling, the waters were near stability for H-Jarosite or poorly crystalline $Fe(OH)_3$ (figure 3-22).
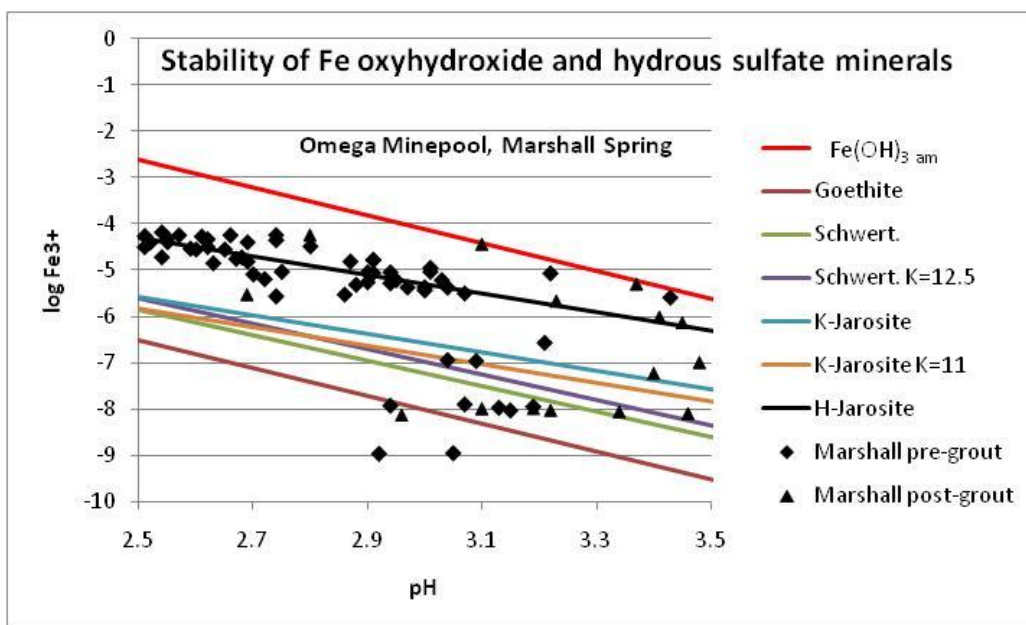
Figure 3-22. Stability of Selected Fe Oxyhydroxide and Hydrous Sulfate Minerals, Omega Mine-pool, and Composition of Marshall Spring. Log activity of SO_4^{2-} fixed at -2.01, log activity of K^+ fixed at -3.76. Pregrout samples (diamond) and post grout (triangle) shown.

Figure 3-23 shows results for the T&T mine-pool. The plot is limited to samples which included measured Eh to estimate Fe(II)/Fe(III) distribution. The WVDEP data source which comprises most of the information for this site does not routinely include Fe(II) analysis or Eh measurement.
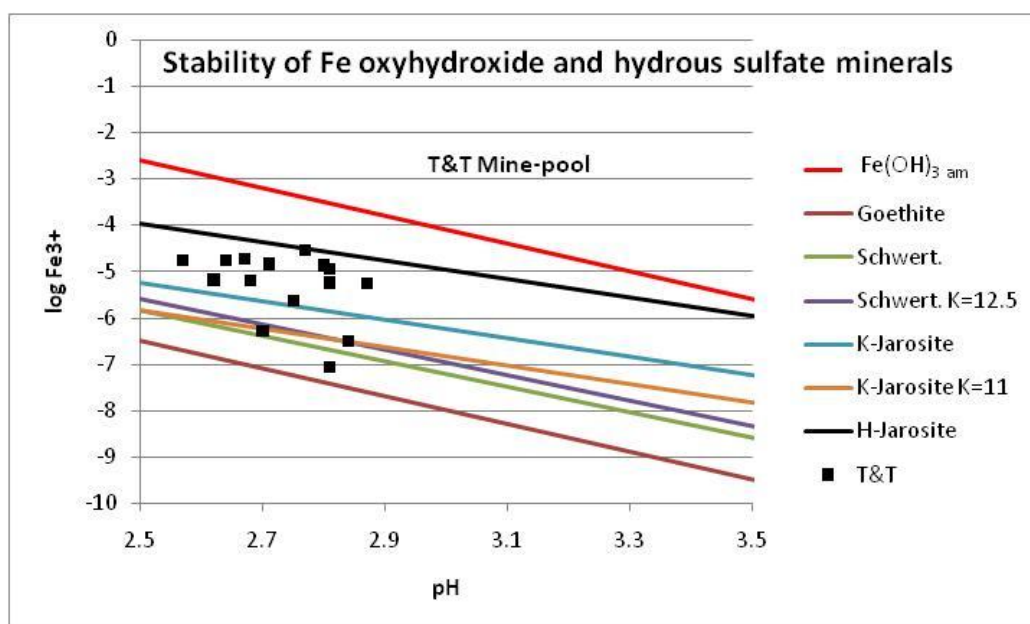
Figure 3-23. Stability of Selected Fe Oxyhydroxide and Hydrous Sulfate Minerals, T&T Mine-pool, and Composition of Waters. Log activity of SO_4^{2-} fixed at -2.48, log activity of K^+ fixed at -4.21.

The waters in figure 3-23 are scattered between K-Jarosite and H-Jarosite, with no clear trend. Either the mine-pool does not approach equilibrium for any single mineral, or the sediments vary sufficiently in composition and crystallinity, that equilibrium is defined within a "window" of conditions.

Figures 3-24a-d are conventional Eh/pH diagrams for selected Fe minerals for the same waters plotted in figures 3-20 to 3-23, and were generated using Geochemist Workbench version 6. Poorly crystalline $Fe(OH)_3$ and H-Jarosite were specified as the oxyhydroxide and hydrous sulfate minerals controlling Fe activity in both mine-pools. Chemical activities for Fe^{2+} and SO_4^{2-} were fixed as the median value of speciated waters for each respective sample point, and that data is included in the caption material for each figure. Hematite, goethite and several other Fe oxyhydroxide minerals were not plotted since they may not be the first minerals to precipitate from mine water. Siderite is not included in figures 3-24a-d, because no direct measurement of aqueous CO_2 was available, and siderite is not stable at the pH values of 2.5 to 3.5 that characterize these mine-pools. To simplify the display, aqueous complexes of Fe and sulfate were not plotted unless they represented the preferred species on significant portions of the diagram. Dark shaded areas in figures 3-24a-d represent Eh/pH conditions where dissolved species are the preferred state, and lighter shading represents an environment where solid phase minerals are likely to form.

Data for the three springs in the Omega mine-pool include about 80 samples at each location from 1994 to 2007, while the T&T mine-pool data include 16 samples from 1994 to 2007. Each figure shows the mine-pool waters near apparent equilibrium for H-Jarosite. Individual samples may be slightly under- or super-saturated, but overall pH/Eh conditions have changed little over a 14 year period. The DEF samples (figure 3-24a) for example plot in a tight cluster spanning less than one pH unit and less than 100 millivolts, respectively. The Marshall Spring samples exhibit somewhat greater scatter, and that is attributable to the grout injection adjacent to the spring. Samples collected prior to grouting exhibit near apparent equilibrium for H-Jarosite, like the other two springs. During grouting and shortly after, the Marshall spring waters were more under-saturated with respect to H-Jarosite.

The complex $FeSO_4^0$ is the preferred state for two Omega mine-pool sites; PM-21 and Marshall waters (figures 3-24 c and d) at Eh/pH conditions bounded by pyrite, $Fe(OH)_3$, and H-Jarosite. Uncomplexed Fe^{2+} is the preferred soluble species in the Omega mine-pool DEF spring and the T&T mine-pool (figures 3-24 a and d). Larger sulfate activity values in the PM-21 and Marshall waters favor $FeSO_4^0$ over uncomplexed Fe^{2+}. As expected, all four mine-pool discharges are far from thermodynamic stability for pyrite. Individual samples are about 200 to 400 millivolts or more from equilibrium with pyrite. Only a few samples in the Omega mine-pool Marshall spring and T&T mine-pool plot within the stability field for poorly crystalline $Fe(OH)_3$. Figures 3-24 a-d like figures 3-20 to 3-23, indicate that hydrous sulfate minerals of the jarosite series are likely controls for Fe solubility in these waters.
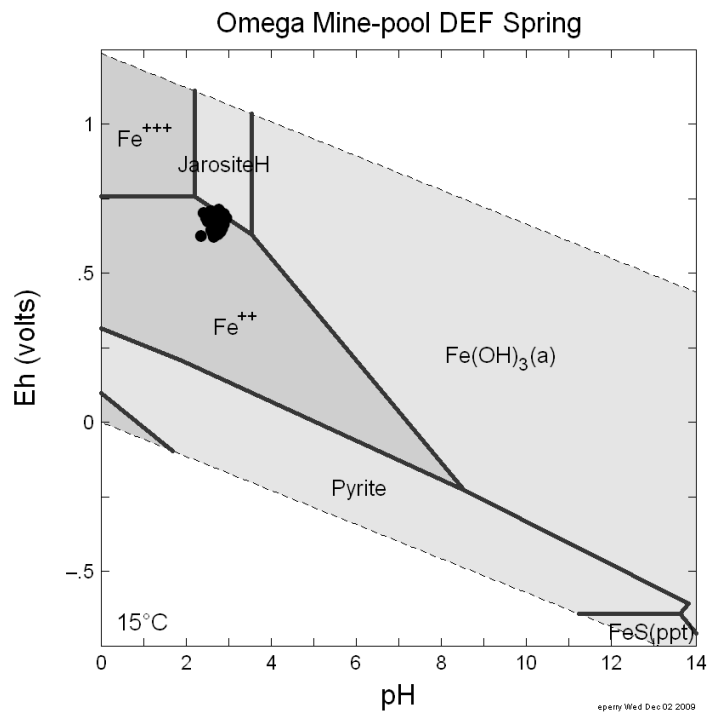
Figure 3-24a. Eh/pH Diagram for Fe Minerals of Omega Mine-pool Spring DEF. H-Jarosite and poorly crystalline Fe(OH)$_3$ specified as controlling minerals. Log Fe^{2+} activity fixed at -2.78, log SO$_4^{2-}$activity fixed at -2.23, log K$^+$ activity fixed at -4.71. Fe-SO$_4$ complexes not shown. Approximately 80 samples plotted.
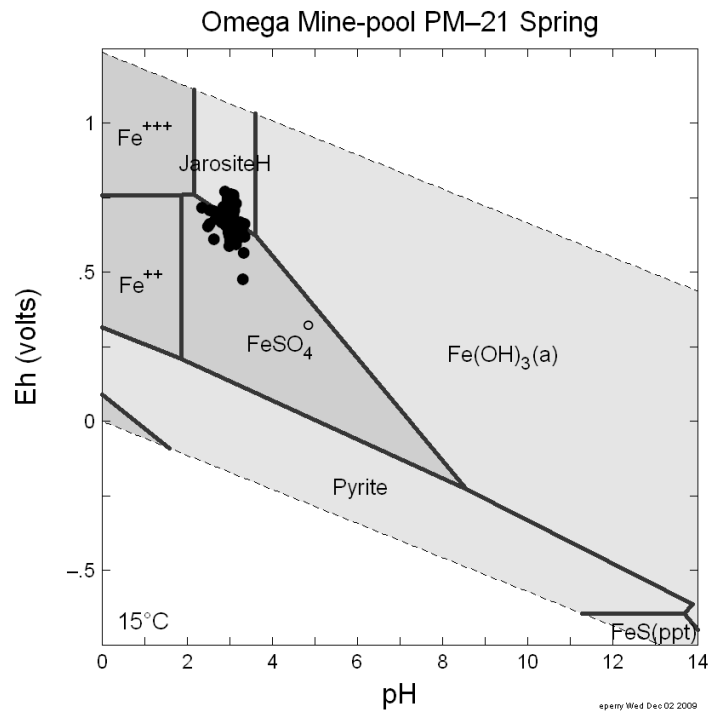
Figure 3-24b. Eh/pH Diagram for Fe Minerals of Omega Mine-pool Spring PM-21. H-Jarosite and poorly crystalline Fe(OH)$_3$ specified as controlling minerals. Log Fe^{2+} activity fixed at -3.51, log SO$_4^{2-}$activity fixed at -2.14, log K$^+$ activity fixed at -3.81 for spring PM-21. Approximately 80 samples plotted.
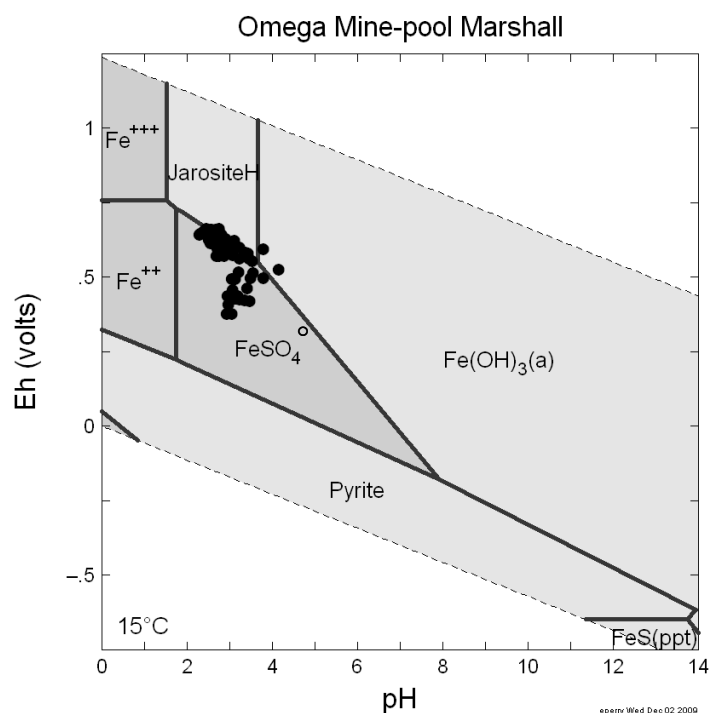
Figure 3-24c. Eh/pH Diagram for Fe Minerals of Omega Mine-pool Marshall Spring. H-Jarosite and poorly crystalline Fe(OH)₃ specified as controlling minerals. Log Fe²⁺ activity fixed at -2.29, log SO₄²⁻ activity fixed at -2.01, log K⁺ activity fixed at -3.76 for Marshall spring. Approximately 80 samples plotted.
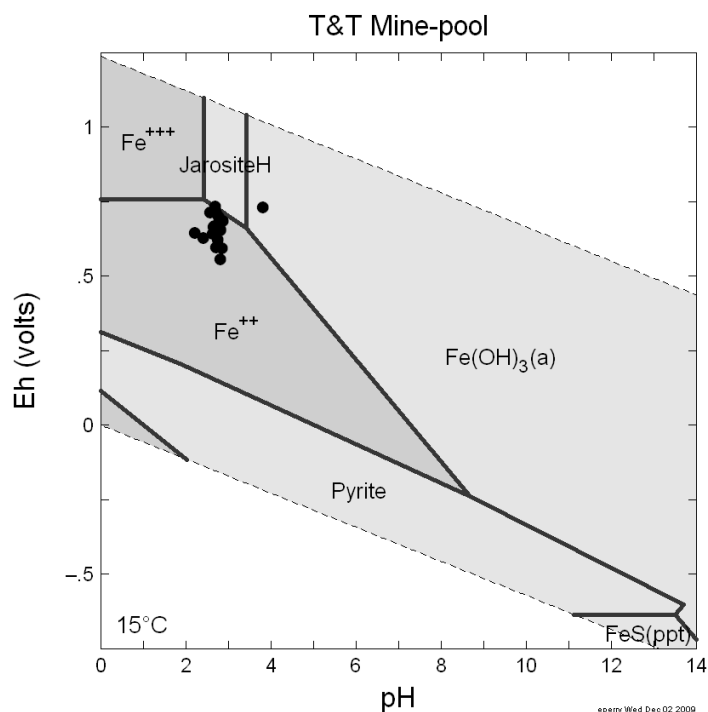
Figure 3-24d. Eh/pH Diagram for Fe Minerals of T&T Mine-pool. H-Jarosite and poorly crystalline Fe(OH)₃ specified as controlling minerals. Log Fe²⁺ activity fixed at -3.70, log SO₄²⁻ activity fixed at -2.48, log K⁺ activity fixed at -4.21 for T&T Mine-pool. Fe-SO₄ complexes not shown. Sixteen samples plotted.

Figures 3-20 to 3-23 include goethite and poorly crystalline $Fe(OH)_3(am)$. These two minerals span about 6 orders of magnitude in solubility, and a range of oxyhydroxides with intermediate solubilities occur in between these end members (Langmuir and Whittemore, 1971; Langmuir, 1997). Langmuir and Whittemore (1971) provided an extensive review of stability of Fe oxyhydroxides including particle size and concentration effects. They observed that the greater the degree of over-saturation for crystalline phases, the faster precipitates formed, and these materials were more soluble. Langmuir and Whittemore also suggest that dissolution reactions for various Fe oxyhydroxide minerals could be written in a common form and thermodynamic stability expressed as a function of Fe^{3+} and OH^- activity:

$$Fe^{3+} \; + \; 3\,OH^- \; \leftrightarrow \; Fe(OH)_3 \; \text{and} \qquad\qquad (3\text{-}33a)$$

$$-pQ = \; - \log\,(Fe^{3+})\,(OH^-)^3 \qquad\qquad (3\text{-}33b)$$

The activity product -pQ ranges from about 37.3 to 43.3 for amorphous to crystalline phases. The -pQ relationship makes it possible to compute an apparent stability for water containing a mixture of Fe oxyhydroxide minerals. The log activities of uncomplexed Fe^{3+} and OH^- were substituted into equation 3-33b and the expression solved for -pQ for the speciated water samples from DEF, PM-21 and Marshall springs in the Omega mine-pool and the T&T mine-pool. These are the same samples plotted in figures 3-20 to 3-23 and 3-24a-d. Figures 3-25 a-c are time series plots of -pQ $Fe(OH)_3$ for the DEF, PM-21 and Marshall springs in the Omega mine-pool.

Table 3-7	
-pQ $Fe(OH)_3$, Omega, T&T Mine-pools	
Site	Median -pQ $Fe(OH)_3$
Omega DEF	39.4
Omega PM-21	38.9
Omega Marshall	39.7
T&T Mine-pool	39.8
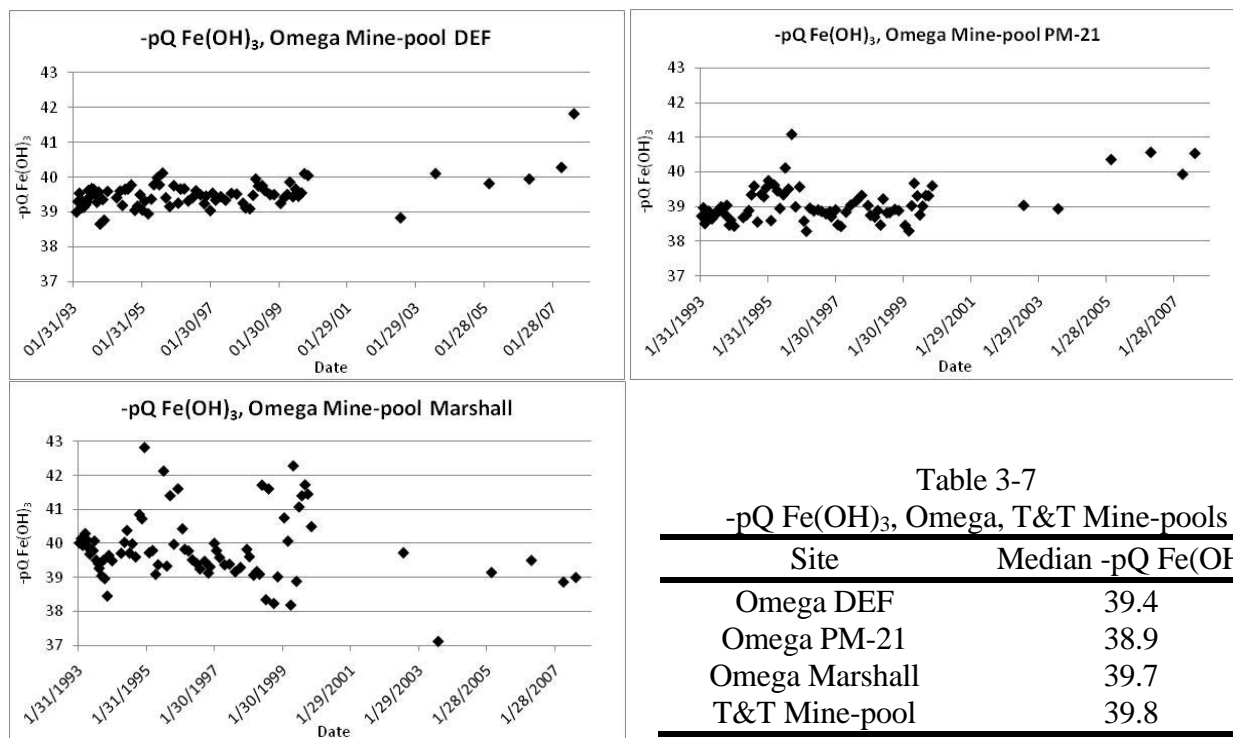
Figures 3-25a-c. Time series of -pQ $Fe(OH)_3$ Values, Omega Mine-pool, DEF, PM-21 and Marshall Springs.

67

Median values for the three springs and the T&T mine-pool are in table 3-7. The median -pQ values range within one order of magnitude and are characteristic of more soluble Fe oxyhydroxides. The long term data for DEF and PM-21 suggest a small increase in -pQ $Fe(OH)_3$ toward less soluble Fe oxyhydroxides. A transformation to more stable mineral phases as the mine-pool ages is consistent with the observations that jarosite, schwertmannite and others are metastable with respect to goethite (Bigham and Nordstrom, 2000; Jonsson et al., 2005). No time series trend is apparent in the Marshall discharge, however. This spring was disturbed by grout injection in 1999, and may have not had sufficient time to establish a discernible long term trend.

3.5 Chemical Flux

Chemical flux or load is a primary factor controlling the magnitude of off-site impacts to aquifers and receiving streams. Clearly, water of given chemical composition flowing at 5 liters per minute will discharge less pollution than one at 25 liters per minute. Nearly all of the chemical analyses for the Omega and T&T mine-pools included an instantaneous flow value compiled by WVDEP, US Dept of Energy or the author. Thus it was possible to compute the chemical flux as:

Flux (kg/day) = Flow(gpm) x 1440 min/day x Concentration (mg/L) x 3.785(L/gal) ÷ $10^{\wedge 6}$ (mg/Kg)

(3-34)

where the constants are units conversion factors. The flux was expressed in moles or kg per day or year by appropriate conversion factors as needed. Iron and sulfate flux were expressed as moles on the basis of 55.85 g/mole for Fe and 96g/mole for sulfate, respectively.

Chemical flux was summarized by estimated yearly totals and by month for both the Omega and T&T mine-pools. Figures 3-26 and 3-27 show estimated yearly chemical flux for total dissolved
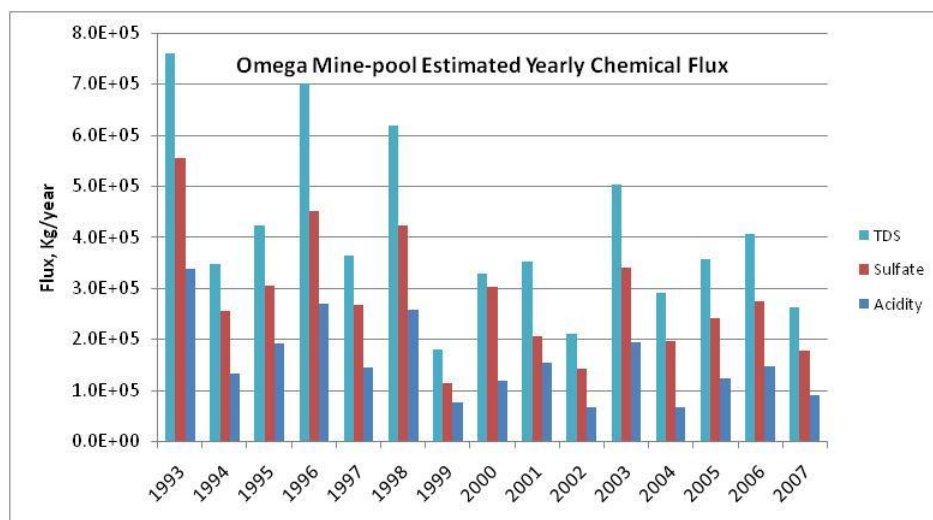
Figure 3-26. Omega Mine-pool Estimated Chemical Flux, Kg/Year, for Total Dissolved Solids, Sulfate and Total Acidity.

68
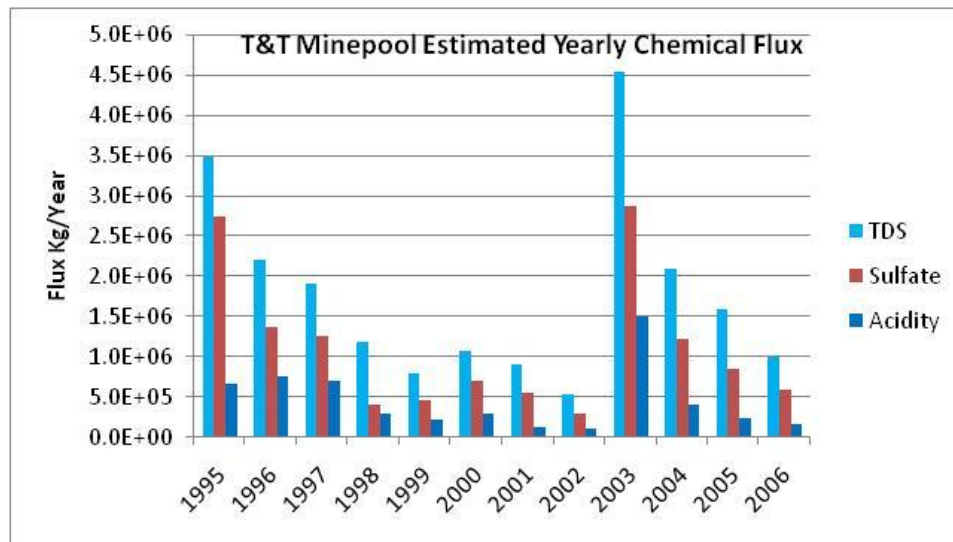
**Figure 3-27. T&T Mine-pool Estimated Chemical Flux, Kg/Year,
for Total Dissolved Solids, Sulfate and Total Acidity.**

solids, sulfate and total acidity in kg/year for the two mine-pools. The Omega mine-pool data in figure 3-26 represent the combined outflow of all discharges, and display an irregular decline in chemical flux from year to year. Flux reached a minimum in 1999, during the period of grout injection. All three flux parameters are significantly correlated with flow (r >0.7), indicating that flow is the dominant component of flux.   Figure 3-27, modified from Perry and Rauch (2004, Appendix A), graphically displays the relationship between sulfate flux and flow in the Omega mine-pool. Hawkins (1994), in an extensive study of surface mine discharges, also found flow to be the dominant component of flux.

.
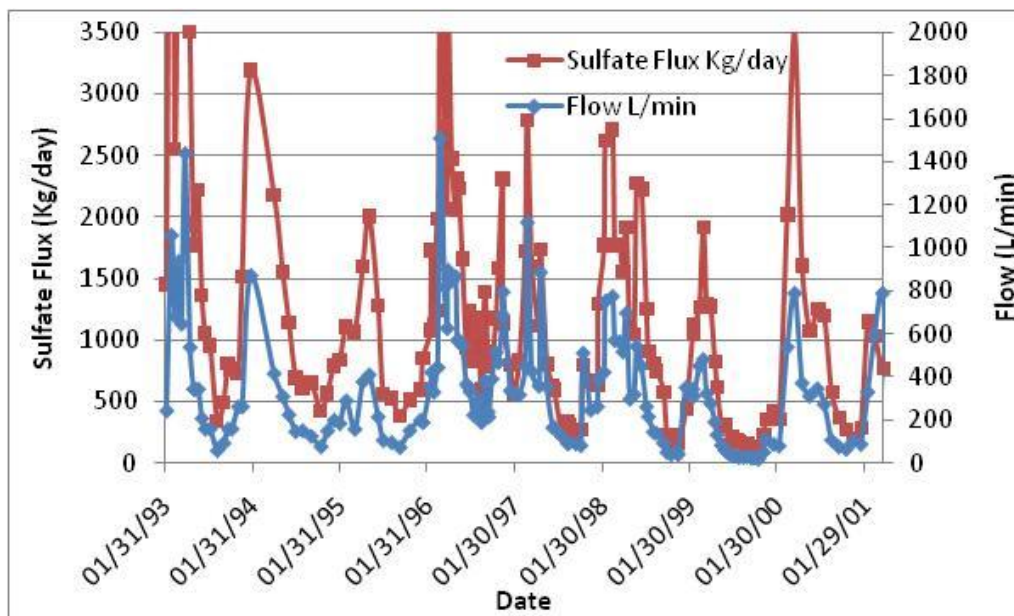
Figure 3-28. Omega Mine-pool Sulfate Flux and Flow, 1993 to 2001.

The T&T mine-pool (figure 3-27), displays a more consistent decline in chemical flux rate to 1999, when limestone injection began. Flux increased during the two year period of in-situ treatment suggesting that the short term effect was to displace stored weathering products. A similar short term increase was noted after grout injection in the Omega mine-pool (Perry and Rauch, 2004; figure 3-26). A large flux surge occurred in 2003 (figure 3-27) in the T&T mine-pool. In April of that year, a rapid buildup in mine pool water level occurred, followed by "blow-out" of high volume flow and increased chemical concentration.The mine-pool water level increase and following blow-out probably occurred after existing flow-paths were blocked or constricted. The cause is speculative but could include subsidence and caving of roof material into mine voids, or blockage by treatment sludge which is periodically injected into part of the mine-works for disposal. Since 2003, the annual flux rate has again declined from year to year in a consistent manner. By 2006, flux rates had declined to about 25% or less of 2003 values.

The two mine-pools exhibit different behaviors with respect to yearly flux. The T&T mine-pool flux exhibits a systematic decline, and except for the injection and blow-out events, does not appear to be affected by shorter term fluctuations in flow or recharge. This mine-pool must have additional ground-water storage that can attenuate high recharge periods. The Omega mine-pool, however, is more responsive to yearly fluctuations in flow and recharge, and appears to have limited extra ground-water storage capacity to attenuate high recharge periods. The T&T mine-works cover about 8.5 times more area than Omega, while the estimated mine-pool volumes differ by a factor of about 2.6.

Flux rates are declining about 3 to 4 times more rapidly in the T&T mine-pool than in the Omega mine-pool. This may be a function of chemical and mineral concentrations in the two mine-pools. While both produce acid drainage, chemical concentrations are about 3 to 5 times greater in Omega, indicating significant ongoing active chemical weathering.

Flux rates exhibit a strong seasonal trend. Figure 3-29a-b and 3-30a-b display monthly flux data over 13 and 14 year periods respectively in the Omega (all discharges combined) and T&T mine-pools. Graph values are median data for each month compiled over the period of record. The Omega mine-pool is further divided into pre and post grout injection. Both mine-pools discharge about 75% ± of the yearly flux in a six month period from January to June. Monthly flux rate did decline in the Omega mine-pool after grouting compared to pre-grouting, and decreases occurred across all months and seasons. The spike in April flux data in the T&T mine-pool resulted from the large blow-out event in April 2003 and another large discharge event in April, 1995. More flow and water quality measurements were taken during these two events, and these extreme conditions are over-represented in the data compilation. Sulfate, Fe and Al fluxes are similar to that shown for TDS and total acidity for both mine-pools. The period of March to about June produces the peak monthly fluxes. Chemical consumption for active or passive treatment is also seasonal, as is the potential impact of untreated discharges to aquifers and surface waters. Baseline sampling for sizing treatment systems should include seasonality criteria.
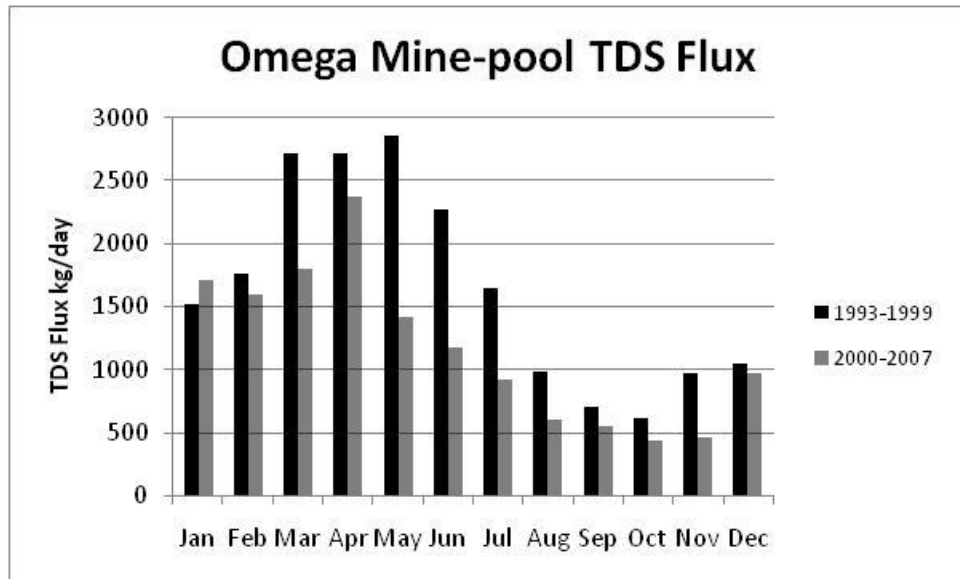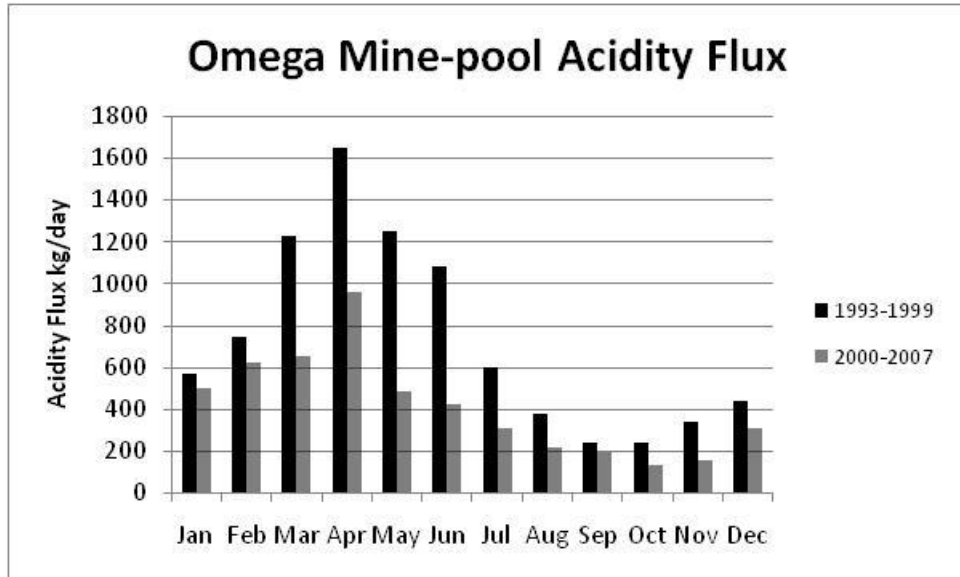
Figure 3-29a-b. Seasonal Distribution of Total Acidity and TDS Flux in Omega Mine-pool.
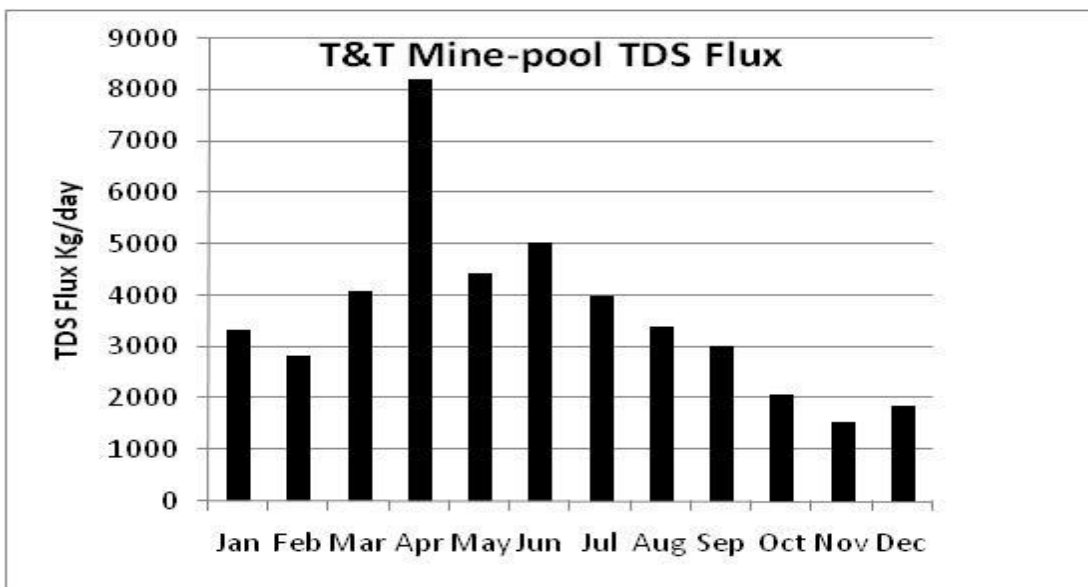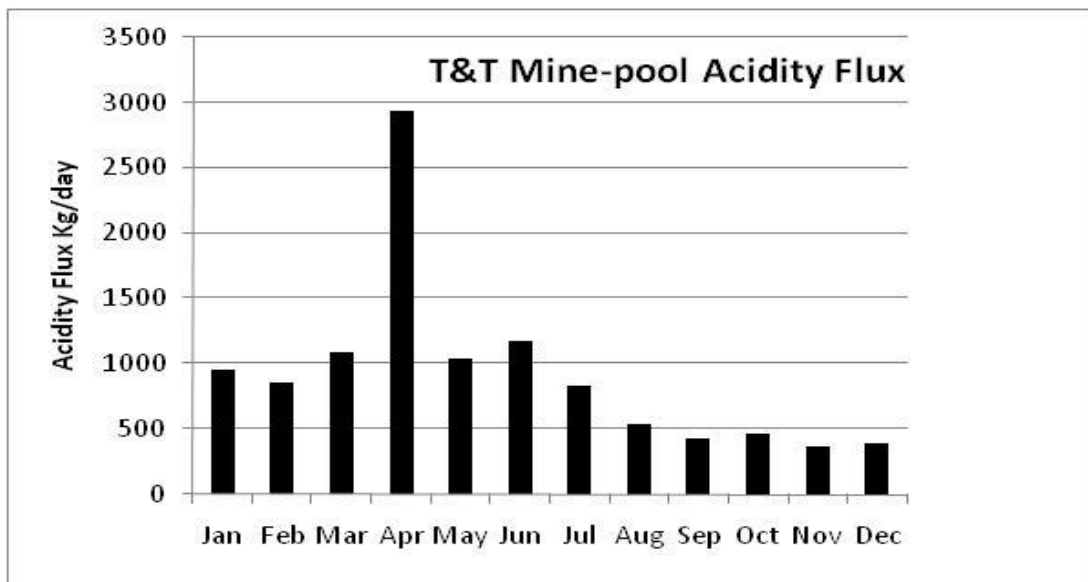
Figure 3-30 a-b. Seasonal Distribution of Total Acidity and TDS Flux in T&T Mine-pool.

Long term Fe and sulfate flux rates were estimated for the Omega and T&T mine-pools as an average over the period of record. The flux rates were normalized to a m^2 of mine-works for comparison between each other, and to three mostly flooded mine-pools (chapter four). Flux rate is expressed as mole/m^2-s, consistent with expression of reaction rate constants. It was hypothesized that flux would be different between unflooded mines and mostly flooded mines. Flux rates in flooded mines were anticipated to be less on the premise of slower pyrite weathering rates under flooded conditions. The Omega and T&T mine-pool discharge rates were determined from monitoring data obtained from West Virginia DEP. Results are shown in table 3-8 and comparison of all five mine-pools is presented in section 4.2.6.

72

Table 3-8
Average Long Term Iron and Sulfate Flux From
Two Partly Flooded and Three Flooded Mine-pools

Mine-pool	Flooding State	Area (Hectares)	Average Q (L/Min)	Fe Flux (mole/m^{2}s)	Sulfate Flux (mole/m^{2}s)
Barnes&Tucker	Flooded	5700	19000	9.49×10^{-9}	3.48×10^{-8}
Hahn	Flooded	5900	13250	7.04×10^{-8}	2.69×10^{-7}
Arden-Westland	Flooded	5100	6600	6.2×10^{-9}	3.48×10^{-8}
Omega	P. Flooded	69	268	3.42×10^{-8}	1.37×10^{-7}
T&T	P. Flooded	588	1139	7.33×10^{-9}	4.72×10^{-8}

3.6 Mine Recharge Rate

Chemical flux is determined in part by mine-pool discharge as described in section 3.5. Mine-pool discharge in turn is a function of ground water recharge. Daily mine-pool discharge and on-site precipitation data collected by WVDEP were summarized into annual and seasonal estimates of recharge rate for the two mine-pools. The estimates include several assumptions as follows:

- Infiltration is assumed to be vertical, such that the area of mine-works and land surface area contributing recharge are equal. McCoy (2002) estimated recharge to underground mines using this method.

- Net ground-water storage change in the mine-pool is zero, and discharge equals recharge.

- Measured drainage points represent mine-pool discharge and mine-pool diffuse leakage is minor.

The first assumption of vertical infiltration neglects the observation that underground mines act as ground-water sinks (Hobba, 1981; Bruhn, 1986) and a ground-water cone of depression may develop. Cifelli and Rauch (1986) showed an "angle of influence" exists in rocks overlying a mine, defining a zone where aquifer dewatering occurs. They estimated the angle of influence at 16 and 24 degrees for two case studies. The land area contributing inflow to the mine may therefore exceed the mine-works area. However, both the Omega and T&T mine-pools underlie hilltops, which limit the amount of additional land area that could contribute inflow. The contributing area is a function of angle, overburden thickness and stratigraphy. Since recharge rates are customarily expressed per unit area of mine-works, infiltration from rocks outside the vertical recharge zone will increase the estimated recharge rate. Neither mine has wells that could be used to estimate the

angle of influence. The T&T mine-pool area was estimated as the sum of the three individual, but hydrologically connected mines; T&T 2, T&T 3 and Ruthbelle.

No net storage change is a reasonable assumption over extended periods of time. Water level measurements in two wells in the T&T mine-pool showed essentially steady state conditions from 2002 to 2007, with the exception of a "blowout" event in 2005.

The third assumption is difficult to quantify, but is based on the premise that hydraulic conductivity and ground-water flow velocity through open or partially collapsed mine-works is several orders of magnitude greater than flow through intact bedrock and soils.

Figure 3-31 and 3-32 display estimated average daily recharge rate for the two mine-pools from 1996 and 1997 respectively, through 2007. Rate was determined as total discharge per unit time divided by mine area. The yearly estimate is a median of the daily values for that year. Total annual precipitation is also plotted. The Omega mine-pool recharge ranges from a minimum of 0.13 to a maximum of 0.59 gal/A-min, with an overall median of 0.36 gal/A-min for the ten year record. The T&T mine-pool average daily recharge rate ranges from 0.17 to 0.46 gal/A-min with an overall median of 0.28 gal/A-min. Behavior of the two mine- pools is similar, and the annual and average daily recharge rate varies by a factor of two to three over the period of record. Both mine-pools exhibited low recharge rates in 1999, and an overall correlation coefficient of $r = 0.53$ when compared to each other. The two mine-pools are sufficiently close (about 27 km) that they can be considered to have similar annual climatic conditions. It was expected that precipitation
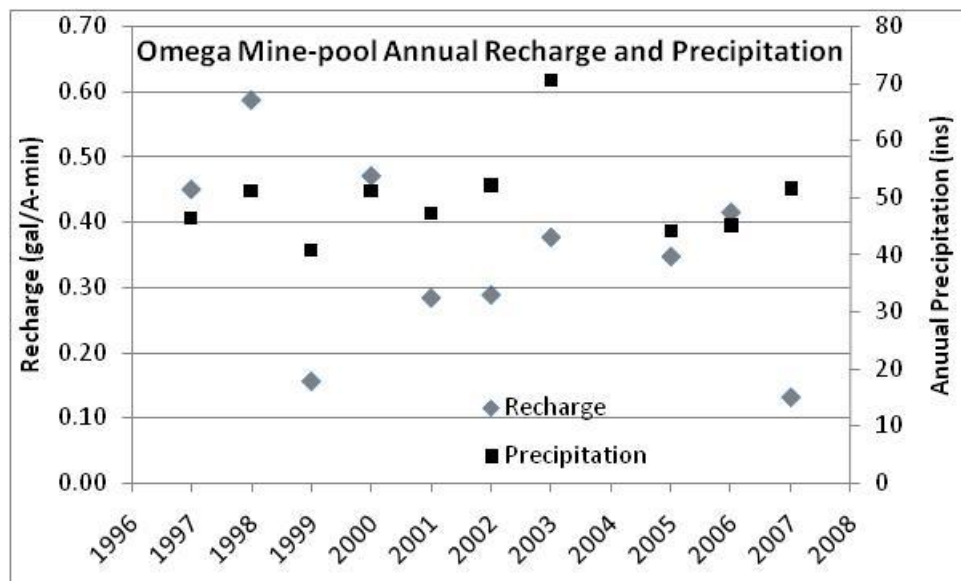
Figure 3-31. Omega Mine-pool Estimated Annual Recharge (gal/A-min) and Annual Precipitation.
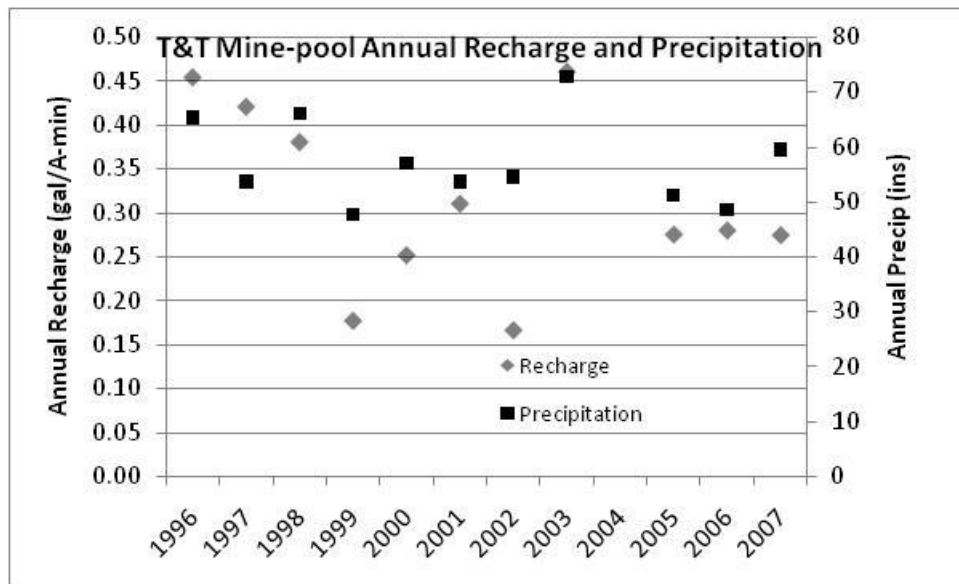
Figure 3-32. T&T Mine-pool Estimated Annual Recharge (gal/A-min) and Annual Precipitation.

would be a principal control on recharge rate, but considerable scatter exists when comparing data on an annual basis.The precipitation/discharge relationship might be resolved further by examining the record in smaller time increments.

A general relationship has been observed to exist between overburden thickness and mine inflow rates, where mine recharge rate decreases for increasing cover. For the Appalachian region, mine water inflow rates have been reported to range from less than 0.05 gal/A-min to rates approaching 1.0 gal/A-min (Crichton, 1927; Parizek, 1974; Stoner et al., 1987; Tieman and Rauch, 1987). Carpenter and Herndon (1933) examined discharge records for 243 underground mines in the Monongahela River basin, and commented that annual precipitation affected mine discharge quantities, especially for mines under thin overburden. They reported a range for recharge rates from 0.21 to 0.84 gal/A-min for mines under 100 to about 300 feet of overburden. Carpenter and Herndon estimated recharge under a "normal" precipitation year to be about 0.69 gal/A-min or about two times the values compiled for the Omega and T&T mine-pools. Another early study by Collins (1923) gave an estimate of 0.62 gal/A-min from a series of measured mine inflow rates from several counties in western Pennsylvania with average overburden depth of 250 feet. Hawkins et al. (2005) reported an average recharge rate of 0.27 gal/A-min for the Barnes&Tucker mine-pool based on pumping records, which is similar to the Omega and T&T mine-pools. The Barnes&Tucker mine-pool is discussed in more detail in chapter four.

The data reported by Carpenter and Herndon (1933), and Collins (1923) all seem to have been conducted on operating mines that were actively removing ground-water inflow. The Omega and T&T mines are however closed, and discharge by gravity flow. Mine inflow rates reported in the literature are often developed from pumping and flow data acquired during active mining, when head differential between the mine-works and overlying aquifers is maximized. After abandonment, flooding can reduce the head differential. Under these circumstances, the head differential between the mine pool and overlying aquifers will diminish, and the inflow rate to the

75

mine pool should decline. In above drainage mines, head increase should be small and recharge may be supplied mostly by fracture flow. Mine differences in flooding state and active versus abandoned status may account for some of the difference between the early studies and these two mine-pools.

Leavitt (1997) developed a recharge estimate equation based on pump records in active mines, most located in northern Appalachia, of the form:

$$L = 1.117*e^{(-0.0045*H)} \tag{3-33}$$

where L is the mine inflow rate in gallons/Acre-min and H is the overburden thickness in feet. Figure 3-33 is a plot of estimated mine inflow rate using Leavitt's relationship. Inflow rate is sensitive to overburden thickness at depths of less than about 500 to 600 feet. Using an average overburden thickness of 150 and 250 feet for the Omega and T&T mine-pools, respectively, Leavitt's equation estimates a recharge rate of 0.56 gal/A-min for the Omega site, compared to 0.36 estimated from site discharge data, or an over-estimate of 56 percent. The T&T mine-pool estimate is 0.36 gal/A-min from Leavitt's equation compared to 0.28 from discharge data, a difference of 28 percent, but providing reasonable agreement between the two methods for the T&T site. Leavitt's equation was derived from a data set with overburden thicknesses greater than
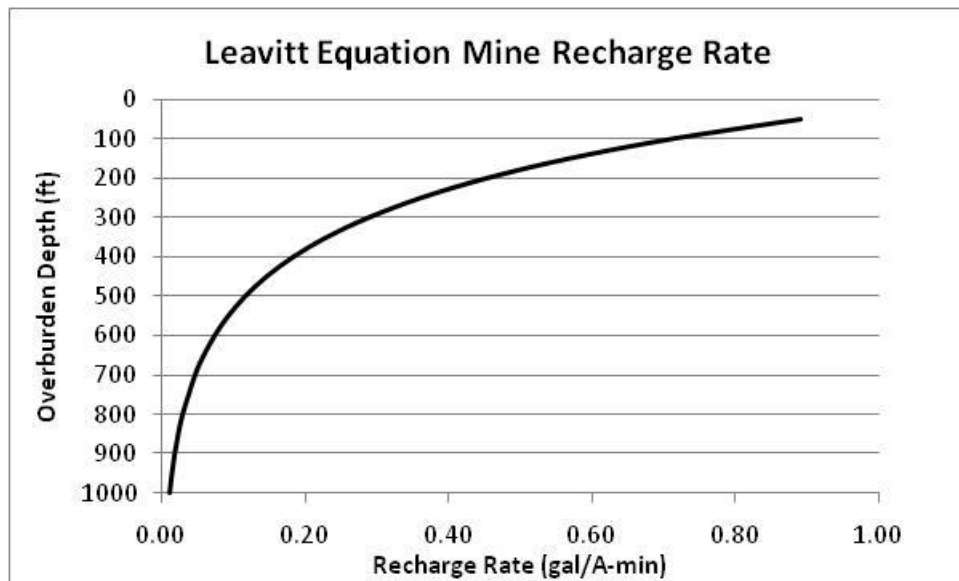
Figure 3-33. Plot of Estimated Recharge vs. Overburden Depth,
Using Leavitt's (1997) Empirical Relationship.

that of the Omega mine, and the predictive relationship may be less accurate for shallow overburden depths. A single value is often specified or described for annual recharge rate to mine-pools. A long-term average or median rate is useful for estimating trends and general conditions but actual rates vary from year to year. The tenth and 90th percentiles for annual recharge in the

Omega and T&T mine-pools are 0.15 and 0.48; and 0.17 and 0.45 gal/A-min, respectively. These values can define a reasonable range of values for mines in similar conditions.

Recharge relationships were also estimated on a seasonal basis by summarizing monthly data over the period of record. Figures 3-34 and 3-35 show the median estimated recharge rate for the two mine-pools, and the estimated fraction of precipitation occurring as recharge. The plots have seasonal trends that are similar to the chemical flux data in figures 3-29 and 3-30. Maximum recharge occurs in March for both mine-pools, with rates exceeding 0.5 and 0.8 gal/A-min, respectively. Minimum recharge rates are very similar for the two mine-pools, declining to 0.11 (Omega) and 0.12 (T&T) gal/A-min in November. These data represent a lower limit or base-flow condition for mine-pools in similar settings.
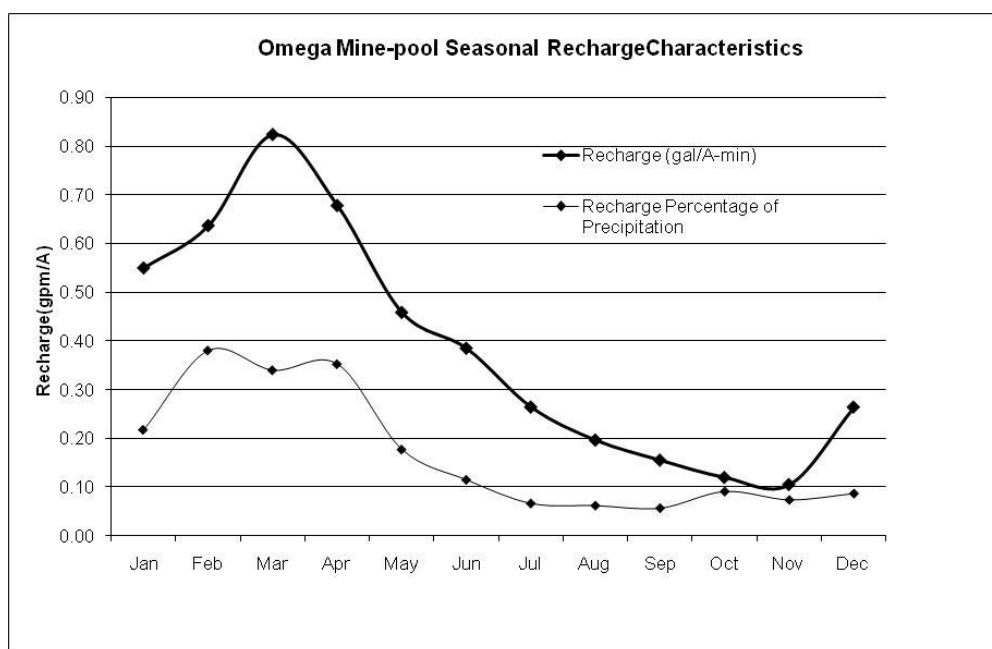
Figure 3-34. Seasonal Distribution of Recharge Characteristics, Omega Mine-pool.
Median monthly recharge rate in gal/A-min based on 1997-2007 flow and
precipitation data.

Both mine-pools exhibit year to year fluctuation in monthly recharge rate and the values in figure 3-34 and 3-35 should be used as trend indicators. The 3 month period of September to November is an overall period of minimal recharge, while maximum recharge occurs in the 6 month period of January to June. The seasonal distribution data between the two pools has a correlation coefficient of $r = 0.94$, confirming similar behavior of the two mine-pools. The percentage of precipitation occurring as recharge is also seasonally distributed, and ranges from about 6 to 38% in the Omega mine-pool, and 6 to 20% in the T&T mine-pool. Minimal values occur during the base-flow period of late summer to autumn, when evapotranspiration (ET) is high, and precipitation can occur as intense short duration storm events. The maximum fraction of precipitation intercepted as recharge is late winter, when ET is low. Hobba (1981) summarizing data from several sources, estimated annual ET as about 50% of total precipitation for the Monongahela River basin. The remaining

50% is divided among runoff, recharge and ground-water storage change. Figures 3-34 and 3-35 show that mine recharge distribution has a strong seasonal component. It should be considered in mine water planning and mitigation.
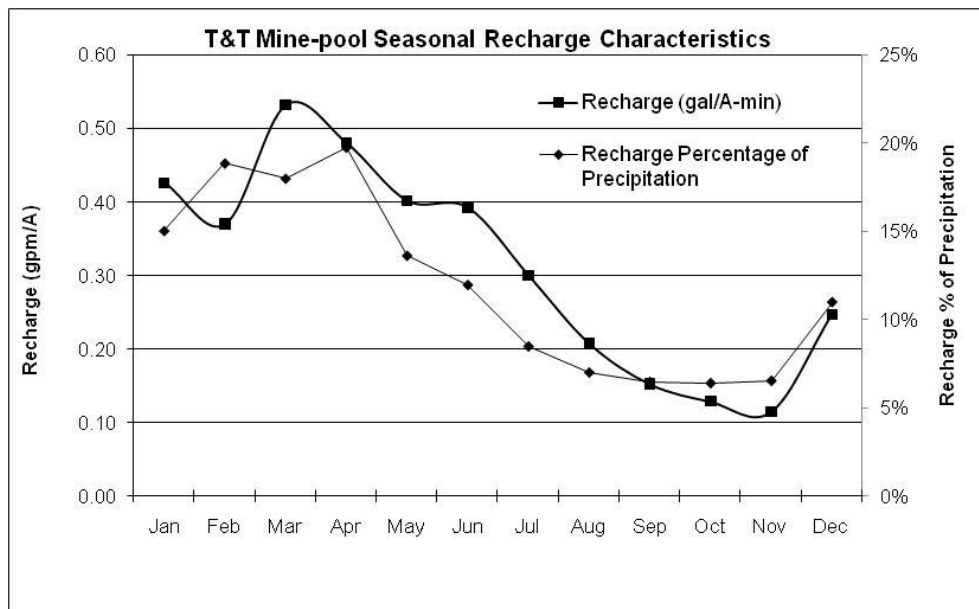
**Figure 3-35. Seasonal Distribution of Recharge Characteristics, T&T Mine-pool.
Median monthly recharge rate in gal/A-min Based on 1996-2007 flow and
precipitation data.**

3.7 Chapter 3 Summary Findings and Observations

In chapter three water quality, chemical flux and recharge characteristics of two partly flooded, acidic mine-pools were examined over a period exceeding ten years. Chemical concentrations and flux declined during the monitoring period, however overall water quality remains severely degraded. Significant short term variations in concentration, flux and flow were common to both mine-pools, but long term trends were also evident. The principal findings and observations for this chapter are summarized as follows:

- Conceptually, partly flooded mines can be viewed as large reactor and leaching chambers, that are regularly supplied with oxygen to oxidize pyrite, and water to rinse soluble weathering products.

- Data for the two mine-pools were obtained from different sources and consistency was an issue. Total Dissolved Solids was a suitable estimator for sulfate concentration, but the relationship was mine specific. Sulfate represented about 58% of TDS in the T&T mine-pool, and 67% in the Omega mine-pool.

- The two mines are an estimated 20 to 30% flooded and discharge by gravity drainage. The Omega mine is a small (68 hectares) complex, with relatively short flow paths,

while the T&T mine-pool includes about 588 hectares of workings in three hydrologically connected mines.

- Both mines had in-situ treatment consisting of grout injection in the Omega mine and limestone injection in the T&T mine-pool. Water quality actually declined for 1 to 2 years after remediation, as stored weathering products were displaced and flushed from each mine. The Marshall discharge, adjacent to the grout injection zone in the Omega mine-pool, has since injection shown an increase of about one pH unit.

- Each site has had some treatment sludge with excess alkalinity injected into the mine-works. The overall effect on mine-pool composition appears minimal or is masked by other processes.

- The Omega mine-pool has multiple discharge points which vary in individual concentration. The overall character of the mine-pool is consistent however, with low pH water (2.5-3.5), and Al and Fe concentrations in the tens to hundreds of mg/L. The T&T mine-pool is also acidic, but with Fe and Al now in the tens of mg/L.

- The cation fraction of the Omega mine-pool has increasing portions of Al and Fe as the mine-pool ages, with Ca and Mg as the other major cations. The anion fraction is dominated by sulfate. The T&T mine-pool is Ca-Mg-SO_4 type water, and is progressively enriched in Al as the mine-pool ages. In both mine-pools, Al concentration is declining more slowly than other components.

- The Omega mine-pool has about 2 to 5 times greater chemical concentrations than the T&T mine-pool even though both are developed in the same coal bed. Only limited site specific geochemical rock data were located for the Omega mine, which indicates pyrite is abundant in this mine and few carbonates are present. The Omega mine-pool continues to undergo intense chemical weathering more than 15 years after closure.

- Simple time series plots of chemical concentration show considerable short term variation and data scatter in both mine-pools. Since the mine-pools are being stressed repeatedly at short intervals by recharge events, short term variability is expected.

- A five point moving average provided smoothed data sets that more clearly displayed seasonality and other subtle trends and features in both mine-pools. Chemical concentrations are inversely related to flow in the Omega mine-pool, increasing during low recharge periods of late summer and autumn.

- The distinct seasonal behavior in the Omega mine-pool suggests the complex has little additional ground-water storage capacity, beyond that in the mine-pool. The T&T mine-pool had little or indistinct seasonality in chemical concentrations, suggesting some

additional storage capacity is available to dampen seasonal effects and variable recharge events.

- The possible differences in storage behavior may result from mine size and topographic position. The Omega mine-pool is small, and ground-water should have a short travel distance within the mine-works to a discharge point. The T&T complex is about 8 times larger, with longer average travel distance. The Omega mine-pool is located almost entirely above the local base level drainage, with about 8 major and several minor springs draining the mine-works. The lowest portion of the T&T mine-pool is located below base level drainage with one major and three smaller outlets. The below drainage portion of the mine-works may provide some dampening effect on seasonal and individual recharge events.

- Time series plots of iron to sulfate mole ratios showed that discharge water from both mine-pools are deficient in dissolved Fe with respect to sulfate, based on pyrite composition. The Fe deficiency increases as the mine-pool ages and approaches a constant value. An estimated 60 to 80 % of the Fe associated with pyrite weathering is missing from aged mine-pool discharge water. A large fraction of the Fe from pyrite weathering is therefore being attenuated within the mine-pool, even in very acidic conditions. The retention mechanisms could include hydrous sulfate minerals, oxyhydroxide minerals, cation exchange or adsorption.

- Iron to sulfate ratio was greatest during high flow periods in the Omega mine-pool indicating flushing of Fe minerals. The ratio declined in low flow conditions indicating more storage during these periods. The T&T mine-pool displayed similar seasonal behavior; the variation was smaller than in the Omega mine. The flushing dependent mole ratios suggest some Fe is attenuated in relatively soluble phases, such as hydrous sulfate minerals.

- Mole ratios may be useful for distinguishing initial flushing from long term leaching. The T&T mine-pool approached steady state $Fe:SO_4$ ratio about 7 years after closure. The initial record for the Omega mine-pool from 1989 to 1993 is sparse. However, after grout injection in 1999, $Fe:SO_4$ ratio rapidly increased then declined slowly approaching a steady state after about 5 years. This second event approximates an initial flush.

- Both mine-pools contained a large excess of sulfate to Al on a mole basis (range from 7:1 to 10:1). These conditions should promote formation of $Al-SO_4$ minerals, including sulfate rich minerals such as alunite or jurbanite.

- Mine-pool chemistry is very responsive to large imposed stresses. Both mine-pools had substantial increases in concentration and flux for several years after in–situ treatment. The T&T mine-pool also experienced a short term major "blowout" event in 2003 resulting in a large flux of pollutants. These events established a new flushing cycle followed by gradual declines in concentration and flux. The T&T "blowout" was not

associated with any anthropogenic activities. Rather it appears to have resulted from disruption of existing flow-paths, rapid head buildup, followed by failure of a barrier, pillars, or other subsidence that rapidly relieved the hydraulic pressure. Roof falls or partial collapse, and pillar failure are extremely difficult to predict on a temporal basis, but can affect chemical flux on short and long term bases by altering ground-water flow patterns.

- Sulfate, Al and Fe(III) form significant amounts of complexes in mine water. Complex formation, in general, increases the quantity of the contributing mineral and element that can dissolve in solution. The distribution of complexes also changed as the mine-pools aged.

- About 70% of total dissolved sulfate was uncomplexed SO_4^{2-} in the Omega mine-pool during initial flushing. $CaSO_4^{°}$ was the second most abundant sulfate species. In the aged mine-pool, uncomplexed SO_4^{2-} had declined to about 50% of the total sulfate, and Fe-SO_4 and Al-SO_4 species had replaced $CaSO_4^{°}$ as the secondary species. The T&T mine-pool had 40 to 50% of total sulfate present as uncomplexed SO_4^{2-}, and $CaSO_4^{°}$ was more abundant in the aged mine-pool after limestone injection.

- Most dissolved Al, about 70% of the total, was present as Al-SO_4 species in both mine-pools. This increases the quantity of Al-SO_4 minerals, and amount of Al that can dissolve. About five times more jurbanite could dissolve in these mine waters because of complex formation, than if dissolved Al was present only as Al^{3+}. The distribution of Al- SO_4 species showed little change as the mine-pools aged.

- About 70 to 80% of Fe(II) is present as uncomplexed Fe^{2+} in these waters and there is little difference by age or mine-pool.

- Ferric iron is a much stronger complexing agent than Fe(II). Seventy to 80% of dissolved Fe(III) occurs as Fe-SO_4 species. In general, this increases the solubility of Fe(III)-SO_4 minerals such as schwertmannite, and amount of Fe(III) that can dissolve.

- Measured Eh and Eh calculated from Fe^{2+}/Fe^{3+} activities had a median difference of -32 millivolts. Results were similar to other studies. Two potential error sources included the necessity to dilute samples containing high Fe concentrations and determining Fe(III) by difference rather than directly. Dilution by a factor of ten or 100 reduced resolution of Fe(II) concentration. Ferric iron may be over-estimated when determined by difference and results in over-estimating Eh.

- Stable Eh readings were obtained within a few seconds indicating well poised systems. Measurements collected from 2002 to 2007 for both mine-pools were consistent, indicating reproducible results and/or stable redox conditions. Individual sample points fell within a range of 50 to 100 millivolts over the five year record.

- Eh readings in acid mine waters can be used to estimate system redox conditions for iron. Fe^{2+}/Fe^{3+} activities are sufficiently large that both can be sensed by the electrode and the couple is readily reversible.

- Measured Eh did not have a consistent relationship with $Fe^{2+}/Fe(OH)_3$, $Fe^{2+}/Goethite$, or $O_2/Pyrite$ redox couples.

- Uncertainty in redox state affects computed saturation index for Fe minerals especially if the water is near equilibrium for a mineral.

- A large number of Fe and Al oxyhydroxides and hydrous sulfates could form in acid mine-pools. They are potential sinks for metals. Many, however, are soluble and dissolve during flushing events.

- Three springs in the Omega mine-pool are near apparent equilibrium for jurbanite ($AlOHSO_4$) and approach stability for alunite ($KAl_3(SO_4)_2(OH)_6$). There is little change in water composition with respect to Al minerals over more than ten years in the Omega mine-pool. Al activity and mineral saturation state in the T&T mine-pool were estimated from indirect methods utilizing charge balance and ionic strength principles. This mine-pool is apparently under-saturated for Al-SO_4 minerals. Neither mine-pool was directly accessible for sediment sampling.

- Both mine-pools approach apparent saturation for H-Jarosite ($H_3OFe_3(SO_4)_2(OH)_6$). With the exception of one spring (Marshall) in the Omega mine-pool, both mine-pools show little change in composition with respect to Fe minerals over time.

- Apparent thermodynamic stability of mine-pool waters with respect to Fe oxyhydroxides was assessed from a modified activity product, -pQ. Both partly flooded mine-pools have -pQ values characteristic of poorly crystalline, soluble Fe oxyhydroxides.

- Common ion effects for sulfate, Fe, Al and Ca can suppress dissolution of less soluble minerals, and complicate interpretation of mine water composition. Some hydrous sulfate minerals lack reliable thermodynamic data and their solubility cannot be assessed quantitatively.

- Annual chemical flux has declined in both mine-pools. The Omega mine-pool flux is irregular from year to year, and after 14 years has declined to about 1/3 of its initial load. The T&T mine-pool has a consistent rate of change in annual chemical flux and has declined more rapidly than the Omega mine-pool. The 2003 "blowout" in T&T increased flux, but it has declined each subsequent year.

- Irregular flux rate in the Omega mine-pool suggests that loading is sensitive to variations in precipitation. Such behavior could result from limited additional ground-water storage in the mine, where large recharge events quickly pass through the mine. The more regular response in the T&T mine-pool suggests a mechanism that dampens response, such as the ability to store additional ground-water recharge during exceptionally wet periods and release it slowly.

- Flux has a strong seasonal component. About 75% of annual chemical flux is discharged in a six month peak recharge period from January to June in both mine-pools.

- Average long term flux rates (mole basis) normalized to mine area are within about one order of magnitude for Fe and sulfate in both mine-pools. Sulfate flux rate is greater than for Fe flux.

- There is no clear distinction in flux rate between partly flooded and mostly flooded mines when normalized to mine area.

- Median annual recharge is 0.28 and 0.36 gal/A-min for the T&T and Omega mines, respectively, varies from year to year, and is at least partly dependent on precipitation and overburden thickness.

- Recharge, like flux, has a seasonal component. Median recharge in spring is from 0.5 to 0.8 gal/A-min for the two mine-pools, and also varies from year to year.

- Both mine-pools approach base-flow conditions of about 0.1 gal/A-min recharge in the autumn.

Chapter 4: Chemical and Hydrologic Properties of Flooded Mines

Flooding and inundation of closed underground mines, tailings and waste rock containing pyrite has been suggested as a useful mine closure practice (Robertson et al., 1997, Jakubick et al., 2002). Stoertz et al. (2001), for example, attributed a pH increase from about 2.7 to greater than 5, and a decline in specific conductance, to flooding in a small underground mine in Ohio. The flooding principle is based on exclusion of oxygen to halt or at least inhibit pyrite oxidation and acid production. In northern Appalachia, mines located mostly or entirely below the local base level drainage usually flood after mine closure. Flooding rate and extent are a function of recharge, potential discharge locations and interaction with other hydrologically connected mines and aquifers. The author describes in this chapter the conceptual development of chemical conditions in closed, flooded underground mines, and applies those concepts to existing mine-pools in West Virginia and Pennsylvania, USA.The final section presents observations and measurements of quantitative ground-water parameters that are useful for managing mine-pools.

Four mostly to fully flooded mine-pools are analyzed in this chapter. Additional background is provided in the conference papers contained in Appendices B, C and D, and by Donovan et al. (1999) for the Hahn and Arden-Westland mine-pools. Some basic information is shown in table 4-1. Three of the mine-pools are located in the Pittsburgh coal bed, which extends over parts of four states in northern Appalachia (Ruppert et al., 1999). It has been mined extensively. The Barnes&Tucker mine-pool is in central Pennsylvania in the Lower Kittanning and Lower Freeport coal beds and has been extensively mined in that locale.

Table 4-1
Summary Information on Four Flooded Mine-pools

Mine-pool	Location	Coal bed	Flooding State	Area
Barnes&Tucker (Lancashire 15)	Cambria County, PA	Lower Kittanning, Lower Freeport	~80% Flooded, Pumped to Control Discharge	5700 Hectares
Hahn (Montour 4,10)	Washington County, PA	Pittsburgh	~70% Flooded, Pumped to Control Discharge	5900 Hectares
Arden-Westland	Washington County, PA	Pittsburgh	~80% Flooded, Pumped to Control Discharge	5100 Hectares
Fairmont	Marion County, WV	Pittsburgh	~100% Flooded, Pumped to Control Discharge	12100 Hectares

How important is flooding to halt the production of acid drainage? Table 4-2 shows paired mine water samples at flooded and partly flooded conditions, from either the same sample point at different flooding states, or two different sample points in the same mine-pool. The first two entries in table 4-2 are located within the city of Fairmont, WV, and are separated from each other by about 0.8 km. Both are located in the Pittsburgh coal bed and are about 80 years old. The acid discharge drains from a small section of unflooded mine-works, while the circumneutral water sample is from a fully flooded section. The flooded section water is lower in

metals, sulfate and Total Dissolved Solids (TDS), and in fact, meets most water quality use standards except for Fe.

Table 4-2
Comparison of Mine Water Composition at Flooded and Partly Flooded Conditions [1]

Mine-pool	Location	Flooding State	Sample Date	pH	Fe	Al	SO$_4$	Total Dissolved Solids
Fairmont	Marion Co., WV	Flooded	4/6/2004	6.68	4.31	0.33	153	442
Fairmont	Marion Co., WV	Partly Flooded	4/6/2004	2.58	15.6	21.3	668	992
Barnes&Tucker	Cambria Co., PA	Flooded	10/6/2005	6.98	38.1	0.06	276	614
Barnes&Tucker	Cambria Co., PA	Partly Flooded	10/6/2005	2.63	73.8	43.9	1037	1496
Hahn	Washington Co., PA	Flooded	2/94-10/95	6.60	87	0.2	1445	2999
Hahn	Washington Co., PA	Partly Flooded	7/84-7/85	4.40	931	20.6	7000	11370
Uniontown	Fayette Co., PA	Flooded	8/05-3/08	6.13	50.0	0.04	691	1286
Uniontown	Fayette Co., PA	Partly Flooded	1974-1975	3.20	113	11	1950	-

(1) pH in S.U., all others in mg/L. Fairmont and Barnes&Tucker data are individual samples collected by the author. Hahn data are medians of n=14 and n=50 analyses, respectively, and were reported by Donovan et al., 1999. n=14 for Uniontown samples 8/05-3/08 collected by the author. 1974-1975 data from Ackenheil Associates (1977).

Similar conditions exist in the Barnes&Tucker samples.The circumneutral water is from the main pumped discharge, fully flooded section of the mine-pool, which has been inundated since about 1970. The acidic water drains from the same stratigraphy and mine complex, but is in a small unflooded section that has been abandoned for at least 50 years.

The Hahn water samples are from the main pumped discharge, but at two different stages of flooding in the mine-pool. The acidic water from 1984-1985 is from the initial filling of the mine-works, and contains very high concentrations of all reported parameters. Ten years later, the mostly flooded mine-pool produced circumneutral water, and metals and TDS had declined significantly. The final data pair in table 4-2 is from a high volume discharge (15,000 L/min), draining fully flooded mine-works in the Pittsburgh coal bed near Uniontown, PA. The mine-works are in a syncline that flooded and began to discharge about 1960, after mining and dewatering ceased. The drainage was still acidic 14 years after closure, but now discharges circumneutral water with reduced concentrations of Fe and sulfate. Anecdotal information obtained from Pennsylvania DEP personnel (Beam, 2005) suggests the pool turned net alkaline about 1980.

The principal difference within each paired data set in table 4-2 is flooding state. Each entry in the unflooded category has acidic drainage and elevated chemical concentrations compared to the flooded sample. These example data illustrate that flooding can profoundly affect mine-pool composition, and suggests flooding stops or at least slows pyrite oxidation.

4.1 Data Acquisition and Sampling

Water quality analyses for the flooded mines were obtained by a combination of methods. These included:

- samples collected by the author for the Fairmont, Barnes&Tucker and Uniontown mine-pools,

- review of published data,

- searching files in various offices of the federal government, and state government in West Virginia and Pennsylvania, and,

- unpublished company monitoring records where accessible

The author collected samples for the Fairmont, Uniontown, and Barnes&Tucker mine-pools following guidelines suggested by Cherceri et al. (1998), US EPA and the USGS. This included appropriate filtering, preservation and containers, and field measured pH, Eh, specific conductance, and dissolved oxygen. Field alkalinity was also run for selected samples. The chemical data used for the Hahn and Arden-Westland mine-pools were originally reported by Donovan et al. (1999), and the mining and flooding history of both is given therein. Some data for the Fairmont and Barnes&Tucker mine-pools were obtained by file searches in government and company monitoring records. Mining and flooding history of the Barnes&Tucker mine-pool is given in Appendix D and by Hawkins et al. (2005). Features of the Fairmont mine-pool are described in Appendix C.

Data discussed in this chapter were obtained from multiple sources, sampled by different individuals, analyzed in different labs, and collected for various purposes and parameters. This introduced some uncertainty and limitations into the analyses. Where feasible, data were examined for quality control using charge balance, conductance/TDS relationships and similar techniques. Data limitations are discussed where appropriate in subsequent sections of this chapter. The Barnes&Tucker, Hahn, and Arden-Westland data sets provide reasonably continuous time series information. The Fairmont mine-pool data are more dispersed. Data from other mine-pools are included in specific analyses, and background information is included as needed.

4.1.1 Sampling Flooded Mines - Spatial Variability

A basic prerequisite for characterizing chemical quality in large mine-pools is the collection of "representative samples". Figures 4-1 and 4-2 are vertical profiles of specific conductance in two mine-pool wells. Chemical samples from the top and bottom of the water columns of these two wells are shown in table 4-3. The vertical conductance profile was done by lowering a Solinst

Conductance/Temperature probe to predetermined depths beginning at the top of the water column, and collecting readings once the instrument had equilibrated with water in that zone. Water quality samples were collected using a Kemmerer sampler that was open at both ends, and lowering it to the predetermined depth. At the appropriate depth, a "messenger" weight sent down the line closed the sampler, and the water was retrieved. The figures and tables illustrate the extent of stratification that can occur in a mine-pool well or flooded shaft, and the significance of sampling techniques.

Figure 4-1 is from the Shannopin mine-pool in Greene County, PA. This mine, covering about 4000 hectares in the Pittsburgh coal bed, closed abruptly in the early 1990's and was abandoned. The conductance profile and chemical samples were collected from a partly inundated shaft while flooding was in process, and the "beach" line between flooded and unflooded sections was nearby. The mine-pool developed over about a ten year period, and is now controlled by pumping. The vertical conductance profile was conducted when mine-pool head increased to about ten meters above coal elevation at this shaft during flooding. No pumping was underway when this profile was collected. Specific conductance was nearly constant from the top of the water column at 47 meters to near top of the coal. At mine level, specific conductance abruptly increased by almost an order of magnitude.
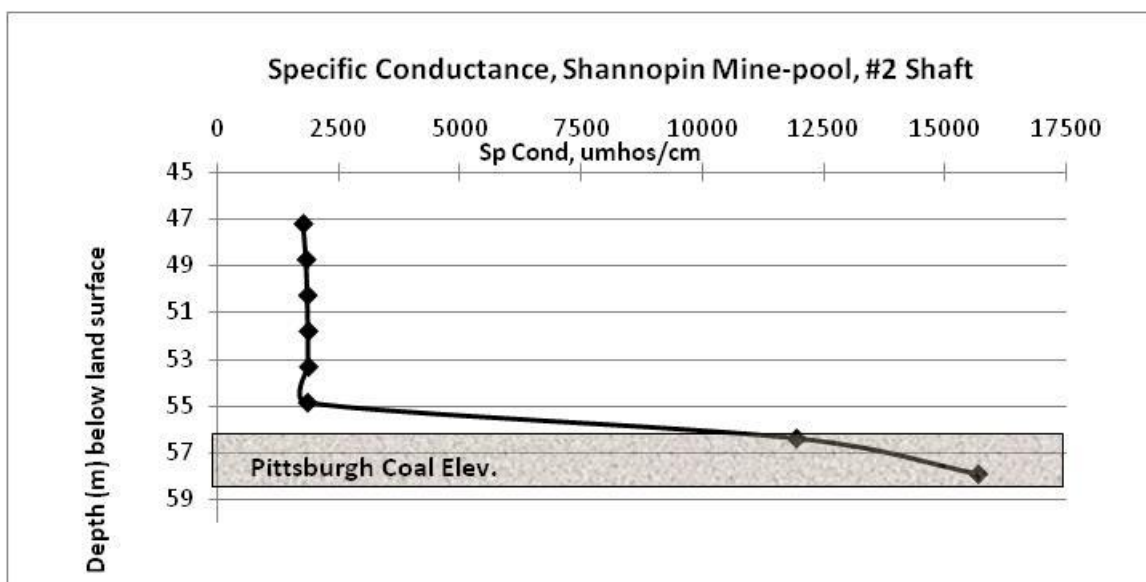
Figure 4-1. Profile of Specific Conductance in a Mine-pool Water Column, Shannopin Mine, Greene Co, PA. Conductance profile measured and chemical samples collected 10/25/2000.

Extreme differences in water chemistry between top and bottom of the water column are evident in table 4-3. Iron concentration, for example, is 160 times greater at the bottom, sulfate is enriched by a factor of about 20, and total acidity exceeds 3000 mg/L. Low pH water at the bottom of the shaft likely represents acid drainage flowing from the unflooded sections just up-dip of the shaft and mixing with the main mine-pool. Higher pH water at the top of the shaft probably represents ground water from the overburden that has undergone only limited mixing with water from the mine-works. The abrupt vertical transition in water chemistry suggests that flow in the mine-pool is laminar with no turbulent mixing.

Figure 4-2 is a conductance profile from the Fairmont mine-pool. Conductance measurements and water quality samples were collected as described previously. The "Siphon" well is in the main ground-water withdrawal structure for the mine-pool (see Appendix C) and represents water at the end of the mine-pool flow-path. The Fairmont mine-pool is essentially 100 percent flooded, and the water chemistry reflects the inundated condition with a measured Eh of 8 millivolts in the bottom of the well. About 5,000 L/min is removed via a pipeline and discharges into an adjacent mine-pool. The turbulent flow has caused some mixing in the well from coal elevation to about 15 m below ground surface. The top few meters of the water column remain chemically distinct, however, as shown in table 4-3. Iron is enriched by a factor of about 36 at the bottom of the water column, sulfate concentration is about five times greater, and alkalinity differs by a factor of about three. The lower pH at the top of the water column compared to water at mine level may reflect differences between a mixture of mine-pool and ground water and mine-pool water only. Turbulent mixing may also introduce oxygen into the top of the water column and promote Fe oxidation, followed by hydrolysis with H^+ production and consumption of alkalinity.
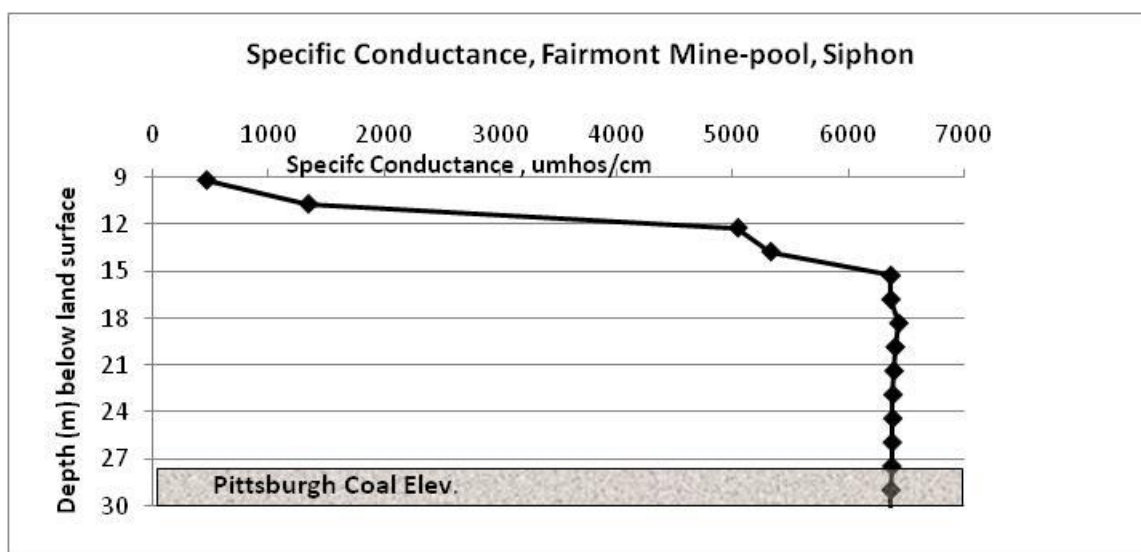
Figure 4-2. Profile of Specific Conductance in a Mine-pool Water Column with Turbulent Flow, Fairmont Mine-pool. Conductance profile measured 2/28/2001 and chemical samples collected 5/2/2001.

The data in figures 4-1 and 4-2 and table 4-3 show that sampling can misrepresent mine-pool conditions, if stratification is not considered. Nuttall and Younger (2004) also found stratification in flooded coal mines in the UK. They describe a case where initial sampling from top of the water column gave data that greatly under-estimated treatment needs. As test pumping was carried out over 50 days, mine-pool water became more mineralized, and Fe concentration increased by a factor of nearly 100. They concluded that stratification is likely in wells and shafts that are recharging gradually, and attempts to pump only the "best" water stratified at the top of the column is likely to fail, because pumping induces turbulent flow and greater mixing. They also noted that metals such as Fe and Zn showed the most extreme stratification, up to two orders of magnitude. Their observations are similar to the Fe data in the Shannopin mine-pool with an enrichment factor of 160. Finally, they noted that water quality changes were likely to be most profound after exchange of at least one shaft volume. Ladwig et al. (1984) also found pronounced chemical

stratification in flooded anthracite mines of eastern Pennsylvania, USA. In most instances, their data also show abrupt transitions in pH, Eh and chemical composition.

Table 4-3
Chemical Composition of Stratified Mine-pool Waters[1]

Sample	pH	Eh	TDS	Alkalinity (Acidity)	Fe	Al	Ca	Mg	Na	SO_4	Cl
Shannopin Top Column	7.75	287	806	272 (-)	8.9	0.25	24.6	6.2	239	299	39
Shannopin Bottom Column	4.65	350	10460	- (3220)	1429	184	201.3	204.8	812	6104	70
Fairmont Top Column	6.37	150	1179	169 (-)	1.7	0.04	10.7	11.9	317	588	52
Fairmont Bottom Column	6.98	8	5182	523 (-)	60.9	0.03	185.7	91.9	1053	3237	141

(1) pH in S.U., Eh in millivolts, Specific Conductance in μmhos/cm, Acidity and Alkalinity as mg/L $CaCO_3$ Eq. All others in mg/L.

A chemical characterization and sampling program in pumped or non-pumped mine-pools must recognize potential for stratification and turbulent mixing. Samples from the top of the water column likely do not represent main mine-pool composition. Treatment or other water management decisions should be based on samples typical of the mine-pool.

Water quality may show significant lateral variation across a mine-pool. Table 4-4 includes analyses from three wells located in the Fairmont mine-pool (Appendix C). They are in different parts of the flow system; a recharge area (mine 38 well), intermediate flow-path (Mine 63) and end of flow-path for the mine-pool (Siphon). The mine-pool has circumneutral pH at each well, in each part of the flow system. Recharge water at Mine 38 is a mixed Na-Ca-HCO_3-SO_4 type; Mine 63 at an intermediate flow-path position is a Na-SO_4-HCO_3 type water, while the siphon at the end

Table 4-4
Spatial Variation in Water Quality of Fairmont Mine-pool[1]

Site	Flow-Path Location	pH (field)	Alkalinity	TDS	Fe	Mn	Ca	Mg	Na	Cl	SO_4
Mine 38	Recharge	7.32	179.8	548	3.44	0.53	60.7	14.1	105.7	34.1	207
Mine 63	Intermediate	7.31	589.6	3301	33.9	0.64	158.4	33.1	853.4	44.2	1697
Siphon	End	7.20	568.7	5194	134.8	1.63	250.6	89.7	1254	119.9	2812

(1) pH in S.U., Alkalinity in mg/L $CaCO_3$, all others in mg/L. TDS = Total Dissolved Solids. Mine-pool samples collected 12/17/2002 by the author.

of flow-path is a Na-SO$_4$ water. Mine-pool composition becomes progressively mineralized and enriched in Na and sulfate as water moves from recharge to discharge areas. Iron concentration is variable, and is enriched by a factor of about 40 from recharge to the end of the flow-path. Location within the mine-pool flow system is another sampling variable.

4.1.2 Pumping Effects on Mine-pool Composition
The Barnes&Tucker mine-pool (Appendix D) is controlled by one pumped discharge, and the quality is affected by the pumping rate. Most water samples collected from October, 2000 to May, 2004 included field notes indicating pumping rate at the time of sample collection. A total of 41 sampling events from that time period were analyzed using summary statistics and nonparametric comparisons. A Mann-Whitney test compared median water chemistry of data grouped by discharge rate. Median water quality values are shown in table 4-5, and each parameter is significantly different by discharge rate at the p=0.05 level of significance.

Raw water quality declines when the pumping rate is increased. Median acidity is about 1.6 times greater at higher discharge rate, while alkalinity decreases from 230 to 169 mg/L.

Table 4-5
Effect of Pumping Rate on Water Quality from Barnes&Tucker Mine-pool[1]

Discharge Rate [2] (L/min)	pH	Alkalinity	Calculated Acidity	Net Alkalinity	Iron	Sulfate	Manganese	Aluminum
12300	6.7	230	58.4	170.7	32.6	298.6	0.60	0.5
24600	6.5	169.3	93.6	52.8	47.7	401.5	1.00	6.5

(1) pH in standard units, Alkalinity, Calculated Acidity and Net Alkalinity in mg/L CaCO$_3$ Eq., all others in mg/L. Values are medians.
(2) 17 samples collected during 12,300 L/min pump discharge rate. 24 samples collected during 24,600 L/min pump discharge rate.

Concentrations of iron, sulfate and manganese also increase about 50, 37 and 68% respectively at higher pumping rates. Total aluminum concentration also increases with pumping rate. Most of the aluminum is likely in suspended or colloidal form, and not dissolved, because of solubility constraints at neutral pH.

Pumping rate effects on water quality show that if stress on the mine-pool is increased, water is delivered from storage areas with more acid weathering products, and/or areas that have undergone less flushing and leaching. These may be zones with slow or limited ground-water circulation within the mine-pool. Winters and Capo (2004), and Aljoe and Hawkins (1991) have suggested that "short circuiting" and preferential flow-paths probably exist in mine-pools.

4.2 Water Quality in Flooded Mines
The chemical composition of large flooded mines in northern Appalachia is significant for the capacity to degrade other aquifers and surface waters. If water quality issues can be overcome , these new aquifers are potential ground-water resources. Discharge rates from flooded mines in this study are on the order of thousands of L/min. While the focus of this study was on mines

discharging polluted water, some mine-pools produce water with quality that is acceptable for use without treatment. Lessing and Hobba (1981), for example reported on mine waters in West Virginia that are used as public water supplies with minimal or no treatment needed. Thus, whether viewed as a pollution source or potential resource, these mine-pools are important regional ground-water features.

Table 4-6 shows the overall composition of five flooded mine-pools, based on the relative abundance of major cations and anions. Each analysis is from the main pumped or flowing discharge point for the mine-pool, and represents water at the end of the flow-path. Median pH, alkalinity, and dissolved solids are also shown. Time flooded ranges from 7 years to as long as 48 years. The mine-pools share a general set of common traits.

Four of five mine-pools have Na as the dominant cation (meq basis) and sulfate is the most abundant anion in each. The Uniontown mine-pool is Ca-Mg-SO_4 water. Alkalinity concentrations range from moderate to very high. With the exception of the Fairmont mine-pool, pH values range from 6.13 to 6.58, suggesting that they are carbonate buffered systems with relatively high pCO. Equilibrium calculations performed with PHREEQCI on some of these data estimated log pCO_2 values of about -0.8 to -1.5. Cravotta (2008a, 2008b) in a detailed study of about 140 mine discharges in Pennsylvania USA found a mean log pCO_2 of minus one for his sample set. Dissolved solids concentrations are more variable, and are inversely related to mine-pool age.

Table 4-6
Water Composition and General Chemistry of Five Flooded Mine-pools[1]

Mine-pool	Location	Years Flooded	Date	n	pH	Alkalinity	TDS	Water Type
Barnes&Tucker	Cambria Co., PA	34-35	4/04-10/05	9	6.39	131	668	Na-SO_4
Hahn	Washington Co., PA	11	1/95-12/95	10	6.58	344	2926	Na-SO_4
Arden-Westland	Washington Co., PA	10	1/95-10/95	10	6.25	138	1841	Na-Ca-SO_4
Fairmont	Marion Co., WV	7-9	4/02-4/04	9	7.55	564	4932	Na-SO_4
Uniontown	Fayette Co., PA	45-48	8/05 - 3/08	13	6.13	224	1286	Ca-Mg-SO_4

(1) pH in S.U., alkalinity in mg/L $CaCO_3$ Eq., and TDS in mg/L. Water types based on dominant cations and anions using median values. n= number of samples.

4.2.1 Mole Ratios
Figures 4-3a-d are time series plots of Fe:SO_4 mole ratio for the Barnes&Tucker, Hahn, Arden-Westland and Fairmont mine-pools. Sample intervals vary from weekly to monthly for most of

the Hahn, Arden-Westland and Fairmont mine-pool samples. The Barnes&Tucker data are based on mean annual water quality data. Assuming pyrite is the principal source of Fe and sulfate in these mine waters, dissolution should yield a mole ratio of one Fe to two SO_4. The one to two ratio is identified by the bold line in each plot. All four mine-pools are deficient in Fe with respect to sulfate. As much as 60 to 80% of the expected Fe is missing, which suggests significant attenuation by mineral formation, adsorption, or exchange. The ratios are greatest during the early flushing and development of the mine-pool, but approach a steady state as the mine-pool ages. The change in slope observed in three of the four plots may indicate the change from initial flushing to long term weathering that has been described by Younger (2000) for flooded coal mines in the UK. This suggests it is in a long term weathering phase. The Fairmont mine-pool, although more recently flooded, shows no obvious change over a 6 year period (figure 4-3d). Iron to sulfate mole ratios in the flooded mines approach a value of about 0.1 to 0.2, long-term. The partly flooded T&T mine described in chapter three also approaches a ratio of about 0.1 long-term. The partly flooded Omega mine (chapter three) has the largest Fe:SO_4
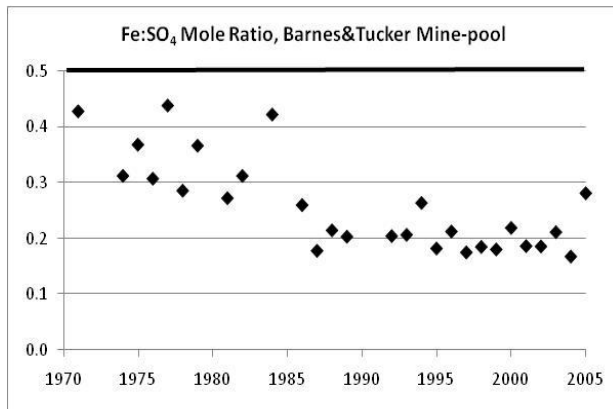
Figure 4-3a. Iron to Sulfate Mole Ratio Barnes&Tucker Mine-pool, Yearly Mean Data.
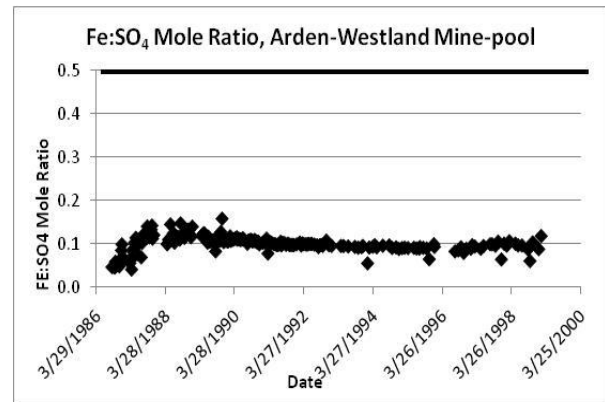
Figure 4-3b. Iron to Sulfate Mole ratio, Arden-Westland Mine-pool.
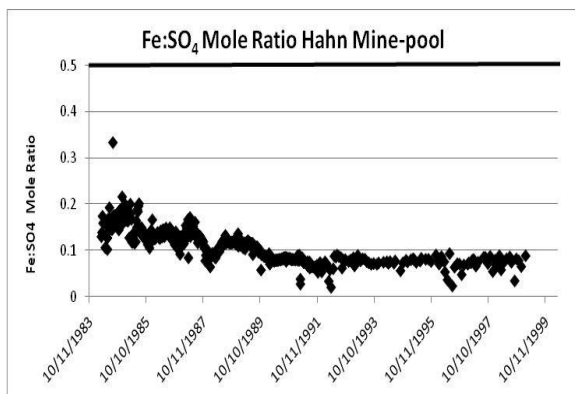
Figure 4-3c. Iron to Sulfate Mole Ratio, Hahn Mine-pool.
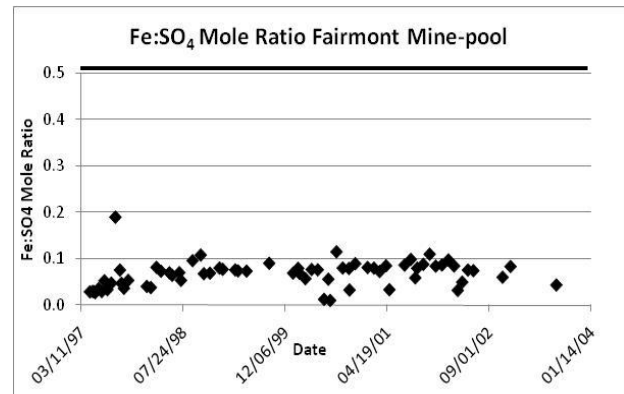
Figure 4-3d. Iron to Sulfate Mole ratio, Fairmont Mine-pool.

ratio, and the least Fe attenuation of any mine examined. Any conceptual or analytical model of Fe circulation in flooded or partly flooded mine-pools needs to account for Fe attenuation in-situ.

Figures 4-4a and 4-4b show time series plots of Ca to carbonate carbon ($H_2CO_3 + HCO_3^- + CO_3^{2-}$) ratio on a milliequivalent basis, and pH, for the Hahn and Arden-Westland mine-pools. The graphs were constructed by speciating samples in PHREEQCI that had pH, alkalinity and major cations and anion reported and assuming a temperature of 15° C. The calculated equilibrium concentrations of carbonate species $CO_{2(aq)}$, HCO_3^-, and CO_3^{2-} were summed and plotted as ratio to Ca concentration. pH is included on the plots to indicate the dominant calcite dissolution process. Following convention, $CO_{2(aq)}$ is represented as H_2CO_3. Calcium data for other mine-pools were not available for long periods and hence are not included here.

The mine-pools in figures 4-4a-b have ratios of about one to ten during initial flushing. If calcite is the only source of soluble Ca and alkalinity in these mine-pools, and carbonate species are conserved in the mine-pool, then the ratios should range from about 0.5 to one depending on pH. At low pH (less than about 5), calcite dissolution is dominated by the reaction:

$$CaCO_3 + 2\,H^+ \leftrightarrow H_2CO_3 + Ca^{2+} \qquad (4\text{-}1)$$

where two milliequivalents of Ca are dissolved and two milliequivalents of H_2CO_3 are produced. Under these conditions, and if there are no other sources or sinks for Ca or carbonate, the Ca to carbonate carbon ratio should approach one.

At circumneutral pH (~7) the dominant dissolution reaction is

$$CaCO_3 + H^+ \leftrightarrow HCO_3^- + Ca^{2+} \qquad (4\text{-}2)$$
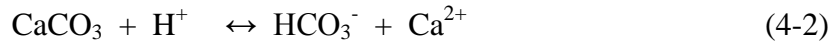
where two milliequivalents of Ca are dissolved and one milliequivalent of HCO_3^- is produced. Under these conditions, and if there are no other sources or sinks for Ca or carbonate, the Ca to carbonate carbon ratio should approach 0.5.

The equilibrium distribution of carbonate species is commonly represented as:

$$CO_{2(g)} + H_2O \leftrightarrow H_2CO_3 \qquad pK= 1.32\ @\ 15°\ C \qquad (4\text{-}3)$$

$$H_2CO_3 \leftrightarrow H^+ + HCO_3^- \qquad pK=6.42\ @\ 15°\ C \qquad (4\text{-}4)$$

$$HCO_3^- \leftrightarrow H^+ + CO_3^{2-} \qquad pK=10.43\ @\ 15°\ C \qquad (4\text{-}5)$$
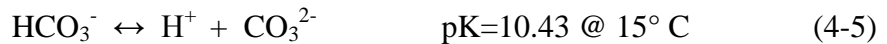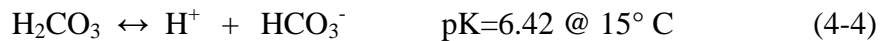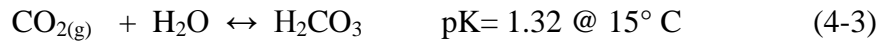
From pH data in figures 4-4a and 4-4b and equations 4-3 to 4-5, the dominant carbonate species under equilibrium conditions in these two mine-pools are H_2CO_3 and HCO_3^-.

The large early Ca to carbonate ratios show that mine-waters initially may have Ca sources other than just calcite, such as gypsum; or that carbonate is lost to other processes, such as gas leakage through fractures. Both mines are below local base level drainage and do not crop out to the surface. They have median pCO_2 values of -1.31 and -1.45 for the Hahn and Arden Westland pools, respectively. The pCO_2 values are more

than 100 times atmospheric conditions and would create a strong gradient for gaseous diffusion. No direct evidence was found for CO_2 gas leakage from either mine.

As the mine-pools age, the Ca to carbonate ratios approaches 0.5 in the Hahn mine-pool and one in the Arden-Westland mine-pool. Based on reported pH of about 6.5 to seven in the aged mine-pools, calcite dissolution with bicarbonate production (equation 4-2) is the dominant reaction. The Ca to carbonate ratio of 0.5 in the mature (after about 1993) Hahn mine-pool corresponds to the expected conditions if calcite controls alkalinity concentration (equation 4-2). The Ca to carbonate ratio of one in the Arden-Westland mine-pool is about twice the expected amount if alkalinity concentration is controlled by
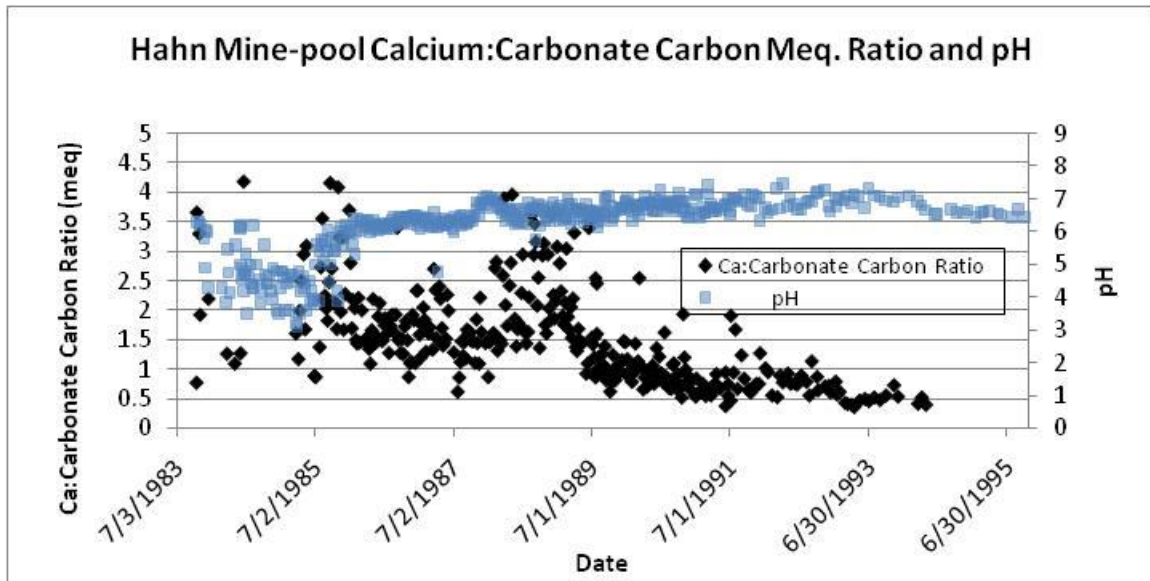
Figure 4-4a. Calcium to Carbonate Carbon Milliequivalent Ratio, Hahn Mine-pool.
Carbonate carbon is sum of H_2CO_3 and HCO_3^-.
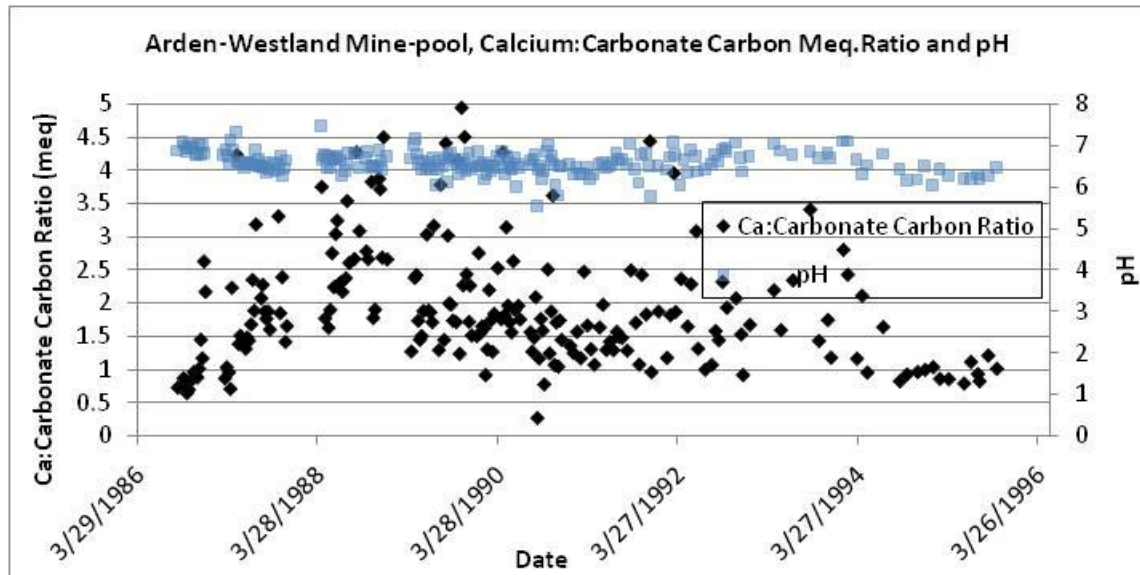
Figure 4-4b. Calcium to Carbonate Carbon Milliequivalent Ratio, Arden-Westland Mine-pool.
Carbonate carbon is sum of H_2CO_3 and HCO_3^-.

94

calcite at circumneutral pH (equation 4-2). Either carbonate is being lost from the mine-pool, or Ca is still being generated from source minerals or processes other than calcite at the end of the monitoring record. Magnesium which can dissolve from dolomite or magnesian calcite, was not included in the calculations.

A large fraction of alkalinity concentration in mine-pools with calcareous rocks may be explained by Ca concentrations and calcite dissolution in the aging mine-pools. Mugunthan et al. (2004) developed a geochemical model of water quality in the Uniontown mine-pool. Their model included significant dissolution of calcite in fractured and caved overburden as the most satisfactory explanation of the observed Ca and alkalinity concentrations. Conceptual models of mine-pool composition should account for sources and sinks of Ca, other elements, and alkalinity.

Each flooded circumneutral mine-pool contains dissolved sulfate as a residual of pyrite weathering. The initial weathering of pyrite produces two moles H^+ as reduced S is oxidized to S(VI) as shown:

$$FeS_2 + 7/2\ O_2 + H_2O\ \rightarrow Fe^{2+} +\ 2\ SO_4^{2-} +\ 2\ H^+ \tag{4-6}$$
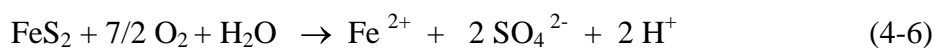
A water like the Fairmont pool siphon in table 4-3 containing 3237 mg/L sulfate, represents over 67 mmoles of H^+ produced and consumed in-situ, or the equivalent of 3350 mg/L total acidity, based on equation 4-6. Conceptual models of flooded circumneutral mine-pools must account for large amounts of in-situ consumption of H^+.

4.2.2 Cation Exchange, Sodium for Calcium and Magnesium

The Barnes&Tucker mine-pool, also called the Lancashire 15 mine-pool (Appendix D) is enriched in sodium and depleted in calcium and magnesium in the end of the flow-path. Table 4-7 shows typical composition of the end of flow-path (main discharge) water and source waters that recharge the mine-pool. The source waters include ground water from unmined strata, leakage from the overlying Lower Freeport mine-pool, and drainage from adjacent unflooded and flooded Lower Kittanning mine-works. The end of flow-path water has greater Na concentration than any of the source waters. Calcium and Mg concentrations are less than all the source waters except ground-water from unmined aquifers. These data are consistent with exchange of adsorbed Na with solution Ca and Mg. The presence of small amounts of exchangeable sodium along a lengthy flow-path would be sufficient to produce a Na-SO$_4$ solution. Cation exchange of adsorbed sodium for dissolved calcium and magnesium is a feasible explanation for the observed behavior, and has been postulated in ground-water flow systems. Back (1966) in a study of water quality evolution in Atlantic Coastal Plain aquifers, observed increasing dominance of sodium over calcium and magnesium the further ground-water moved along its flow-path. Stoner et al. (1987) suggested cation exchange occurred in ground-water in Greene County, PA. Ground-water moving from recharge areas on ridge tops and hill slopes became enriched in Na as it moved to discharge areas in valley bottoms and foot slopes. Appelo et al. (1998), reported studies of pyrite oxidation and calcite weathering in a sandy aquifer, where they noted cation exchange of Ca and Na, and H^+ as well. Capo et al. (2001) and Coulson et al. (1999) identified cation exchange as a probable mechanism explaining evolution and chemical composition of mine waters in flooded underground works in the Pittsburgh coal bed.

Table 4-7
Composition of Source and End of Flow-path Waters Showing[1]
Sodium Enrichment and Calcium and Magnesium Depletion, Barnes&Tucker Mine-pool

Source Water	pH	Alkalinity	Fe	Al	Ca	Mg	Na	SO$_4$
Flooded L.K[2]	6.4	63	62	0.1	96	30	70	417
Unflooded L.K.	2.8	0	113	44	85	34	35	767
Lower Freeport	6.3	124	0.3	0.2	75	19	11	157
Ground-water[3]	7.0	142	0.3	0.1	43	6	2	27
Main Discharge	6.55	137	40	0.2	**40**	**15**	**159**	390

(1) pH in S.U., alkalinity and acidity in mg/L CaCO$_3$ Eq.; all others in mg/L.

(2) L.K. = Lower Kittanning coal bed.

(3) Recharge ground-water from unmined area strata. Data from McElroy, 1998.

4.2.3 Sulfate Complexes

The speciation of elements in flooded mine-pools and the solid phase aquifer matrix partly controls the quantity of those elements in solution. The sulfate ion can form aqueous complexes with various cations, and these complexes can comprise a significant percentage of the total cation element in solution. Mine-pools in this study contain substantial concentrations of sulfate, Fe and other major and minor elements. Five flooded mine-pool waters encompassing a range of Fe, sulfate and Ca concentrations were speciated in PHREEQCI and the amounts of soluble complexes were tabulated. Composition of the waters is shown in table 4-8 and the distribution of sulfate, Fe and Ca is shown in figures 4-5 to 4-7. The five mine-pools are as previously described in this chapter and samples are from the principal discharge point. No pe (Eh) measurements were available for the Hahn mine-pool. As described in section 5.2.3, pe for the Hahn samples was assigned a value of zero. This represents an estimated upper bound of redox conditions that allows soluble Fe in the concentrations observed, if Fe solubility is controlled by Fe(OH)$_3$ minerals. The early sample for the Hahn mine-pool was taken as initial flooding was near completion, and the late sample after the mine-pool reached circumneutral pH.

Figure 4-5 shows distribution of the most abundant S(VI) species, expressed as a percentage of total S(VI) present. Uncomplexed sulfate ion is the most abundant species present in each mine water, comprising from 68 to 90% of the total. Lesser but significant percentages of sulfate are complexed with Ca, Fe, Mg and Na. Figure 4-6 shows the distribution of the three most abundant Ca species. Uncomplexed calcium comprises 55 to 83 % of the total Ca. However, CaSO$_4^0$ is 15 to 44% of total Ca. The abundance of this complex permits greater amounts of solid phase minerals containing Ca or sulfate, such as gypsum, to dissolve. Figure 4-7 shows distribution of the most abundant Fe(II) species. Uncomplexed Fe^{2+} comprises 50 to 72% of total Fe(II). Like calcium, a significant

fraction of Fe(II) complexes with sulfate. Ten to 38% of total Fe(II) is in the complex $FeSO_4^0$, which enhances dissolution of minerals containing Fe^{2+} or sulfate. The abundance of cation-sulfate complexes enhances dissolution of minerals containing the corresponding elements, and allows larger concentrations to remain dissolved in these mine-pools.

Table 4-8
Chemical Composition of Five Mine-pools Speciated in PHREEQCI

Mine-pool (Sample Date)	pe	pH	Alkalinity	Fe	Al	Ca	Mg	Na	SO$_4$	Cl
Uniontown (8/05)	3.75	6.19	220	50.4	0.02	175	65.3	87.8	700	25
Barnes& Tucker (8/05)	2.94	6.55	137	40	0.2	40	15	159	390	7
Fairmont (7/04)	0.26	7.10	561	70.4	0.05	208	81	1060	2850	123
Hahn Early (7/84)	0	4.7	<1	1008	24.3	367	210	2220	6650	693
Hahn Late (6/95)	0	6.52	386	88	0.21	150	50	770	1350	310

(1) pH in S.U., alkalinity in mg/L CaCO$_3$ Eq.; all others in mg/L.
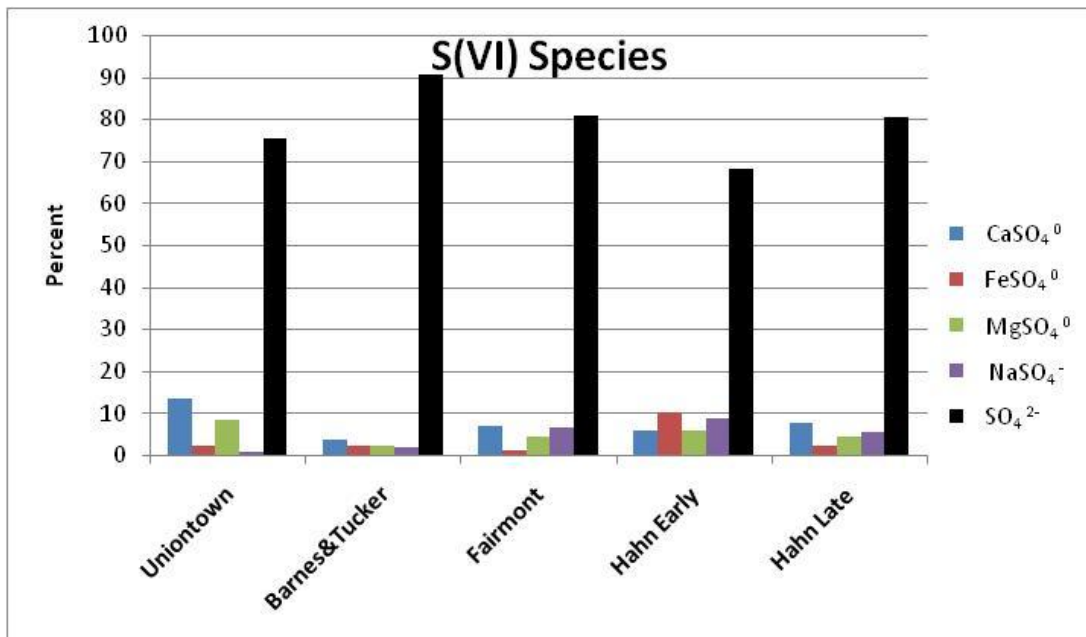
Figure 4-5. Distribution of Most Abundant S(VI) Species in Five Flooded Mine-pools.
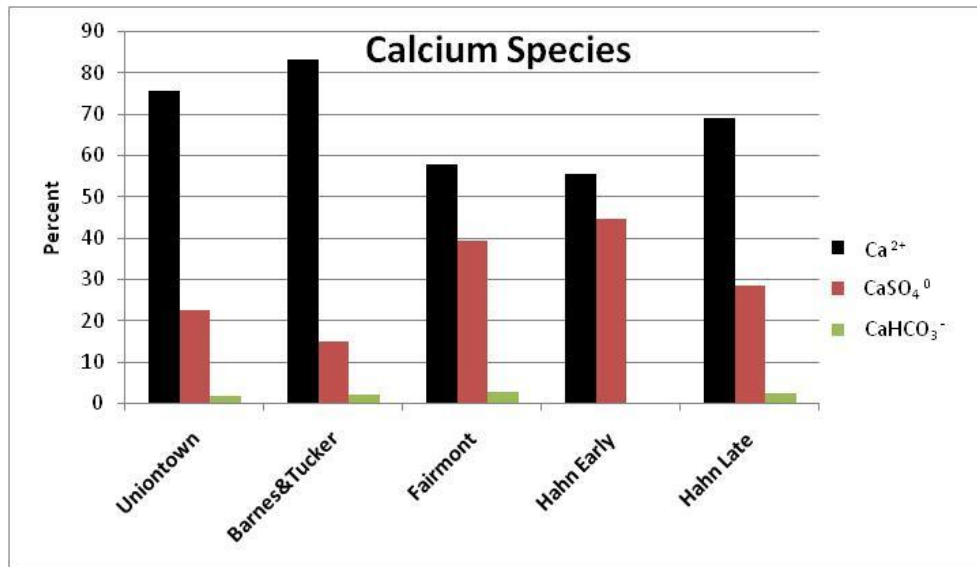
Figure 4-6. Distribution of Most Abundant Calcium Species in Five Flooded Mine-pools.
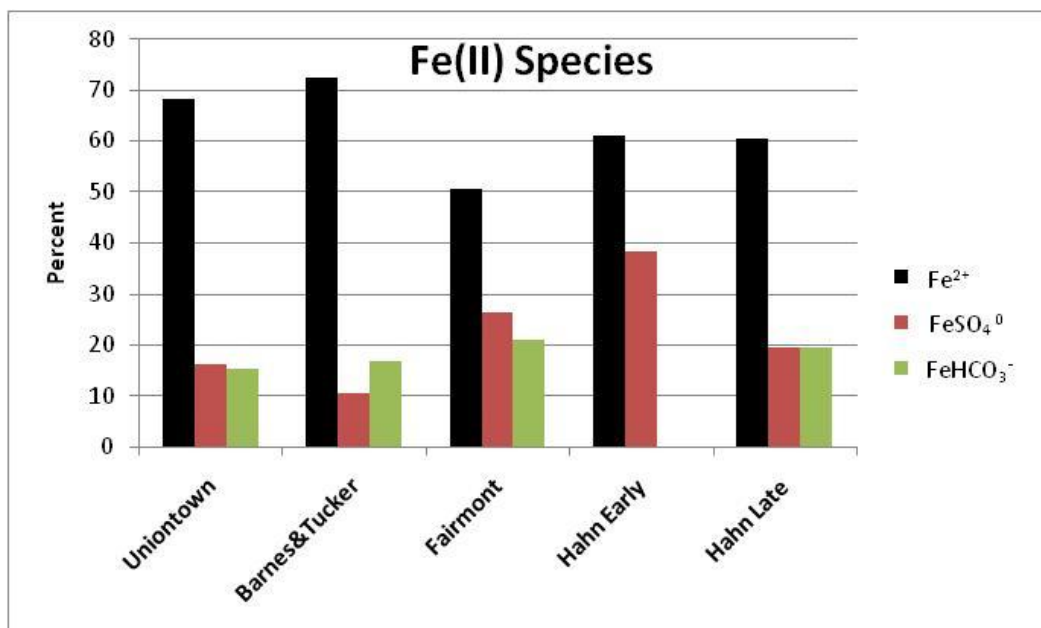
Figure 4-7. Distribution of Most Abundant Fe(II) Species in Five Flooded Mine-pools.

4.2.4 Mineral Solubility Controls

Minerals including oxyhydroxides, sulfates, hydroxysulfates, and carbonates can control the composition of mine waters (Nordstrom, 1982a; Rose and Cravotta, 1998). Mineral saturation indices were calculated in PHREEQCI. Selected mineral saturation indices for the five mine-pool waters (table 4-8) are summarized in table 4-9, where positive indices represent super-saturation; negative values signify under-saturation and zero values symbolize equilibrium between the mineral and the mine water. Mineral solubility controls are inferred from the saturation indices. Collection of sediments for mineral verification was not possible because the mines are closed and flooded. The Fairmont

98

mine-pool is slightly over-saturated for calcite and at apparent equilibrium for dolomite. Carbonate equilibrium seems to control Ca, Mg and alkalinity in this mine-pool.

Table 4-9
Mineral Saturation Indices and log pCO_2 for Five Flooded Mine-pools

Mine-pool (Sample Date)	Calcite $CaCO_3$	Dolomite $CaMg(CO_3)_2$	Siderite $FeCO_3$	$Fe(OH)_3$	$Fe_3(OH)_8$	Goethite $FeOOH$	Gypsum $CaSO_4*2 H_2O$	log pCO_2
Uniontown (8/05)	-1.00	-2.22	0.65	0.67	-0.18	6.18	-0.67	-0.88
Barnes& Tucker (8/05)	-1.60	-3.43	0.65	0.30	-0.65	5.79	-1.70	-1.13
Fairmont (7/04)	0.10	0.00	1.80	-0.74	-1.32	4.74	-0.34	-1.42
Hahn Early (7/84)	-4.66	-9.36	-1.95	-6.53	-16.56	-1.04	-0.03	-1.52
Hahn Late (6/95)	-0.64	-1.56	1.29	-1.99	-4.76	3.49	-0.63	-0.99

Donovan et al. (2003) discussed mineral saturation indices in the Hahn mine-pool. They describe an early phase after flooding was complete where mine-pool waters were near equilibrium for calcite and gypsum and concluded that gypsum was likely controlling Ca and sulfate concentrations. As the mine-pool aged, concentrations declined and the waters became under-saturated for both calcite and gypsum. The gypsum index of -0.03 for the early Hahn sample and -0.63 for the late Hahn sample in table 4-9 is consistent with Donovan et al.'s findings.

The Uniontown and Barnes and Tucker mine-pools have aged past the initial flushing and are under-saturated for calcite, dolomite and gypsum. No data were found for early flushing of these mine-pools (circa 1960-1970) to calculate saturation state for those minerals. Log pCO_2, calculated from pH and alkalinity relationships is as much as 400 times atmospheric levels. The high pCO_2 values suggest the mine-pools do not readily exchange gases with the above–ground atmosphere, and that there are gases likely causing active chemical weathering of rock within the mines. On several sampling events at the Fairmont mine-pool, the author observed that sample waters would begin to visibly exsolve gas if allowed to stand open to the surface atmosphere for more than a few minutes. Sample collection was conducted so as to minimize aeration and gas exchange.

Four of five mine waters are over-saturated for siderite, suggesting this mineral should be forming. However, no visual indications of solid phase siderite were found in any samples or filtered materials. The formation of siderite is usually described as a microbially mediated process involving reduction of Fe oxide minerals and precipitation as a carbonate (Ehrlich, 2002, Roh et al., 2003). Conditions favoring siderite formation include low sulfide and sulfate concentration, low Eh, high Fe to Ca ratio, and abundant carbonate. In mine-pools, the Fe source is likely to be sulfide mineral oxidation, not Fe

oxide reduction, and the mine-pools contain high sulfate concentrations. Both conditions differ from the formation model described.

Siderite composition is influenced by depositional environment. Siderite formed in freshwater environments is relatively pure, while marine based siderite has extensive substitution of Mg and Ca for Fe (Mozley, 1989). The apparent super-saturation for siderite, deviation from the depositional model and equilibrium or near equilibrium conditions for dolomite and calcite suggest that siderite does not control Fe or carbonate in these mine-pools.

Table 4-9 includes saturation indices for three Fe oxide minerals of varying solubility including poorly crystalline $Fe(OH)_3$, $Fe_3(OH)_8$ and goethite, $FeOOH$. Water draining from mines often contains a mix of Fe-oxyhydroxide minerals (Karathanasis and Thompson, 1995; McCarty et al., 1998; Bowell and Bruce, 1995; Kaires et al. 2005). The solubility of Fe oxyhydroxide minerals spans over 6 orders of magnitude (Langmuir, 1997). Thus it becomes difficult to determine which Fe mineral, if any, is controlling soluble iron. Four of the five mine waters are orders of magnitude over-saturated for goethite, and so it is unlikely that it controls soluble Fe. Langmuir (1997), notes that minerals that are greatly over-saturated are unlikely controls for the component elements, due to slow kinetics or other barriers. Every water is under-saturated for $Fe_3(OH)_8$, and this mineral is unlikely to control soluble Fe. The two oldest mine-pools, Uniontown and Barnes and Tucker, are over-saturated for the poorly crystalline $Fe(OH)_3$, but the other three waters are under-saturated. Examining saturation indices for the three different Fe hydroxide minerals does not give clear indication of which mineral(s) might be controlling Fe activity in the flooded mine-pools.

Langmuir and Whittemore (1971) provided an extensive review of stability of Fe oxyhydroxides including particle size and concentration effects. They observed that the greater the degree of over-saturation for crystalline phases, the faster precipitates formed, and these materials were more soluble. The conditions described are similar to circumneutral mine-pools in table 4-9, where high soluble Fe concentration leads to significant over-saturation for goethite. Langmuir and Whittemore also suggest that dissolution reactions for various Fe oxyhydroxides including goethite, hematite, $Fe(OH)_3$ and others could be rewritten in a common form based on Fe^{3+} and OH^- activities, and thermodynamic (equilibrium) stability expressed as:

$$Fe^{3+} \quad + \quad 3\,OH^- \quad \leftrightarrow \quad Fe(OH)_3 \tag{4-6a}$$
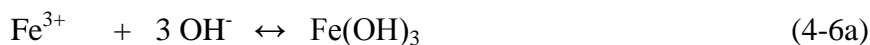
$$-pQ = -\log [(Fe^{3+})\,(OH^-)^3] \tag{4-6b}$$

Langmuir and Whittemore (1971) report that the activity product -pQ for different Fe oxyhydroxide minerals ranges from about 37.3 to 43.3 for amorphous $Fe(OH)_3$ to hematite. The -pQ relationship makes it possible to compute an apparent stability for water containing a mixture of Fe oxyhydroxide minerals, that is, which Fe oxyhydroxide mineral could precipitate from the mine water. Three of the five mine waters had field measured Eh (pe) and pH data. The distribution of Fe(II) and Fe(III) species was calculated in PHREEQCI assuming redox equilibrium among Fe species. The log activities of uncomplexed Fe^{3+} and OH^- were substituted into equation 4-6b and the

expression was solved for -pQ. The pe for the Hahn mine waters was estimated based on solubility of poorly crystalline $Fe(OH)_3$ and reported Fe concentrations. Several runs of PHREEQCI were conducted varying the system pe until the waters were able to contain the reported Fe concentrations without super-saturation. A pe of 0 was assigned to the Hahn mine waters for further calculations, and Fe^{2+} and Fe^{3+} activities are therefore estimates. The $Fe(OH)_3$ activity products for the three mine waters have measured -pQ ranging from 37.5 to 39.0, implying that more soluble forms of Fe oxyhydroxides are controlling soluble Fe activity (table 4-10). It is consistent with the observations of Langmuir and Whittemore (1971) that waters highly over-saturated for goethite tended to produce more soluble

Table 4-10
$Fe(OH)_3$ Activity Product

Mine-pool (Sample Date)	-pQ	log Fe^{3+} Activity	log OH- Activity
Uniontown (8/05)	37.5	-13.00	-8.16
Barnes& Tucker (8/05)	38.0	-13.96	-7.99
Fairmont (7/04)	39.0	-17.15	-7.28
Hahn Early (7/84)	44.8	-15.73	-9.68
Hahn Late (6/95)	40.2	-16.66	-7.86

precipitates. Ferris et al. (1989), found ferrihydrite (ferric hhydroxide) was the principal Fe oxhydroxide precipitating from coal refuse drainage. Less soluble goethite and hematite were minor components. The two waters from the Hahn mine-pool have activity products suggesting less soluble iron minerals control soluble Fe, but the calculations depend on the estimate of pe, which determines Fe^{3+} activity. These estimates are considered less reliable than the -pQ values generated from measured pe.

Figures 4-8a and 4-8b are Eh/pH diagrams for Fe and Fe bearing minerals for four of the flooded mine-pools included in table 4-9. Log iron, log sulfate, and log bicarbonate activities are fixed at -3.47, -2.52 and -2.45, respectively in both diagrams. These values represent conditions in the Uniontown mine-pool water and are similar to chemical activities in the three other samples. In figure 4-8a, $Fe(OH)_3$ is assumed to control Fe activity. The Fe minerals siderite and goethite are not included on the plot since it is considered less likely that they control soluble Fe. Consistent with the saturation indices in table 4-9, the Uniontown and Barnes&Tucker waters plot within the stability field for $Fe(OH)_3$, while the Fairmont mine-pool water is slightly under-saturated. The Hahn mine-pool water is based on estimated pe, so its location on the Eh-axis of the plot is less certain. The plots were generated in Geochemist Workbench, version 6.

The boundaries in figure 4-8a are drawn based on chemical activities for the Uniontown mine-pool water. Plot boundaries for the other three waters differ slightly from that shown in Figure 4-8a, based on the chemical activities for each water. However, the four waters are similar so that the errors introduced by plotting all samples on one graph are small. For example, the calculated log ferrous iron activities for the four waters ranged from -3.37 to -3.62, and log bicarbonate activities ranged from -2.23 to-2.50.
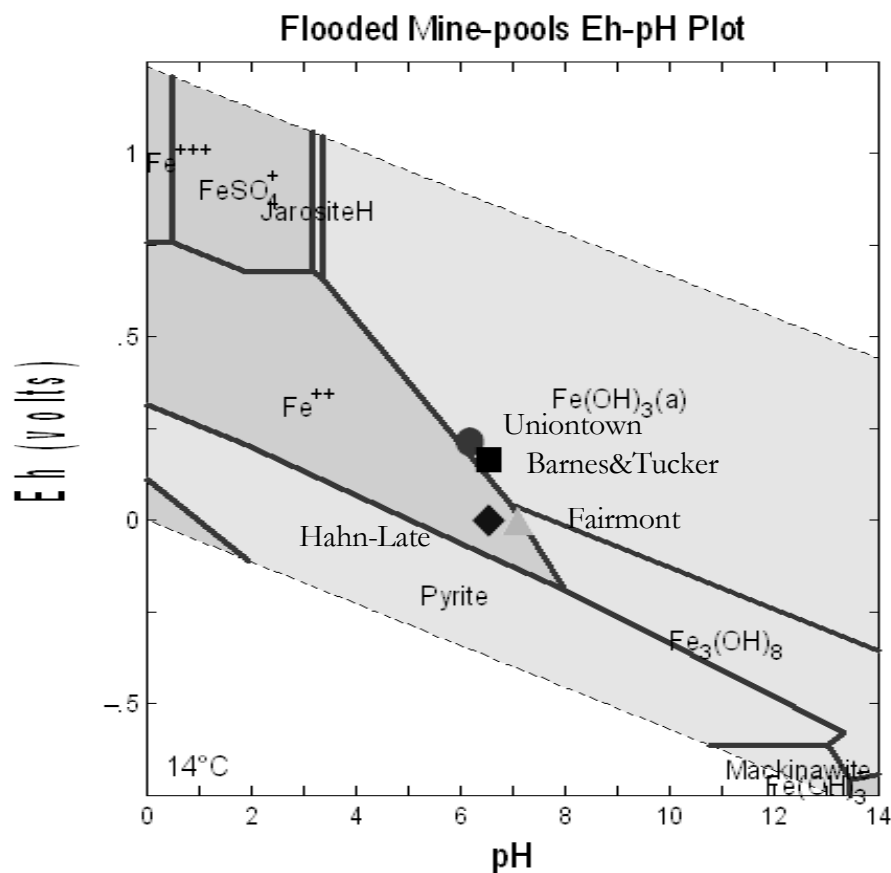
Figure 4-8a. Eh/pH diagram for Iron in Four Flooded Mine-pools. Fe(OH)₃(am) specified as controlling mineral. Diagram based on log Fe²⁺molar activity = -3.47 (total Fe(II)=8.95x10⁻⁴ mole/L), log sulfate molar activity = -2.522 (total sulfate = 7.29x10⁻³mole/L), log HCO₃⁻ molar activity =-2.45(total HCO₃⁻= 4.11x10⁻³ mole/L). See table 4-9 for mineral saturation indices.

The plotting of mine waters at or near apparent equilibrium for Fe(OH)₃ has also been noted by Gang and Langmuir (1974) in streams and ground-waters in the bituminous coal region of Pennsylvania, USA. An examination of Fe, pH, Eh and other chemical data reported from Ladwig et al. (1984) suggests that the anthracite mine-pools they studied were also near apparent equilibrium for poorly crystalline Fe(OH)₃.

Figure 4-8b does include the stability field for the iron carbonate siderite. The Fairmont and Hahn mine-pools plot within the siderite field and the Uniontown and Barnes&Tucker mine-pools are near the boundary between siderite and Fe(OH)₃, indicating siderite formation is thermodynamically possible in these mine-pools. However, no visual evidence of siderite precipitation was found in any sediment filtered from these mine waters, and little indication of siderite formation from mine water was found in the surveyed literature.

Figure 4-8b. Eh/pH diagram for Iron in Four Flooded Mine-pools. Fe(OH)₃(am) specified as controlling mineral. Diagram based on log Fe²⁺activity = -3.47 (total Fe(II)=8.95x10⁻⁴ mole/L), log sulfate activity = -2.522 (total sulfate = 7.29x10⁻³mole/L), log HCO₃⁻ activity =-2.45(total HCO₃⁻= 4.11x10⁻³ mole/L). See table 4-9 for mineral saturation indices.

The distribution of total dissolved Fe(II) and Fe(III) used to construct figures 4-8a and 4-8b was calculated from Eh (pe) measurements and the half reaction:

$$Fe^{2+} \leftrightarrow Fe^{3+} + e^- \quad \log K = -13.02 \ @ \ 25° \ C \quad (4-7)$$

The Fe(III) activities calculated for the four mine-pools from equation 4-7 are 10^{-7} mole/L or less, and are too small to provide reliable measured Eh based on the Fe^{2+}/Fe^{3+} couple (Nordstrom, 2000). Back and Barnes (1965) examined the relationship between Eh and iron content in US Coastal Plain ground-waters. They compared measured Eh to values calculated from couples $Fe^{3+}/Fe(OH)_3$ and Fe^{3+}/Fe_2O_3. They concluded that measured Eh was associated more closely with $Fe^{3+}/Fe(OH)_3$, but that Fe solubility was best described as intermediate between the two minerals. They also noted that at pH greater than about 5.0, Fe(III) concentration was so small as to be undetectable, and all measured Fe should be regarded as ferrous.

A limited set of Fe(II) samples was collected on several occasions from the Fairmont, Uniontown, and Barnes&Tucker mine-pools. The purpose was to compare measured Eh

with Eh calculated from Fe(II)/Fe(III) distribution in the samples. The author collected samples for Fe(II) analysis using opaque bottles and HCl preservative. Each sample was analyzed by complexing with phenanthroline and spectrophotometer measurement. Samples reported back as essentially all Fe(II). Most samples had to be diluted for analysis, and this limited resolution. Therefore, dissolved Fe(II) was equivalent to total dissolved Fe, and Fe(III) could not be reliably estimated from the analyses. For flooded mine-pools with very low concentrations of Fe(III), Fe(II)/Fe(III) distribution may have to be estimated from measured Eh, rather than Fe speciation techniques. Redox dependent solubility relationships for Fe minerals are then based on measured Eh and assumption of equilibrium. The difficulties in reliably measuring small amounts of Fe(III) in flooded mines-pools are similar to the observations of Barnes and Back (1965) and Nordstrom (2000).

Ground-water redox measurements can be difficult to interpret. Lindberg and Runnells (1984) compared measured Eh and Eh values calculated from various redox couples for over 600 waters of diverse compositions. They found large discrepancies between measured and calculated Eh. They concluded that many waters were at internal disequilibrium, because the reaction kinetics of some redox couples were too slow and different redox couples may have different Eh in the same water. However, the Fe^{2+}/Fe^{3+} couple provided the best agreement between and measured and calculated values. Nordstrom et al. (1979), compared measured and calculated Eh in acid oxidized mine waters. The calculated values were derived from the Fe^{2+}/Fe^{3+} couple over a range of about +600 to +800 millivolts, and measured and calculated values were usually within about 30 millivolts. A later paper by Nordstrom (2000) was more cautious about the use of Eh. At more reduced conditions, approaching those measured in flooded mine-pools, measured Eh was greater than calculated. The deviation was attributed in part to the decreasing Fe^{3+} activity, and the difficulty of the electrode detecting small amounts of uncomplexed ferric iron. Nonetheless, used carefully, redox measurements based on Fe^{2+}/Fe^{3+} were deemed to have value in characterizing iron rich mine water. Christensen et al. (2000) in a review of redox characterization techniques concluded that the Fe^{2+}/Fe^{3+} couple was reversible, and sufficiently rapid to be useful in ground-water studies.

4.2.5 Sulfate Reduction in Flooded Mine-pools

Water samples collected from the Barnes&Tucker, Fairmont and Uniontown mine-pools sometimes had the odor of H_2S gas. Field tests for dissolved sulfide using a methylene blue procedure were conducted at each of these mine-pools at least two different times and trace levels corresponding to the detection limit of 0.01 mg/L or greater were detected each time. A biological activity reaction test (BART) for sulfate reducing bacteria (SRB) was also conducted for each mine-pool. An aqueous sample was collected using sterile techniques and inoculated in a sealed container with media specific for SRB. A strong positive reaction was obtained in each test, indicating the presence of SRB in the three mine-pools. These observations all suggested that sulfate reduction might be taking place in flooded mine-pools.

A classic paper by Baas-Becking et al. (1960) contains a series of plots showing the range of Eh and pH conditions measured for different reduction/oxidation processes, including microbial sulfate reduction. The compiled sulfate reduction data showed most reported

measurements between pH 6 to 8.5 and Eh normally between +100 to -300 millivolts. These conditions generally match the flooded mine-pools discussed in this chapter.

Pyrite formation is usually described as a microbially mediated sequence of sulfate reduction, then Fe monosulfide (FeS) formation, followed by gradual conversion to FeS_2 (Schoonen and Barnes, 1991; Morse et al., 1987). Precipitated FeS, mackinawite and gregite are metastable with respect to pyrite (Berner, 1967). Berner (1970), describing the formation of pyrite in marine sediments, noted that metabolizeable organic matter is an important factor controlling pyrite formation. Flooded mine-pools contain large amounts of organic matter in the form of residual coal and other carbonaceous rock, but no data were found that addressed sulfate reduction in these conditions, especially whether these organic compounds are suitable for SRB. Other investigators have noted that sulfate reduction rates are temperature and concentration dependent (Herlihy and Mills, 1985).

Langmuir (1997) presents a redox "ladder" showing the theoretical sequence of reduction in ground-waters. Fe(III) reduction occurs before sulfate reduction, and that sequence has also been described in several large scale aquifer studies (Champ et al., 1979). A paper by Postma and Jakobsen (1996), however argues that Fe(III) and sulfate reduction can occur simultaneously depending on the stability of iron oxide minerals in the aquifer.

After reviewing field conditions and literature, the apparent equilibrium Eh needed to form FeS was calculated for the five mine-pool samples identified in tables 4-7 and 4-8. The reactions are:

$$FeS + H^+ \leftrightarrow Fe^{+2} + HS^- \quad \log Keq = -4.648 \tag{4-8}$$

$$H_2S \leftrightarrow HS^- + H^+ \quad \log Keq = -6.994 \tag{4-9}$$

$$SO_4^{-2} + 10H^+ + 8e^- \leftrightarrow H_2S + 4H_2O \quad \log Keq = 40.644 \tag{4-10}$$
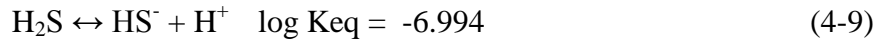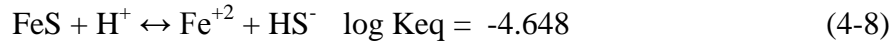
with log k values from the Wateq database in PHREEQCI. Subtracting equation 4-9 and 4-10 from 4-8 gives:

$$FeS + 4H_2O \leftrightarrow Fe^{+2} + SO_4^{-2} + 8H^+ + 8e^- \quad \log Keq = -37.565 \tag{4-11}$$

and

$$\log Fe^{+2} + \log SO_4^{-2} + 8 \log H^+ + 8 \log e^- = -37.565 \tag{4-12}$$
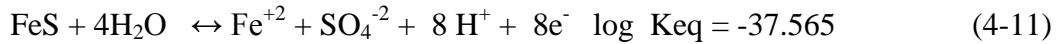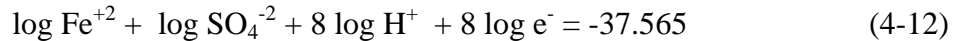
Chemical activities for sulfate, Fe^{2+}, pH, and computed equilibrium redox conditions are shown in table 4-11. Measured redox values are also shown for the Uniontown, Barnes&Tucker and Fairmont mine-pools.

Table 4-11
Equilibrium Redox Conditions for Sulfate Reduction to FeS

Mine-pool (Sample Date)	log SO_4^{-2} Activity	log Fe^{2+} Activity	log H^+ Activity	FeS Formation Equilibrium Eh (millivolts)	Equilibrium Eh (millivolts) 0.01 mg/L Sulfide	Measured Eh (millivolts)
Uniontown (8/05)	-2.52	-3.477	-6.13	-129	-110	+214
Barnes& Tucker (8/05)	-2.81	-3.615	-6.39	-147	-125	+222
Fairmont (7/04)	-2.02	-3.607	-7.10	-184	-169	-15
Hahn Early (7/84)	-1.84	-2.45	-4.70	-32	-	-
Hahn Late (6/95)	-2.29	-3.37	-6.52	-150	-	-

The equilibrium redox values for FeS formation are about 169 to 370 millivolts less than measured Eh for three mine-pools. As noted previously, trace levels of dissolved sulfide (0.01 mg/L or more) were detected in three mine-pools. The three mine-pools were speciated in PHREEQCI with the solutions including 0.01 mg/L dissolved sulfide (H_2S and HS^-) assuming equilibrium. The estimated redox conditions for the S(VI)/S(-II) couple (reaction 4-10) are within 15 to 22 millivolts of thermodynamic equilibrium for FeS formation (reaction 4-11). If S(-II) activity is greater than that represented by 0.01 mg/L concentration, then computed redox approaches FeS stability more closely. Though direct evidence is lacking, the field measurements and calculations suggest that sulfate reduction and FeS precipitation are possible in these flooded mine-pools.

The difference between measured Eh and computed Eh for the S(VI)/S(-II) couple are consistent with reported findings of Lindberg and Runnells (1984) that a water may have more than one apparent Eh where different redox couples are present.

4.2.6 Flux Rate of Iron and Sulfate
Long term Fe and sulfate flux rates were estimated for three mine-pools with one principal discharge point, reported pumping rates and chemical concentration data. It was hypothesized that flux would be similar among the flooded mines and less than that for the partly flooded mines, as pyrite weathering rates were expected to be less under flooded conditions. The fluxes (mole basis) were normalized to a m^2 of mine-works for comparison among each other, and to the two partly flooded mine-pools in chapter three. The mine areas were determined from the plan view extent of mining to provide a consistent basis for comparison. The actual exposed rock surface area is larger and includes roof, floor and pillar surfaces, and surfaces of fractured and disaggregated rocks. A consistent defensible technique for estimating rock surface area from mine map

information was not developed, due to the uncertainty of estimating the extent of caving or "gob" and particle sizes. Since the flux rates in table 4-12 are based on less than actual surface area, the values are probably overestimated, but do provide a consistent basis for comparison. The Barnes&Tucker mine-pool flux was estimated from reported yearly average discharge rate and chemical concentration. The Hahn and Arden-Westland mine-pools had reported long term pumping rates (Donovan et al., 1999; Pennsylvania DEP unpublished records). The Omega and T&T mine-pool discharge rates were determined from monitoring data obtained from West Virginia DEP. Results are shown in table 4-12.

Table 4-12
Average Long Term Iron and Sulfate Flux from
Three Flooded and Two Partly Flooded Mine-pools

Mine-pool	Flooding State	Area (hectares)	Average Q (L/Min)	Fe Flux (mole/m^{2}s)	Sulfate Flux (mole/m^{2}s)
Barnes&Tucker	Flooded	5700	19,000	9.49×10^{-9}	3.48×10^{-8}
Hahn	Flooded	5900	13,250	7.04×10^{-8}	2.69×10^{-7}
Arden-Westland	Flooded	5100	6600	6.2×10^{-9}	3.48×10^{-8}
Omega	Partially Flooded	69	268	3.42×10^{-8}	1.37×10^{-7}
T&T	Partially Flooded	588	1139	7.33×10^{-9}	4.72×10^{-8}

The flux values range over about an order of magnitude for both Fe and sulfate. There is no clear distinction in flux rate between flooded and partly flooded mines. Normalized flux rates therefore appear to be a function of flushing and transport. Chemical reaction rate does not seem to be a limiting factor. Pyrite weathering rates are on the order of 10^{-10} mole/m^{2}s (Williamson and Rimstidt, 1994), where area refers to pyrite mineral surface. To sustain the average flux rates in table 4-12, available pyrite surface area would be on the order of about ten to 100 m^2 per one m^2 of mine-pool. These values may appear large, but are well within the range of surface areas reported for common minerals (Langmuir, 1997). Weathering rates are sometimes reported on the basis of whole rock mass, rather than specific minerals. Sheetz et al. (2009) for example, measured surface areas of 12 to 17 m^2/g rock, for three shales from Upper Pennsylvanian rocks used in column weathering tests.

Although the flux rates in table 4-12 are not distinguishable on the basis of flooding state, they do provide a range of values to estimate expected loading rates from mine-works of known size.

4.3 A Conceptual Model of Water Quality in Flooded Mines
The preceding sections of this chapter identified some fundamental characteristics of flooded mine-pools, which can be used to develop a conceptual model of geochemical processes at work. A robust model should incorporate feasible reactions, appropriate mineral constraints and representative hydrogeologic conditions. A flooded mine-pool model should incorporate the following processes:

- Shift from initial acid oxidizing to circumneutral reduced conditions
- Consumption of acidity in-situ and production of alkalinity.
- Cation exchange
- Attenuation of iron in-situ
- Sulfate reduction (possible)

Several studies of ground-water and surface water interaction with acid drainage were examined for common factors. Zhu and Burden (2001) stress the importance of aquifer mineralogy in constructing a ground-water reactive transport model for acid tailings. In their study, the distance of acid plume migration was sensitive to the amount of calcite in the aquifer, and Al was at apparent equilibrium with jurbanite. Broshears et al. (1996) modeled the mobility of acid drainage constituents entering a stream. They concluded that Fe and Al mobility were probably controlled by oxyhydroxides, and carbonate dissolution buffered pH. Berger et al. (2000) modeled acid drainage discharge from a waste rock pile. The principal mechanisms controlling metals were mixing with non-polluted streams, limestone dissolution from underlying bedrock, and adsorption onto oxide surfaces. Filipek et al. (1987) also identified mixing and oxyhydroxide precipitation as controls on mine water draining from an abandoned metal mine in California. They also found some waters were at apparent saturation for jurbanite and jarosite. Finally Appelo et al. (1998) identified calcite dissolution and cation exchange as significant processes in an aquifer containing pyrite. Metal control by oxyhydroxides, carbonate dissolution, mixing, and ion exchange are common processes in these studies.

A conceptual model was formulated based on the observed mine-pool properties and hypothesized processes described in the preceding paragraphs. It is illustrated in flow chart fashion in figure 4-9. A model based on Pittsburgh coal bed mine-pools was tested in PHREEQCI and is fully described in Appendix B. It also includes pH dependent sulfate sorption and oxyhydroxides as possible sinks for Fe and Al.

A simple model of the mostly flooded Barnes&Tucker mine-pool is described in Appendix D. It also includes oxyhydroxide controls on Fe and cation exchange. It includes a small amount of continuing pyrite oxidation in unflooded sections of the mine-pool, and mixing of various source waters. Complete results are shown in Appendix D.

Initial flooding solution
Acid-Oxidized Environment

+

Recharge Water

Acid Neutralization

Sulfate Salts Dissolution

Carbonate Dissolution

Alkalinity

Ion Exchange

Sulfate Reduction ?

Iron Oxide Reduction?

Sulfide Precipitation?

Carbonate precipitation ?

End of Flowpath
Alkaline-Reduced Environment
Prevent Sulfide Oxidation
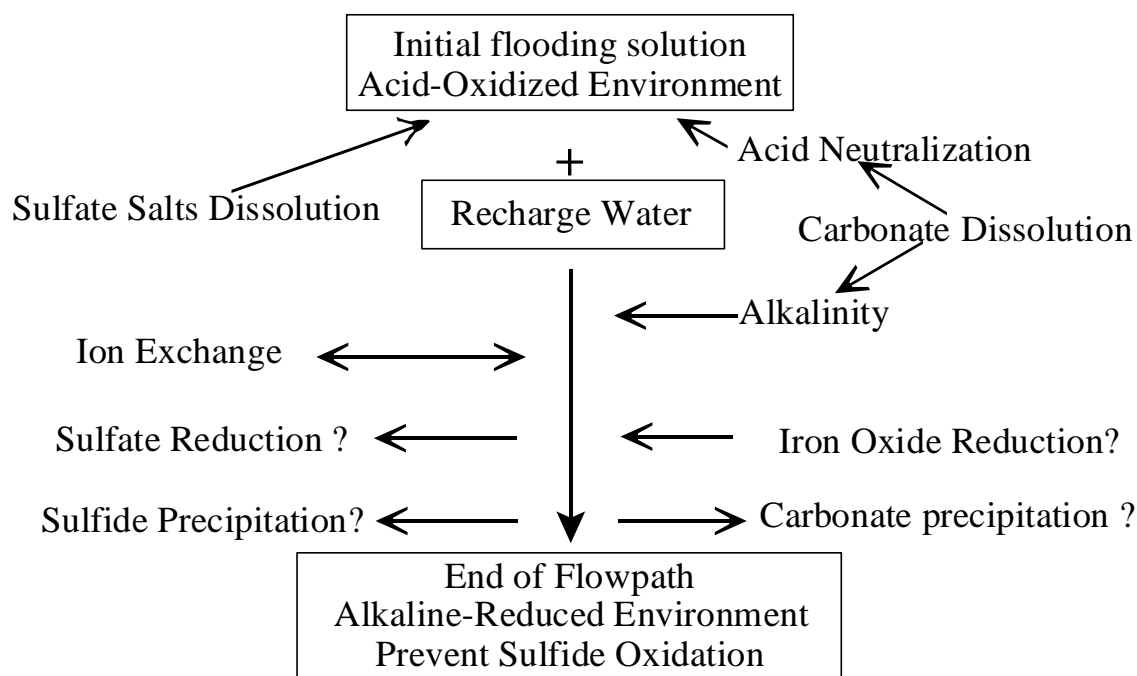
Figure 4-9. Conceptual Model of Geochemical Processes in Flooded Mine-pools.

4.4 Fluid Storage and Transmissivity in Flooded Mine-pools

Water storage and transmissivity properties of flooded mine-pools affect the volume and rate of recharge and discharge, and hence chemical flux. Strategies for managing or remediating mine-pools are therefore partly dependent on the quantitative hydrogeologic properties of the mine-pool. A small set of storage and transmissivity data were generated from monitoring wells in the Fairmont and Uniontown mine-pools, based on principles of aquifer response to atmospheric loading, and one aquifer (pump) test. Furbish (1991), Ritzi et al. (1991) and Rojstaczer (1988) outline many of the principles where storage and transmission properties of confined aquifers can be estimated from changes in water level (head) data and atmospheric pressure. Seo (2001) and Mehnert et al. (1999) liken barometric efficiency to small scale slug tests that are useful for estimating specific storage (S_s), transmissivity (T) and hydraulic conductivity (K). The effect of atmospheric pressure on head was recognized as early as 1940 by Jacob (cited by Furbish, 1991). Much of the subject literature is concerned with correcting pump test and other head data for the confounding effects of atmospheric pressure variation.

Vented pressure transducers were installed in four monitoring wells in the Fairmont mine-pool and one well in the Uniontown mine-pool. The transducers were programmed to record water level and temperature on an hourly basis. These data were paired with hourly barometric pressure readings obtained from National Oceanic and Atmospheric Administration (NOAA) records for nearby weather stations. For the Fairmont mine-pool, pressure data were obtained for the Morgantown, WV airport about 24 km away. Pressure data for the Uniontown mine-pool were obtained for the station at the Uniontown, PA airport about 8 km away. Characteristics of the different wells are

summarized in table 4-13. The author also reviewed mine maps, drill logs and well installation details for the Fairmont and Uniontown wells, and several borings had been inspected with a down-hole camera prior to casing installation.

Table 4-13
Wells Used in Storage and Transmissivity Estimates

Mine-pool (Mine)	Well Depth (meters)	Comments
Fairmont (Beth 41, North)	107	In partially collapsed void, fully flooded.
Fairmont (Joanne)	134	In coal pillar, fully flooded
Fairmont (Federal 1)	88	In open void, fully flooded
Fairmont (Beth 41, West)	107	In coal pillar, fully flooded
Uniontown	15	In coal pillar, fully flooded

Figure 4-10 displays a time series plot of hourly head and barometric pressure for a well in the Fairmont mine-pool, Beth 41, North mine. The two parameters are inversely related; head declines as atmospheric pressure increases, and head increases when pressure declines. This behavior is characteristic of confined aquifers whose elastic storage is derived from compressibility of the aquifer matrix and water.
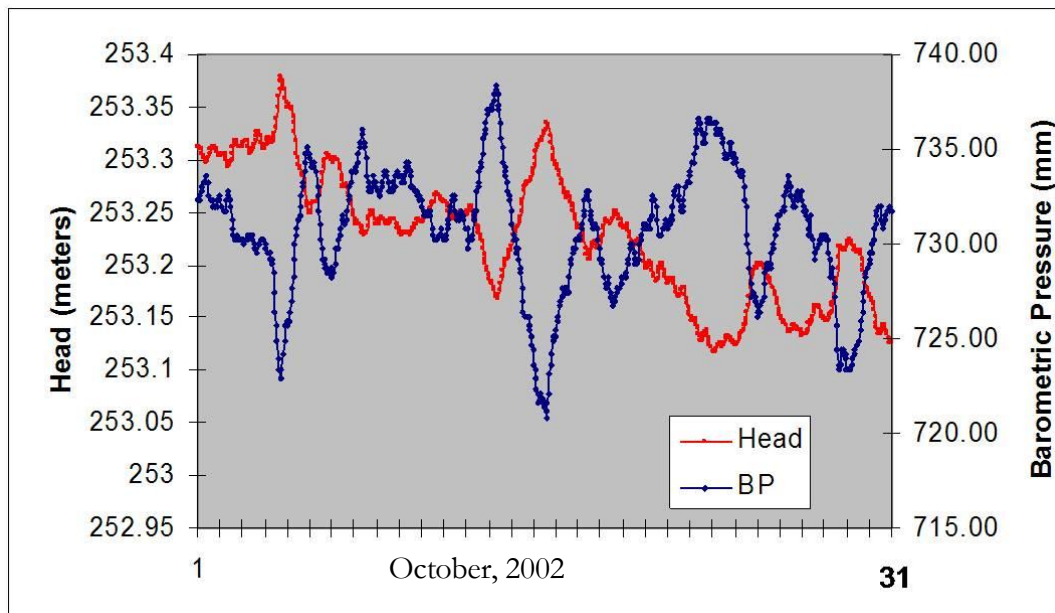
Figure 4-10. Time Series Plot of Aquifer Head and Barometric Pressure, Fairmont Mine-pool, Beth 41 Mine.

Close inspection of the head data also reveals a declining trend, independent of barometric effects. The head decline is seasonal, and this underlying influence was

removed from the data set by linear regression methods. A least squares regression gave an estimate of the slope of the head loss/day. Davis and Rasmussen (1993), and Rasmussen and Crawford (1997) found regression to be satisfactory for removing underlying trend effects. Davis and Rasmussen (1993) also found that regression gave similar results to a method originally described by Clark (1967). Clark's technique uses a set of simple rules to identify which members in a time series respond like a barometer. A head change of zero, for example, between successive measurements is excluded from barometric efficiency calculations. Head response to atmospheric loading can be either instantaneous or delayed (Rasmussen and Crawford, 1997; Hare and Morse, 1997; Seo, 2001). In a well, the response should be instantaneous, and examination of time series data showed no apparent lag between pressure and head change, and calculations were then based on that premise.

Multiple estimates of barometric efficiency were generated for each well. The paired head and pressure readings were examined in time series plots. Periods showing a significant barometric pressure change were identified, preferably encompassing at least a 24 hour period. Figure 4-10 shows 4 distinct pressure declines in October, 2002, and these subsets were extracted for analysis. Three periods of distinct barometric pressure increase are also present and these subsets could be extracted for analysis. For each well, barometric efficiency was determined for both increasing and decreasing barometric pressure trends. Daily precipitation data were also examined for potential influence of significant recharge events. Most data sets for barometric efficiency were obtained during periods lacking large precipitation events, typically September through November.

Barometric efficiency (BE) was estimated as follows:

$$BE = (y_w * dh)/dP_a \qquad (4\text{-}13)$$

where y_w is the unit weight of water; dh is the head change; and dP_a is the change in atmospheric pressure. "Tidal efficiency" (TE) was estimated as follows:

$$TE = 1 - BE \qquad (4\text{-}14)$$

Specific Storage (S_s) was estimated as follows:

$$TE = (p_w * g * B_p)/ S_s \qquad (4\text{-}15)$$

after rearranging this equation, where p_w is fluid density, g is the gravitational acceleration constant; and B_p is compressibility of the aquifer matrix, either measured or estimated; and TE is "tidal efficiency".

Finally, porosity, n is estimated from:

$$BE = (p_w g n B_w)/ S_s \qquad (4\text{-}16)$$

after rearranging this equation where S_s, p_w and g are as previously defined, and B_w is fluid compressibility.

Equation 4-12 includes a term, B_p, for compressibility of the aquifer matrix. Domenico and Schwartz (1990) compiled values for vertical compressibility of sediments and rocks.

They report a range of 6.9 to 3.3 x 10^{-10} m^2/N for "fissured rock", while Freeze and Cherry (1979) report a wider range of 10^{-8} to 10^{-10} m^2/N, and 10^{-11} for "sound rock". Initial calculations included a sensitivity analysis for B_p, varying over the range of 10^{-8} to 10^{-11}. Estimated porosity, n, was greater than 100% when B_p was specified as 10^{-9} m^2/N, indicating the aquifer compressibility estimate was too large. When B_p was assigned a value of 10^{-10} m^2/N, this produced reasonable estimates of porosity, while a B_p value of 10^{-11} m^2/ N, produced small values (< 3%) for porosity (n). Based on examination of borehole videos and drilling logs for several Fairmont mine-pool wells which indicated partially open mine voids, low n values were deemed unreasonable. A compressibility index (B_p) value of 10^{-10} m^2/N was used for all subsequent estimates.

Table 4-14 shows average values of barometric efficiency (BE), "tidal efficiency" (TE), specific storage (S_s), and porosity (n) estimated from head and atmospheric pressure data. Specific storage, S_s was estimated to be on the order of 1.5 to 4.5 x 10^{-6}/m, and porosity estimates ranged from about 17 to 44% at three different wells. For individual wells, estimated porosity values from multiple analyses were generally within 25% relative difference. Three wells were completed in partially caved zones and crushed coal pillars, based on drilling and borehole camera observations. The fourth well was completed in an open void in the Federal 1 mine and reports a correspondingly high porosity of 82%.

Since coal recovery typically ranged from at least 50 to upwards of 80%, porosity data for three wells suggests the mine-pool aquifer thickness exceeds the coalbed thickness, by perhaps two to five times. For example, a porosity of 25% in an area with 50% coal removal suggests the void space may now be distributed over a thickness of two times the original mining height. The storage coefficient, S, for the aquifer, is estimated from:

$$S = S_s b \qquad\qquad (4\text{-}17)$$

where Ss is specific storage and b is saturated aquifer thickness in consistent units.

The estimated storage coefficient, S, ranges from about 3.4 x 10^{-6} to 1.5 x 10^{-5} as aquifer thickness b ranges from 2 (~4 meters) to 5 (~ten meters) times coal height. The high porosity estimate and intact open void in the Federal 1 well implies that aquifer thickness in this location is similar to coal height and the roof rock acts as a confining layer. The apparent low storage coefficient for the Fairmont mine-pool results in relatively large drawdown when it is pumped.

The fraction of storage attributable to water compression and expansion is indicated by barometric efficiency, and the water derived from matrix compression and expansion is attributed to "tidal efficiency" in table 4-14.

The principal disadvantage of barometric calculations is the sensitivity of the calculations to small changes in head and atmospheric pressure data. The small head changes also imply that only aquifer material near the well is being tested.

The values in table 4-14 are similar to results reported by Sahu (2004) for a mostly flooded underground mine in Ohio. Using barometric efficiency calculations, Sahu estimated specific storativity in five wells to range from 1.7 x 10^{-6} to 1 x 10^{-5} and porosity from 0.31 to 0.52. Using an amplitude ratio method described by Mehnert et al. (1999),

Sahu also estimated transmissivity as ranging from 1×10^{-5} to 4×10^{-6} m^2/s , and hydraulic conductivity on the order of 10^{-6} m/s. Sahu analyzed recharge/discharge characteristics of the Ohio mine-pool and concluded that it had overall low storage.

Table 4-14
Specific Storage, Porosity and Storativity Estimated from Head and Barometric Pressure[1]

Mine-pool (Mine)	B.E.	T.E	Specific Storage (Ss)	Porosity, (n)
Fairmont (Beth 41, North)	0.65	0.35	2.9×10^{-6}/m	0.44
Fairmont (Joanne)	0.45	0.55	1.8×10^{-6}/m	0.19
Fairmont (Federal 1)	0.78	0.22	4.5×10^{-6}/m	0.82
Fairmont (Beth 41,West)	0.42	0.58	1.7×10^{-6}/m	0.17

(1) B.E.= Barometric Efficiency; T.E. = "Tidal Efficiency".

Pressure transducer readings in one well in the Uniontown mine-pool recorded periodic pumping of the mine-pool. A coal reprocessing company located about three km from the well provided information to the author about their pumping rates and schedule in sufficient detail to permit analysis via time drawdown methods. Transmissivity was estimated using the Theis equation for radial flow to pumping wells in confined aquifers. Data transformation and curve fitting were conducted in Aqtesolv for Windows, version 4.1. A semi-log plot of drawdown versus time is shown in figure 4-11. Some deviation
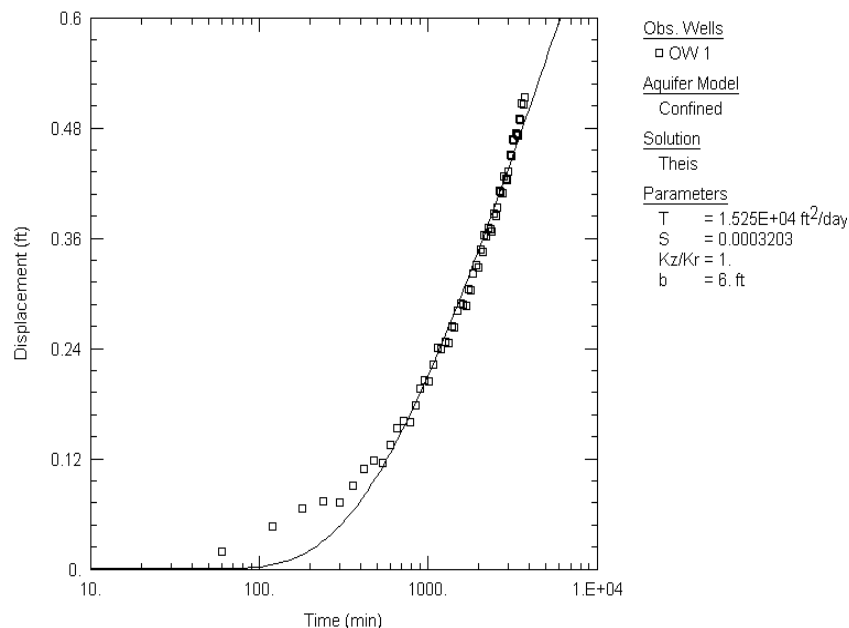
Figure 4-11. Uniontown Mine-pool, semi-log Plot of Aquifer Drawdown vs. Time
and Estimated Transmissivity and Storativity Using Theis Method.

from the type curve is apparent in early pumping data, but with better fit in late data. The estimated transmissivity, assuming a six foot (~ two meter) thick aquifer, was 1.5×10^4

ft^2/day (1.6 x 10^{-2} m^2/s). Storativity was estimated at 3.2 x 10^{-4}, equivalent to specific storage of about 1.6 x $10^{-4}/m$. The storage values are about one to two orders of magnitude larger than in the Fairmont mine-pool but are also subject to uncertainty of identifying aquifer thickness. The data were also analyzed using several other solutions for leaky confined aquifers, but results showed little variation.

Figure 4-12 is a time series plot of head measurements in the Fairmont mine-pool. In April 1997, a siphon system began operating in the mine-pool to prevent mine water from discharging into overlying streams. The graph shows head response to a pumping rate of about 4500 L/min. The Williams mine well is located 18 km from the siphon, but head declined about 4 meters after pumping began. The Fairmont mine-pool is subdivided into individual mines separated by barrier pillars. The internal barrier pillars, and confined aquifer with elastic storage and apparent low storativity, explains the large drawdown
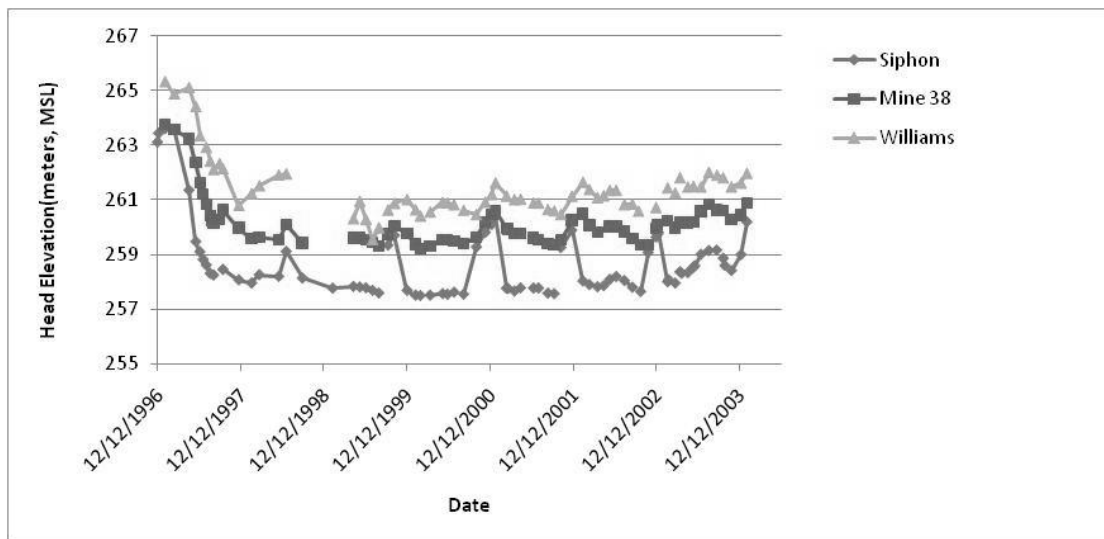
Figure 4-12. Fairmont Mine-pool. Head Response to Pumping in Three Mines. Pumping Started April, 1997 at Siphon. Williams Mine is 18 km from Siphon. Mine 38 is 2.5 km from Siphon.

observed at distance. This behavior has practical significance for controlling head in flooded confined mine-pools. The Barnes&Tucker mine-pool exhibits a similar response to pumping, with head declines of 6 meters at a distance of about 16 km (Hawkins et al., 2005).

4.5 Chapter 4 Summary Findings and Observations
In Chapter four water quality characteristics and geochemical processes in flooded underground mines were examined. The data and observations were drawn from mines in West Virginia and Pennsylvania that have been flooded for as much as 45+ years. These included observations on:

- Flooding effects on chemical composition

- Obtaining "representative" mine-pool samples for chemical analysis

- Chemical characteristics of flooded mine-pools

- Fluid storage and transmissivity in flooded mine-pools.

The principal findings and conclusions for mine-pools of this chapter are summarized as follows:

- Flooding profoundly affects aqueous chemistry of flooded mine-pools. Each mine-pool initially contained or discharged low pH waters, or discharges acid water from small unflooded sections. After flooding, mine water shifted to circumneutral, net alkaline conditions, although Fe, sulfate and TDS remained elevated. The typical pH shift was three to four S.U. The Fairmont and Uniontown mine-pools are nearly 100% flooded, while the remaining mines are 70 to 80% inundated.

- Extreme vertical stratification of chemical conditions can occur in mine-pool wells and shafts. Transitions can be abrupt, and include one to two order of magnitude changes in parameter concentrations. Water samples should be collected at mine level, in the mine-pool, to represent conditions. Samples collected at the beginning of a pumping cycle may not represent long term conditions, as turbulent flow and mixing occur over time.

- Varying stress on the mine-pool, in the form of changing pumping rates, may affect discharge quality. The Barnes&Tucker mine-pool discharge water quality declined as pumping rate increased. The behavior suggests that flushing within the mine-pool is not uniform, with preferred flow-paths and short circuiting. Some sections of the mine-pool may have limited fluid exchange, unless the mine-pool is stressed.

- Mine-pool water quality exhibits spatial variability. Concentrations of Fe, sulfate, Ca and other parameters vary among different wells in the Fairmont and Barnes&Tucker mine-pools and are partly related to location in the mine-pool flow system. Waters in recharge zones, at the beginning of the mine-pool flow-path are the least mineralized. Water becomes more mineralized as it migrates through the mine-pool flow system. In the Fairmont mine-pool, dissolved solids increased by a factor of about ten from recharge to end of flow path waters. Location in the flow system is a water sampling variable.

- Flooded mine-pools were $Na-SO_4$, $Ca-Mg-SO_4$ or mixed cation-SO_4 composition.

- Flooded mine-pools are deficient in Fe with respect to sulfate; indicating most iron originally liberated by pyrite oxidation has been retained in the mine-pool. About 60 to 80% of the Fe is "missing" from the discharge waters. Iron retention, estimated from ion ratios, was lowest during initial flooding and increased with age.

- Flooded mine-pools consume large amounts of acidity in-situ. Two moles of H^+ generated per mole of sulfide to sulfate oxidation, are mostly consumed within the flow system. Net alkaline waters are discharged from each flooded mine-pool.

- Cation exchange of Na for Ca and Mg is a prominent feature in flooded mine-pools. End of flow-path waters in the Fairmont and Barnes&Tucker mine-pools are enriched in Na with respect to their source waters.

- Geochemical modeling simulations described in Appendix B and summarized in chapter four show that carbonate weathering can be a significant source of acid neutralization and alkalinity. Some sulfate adsorption to Fe oxide sediment surfaces is possible at low pH, and some Fe may be retained in mine-pools by ion exchange

- Iron behavior is difficult to model because of the number of possible sources and sinks.

- Flooded mine-pools contain little or no detectable oxygen, a condition that favors inhibition of pyrite oxidation. Small unflooded sections can, however, support continuing oxidation and mobilization of weathering products.

- Sulfate complexes with Ca, Fe and other elements increases solution concentration of those parameters and allows more dissolution of the source minerals. Fifteen to 40 % of total dissolved Ca was complexed with sulfate in five flooded mine-pools, and ten to 40 % of total dissolved Fe(II) was complexed with sulfate.

- Flooded mine-pools may approach saturation for one or more minerals especially during early flooding. Gypsum, calcite, dolomite and Fe oxyhydroxides were near apparent equilibrium in several mine-pools. Iron data are more difficult to interpret due to the wide solubility range for Fe oxyhydroxides. The waters tend become under-saturated for these minerals as the mine-pool ages.

- Computed pCO_2 values are up to several hundred times atmospheric conditions, suggesting that either the mine-pools do not readily exchange gases with the outside atmosphere, and that chemical weathering of carbonates is ongoing. Altenatively, a strong gas diffusion gradient is present that would promote carbon dioxide leakage from the mine.

- Apparent thermodynamic stability of mine-pool waters with respect to Fe oxyhydroxides was assessed from a modified activity product, -pQ. Most -pQ values indicate equilibrium with more soluble, less crystalline forms of Fe

oxyhydroxides. Mine waters in this study are more likely to form amorphous Fe precipitates than goethite or hematite.

- Eh/pH plots based on field measured values show mine-pool waters near equilibrium with respect to poorly crystalline $Fe(OH)_3$ and over-saturated with respect to siderite.

- Fe(III) concentration is difficult to quantify in flooded mine-pools, because it is present in such low amounts. Attempts to measure Fe(II)/Fe(III) with wet chemistry methods are limited by the necessity of diluting samples with high Fe so that the solution is within range of the spectrophotometer. For flooded mine-pools with very low concentrations of Fe(III), Fe(II)/Fe(III) distribution may have to be estimated from measured Eh, rather than Fe speciation techniques.

- In spite of difficulties associated with obtaining and interpreting Eh measurements, subject literature suggests Fe is one element where useful, quantitative readings can be obtained.

- Sulfate reduction may occur in flooded mine-pools. A strong positive response for sulfate reducing bacteria was obtained for several mine-pools and H_2S was also detected in mine waters. Computed Eh for the S(-II)/S(VI) couple approaches conditions of FeS formation in one mine-pool.

- Long term flux rates of Fe and sulfate, normalized to $1\ m^2$ of mine-works, varied about one order of magnitude for each parameter. There was no discernible difference in flux rate between flooded and partly flooded mines. Normalized flux rates are likely over-estimated since total rock surface area in caved and fractured rock exceeds plan view mine area. The actual exposed rock surface area is larger and includes roof, floor and pillar surfaces, and surfaces of fractured and disaggregated rocks. Normalized flux rates do provide a consistent basis for comparison, however.

- Mine-pools can be partly recharged by leakage from adjacent or overlying mine-pools as well as ground water infiltration from unmined strata. Recharge from other mine-pools can affect mine-pool composition.

- Flooded mine-pools that are subdivided by barrier pillars can be visualized as a series of compartments, each with high internal hydraulic conductivity and low gradient. Overall head and flow between compartments is controlled by hydraulic conductivity, thickness and gradient of the barrier pillars.

- Flooded mine-pools behave as confined or leaky confined aquifers. Aquifers are thin, on the order of coal thickness, to several times coal thickness, depending on the magnitude of collapse and fracturing of the overlying rock.

- Flooded mine-pools have low specific storage, on the order of 10^{-6}/m. The low values result in part from the low compressibility of the aquifer matrix.

- Head in confined mine-pools responds to pumping over distances of tens of km. This behavior has practical significance, in that large mine-pools can be controlled by a single pumping facility.

Chapter 5: Temporal Trends and Geochemical Behavior of Mine-pools

Drainage from closed underground coal mines is a significant source of water pollution in northern Appalachia and elsewhere (Kleinmann et al.; 2000; Younger, 1997). Long term chemical composition of mine-pools is of interest to government, industry and environmental organizations who estimate cost and duration of treatment, and select optimal mine closure techniques. The rate and degree of improvement or pollution abatement and the steady-state composition of mature mine-pools is the subject of this section based on the following observations and questions:

- How fast does water quality improve? In general, coal mine-pools have been observed to discharge the poorest water quality in the initial flush, followed by a gradual improvement in composition (Younger, 2000). Is improvement solely a function of time, geochemical conditions, hydrologic processes or a combination of variables?

- To what degree does water quality improve? Is complete abatement and return to background conditions a realistic expectation? Or, will the mine-pool have low but objectionable concentrations of metals, acidity, dissolved solids or other parameters for an indefinite period of time?

Long term data sets from five mine-pools, ranging from about ten to 35 years duration, were examined to address these questions. The general geologic and hydrologic setting and history of these mine-pools is described in chapters three and four, appendices A-D and by Donovan et al. (1999). The five mine-pools include two sites that are mostly unflooded, and discharge acidic water. The remaining three are mostly flooded and discharge circumneutral water. Essential features are included here in the discussion as needed.

Three principal tasks are described in this section:

- Estimate in-situ neutralization of mine-pools by a combination of processes including introduction of alkalinity from recharge water, and dissolution of carbonate and other minerals.

- Statistical fits, including decay function, of solution chemistry versus time to estimate the rate of change in concentration or flux. Regression techniques are used to estimate the time to attain reduction in concentrations of Fe, Al, SO_4 and dissolved solids.

- Estimate the constraints on long term solution chemistry as it approaches a steady state condition using equilibrium and kinetic calculations. The kinetics of pyrite oxidation has been extensively studied as reported by Williamson and Rimstidt (1994), and Rimstidt and Vaughn (2003).

5.1 Other Long Term Mine-pool Studies

Most of the published work on long term chemical behavior of mine-pools comes from either the United Kingdom (U.K.), or the Appalachian region of the U.S.A. Glover (1983) observed that drainage from flooded underground coal mines in Great Britain showed about a 50% reduction in iron concentration for each pool volume discharged, implying an exponential decay. Younger (2000), found that Fe concentrations became asymptotic at values of about one to 40 mg/L in drainage from British coal mines after flushing for a period of a few years to several decades. Younger (1997), also characterized British mine waters as having "juvenile" and "vestigial" acidity. The latter is removed in the first flush of the mine-pool, usually within 40 years. Juvenile acidity resulting from ongoing pyrite oxidation is projected to last for hundreds of years. Wood et al. (1999), concluded that pollution from closed underground coal mines in Scotland was most severe in the first few decades, and that iron (Fe) concentrations would decline to 30 mg/L or less within 40 years.

Younger and Thorn (2006) estimated that initial flooding of a recently closed coal mine in the U.K. would produce acidic water, based on observations of flowpath, and analyses of water encountered during mining. They correctly predicted the acidic nature of the discharge, but the actual Fe concentration was more than three times greater than predicted. They suggest that better understanding of flowpaths in mine-pools could improve water quality prediction.

Demchek et al. (2004) reported that iron concentration had decreased an average of about 80% in 44 free-draining underground mine discharges in West Virginia over a 30 year period. This study includes mines in the same coal beds, Upper Freeport and Pittsburgh, as in this work. Demchek et al. compared water quality from a 1968 survey with drainage in 1999-2000, and found that acidity had decreased an average of 56% in Upper Freeport mines. Overall, iron concentrations declined about 80%, and sulfate declined about 50 to 75%. The average data included substantial variation among individual mines. Thus, while most mines show improvement in water quality, the rate and degree of chemical change seems to be influenced by site specific factors. More recently, Skousen et al. (2006) supplemented the 2004 study with some additional data. They concluded that seasonal variation should be examined further to quantify the effect of flow on underground mine chemistry. Skousen et al.'s study included a large number of mines, but with a limited number of sample events through time. Short term features are therefore difficult to identify and evaluate. All of the mines in Skousen et al.'s study were abandoned at closure, and there is no continuing legal obligation for a company (if it still exists), or for a government entity, to continue systematic water quality monitoring of underground mines abandoned before 1977.

Donovan et al. (2003) describe the flooding history and chemical evolution of a below drainage underground mine in the Pittsburgh coal bed in southwestern Pennsylvania. They describe three phases of water chemistry, including an initial flooding phase of peak concentrations of Fe and other pollutants over a two year period. Second was a transition phase lasting two to four years with decline in iron and other parameter concentrations;

and a third phase, where Fe declined to less than ten percent of initial concentration, and net alkaline conditions developed. This data set, called the Hahn discharge, is one of the five sites analyzed in this section.

Perry and Rauch (2004, Appendix A) found that a first order decay function described the decrease in acidity, Fe, Al, and sulfate and other parameters for the first eight years of record of the Omega mine-pool, located near Morgantown, West Virginia. This small free-draining mine showed strong seasonal influences in pollutant flux and concentration, with flux rates two to three times higher in spring high discharge season, compared to the fall low flow season. Sulfate, Fe and acidity concentrations were projected to decline by half over a six to eight year period. The decline in Al concentration, however, was two to three times slower than for other parameters. The Omega mine-pool is one of the five sites analyzed in this section.

Perry et al. (2005, Appendix D) found that after 14 years and pumping approximately 21 pool volumes, Fe and sulfate concentrations in the Lancashire 15 mine-pool had declined to about 20 % of their initial values. In 1986, leakage from an overlying mine complex further diluted the Lancashire 15 mine-pool. Since 1986, Fe and sulfate concentrations have continued a slow, irregular decline at the rate of one to two mg/L/year for Fe and about ten to 15 mg/L/year for sulfate. The long term concentration trends can be described with exponential models, which project that objectionable Fe levels may persist for decades. The Lancashire 15 mine-pool, also referred to as Barnes&Tucker, is one of the five sites analyzed in this chapter.

Koryak et al. (2004) summarized more than 30 years of stream monitoring data in several major tributaries of the Allegheny River in northern Appalachia. This area has been degraded by acid drainage from abandoned coal mines. They found over three decades a steady decreasing trend in acidity, and associated increases in pH and alkalinity. Since the 1970s, acidity had declined by an average of 63%. They attributed the water quality improvements to "exhaustion" of pyritic materials. The stream data are an indirect gage of the acid loading in the watershed. The observed time frames and relative improvements are consistent with the behavior described for mine-pools.

Younger (2000) described a simplified generic model for estimating iron behavior in flooded mines in the U.K. Younger's philosophy of using a simple approximation is similar to the approach taken in this work. Younger examined 81 discharge records from closed, mostly to fully flooded mines, and made the following observations:

- Flushing could be described using decay functions.

- The main period of flushing lasted about four times as long as the flooding period.

- The ratio of initial or short term to long term Fe concentration was about eight to one.

- Fe concentration was related to sulfur content of the strata and distance to outcrop.

Younger examined a simple batch reactor flow model to describe flushing of the form:

$$t_f = V_0/Q \qquad (5\text{-}1)$$

where t_f = flushing time.

V_0 = Pore volume (mine-pool volume).

Q = Discharge Rate, at steady state is equal to recharge.

Younger found the batch reactor model underestimated flushing time for the discharges. He attributed the lack of fit to flow-path tortuosity, which is not accounted for in a simple batch reactor.

Younger (2000) also attempted to describe mine-pool flushing using an advection-dispersion equation. He was able to obtain a good fit between model and actual discharge data for one mine by adjusting several parameters in the equation. Younger commented on the difficulty of measuring several of the variables in the equation, and stated that it was possible to obtain model fits simply by continually adjusting parameters.

Finally, Younger, building on the work of Glover (1983), devised a simple relationship:

$$t_f = (R_f/2)^*t_r \qquad (5\text{-}2)$$

where t_f = flushing time,

R_f = ratio of initial concentration to final concentration.

t_r = time to flooding, assumed equal to half life for Fe.

Younger obtained reasonable agreement with discharge data for the part of the record that exhibited exponential decline; that is, before the time-concentration curve approaches asymptotic conditions.

There is anecdotal and observational evidence suggesting that water pollution from closed mines will persist on a time scale of decades. The author has observed underground coal mines abandoned for 80 to 100 years in northern Appalachia and the Illinois basin that still discharge water with Fe concentration exceeding most Fe water quality standards. The Argo drainage tunnel in Colorado, completed in the 1890's and designed to drain gold and silver mine-works, still discharges acidic water (pH~3.2) with elevated metals (Al, Cu, Fe, Zn) concentrations (Miller et al., 2007).

5.2 In-Situ Acid Neutralization

An initial examination of the five mine-pool data sets revealed that a large fraction of pyrite oxidation acidity is "missing" from coal mine-pool waters, even in acid mine waters. This missing acidity has been termed "neutralization" and is attributed to H^+ consumption by weathering (Hollyday and McKenzie, 1973; James, 1984). Apparent in-situ consumption of acidity reduces the impact of mine waters to receiving streams and aquifers, the burden for conventional chemical or passive treatment; and perhaps duration of pollution. The mechanisms supporting in-situ acid consumption could include alkaline ground-water recharge, dissolution of carbonate minerals, dissolution of alumino-silicate minerals, and exchange and adsorption reactions.

Hollyday and McKenzie (1973) calculated "Neutralization Ratios" based on cation and anion composition, and pH. Hollyday and McKenzie's computation methods are shown as:

$$\text{Acid Neutralization Ratio} = [\sum(Ca^{2+}, Mg^{2+}, Na^+, K^+)-\sum(Cl^-, F^-)]/(SO_4^{2-}) \quad (5\text{-}3)$$

where parameters are expressed in meq/L. The numerator is a gross estimate of alkalinity, produced from the dissolution of carbonates and other acid consuming reactions. The sulfate denominator represents the acidity produced via pyrite oxidation.

Both Hollyday and McKenzie (1973) and James (1984) reported that, in general, more than 60% of the acidity projected from pyrite oxidation was absent from the discharge water, even in mine waters with low pH.

James (1984) subsequently modified the Acid Neutralization Ratio to account for the presence of Al, Fe(II) and HSO_4^-. He calculated strong acid neutralization ratio as:

$$[\sum(Ca^{2+}, Mg^{2+}, Na^+, K^+, Al^{3+}, HSO_4^-)-\sum(Cl^-, F^-)]/[(SO_4^{2-})-(Fe^{2+})] \quad (5\text{-}4)$$

where parameters are expressed in meq/L.

For waters containing appreciable Al, dissolution of an alumino-silicate is an acid consuming reaction. Complete kaolinite dissolution consumes three moles of H^+ per mole of Al as follows:

$$Al_2Si_2O_5(OH)_4 + 6\,H^+ \rightarrow 2\,Al^{3+} + 2\,H_4SiO_4 + H_2O \quad (5\text{-}5)$$
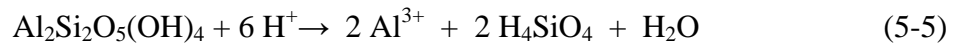
The bisulfate ion HSO_4^- is included in James' equation since its formation consumes one mole of H^+. At pH values approaching two, bisulfate from H_2SO_4 dissociation, with a pK_a of 1.99 at 25° C, constitutes a noteworthy fraction of total sulfate in solution. Ferrous iron is subtracted in James' expression, since it represents acidity not yet produced by oxidation and hydrolysis. James' (1984) method is an improvement for waters containing significant amounts of soluble Al, ferrous Fe, or low pH.

Morin et al. (1988) describe neutralization of an acidic ground-water plume initially by carbonate, then by hydroxide and finally by alumino-silicate dissolution. Bains et al. (2000) and Blowes et al. (1992) have described similar reaction sequences for acid ground-water migrating from tailings impoundments.

Neutralization ratio was estimated three ways in this study:

- The first was a simple mass balance calculation based on pyrite stoichiometry, sulfate and acidity concentrations.

- The second set of calculations used the James (1984) method (equation 5-4) for three data sets that contained major cation and anion analysis for at a least a significant portion of the record.

- The third method involved speciating the solutions based on equilibrium calculations and summing solution complexes that either consume or liberate H^+. Speciation calculations were performed using PHREEQCI (Parkhurst and Appelo, 1999), for one acidic mine-pool (Omega) and one circumneutral mine-pool (Hahn).

5.2.1 Neutralization from Mass Balance Difference Sulfate and Observed Acidity

A simple approximation of in-situ neutralization may be derived from sulfate concentration and a measure of the acidity attributable to pyrite oxidation. The summary reaction for pyrite oxidation shows that four moles of H^+ are produced for two moles of sulfate as follows:

$$FeS_2 + 15/4\, O_2 + 7/2\, H_2O \rightarrow Fe(OH)_3 + 4\, H^+ + 2\, SO_4^{2-} \qquad (5\text{-}6)$$

Maximum acid production (MAP) was calculated based on equation 5-6, subject to the following assumptions:

- All measured sulfate is derived from pyrite oxidation within the mine.

- No sulfate is retained in the mine-pool by precipitation or adsorption reactions.

- Iron retained in the mine-pool has undergone oxidation and hydrolysis, producing its full complement of H^+ in-situ.

The first assumption is approximately correct, because sulfate concentration in ground-waters entering Appalachian mine-pools is usually small relative to the mine-pool composition. For example, ground-water recharging the Barnes&Tucker mine-pool contains an average of about 27 mg/L sulfate, based on data collected by McElroy (1998). Similar sulfate concentrations, about 40 mg/L average, were reported by Hobba (1984) for ground water of the Monongahela group rocks overlying the Pittsburgh coal bed. The "background" recharge water values are less than five percent of the concentrations observed in the mine-pools that they enter.

The second assumption, that no sulfate is retained by precipitation or adsorption reaction, is mine-pool specific. A series of jarosite minerals of composition $MFe_3((SO_4)_2(OH)_6$ may form under acid oxidizing conditions, such as exists in the Omega and T&T mine-pools. M is typically K^+, Na^+, or H^+, but may include other metals as well. Gypsum, melanterite, halotrichite, schwertmannite (an Fe-hydroxy-sulfate), and many other minerals are also potential sinks for sulfate in acidic or partly flooded mine-pools. Melanterite and other highly soluble minerals may be flushed from the mine. Schwertmannite has been reported to gradually dehydrate, liberate sulfate and form goethite over a period of several years (Bigham et al., 1996; Jonsson et al., 2005). Alunite is an Al-sulfate mineral with composition analogous to jarosite, where Al replaces Fe. In general, sulfate bearing solids are more likely to form in unflooded than in flooded mines or mine sections. The third assumption may not be completely correct if short term storage of Fe salts is significant.

Sulfate adsorption on Fe oxy-hydroxide precipitates that is pH dependent has been reported (Rose and Elliot, 2000), with increased retention at low pH. Given the potential for sulfate adsorption and mineral formation, the second assumption of conservative sulfate behavior may not always be fully met. In this instance, if sulfate is retained in the mine-pool, estimated acid production will be less than the actual amount.

Noting these assumptions, estimated maximum acid production (EMAP) within the five mine-pools studied was calculated as:

$$EMAP = [SO_4(mg/L)*1mmole/96\ mg]*[\ 100\ mg\ CaCO_3\ Eq] \qquad (5\text{-}7)$$

where two mmole of H^+ are produced per mmole sulfate and two mmole of H^+ are consumed per mmole $CaCO_3$.

Total acidity can be calculated from dissolved metals and pH as:

$$Acidity_{total} = 50[(2*Fe(II)/56) + (2*Mn/55) + (3*Al/27) + (\ 1000*10^{\wedge -pH})] \qquad (5\text{-}8)$$

However, for the purpose of estimating mine water acidity directly attributable to pyrite weathering, equation 5-8 was modified to include only Fe(II) and H^+. Fe(II) represents H^+ that will be produced from iron oxidation and subsequent hydrolysis. pH represents H^+ that has already been generated within the mine-pool from sulfide oxidation. The sum of these two parameters is acidity that can be attributed to sulfide oxidation, and is termed "pyrite acidity" (equation 5-9).

$$Acidity_{pyrite} = 50[(2*Fe/56) + (\ 1000*10^{\wedge -pH})] \qquad (5\text{-}9)$$

Total dissolved Fe is presumed to originate from pyrite and represents acidity not yet generated by metal hydrolysis, while pH represents acid generation that has already occurred from pyrite. The difference in acidity between equations 5-9 and 5-7 is termed neutralization and represents mineral weathering, recharge water or other processes.

The total and "pyrite acidity" calculations assumes that metal hydrolysis and H^+ comprise all of the mine water acidity. Carbonate acidity is not included, and is assumed to be negligible. Kirby and Cravotta (2005), and Cravotta and Kirby (2005) discuss, in detail, theoretical and practical aspects of acidity measurements in mine waters. They concluded that Fe should be represented as Fe(II) in acidity calculations after examining Fe speciation in mine water. Acidity calculations for the five mine-pools followed this convention unless noted otherwise.

A Neutralization Ratio was then calculated as:

$$\text{Neutralization Ratio} = [(\text{EMAP- Acidity}_{pyrite})/\text{EMAP}]*100 \qquad (5\text{-}10a)$$

The "missing acidity" or neutralization is represented by the difference between estimated maximum acid production (EMAP) and acidity still present that can be attributed to pyrite (Fe and H^+). Dissolved metals such as Al and Mn, are assumed to represent in-situ neutralization, that is, acid consumption within the mine-pool. Carbonate alkalinity is assumed to be absent. If measurable alkalinity is present, then equation 5-10 must be modified by adding alkalinity to the numerator as follows:

$$\text{Neutralization Ratio} = [(\text{EMAP- Acidity}_{pyrite} + \text{Alkalinity})/\text{EMAP}]*100 \qquad (5\text{-}10b)$$

For mine waters that are net alkaline, the neutralization ratio can exceed 100%.

Median data in table 5-1 show mine-pool quality conditions soon after closure, and after about ten to 35 years of continued weathering, ground-water recharge and discharge. In each mine-pool, acidity and metals concentration have declined significantly through time, although water quality remains poor, especially in the acidic mine-pools. Iron concentrations remain elevated in all mine-pools. The two acidic mine-pools, Omega and T&T, and the acidic Sterling 1 sub-pool in Barnes&Tucker, contain significant dissolved aluminum, indicating the dissolution of alumino-silicates and/or aluminum oxyhydroxides. Dissolution of aluminum minerals in-situ is an acid consuming reaction, as shown for kaolinite weathering in equation 5-5. Pyrite acidity, attributable to Fe and H^+, and calculated from equation 5-9, is 65 to 70% of the total acidity (equation 5-8) soon after flooding in the acidic pools. Pyrite acidity declines to about 55% of total acidity as the mine-pools age.

Table 5-1 also shows neutralization ratios computed from equation 5-10a and 5-10b. The acidic sites, Omega, T&T, have neutralization ratios (equation 5-10a) of about 61 to 65% in early flushing, indicating considerable acid consumption is occurring. The ratios increase to 73 % and 83 % as the mine-pools age, and are over 70% in the 50+ year old Sterling 1 sub-pool. The main Barnes and Tucker discharge increased from 58 to 86% neutralization ratio as it aged. The Hahn and Arden-Westland mine-pools had 77 and 88% neutralization respectively, in early flooding. Three mine-pools, Hahn, Arden-Westland and Barnes and Tucker after flooding, contained water with measureable alkalinity. Neutralization ratio (equation 5-10b) that includes carbonate alkalinity is also

shown in table 5-1 for these three sites. Each of these mine-pools developed net alkaline water as they aged and have neutralization ratios exceeding 100%. Neutralization in each mine-pool is discussed in more detail in following sections.

Table 5-1
Summary Water Quality Characteristics of Five Mine-pools[(1)]

Mine-pool	Date	pH	Total Acidity	Pyrite Acidity	Alkalinity	Fe	Al	SO$_4$	Neut. Ratio 1	Neut. Ratio 2
Omega	1993	2.86	2200	1440	-	772	137	3915	64.6	-
Omega	2007	2.63	1075	560	-	248	92	2021	73.3	-
T&T	1996	2.6	700	509	-	227	39.7	1270	61.5	-
T&T	2006	2.79	300	162	-	44.2	26.3	964	83.8	-
Hahn	1984-1985	4.4	1831	1667	70	931	20.6	7000	77.1	81.8
Hahn	1994-1995	6.6	158	156	360	87	0.2	1445	89.6	113.4
Arden-Westland	1986-1987	6.75	148	139	219	78	0.2	1170	88.6	102
Arden-Westland	1998-1999	6.8	131	127	146	71	0.1	888	86.2	102
Barnes& Tucker (Duman)	1971	4.1	1500	1499	8	837	-	3432	58.0	-
Barnes& Tucker (Duman)	2005	6.60	71	56	197	31	0.2	390	86.2	148
Barnes& Tucker Sterling 1	2005	2.69	495	263	-	78	39	930	72.8	-

(1) Values are median data for the specified time period. pH in S.U.; acidity and alkalinity in mg/L CaCO$_3$ Eq.; Fe, Al, SO$_4$, in mg/L. Total acidity from equation 5-8, pyrite acidity from equation 5-9. Neut. Ratio 1 is Neutralization Ratio calculated from equation 5-10, carbonate alkalinity not included. Neut. Ratio 2 includes carbonate alkalinity.

5.2.1.1 Neutralization in the Partly Flooded, Acidic Omega Mine-pool

Figure 5-1 shows the neutralization ratio, calculated using equation 5-10a, over a 14 year period from 1993 to 2007 for the Omega Main Treatment Inlet. All drainage from the mine-pool is routed to this inlet by a series of pipelines. The samples are taken just before the raw water enters chemical treatment facilities at approximately monthly intervals. A great deal of scatter is evident in figure 5-1, but between about 60 and 80 % of the maximum acid production has been consumed before the drainage enters the treatment facilities. The overall median neutralization ratio is 66%.
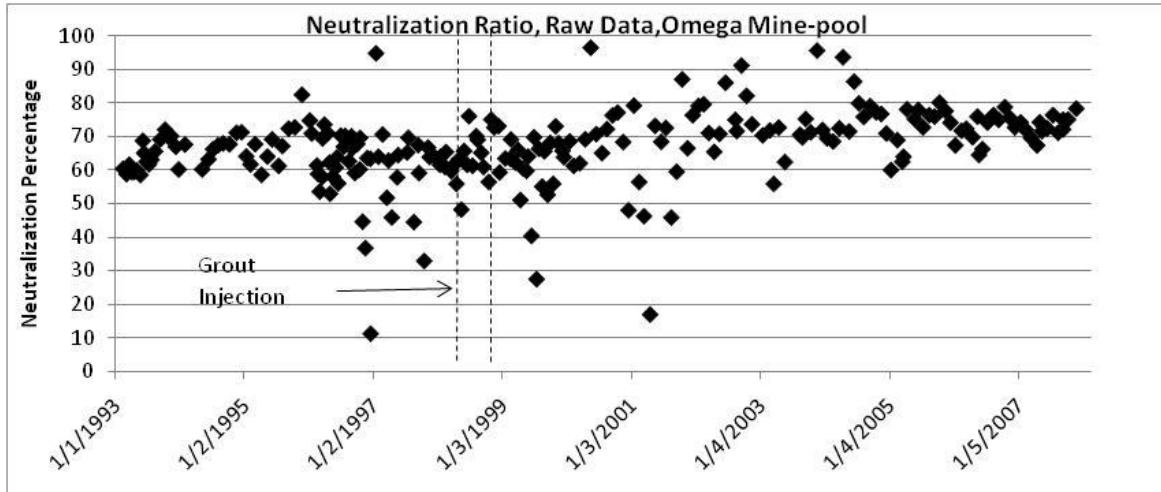
Figure 5-1. Neutralization Ratio for Raw Data, Omega Mine-pool, Main Treatment Inlet.

Figure 5-2 displays the same data set after applying a simple five point moving average, to show trends more clearly. Since samples were collected roughly at monthly intervals, or sometimes more frequently, the smoothed mean includes as much as five months temporal trend. Smoothing can cause an apparent lag in seasonal or trend display. Figure 5-2 shows a pronounced seasonal trend; with maximum neutralization of 70 to 80% occurring in the fall season, and corresponding to low flow period. Minimum neutralization of around 50% occurs in spring season, corresponding to high flow periods. This trend may result from seasonal accumulation and flushing of metal sulfate salts (Perry and Rauch, 2004, Appendix A). They reported that about 75% of yearly acid and metal flux was discharged during high flow periods of a few months per year at this mine.
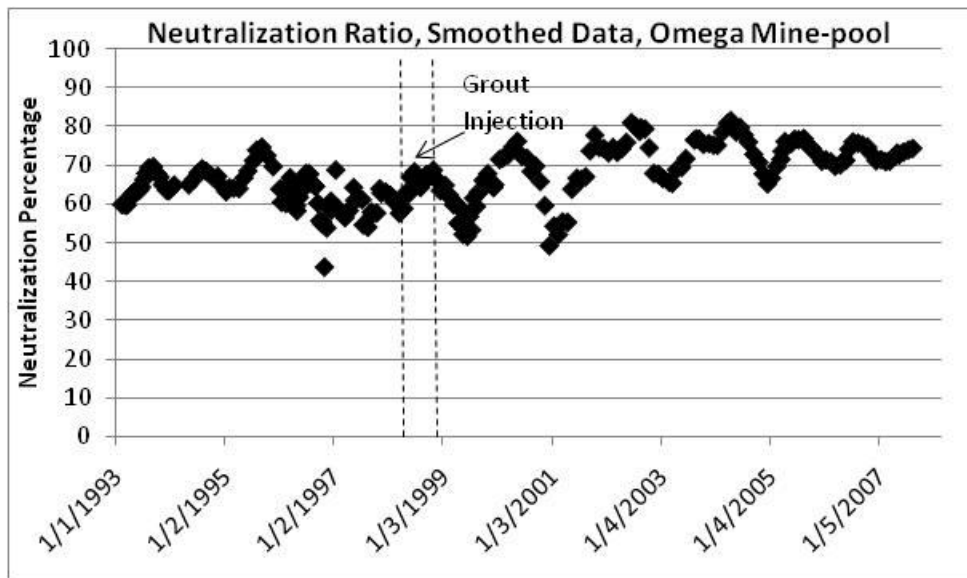

Figure 5-2. Neutralization Ratio for Omega mine-pool, Main Treatment Inlet, Smoothed Data.

Neutralization ratio was depressed during late 1998 and all of 1999. This corresponds to grout injection in part of the mine-works. During grout injection, and for a period of about one year following, chemical concentrations of sulfate and other parameters increased in mine waters draining this section of the mine-works. The chemical concentration increase is interpreted as displacement and flushing of soluble weathering products, including hydrous-sulfate metal salts, such as melanterite, copiapite and similar minerals. The short term deterioration in water quality is discussed more detail by Perry and Rauch (2004, Appendix A). In 2000, neutralization ratio increased about eight percent over pre-grouting conditions, suggesting some benefit of additional in-situ neutralization from the grout mix. Overall median neutralization ratio was 64% before grout injection, and about 72% after grouting. It has remained between about 70 and 80% through 2007.

The trend data in figure 5-2 show that the over the 14 year period of record, neutralization ratio has remained relatively stable, except when the system was stressed during grout injection and seasonal fluctuations.

Figure 5-3 shows smoothed (five point moving average) neutralization percentage data for the Marshall discharge at the Omega mine. This drainage is located at the down-dip end of the mine-works and in close proximity to a section that was grouted with a flyash and cement mix. It is the largest flow of any drainage at the mine, comprising about 50%
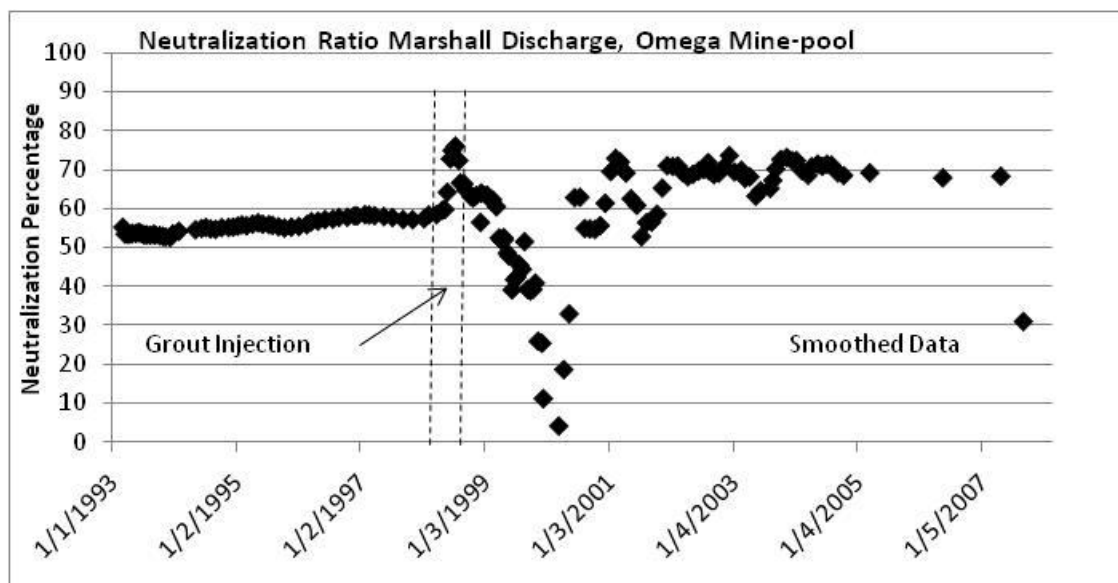

Figure 5-3. Neutralization Ratio for Omega Mine-pool, Marshall Discharge, Smoothed Data.

of the total discharge. It has some of the poorest quality water encountered in the mine-pool, with total acidity often exceeding 5000 mg/L $CaCO_3$ prior to grout injection.

Grouting response is clearly displayed in figure 5-3. Before grouting in 1998, about 50 to 60% of acidity was consumed in-situ. When grouting commenced in October, 1998, a brief and rapid rise to about 75 % neutralization occurred. This was quickly followed by a

decline, which lasted about one year, to as low as four percent neutralization in March, 2000. The rapid fluctuations are likely due to close proximity of the discharge to the grout zone, and short term neutralization by acid consuming grout material, followed by displacement of acid weathering products that had accumulated in the mine. Welch et al. (2008) showed that jarosite, for example, could dissolve congruently, liberating soluble Fe and sulfate at pH values like that in the Omega mine-pool. Acid neutralization continued to fluctuate until 2002, about four years after grout injection, and has remained at about 70%.

5.2.1.2 Neutralization in the Partly Flooded, Acidic T&T Mine-pool
Like the Omega mine, the T&T mine complex is located above base level drainage in a sequence of rocks that contain few carbonates. The T&T drainage also shows poor water quality, typified by low pH, and elevated acidity, metals and sulfate. Over the ten year period from 1996 to 2006, all chemical concentrations declined in the principal discharge. The largest improvements were declines in Fe, and consequently acidity. Sulfate, Al and pH showed the smallest improvements. These same trends also occur in the Omega mine-pool (table 5-1).

Neutralization percentage in the T&T mine-pool averaged about 72% for the period of record (figure 5-4, smoothed data five point moving average), and was calculated using equation 5-10a. The behavior is similar to the Omega mine-pool. The T&T raw data were collected at monthly intervals or less, and the smoothed means include a maximum of five months. Neutralization Ratio actually declined from 70 to about 50% during the first few years after closure. This period was characterized by high volume discharges sometimes exceeding 7,000 L/minute, and is similar to the "first flush" behavior described for flooding underground coal mines in the United Kingdom (Younger, 2000).
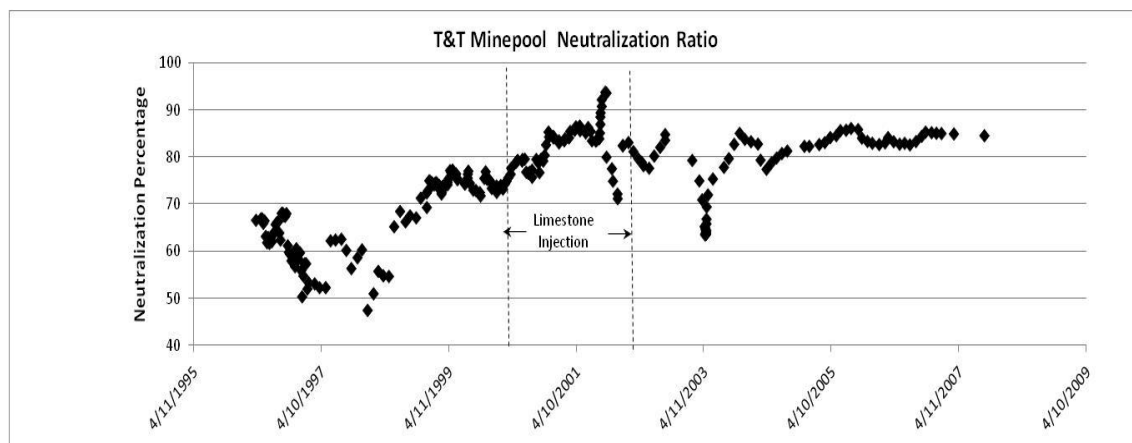

Figure 5-4. Neutralization Ratio for T&T Mine-pool, Smoothed Data.

The extreme flows and flushing of acid weathering products likely caused the decline in neutralization percentage. The mine-pool includes about 560 hectares of workings, of which about 20% are flooded. Approximately 65,000 metric tons of limestone byproduct

(70% CaCO$_3$ Eq.) were injected into the mine from late 1999 to late 2001 in an attempt to treat acid water in-situ.

Neutralization Ratio in the T&T mine-pool increased from about 65 to 85% over a three year period from 1998 to 2001 after limestone injection. There were two rapid short term fluctuations in 2001 and 2003. Both events included a brief rapid increase in mine-pool head, followed by a large volume short duration discharge of very poor quality water. After 2004, neutralization ratio has usually exceeded 80%.

Injecting a large mass of limestone into the mine-works should have had a beneficial effect on acid production and leaching. Post injection neutralization ratio is about 12% greater than immediately prior to treatment, and the amount of "pyrite acidity" did decrease during limestone injection. Injection did not; however produce large shifts in pH, as might be expected after adding large amounts of calcium carbonate to the system. The mine-pool discharge water is slightly under-saturated for gypsum and jurbanite since limestone injection. These minerals could control Ca, Al and sulfate concentrations, which may mask neutralization effects.

5.2.1.3 Neutralization in the Flooded, Neutral, Barnes&Tucker Mine-pool
The Barnes&Tucker mine-pool, located in Cambria county, Pennsylvania is pumped drainage from a mostly flooded underground mine in the Lower Kittanning coal bed within the Kittanning formation, Allegheny group. It is partially overlain by a second set of flooded mine-works in the Lower Freeport coal bed. The two mine-pools are hydraulically connected as shown by pumping and other data (Hawkins et al., 2005). The mine-pool has been flooded for over 35 years, after closing in 1969, and filling by with ground water by 1970. Further details of the chemical composition of the mine-pool are described by Perry et al. (2005, Appendix D). Summary data in table 5-1, show that the discharge was initially acidic with Fe and sulfate exceeding 800 and 3400 mg/L, respectively.

Neutralization ratio in figure 5-5 is based on yearly average values from the main discharge, called Duman, and was calculated using equation 5-10b, which includes carbonate alkalinity. In the first years after flooding and during the initial flush, neutralization ratio was about as low 40%, but rapidly increased to between 60 and 80%. In 1986, mine-works in an overlying coal bed were abandoned and allowed to flood. Flooding of the overlying mine-works and the vertical connection between the two mines necessitated an increase in pumping rate, and increased alkalinity concentration in the Barnes and Tucker mine-pool. The upper mine-works contained water with alkalinity of about 150 mg/L CaCO$_3$ Eq. and negligible amounts of Fe (unpublished monitoring records, Lloyd, 2004). Flooding of the overlying mine-works and the vertical connection between two coal beds resulted in a rapid increase in neutralization ratio to about 140%. Neutralization ratio has remained between about 90 and 140% since that time.

Neutralization ratio was also estimated for drainage emanating from an unflooded section of the Barnes&Tucker works in the same Lower Kittanning coal bed. The discharge, called Sterling 1, drains mine-works that were closed about 1960. Unlike the flooded pool, the Sterling 1 drainage is acidic with pH less than 3.0 (table 5-1). Monitoring data

from the mid 1980s, mid 1990s and 2004-2005 have a median neutralization ratio of about 73%.
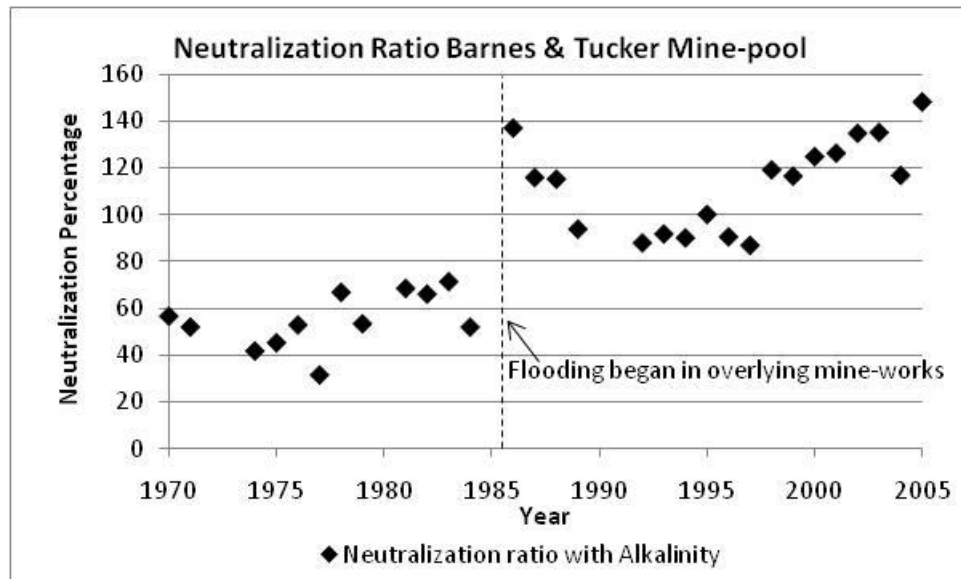

**Figure 5-5 Neutralization Ratio, Mostly Flooded, Circumneutral,
Barnes &Tucker Mine-pool, Yearly Average Data.**

In-situ neutralization is less efficient in the Sterling 1 drainage. The only difference between the Duman and Sterling 1 discharges is flooding state (flooded vs. unflooded). The Sterling 1 discharge neutralization ratio is similar to the behavior of the Omega and T&T mines described previously.

5.2.1.4 Neutralization in the Flooded, Circumneutral Hahn Discharge Mine-pool
The Hahn discharge, located in Washington County, Pennsylvania, is pumped drainage from a mostly flooded underground mine (Montour 4) in the Pittsburgh coal bed. Some characteristics of the drainage quality at this mine have been described by Donovan et al. (2003). Early discharge water from the mine-pool was highly mineralized, containing over 900 mg/L Fe and 7000 mg/L sulfate (table 5-1).

The mine closed in 1980 when a barrier failed between Montour 4 and an up-dip mine, and the works began to flood The Hahn drainage was initially acidic, but produced circumneutral pH water about five years after mine abandonment, and net alkaline water after about ten years. The mine-pool includes about 5900 hectares, of which over 70% is flooded. The pool is pumped as a controlled discharge at about 13,250 L/minute, and has an estimated residence time of about 4 years. No seasonal effects were found in neutralization ratio. Pumping dampens seasonal influences, if any occur. The mine-pool was near saturation with respect to calcite after initial flooding (Donovan et al., 2003).

Figure 5-6 shows neutralization ratio calculated with (equation 5-10b), and without including alkalinity (equation 5-10a) for the Hahn discharge. Neutralization Ratio computed with alkalinity has always been at least 80% and approached 120% about 20

years after mine closure. The continuing increase in neutralization ratio is a function of the decline in estimated maximum acidity, and simultaneous increase in mine-pool alkalinity through time. Neutralization ratio calculated without alkalinity stabilized at about 90% in 1990, about ten years after mine closure and the start of flooding. Sulfate and iron, the two parameters that exert the greatest influence on the calculated neutralization ratio (excluding alkalinity) are decreasing in concentration at about the same rate. There is no statistically significant change ($p = 0.01$) in neutralization ratio (excluding alkalinity), after about 1990. The plot and statistics indicate establishment of a near steady state condition in this form of neutralization ratio. This suggests that the initial flushing event was completed at this time. The time scale corresponds to about one and one half pool volumes of discharge, after flooding was complete in 1984, and a four year residence time.
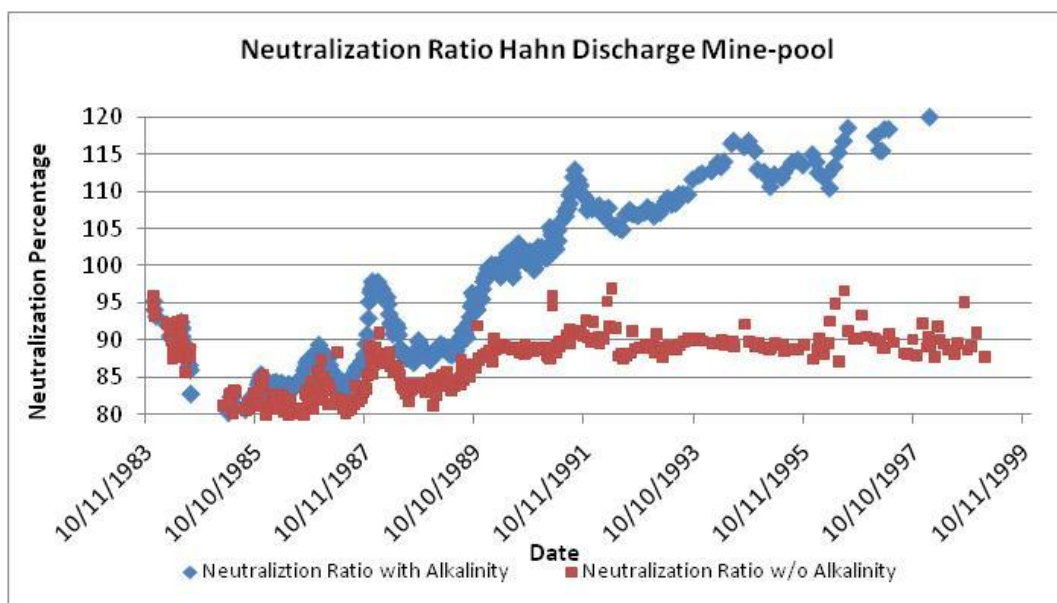

Figure 5-6. Neutralization Ratio, Computed with Alkalinity (Blue) and without Alkalinity (Red) Mostly Flooded, Circumneutral Hahn Discharge Mine-pool.

5.2.1.5 Neutralization in the Arden-Westland Discharge, Westland Mine

The Arden-Westland discharge is from a pumped mine-pool in the Arden-Westland mine in Washington County, Pennsylvania. It is located about 16 km southwest of the Hahn discharge, and is also in the Pittsburgh coal bed. The Westland mine covers about 5100 hectares. It is estimated to be about 80% flooded, based on examination of mine maps and water level data. The Westland mine actually surrounds and discharges through the smaller Arden mine-works, which ceased operating in the 1940s. The inclusion of water from the older Arden-Westland mine-works complicates interpretation of mine-pool chemistry.

The Westland mine closed in 1980 and was flooded by 1986. Donovan et al. (1999) estimated a 4 year residence time for the mine-pool. Unlike the Hahn drainage, Arden-Westland discharge waters are under-saturated for calcite (Donavan et al., 1999). No

133

water quality data for the period 1980 to 1986 were located, so the early mine flooding history is not addressed.

Table 5-1 shows summary water quality characteristics of the mine-pool in 1986 soon after flooding was complete, and after flushing an estimated four to five pool volumes by 1998. Unlike the Hahn discharge, the Arden-Westland drainage did not display dramatic declines in pollutant concentrations after flooding. Neither did the Arden-Westland discharge acidic water in the initial period of record. Metals, sulfate and acidity were roughly an order of magnitude lower than early discharge chemistry of the Hahn. The early Arden-Westland discharge water is similar to the later Hahn water composition.

Figure 5-7 shows neutralization ratio for the Arden-Westland discharge, calculated with alkalinity (equation 5-10b), and without alkalinity (equation 5-10a). The early period of record shows a rapid decline in neutralization ratio by either method. This may represent the end of the initial flushing event rinsing accumulated acid weathering products from the mine. Figure 5-7 shows that the mine-pool approaches 100% neutralization with alkalinity by 1992, or about 6 years after flooding was complete. The decline in metals concentrations, and estimated maximum acid production, which is calculated from sulfate concentration, is slower in the Arden-Westland mine-pool than the Hahn drainage. Sufficient alkalinity enters, or is generated in the Arden-Westland mine-pool, to approach 100% neutralization.
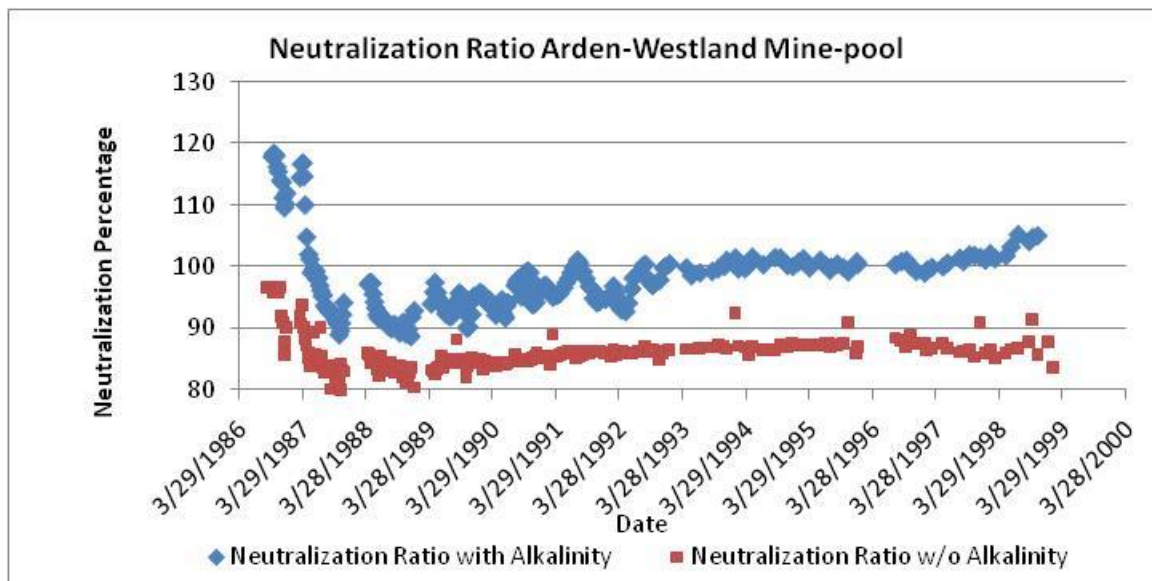

Figure 5-7. Neutralization Ratio, Computed with Alkalinity (Blue) and without Alkalinity (Red) Mostly Flooded, Neutral Arden-Westland Mine-pool.

Figure 5-7 shows that neutralization ratio, excluding alkalinity, reached a near steady condition by about 1992, or six years after flooding was complete. It is equivalent to flushing about 1.5 pool volumes after flooding was complete, and is similar to the behavior of the Hahn discharge. No seasonal effects on neutralization ratio including or excluding alkalinity were identified. Pumping dampens seasonal influences, if any occur.

5.2.2 Neutralization Estimate by Mass Balance Cation Sum Methods

Neutralization ratio was also calculated for three mine-pools, one acidic (Omega) and two alkaline (Hahn and Arden-Westland) using the cation/anion summation strong acid neutralization ratio method described by James (1984) and shown in equation 5-4. The three mine-pools have major cation/anion analysis for at least a portion of the monitoring record. The average neutralization ratio derived from James cation/anion summation method (equation 5-4), and the ratio obtained from equation 5-10a for the same sample subsets are summarized in table 5-2. Equation 5-10a and James' method both estimate total acid production from sulfate concentration. Both methods are subject to underestimating total acid production if some sulfate is retained in the mine-pool. Rose and Elliot (2000) reported that some sulfate was adsorbed to Fe oxyhydroxides surfaces at low pH. The two methods differ where James estimates neutralization equivalent from cation concentrations, while equation 5-10a estimates neutralization by difference between maximum acid production and observed Fe and H^+. Results from equation 5-10a are identified as the difference method in table 5-2.

The average difference between James' (1984) method and equation 5-10a was only about 4% for the Omega mine-pool and about 7 to 8% for the two alkaline mine-pools. Differences between methods for individual sample events were usually less than 10%. James (1984) cation summation method was consistently less than the difference method in the Hahn and Arden-Westland mine-pools. The difference method, equation 5-10a, is a lumped parameter that does not provide an account of the contributing components. Therefore it can't be readily resolved as either over or underestimating in–situ neutralization. It is possible that James method may under-estimate neutralization if other cations, for example Zn, are present in mine water, but are not included in the calculation.

Table 5-2
Neutralization Ratio by Cation Sum and Mass Balance Difference Methods

Mine	n	Mean Neutralization Ratio, James (1984) Cation Summation Method	Mean Neutralization Ratio, Mass Balance Method (equation 5-10a)	Mean Neutralization Ratio, Speciation Method
Omega	76	68.7 %	63.9%	73.5
Hahn (Montour 4)	420	87%	95%	90.6
Arden-Westland	220	89%	96%	-

The two methods give similar results, and either should be useful for characterizing the extent of in-situ neutralization. The mass balance by difference method (5-10a) can be used on acid waters with more limited analytical parameters. Neutralization ratio in mine waters with measurable carbonate alkalinity should be calculated using equation 5-10b or a modified form of James method that includes bicarbonate and carbonate ions.

5.2.3 Neutralization Ratio From Speciated Mine Water Solutions

The third method for estimating neutralization ratio consisted of speciating water data from two mine-pools, one acidic (Omega) and one circumneutral (Hahn-Montour 4). The purpose was to determine whether quantifying complexes and reactions that either consume or produce H^+ should be included in a neutralization calculation. The alternative was that contribution of solution complexes is small enough that they can be neglected without causing serious error. Carbonate and bicarbonate species were not included in the speciation tabulation to allow direct comparison to James' method and equation 5-10a. For mine waters with measureable alkalinity like the Hahn-Montour 4 discharge, a complete accounting of in-situ neutralization should include carbonate and bicarbonate species

Solutions reporting major cations and anions were speciated using PHREEQCI (Parkhurst and Appelo, 1999). For the Omega mine-pool, this included about 75 sample events with reported dissolved constituents of Fe^{2+} (Fe(II)) and Fe^{3+} (Fe(III)). The redox state of the water was calculated assuming equilibrium with the Fe(II)/Fe(III) couple. A small number of samples collected by the author at the Omega mine-pool included field measured Eh and redox state for these samples is based on that measurement. The measured and calculated Eh readings, while collected at different time periods, were consistent.

No Eh or Fe(II)/Fe(III) data were available for the Hahn discharge. Redox state was initially calculated for about 420 Hahn samples using the PHREEQCI default of pe equal to four. The results of this run showed over-saturation for $Fe(OH)_{3(am)}$ and other less soluble Fe oxyhydroxide minerals for many samples. The pe was adjusted to zero to represent more reduced conditions in several subsequent runs. This produced solutions that were slightly under-saturated for $Fe(OH)_{3(am)}$. A pe of zero therefore approximately represents a Hahn mine-pool redox state that could contain the concentrations of dissolved Fe reported in the data set, without exceeding saturation for an Fe hydroxide mineral. These adjusted runs were used to estimate distribution of redox-sensitive species of Fe for the Hahn mine-pool.

Acid consuming and acid producing species were identified, and their contributions to overall neutralization quantified by modifying equation 5-10a. The concept is summarized as:

Neutralization Ratio =
$$((EMAP - (Acidity_{pyrite} + H^+ \, Production - H^+ \, Consumption))/EMAP)*100 \qquad (5-11)$$

where:

EMAP = Estimated Maximum acid production, based on sulfate concentration as defined in equation 5-7.

$Acidity_{pyrite}$ = pH, and H^+ not yet produced, represented by soluble iron that has not hydrolyzed, as defined in equation 5-9.

H^+ Production = hydrolysis complexes and solution H^+.

H^+ Consumption = oxidation of Fe(II) to Fe(III), and formation of HSO_4^- and related species.

Tables 5-3 and 5-4 summarize the acid producing and acid consuming complexes and reactions, respectively. Log K data are for 25 ° C and are drawn from the PHREEQCI databases. Table 5-3 includes a series of hydrolyzed complexes of Fe, Al, Ca and Mg that produce H^+. The principal H^+ consuming processes in table 5-4 are the oxidation of ferrous to ferric Fe, and the formation of bisulfate and related complexes. The calculated equilibrium concentrations of the components in table 5-3 were summed, and then included as H^+ Production in equation 5-11. The acid consuming complexes and reactions in Table 5-4 were likewise included in equation 5-11 as H^+ consumption. The last four entries in table 5-4 are metal bisulfate complexes. They are included as indirect acid consumers because the bisulfate ion consumes one mole of H^+.

Table 5-3
Solution Complexes With Hydrolysis That Produce H^+

Reaction	Moles H^+ Produced	log K
$Ca^{+2} + H_2O = CaOH^+ + H^+$	1	-12.78
$Mg^{+2} + H_2O = MgOH^+ + H^+$	1	-11.44
$Al^{+3} + H_2O = AlOH^{+2} + H^+$	1	-5.0
$Al^{+3} + 2H_2O = Al(OH)^{2+} + 2H^+$	2	-10.1
$Al^{+3} + 3H_2O = Al(OH)_3 + 3H^+$	3	-16.9
$Al^{+3} + 4H_2O = Al(OH)^{4-} + 4H^+$	4	-22.7
$Fe^{+3} + 2H_2O = Fe(OH)^{2+} + 2H^+$	2	-5.67
$Fe^{+3} + 3H_2O = Fe(OH)_3 + 3H^+$	3	-12.56
$Fe^{+3} + 4H_2O = Fe(OH)_4^- + 4H^+$	4	-21.6
$Fe^{+2} + 2H_2O = Fe(OH)_2 + 2H^+$	2	-20.57
$Fe^{+2} + 3H_2O = Fe(OH)_3^- + 3H^+$	3	-31.0
$3Fe^{+3} + 4H_2O = Fe_3(OH)_4^{+5} + 4H^+$	4	-6.3
$2Fe^{+3} + 2H_2O = Fe_2(OH)_2^{+4} + 2H^+$	2	-2.95
$Fe^{+2} + H_2O = FeOH^+ + H^+$	1	-9.5
$Fe^{+3} + H_2O = FeOH^{+2} + H^+$	1	-2.19

Table 5-4
Solution Complexes and Reactions That Consume H^+

Reaction	Moles H^+ Consumed	log K
$Fe^{2+} + 1/4\ O_2 + H^+ = Fe^{3+} + 1/2\ H_2O$	1	7.76
$H^+ + SO_4^{-2} = HSO_4^-$	1	1.98
$Fe^{+2} + HSO_4^- = FeHSO_4^+$	1 from HSO_4^-	1.08
$Fe^{+3} + HSO_4^- = FeHSO_4^{+2}$	1 from HSO_4^-	2.48
$Ca^{+2} + HSO_4^- = CaHSO_4^+$	1 from HSO_4^-	1.08
$Al^{+3} + HSO_4^- = AlHSO_4^{+2}$	1 from HSO_4^-	0.46

The mean neutralization ratio using speciation calculations was 73.5 % for the Omega mine-pool (see table 5-2), compared to 68.7% using James (1984) method, or 63.9 % using the difference method based on equation 5-10a. The inclusion of hydrolysis species from table 5-3 had minimal affect on results, and typically comprised less than one percent of the acid generating capacity of the system. Fe(II)/Fe(III) oxidation accounted for about 80% of the H^+ consumption in speciation calculations, and is the main factor that produces results different from the other two methods. The mean distribution of acid producing and acid consuming complexes and processes, expressed in $CaCO_3$ Eq., and is shown in figure 5-8 for the Omega mine-pool.
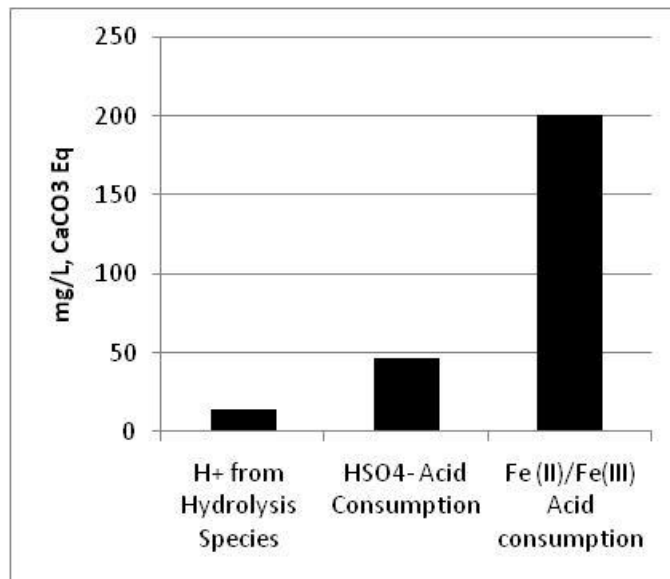
Figure 5-8. Mean Acid Producing and Acid Consuming Solution Complexes and Reactions, Omega Mine-pool. Concentrations in mg/L $CaCO_3$ Eq.

In oxidizing environments like the Omega mine-pool, speciating the solution chemistry will probably yield a higher estimate of in-situ neutralization. This is mostly due to H^+ consumption in Fe(II)/Fe(III) oxidation. If sufficient data are available to characterize Fe species distribution, speciating the water data may provide an improved estimate of in-situ neutralization.

Mean neutralization in the Hahn mine-pool was 90.6% using speciated data, compared to 87% by James (1984) cation sum method and 95% from the difference approach in equation 5-10a. Unlike the Omega mine-pool, Fe resides overwhelmingly as Fe(II) and minimal H^+ consumption occurs from Fe oxidation. Hydrolysis and HSO_4^- species had negligible effect on neutralization estimates.

James (1984), equation 5-10a, and the speciation method presented here, are all designed for acid waters without measureable alkalinity. A complete accounting of neutralization in mine-pools with alkalinity should include contribution of carbonate species. Equation 5-10b is one such approach. James method and the speciation method could be modified to include carbonate species.

The observed differences among methods are relatively small and each technique is suitable for estimating in-situ neutralization for planning purposes. The method of choice will be determined by the available data. In reduced mine-pool environments where Fe(II)/Fe(III) oxidation is restrained, there is little advantage to speciating solution composition to estimate in-situ neutralization.

5.2.4 Sources of In-Situ Neutralization

The apparent acid neutralization ratio of 60 to 80 percent in the Omega and T&T mine-pools is remarkable considering that the rock strata in this geological section near the mined Upper Freeport coal bed contain few carbonates (Hennen and Reger, 1913). Limited Acid Base Accounting analyses of roof and floor rock material of the Omega mine (EPRI, 2001) show a large excess of acid generating capacity and little carbonate present. Where does the in-situ neutralization originate? The following processes were considered:

- Alumino-silicate weathering and dissolution of oxyhydroxides
- Recharge water alkalinity
- Carbonate weathering
- Sulfate reduction
- Cation exchange and adsorption reactions

Mine-pool aquifers include some overburden rocks that have been disrupted by mining. Kendorski (1993) proposed a five layer subsidence model, and a zone of fracturing extending up to 24 times mine height which includes a collapsed overburden zone estimated as six to ten times mine height. The extent and severity of sagging, cracking, bedding plane separation, breakage and collapse of the overlying strata is a function of the type of mining and remaining support, and strength characteristics of the overburden rocks. Collapse and breakage can be near instantaneous, as in long wall mining, or may occur over years as pillars and roof supports weaken. Subsidence adds chemical and mineralogical content of overburden rocks to mine-pool chemistry.

Most of the water quality data in this study were originally collected for monitoring purposes, not research. Consequently, complete suite tests, redox measurements, mineralogical samples and other data useful for detailed source analyses are not available for many water samples. However, some partitioning of processes is possible.

Table 5-5 summarizes chemical characteristics of ground-waters recharging the five mine-pools. Recharge water sulfate ranges from about 14 to 53 mg/L and is an order of magnitude or more lower than corresponding mine-pool water in table 5-1. Calcium, Mg, and Na concentrations in recharge waters are also significantly less than mine-pool waters. The contrasting water compositions in tables 5-1 and 5-5 show that substantial chemical weathering of various minerals must be occurring in mine-pools, and that the weathering reactions include in-situ H^+ consumption as well as H^+ generation. Data in table 5-5 for the Omega and T&T mine-pools are site-specific overburden ground water samples, while data for the other three were estimated from published well records in the locale.

Table 5-5
Chemical Characteristics of Recharge Waters for Five Mine-pools[1]

Mine-pool	pH	Alkalinity	Fe	Al	SO_4	Ca	Mg	Na
Omega	7.2	100	0.4	0.05	14	40	10	3.5
T&T	6.7	120	0.6	0.2	21	39	9	3.9
Hahn Arden-Westland	7.4	260	0.3	-	53	76	17	30
Barnes&Tucker	7.0	142	0.3	0.1	27	43	6	2

(1) pH in S.U., alkalinity in mg/L $CaCO_3$ Eq., Fe, Al, SO_4, Ca, Mg and Na in mg/L. Recharge water composition from ground-water samples at T&T and Omega, data from Williams et al. (1993), for Hahn and Arden-Westland, and data from McElroy (1998), for Barnes&Tucker.

5.2.4.1 Neutralization from Aluminum Mineral Weathering

The Omega and T&T mine-pool discharges contain high concentrations of dissolved Al. Ground-waters circulating in non-acidified overburden aquifers contain insignificant amounts of soluble Al (see table 5-5). Soluble Al must be generated by weathering reactions within the mine-works.

Alumino-silicate minerals are generally slow to dissolve in low temperature settings. Jambor et al (2002) found that alumino–silicates did contribute a small amount to the Neutralization Potential test and tended to react at rates five to eight orders of magnitude slower than for carbonates. Both Jambor et al. (2002), and Eary and Williamson (2006), report that feldspar minerals react too slowly to provide effective acid neutralization, while other mineral such as calcic plagioclase were more significant acid neutralizers. Rate data, summarized by Palandri and Kharaka (2004), show kaolinite dissolution to be ten orders of magnitude slower than calcite under acid conditions. The acid weathering constant for kaolinite is about 100 times faster than at neutral pH, however. The slow weathering rates for alumino-silicate minerals are compensated by their abundance in rocks and sediments.

The concentrations of soluble Al and Si measured in the acidic Omega and T&T mine-pools are indicative of alumino-silicate dissolution. These drainages are relatively rich in Mg when compared to recharge water composition, and the mineral chlorite as one Mg source is commonly present in these rocks (Dulong et al., 2002). The complete dissolution of chlorite consumes H^+ as follows:

$$Mg_5Al_2Si_3O_{10}(OH)_8 + 16\,H^+ \rightarrow 5\,Mg^{2+} + 2\,Al^{3+} + 3\,H_4SiO_4 + 6\,H_2O \qquad (5\text{-}12)$$
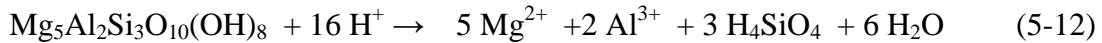
If Al is subsequently precipitated as hydroxide, the net acid consumption is still ten mmoles of H^+ per mmole of chlorite consumed. Weathering of other alumino–silicates is also typically acid consuming. Dolomite dissolution is another potential Mg source.

The dissolution of Al hydroxides also consumes three moles of H^+ per mole of Al:

$$Al(OH)_3 + 3\,H^+ \quad \leftrightarrow \quad Al^{3+} + 3\,H_2O \qquad\qquad (5\text{-}13)$$

As shown in equation 5-5, congruent dissolution of Al bearing minerals like kaolinite also consumes three moles of H^+ per mole of Al produced.

Two conditions favor acid neutralization by alumino-silicates; a very aggressive chemical weathering environment, or a lengthy residence time in the mine-pool. The aggressive weathering environment exists within the Omega and T&T mine-pools, characterized by solution pH of less than 3.0. That condition has persisted in those two mine-pools for more than ten years.

An average mine-pool residence time has been estimated from discharge records for the five mine-pools, and ranges from as little as 6 months to about 4 years. These estimates are based on a simple flow-through model and do not account for short circuiting, tortuosity, or no-flow zones. Nonetheless, these estimates suggest relatively short residence times in comparison to other bedrock aquifers and flow systems in Upper Pennsylvanian age rocks of the Appalachian region.

The fraction of in-situ neutralization provided by alumino-silicate and oxyhydroxide mineral weathering was estimated, based on three moles of H^+ per mole of Al for the Omega and T&T mine-pools, and assuming the increases in Al concentration result from mineral weathering in the mine-pool.

Figure 5-9 is a time series plot of "pyrite acidity" (equation 5-9), H^+ consumption attributed to aluminum mineral weathering, and H^+ consumption attributed to Ca, Mg, Na
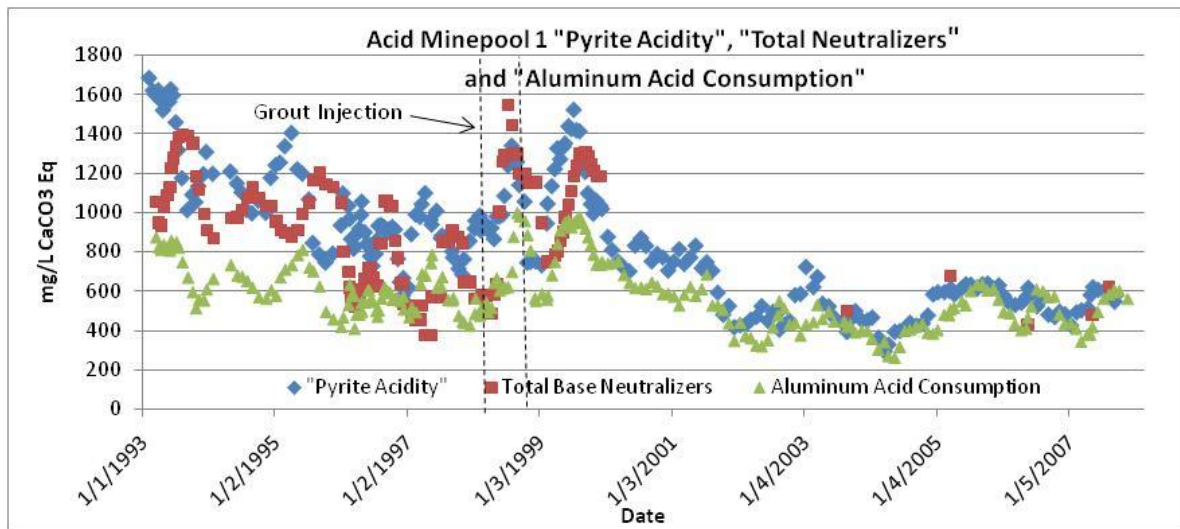
Figure 5-9. "Pyrite Acidity"(Blue), Base Neutralizers (Red), and H^+ Consumption from Alumino-Silicate Mineral Weathering (Green), Omega Mine-pool.

and K mineral weathering ("total neutralizers") in the Omega mine-pool. H^+ consumption was compiled as three moles H^+ per mole Al, two moles H^+ per mole of Ca and Mg, and one mole H^+ for Na and K. Each parameter is plotted as mg/L $CaCO_3$ Eq., the customary

units for reporting acidity and alkalinity, to facilitate direct comparison. Al mineral dissolution averages the equivalent of 465 mg/L acid consumption, or about 40 % of the total neutralization occurring in the mine-pool. All three parameters decrease as the mine-pool ages, showing declining weathering capacity. The effects of grout injection in 1999 are clearly visible, displacing accumulated weathering products as a short term increase in acidity, bases and Al.

Weathering of Al minerals is still occurring after 14 years. The long-term average dissolved Al content is equivalent to consuming about 1.5 mmoles of kaolinite per liter of mine-pool solution.

Figure 5-10 shows the distribution of pyrite acidity, base neutralizers and H^+ consumption attributed to weathering of alumino-silicates and oxyhydroxide mineral weathering in the T&T mine-pool. The data were compiled in the same manner as in the Omega mine-pool. Aluminum mineral dissolution averages the equivalent of 195 mg/L acid consumption, or about 20 % of the total neutralization occurring in the mine-pool.
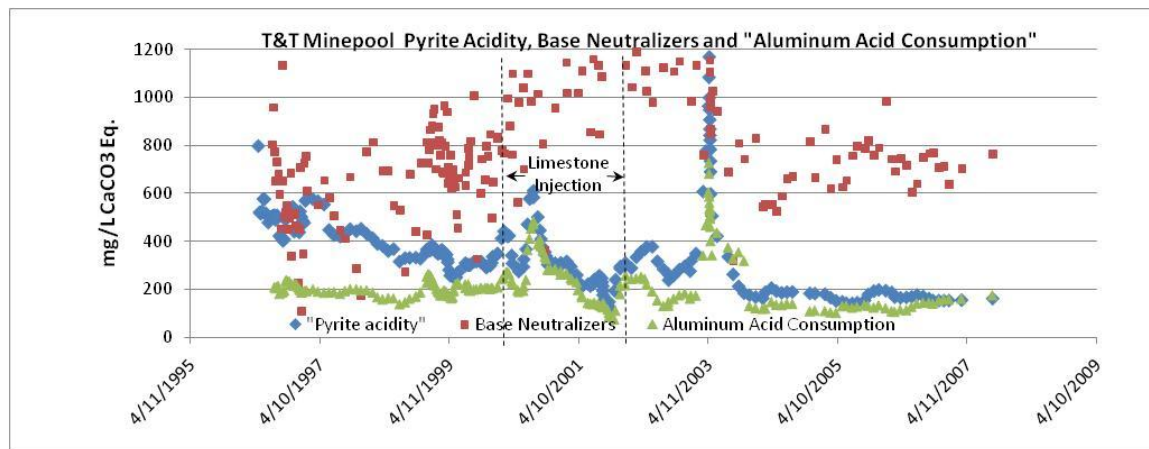
Figure 5-10. "Pyrite Acidity", Base Neutralizers, and H^+ Consumption from Alumino-Silicate Mineral Weathering, T&T Mine-pool.

The long-term average dissolved Al content is equivalent to consuming about 0.7 mmoles of kaolinite per liter of mine-pool solution.

Aluminum concentrations in the three circumneutral mine-pools, Hahn, Arden-Westland and Barnes&Tucker, are minimal, due to solubility constraints. Thus, there is little direct evidence of alumino-silicate weathering in these mines. However, Al dissolution could occur in the small unflooded and presumably acidic sections, with subsequent secondary mineral formation within the pool.

The Al–sulfate mineral jurbanite is at apparent saturation or super saturation in the Omega mine-pool (Perry and Rauch, 2004, Appendix A) and approaches saturation in the T&T mine water discharge. Direct examination of solids to confirm or refute the presence of a mineral phase is not possible, because the mine-works are not directly accessible for sediment sampling. Jurbanite could form as an alteration product of kaolinite in sulfate

rich environments, or as a hydrolysis precipitate product, and is stable in low pH environments of about three to five (Nordstrom, 1982b):

$$Al_2Si_2O_5(OH)_4 + 2\,SO_4^{2-} + 11\,H_2O + 4\,H^+ \leftrightarrow$$

$$2\;AlOHSO_4*5\,H_2O + 2\,H_4SiO_4\;\;\text{or} \qquad (5\text{-}14)$$

$$Al^{3+} + SO_4^{2-} + 6\,H_2O \leftrightarrow AlOHSO_4*5\,H_2O + H^+ \qquad (5\text{-}15)$$
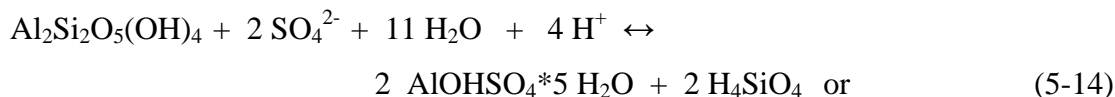
The possible presence of a mineral phase limiting Al solubility shows that the discharge chemistry, while containing high concentrations of dissolved Al, may actually underestimate the full extent of alumino-silicate mineral dissolution.

Should aluminum mineral weathering be counted as in-situ neutralization? Soluble Al, a component of mineral acidity in mine-pool waters, is usually removed during water treatment by base addition and hydrolysis. That neutralization process neutralizes the three moles H^+ generated per mole Al that is precipitated, equal to that originally consumed. In this case, Al weathering produces a net neutralization of zero. Partial hydrolysis, as shown in equation 5-15, generates one mole H^+ per mole Al, with a net neutralization of two moles H^+ per mole Al.

The in-situ neutralization data for the Omega and T&T mine-pools were recalculated to exclude acid consumption by alumino-silicate weathering, assuming that zero net neutralization describes the fate of dissolved Al draining from the mine-pool. The remaining neutralization, termed "effective neutralization" is attributable to other sources, including carbonates, recharge water alkalinity or other processes that do not regenerate acidity elsewhere in the system.

Effective Neutralization is calculated as:

$$\text{Effective Neutralization Ratio} = [(EMAP - Acidity_{total})/EMAP]*100 \qquad (5\text{-}16)$$

Where EMAP and $Acidity_{total}$ are as defined in equation 5-7 and 5-8, respectively. $Acidity_{total}$ is computed from Fe(II), Al, Mn and H^+, and equation 5-16 simply assigns soluble aluminum exiting the mine-pool a net acid production/neutralization of zero.

Figures 5-11 and 5-12 show mean Neutralization Ratio and Effective Neutralization Ratio values for the Omega and T&T mine-pools. Both of these mine-pools contain concentrations of dissolved Al in the tens to more than 100 mg/L. The data are grouped by all records, pregrout or limestone injection and post injection. No calculations were performed for the Hahn, Arden-Westland and the Barnes&Tucker mine-pools, because their waters contain only small amounts of soluble Al.

"Effective neutralization" in the Omega mine-pool is about 20 to 25% less when dissolved Al from mineral dissolution is excluded as a neutralization process. Nonetheless, nearly half of the maximum acid production is unaccounted for and is

attributed to in-situ neutralization. Even after 14 years of aggressive chemical weathering, other minerals or processes must still be supplying acid neutralization to the Omega mine-pool.

A similar trend is apparent in the T&T mine-pool. In-situ neutralization is reduced about 11 to 15% when dissolved Al from mineral dissolution is excluded. However, even with this conservative assessment of neutralization, more than half of the projected maximum acid production is "missing" and is attributed to in-situ neutralization. Other minerals or processes must still be consuming H^+ after more than ten years of weathering in a highly acidic environment.
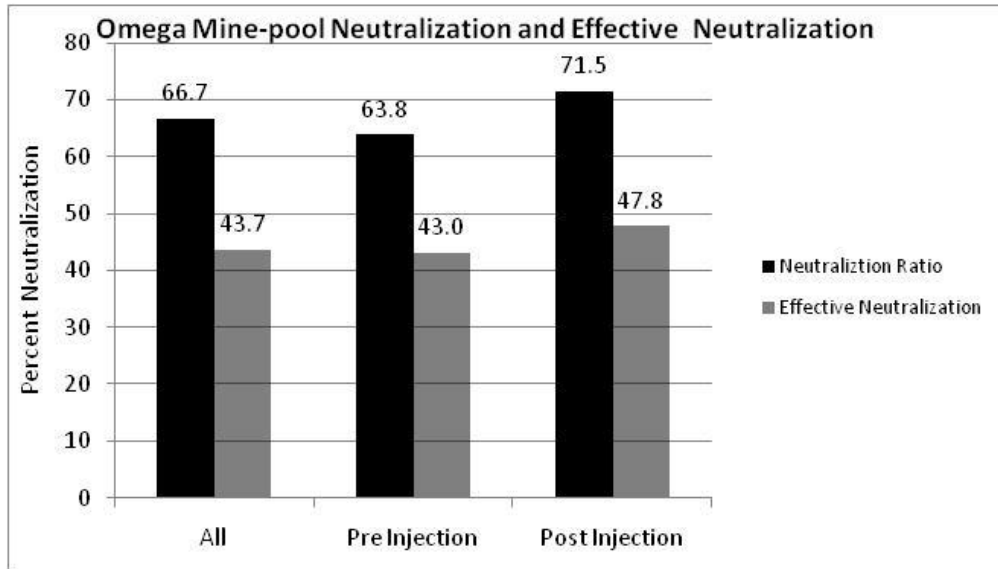
Figure 5-11. Mean Neutralization Ratio and Effective Neutralization Ratio Percentages (Excluding H^+ Consumption by Al Minerals), Omega Mine-pool.
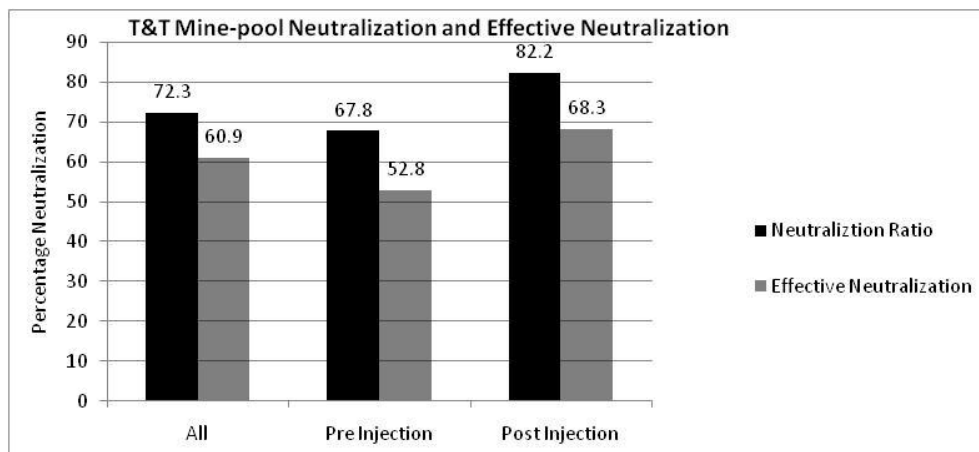
Figure 5-12. Mean Neutralization Ratio and Effective Neutralization Ratio Percentages (Excluding H^+ Consumption by Al Minerals), T&T Mine-pool.

144

Both mines have increased effective neutralization after grout or limestone treatment. The improvements were a relatively modest gain of about five percent over pre-treatment conditions for Omega, and over 15% for T&T. Neutralization data can be used to assess the effectiveness and efficiency of in-situ abatement techniques.

5.2.4.2 Neutralization by Recharge Water

The contribution of recharge water to in-situ neutralization was assessed using a mass balance approach and assuming fixed flow-through conditions. The long term net storage change, ΔS, in the mine-pool volume is presumed to be zero. This assumption is justified by relatively constant pumping rates and water levels in the Hahn, Arden-Westland and Barnes&Tucker mine-pools. The Omega and T&T mine-pools do fluctuate on a short term basis, but display no obvious long term head or discharge changes. Chemistry of recharge water entering mine-pools from overlying aquifers was assessed from a combination of sampling by the author, and review of published background water data. Recharge water alkalinity assigned to each mine is shown in table 5-5, and was assumed to be constant through time. For the Omega and T&T mine-pools, site specific water data are similar to the average bicarbonate data reported by Hobba (1984) for rocks of the Allegheny group. Recharge alkalinity was potentially significant since it represents an essentially inexhaustible source of acid consumption. Recharge water alkalinity neutralizes acidic mine water as:

$$HCO_3^- \; + \; H^+ \; \leftrightarrow \; H_2CO_3 \qquad\qquad (5\text{-}17)$$

Recharge water neutralization is expressed as percentage of the total neutralizers:

$$\% \text{ Recharge Neutralization } = (\text{Recharge Alkalinity}/(\text{EMAP- Acidity}_{pyrite}))*100 \qquad (5\text{-}18)$$

where EMAP and Acidity$_{pyrite}$ are as defined in equation 5-7 and 5-9. The difference of EMAP- Acidity$_{pyrite}$ is an estimate of the total strong acid neutralization, including alumino-silicate dissolution without differentiating sources. The median results are in table 5-6, summarized for all data, early and late phases of pool flooding. A time series for the Hahn discharge is shown in figure 5-12.

Recharge water alkalinity has the smallest contribution to in-situ neutralization in the two acidic mine-pools; only about 5 to 7% in Omega and 12 to 14 % in T&T. Further, the recharge water neutralization is essentially constant or near steady state for a period of more than ten years in both pools. Mineral weathering, including consumption of alumino-silicates and oxhydroxides, continues to be to the principal source of H^+ consumption in these two mines. Recharge water alkalinity does not contribute significantly to neutralization in strongly acidic, aggressive weathering environments like the Omega and T&T mine-pools.

Figure 5-13 shows a trend of increasing recharge water neutralization of the Hahn mine-pool as it ages. The other alkaline mine-pools also show increasing recharge water neutralization through time as mineral weathering declines (table 5-6). Figure 5-12 shows that recharge water neutralization was minor comprising less than ten percent of total

neutralizers. Soon after flooding was complete in 1984, recharge neutralization steadily increased afterwards and was 25 to 30% of the total neutralizers by 1999. Recharge water contributes to in-situ neutralization, and becomes more important as alkaline mine-pool water ages. This results from recharge water alkalinity remaining constant while acid production and sulfate concentration decline as the mine-pool ages. Recharge alkalinity, while important, is not the dominant neutralization process in the Hahn, Arden-Westland and Barnes&Tucker mine-pools.

Table 5-6
Fraction of Neutralization
Supplied From Recharge Water Relative to Estimated Total Neutralization [1]

Mine-pool	Recharge Alkalinity	All data	Early Phase	Late Phase
Omega	100	6% (1677)	Pre-inject 5.7% (1765)	Post-inject 6.3% (1579)
T&T	120	12.3% (1002)	Pre-inject 13.9% (908)	Post-inject 12% (998)
Barnes&Tucker	142	29% (488)	Pre-flood 15.6% (908)	Post-flood 39.5% (360)
Hahn	260	7.6% (3406)	Initial Flush 4.6% (5653)	Post-flush 19% (1337)
Arden-Westland	260	21.3% (1220)	Initial Flush 20% (1316)	Post-flush 32% (801)

(1) Recharge alkalinity in mg/L $CaCO_3$ Eq. Values in parentheses are estimated total neutralizers in mg/L $CaCO_3$ Eq. Early phase is initial flooding and flushing, late phase is long term weathering.
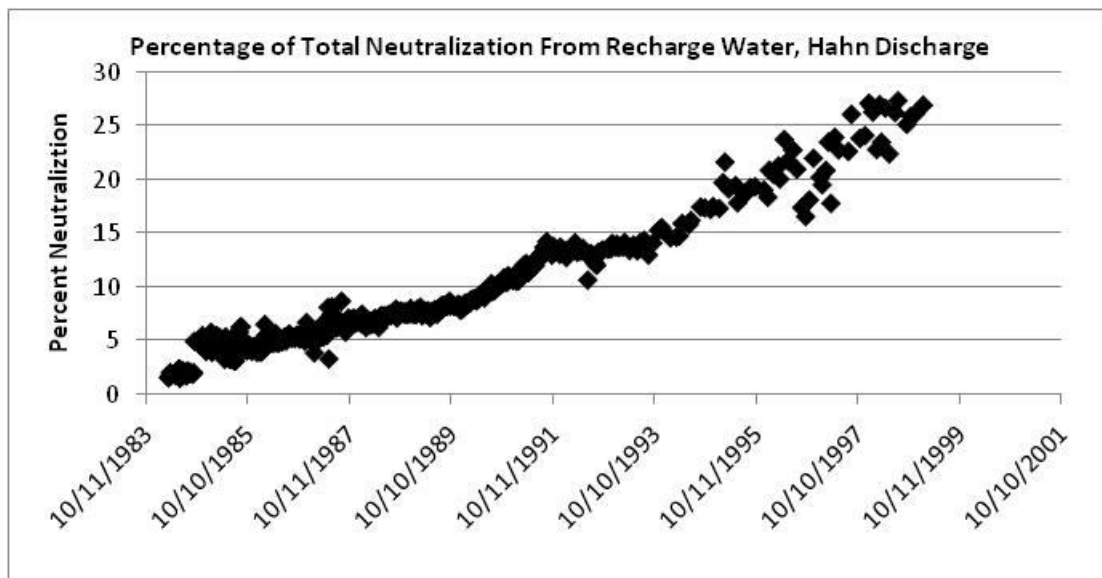
Figure 5-13. Estimated Percentage of Neutralization Supplied by Recharge Water, Hahn Mine-pool Discharge.

146

5.2.4.3 Neutralization by Carbonate Mineral Weathering

Carbonate minerals are the most obvious source minerals to provide in-situ neutralization in a mine-pool aquifer. The increase in mine-pool Ca and Mg concentrations over that supplied by ground water recharge could represent weathering of carbonates within the mine-pool, and perhaps of other minerals such as chlorite as a Mg source. The additional mine-pool Ca and Mg sum exceeding recharge water concentration was converted to $CaCO_3$ Eq., as if it all represents carbonate mineral neutralization. The amount of total neutralizers calculated from equation 5-10 (difference method), and neutralization attributed to increased mine-pool Ca and Mg were compiled for the Hahn discharge, and parts of the Omega and Arden-Westland records. Results are shown figure 5-14 to 5-16 and represent median values.
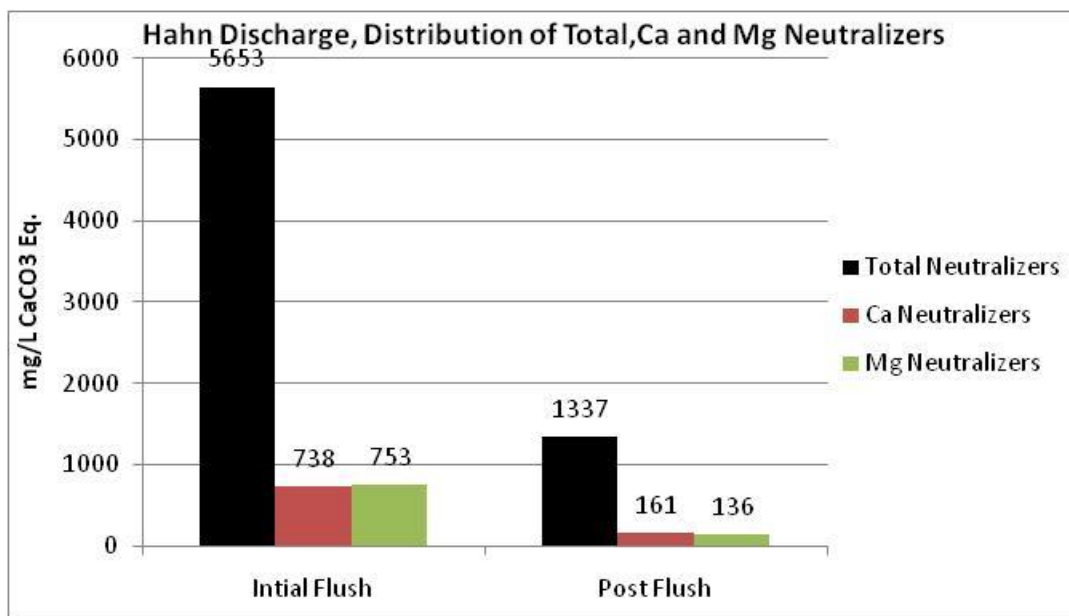
Figure 5-14. Hahn Discharge Distribution of Total
Ca and Mg Neutralization in Initial Flushing and Post Flushing.

The Hahn discharge has extremely high neutralization values, exceeding 5000 mg/L $CaCO_3$ Eq. during initial flushing (fig 5-14). Calcium and Mg combined represent about 1500 mg/L, or 26% of the total neutralizers. The remainder is attributed to Na, which was present in excess of 2000 mg/L initially. Donovan et al. (2003) report that the pool was near saturation for calcite during initial flushing, so it seems likely that mine-pool carbonate dissolution accounts for part of the observed Ca and Mg. Post-flushing neutralization values declined to less than 20% of initial conditions as shown in figure 5-14, and Ca and Mg account for 22% of the total. The post-flushing waters are under-saturated for calcite (Donovan, 2003), so carbonate contribution is less certain.

The acidic Omega discharge (figure 5-15) had median neutralization of 1765 mg/L $CaCO_3$ Eq., of which about 51% was attributable to Ca and Mg. The remainder is mostly accounted for by weathering of Al minerals (section5.2.4.1). The waters are orders of magnitude under-saturated for calcite and the Mg bearing mineral chlorite, but are

slightly under-saturated for gypsum as determined from equilibrium calculations in PHREEQCI.

The Arden-Westland drainage (figure 5-16) had the lowest total neutralizers, and Ca and Mg accounted for almost 70% of the total. Sodium accounted for most of the remaining neutralization. The waters were under-saturated for both calcite and gypsum as determined by equilibrium calculations in PHREEQCI.
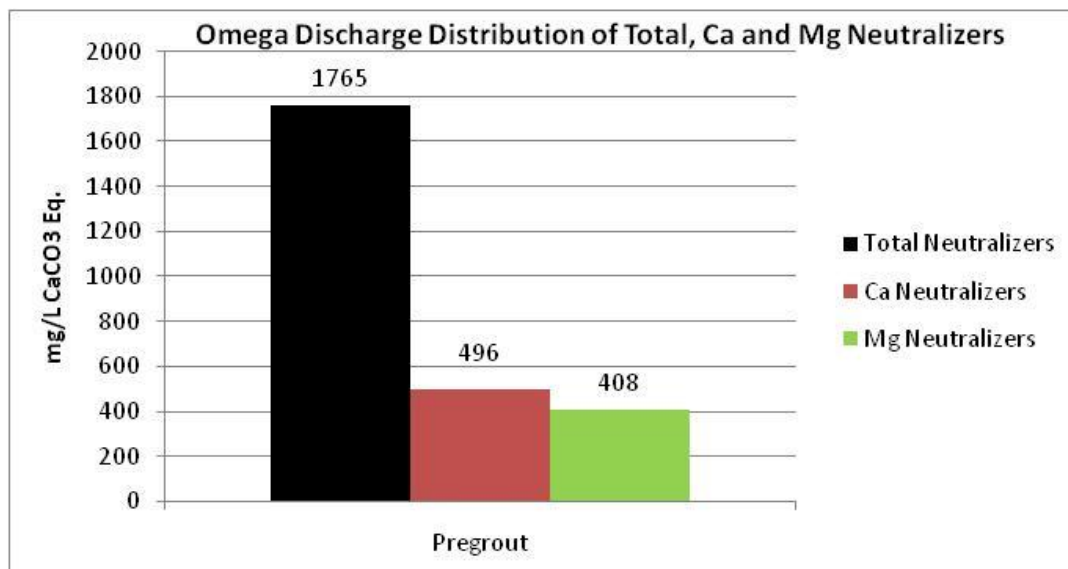
Figure 5-15. Omega Discharge Distribution of
Total Ca and Mg Neutralization before Grout Injection.
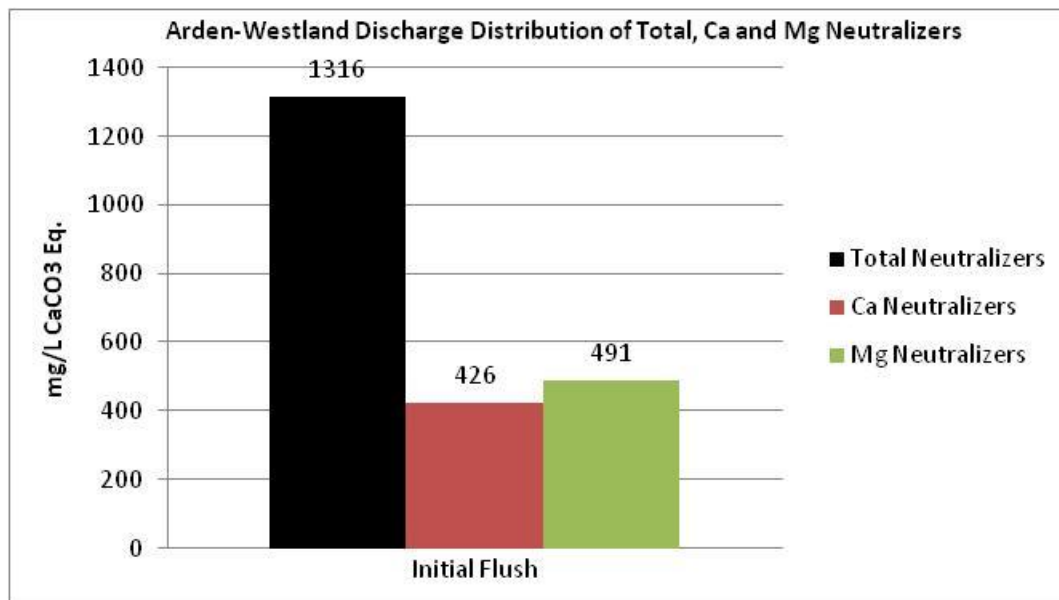
Figure 5-16 Arden-Westland Discharge Distribution of Total
Ca and Mg Neutralization in Initial Flushing.

All three mines show significant consumption of Ca and Mg minerals, although the precise source(s) can only be inferred from solubility considerations, solution composition and general mineralogy of the rocks. Solubility controls complicate interpretation of the discharge chemistry. Gypsum controls on soluble Ca could not be discounted for the Omega and Hahn mine-pools, and common ion effects of Ca-gypsum-calcite could control Ca. Appendix B describes inverse modeling of water quality evolution in Pittsburgh coal bed mine-pools. Those models show that carbonate dissolution, and other mineral reactions, including gypsum dissolution could explain the generation of alkaline mine waters and changes in solution composition. Modeling results described in Appendix B suggest that carbonate dissolution is probably the single most important mineral neutralization mechanism in mine-pools. Magnesium has potential source minerals other than carbonates, such as chlorite, and changes in Mg concentration could not be assigned solely to carbonate minerals.

5.2.4.4 Neutralization by Sulfate Reduction

Sulfate reduction occurs in oxygen poor environments, like flooded mine-pools, and produces bicarbonate alkalinity. At pH 7 and 25ºC, the equilibrium sulfide-sulfate redox couple is -217 mill volts (Langmuir, 1997). Sulfate reduction is unlikely to take place in aerated Omega and T&T mine-pools, where dissolved oxygen levels of one to more than five mg/L were measured by the author. The flooded sections of Arden-Westland, Hahn and Barnes&Tucker, however, may provide suitable conditions. The reaction is driven by heterotrophic bacteria such as the genus *Desulfovibrio* and is often represented as:

$$2\,CH_2O + \ SO_4^{2-} \ \rightarrow \ H_2S \ + 2\,HCO_3^- \ or \hspace{2cm} (5\text{-}19a)$$

$$CH_4 + \ SO_4^{2-} \ \rightarrow \ HS^- \ + 2\,HCO_3^- \ + H_2O \hspace{2cm} (5\text{-}19b)$$

where CH_2O represents organic compounds, CH_4 (methane), or other simple organic molecules. The optimal pH range for *Desulfovibrio* is between about 6 and 8 (Baas Becking et al., 1969). Other microbes may also participate in or facilitate sulfate reduction (Barton, 1995).

The Estimated Maximum Acid Production (EMAP), equation 5-7, is based on two moles of H^+ produced per mole of SO_4^{2-}. Sulfate reduction, as in equation 5-19, reduces the quantity of EMAP, and produces two moles bicarbonate alkalinity per mole of S reduced. If the reaction proceeds further to sulfide precipitation, H^+ is regenerated as in the formation of FeS:

$$Fe^{2+} \ + \ H_2S \ \rightarrow FeS \ + \ 2\,H^+ \hspace{2cm} (5\text{-}20)$$

Biological Reactivity Test (BART) vials were inoculated with raw mine water at the Omega, T&T, and Barnes&Tucker mine-pools. The BART vials contained nutrient media for specified groups of microbes, and could be used for presence or absence determinations. The acidic and oxygenated Omega and T&T mine-pools returned a negative response to sulfate-reducing bacteria (SRBs). The oxygen–poor and mostly flooded Duman discharge of the Barnes&Tucker mine-pool produced a strong positive

response for SRBs, however. Trace amounts of dissolved sulfide were also detected in field tests, and the characteristic "rotten egg" odor of H_2S was detectable. While sulfate reduction was not directly measured in the mine-pool, circumstantial evidence suggests it is likely to occur in flooded circumneutral mine waters. Mine waters collected by the author from several wells in a large circumneutral (pH~7) mine-pool near Fairmont, WV, have also tested positive for SRBs.

5.2.4.5 Neutralization from Oxyhydroxide Minerals
Dissolution of existing metal oxyhydroxide minerals represent yet another potential in-situ neutralization mechanism for strong acidity as shown by:

$$Fe(OH)_3 + 3 H^+ \leftrightarrow Fe^{3+} \ 3 \ H_2O \qquad (5\text{-}21)$$
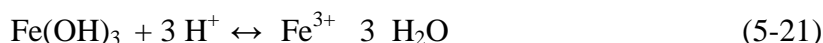
The reaction is reversible depending on pH. During the initial acidification of a mine-pool aquifer, reaction 5-21 could be driven to the left and dissolve existing oxyhydroxide minerals with subsequent H^+ neutralization. A simple calculation suggests this could provide substantial strong acid consumption in the short term. For a mine-pool aquifer with 20% water filled porosity, 80% rock matrix with specific gravity of 2.6, and the rock matrix contains one percent $Fe(OH)_3$, a large quantity of hydroxide mineral is potentially available to react. In one m^3 of aquifer, total $Fe(OH)_3$ is:

 mmoles $Fe(OH)_3$ = 0.8 m^3 x 2.6g/cm^3 x $10^6 cm^3/m^3$ x 0.01 x 10^3mg/g x 1 mmole/103.85 mg

or about 200,000 mmoles of $Fe(OH)_3$. The 20% water filled aquifer contains 200 liter/m^3 of fluid. Potentially about 1000 mmoles of hydroxide per liter of solution is available. Only a very small fraction of the hydroxide need react to provide significant H^+ consumption. The system potentially renews itself as the water flows into the next unit of aquifer matrix.

Oxyhydroxide neutralization likely represents a temporary acid consumption mechanism. The reaction is reversible, and as neutralization of acidic mine-pool increases pH, oxyhydroxides precipitate and acidity is regenerated. Therefore these types of reactions are not likely to be a significant source of strong acid production. Kinetic considerations also constrain the rate of oxyhydroxide dissolution.

5.2.4.6 Neutralization by Cation Exchange Cation exchange is another reversible reaction that may remove H^+ from solution. Back (1966) in describing hydrochemical facies for ground water, concluded that Na was exchanging for Ca in Atlantic Coastal Plain aquifers as ground water moved through the aquifer. Back also observed that the composition of the water depended on its location in the flow system. Perry et al. (2005, Appendix D) concluded that sorbed Na exchanges into the aquifer for Ca and Mg in the Barnes&Tucker mine-pool. The end of flow path Duman discharge is enriched in Na and depleted in Ca and Mg compared to its' source waters. The Barnes&Tucker mine-pool has a maximum flow path of about 16 km. H^+ could be removed from mine-pool water by exchange for Na^+ as graphically illustrated in figure 5-17.

A large number of exchange sites are potentially available in an extended flow system. Using the same mine-pool aquifer example described above for hydroxide neutralization; 20% water filled porosity, 80% rock matrix; and assuming a modest cation exchange capacity of 2 meq/100 g of rock, the amount of exchangers is:
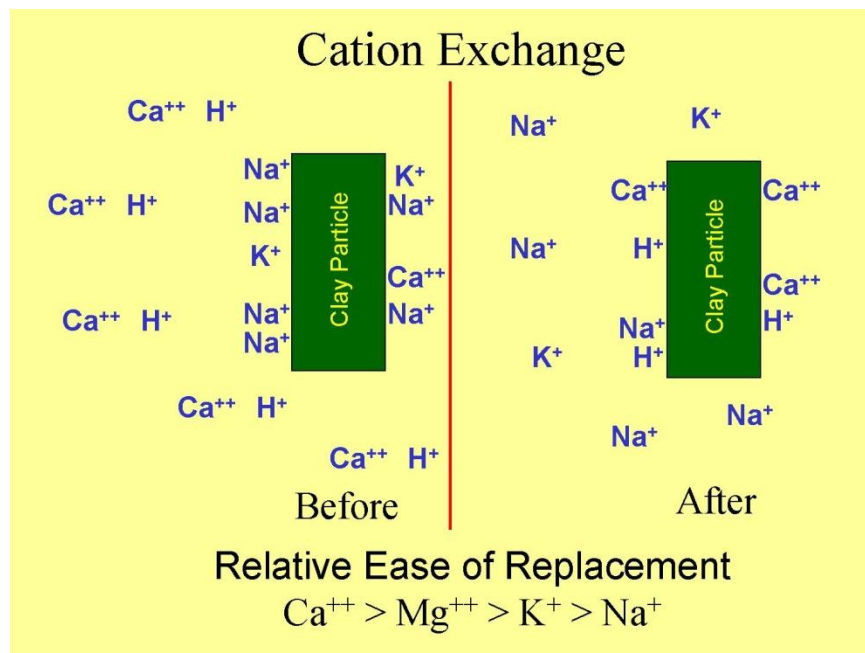

Figure 5-17. Conceptual Cation Exchange in Acid Waters. H$^+$ is Adsorbed to Exchange Sites on Clays. The Reactions are Reversible if Solution Composition Changes.

Total Exchangers (meq) = 0.8 m^3 x 2.6g/cm^3 x 10^6 cm^3/m^3 x 2 meq/100 g

or 41,600 meq in one m^3 of aquifer. In the 200 L of aquifer solution, potentially about 208 meq of exchangers are available per liter of solution. Like hydroxide neutralization, only a small fraction of the exchange capacity need react with the solution to provide significant attenuation of H$^+$. As with the hydroxide minerals, the system potentially renews itself as the water flows into the next unit of aquifer matrix. The exchange reactions are potentially reversible if solution composition changes. The H$^+$ exchange capacity is finite. Thus, long term acid attenuation by exchange reactions is probably limited.

5.3 Decay Functions for Estimating Time Dependent Chemical Composition
This section presents results of fitting decay functions to time series chemical data to describe the rate of change, and estimate future mine-pool chemical composition.

Time series plots of chemical concentrations in the five mine-pools often exhibited curvilinear behavior. Figure 5-18, iron concentration in the Hahn discharge, exemplifies this trend. A log-log scale (base ten) plot of concentration vs. time (figures 5-19 and 5-20) are similar to idealized plots of first or second order rates laws, like those shown by Langmuir (1997). The X-axis is log scale base ten in days, and the Y axis is log scale

base ten Fe concentration in mg/L in figures 5-19 and 5-20. This suggests the long-term chemical trends can be represented by an exponential expression which describes the rate of change as a function of time, and that the changes are related to fundamental chemical principles.
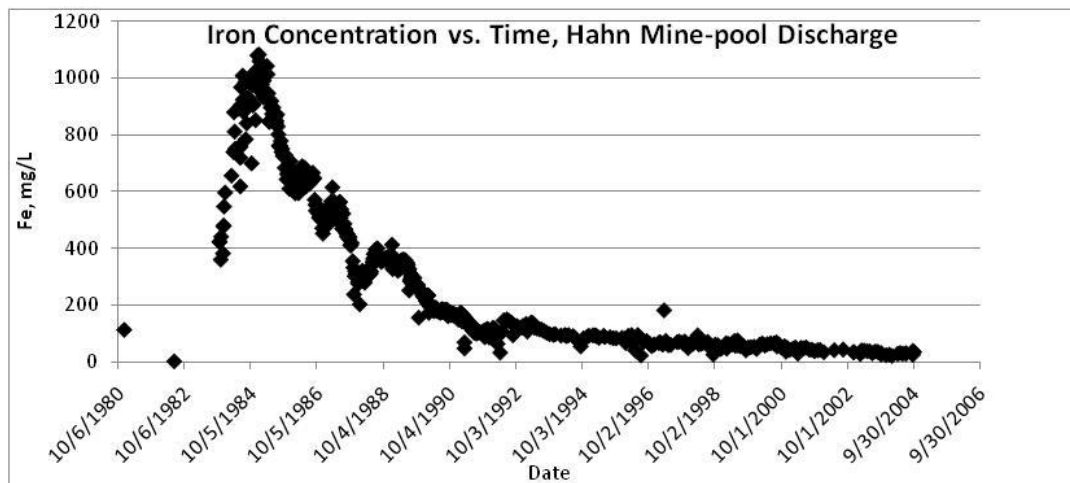
Figure 5-18. Time Series Plot of Fe Concentration, Hahn Discharge, Showing Exponential Rate of Change.
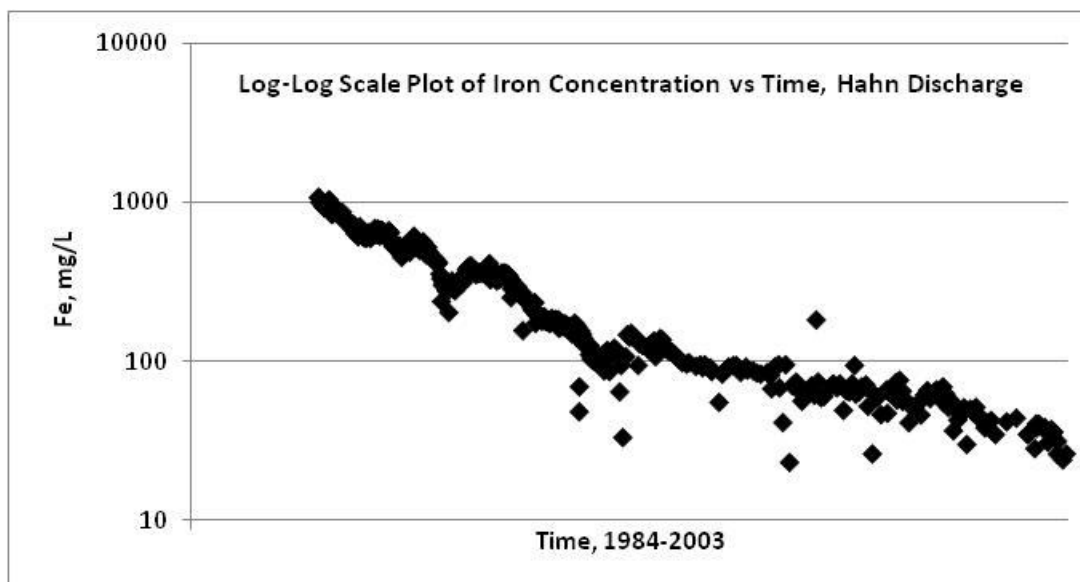
Figure 5-19. Log–log Scale Plot of Iron vs. Time Hahn Discharge. Same Data as Figure 5-18. X-axis is log Scale Base 10, Days, from 1984-2003. Y Axis is log Scale Base 10. Fe concentration in mg/L.
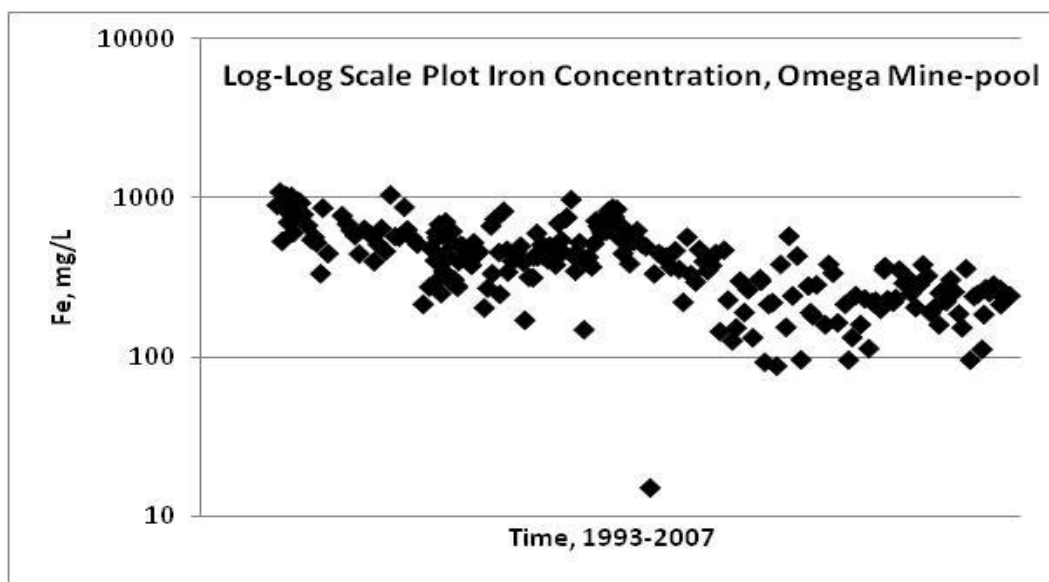
Figure 5-20. Log–log Scale Plot of Iron vs. Time Omega Mine-pool Discharge.
X-Axis is log Scale Base 10, Days, 1993-2007. Y Axis is log Scale Base 10, Fe in mg/L.

The behavior of many chemical and biological systems has been described using a first order function of the general form:

$$C_t \quad = \quad C_o \, x \, e^{-kt} \tag{5-22}$$

where: C_t = concentration at time t
  C_o = concentration at time zero
   e = base e, approximate value of 2.718
   k = decay constant, rate of concentration change per unit time
   t = time

The function in equation 5-22 is sometimes used to describe radioactive decay. The changes with time in mine-pool chemistry are not radioactive processes and therefore, strictly speaking, are not decay processes, but are a rate of change with a similar mathematical description. Gzyl and Banks (2007) use the term "decay" to describe the rate of change in pH and sulfate concentration in flooding Polish coal mines. The term decay is used for convenience in this chapter in the context of describing rate of change in mine-pool chemical concentration.

Decay constants (k) were estimated for chemical parameters Fe, Al, sulfate, total dissolved solids (TDS), and total acidity, where data were available. Aluminum decay constants were computed just for the Omega and T&T mine-pools because only these two sites had appreciable concentrations of Al.

5.3.1 Method for Estimating Decay Constants
Four of the five mine-pools had distinct changes in chemical composition that were related to flooding phase or in-situ treatment. Only the Arden-Westland mine-pool lacked

distinct changes, and the early flooding record was not available for this site. The monitoring record was analyzed for decay behavior in several ways including:

- A single decay function for the entire period of record, assuming flooding phase or in-situ treatment had no effect on decay.
- Dividing the record into pre and post in-situ treatment and computing separate decay values for each period.
- Computing decay on data smoothed with a 5 point moving average.
- Computing decay based on yearly average values.
- Dividing the record based on flooding phases, and computing separate decay values for each period.
- Examining log-log scale plots of concentration against time for rate changes, manifested by change in slope.

Because each mine-pool has a unique history, and different record of sampling and analyses, not all of the above techniques were used for each mine-pool. Pertinent details of each mine-pool history are contained in chapter three and Appendix A for the Omega and T&T mine-pools, chapter four and Donovan et al. (1999) for Hahn, Arden-Westland, and chapter four and Appendix D for the Barnes&Tucker mine-pool. The principal events and observations used to subdivide the record for each mine-pool are summarized as follows.

Omega mine-pool – Grout injection in one section of the mine for drainage control and in-situ treatment. Separate decay constants estimated for pre and post grout injection records, and one set of k values for the entire period of record. Post grouting subdivided based on apparent mineral solubility controls. Smoothed data and yearly averages used to approximate the full record.

 T&T mine-pool – Limestone injection for in-situ treatment. Separate decay constants estimated for pre and post limestone injection records and one set of k values for the entire period of record. Post limestone injection subdivided based on apparent mineral solubility controls. Smoothed data and yearly averages used to approximate the full record.

Hahn (Montour 4) mine-pool – Initial flushing phase, followed by pumping to maintain constant pool elevation. Separate decay constants estimated for initial flushing phase and constant head phase, and one set of k values for the entire period of record.

Arden-Westland mine-pool - Initial flushing phase, transition period and long term flushing with pumping to control pool elevation. Separate decay values for each period and one set of k values for the entire period.

Barnes and Tucker mine-pool – Flooded phase with pumping to maintain constant pool elevation. Flooding of overlying vertically connected mine-works, with increased pumping to maintain constant pool elevation. Separate decay constants estimated for

before and after flooding overlying mine-works, and one set of k values for the entire period of record, using yearly average values.

The decay constant, k, was estimated by rearranging equation 5-22, to give the following:

$$C_t/C_o = e^{-kt} \qquad\qquad (5\text{-}22b)$$

$$\ln(C_t/C_o) = -kt \qquad\qquad (5\text{-}22c)$$

$$k = -\ln(C_t/C_o)/t \qquad\qquad (5\text{-}22d)$$

An X-Y plot of ln(Ct/Co) and t should yield a straight line with a slope of k. If concentration data are expressed in consistent units, then k has dimensions of t^{-1}.

Figures 5-21 and 5-22, respectively, show Fe data from the Hahn discharge (flooded mine) and Fe data from the Omega mine-pool discharge (unflooded mine) plotted in this manner. These are the same monitoring records shown in the log-log plots in figs 5-19 and 5-20, respectively.

 In general, water quality data at the Hahn discharge followed a fairly distinct curvilinear trend pattern. The Hahn drainage was therefore expected to provide a good fit to a natural log decay function. Slope of the plot was determined using least squares linear regression techniques. Figure 5-21 shows good agreement between the iron data and the log function. An R^2 of 89% was obtained for this plot and the results are statistically significant (p<0.01).
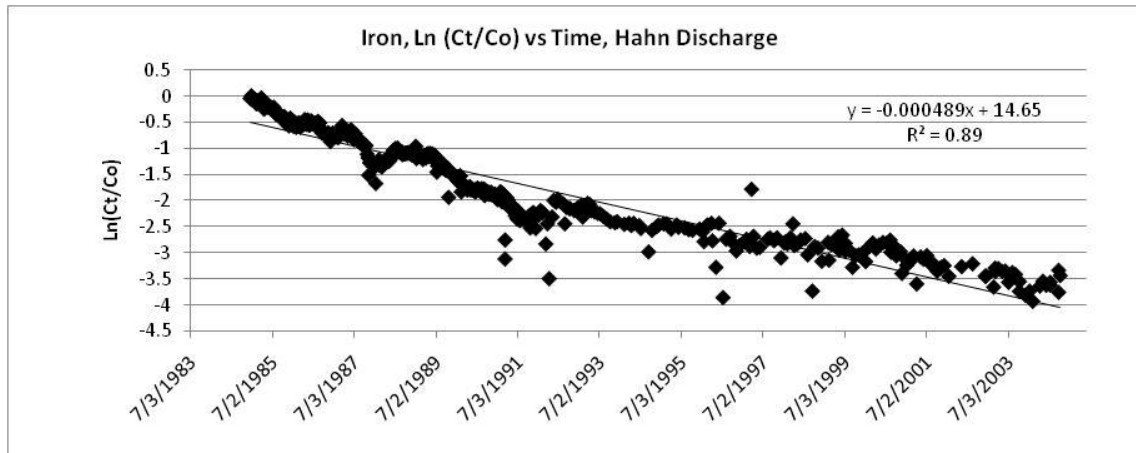
Figure 5-21. Plot of Ln(Ct/Co), Iron Concentration, Against t, Time, Hahn Discharge. Slope Equal k, Decay Constant.

While the overall fit is good, closer examination of figure 5-21 reveals that the data do not plot on one continuous slope. There is a small but distinct slope change occurring about 1992. While a single decay function might provide adequate estimates of decay, two constants represent the two different stages of early flushing and long term conditions. This large, mostly flooded mine-pool displays relatively small short term

variation. Therefore concentration changes estimated from properly derived decay functions should have a relatively narrow confidence interval.
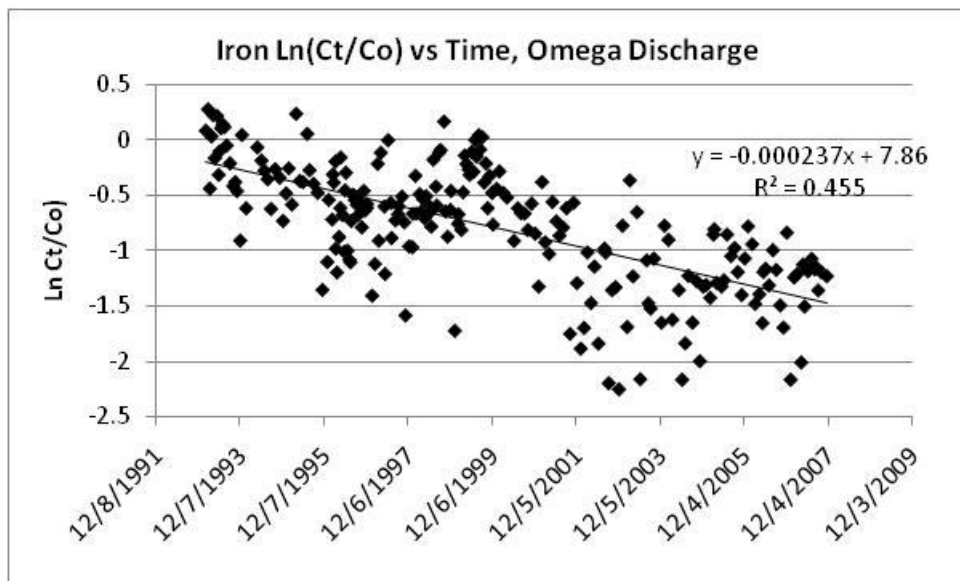
**Figure 5-22. Plot of Ln(Ct/Co), Iron Data Against t, Time,
Omega Mine. Slope Equal k, Decay Constant.**

Figure 5-22 shows much greater data scatter in the mostly unflooded Omega mine-pool. A slope change occurs about 1998, corresponding to grout injection. The regression model and slope for the entire data set are significant (p<0.01), but with a lower R^2 of about 45%. Since grouting affects the decay sequence, concentration estimates could be improved by subdividing the record into pre and post grout conditions. Data from the mostly unflooded Omega and T&T mine-pools have large short term variations. Concentration estimates derived for these mine-pools have a relatively wider confidence interval than for pools like the Hahn discharge.

Decay constants were derived by identifying slope breaks on log-log plots, identifying known events such grout injection, and using the natural log function and regression techniques illustrated in figures 5-21 to 5-22 for the other parameters across the five mine-pools.

5.3.2 Computed Chemical Decay Constants
Decay constants based on concentration data for Total Acidity, Fe, Al, sulfate and TDS for the five mine-pools are shown in tables 5-7 (acidic, partly flooded Omega and T&T mines) and 5-8 (mostly flooded circumneutral Hahn, Arden-Westland and Barnes&Tucker mines) in units of day^{-1}. Table 5-8 also includes constants for pH in the Hahn, Arden-Westland and Barnes&Tucker mine-pools. The tables also contain the percentage coefficient of variation (R^2) to illustrate the strength of the derived relationships. Decay constants that were not statistically significant at p=0.05 are highlighted in italics and shown as N.S. for R^2.

Table 5-7

Chemical Concentration Decay Constants (d^{-1}) Estimated Using Different Data for Two Acidic Mostly Unflooded Mines

Mine	Period of Record	Total Acidity k(d^{-1})	R^2	Iron k(d^{-1})	R^2	Aluminum k(d^{-1})	R^2	Sulfate k(d^{-1})	R^2	TDS k(d^{-1})	R^2
Omega all data	3/93 to 11/07	-2.35×10^{-4}	21.5	-2.59×10^{-4}	45.5	-1.09×10^{-4}	9.1	-1.31×10^{-4}	26.2	-1.05×10^{-4}	54.0
Omega all data, smoothed	3/93 to 11/07	-1.47×10^{-4}	44.5	-2.39×10^{-4}	65.5	-8.4×10^{-5}	20.9	-1.16×10^{-4}	39.7	-1.03×10^{-4}	36.8
Omega , yearly average	3/93 to 11/07	-1.56×10^{-4}	64.7	-2.43×10^{-4}	79.1	-9.1×10^{-5}	79.1	-1.25×10^{-4}	59.6	-1.1×10^{-4}	58.1
Omega, pre-grouting	3/93 to 1/97	-2.92×10^{-4}	21.5	-3.86×10^{-4}	28.4	-1.97×10^{-4}	10.6	-4.46×10^{-4}	61.4	-3.5×10^{-4}	54.0
Omega, pre-grouting, smoothed	3/93 to 1/97	-2.90×10^{-4}	43.4	-4.27×10^{-4}	68.5	-2.27×10^{-4}	34.3	-4.64×10^{-4}	82.0	-3.75×10^{-4}	75.8
Omega post-grouting	6/99 to 9/07	-2.73×10^{-4}	22.7	-2.47×10^{-4}	8.4	-1.3×10^{-4}	4	-1.21×10^{-4}	12.1	-1.16×10^{-4}	16.1
Omega post-grouting, smoothed	6/99 to 9/07	-2.0×10^{-4}	33.9	-3.01×10^{-4}	48.2	-1.54×10^{-4}	23.7	-1.43×10^{-4}	29.5	-1.48×10^{-4}	31.6
Omega immediate post-grouting	6/99 to 1/05	-5.99×10^{-4}	41.4	-9.2×10^{-4}	20.2	-5.4×10^{-4}	21.2	-4.56×10^{-4}	18.4	-4.69×10^{-4}	20.6
Omega immediate post-grouting, smoothed	6/99 to 1/05	-5.34×10^{-4}	79	-6.66×10^{-4}	80.1	-4.64×10^{-4}	70.5	-3.89×10^{-4}	76.8	-3.94×10^{-4}	79.5
Omega post-grouting, long term	1/05 to 9/07	*-1.3×10^{-4}*	N.S.	-2.57×10^{-4}	6.9	*-1.4×10^{-4}*	N.S.	*-1.18×10^{-4}*	N.S.	*-1.02×10^{-4}*	N.S.
Omega post-grouting, long term, smoothed	1/05 to 9/07	-1.58×10^{-4}	13.2	-2.66×10^{-4}	39.7	-1.46×10^{-4}	6.4	-1.43×10^{-4}	7.9	-1.23×10^{-4}	5.6
T&T, all data	4/94 to 9/07	*-1.08×10^{-4}*	N.S	-3.26×10^{-4}	19.7	-1.01×10^{-4}	4.7	-3.06×10^{-4}	5.6	*-1.2×10^{-5}*	N.S.
T&T, all data, smoothed	4/94 to 9/07	-1.62×10^{-4}	17.3	-3.86×10^{-4}	45.1	-6.2×10^{-5}	2.6	-1.05×10^{-4}	11.8	*-1.5×10^{-5}*	N.S.
T&T, all data, yearly average	4/94 to 9/07	-2.54×10^{-4}	49.3	-4.84×10^{-4}	65	-1.78×10^{-4}	30.9	-1.71×10^{-4}	31.5	*-2.3×10^{-5}*	N.S.
T&T, pre-injection	4/94 to 11/96	-1.85×10^{-4}	13.3	-3.96×10^{-4}	8.9	*3.9×10^{-5}*	N.S.	-4.37×10^{-4}	33.5	-5.67×10^{-4}	12.2
T&T, pre-injection, smooth	4/94 to 11/96	-2.36×10^{-4}	13.3	-6.46×10^{-4}	17.4	*-6.2×10^{-5}*	N.S.	-4.75×10^{-4}	49.3	*-2.9×10^{-5}*	N.S.
T&T, pre-injection, long term	11/96 to 11/99	*-1.78×10^{-4}*	N.S	-2.91×10^{-4}	4.2	*-4.8×10^{-5}*	N.S.	-2.13×10^{-4}	6.3	-2.22×10^{-4}	4.8
T&T, post-injection	10/01 to 9/07	-5.99×10^{-4}	26.8	-9.44×10^{-4}	23	-5.26×10^{-4}	16.5	-3.20×10^{-4}	23.4	-3.58×10^{-4}	17.0
T&T, post-injection, smoothed	10/01 to 9/07	-6.47×10^{-4}	35.3	-1.05×10^{-3}	47.3	-5.57×10^{-4}	28.1	-4.36×10^{-4}	42.3	-4.59×10^{-4}	42.7
T&T, post-injection, long term	1/04 to 9/07	*-1.31×10^{-4}*	N.S	-4.29×10^{-4}	20.4	*-9.4×10^{-5}*	N.S.	*-5.8×10^{-5}*	N.S.	*-2.2×10^{-5}*	N.S.
T&T, post-injection, long term, smoothed	1/04 to 9/07	*-4.2×10^{-5}*	N.S	-2.96×10^{-4}	34.8	*-3.7×10^{-5}*	N.S	*-4.0×10^{-5}*	N.S	6.4×10^{-5}	14.0

Table 5-8
Decay Constants (d^{-1}) Estimated from Chemical Concentration for Three Mostly Flooded Circumneutral Mine-pools

Mine	Period of Record	Total Acidity $k(d^{-1})$	R^2	Iron $k(d^{-1})$	R^2	Sulfate $k(d^{-1})$	R^2	TDS $k(d^{-1})$	R^2	pH $k(d^{-1})$	R^2
Hahn all data	12/84 to 10/04	-4.88×10^{-4}	87	-4.89×10^{-4}	89	-4.18×10^{-4}	95	-4.14×10^{-4}	96	6.8×10^{-4}	44
Hahn, initial flush	12/84 to 8/91	-8.28×10^{-4}	75	-8.16×10^{-4}	74	-4.76×10^{-4}	75	-4.33×10^{-4}	76	1.1×10^{-3}	47
Hahn, long term	5/93 to 10/04	-2.89×10^{-4}	68	-2.99×10^{-4}	69	-2.72×10^{-4}	47	-4.63×10^{-4}	49	5.2×10^{-4}	5
Arden-Westland all data	1/89 to 2/99	-2.50×10^{-4}	81	-2.48×10^{-4}	80	-1.64×10^{-4}	77	-1.29×10^{-4}	76	*-1.0×10^{-5}*	N.S
Arden-Westland initial flush	1/89 to 5/91	-3.55×10^{-4}	33	-3.55×10^{-4}	32	-1.78×10^{-4}	14	-1.84×10^{-4}	20	*5.0×10^{-5}*	N.S
Arden-Westland transition	2/92 to 8/96	-3.52×10^{-4}	84	-3.53×10^{-4}	84	-2.55×10^{-4}	69	-2.09×10^{-4}	71	*2.3×10^{-5}*	N.S
Arden-Westland long term	8/96 to 10/99	*-5.6×10^{-5}*	N.S	*-4.5×10^{-5}*	N.S	-1.08×10^{-4}	12	*-1.6×10^{-5}*	N.S	-1.2×10^{-4}	21
Barnes&Tucker All data	1971-2005	-2.20×10^{-4}	87	-2.23×10^{-4}	86	-1.31×10^{-4}	87	-		7.08×10^{-4}	15
Barnes&Tucker Pre-flooding	1971-1984	-2.52×10^{-4}	29	-2.52×10^{-4}	54	-1.75×10^{-4}	68	-		1.81×10^{-3}	6.7
Barnes&Tucker Post-flooding	1985-2005	-1.12×10^{-4}	66	-1.12×10^{-4}	67	-1.05×10^{-4}	75	-		*3.0×10^{-5}*	N.S

The significant decay constants span about one order of magnitude, around 10^{-4}/day, regardless of the degree of flooding, or stage of flooding (initial flush or long term). The only exceptions are rapid pH increases in the early phases of flooding in the Hahn and Barnes&Tucker mine-pools where k is about 1×10^{-3}/day, several scenarios where the decay constant is statistically insignificant, and Al decay for parts of the record in the Omega and T&T mine-pools. The relatively narrow range of decay constants suggests that k is not greatly influenced by chemical conditions, but may be in part, a function of physical conditions of mine-pool flow and leaching efficiency. All five mines are in the northern Appalachian plateau with similar hydrogeologic and climatic controls.

The two mostly unflooded mines have the most complex history and leaching behavior. This is reflected in the number of subdivisions of the record for the T&T and Omega mine-pools. Both had episodes of grout or limestone injection approximately midway through the monitoring record, and both had periods of statistically insignificant decay rates for some parameters. Because the raw data exhibit large short term variations, decay constants were also calculated on smoothed data generated from a five point moving average and yearly averages. As expected, smoothing and combining data increased the R^2 values. In many instances, decay constants computed on raw, smoothed or yearly average data were within about 20% of each other; some parameters exhibited larger differences. The use of smoothed data also enabled resolution of decay constants that could not be determined on the raw data. Table 5-7, Omega mine-pool post grouting, from 1/05 to 9/07 had statistically insignificant decay values based on raw data. The smoothing function reduced variation sufficiently to identify statistically significant decay values without disrupting data trends.

The three mostly flooded mine-pools (table 5-8) have decay constants spanning less than one order of magnitude, excluding pH change. The Hahn discharge, initial flush, has a high rate of change for Fe. With few exceptions, R^2 values exceed 50%, and approach 90% for some parameters, indicating relatively robust estimates for k. The exceptions include Arden-Westland long term conditions.

pH changes were rapid during early flushing in the Hahn and Barnes&Tucker mine-pools, and are on the order of about -1×10^{-3}/d. Gzyl and Banks (2007) reported decay constants of about -3 to -5×10^{-3}/d for pH and sulfate concentration in flooding underground coal mines in Poland. The pH rate change in their study is similar to early flushing values derived here. Sulfate decay however is about three to ten times faster than for this study. Gzyl and Banks' decay values were derived for one mine which has low ionic strength waters, with sulfate concentration reported between 85 and 442 mg/L, and a rapid flooding rate in comparison to the three mostly flooded mines in this study. The chemical and flooding disparity, and perhaps hydrogeologic factors, may account for difference of up to an order of magnitude between the Polish and Appalachian mine-pools. The results do suggest however, that a range of mine water pollutant decay rates can be estimated that encompass a range of conditions.

Mack and Skousen (2008) reported a survey of acidity decay in about 40 above drainage mines in West Virginia. Their surveyed mines included the T&T complex described in this study, and other older mines in the Upper Freeport and Pittsburgh coal beds. Most of the mines had been

closed for 50 to 70 years. They plotted acidity decay curves with k of two, five and ten percent per year and compared them to time series plots of acidity concentration. They concluded that most mines best fit a five percent per year decay curve, or about -1.4 x 10^{-4}/day. The T&T mine-pool mean annual acidity most closely approximated a ten percent decay, or about -2.7 x 10^{-4}/day. This study estimated a very similar value for mean acidity decay at -2.54 x 10^{-4}/day, using the regression techniques described previously. The two and five percent per year decay curves that Mack and Skousen used are well within the range of decay constants computed in this study. Mack and Skousen's data, and this study's results, suggest it is possible to define chemical concentration decay estimates within about one order of magnitude for mines in similar hydrogeologic and geochemical settings.

The lower R^2 values found with the mostly unflooded Omega and T&T mine-pools are influenced by discharge characteristics. These two mines are gravity drained, and exhibit transient short term and seasonal variation in flow and chemical concentrations. The decay equation models longer term trends, and do not accommodate the transient conditions characteristic of these two mine-pools. In contrast, the three mostly flooded Hahn, Arden-Westland and Barnes&Tucker mine-pools are pumped at more or less constant rates, and the flow system approaches steady state conditions.

The decay constants in tables 5-7 and 5-8 are summarized graphically by parameter, degree of flooding, and flushing stage in figure 5-23, with median values for the five mine-pools combined. Overall, Fe has the most rapid median decay or rate of concentration decrease, of the five parameters. Aluminum, which was compiled only for the two acidic mostly unflooded mines, and total dissolved solids change for all five mines, have the slowest overall decay. Total acidity and sulfate have intermediate decay rates. For every parameter, decay is most rapid during early flushing stage.

Relative decay of the five parameters is influenced by geochemical conditions in the mine-pools. In the moderately oxidizing conditions of the Omega and T&T mine-pools, there are several possible sinks for iron, including formation of oxide, oxyhydroxide, and sulfate minerals, and adsorption/exchange reactions. Both mine-pools are near apparent equilibrium for jarosite, and over-saturated for more crystalline forms of Fe oxyhydroxide. Iron decay may reflect in part, formation of solid phases that remain in these mine-pools. In the mostly flooded mine-pools, Fe resides largely as Fe(II), and the waters are under-saturated for common Fe(II) minerals. There are no obvious mineral sinks for Fe(II), and decay is likely dependent on the recharge and exchange rates of mine-pool water.

In the Omega and T&T mine-pools, Al is near or approaches apparent equilibrium with jurbanite, and the pools are under-saturated for several alumino-silicate minerals. Even with relatively slow alumino-silicate weathering rates, the two mine-pools remain capable of supplying soluble Al, and consequently have a slow Al decay rate. In these two mine-pools, overall decay constants for total dissolved solids are similar to Al. These two parameters are projected to have the slowest rates of concentration change.
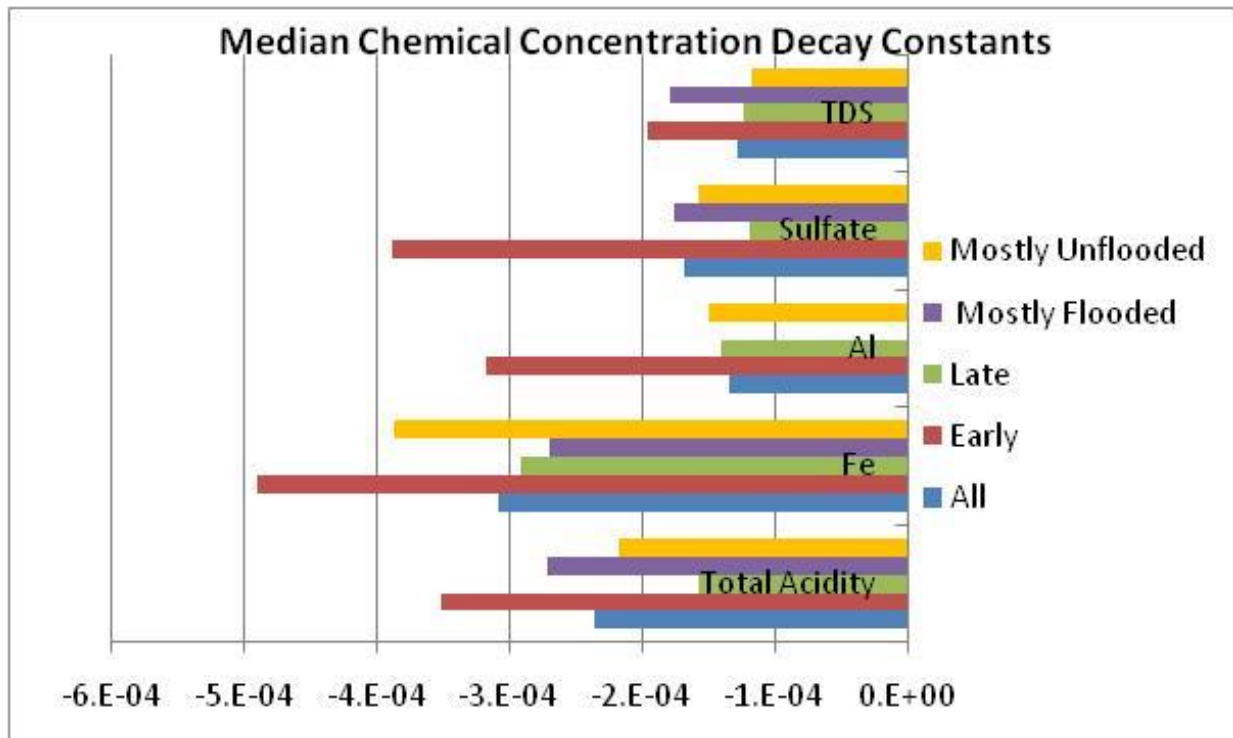
**Figure 5-23. Chemical Concentration Decay Constants by Parameter,
Degree of Flooding and Flushing Stage. Median Values for Five Mine-pools.**

Figure 5-24 compares median decay constants as a ratio of mostly flooded to mostly unflooded, and ratio of early flushing to late leaching constants for the five mine-pools. The mostly flooded mines decay faster for total acidity, sulfate and dissolved solids in comparison to the mostly unflooded mines. Iron, however, is exceptional, with a slower decay rate in flooded mines. The
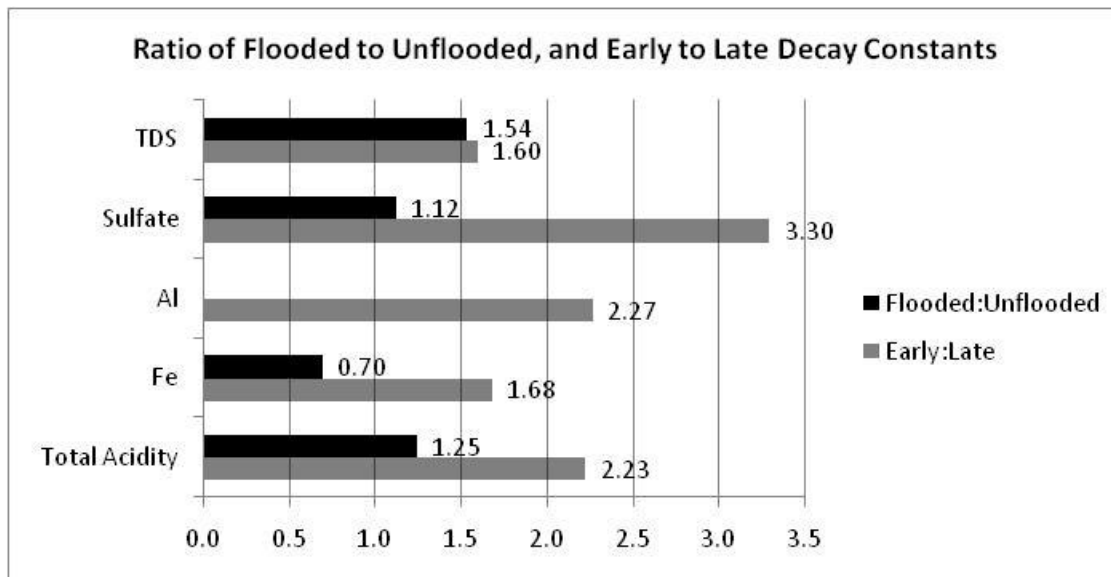
**Figure 5-24. Comparison of Chemical Decay Constants Mostly Flooded to Mostly Unflooded,
and Early Flushing to Late Leaching, for Five Mine-pools.**

161

implication is that flooding reduces weathering rates, in particular oxidation reactions, hence the decline in concentration is more rapid. The slower iron decay in flooded conditions suggests that soluble Fe may be generated from sources other than pyrite, such as the dissolution of Fe oxyhydroxide minerals. No redox measurements of the Hahn and Arden-Westland mine-pools are available, and the tendency for these mine-pools to dissolve Fe oxyhydroxides can only be approximated from indirect means. In section 5.2, the Hahn mine-pool was estimated to be reduced enough to at least dissolve more soluble forms of $Fe(OH)_3$.

Six Eh measurements were made in the Doman (main) discharge from the mostly flooded Barnes&Tucker mine-pool over an 18 month period by the author. Measured Eh ranged from +160 to +290 millivolts. The calculated indices were slightly under-saturated for poorly crystalline forms of Fe oxyhydroxides. These lines of evidence are indirect, but show that it is possible that Fe in mostly flooded, reduced mine-pools could be generated from dissolution of Fe oxide minerals.

Figure 5-24 also shows a comparison of decay constants for early flushing versus late or long term conditions. Early decay ranges from about 1.5 to 3 times faster than late decay for the five parameters, with the largest disparity reported for sulfate. In all parameters, the difference is likely attributed to the initial flush of accumulated and highly soluble minerals, followed by continued weathering and slower leaching of soluble minerals. Younger (1997, 2000), and Wood et al. (1999) have made similar observations to explain the discharge quality of coal mines in the U.K.

Tables 5-7 and 5-8, and figure 5-24 show that early flushing and long term conditions should be assigned separate decay values to model chemical concentration decay in mines. How should early and late decay periods be identified? For several mine-pools, events including grout injection and flooding of other mine-works clearly signal a change in conditions. Earlier in this chapter, the use of log-log scale plots was presented as a means of identifying flooding and flushing stages. A third mechanism is chemical ratios.

In chapter three and four, mine water iron to sulfate mole ratios were plotted on the assumption of pyrite stoichiometry, or one mmole Fe per two mmoles sulfate. These plots show the largest ratios present early in the monitoring record, then declining to a near constant value, with time series slope approaching zero. The approach of a near constant ratio approximately coincides with the demarcations made from log-log scale plots. A constant ratio also suggests that the initial transient flushing condition has passed and the mine-pool is in long term leaching. Figure 5-25 a and b are plots of Fe to sulfate mole ratios for the Hahn and Omega mine-pools, respectively.

The ratio approached near constant value in late 1989 in the Hahn mine-pool, about five years after flooding was complete. It is equivalent to the exchange of about 1.25 pool volumes. The mostly flooded Arden-Westland mine-pool displayed a near constant element ratio by 1991, about five years after flooding was complete. Based on an average four year residence time, the Arden-Westland mine-pool Fe to sulfate ratio also stabilized after discharging about 1.25 pool

volumes. For the mostly flooded Barnes and Tucker mine-pool, the ratio stabilized after about four years or about eight pool volumes.
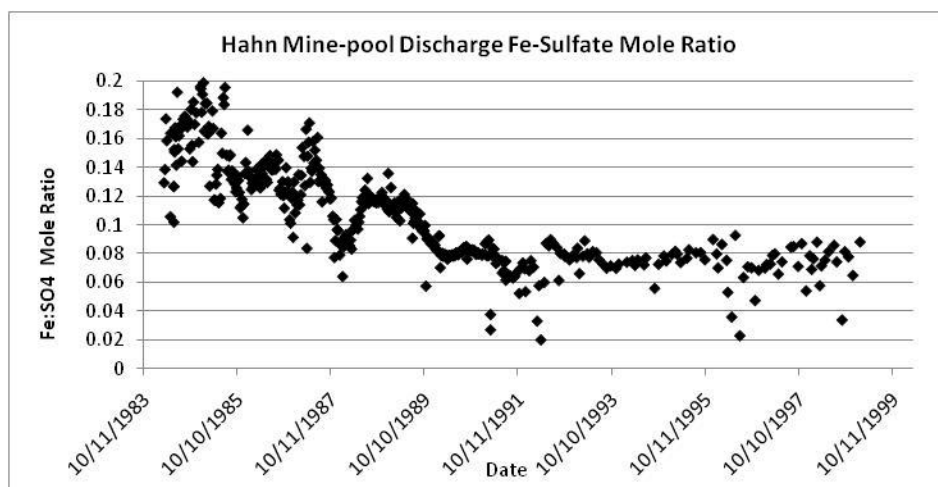
Figure 5-25a. Fe to Sulfate Mole Ratio, Hahn Mine-pool.
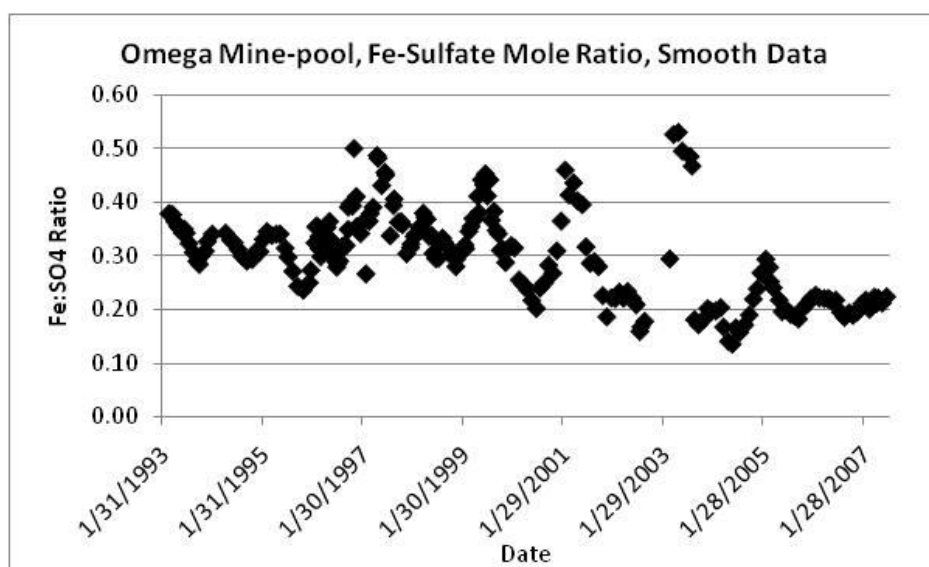
Figure 5-25b. Fe to Sulfate Mole Ratio, Omega Mine-pool.

The slope change in the Omega mine-pool (fig 5-25b) is not as obvious, but occurred around mid 1997, or about seven years after mine closure. Part of the monitoring record in this period is absent, so the exchange of water is a broad estimate of about 12 pool volumes. The T&T mine-pool Fe to sulfate ratio stabilized about mid 1998, or four years after mine closure. This is equivalent to about eight pool volumes of water exchange.

For two of the three mostly flooded mines, Hahn and Arden-Westland, Fe to sulfate ratio approached a constant value after the mine-pool flushed slightly more than one pool volume. The two acidic mostly unflooded mines had less distinct slope changes, and exchanged an estimated eight to ten pool volumes before stabilizing. The contrast between flooded and mostly unflooded mines could be attributed to the active ongoing chemical weathering in the aerated partly flooded

mine-pools, and less aggressive weathering in the mostly flooded mines. Element ratios can be a useful tool for separating initial flushing and long term leaching periods.

5.3.3 Estimated Decay Times for Chemical Parameters

Decay constants were used to estimate time dependent chemical concentration decline in two ways. The first was to estimate the time required for the chemical parameter to decay to a specified fraction of 0.5, 0.1, 0.05, and 0.01 of the starting concentration C_0. The second approach estimated the time required to reach a specified concentration.

Tables 5-9 to 5-13 show the estimated decay times in years to reach specified fractions of starting concentration, respectively, for the five parameters of total acidity, Al, Fe, sulfate and total dissolved solids (TDS). The estimates are derived from the decay constants in tables 5-7 and 5-8, using the single k value derived for all data. Equation 5-22 was solved for time t using specified fractions of C_t/C_0 and the previously determined decay constant. The time estimates in this set of calculations are only dependent on the value of "k", the decay constant. For all parameters and decay constants, the "half life" or time for concentration to decline to 50% of initial conditions ranges from about three to 18 years, with most estimates between about seven to 15 years. Time to reach ten percent of initial concentration (t0.1 in the tables), ranges from about two to 60 years for all parameters and decay constants. Most are between 15 and 40 years. Time to reach five percent of initial concentration ranges from about three to 78 years. Most estimates are greater than 20 years. Finally, the estimated time to reach one percent of initial concentration ranges from at least 15 to more than 100 years. Many estimates exceed 40 years. Several entries had statistically insignificant decay constants, for which time dependent concentrations were not estimated. These rates are too small to resolve. This implies longer decay times, or large variation in the data set, masking a statistically identifiable trend.

This initial summary has two significant implicit assumptions:

- Hydrogeologic conditions will remain constant through time, and
- Geochemical conditions will remain constant through time.

The hydrogeology of closed mines can be affected by pumping, and flooding or dewatering of hydrologically connected mines and aquifers. Effects from adjacent mines will be site-specific. A second issue is the alteration in aquifer properties of the mine-pool by continued physical weathering, pillar crushing and collapse of roof rock. The significance of continued weathering of aquifer rocks in underground mines is not developed here. However, Hawkins (2004) reported that hydraulic conductivity of surface mine-spoil more than 2.5 years old was less than for newly reclaimed rocks. He attributed this in part to continued physical weathering. Rhem et al. (1980) also reported that hydraulic conductivity decreased with age on surface mine spoil in North Dakota. A plausible effect of decreasing hydraulic conductivity in underground mine gob would be to reduce ground-water flow velocity and removal of chemical constituents, and hence reduce decay rates. The assumption of constant hydrogeologic conditions over a prolonged period may not be completely robust.

Table 5-9
Estimated Decay Time for Total Acidity to Decline to 50, 10, 5 and 1% of Initial Concentration

Mine	Initial Concentration C_0 (mg/L)	t 0.5 (years)	t 0.1 (years)	t 0.05 (years)	t 0.01 (years)
Omega, all, 3/93 to 11/07	3169	8.1	26.8	34.9	53.7
Omega, pregrout, 3/93-1/97	3169	4.0	13.1	17.1	26.3
Omega, postgrout 6/99-9/07	2061	9.9	33	43	66.1
T&T all data, 4/94-9/07	750	17.6	58.4	76	116.8
T&T, pre inject, 4/94-11/96	750	3.5	11.5	15.0	23.0
T&T, long term 1/04-9/07	566	N.S.[1]	N.S.	N.S.	N.S.
Hahn all data, 12/84 -10/04	2123	3.9	12.9	16.8	25.9
Hahn, early data, 12/84-8/91	2123	2.3	7.7	9.9	15.2
Hahn, late data, 5/93-10/04	216	6.6	21.8	28.4	43.7
Arden-Westland all, 1/89-2/99	307	7.6	25.2	32.8	50.5
Arden-Westland, early 1/89-5/91	307	6.9	22.8	29.6	45.5
Arden-Westland, long term 8/96-2/99	118	N.S.	N.S.	N.S.	N.S.
Barnes&Tucker all data	1647	8.6	28.7	37.3	57.3
Barnes&Tucker, pre flooding	1647	7.5	25.0	32.6	50.1
Barnes&Tucker post flooding	133	17.0	56.3	73.3	112.6

(1) N.S. = Decay constant not statistically significant. No time estimate calculated.

The second assumption, that geochemical conditions remain constant through time may also be suspect. As the mine-pool solution becomes increasingly dilute, concentrations of Fe and other elements could be controlled by mineral solubility. This prospect is examined in section 5.5.

The decay estimates summarized in tables 5-9 to 5-13 illustrate two observations of practical significance about temporal trends in water composition:

- A relatively rapid initial decline on the order of a few years to ten to 20 years. Water treatment needs are at a maximum during this time.

- A much slower decline, where water treatment demands are reduced, but are likely needed over a longer period, spanning multiple decades.

Table 5-10
Estimated Decay Time for Aluminum to decline to 50, 10, 5 and 1% of Initial Concentration

Mine	Initial Concentration C_0 (mg/L)	t 0.5 (years)	t 0.1 (years)	t 0.05 (years)	t 0.01 (years)
Omega, 3/93 to 11/07	147	17.4	57.9	75.3	115.7
Omega, pregrout, 3/93-1/97	147	7	23.1	30.1	46.2
Omega, postgrout 6/99-9/07	111	14.8	49.3	64.1	98.6
T&T all data, 4/94-9/07	46	18.8	62.4	81.2	124.9
T&T, pre inject, 4/94-11/96	46	0.7	2.2	2.8	4.3
T&T, long term 1/04-9/07	44	N.S.[1]	N.S.	N.S.	N.S.

(1) N.S=Decay constant not statistically significant. No time estimate calculated.

Table 5-11
Estimated Decay Time for Iron to decline to 50, 10, 5 and 1% of Initial Concentration

Mine	Initial Concentration C_0 (mg/L)	t 0.5 (years)	t 0.1 (years)	t 0.05 (years)	t 0.01 (years)
Omega, all, 3/93 to 11/07	839	7.3	24.4	31.7	48.7
Omega, pre-grout, 3/93-1/97	839	3.9	12.9	16.7	25.7
Omega, post-grout 6/99-9/07	600	6.7	22.2	28.9	44.1
T&T all data, 4/94-9/07	316	5.8	19.3	25.2	38.7
T&T, pre-inject, 4/94-11/96	316	4.9	16.2	21.1	32.4
T&T, long term 1/04-9/07	123	4.4	14.7	19.1	29.4
Hahn all data, 12/84 -10/04	1030	3.9	12.9	16.8	25.9
Hahn, early data, 12/84-8/91	1030	2.3	7.7	10.1	15.5
Hahn, late data, 5/93-10/04	121	6.3	21.1	27.4	42.2
Arden-Westland all, 1/89-2/99	165	7.7	25.4	33.1	50.9
Arden-Westland, early 1/89-5/91	121	5.3	17.8	23.1	35.5
Arden-Westland, long term 8/96-2/99	63	N.S.[1]	N.S.	N.S.	N.S.
Barnes&Tucker all data	920	8.5	28.3	36.8	56.6
Barnes&Tucker, pre flooding	920	7.5	25	32.6	50.1
Barnes&Tucker, post flooding	74	17	56.3	73.3	112.6

(1) N.S.=Decay constant not statistically significant. No time estimate calculated.

Table 5-12
Estimated Decay Time for Sulfate to decline to 50, 10, 5 and 1% of Initial Concentration

Mine	Initial Concentration C_0 (mg/L)	t 0.5 (years)	t 0.1 (years)	t 0.05 (years)	t 0.01 (years)
Omega, all, 3/93 to 11/07	4016	14.5	48.1	62.6	96.3
Omega, pregrout, 3/93-1/97	4016	3.9	13.0	16.9	26.0
Omega, postgrout 6/99-9/07	3242	15.3	50.9	66.2	101.7
T&T all data, 4/94-9/07	2885	6.2	20.6	26.8	41.2
T&T, pre inject, 4/94-11/96	2885	1.8	5.9	7.7	11.9
T&T, long term 1/04-9/07	1655	N.S.[1]	N.S.	N.S.	N.S.
Hahn all data, 12/84 -10/04	8300	4.6	15.2	19.7	30.3
Hahn, early data, 12/84-8/91	8300	4.0	13.2	17.2	26.5
Hahn, late data, 5/93-10/04	1838	7.0	23.2	30.2	46.4
Arden-Westland all, 1/89-2/99	1672	11.6	38.5	50.0	76.9
Arden-Westland, early 1/89-5/91	1672	10.7	35.4	46.1	70.9
Arden-Westland, long term 8/96-2/99	1060	17.6	58.4	76.0	116.8
Barnes&Tucker all data	3692	12.8	42.6	55.4	85.2
Barnes&Tucker, pre flooding	3692	10.8	36.0	46.9	72.1
Barnes&Tucker post flooding	597	18.1	60.1	78.1	120.2

(1) N.S.=Decay constant not statistically significant. No time estimate calculated.

Table 5-13
Estimated Decay Time for TDS to decline to 50, 10, 5 and 1% of Initial Concentration

Mine	Intial Concentration C_0 (mg/L)	t 0.5 (years)	t 0.1 (years)	t 0.05 (years)	t 0.01 (years)
Omega, all, 3/93 to 11/07	5315	18.1	60.1	78.1	120.2
Omega, pre-grout, 3/93-1/97	5315	5.5	18.3	23.8	36.6
Omega, post-grout 6/99-9/07	4972	14.2	47.1	61.2	94.2
T&T all data, 4/94-9/07	2194	N.S. [1]	N.S.	N.S.	N.S.
T&T, pre-inject, 4/94-11/96	2194	3.3	11.1	14.5	22.3
T&T, long term 1/04-9/07	2894	N.S.	N.S.	N.S.	N.S.
Hahn all data, 12/84 -10/04	11400	4.6	15.2	19.7	30.3
Hahn, early data, 12/84-8/91	11400	4.4	14.6	19.0	29.1
Hahn, late data, 5/93-10/04	3952	4.1	13.6	17.7	27.2
Arden-Westland all, 1/89-2/99	3074	14.7	48.9	63.6	97.8
Arden-Westland, early 1/89-5/91	3074	10.7	35.4	46.1	70.9
Arden-Westland, long term 8/96-2/99	2222	N.S.	N.S.	N.S.	N.S.
Barnes&Tucker all data	Insuffucient Data	-	-	-	-
Barnes&Tucker, pre flooding	Insuffucient Data	-	-	-	-
Barnes&Tucker, post flooding	Insuffucient Data	-	-	-	-

(1) N.S.= Decay constant not statistically significant. No time estimate calculated.

The second decay time estimate used a specific parameter concentration as a target value. The target values were selected on the basis of established water quality values for specific uses or discharge standards. The estimates then provide an indication of the time required to approach suitability for various uses. The decay equation (equation 5-22) was solved for time t, using the initial and target concentrations, and previously calculated decay constant. The time estimates in this set of calculations are dependent on the starting concentration C_0 and the decay constant, "k". Target concentrations of 10, 3.5 and 1 mg/L were selected for Fe. One mg/L Fe is a suggested water quality standard for aquatic life (US EPA, 1986a), while the 3.5 mg/L is a 30 day average National Pollutant Discharge Elimination System (NPDES) discharge standard for coal mines. The regulatory standards are described in Title 40, Part 434 of the Code of Federal Regulations. A target concentration of one mg/L was selected for Al, which is similar to the recommended standard of 0.75 mg/L for aquatic life (US EPA, 1986b). Target values of 500 mg/L total dissolved solids, and 250 mg/L for sulfate were selected based on national secondary drinking water standards. Those standards are found in Title 40, part 143 of the Code of Federal Regulations. A target value of 300 mg/L acidity was selected as a condition where passive treatment systems that add alkalinity might be feasible (Hedin et al., 1994).

The estimated times to attain target concentration values are shown in figures 5-26 to 5-30 and table 5-14 for the five mine-pools. Concentration data in the graphs (y-axis) are log base ten scale to more clearly display the difference in decay rate. Iron decay with the exception of T&T post injection data and Hahn early flushing, ranges from 27 to 75 years to reach 3.5 mg/L Fe.

Aluminum decay to one mg/L is estimated to require 69 to more than 100 years in the acidic mostly unflooded mines. Sulfate decay to 250 mg/L is estimated to require between 15 and 58 years. The shortest decay times are for total acidity to reach 300 mg/L, requiring less than 30 years for all scenarios. Parts of the Hahn, Arden-Westland and Barnes&Tucker records are already less than 300 mg/L total acidity. Several decay scenarios have statistically insignificant rates and no estimates were calculated. They are too small to resolve. This implies longer decay.
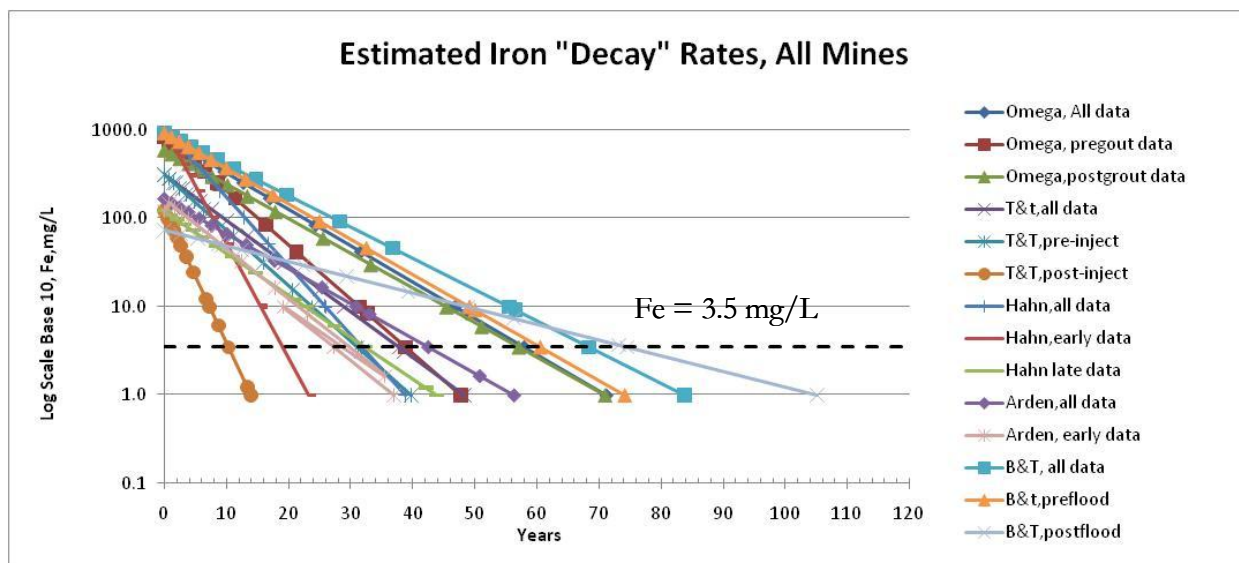
Figure 5-26. Estimated Time in Years for Iron to "Decay" to 3.5 mg/L, for Five Mines and Different Flooding Phases. Concentration Axis is log Base 10 Scale. See table 5-14 for Numeric Values.

Total dissolved solids decay estimates to attain 500 mg/L were between 12 and 24 years, with the exception of the Omega mine-pool post-grouting or for the combined Omega data. This set of estimated decay times also implies near steady conditions in physical and chemical properties through time.
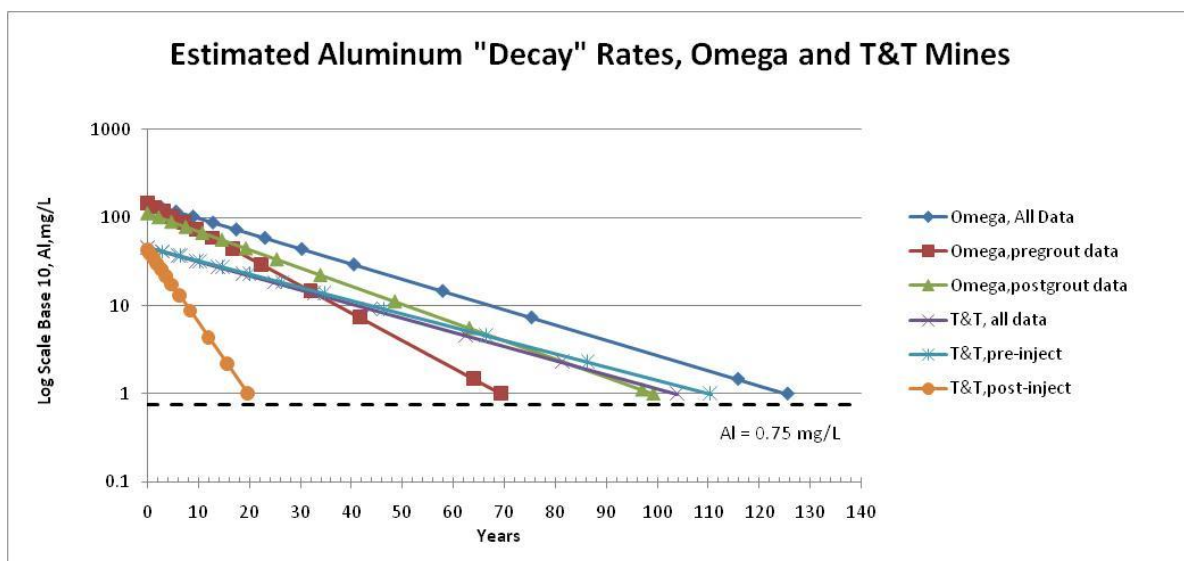
Figure 5-27. Estimated Time in Years for Aluminum to "Decay" to One mg/L, for Five mines and Different Flooding Phases. Concentration Axis is log Base 10 Scale. See table 5-14 for Numeric Values.

The target concentration estimates show that mine-pool waters of these starting chemical compositions are likely to require decades to achieve acceptable chemistry. Excluding total acidity, most parameter decay estimates are between 20 and 70 years to achieve target concentrations.
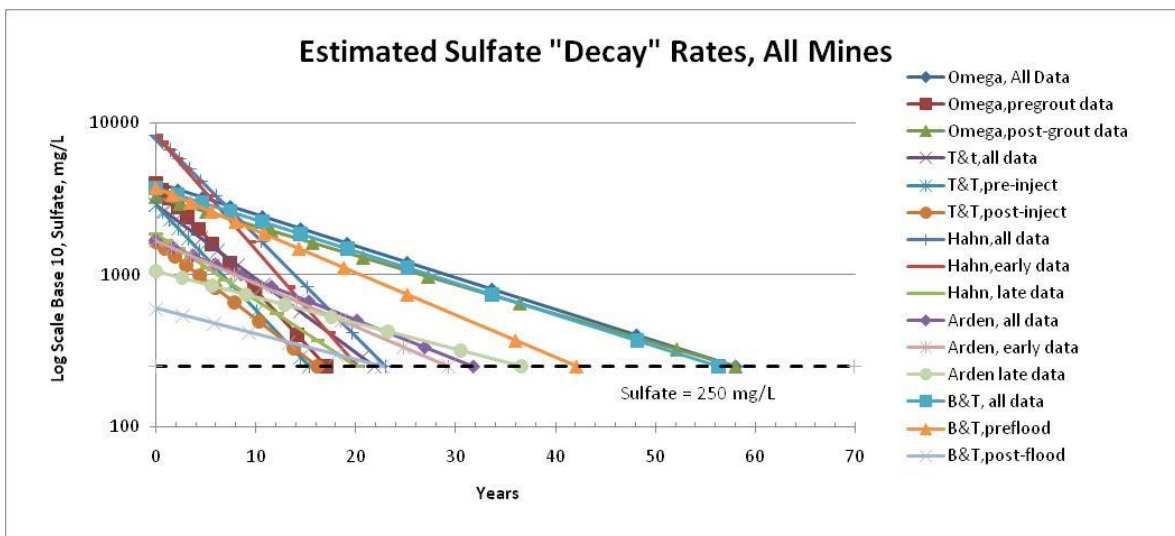
Figure 5-28. Estimated Time in Years for Sulfate to "Decay" to 250 mg/l, for Five Mines and Different Flooding Phases. Concentration Axis is log Base 10 Scale. See table 5-14 for Numeric Values.
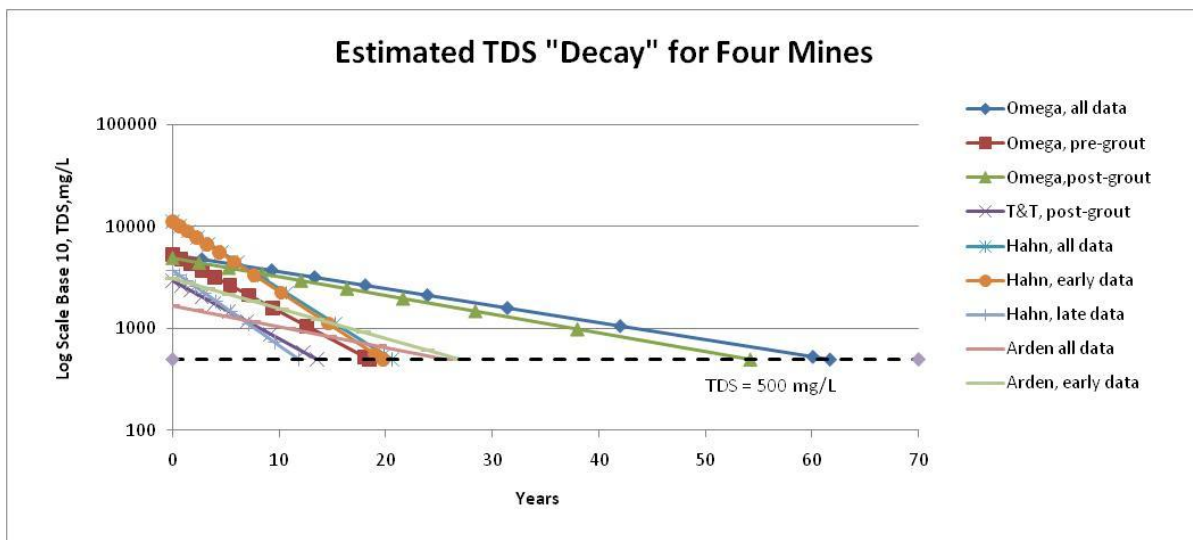
Figure 5-29. Estimated Time in Years for Total Dissolved Solids to "Decay" to 500 mg/L, for Five Mines and Different Flooding Phases. Concentration Axis is log Base 10 Scale. See table 5-14 for NumericValues.

Table 5-14
Estimated Years to Attain Target Parameter Concentration
Based on "Decay" Calculation, And Initial Concentration (C_o) [1]

Mine	Fe, 10 mg/L	Fe, 3.5 mg/L	Fe, 1 mg/L	Al, 1 mg/L	Sulfate, 250/mg/L	TDS, 500 mg/L	Acidity, 300 mg/L
Omega, All data	47 yrs (839mg/L)	58 yrs (839mg/L)	71 yrs (839mg/L)	125 yrs (147/mg/L)	58 yrs (4016mg/L)	62 yrs (5315 mg/L)	28 yrs (3169mg/L)
Omega, Pre-grout	31 yrs (839mg/L)	39 yrs (839mg/L)	48 yrs (839mg/L)	69 yrs (147/mg/L)	17 yrs (4016mg/L)	19 yrs (5315mg/L)	22 yrs (3169mg/L)
Omega, Post-grout	45 yrs (600mg/L)	57 yrs (600mg/L)	71 yrs (600mg/L)	102 yrs (111mg/L)	58 yrs (3242mg/L)	54 yrs (4972mg/L)	19 yrs (2061mg/L)
T&T, All data	29 yrs (316mg/L)	38 yrs (316mg/L)	48 yrs (316mg/L)	104 yrs (46 mg/L)	22 yrs (2885mg/L)	N.S.	23 yrs (750 mg/L)
T&T, Pre-inject	24 yrs (316 mg/L)	31 yrs (316 mg/L)	40 yrs (316 mg/L)	110 yrs (46 mg/L)	15 yrs (2885mg/L)	N.S.	12 yrs (750 mg/L)
T&T, Post-inject	5 yrs (123 mg/L)	7 yrs (123 mg/L)	10 yrs (123 mg/L)	21 yrs (44 mg/L)	16 yrs (1655mg/L)	9 yrs (2894 mg/L)	4 yrs (630 mg/L)
Hahn, all data	26 yrs (1030mg/L)	32 yrs (1030mg/L)	39 yrs (1030mg/L)		22 yrs (8300mg/L)	20 yrs (11400mg/L)	11 yrs (2018mg/L)
Hahn, early data	16 yrs (1030mg/L)	19 yrs (1030mg/L)	23 yrs (1030mg/L)		19 yrs (8300mg/L)	20 yrs (11400mg/L)	7 yrs (2018mg/L)
Hahn, late data	22 yrs (121mg/L)	32 yrs (121mg/L)	43 yrs (121mg/L)		20 yrs (1838mg/L)	12 yrs (3685 mg/L)	
Arden-Westland, all data	31 yrs (165mg/L)	43 yrs (165mg/L)	56 yrs (165mg/L)		32 yrs (1670mg/L)	24 yrs (3074 mg/L)	
Arden-Westland early data	19 yrs (121mg/L)	27 yrs (121mg/L)	37 yrs (121mg/L)		25 yrs (1670mg/L)	24 yrs (3074 mg/L)	
Arden-Westland late data	N.S.	N.S.	N.S.		31 yrs (1060mg/L)	N.S.	
B&T, All data	56 yrs (920mg/L)	68 yrs (920mg/L)	84 yrs (920mg/L)		56 yrs (3692mg/L)		21 yrs (1647mg/L)
B&T, Pre-flood	49 yrs (920mg/L)	61 yrs (920mg/L)	74 yrs (920mg/L)		42 yrs (3692mg/L)		30 yrs (1647mg/L)
B&T, Post-flood	49 yrs (74mg/L)	75 yrs (74mg/L)	105 yrs (74mg/L)		23 yrs (597 mg/L)		

(1) No Aluminum decay values for Hahn, Arden-Westland, and B&T mine-pools, because the waters are circumneutral and contain little dissolved Al. TDS decay values for the T&T all data record and T&T pre-inject record are not statistically significant. TDS data not reported for most of the B&T period of record. Acidity decay value for T&T pre-injection data record is not statistically significant. Acidity decay values for Hahn late data, Arden-Westland, and B&T post flooding are near or less than the target concentration of 300 mg/L.
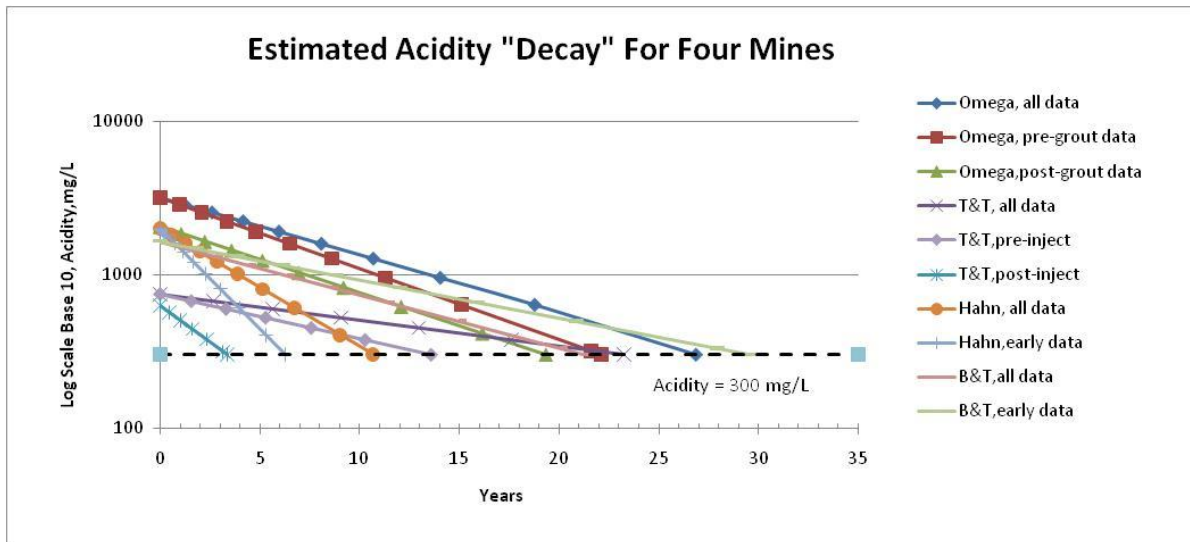
Figure 5-30. Estimated Time in Years for Total Acidity to "Decay" to 300 mg/L, for Four Mines and Different Flooding Phases. Concentration Axis is log Base 10 Scale. See table 5-14 for Numeric Values.

5.3.4 Sensitivity Analysis of Decay Constants

The decay constants presented in this chapter were derived by regression analysis, and hence are "best fit" estimates of the slope of the fitted equation. Sensitivity of the decay constant estimate was evaluated against the initial concentration C_0, and by examining the range of plus or minus two standard deviations of the estimate of "k".

Estimating the decay constant k is not sensitive to the specified value of the initial concentration C_0. This is graphically illustrated in figure 5-31. Equation 5-22 uses the ratio C_t/C_0 to generate values to plot against time. If C_0 is changed by an amount b, then the ratio for every
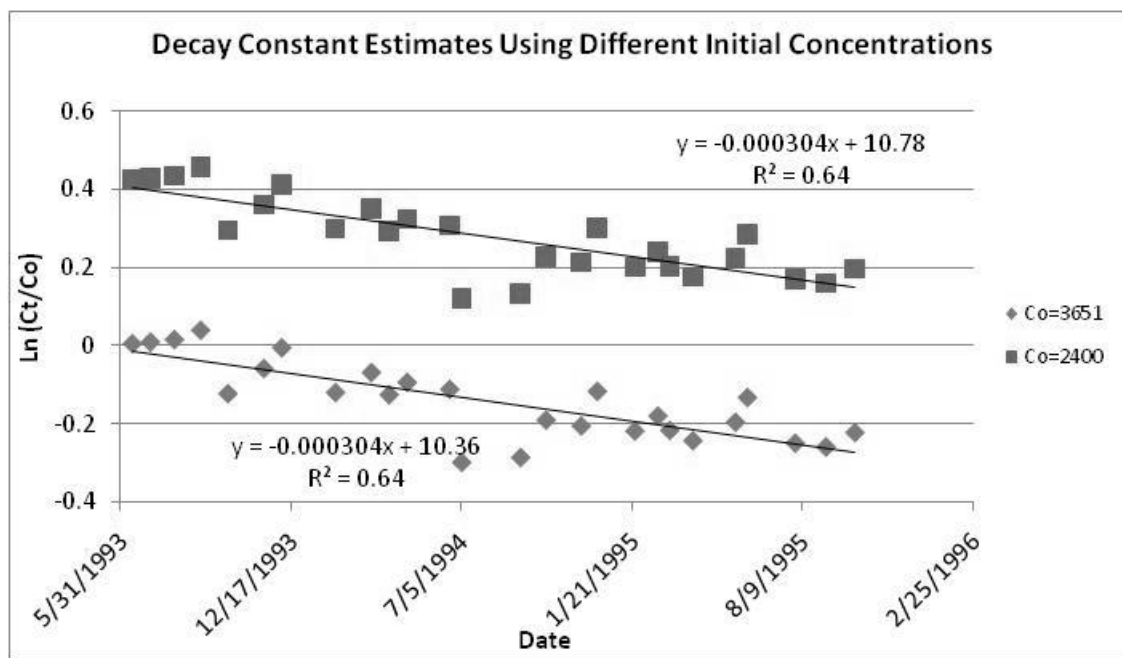
Figure 5-31. Estimating Decay Constant Using Different Initial Concentrations on the Same Data Set.

171

datum point becomes $C_t/(C_0-b)$. The variance, distribution of residuals about the fitted line and slope ("k") will remain the same. Only the line intercept value will change. Figure 5-31shows data points fitted to regression lines using C_0 values of 3651 and 2400 mg/L. The example data are TDS measurements from the Hahn mine-pool. Both regressions produce a decay constant of -3.04×10^{-4}/d and R^2 values of 64%, but with different y intercepts. A "correct" initial concentration is only needed if the function is extrapolated back to time t=0.

Table 5-15 shows "best fit" estimates of decay constants, and a constant at +2 standard deviations (95th percentile) from the best fit value. The latter represents an upper bound of decay rate, and hence a minimum time for pollutant concentrations to decrease. The table includes constants fitted to the entire period of record. The two mostly unflooded mines, Omega and T&T, have the largest variation about the regression and range of decay constant. The largest is for total acidity at the Omega mine-pool where k at the 95th percentile is 1.35×10^{-4}/d greater than the best fit value. This gives a time range of 17 to 27 years for total acidity to decay to 300 mg/L. Other parameters in mostly unflooded mines range from 0.31 to 0.92×10^{-4}/d difference in decay constant values. The range in decay constant values produces a wider confidence interval when estimating pollutant decay behavior.

The three mostly flooded mines have smaller variances and range of decay constants. The largest difference is 0.24×10^{-4}/d for Fe in the Barnes&Tucker mine-pool. This produces a time range of 19 to 21 years for total acidity to decline to 300 mg/L. The smaller range of estimated decay constants in mostly flooded mines produces a smaller confidence interval for time dependent behavior. The standard deviation values in table 5-16 can be used to estimate upper and lower bounds on the decay constant, and minimum and maximum decay times.

Table 5-15
Range of Decay Constant Values [1]

	Total Acidity	Iron	Aluminum	Sulfate	TDS
Omega All Data					
Best Fit k	-2.35×10^{-4}	-2.59×10^{-4}	-1.09×10^{-4}	-1.31×10^{-4}	-1.05×10^{-4}
+2 Std Dev k	-3.70×10^{-4}	-3.38×10^{-4}	-1.62×10^{-4}	-1.62×10^{-4}	-1.88×10^{-4}
T&T All Data					
Best Fit k	N.S.	-3.26×10^{-4}	-1.01×10^{-4}	-3.06×10^{-4}	N.S.
+2 Std Dev k		-4.04×10^{-4}	-1.71×10^{-4}	-3.98×10^{-4}	
Hahn All Data					
Best Fit k	-4.88×10^{-4}	-4.89×10^{-4}	no data	-4.18×10^{-4}	-4.14×10^{-4}
+2 Std Dev k	-4.89×10^{-4}	-5.04×10^{-4}		-4.27×10^{-4}	-4.22×10^{-4}
Arden-Westland All Data					
Best Fit k	-2.50×10^{-4}	-2.48×10^{-4}	no data	-1.64×10^{-4}	-1.29×10^{-4}
+2 Std Dev k	-2.52×10^{-4}	-2.65×10^{-4}		-1.76×10^{-4}	-1.39×10^{-4}
B&T All Data					
Best Fit k	-2.20×10^{-4}	-2.23×10^{-4}	no data	-1.48×10^{-4}	no data
+2 Std Dev k	-2.52×10^{-4}	-2.57×10^{-4}		-1.68×10^{-4}	

(1) Constant values in day^{-1}.

5.3.5 Sensitivity Analysis of Decay Time Estimates

The sensitivity of estimated time for pollutant decay was evaluated by varying two parameters in equation 5-22, the decay constant "k" and initial concentration "C_0". Table 5-16 shows the estimated decay times to a target concentration, computed by varying "k" from the best fit and 95th percentile values shown in table 5-15. Decay times for the mostly flooded Hahn and Arden-Westland mine-pools are essentially unchanged, regardless of whether the best fit or 95th percentile value of k is used. The Barnes&Tucker mine-pool estimates differ from six to 12 years. The more variable, mostly unflooded mine-pools, differ by ten to 15 years for estimates of iron, sulfate and total acidity. The largest difference occurs for aluminum and results from two factors; a low target concentration of one mg/L, and small decay constants. Unfortunately, the T&T total acidity and total dissolved solids data have large variances, and single statistically significant decay constants could not be resolved for the entire monitoring record.

The results in table 5-16 show that chemical concentration decay in mines approaching steady state condition can be estimated within a narrow confidence of range of a decade or less. The mostly unflooded mines, which are characterized by numerous short term transient events, have a somewhat broader range of about one to two decades for most parameters. Regardless of the k values used, the time estimates to approach target concentrations are on the order of multiple decades.

Table 5-16
Range of Decay Times in Years from Best Fit and 95th Percentile Values of k

	Total Acidity Decay Time to 300 mg/L	Iron Decay Time to 1 mg/L	Aluminum Decay Time to 1 mg/L	Sulfate Decay Time to 250 mg/L	TDS Decay Time to 500 mg/L
Omega All Data					
Best Fit k	27 yrs	71 yrs	126 yrs	58 yrs	62 yrs
+2 Std Dev k	17 yrs	56 yrs	84 yrs	47 yrs	34 yrs
T&T All Data					
Best Fit k	N.S.	48 yrs	104 yrs	22 yrs	N.S.
+2 Std Dev k		39 yrs	61 yrs	17 yrs	
Hahn All Data					
Best Fit k	24 yrs	39 yrs	no data	23 yrs	21 yrs
+2 Std Dev k	24 yrs	38 yrs		23 yrs	20 ysr
Arden-Westland All Data					
Best Fit k	<1	56 yrs	no data	32 yrs	26 yrs
+2 Std Dev k	<1	53 yrs		30 ysr	24 yrs
B&T All Data					
Best Fit k	50 yrs	84 yrs	no data	56 yrs	no data
+2 Std Dev k	44 yrs	73 yrs		44 yrs	

The second time sensitivity analysis varied the value for initial concentration C_0. The initial concentration was selected by identifying the single measurement, or more commonly, group of plotted measurements, that showed the beginning of a declining concentration trend. The median was used to represent the value for C_0 for a group of measurements.

Decay time estimates to achieve a target concentration were calculated using a single value for k while varying C_0 by plus or minus one, three, five, ten and 20 percent. This analysis was conducted for one mostly unflooded site, the Omega mine-pool, and one mostly flooded mine-pool, the Hahn discharge. These two mines had the greatest and smallest variances in parameters estimates respectively. The results are shown in figures 5-32 to 5-36.
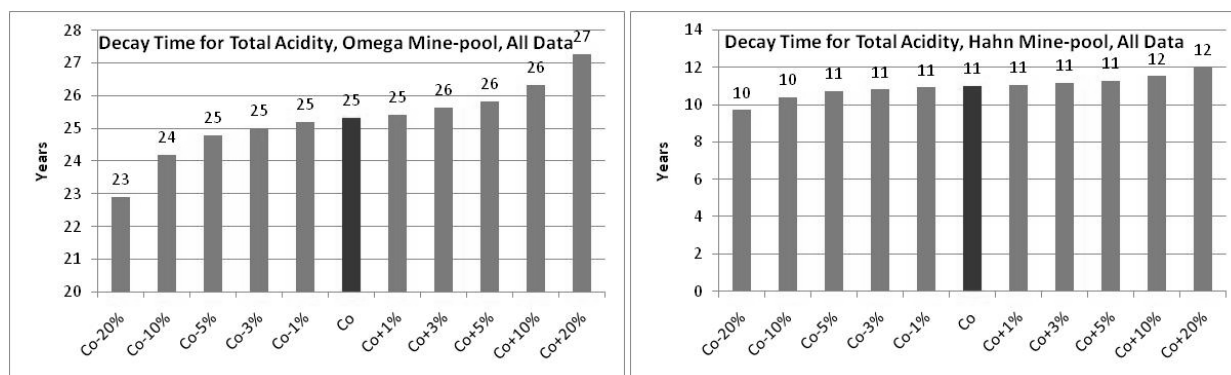
Figure 5-32. Estimated Decay Times for Total Acidity to Reach 300 mg/L, Based on Different Starting Concentrations, Omega and Hahn Mine-pools. Black bars indicate C_0. Gray bars show C_0 varied by 1, 3, 5, 10 or 20%. Decay time in years.
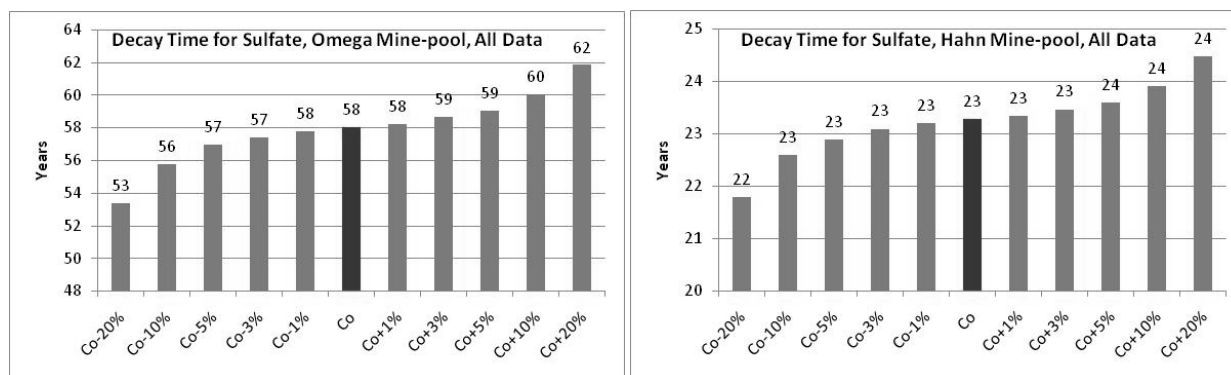
Figure 5-33. Estimated Decay Times for Sulfate to Reach 250 mg/L, Based on Different Starting Concentrations, Omega and Hahn Mine-pools. Black bars indicate C_0. Gray bars show C_0 varied by 1, 3, 5, 10 or 20%. Decay time in years.
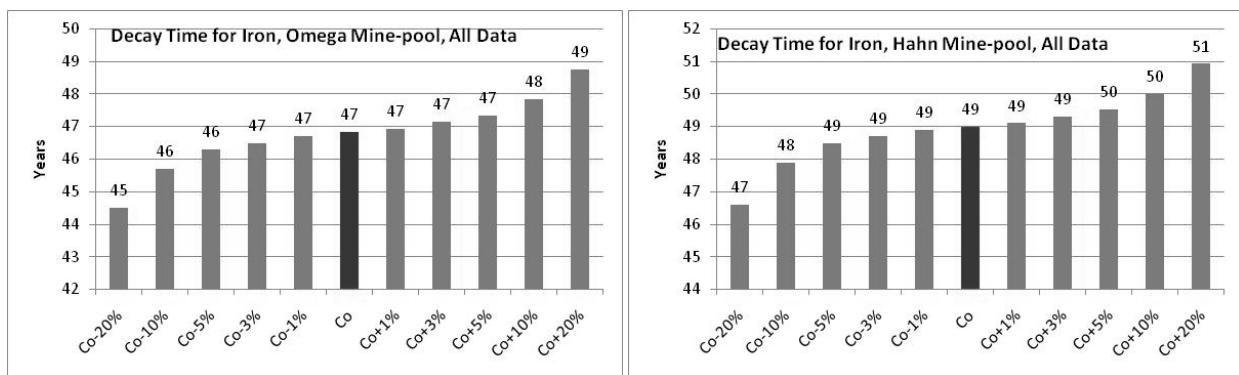
Figure 5-34. Estimated Decay Times for Iron to Reach 10 mg/L, Based on Different Starting Concentrations, Omega and Hahn Mine-pools. Black bars indicate C_0. Gary bars show C_0 varied by 1, 3, 5, 10 or 20%. Decay time in years.
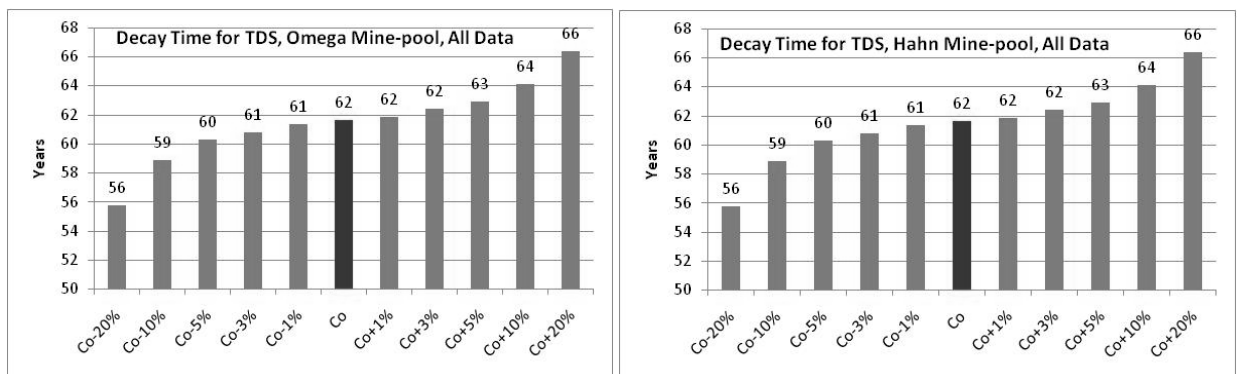
Figure 5-35. Estimated Decay Times for TDS to Reach 500 mg/L, Based on Different Starting Concentrations, Omega and Hahn Mine-pools. Black bars indicate C_0. Gary bars show C_0 varied by1, 3, 5, 10 or 20%. Decay time in years.
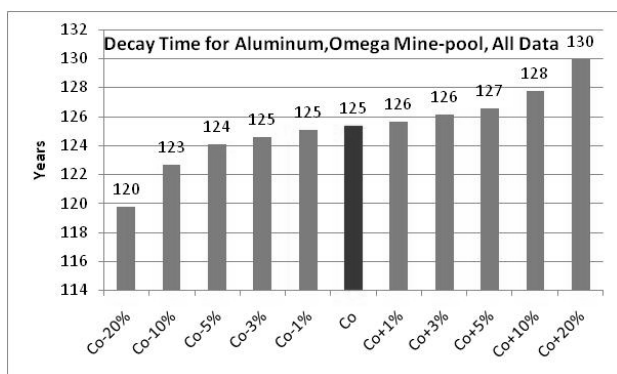
Figure 5-36. Estimated Decay Times for Aluminum to Reach One mg/L, Based on Different Starting Concentrations, Omega Mine-pool. Black bars indicate C_0. Gray bars show C_0 varied by 1, 3, 5, 10 or 20%. Decay time in years.

Varying the C_0 for total acidity by plus or minus 20% changed the estimated decay time by +/- one year in the Hahn mine-pool, and +/- five years in the Omega mine-pool (figure 5-29). Estimated decay time for sulfate ranged from 53 to 62, and 22 to 24 years, while Fe varied from 45 to 49 and 47 to 51 years, respectively for the Omega and Hahn mine-pools (figures 5-30 and

175

5-31). Total Dissolved Solids decay estimates varied over a range of ten years for both mine-pools (figure 5-32). Aluminum decay estimates also ranged over a ten year span as C_0 was varied. This set of sensitivity analyses, like the preceding evaluations, show limited response to variations in the decay equation. Regardless of the C_0 values used, the time estimates to approach target concentrations are on the order of multiple decades.

5.3.6 Decay Estimates Using Flushing Phases
Examining the R^2 values in tables 5-7 and 5-8 suggests that estimation of chemical concentration decay could be improved by assigning separate decay values to represent initial flushing (early data) and long term leaching conditions (late data). Figures 5-37 to 5-45 are time series plots of raw data decay estimated from a single k value, and decay estimated in two phases, early and late data. The fit of the decay lines was assessed by tabulating residuals (difference of raw data minus decay estimate) and expressing the difference as a percentage of the raw data. The median residual percentages for fitting all data to single k value, and by estimating early and late decay from two separate constants are shown in table 5-17.

Table 5-17
Decay Curve Fitting Median Residual Percentages, Hahn and Omega Mine-pools[1]

Hahn Mine-pool	Total Acidity	Iron	Aluminum	Sulfate	Total Dissolved Solids
Single k Residual Percentage	39%	31.2%	-	6.8%	6.2%
2 Phase k Residual Percentage	14%	6.6%	-	0.4%	7.5%
Omega Mine-pool	Total Acidity	Iron	Aluminum	Sulfate	Total Dissolved Solids
Single k Residual Percentage	12.1%	16.5%	3.1%	18.3%	16.0%
2 Phase k Residual Percentage	10.2%	19.8%	3.4%	11.1%	15.1%

(1) Entries are median values of (raw data minus calculated data)/(raw data), expressed as percentage.

Residuals, or the difference between observed and fitted data, generally improved (decreased) when decay was modeled using two separate data phases constants compared to a single constant to represent concentration change through time. The fit for total acidity and Fe improved significantly, and sulfate residuals were less than one percent for the Hahn mine-pool (table 5-17, figures 5-37 and 5-38). Iron and total acidity were over-estimated in the middle part of the monitoring record using a single decay constant. A two phase decay model largely eliminated this difference. A single k calculation for TDS provided a slightly smaller median residual than decay modeled with two constants for the Hahn mine-pool.
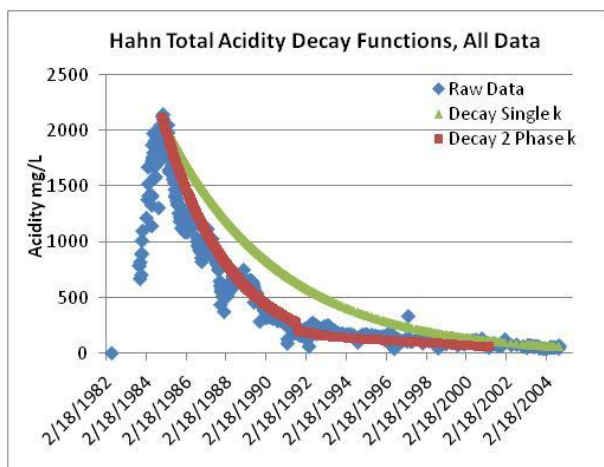
Figure 5-37. Total Acidity Decay Functions, Hahn Mine-pool.
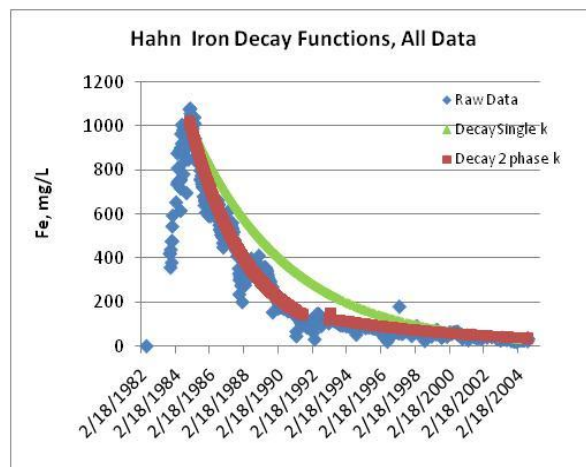
Figure 5-38. Iron Decay Functions, Hahn Mine-pool.
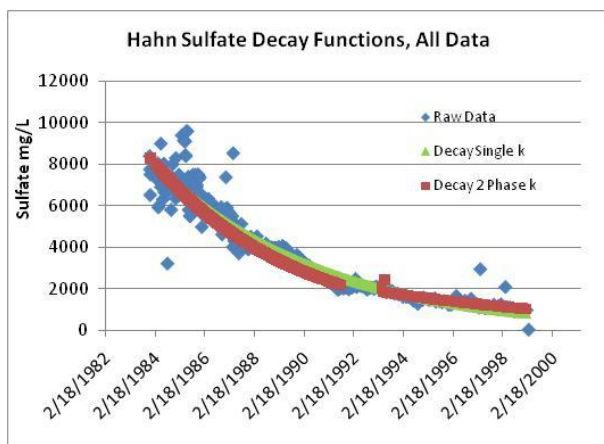
Figure 5-39. Sulfate Decay Functions, Hahn Mine-pool.
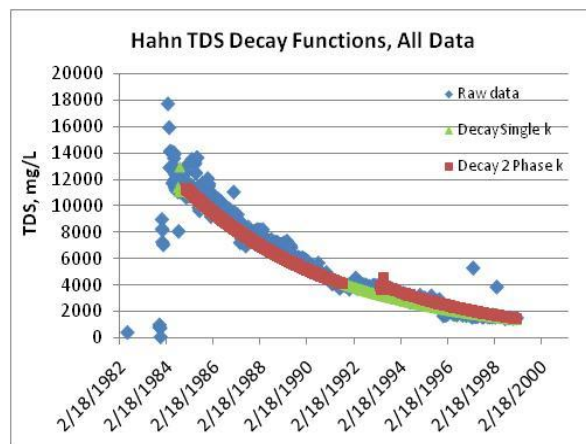
Figure 5-40. Total Dissolved Solids Decay Functions, Hahn Mine-pool.
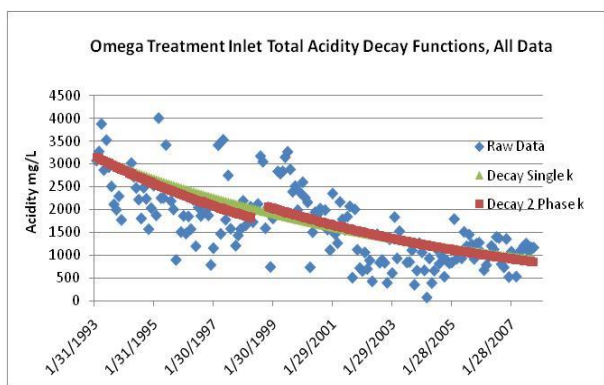
Figure 5-41. Total Acidity Decay Functions, Omega Mine-pool.
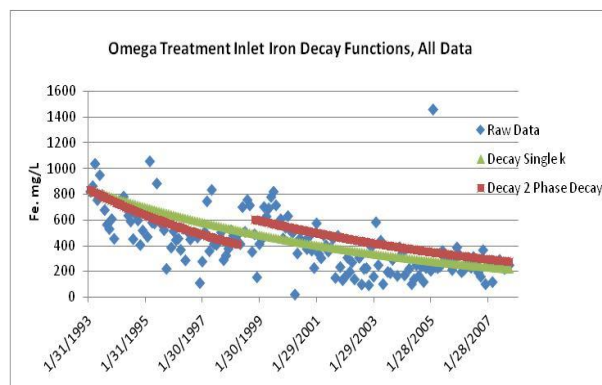
Figure 5-42. Iron Decay Functions, Omega Mine-pool.

177
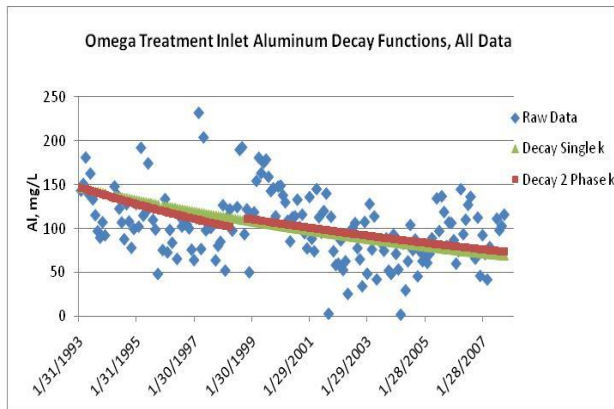
Figure 5-43. Omega Mine-pool, Aluminum Decay Functions.
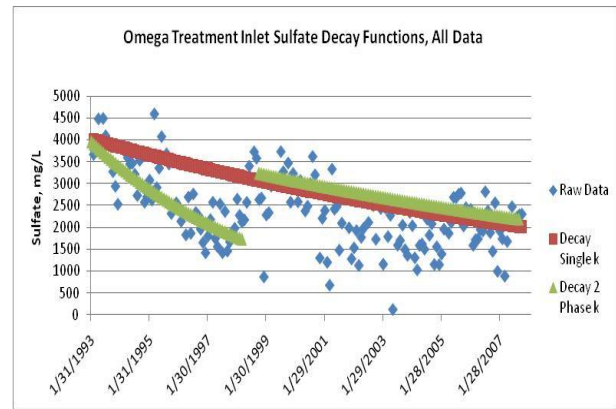
Figure 5-44. Omega Mine-pool, Sulfate Decay Functions.
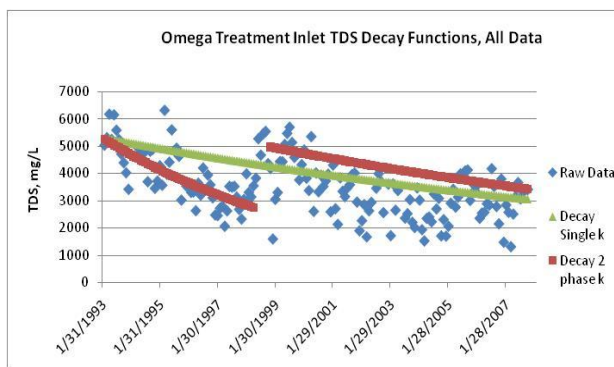
Figure 5-45. Omega Mine-pool. Total Dissolved Solids Decay Functions.

Improvements in data fiting were also found in the Omega mine-pool using a two phase decay model. Residual percentages for total acidity, sulfate and total dissolved solids decreased. Aluminum decay displayed little difference in residual percentage using a one or two phase decay model, while iron residual increased when based on a two phase decay. Figures 5-44 and 5-45 also display the effects of grout injection on sulfate and total dissolved solids decay, respectively. For both parameters, decay was faster prior to grouting. Post-grouting, there is a large increase in chemical concentration, and a decline in the decay rate. Iron behaved in similar fashion (figure 5-42), but the chemical concentration initial increase was less. Aluminum decay was the parameter least affected by grouting. This may result from solubility controls on Al concentration, maintaining mine water at or near saturation for the Al mineral jurbanite. Mineral solubility in the Omega mine-pool in addressed in more detail in chapter three.

Data presented in figures 5-37 to 5-45 and table 5-17, show that in general, agreement between raw and calculated decay data can be improved using a two phase decay model. The poorest fit usually occurred in the middle of a curve, at the expense of closer agreement at the beginning and end of the decay line. This systematic error suggests that the decay function does not completely describe the physical and chemical processes at work. Neither does the decay equation accommodate short term and seasonal variations in chemical composition. The decay function is useful however, as a trend estimator.

5.3.7. Controls on the Decay Constant
The decay constant values generally ranged over about one order of magnitude, suggesting that there might be underlying controls on the magnitude of k. These could be either physical, chemical, or a combination of features. Dissolution rates for moderately soluble minerals are rapid relative to diffusion of reactants and products within mineral grains and bulk solution. Therefore, diffusion was considered a potential control on decay rate. Surface controlled reactions for these moderately soluble minerals are also often rapid relative to the flushing provided by ground-water flow. For example, many limestone aquifers are slightly under-saturated for calcite. This condition suggests that calcite dissolution is rapid enough to approximately compensate for dissolution transport away from the calcite grain. Transport at the macroscale was also considered a potential control on decay rate.

An initial analysis of macroscale variables included mine recharge rate, percent flooded, mine area, average residence time, maximum flow-path length and initial chemical concentration. These parameters were compared with decay constant values for all monitoring data, early or initial flushing phase, and late or long term leaching. Only sulfate and total dissolved solids decay showed any appreciable correlation with the macroscale parameters. Sulfate decay was correlated with initial concentration (r = 0.60), and total dissolved solids with mine area (r=0.62), maximum flow-path length (r=0.63), residence time (r=0.44) and initial concentration (r=0.55). The small size of the data set precludes more rigorous statistical analysis. The decay parameters were however, correlated with each other as shown in table 5-18. The magnitude of the five decay parameters was greater or lesser as a group when considered on mine by mine basis. This suggests decay is influenced by mine specific chemical or transport properties, while the lack of a strong relationship to macroscale features implies that transport control may be at the microscale. This initial analysis prompted a closer examination of the effects of diffusion and flushing rate on mine water decay functions.

Table 5-18
Correlation coefficents (r) among decay constant (k) parameters

Parameter	Total Acidity	Fe	Al	Sulfate
Fe	0.87			
Al	0.98	0.98		
Sulfate	0.48	0.36	0.36	
Total Dissolved Solids	0.57	0.98	0.98	0.85

Berner (1978) described a simple box model calculation to illustrate the effects of flushing and diffusion on mineral dissolution rates. Berner's equations are based on conservation of mass principles. The rate of concentration change affected by flushing is expressed as:

$$\frac{dc}{dt} = R - \frac{F}{V}\, c \qquad\qquad (5\text{-}23)$$

where:
c = concentration dissolved
t = time

F = Flushing rate (mass/time)
V = Unit Fluid Volume
R = Dissolution Rate, (mass/volume-time)

At high flushing rates (high ground-water flow velocities) a maximum dissolution rate is reached, controlled by the surface reaction rate on the mineral grain. At the other extreme, where flushing rate is small (low ground-water flow velocity) compared to mineral reaction rate, chemical concentration approaches saturation, and flushing or flow rate is the controlling factor. This is illustrated by the case of a limestone aquifer near saturation for calcite described previously.

In the case of small ground-water flow rates and slow flushing, Berner (1978) notes that $c \approx C_{eq}$, or equilibrium concentration for a specified mineral phase. Under these conditions,

$$R \approx (F/V) \, C_{eq} \qquad\qquad (5\text{-}24)$$

or the dissolution rate is approximated as the product of flushing frequency and equilibrium concentration. If flushing frequency and equilibrium concentration values are known, then dissolution rate can be estimated.

In the case of rapid flushing of the mine-pool, Berner notes that:

$$R \approx k \, C_{eq} \qquad\qquad (5\text{-}25)$$

where k is approximated as the product of the dissolution rate constant for a specified mineral and equilibrium concentration.

A consistent set of values for R could explain the observed magnitude of decay constants. Slow flushing conditions were deemed to be the more likely scenario since most of the mine-pools were near equilibrium for some minerals, especially during early flushing. Equation 5-24, slow flushing rate conditions, was used to estimate R for sulfate for the five mine-pools. Sulfate calculations were successively performed assuming solution control by gypsum, pyrite, and for the two acidic mine-pools, jurbanite. Single sample analyses, deemed typical of early flushing and long-term conditions, were selected for analysis.

Flushing rate, F in equation 5-24, was estimated as the inverse of the residence time in units of day^{-1}, treating the mine-pool as simple box model with uniform flow conditions. For convenience, the unit volume of fluid was taken as one liter. The equilibrium concentration, C_{eq}, for the solute was determined using PHREEQC and equilibrating the solution chemistry to a saturation index of zero for gypsum, pyrite, or jurbanite. Input data and estimated dissolution rates, R, are shown in table 5-19.

Table 5-19
Apparent Dissolution Rate, R, for Sulfate,
Estimated from Different Mineral Controls and Slow Flush Rate Equation.

Mine-pool	Phase	Flush Rate F (d^{-1})	Sulfate, Gypsum Control		Sulfate, Pyrite Control		Sulfate, Jurbanite Control	
			C_{eq} Mol/L	R Mol/L-s	C_{eq} Mol/L	R Mol/L-s	C_{eq} Mol/L	R Mol/L-s
Omega	Early	7.40E-03	4.64E-02	4.20E-09	4.30E-02	3.91E-9	4.22E-02	3.83E-09
Omega	Late	7.40E-03	4.33E-02	3.76E-09	3.98E-02	3.47E-9	3.82E-02	3.33E-09
T&T	Early	6.85E-03	2.76E-02	2.30E-09	2.00E-02	1.69E-9	2.30E-02	1.93E-09
T&T	Late	6.85E-03	1.90E-02	1.54E-09	8.76E-03	7.27E-10	1.03E-02	8.48E-10
Hahn	Early	6.85E-04	8.78E-02	1.17E-09	8.75E-02	1.17E-9		
Hahn	Late	6.85E-04	2.79E-02	2.81E-10	1.92E-03	7.55E-11		
Arden-Westland	Early	6.85E-04	2.49E-02	2.36E-10	1.88E-02	1.88E-10		
Arden-Westland	Late	6.85E-04	1.97E-02	1.67E-10	9.39E-03	8.61E-11		
B&T	Late	5.48E-03	1.74E-02	1.11E-09	4.74E-03	3.06E-10		

Dissolution calculations based on slow flushing rates did not provide a uniform set of values. The apparent dissolution rates, R, are on the order of 10^{-9} to 10^{-11} mol/L-s, regardless of which mineral is specified as controlling sulfate concentration. The dissolution rate is most influenced by flushing rate, not the choice of controlling mineral. The range of computed values is about 25, 50 and 5 times for gypsum, pyrite and jurbanite calculations, respectively. This is similar to the range for the decay constants themselves. Mineral mass and surface areas per unit volume of the mine-pools are not known. However, the estimated dissolution rates could support continued weathering of the duration actually observed, with relatively small amounts of accessible minerals. Thus, slow flushing relative to mineral dissolution reaction rates, in conjunction with mineral saturation data in chapters three and four provide indirect evidence that the decay constant is at least partly a transport function.

The dissolution rates in table 5-19 (mole/L-s), combined with dissolution rate constants (mole/m^2-s) could be used to estimate specific mineral surface area per liter of solution. Published rate constants for gypsum are log k = -2.79; and for pyrite, log k= -7.52 in acid solution, and log k = -4.55 in neutral solution (Palandri and Kharaka, 2004). No published rate data were found for jurbanite dissolution. Inspecting the values for k, it is apparent that the computed mineral surface areas per liter of solution will be large, and the values will vary significantly, depending on which mineral is specified as controlling sulfate concentration. Surface area measurements estimated in this manner are therefore not reliable.

A set of calculations using equation 5-25, assuming rapid flushing relative to dissolution, was also compiled using the same samples and flushing rates as in table 5-19. Equation 5-25 requires a dissolution rate constant, designated k, and the equilibrium concentration C_{eq}. Rate constants for gypsum and pyrite were taken from data compiled by Palandri and Kharaka (2004). Results are shown in table 5-20.

Table 5-20
Apparent Dissolution Rate, R, for Sulfate,
Estimated from Different Mineral Controls and Rapid Flush Rate Equation

Mine-pool	Phase	Flush Rate F (d^{-1})	Sulfate, Gypsum Control		Sulfate, Pyrite Control		Sulfate, Jurbanite Control	
			C_{eq} Mol/L	R Mol/L-s	C_{eq} Mol/L	R Mol/L-s	C_{eq} Mol/L	R Mol/L-s
Omega	Early	7.40E-03	4.64E-02	7.53E-05	4.30E-02	1.18E+02	4.22E-02	-
Omega	Late	7.40E-03	4.33E-02	7.02E-05	3.98E-02	1.09E+02	3.82E-02	-
T&T	Early	6.85E-03	2.76E-02	4.48E-05	2.00E-02	5.49E+01	2.30E-02	-
T&T	Late	6.85E-03	1.90E-02	3.07E-05	8.76E-03	2.41E+01	1.03E-02	-
Hahn	Early	6.85E-04	8.78E-02	1.42E-04	8.75E-02	5.52E+01		
Hahn	Late	6.85E-04	2.79E-02	4.52E-05	1.92E-03	2.24E+05		
Arden-Westland	Early	6.85E-04	2.49E-02	4.03E-05	1.88E-02	4.83E+04		
Arden-Westland	Late	6.85E-04	1.97E-02	3.19E-05	9.39E-03	2.41E+04		
B&T	Late	5.48E-03	1.74E-02	2.82E-05	4.74E-03	1.22E+4		

For rapid flushing rates, dissolution estimates are strongly influenced by the choice of controlling mineral. Dissolution estimates of sulfate based on pyrite control produced R values that are unreasonably high for the geochemical system being considered. Even the values derived for gypsum control indicate a rapid rate of weathering that would deplete the source mineral within a short time. These results indicate that rapid flushing relative to dissolution is not an appropriate model for these mine-pools.

Berner (1978) also describes a box model calculation for diffusion controlled dissolution as:

$$R = \frac{D\, p\, A\, (Ceq - C)}{r}$$ (5-26)

where:
R = Dissolution Rate
C= concentration in outer solution
Ceq = Equilibrium or saturation concentration
r = spherical radius of dissolving crystal
D = diffusion coefficient
p = porosity
A = Surface Area of mineral per unit volume of solution

If dissolution is strictly diffusion controlled, the dissolution rate is directly dependent on the degree of under-saturation. However, Berner also notes that equation 5-26 requires modification if dissolution is influenced by surface reactions, such as the buildup of a weathering rind on the mineral grain itself. In that case, diffusion in solution, and diffusion through the weathering rind may control the rate of reaction. That two phase weathering and diffusion process has been described for pyrite, and is reviewed in the next section.

5.4 Application of Pyrite Weathering Kinetics to Mine-pools

Pyrite weathering rates are a principal determinant in estimating the intensity and longevity of acid production in sulfide bearing rocks. Lowson (1982), Nordstrom (1982a), and Rimstidt and Vaughan (2003), among others, provide detailed reviews of the oxidation process and discussion of controlling factors, including oxygen availability and microbial catalysis. This section contains a brief review of the literature on weathering rates and controlling variables, and the implications for mine-pool pollution production over time.

Pyrite weathering is characteristically described as a four step cyclic process involving decomposition of the mineral, and oxidation of sulfur and iron in the presence of water and oxygen (Nordstrom, 1982a). The individual steps are shown below and graphically in figure 5-46:

$$FeS_2 + 7/2\ O_2 + H_2O \rightarrow Fe^{2+} + 2\ SO_4^{2-} + 2\ H^+ \qquad (5\text{-}27a)$$

$$Fe^{2+} + 1/4\ O_2 + H^+ \rightarrow Fe^{3+} + 1/2\ H_2O \qquad (5\text{-}27b)$$

$$Fe^{3+} + 3\ H_2O \rightarrow Fe(OH)_3 + 3\ H^+ \qquad (5\text{-}27c)$$

$$FeS_2 + 14\ Fe^{3+} + 8\ H_2O \rightarrow 15\ Fe^{2+} + 2\ SO_4^{2-} + 16\ H^+ \qquad (5\text{-}27d)$$
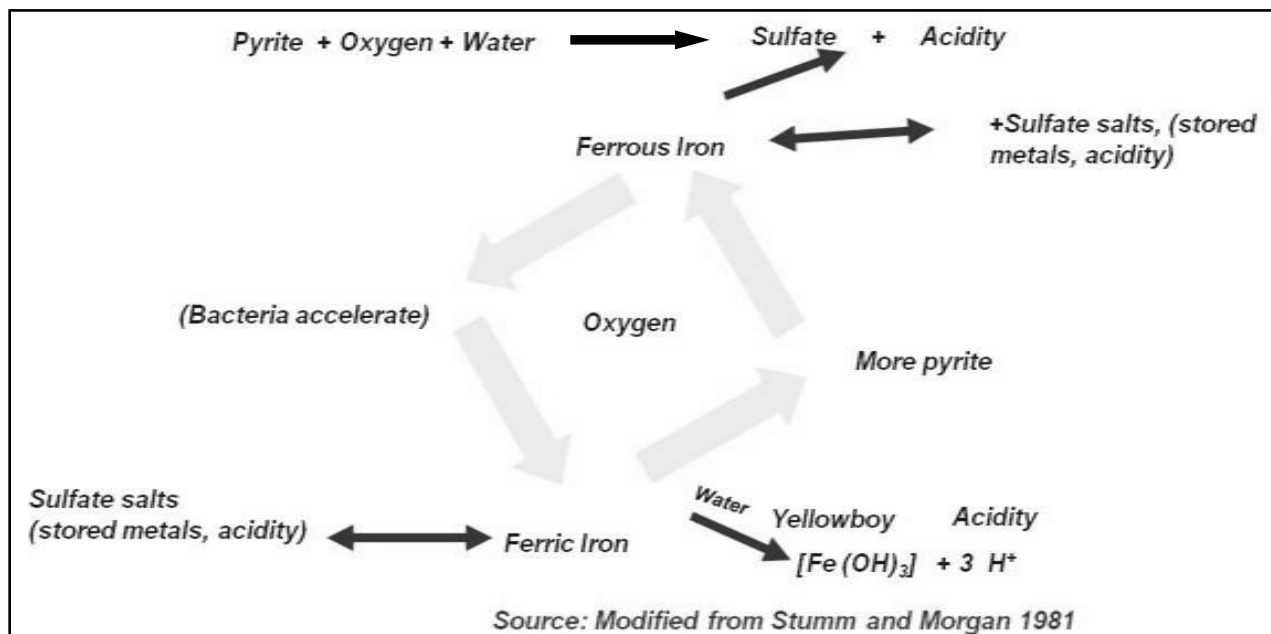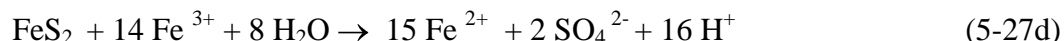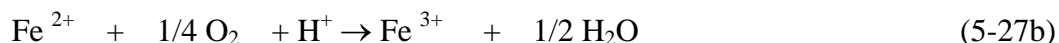
Figure 5-46. Pyrite Oxidation Process. Source, Modified From Stumm and Morgan, 1981.

The ultimate driver of the system is oxygen availability, since it is required in both the initial decomposition (equation 5-27a), and for the Fe(II)/Fe(III) couple (5-27b). Much of the literature on pyrite kinetics and field scale control technology has therefore focused on the role of oxygen.

Hammack and Watzlaf (1990) examined oxygen effects in small and large scale column studies under abiotic and biotic conditions. They found that pyrite weathering was independent of oxygen content at values greater than one percent pO_2 when Acidthiobacillus bacteria were present. At oxygen concentrations less than one percent, pyrite consumption rate was proportional to pO_2. They concluded that disposal in an anoxic environment was necessary to halt pyrite oxidation. A mostly to fully flooded mine-pool may be sufficiently oxygen depleted to stop or substantially slow pyrite oxidation.

Williamson and Rimstidt (1994) published a summary paper that provides rate laws for pyrite oxidation based on oxygen concentration, pH, ferrous/ferric iron ratios, and Eh and pH. These relations were derived from their own experiments, and compilation of other published rate data from Smith and Shumate, (1970), Mckibben and Barnes (1986), Nicholson et al. (1988), Moses and Herman (1991) and Lowson (1982), and reviews of other studies. Williamson and Rimstidt's derived rate laws are:

$$r = 10^{-8.19} \frac{m\,DO^{0.5}}{m\,H^{+\,0.11}} \tag{5-28}$$

where r is pyrite consumption rate in mole/m^2-s, DO is dissolved oxygen concentration in mole/L, and H$^+$ is in mole/L. The rate function is applicable over a range of two to ten for pH and four orders of magnitude of DO. A second rate law based on ferrous/ ferric iron ratio is:

$$r = 10^{-8.58} \frac{m\,Fe^{3+\,0.30}}{m\,Fe^{2+\,0.47}\,m\,H^{+\,0.32}} \tag{5-29}$$

where r is pyrite consumption rate in mole/m^2-s, Fe^{3+} concentration is in mole/L and H$^+$ concentration is in mole/L. Equation 5-29 is applicable in pH range 0.5 to 3.0 in the absence of oxygen. When oxygen is present, the rate law is:

$$r = 10^{-6.07} \frac{m\,Fe^{3+\,0.93}}{m\,Fe^{2+\,0.40}} \tag{5-30}$$

and is in units consistent with equation 5-28. Equation 5-30 is also limited to a pH range of 0.5 to 3.0.

Two water sample analyses from each of the five mine-pools were selected for estimating pyrite oxidation rate under contrasting pH, dissolved oxygen, and ferrous/ferric iron conditions. All samples were selected from the long term discharge phase of the record, after the initial flushing event. These samples should therefore present mostly a component of ongoing pyrite oxidation. The author collected dissolved oxygen, Eh, and ferrous iron measurements from three mine-pools Omega, T&T and Barnes&Tucker, on multiple sampling events. No such measurements are available for the Arden-Westland and Hahn mine-pools. However, inspection of the chemical data for these two (see chapter four) suggests that they must be oxygen-poor, reduced mine-pools. Both contain significant dissolved iron concentrations in circumneutral pH waters. These concentrations can only be maintained if Fe resides almost entirely as Fe(II). Since the rate of Fe(II) to Fe(III) conversion at circumneutral pH is rapid, with a half life on the order of hours, the persistence of Fe(II) in these mine-pools suggests that little or no oxygen is available.

Finally, in section 5.2 of this study, Eh of these two mine-pools was estimated to be on the order of zero millivolts to maintain soluble iron below saturation for common hydroxide/oxide minerals. Dissolved oxygen in the Barnes and Tucker mine-pool approached the lower instrument detection limit of 0.01 mg/L. This value was also assigned to the Hahn and Arden-Westland mine-pools. A value of 0.1 mg/L was also assigned to test sensitivity of r to varying dissolved oxygen concentrations. Data for estimating for pyrite oxidation rates are shown in table 5-21. Results using the general rate law in equation 5-28 are shown in figure 5-47 and table 5-21. Calculated rates from Fe^{2+}/Fe^{3+} ratios for the acid mine-pools are also in table 5-21.

Pyrite consumption rates for the four acid samples with abundant dissolved oxygen, calculated with the general rate law, are about an order of magnitude faster than for the circumneutral, low oxygen mine-pools. These results agree with a conceptual model of ongoing oxidation in aerated, partly flooded mines, while weathering rates are slowed in flooded mines. Even when input dissolved oxygen is increased to 0.1 mg/L for the Hahn and Arden-Westland mine-pools, the calculated pyrite consumption rates are still two to three times slower than in the Omega and T&T mine-pools. Conversely, if dissolved oxygen is restricted to less than 0.01 mg/L in the flooded Hahn and Arden-Westland mine-pools, the calculated consumption rates are further reduced. Pyrite consumption rates computed from Fe^{2+}/Fe^{3+} ratios (equation 5-29) for the acid samples were similar or slightly larger (two to five times) than the rates from the general law (equation 5-27). The value for T&T 2008 is outside the suggested pH range for equation 5-30, and is considered a less reliable estimate.

The magnitude of the pyrite consumption rate estimates for the five mine-pools is similar to values reported in laboratory and small scale tests. Lappako and Anston (2006) reported pyrite consumption rates ranging from 4 x 10^{-10} to 1.8 x 10^{-9} mole/m^2-s for pyrite-bearing rocks from a
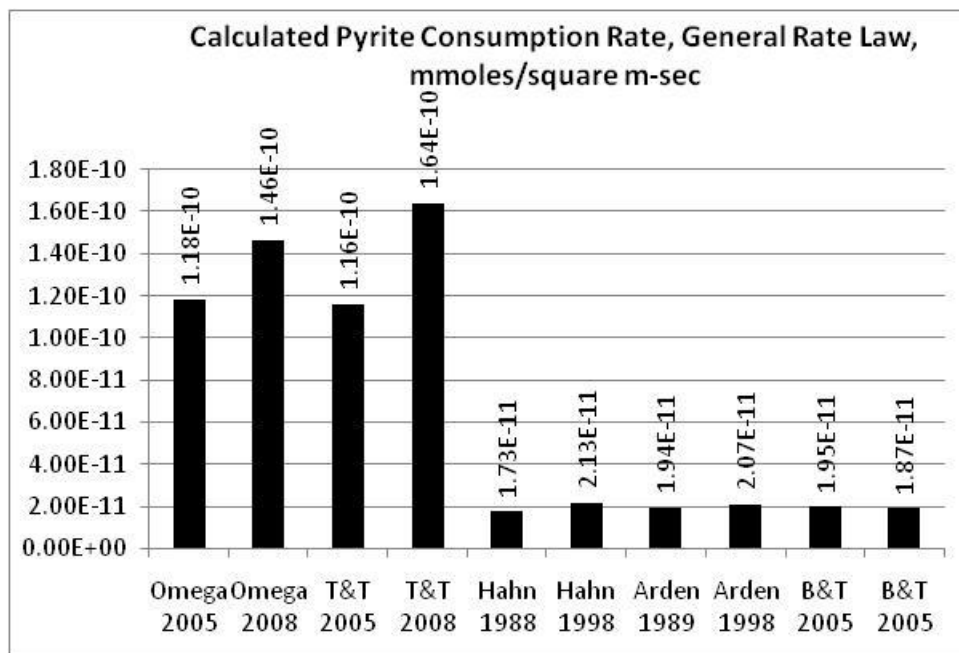
Figure 5-47. Calculated Pyrite Consumption Rate Using Williamson and Rimstidt's (1994) General Rate Law with Dissolved Oxygen and pH.

Table 5-21
Data for Estimating Pyrite Oxidation Rate
in Five Mine-pools with Williamson and Rimstidt's (1994) Rate Laws

Mine-pool	pH	Dis. O_2 mg/L	Dis. O_2 mole/L	Fe^{2+} mole/L	Fe^{3+} mole/L	Rate, r[1] from pH and DO	Rate, r[1] from Fe^{2+} and Fe^{3+}
Omega 2005	2.53	2.97	9.28E-05	1.39E-03	2.62E-04	1.18E-10	5.52E-09
Omega 2008	2.73	4.12	1.29E-04	3.20E-03	1.62E-05	1.46E-10	2.97E-10
T&T 2005	2.57	2.8	8.75E-05	1.21E-04	5.91E-05	1.16E-10	3.67E-09
T&T 2008	4.36	2.27	7.09E-05	6.19E-04	1.66E-06	1.64E-10	6.89E-11
Hahn 1988	6.18	0.01	3.13E-07			1.73E-11	
Hahn 1998	7.00	0.01	3.13E-07			2.13E-11	
Arden-Westland 1989	6.63	0.01	3.13E-07			1.94E-11	
Arden-Westland 1998	6.90	0.01	3.13E-07			2.07E-11	
B&T 2005	6.67	0.01	3.13E-07			1.95E-11	
B&T 2005	6.50	0.01	3.13E-07			1.87E-11	
Hahn 1988	6.18	0.1	3.13E-06			5.46E-11	
Hahn 1998	7.00	0.1	3.13E-06			6.72E-11	
Arden-Westland 1989	6.63	0.1	3.13E-06			6.12E-11	
Arden-Westland 1998	6.90	0.1	3.13E-06			6.55E-11	

(1) Rate in mole/m^2-s.

Minnesota mine. Glesiner et al. (2006), studying the effects of oxygen concentration on Acidthiobacillus activity, reported pyrite oxidation rates on the order of 5 x10^{-10} mole/m^2-s with a range of 7 x 10^{-12} to 8.9 x 10^{-10}, and the rate was directly proportional to oxygen content. Other studies have reported pyrite weathering rates on the basis of mg SO_4/g rock-unit time. As summarized by Hammack and Watzlaf (1990) consistent data from five other studies compared favorably with their own.

Jerz and Rimstidit (2004), measured pyrite oxidation rates in moist air, conditions that are analogous to aerated sections of underground mines. They found the oxidation rate to be a function of pO_2 and time. Oxidation rate decreased over time, which was attributed to the formation of a thin surface layer of ferrous sulfate, possibly melanterite. The scenario described could also occur in unsaturated mine-works, where weathering products accumulate on particle surfaces, temporarily slowing pyrite consumption. Jerz and Rimstidt also note that the volume increase associated with hydrous ferrous sulfate formation could wedge apart rock fragments exposing more surface area. For partly flooded mines where the inundated zone fluctuates seasonally, and in response to individual recharge events, soluble ferrous sulfate is likely to be rinsed from the mineral surface. Less soluble minerals such as jarosite may persist, however.

The calculated pyrite consumption rates in table 5-21 provide a useful comparison among acidic, partly flooded and circumneutral and flooded mine-pools, but may overestimate actual field weathering. The rate equations reported by Williamson and Rimstidt (1994) and similar studies are usually based on laboratory scale experiments, using clean pyrite grains or rock fragments in a liquid suspension. Test time is often on the order of days or weeks. Weathering conditions are

optimal or near optimal, and the derived values likely represent an upper bound on expected rate. Transport of reactants by advection and diffusion, especially of oxygen, and of products including Fe and H^+ may limit field oxidation rate.

Schnoor (1990) reported a study comparing weathering rates in laboratory columns and batch tests to field weathering in a small watershed using dissolved silica as a tracer. He concluded that field weathering was one to two orders of magnitude slower than lab testing based on his experiments and similar studies. Hood and Oertel (1984) used a leaching column method to simulate coal mine water quality, and compared results to field weathering. They estimated that lab weathering was about 1.5 orders of magnitude faster than field weathering.

A series of pyrite oxidation models incorporating transport and chemical weathering rates have been developed since the 1970's, including one devised for underground mines. Morth et al. (1972) developed a model for acid production based on a small partly flooded underground mine in Ohio. This pioneering modeling effort assumed chemical weathering takes places largely at the surface of the rock fragment and in fractures. Oxygen supply was assumed to be driven by barometric pressure fluctuations, and diffusion in the mine atmosphere. Morth et al. also coupled the acid production model to a quantitative hydrology module to account for transport and pollutant flux. They reported good agreement between predicted and measured parameters for several simulations encompassing a range of flow conditions. This initial model seems not to have been pursued further. The model was not designed for flooded mines.

Jaynes et al. (1984a, 1984b) developed a model to simulate acid drainage production in surface mines. As such, the model assumes oxygen transport from the surface through an unsaturated zone to, and into, pyrite bearing rock fragments. A key feature of this model is oxygen supply by gaseous diffusion, both within the unsaturated zone, and within individual rock fragments. The governing equations for oxidation within rock fragments as presented by Jaynes et al. are a form of the "shrinking core" reaction model. The general form and derivation is described by Levenspiel, 1972. The shrinking core model for oxygen flux into pyrite grains is illustrated in figure 5-48. Oxygen supply to the reaction site is assumed to be the limiting factor controlling overall pyrite oxidation. Oxidation starts at the surface of the grain, and proceeds as a uniform weathering front to the center. A weathering rind or ash layer forms as the oxidation product, so that the overall dimensions of the fragment remain the same. Soluble products counter-diffuse out of the fragment at a rate equal to inward oxygen migration. Oxygen and products must diffuse through the ash layer, which increases in thickness as weathering progresses. With these simplifying assumptions, an oxygen flux rate can be estimated, which in turn controls the pyrite oxidation rate. Wunderly et al., (1996) and Jaynes et al., (1984a) describe an oxygen flux equation based on the shrinking core model. Their respective notations differ, but are equivalent expressions. Oxygen flux is calculated by Wunderly et al. (1996) as:

$$d \; mass \; O_2 \, / \, dt = \; 4 \, \pi \, D \, (\frac{R \, r_x}{R - r_x}) \; Uw \qquad \qquad (5\text{-}31)$$

where:

D is the diffusion coefficient in the weathered rim of the grain

R is the whole grain radius

r_x is the radius of the unreacted grain core

U_W is the oxygen concentration at the outer surface of the particle.
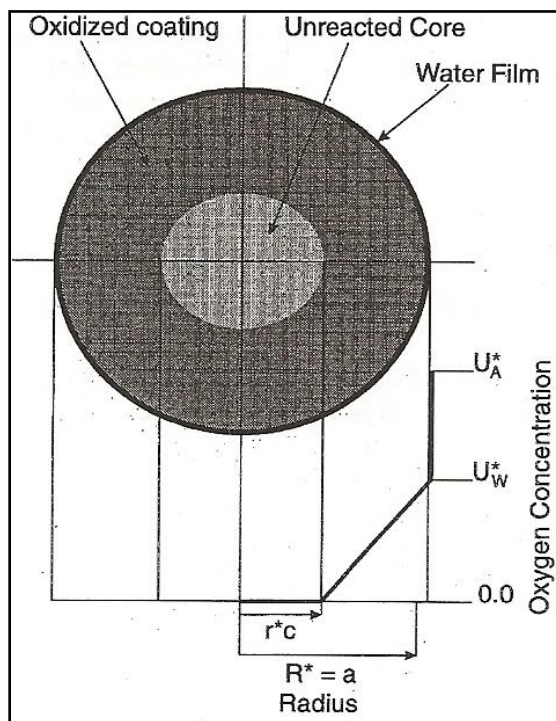
Figure 5-48. Shrinking Core Model of Pyrite Oxidation by Oxygen Diffusion. Modified fromWunderly et al., 1996.

If oxygen concentration and the diffusion coefficient are constants, oxygen flux and hence, pyrite oxidation, depends only on the position of the weathering front, r_x, within the grain. Figure 5-49 shows the relative oxygen flux as a fraction of the grain weathered. This graph was constructed by assigning a grain radius of one, and successively reducing the unreacted core radius in 100 steps. Oxygen concentration at the outer surface was maintained at one mg/L and the diffusion coefficient was selected from Bains et al (2000), who used the model developed by Wunderly et al. (1996).

Figure 5-49 shows three significant effects. The total change in oxygen flux rate spans about seven orders of magnitude as weathering progresses from the outer surface to the center of the grain. Thus oxidation rates and acid production will slow. Second, oxygen flux decreases rapidly with formation of even a very thin weathering rind. Third, diffusion controlled pyrite weathering will proceed for extended time frames before the source mineral is exhausted, albeit with declining acid production. The shape of the flux curve is similar to a time series plot of total

acidity, sulfate or other parameters related to acid production in mine-pools described earlier in this chapter. Oxygen diffusion is a probable micro-scale transport control on acid generation.
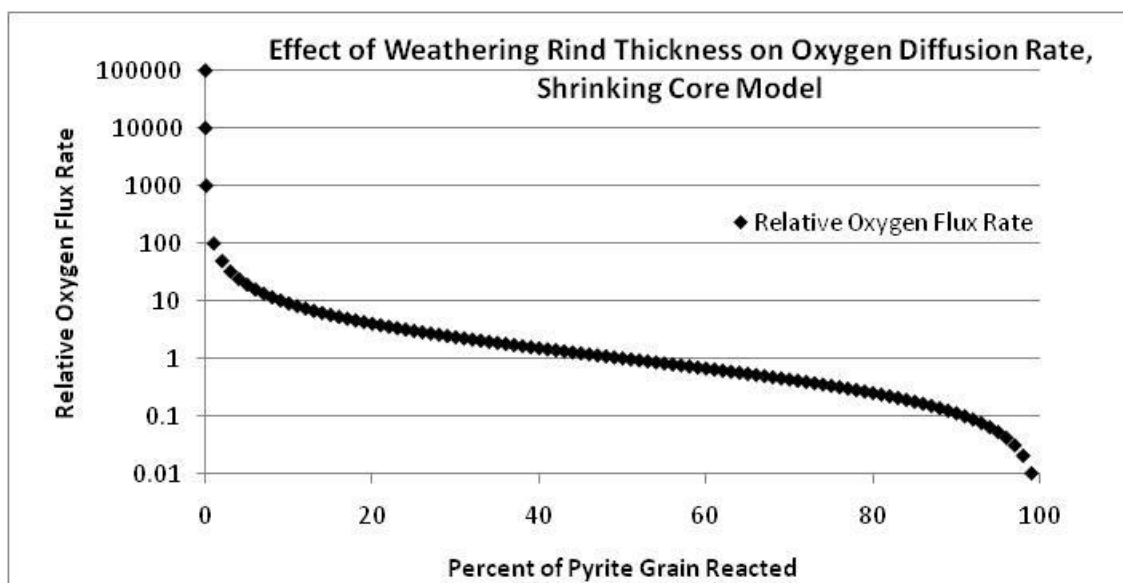
Figure 5-49. Relative Oxygen Flux Rate and Percent of Pyrite Grain Reacted.

The shrinking core model has some caveats when applied to pyrite weathering in mine-pools. First is the assumption of a uniform ash layer. If all or part of the reacted outer zone is rinsed, or diffuses away from the particle, oxygen reaches the unreacted core more rapidly. A second consideration is physical weathering of the rock or mineral grain, opening fractures and exposing new mineral surfaces to chemical attack. The magnitude of these exceptions to the shrinking core model is difficult to quantify, however.

Jaynes et al. (1984b) reported several simulations of acid drainage in surface mines using their model which is similar in concept to Wunderly et al. (1996). For simulations exceeding 25 years, they found for most runs, that less than half of the specified pyrite content had reacted. In addition to diffusion, changing tortuosity and particle size also affected the simulated weathering rates by altering oxygen transport. Their simulated water chemistry was in general agreement with samples measured from reclaimed mines.

Wunderly et al. (1996) also developed a model coupling oxygen diffusion and pyrite oxidation. Geochemical calculations were based on assumption of local thermodynamic equilibrium. Like Jaynes et al., their model, PYROX, is based on an assumption that oxygen transport to the reaction site limits the pyrite oxidation rate. Their model was evaluated using data from a tailings impoundment which included a vadose zone over saturated tailings. Their simulations were in good agreement with observed weathering and mineral reactions. Because the tailings are relatively fine grained, they concluded that convection was an unlikely transport mechanism for oxygen. Pantelis and Ritchie (1991) observed that convection is significant only in coarse grained materials with high permeability. Bains et al. (2000) used a variant of the PYROX model

to simulate 35 years of tailings weathering. They also found good agreement between simulations and actual conditions.

The literature describing pyrite oxidation and reactive transport modeling provide several useful observations for mine-pools:

- Pyrite oxidation rates are fast if reactants are not limiting. Rates are directly proportional to oxygen content. Table 5-21 shows that oxidation in acidic, aerated mine-pools is more rapid than in flooded mines.

- Oxygen availability and transport at the macro and micro-scale can profoundly affect oxidation rate. In flooded mine-pools, the primary macro-scale transport is advection by flowing ground-water. In partly flooded mines, barometric pressure fluctuations can supply oxygen through fractures, subsidence cracks and other openings (Morth et al., 1972). Oxygen diffusion is an important control at the micro-scale within rock and mineral surfaces, shown in both experiments and analytical simulations.

- Diffusion can reduce pyrite oxidation rate, and hence flux of acid weathering products. This is expressed as declining flux as weathering slows and the mine-pool ages.

- Diffusion rate constraints effectively extend the weathering period for pyrite, which otherwise would be rapidly consumed.

A declining flux implies that at some future state, mine-pool waters should contain negligible concentrations of pyrite weathering products. Either the oxidation rate slows because of diffusion constraints on oxygen supply, or the mineral is depleted. From a mass balance consideration, complete depletion of pyrite is unlikely on a time scale of decades As pyrite oxidation slows and the mine-pool ages, could the mobility of Fe, Al, sulfate or other chemicals be controlled by others minerals? That prospect is examined in section 5.5.

5.5 Metal Solubility Controls in Aging Mine-pools

Time series plots of chemical concentration for pyrite weathering products such as figure 5-18, Fe concentration in the Hahn mine-pool, exhibit decreases in both absolute concentration and rate of change with time. The following questions arise when considering these time series plots:

- Will concentrations continue to decline until they reach background conditions? Or,

- Will the mine-pool establish a new chemical composition as its baseline condition?

The solution to these questions can determine how long treatment is needed to achieve specified water quality, or when the mine-pool may be viewed as a ground-water resource, rather than a liability.

The form of the decay function described in previous sections implies a continuing decline in concentration. It has no provision for recognizing geochemical or hydrologic processes that might stop the decay process and establish a steady state condition. Mineral solubility constraints are one such process that could control chemical composition of aged mine-pools.

The author has collected water samples from mine-pools ranging up to about 100 years old, and has found that small concentrations of Fe, sulfate and Al, and sometimes low pH, persist. The waters remain unsuited for most uses, although the concentrations of parameters are small relative to newly formed mine-pools in analogous hydrogeologic and geochemical settings.

Two samples from mine-pools aged about 60 and 90 years were selected for analysis of possible long term geochemical controls on Fe and Al. The first site is the Ruthbelle mine-pool discharge. This mine is located immediately adjacent to the T&T mine-pool, Upper Freeport coal bed in Preston County, WV. Mining dates to the 1950's, and because the mine is hydrologically connected to the T&T complex, drainage from the Ruthbelle mine has been monitored by the West Virginia DEP since the mid 1990s. The author has sampled the Ruthbelle drainage on six different dates. An analysis deemed representative is shown in table 5-22. The Ruthbelle drainage represents the case of an acidic, partly flooded aged mine-pool. A second analysis is from the Acme mine-works, in Marion County, West Virginia (table 5-22) and is among four collected by the author from this site. Mining dates from the 1920s in the Pittsburgh coal bed, and the mine-pool discharge at the up-dip entries. The Acme mine-pool represents the case of a flooded circumneutral mine-pool and is in the same coal bed with similar geology as the Hahn and Arden-Westland mine-pools.

Table 5-22[1]

Chemical Composition of Aged Acidic, Partly Flooded and Circumneutral Flooded Mine-pools

Mine[2]	pe	pH	Alkalinity	Fe	Al	SO_4	Ca	Mg	Na	Cl	Si
Ruthbelle (partly flooded)	13.03	2.68	-	6.63	4.76	235	40.5	14.1	1.3	5	6.8
Acme (flooded)	1.83	6.25	263	5.15	0.05	543	104.3	39.8	165	6	5

(1) Alkalinity in mg/L $CaCO_3$ Eq. Elements in mg/L. pH in S.U.
(2) Ruthbelle sample collected 5/17/05. Acme discharge sampled 6/8/08.

Both mine-pools contain relatively small amounts of dissolved iron, and the Ruthbelle water also has about five mg/L of dissolved Al. These metals concentrations, while easily treatable, generally exceed standards for most water uses, and thus remain problematic.

A set of mineral solubility calculations were run for both waters in PHREEQCI (Parkhurst and Appelo, 1999) to estimate saturation indices for common iron and aluminum minerals. Results are shown in table 5-23. The Ruthbelle water is under-saturated for all of the more soluble Fe oxide, hydroxide and sulfate minerals shown in the table. It is over-saturated by more than three

orders of magnitude for the crystalline and less soluble oxyhydroxide goethite. It is also under-saturated for three minerals that potentially control Al availability; jurbanite, kaolinite and poorly crystalline $Al(OH)_3$. The Acme discharge is also under-saturated for more soluble Fe minerals and more than three orders of magnitude over-saturated for goethite. Aluminum concentrations are low in the Acme water, and may be controlled by a less soluble form of $Al(OH)_3$, alumino-silicates such as kaolinite, or alumino-sulfates such as alunite.

Both waters are more than three orders of magnitude over-saturated for goethite. This degree of over-saturation indicates that goethite is likely not the controlling mineral for Fe in either water. Either goethite is not present; the kinetics are so slow that its formation isn't satisfactorily addressed with equilibrium calculations, or Fe is controlled by another mineral. A number of weathering studies suggest that goethite sometimes forms as the more stable alteration product of other oxide and hydroxide minerals (Schwertmann and Taylor, 1977; Macalady et al., 1990). In mine waters and sediments goethite has been reported to form from ferrihydrite and schwertmannite (Kim et al., 2002; Jonsson et al., 2005). The total range of Fe oxide solubility can span seven orders of magnitude (Langmuir, 1997), thus control of Fe solubility in aging mine-pools may be a function of which minerals are present and the degree of crystallinity. Sediments precipitating from mine waters often contain a mixture of Fe minerals ranging from poorly crystalline to sulfate bearing to goethite (Karathanasis and Thompson, 1995; McCarty et al., 1998; Bowell and Bruce, 1995; Kaires et al. 2005). Since more soluble Fe minerals are common in mine water sediments, and both waters in table 5-23 are under-saturated for them, this analysis considered poorly crystalline $Fe(OH)_3$ as a potential control. Jarosite is unlikely to influence the Acme mine water composition, since this mineral is over-saturated by 11 orders of magnitude and characteristically forms in acid oxidizing environments (Nordstrom, 1982a).

Table 5-23
Mineral Indices of Aged Acidic, Partly Flooded, and Circumneutral Flooded Mine-pools

Mine	$Fe(OH)_3$	$Fe_3(OH)_8$	Goethite	K-Jarosite	Schwertmannite	Jurbanite	Kaolinite	$Al(OH)_3$
Ruthbelle (partly flooded)	-2.06	-14.07	3.29	-1.86	-2.72	-1.52	-9.63	-8.28
Acme (flooded)	-2.07	-6.54	3.41	11.13	-15.06	-0.80	5.49	-0.51

Examining the chemical composition and mineral saturation index data in tables 5-22 and 5-23, there are no obvious mineral controls that would further reduce Fe and Al concentrations. All the minerals in table 5-23 are, however, influenced by pH and/or Eh (pe) conditions. Therefore, a series of simulations were conducted using PHREEQCI where pH and Eh (pe) were varied to examine effects on mineral solubility. The simulations were run in 100 steps as follows:

- The acidic Ruthbelle discharge was treated by addition of calcite at the rate of five mmole/L to adjust pH.

- A second simulation for the Ruthbelle water included calcite addition as before, plus the introduction of 0.1 mmole of dissolved oxygen to adjust pH and Eh.

- The circumneutral Acme mine water had 0.01 or 0.05 mmole dissolved oxygen added to adjust Eh.

The oxygen values were selected to represent conditions in a partly flooded mine-pool and introduction of small O_2 amounts into a flooded mine-pool. The minerals listed in table 5-23 were assumed to be absent initially, but were allowed to precipitate if the solution reached saturation for that mineral. The quantity of remaining soluble Fe and Al were tabulated through each step. The initial run for each water considered all the minerals in table 5-23 as potential controls. Subsequent runs removed certain minerals to examine the effects of specific components. Remaining soluble Al and Fe were plotted as a function of pH or Eh (pe). The pH or pe at which saturation occurred for specific minerals was calculated by substituting chemical activities into the appropriate equilibrium expression.

Figure 5-50 shows the first set of simulation results for adding calcite, and calcite plus oxygen to the acidic Ruthbelle discharge. The initial Fe concentration of 6.53 mg/L (left Y axis) was reduced by mineral formation as pH increased. The first simulation considered K-Jarosite, schwertmannite and $Fe(OH)_3$ as the potential controls on soluble Fe, with no added oxygen, and
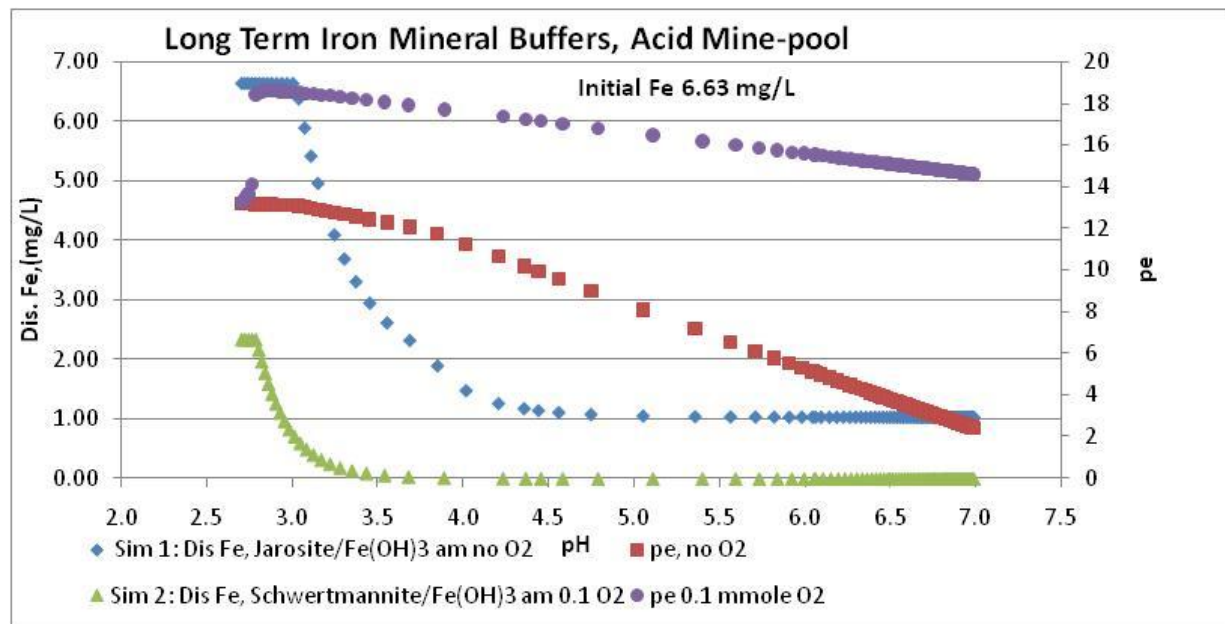
**Figure 5-50. Simulation Results of Long Term Iron Solubility Controls
in the Aged Acid Ruthbelle Mine-pool. Initial sulfate and potassium
concentrations are 235 mg/L, and 1.15 mg/L, respectively.**

pH as the only variable. Saturation for schwertmannite was not achieved, and K-Jarosite and $Fe(OH)_3$ were the only minerals controlling Fe. Soluble Fe was reduced to about one mg/L by

formation of K-Jarosite and $Fe(OH)_3$. The remaining soluble Fe is Fe(II), and absent an oxidizer in this simulation, ferrous iron cannot react to form K-Jarosite or $Fe(OH)_3$. Redox, expressed by pe, declined sharply during the simulation to about two, as oxidized species were precipitated. The complete lack of oxygen was considered unrealistic and was revised in the next run.

The equilibrium saturation pH for K-Jarosite saturation is 2.99, and 3.84 for $Fe(OH)_3$ am. They were calculated from the following solubility expressions and appropriate chemical activity values:

$$KFe_3(SO_4)_2(OH)_6 + 6 H^+ \leftrightarrow K^+ + 3 Fe^{+3} + 2 SO_4^{-2} + 6 H_2O \quad \log Kt = -8.05 \quad \text{(5-31)}$$

$$Fe(OH)_3 + 3 H^+ \leftrightarrow Fe^{+3} + 3 H_2O \quad \log Kt = 4.89 \quad \text{(5-32)}$$
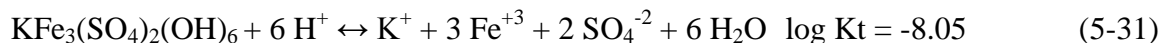
The second Fe simulation for the Ruthbelle discharge included the addition of 0.1 mmole/L (3.2 mg/L) of oxygen, which is similar to actual conditions. The potential iron sinks included schwertmannite, $Fe(OH)_3$ and K-Jarosite. Schwertmannite is an Fe oxyhydroxysulfate mineral of variable composition. It has been found in mine waters in Asia and North America (Bigham et al., 1990; Bigham et al., 1996; Yu et al., 1999). Because of poor crystallinity and variable composition, the reported solubility varies (Yu et al., 1999). The average composition and log K reported by Yu et al. were used to simulate schwertmannite behavior.

The second simulation of Ruthbelle water, adding oxygen and calcite, essentially reduced soluble iron to zero. The equilibrium pH for schwertmannite saturation was 2.79 and 3.79 for $Fe(OH)_3$. They were calculated from equation 5-33 and 5-32. The inclusion of oxygen permitted conversion of Fe(II) to Fe(III) in the simulation, and maintained overall oxidizing conditions in the mine-pool, similar to actual conditions.

$$Fe_8O_8(OH)_{4.4}(SO_4)_{1.8} + 20.4H^+ \leftrightarrow 8 Fe^{+3} + 12.4H_2O + 1.8SO_4^{-2} \quad \log k = 10.5 \quad \text{(5-33)}$$
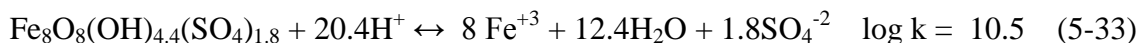
Both Ruthbelle simulations show that if pH is increased to about 3.8 or greater, Fe could be removed as $Fe(OH)_3$ before complete neutralization of the mine-pool is achieved. As the mine-pool sediments age and transition towards goethite, they should be less soluble.

Schwertmannite solubility is highly sensitive to Fe^{3+} activity, as seen in equation 5-33. Thus redox status influences which minerals actually control Fe solubility. The simulations show that Fe may be controlled by K–Jarosite or schwertmannite at pH as low as about three, but both minerals are considered metastable with respect to goethite (Jonsson et al., 2005; Bigham et al., 1996). The range of pH and Eh control by schwertmannite may fluctuate, since the mineral's solubility and composition varies (Yu et al. 1999).

Figure 5-51 shows simulation results for soluble Al in the Ruthbelle drainage with addition of calcite. Jurbanite, kaolinite, and poorly crystalline $Al(OH)_3$ were considered potential controls. The T&T mine-pool adjacent to Ruthbelle has apparent saturation for jurbanite, and kaolinite is a

common clay mineral in these strata (Dulong et al., 2002). The initial simulation included all three minerals, followed by runs where Al was considered to be controlled by one mineral only.
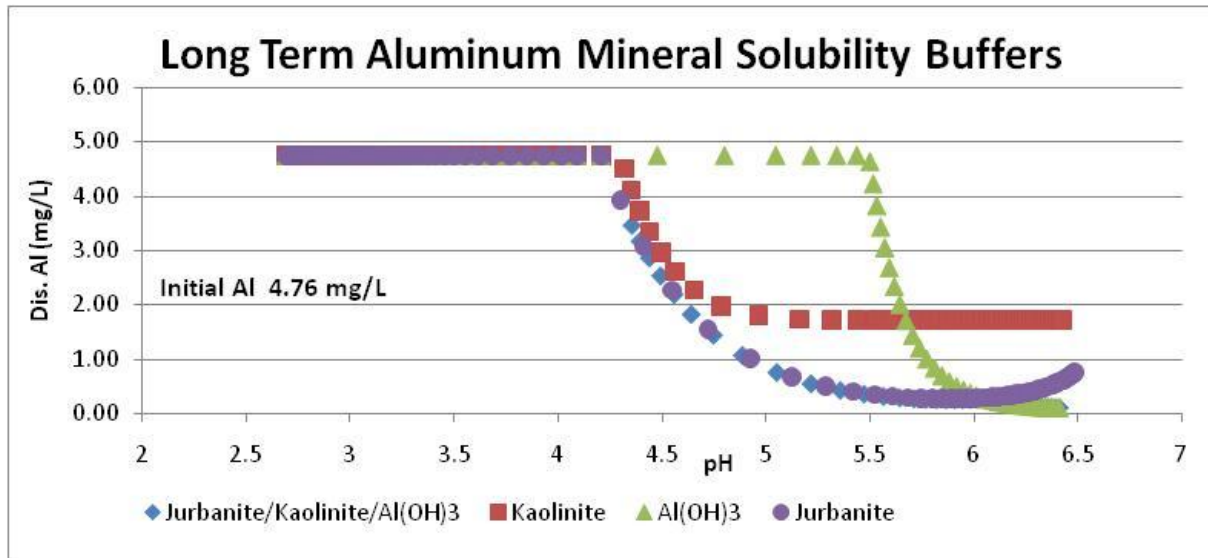
Figure 5-51. Simulation Results of Long Term Aluminum Solubility Controls in the Aged Acid Ruthbelle Mine-pool. Initial sulfate and silica concentrations are 235 and 6.8 mg/L respectively.

The initial run showed soluble Al to be controlled successively by jurbanite, kaolinite and Al(OH)$_3$ as pH increased. The equilibrium pH for jurbanite saturation was 4.21, kaolinite equilibrium pH was 4.35, and equilibrium pH for Al(OH)$_3$ saturation was 6.06. Soluble Al was reduced to about 0.1 mg/L. Equilibrium pH was calculated for the three minerals from the expressions shown in equation 5-34, 5-35 and 5-36 with appropriate chemical activities.

$$AlOHSO_4 + H^+ = Al^{+3} + SO_4^{-2} + H_2O \qquad \log Kt = -3.23 \qquad (5\text{-}34)$$

$$Al_2Si_2O_5(OH)_4 + 6\ H^+ = 2\ Al^{+3} + 2\ H_4SiO_4 + H_2O \quad \log Kt = 8.74 \qquad (5\text{-}35)$$

$$Al(OH)_3 + 3\ H^+ = Al^{+3} + 3\ H_2O \qquad \log Kt = 11.78 \qquad (5\text{-}36)$$

A second run, using kaolinite as the only Al buffer, is also shown in figure 5-47. Soluble Al was reduced to about 1.7 mg/L. Kaolinite formation and additional Al removal was constrained by depleting available Si. In the mine-pool, weathering of other silicates could provide additional Si, and kaolinite would limit soluble Al.

A third run used Al(OH)$_3$ as the only mineral sink in the Ruthbelle water. Soluble Al was reduced to about 0.1 mg/L, but mineral saturation and formation was not attained until pH reached about 5.6.

195

The final run simulating Al control used jurbanite as the controlling mineral. Soluble Al was reduced to a minimum of about 0.26 mg/L at pH of 5.9. At pH greater than 6, jurbanite solubility increased as did soluble Al. The equilibrium pH for jurbanite saturation was 4.3.

The simulations show that if Ruthbelle mine-pool pH is increased to about 4.3 or greater, soluble Al can be reduced. The lowest concentrations are attained if $Al(OH)_3$ is the controlling mineral. Kaolinite formation could also effectively control soluble Al with sufficient available Si and reaction time.

The second set of simulations was performed using the circumneutral mine-pool waters from the Acme mine (tables 5-22 and 5-23). Iron is the metal of concern in this water and redox state is the primary variable to test. As in the Ruthbelle waters, goethite is over-saturated by more than three orders of magnitude, suggesting it is not controlling soluble Fe. The possible controls were considered to be schwertmannite and poorly crystalline more soluble $Fe(OH)_3$. Siderite was also considered as a potential control, but is somewhat under-saturated with an index of about -0.2. A small amount of oxygen, either 0.01 or 0.05 mmoles, was added in different runs to simulate O_2 introduction by recharge or planned oxidation. No pyrite or other oxidizable minerals were present in the simulation. Fe(II) was allowed to oxidize to Fe(III), and distributions of the ferrous and ferric iron species were a function of pe. Results are shown in figure 5-52, with soluble Fe plotted against pe.

The addition of a small quantity of oxygen increased pe and the activity of Fe^{3+}, beginning with the first step in each run. Soluble Fe was reduced to about 2.9 mg/L when oxygen supply was limited for either schwertmannite or $Fe(OH)_3$ (fig 5-48). However, the run results show that even a small shift in pe of less than 0.5 units is sufficient to affect mineral precipitation and soluble Fe. When oxygen supply was increased, soluble Fe was essentially reduced to zero by either mineral, as pe increased to about 6.
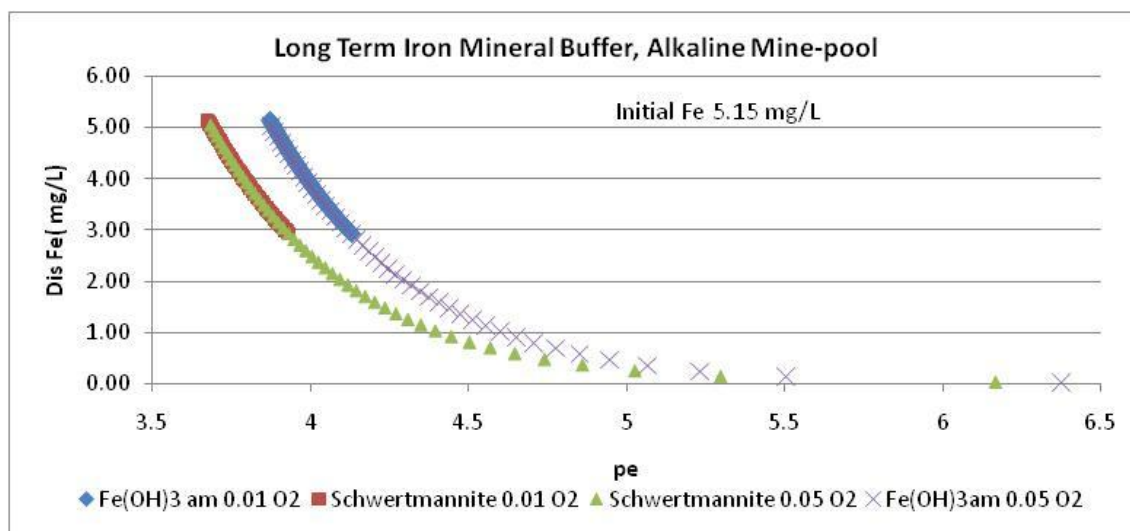
Figure 5-52 Simulation Results of Long Term Iron Solubility Controls in the Aged Circumneutral Acme Mine-pool.

196

The persistence of low concentrations of soluble Fe and Al in the aged Ruthbelle and Acme mine-pools suggests that long term chemistry may be influenced by mineral solubility. Solubility calculations for both waters did not clearly identify any controlling phases that might further reduce concentrations. Both Fe and Al have multiple potential source and sink minerals of varying solubility and reaction rates. The simulation results for both waters show that dissolved metals can be reduced by manipulating pH and redox status, and that the magnitude of change required is not large. Other processes including ion exchange and adsorption/desorption were not explicitly included in these simulations, but could also affect soluble metals concentrations.

5.6 Chapter 5 Summary Findings and Observations

Chapter 5 examined long term trends in water chemistry for two partly flooded, acidic and three mostly flooded circumneutral mine-pools. The available monitoring records encompassed about to 12 to 35 years of post closure water data. The analyses included the following:

- Evaluated in-situ neutralization of acidity;

- Estimated decay constants to describe the rate of chemical concentration change;

- Examined factors that may control or contribute to the magnitude of the decay constant, including macro and micro scale transport processes.

- Conducted simulations of aged mine-pool waters to identify controls on dissolved metals concentrations.

The principal findings and conclusions of this chapter are summarized as follows:

- A large fraction of the strong acid (H^+) acidity attributable to pyrite oxidation was missing from all five mine-pools. The missing acidity is described as in-situ neutralization and exceeds 100% in the flooded net alkaline mine-pools. Significantly, the two acid mine-pools had neutralization ratios on the order of 60 to 70%. Thus, even in acidic mine-pools, water treatments needs are substantially reduced by the acid-consuming weathering reactions. In-situ neutralization includes consumption by weathering of carbonates, alumino-silicates and oxyhydroxides, and alkaline recharge from ground-water infiltration. Bicarbonate alkalinity from sulfate reduction in flooded mine-pools, and exchange and adsorption reactions may also contribute to apparent neutralization.

- Neutralization ratios computed from strong acid (H^+) acidity persist or even increase through the monitoring record for all five mine-pools. Thus water treatment needs or off site impacts are not likely to increase over time.

- Mineral weathering constituted about 60 to 95% of the in-situ neutralization of the strong acid (H^+) acidity, depending on mine-pool age and flooding state. Mineralogy of

the residual coal, floor and roof rock is the principal control on in-situ weathering. The Omega and T&T mine-pools are in a sequence of rocks with few carbonates and have limited acid consuming capacity. The Hahn and Arden-Westland mine-pools are in rocks containing a series of calcareous rocks with significant acid consumption capacity.

- Mineral weathering was reflected by increased concentrations of Ca, Mg and Al in acidic mine-pools. Elevated Ca and Mg probably reflect carbonate weathering, but could include consumption of other minerals. Specific minerals involved could not be directly identified, but were inferred from solution composition and solubility considerations.

- Significant consumption of alumino-silicates and or Al-oxyhydroxides is occurring in the two acidic Omega and T&T mine-pools. After more than ten years of weathering, the two mine-pools are discharging soluble Al equivalent to consuming about 0.7 and 1.5 mmole kaolinite per L of solution.

- Interpreting Al and sulfate behavior is complicated by apparent equilibrium for jurbanite in the two acid mine-pools. Acid production in these mine-pools may be underestimated if sulfate bearing minerals are retained in place.

- Soluble Al exiting the mine-pool should not be included as an overall neutralization process. The H^+ originally consumed in mineral weathering is offset by hydrolysis in water treatment yielding a net neutralization of zero. Some weathering reactions in the mine-pool, for example jurbanite/kaolinite transformation, can be net acid consuming.

- Two methods for estimating neutralization ratio, cation summation and neutralization by difference produced similar estimates. Either can provide a useful estimate of in-situ weathering.

- Estimating neutralization based on speciated solutions was useful for acidic waters containing appreciable Fe(III). In these waters, accounting for H^+ consumption by Fe(II)/Fe(III) oxidation did change the overall neutralization ratio. In waters dominated by Fe(II) there was little advantage to speciating solutions.

- Long term chemical concentration data often fit a first order type reaction plot. The general form of the decay (chemical concentration decline) equation was adequate to estimate the long term trends for total acidity, Fe, Al, sulfate and TDS. Computed decay (k) constants, with few exceptions, range within one order of magnitude. The rates are on the order of 10^{-4}/d.

- Percentage coefficient of variation (R^2) values approached 90 % for some the flooded mine-pools, indicating robust estimates for computed decay constants. R^2 were generally

lower for the unflooded acidic mine-pools due to the higher variation inherent in these data sets.

- Chemical concentration decay can be divided into early and late mine-pool history phases. The early phase includes the flushing of accumulated salts and acid weathering products including "vestigial" acidity. Concentrations decline most rapidly during the early flushing phase. The late phase includes the continued weathering of pyrite and other minerals and removal of "juvenile acidity". Concentration ratios of Fe to sulfate may be a useful method to separate early and late phase decay.

- Some long term data such as pH in the acidic Omega and T&T mine-pools had statistically insignificant chemical decay values. The rate of change is too small to be resolved in these data.

- Early phase chemical decay was about 1.5 to three times faster than late phase decay. Separate decay values should be used to model early and late phase water quality conditions. Using early and late phase decay reduces differences between predicted and actual values.

- With exception of Fe, flooded circumneutral mines have slightly faster decay rates (1.2 to 1.5 times) than unflooded acidic mines. Iron decay is slower in flooded compared to unflooded mines. Unflooded mines have a more oxidizing environment, and conditions are more favorable for the in–situ retention of Fe by formation of less soluble Fe (III) minerals. Flooded mines, in contrast, are dominated by ferrous Fe, which is soluble over a wider pH range and less likely to be immobilized in situ.

- Al has a slower decay (1.5 to two times) compared to Fe, SO_4, and total acidity. The slower Al decay rate may result from continued addition of Al to the system by ongoing alumino-silicate weathering and solubility controls from minerals such as jurbanite and alunite. Al decay was only computed for two acid mine-pools. The circumneutral pools had insignificant concentrations of soluble Al.

- Time frames to reach specified water quality concentrations were on the order of decades. In general, most chemical decay predictions ranged from about 30 to 70 years duration. Aluminum was predicted to have the longest decay period, in some instances exceeding 100 years. The range of statistical uncertainty can span one to two decades for these long term estimates.

- Decay rates are useful for long term chemical value trend estimates. They are less useful for estimating concentration at specific points in time. The decay function does not explicitly account for seasonal variation or other short term changes.

- The chemical decay constant is a lumped variable that includes both chemical reaction and transport elements. It is weakly related to physical parameters including maximum flow path length, recharge rate and residence time. However the small size of the data set (five mines) precluded a rigorous analysis.

- Chemical decay constants were correlated among themselves on a mine by mine basis, suggesting site specific influence.

- A simple model of slow flushing of the mine-pool relative to mineral dissolution rates produced reasonable results. A model assuming rapid flushing relative to mineral dissolution produced results deemed unreasonable. This analysis implies that transport controls observed decay more than chemical kinetics.

- Pyrite oxidation rates estimated from published rate data were about an order of magnitude faster in unflooded mines compared to flooded mines. The rates are sensitive to oxygen content. A faster oxidation rate for pyrite in unflooded mines might be reflected as overall slower chemical decay when compared to flooded mines. Flooded mines do have slightly higher decay rates (1.2 to 1.5 times) for four of five parameters, but the differences cannot be assigned to chemical weathering with certainty.

- A literature review of selected pyrite oxidation models for tailings, spoil piles and underground mines found that all incorporate oxygen diffusion as a rate limiting process. Diffusion is treated on two scales, as oxygen transport through the rock pile or mine-pool water, and as a shrinking core model of oxygen movement within individual grains. In the shrinking core model, oxygen diffusion and corresponding weathering rates are highly sensitive to the position of the grain weathering front and buildup of a reacted layer. Transport at the micro scale could influence decay rates.

- Advective transport of oxygen and weathering products in flooded mines could influence chemical decay rates, and airflow driven by barometric changes may be important for oxygen transport in partly flooded mines.

- The chemical decay constants have no provision for complying with mineral solubility constraints as the mine-pool ages. Samples of aged mine-pools seem to retain dissolved metals such as Fe and Al in the range of a few to a few tens of mg/L. These concentrations are larger than might be estimated using decay constants.

- Simulations of aged mine-pools, including acid water with dissolved Fe and Al, and a circumneutral water with dissolved Fe, showed that metals will not likely be removed by mineral precipitation. However, relatively small manipulation of pH and Eh (pe), simulated by the addition of calcite and oxygen, could effectively remove metals. The large solubility range for Fe oxyhydroxide minerals was the greatest uncertainty in the simulations.

LITERATURE CITED

Ackenheil Associates, 1977. Operation Scarlift Report Redstone Creek and the Uniontown Syncline, prepared for the Pennsylvania Dept of Environmental Resources, Harrisburg, PA, Project 141-2.

Adams, R., and P. Younger, 2001. A Strategy for Modeling Ground Water Rebound in Abandoned Deep Mine Systems, Ground Water, Vol 39, No.2, p 249-261.

Aljoe, W., and J. Hawkins, 1991. Investigation and Characterization of Groundwater Flow Systems in Abandoned Underground Coal Mines, in Proceedings National Meeting of the American Society for Surface Mining and Reclamation, p 241-259.

Alpers, C,, Jambor, J., and D. Nordstrom (eds), 2000. Sulfate Minerals: Crystallography, Geochemistry and Environmental Significance, Reviews in Mineralogy and Geochemistry Vol. 40, Mineralogical Society of America and Geochemical Society, 608 pps.

Appalachian Regional Commission, 1969. Acid Mine Drainage in Appalachia. Congressional House Doc. No. 91-180. Volumes I, II, and III

Appelo, C., and D. Postma, 1993. Geochemistry, Groundwater and Pollution, A.A. Balkema, Rotterdam, Netherlands, 536 pps.

Appelo, C., Verweij, E. and H. Schafer, 1998. A Hydrogeochemical Transport Model for an Oxidation Experiment with Pyrite/Calcite/Exchangers/Organic Matter Containing Sand, Applied Geochemistry, Vol. 13, p 257-268.

Arkle, T., Beissel, D., Larese, R., Nuhfer, E., Patchen, D., Smosna, R., Gillespie, W., Lund, R, Norton, C., and H. Pfefferkorn, 1979. The Mississippian and Pennsylvanian (Carboniferous) Systems in the United States, West Virginia and Maryland. US Geological Survey Professional Paper 1110-D.

Auque, L., Gimeno, M., Gomez, J., and A. Nilsson, 2008. Potentiometrically measured Eh in groundwaters from the Scandinavian Shield, Applied Geochemistry, Vol. 23, p 1820-1833.

Baas Becking, L., Kaplan, I., and D Moore, 1960. Limits of the Natural Environment in Terms of pH and Oxidation-Reduction Potentials, Journal of Geology, Vol. 68, p 243-284.

Back, W., and I. Barnes, 1965. Relation of Electrochemical Potentials and Iron Content to Ground-water Flow Patterns, US Geological Survey Professional Paper 498-C.

Back, W., 1966. Hydrochemical Facies and Ground-Water Flow Patterns in Northern Part of Atlantic Coastal Plain, US Geological Survey Professional Paper 498-A.

Bains, J., Blowes, D., Robertson, W. and E. Frind, 2000. Modelling of Sulfide Oxidation With Reactive Transport At A Mine Drainage Site, Journal Contaminant Hydrology Vol. 41, p 23-47.

Baron, D., and C. Palmer, 1996. Solubility of Jarosite at 4-35°C, Geochemica et Cosmochemica Acta, Vol. 60, p 185-195.

Barton, L. (ed.), 1995. Sulfate-Reducing Bacteria, Biotechnology Handbooks 8. Plenum Publishing, New York, NY, 336 pps.

Bayless, E., and G. Olyphant, 1993. Acid Generating Salts and Their Relationship to the Chemistry of Groundwater and Storm Runoff at an Abandoned Mine Site in Southwestern Indiana, USA. Journal of Contaminant Hydrology, Vol. 12, p 313-328.

Beam, R., 2005. Personal Communication, 2005, Pennsylvania Dept Environmental Protection, Ebensburg, PA

Berger, A., Bethke, C., and J. Krumhansel, 2000. A Process Model of Natural Attenuation in Drainage From a Historic Mining District, Applied Geochemistry, Vol. 15, p 655-666.

Berner, R., 1967. Thermodynamic Stability of Sedimentary Iron Sulfides, American Journal of Science, Vol. 265, p 773-785.

Berner, R., 1970. Sedimentary Pyrite Formation, American Journal of Science, Vol. 268, p 1-23.

Berner, R., 1978. Rate Control of Mineral Dissolution Under Earth Surface Conditions, American Journal of Science, Vol. 278, p 1235-1252.

Berryhill, H., Schweinfurth, S., and B. Kent, 1971. Coal-Bearing Upper Pennsylvanian and Lower Permian Rocks, Washington Area, Pennsylvania, U.S. Geological Survey Professional paper 621.

Bigham, J., Schwertmann, U., Carlson, L., and E. Murad, 1990. A Poorly Crystallized Oxyhydroxysulfate of Iron Formed by Bacterial Oxidation of Fe(II) in Acid Mine Waters, Geochemica et Cosmochemica Acta, Vol. 54, p 2743-2758.

Bigham, J., Schwertman, U., Traina, S., Winland, R. and M. Wolf, 1996. Schwertmannite and the Chemical Modeling of Iron in Acid Sulfate Waters, Geochemica et Cosmochemica Acta, Vol. 60 No. 12, p 2111-2121.

Bigham, J. and D. Nordstrom, 2000. Iron and Aluminum Hydroxysulfates from Acid Sulfate Waters, in Alpers, C., Jambor, J. and D. Nordstrom(eds), Sulfate Minerals: Crystallography, Geochemistry and Environmental Significance, Reviews in Mineralogy and Geochemistry, Vol. 40, Mineralogical Society of America and Geochemical Society, 608 pps.

Blowes, D., Jambor, J., Appleyard, E., Reardon, E., and J. Cherry, 1992. Temporal Observations of the Geochemistry and Mineralogy of a Sulfide-rich Mine Tailings Impoundment, Heathe Steele Mines, New Brunswick, Exploration and Mining Geology, I, No.3, p 251-264.

Booth, C., 1986. Strata Movement Concepts and the Hydrogeological Impact of Underground Coal Mining, Ground Water, Vol. 24, p 507-515.

Booth, C., 2007. Confined-Unconfined Changes Above Longwall Coal Mining Due to Increases in Fracture Porosity, Environmental and Engineering Geoscience. Vol. XIII, No. 4, p 355-367.

Bowell, R., and I. Bruce, 1995. Geochemistry of Iron Ochres and Mine Waters from Levant Mine, Cornwall, Applied Geochemistry, Vol. 110, p 237-250.

Brady, K., Hornberger, R., and G. Fleeger, 1998. Influence of Geology on Post Mining Water Quality: Northern Appalachian Basin. in Coal Mine Drainage Prediction and Pollution Prevention in Pennsylvania, Pennsylvania Dept. of Environmental Protection, Harrisburg, PA.

Brant, R. and W. Foster, 1959. Magnesian Halotrichite from Vinton County, Ohio, Ohio Journal of Science, Vol. 59, No. 3, p 187-191.

Broshears, R., Runkel, R., Kimball, B., Mcknight, D., and K. Bencala, 1996. Reactive Solute Transport in an Acidic Stream: Experimental pH Increase and Simulation of Controls on pH, Aluminum and Iron, Environmental Science and Technology, Vol. 30, No. 10, p 3016-3024.

Bruemmer, G., Gerth, J., and K. Tiller, 1988. Reaction Kinetics of the Adsorption and Desorption of Nickel, Zinc and Cadmium by Goethite I, Adsorption and Diffusion of Metals, Journal of Soil Science, Vol. 39, p 37-52.

Bruhn, R., 1986. Influence of Deep Mining on the Ground Water Regime at a Mine in Northern Appalachia, in Proceedings 2nd Workshop on Surface Subsidence Due to Underground Mining, West Virginia University, Morgantown, WV, p 234-248.

Bucek, M., and J. Emel, 1977. Long Term Effectiveness of Close Down Procedures—Eastern Underground Coal Mines. HRB Singer Inc, for US Environmental Protection Agency, EPA-600/7-77-083.

Burby, T., Younos, T., and E. Anderson, 2000. Hydrologic Analysis of Discharge Sustainability from an Abandoned Underground Coal Mine, Journal of the American Water Resources Association, Vol. 36, No. 5, p 1161-1172.

Callaghan, T., Fleeger, G., Barnes, S., and A. Dalbarto, 1998. Groundwater Flow on the Appalachian Plateau of Pennsylvania. in Coal Mine Drainage Prediction and Pollution Prevention in Pennsylvania, Pennsylvania Dept. of Environmental Protection, Harrisburg, Pa.

Capo, R., Winters, W., Weaver, T., Stafford, S., Hedin, R., and B. Stewart, 2001. Hydrogeologic and Geochemical Evolution of Deep Mine Discharges, Irwin Syncline, Pennsylvania, in Proceedings West Virginia Surface Mine Drainage Task Force Symposium, Morgantown, WV, 10 pps.

Carlson, L., and U. Schwertmann, 1990. The Effect of CO_2 and Oxidation Rate on the Formation of Goethite Versus Lepidocrocite From an Fe(II) System at pH 6 and 7, Clay Minerals, Vol. 25, p 65-71.

Carpenter, L., and L. Herndon, 1933. Acid Drainage from Bituminous Coal Mines, West Virginia University Engineering Station Bulletin 10, Morgantown, WV, 38 pps.

Champ, D., Gulens, J., and R. Jackson, 1979. Oxidation-Reduction Sequences in Ground Water Flow Systems, Canadian Journal of Earth Science. Vol. 16, p 12-23.

Cherceri, L., Greenburg, A., and A. Eaton, 1998. Standard Methods for the Examination of Water and Waste Water, 20th edition, American Public Health Association, Washington, DC.

Chen, M., Soulsby, C., and P. Younger, 1999. Modelling the Evolution of Minewater Pollution at the Polkemmet Colliery, Almond Catchment, Scotland, Quarterly Journal of Engineering Geology, Vol. 32, p 351-362.

Christensen, T., Bjerg, P., Banwart, S., Jakobsen, R., Heron, G., and H. Albrechsten, 2000. Characterization of Redox Conditions in Groundwater Contaminant Plumes, Journal of Contaminant Hydrology, Vol. 45, p 165-241.

Cifelli, R., and H. Rauch, 1986. Dewatering Effects From Selected Underground Coal Mines in North-Central West Virginia, in Proceedings of Second Workshop on Surface Subsidence Due to Underground Mining, West Virginia University, Morgantown, WV, p 249-263.

Clark, W., 1967. Computing the Barometric Efficiency of a Well. Journal of Hydraulics Division, American Society of Civil Engineers, Vol. 93, p 93-98.

Cleveland, W., and I. Terpenning, 1982. Graphical Methods for Seasonal Adjustment, Journal American Statistical Association, Vol. 77, No. 377, p 52-62.

Cleveland, W., and S. Devlin, 1988. Locally Weighted Regression: An Approach to Regression Analysis by Local Fitting, Journal American Statistical Association. Vol. 83, No. 403, p 596-610.

Collins, C., 1923. Pollution of Water Supplies by Coal Mine Drainage, in Engineering News Record, Vol. 91, No.16, p 638-641.

Coulson, A., Hendricks J., and J. Knapp, 1999, Cation Exchange and High Alkaline Mine Water A Case Study, in Proceedings West Virginia Surface Mine Drainage Task Force Symposium, Morgantown, WV, 11 pps.

Cravotta., C., 1994. Secondary Iron-Sulfate Minerals as Sources of Sulfate and Acidity: Geochemical Evaluation of Acidic Groundwater at a Reclaimed Surface Coal Mine in Pennsylvania, in Alpers, C. and Blowes, D. (eds), Environmental Geochemistry of Sulfide Oxidation, American Chemical Society Symposium Series 550, p 345-364.

Cravotta., C., and C. Kirby, 2005. Net Alkalinity and Acidity 2: Practical Considerations, Applied Geochemistry, Vol. 20, p 1941-1964.

Cravotta, C., 2008a. Dissolved Metals and Associated Constituents in Abandoned Coal Mine Discharges, Pennsylvania, USA. Part 1: Constituent Quantities and Correlations, Applied Geochemistry 23, p 166-202.

Cravotta, C., 2008b. Dissolved Metals and Associated Constituents in Abandoned Coal Mine Discharges, Pennsylvania, USA. Part 2: Geochemical Controls on Constituent Concentrations, Applied Geochemistry, Vol. 23, p 203-226.

Crichton, A., 1927. Disposal of Drainage from Coal Mines, American Society of Civil Engineers Proceedings, Vol. 53, p 1656-1666.

Crouch, T., Collins, H., and J. Helgesen, 1980. Abandoned Subsurface Coal Mines as A Source of Water for Coal Conversion in Eastern Ohio. Report of Investigations 118, Ohio Dept. of Natural Resources, Division of Geological Survey, Columbus, OH.

Davis, A., and D. Ashenberg, 1989. The Aqueous Geochemistry of the Berkeley Pit, Butte, Montana, U.S.A., Applied Geochemistry Vol. 4, p 23-26.

Davis, J., and D. Kent, 1990. Surface Complexation Modeling in Aqueous Geochemistry, Reviews in Mineralogy, Mineral Water Interface Geochemistry, Mineralogical Society of America, Vol. 23, p 177-260.

Davis, R., and T. Rasmussen, 1993. A Comparison of Linear Regression With Clark's Method for Estimating Barometric Efficiency of Confined Aquifers. Water Resources Research, Vol. 29, No. 6, p 1849-1854.

Demchek, J., Skousen, J. and L. McDonald, 2004. Longevity of Acid Discharges From Underground Mines Located Above the Regional Water Table, Journal Environmental Quality Vol. 33, p 656-668.

Domenico, P., and F. Schwartz, 1990. Physical And Chemical Hydrogeology, John Wiley & Sons Inc, New York, NY, 824 pps.

Donaldson, A., Presley, M., and J. Renton (eds.), 1979. Carboniferous Coal Guidebook, West Virginia Geological and Economic Survey, Morgantown, WV, 3 volumes.

Donaldson, A., Renton, J., Kimutis, R., Linger, D., and M. Zaidi, 1979. Distribution Pattern of Total Sulfur Content In the Pittsburgh Coal, Carboniferous Coal Guidebook, Bulletin B-37-3, West Virginia Geologic and Economic Survey, Morgantown, WV.

Donovan, J., Fletcher, J., Strager, M..and E. Werener, 1999. Hydrogeological and Geochemical Response to Mine Flooding in the Pittsburgh Coal Basin, Southern Monongahela River Basin,

West Virginia University, National Mined Land Reclamation Center Project WV-132, Final report to US Environmental Protection Agency, 113 pps.

Donovan, J., Leavitt, B., and E. Werner, 2003. Long-Term Changes in Water Chemistry As a Result of Mine Flooding in Closed Mines of the Pittsburgh Coal Basin, USA, in Proceedings 6th International Conference on Acid Rock Drainage, p 869-875.

Donovan, J, and B. Leavitt, 2004. The Future of Mine-Water Discharges From Underground Coal Mines of The Pittsburgh Coal Basin, WV-PA, in R. I. Barnhisel (ed) Proc. Joint Conference American Society Mining and Reclamation 21st Annual National Conference and 25th West Virginia Surface Mine Drainage Task Force Symposium, p 518-528.

Dulong, F., Fedorko, N., Renton, J., and C. Cecil, 2002. Chemical and Mineralogical Analyses of Coal-Bearing Strata in the Appalachian Basin, US Geological Survey Open file report 02-489.

Dzombzk, D., and F. Morel, 1990. Surface Complexation Modeling–Hydrous Ferric Oxide, John Wiley & Sons, New York, NY, 393 pps.

Eary, E., and M. Williamson, 2006. Simulations of the Neutralizing Capacity of Silicate Rocks in Acid Mine Drainage Environments, in Proceedings 7th International Conference on Acid Rock Drainage, American Society for Surface Mining and Reclamation, p 564-577.

Eary, L., 1999. Geochemcial and Equilibrium Trends in Mine Pit Lakes, Applied Geochemistry, Vol. 14, p 963-987.

Edmunds, W., Berg, T., Sevon, W., Piotrowski, R., Heyman, L., and L Rickard, 1979. The Mississippian and Pennsylvanian (Carboniferous) Systems in the United States, Pennsylvania and New York. US Geological Survey Professional Paper 1110-B.

Ehrlich, H., 2002. Geomicrobiology, 4th ed. Marcel Dekker, New York, NY, 768 pps.

EPRI, 2001, Omega Mine Injection Program: Monongalia County, West Virginia, report prepared by GAI Consultants for Electric Power Research Institute, Allegheny Energy Supply, and US Dept of Energy, EPRI, Palo Alto, CA, 169 pps.

Ferris, F., Tazaki, K., and W. Frye, 1989. Iron Oxides in Acid Mine Drainage Environments and Their Association With Bacteria, Chemical Geology, Vol. 74, p 321–330.

Filipek, L., Nordstrom, D. and W. Ficklin, 1987. Interaction of Acid Mine Drainage and Sediments of West Squaw Creek in the West Shasta Mining District, California, Environmental Science and Technology, Vol. 21, No. 4, p 388-396.

Freeze, R., and J. Cherry, 1979. Groundwater, Prentice Hall, Englewood Cliffs, NJ, 604 pps.

Furbish, D., 1991. The Response of Water Level in a Well to a Time Series of Atmospheric Loading Under Confined Conditions. Water Resources Research, Vol.27, No. 4, p 557-568.

Gang, M., and D. Langmuir, 1974. Controls on Heavy Metals in Surface and Ground Waters, Affected by Coal Mine Drainage, in Proceedings 5th Symposium Coal Mine Drainage Research, National Coal Association, Washington DC, p 39-69.

Giehyeon, L., Bigham, J., and G. Faure, 2002. Removal of Trace Metals by Coprecipitation with Fe, Al and Mn from Natural Waters Contaminated With Acid Mine Drainage in the Ducktown Mining District, Tennessee. Applied Geochemistry, Vol 17, No. 5, p 569-581.

Gleisner, M., Herbert, R., and P. Kockum, 2006. Pyrite Oxidation by *Acidithiobacillus ferrooxidans* at Various Concentrations of Dissolved Oxygen, Chemical Geology, Vol. 225, p 16-29.

Glover, H., 1983. Mine Water Pollution- An Overview of Problems and Control Strategies in the United Kingdom, Water Science Technology, Vol. 15, p 59-70.

Gray, T., Moran, T., Broschart, D., and G. Smith, 1998. Plan for Injection of Coal Combustion Byproducts into the Omega Mine for the Reduction of Acid Mine Drainage, in Proceedings of the Nineteenth Annual West Virginia Surface Mine Drainage Task Force Symposium. 9 p.

Growitz, D., 1967. Geochemistry of Mine Water, Northern Bituminous Field, West Virginia, MSc Thesis, West Virginia University, Morgantown, WV, 31 pps.

Gwin, Dobson, & Foreman, 1972. West Branch Susquehanna River Mine Drainage Pollution Abatement Project, Operation Scarlift, prepared for Commonwealth of Pennsylvania, Harrisburg, PA, 181 p.

Gzyl, G. and D. Banks, 2007. Verification of the First Flush Phenomenon in Mine Water from Coal Mines in the Upper Silesian Coal Basin, Poland, Journal of Contaminant Hydrology, Vol. 92 p 66-86.

Hammack, R., and G. Watzlaf, 1990. The Effect of Oxygen on Pyrite Oxidation, in Proceedings Annual Meeting American Society for Surface Mining and Reclamation, Vol. 1, p 33-41.

Hammarstrom, J., Seal, R., Meier, A., and J. Kornfeld, 2005. Secondary Sulfate Minerals Associated with Acid Drainage in the Eastern US: Recycling of Metals and Acidity in Surficial Environments, Chemical Geology Vol. 215, p 407-431.

Hare, P., and R. Morse, 1997. Water-Level Fluctuations Due to Barometric Pressure Changes in an Isolated Portion of an Unconfined Aquifer, Ground Water, Vol. 35, No. 4, p 667-671.

Harrison, J., and V. Berkheiser, 1982. Anion Interactions With Freshly Prepared Hydrous Iron Oxides, Clays and Clay Minerals, Vol. 30, p 97–102.

Hawkins, J., 1994. Assessment of Contaminant Load Changes Caused by Remining of Abandoned Coal Mines, in Proceedings International Land reclamation and Mine Drainage Conference and Third International Conference on the Abatement of Acidic Drainage, US Bureau of Mines Special Publication SP 06A-94, Vol.1, p 20-29.

Hawkins, J. 2004. Predictability of Surface Mine Spoil Hydrologic Properties in the Appalachian Plateau. Ground Water, Vol. 42, No.1, p 119-125.

Hawkins, J., Perry, E., and M. Dunn, 2005. Hydrologic Characterization of a Large Underground Mine Pool In Central Pennsylvania, in R. I. Barnhisel (ed) Proc. Conference American Society Mining and Reclamation 22st Annual National Conference, p 487-503.

Hedin, R., Nairn, R., and R. Kleinmann, 1994. Passive Treatment of Coal Mine Drainage, US Bureau of Mines IC 9389.

Helsel, D., and R. Hirsch, 1992. Statistical Methods in Water Resources, Elesevier Studies in Environmental Science 49, Amsterdam, Netherlands, 529 pps.

Hennen, R., and D. Reger, 1913. West Virginia Geological Survey County Reports, Marion, Monongalia and Taylor counties, Wheeling News Litho Co, Wheeling, WV, 844 pps..

Herlihy, A., and A. Mills, 1985. Sulfate Reduction in Freshwater Sediments Receiving Acid Mine Drainage, Applied and Environmental Microbiology, Vol. 49, No.1, p 179-186.

Hirsch, R., Slack, J. and R. Smith, 1982. Techniques of Trend Analysis for Monthly Water Quality Data. Water Resources Research, Vol. 18, No. 1, p 107-121.

Hirsch, R., and J. Slack, 1984. A Nonparametric Test for Seasonal Data With Serial Dependence, Water Resources Research, Vol. 20, No. 6, p 727-732.

Hirsch, R., Alexander, R., and R. Smith, 1991. Selection of Methods for the Detection and Estimation of Trends in Water Quality. Water Resources Research, Vol. 27, No. 5, p 803-813.

Hobba, W., 1981. Effects of Underground Mining and Mine Collapse on the Hydrology of Selected Basins in West Virginia. RI-33, West Virginia Geological and Economic Survey, Morgantown, WV.

Hobba, W., 1984. Ground-Water Hydrology of the Monongahela River Basin. US Geological Survey in cooperation with the West Virginia Dept of Natural Resources, One Sheet Atlas, Charleston, WV.

Hollyday, E., and S. McKenzie, 1973. Hydrology of the Formation and Neutralization of Acid Waters Draining From Underground Mines of Western Maryland, Report of Investigations 20, Maryland Geological Survey, Baltimore, MD, 50 pps.

Hood, W., and A. Oertel, 1984. A Leaching Column Method for Predicting Effluent Quality from Surface Mines, in Proceedings 1984 Symposium on Surface Mining, Hydrology, Sedimentology and Reclamation, University of Kentucky, p 271-277.

Jakubick, A., Jenk, U., and R. Kahnt, 2002. Modelling of Mine Flooding and Consequences in the Mine Hydro-Geological Environment: Flooding of the Koenigstein Mine, Germany. Environmental Geology, Vol. 42, p 222-234.

Jambor, J., Nordstrom, D. and C. Alpers, 2000. Metal-sulfate Salts From Sulfide Mineral Oxidation, in Sulfate Minerals Crystallography, Geochemistry and Environmental Significance, Reviews in Mineralogy and Geochemistry Vol. 40, p 305-350.

Jambor, J., Dutrizac, J., Groat, L., and M. Raudsepp, 2002. Static Tests of Neutralization Potentials of Silicate and Aluminosilicate Minerals, Environmental Geology, Vol. 43, p 1–17.

James, C., 1984. Characterization of Water Quality For Deep Mine Effluents of Upper Freeport And Bakerstown Coal Mines In Central Preston County, West Virginia. MS Thesis, Dept of Geology and Geography, West Virginia University, Morgantown, WV, 157 pps.

Jaynes, D., Rogowski, A., and H. Pionke, 1984a. Acid Mine Drainage From Reclaimed Coal Strip Mines 1. Model Description, Water Resources Research, Vol. 20, No. 2, p 233-242.

Jaynes, D., Pionke, H., and A. Rogowski, 1984b. Acid Mine Drainage From Reclaimed Coal Strip Mines 2. Simulation Results of Model, Water Resources Research, Vol. 20, No. 2, p 243-250.

Jerz, J., and D. Rimstidt, 2004. Efflorescent Iron Sulfate Minerals: Paragenesis, Relative Stability, and Environmental Impact, American Mineralogist Vol. 88, p 1919-1932.

Johnson, C., and J. Skousen, 1995. Minesoil Properties of 15 Abandoned Mine land Sites in West Virginia, Journal of Environmental Quality, Vol. 24, p 635–643.

Jonsson, J., Persson, P., Sjoberg, S., and L. Lovgren, 2005. Schwertmannite Precipitated from Acid Mine Drainage: Phase Transformation, Sulphate Release and Surface Properties, Applied Geochemistry, Vol. 20, p 179-191.

Kaires, C., Capo, R., and G. Watzlaf, 2005. Chemical and Physical Properties of Iron Hydroxide Precipitates Associated with Passively Treated Coal Mine Drainage in the Bituminous Region of Pennsylvania and Maryland, Applied Geochemistry, Vol. 20, p 1445-1460.

Karathanasis, A., and Y. Thompson, 1995. Mineralogy of Iron Precipitates in a Constructed Acid Mine Drainage Treatment Wetland, Soil Science Society of America Journal. Vol. 59, p 1773-1781.

Kendorski, F., 1993, Effect of High Extraction Mining on Surface and Ground Waters, in Proceedings 12th Conference on Ground Control in Mining, West Virginia University, Morgantown, WV, p 412-425.

Kernic, J. 1999. Barnes and Tucker Company, Lancashire 15 and 20 Mines, Cambria County, Mine Pool and Discharge Report, unpublished report prepared for Pennsylvania Dept Environmental Protection, McMurray, PA, 11 pages.

Kim, J., Kim, S., and K. Tazaki, 2002. Mineralogical Characterization of Microbial Ferrihydrite and Schwertmannite, and Non-Biogenic Al-Sulfate Precipitates From Acid Mine Drainage in the Donghae Mine Area, Korea, Environmental Geology Vol. 42, p 19-31.

Kim, J., and S. Kim, 2003. Environmental, Mineralogical, and Genetic Characterization of Ocherous and White Precipitates from Acid Drainages in Taebaeg, Korea, Environmental Science and Technology, Vol. 37, No. 10, p 2120-2126.

Kirby, C., and C. Cravotta, 2005. Net Alkalinity and Acidity 1: Theoretical Considerations. Applied Geochemistry, Vol. 20, p 1920-1940.

Kittrick, J., Fanning, D., and L Hossner (eds), 1982. Acid Sulfate Weathering, Soil Science Society of America Special Publication 10, 234 pps.

Kleinmann, R., Hornberger, R., Leavitt, B., and D. Hyman, 2000. Introduction and Recommendation, The Nature of the Problem, In Prediction of Water Quality at Surface Coal Mines, Acid Drainage Technology Initiative, Prediction Workgroup, National Mined Land Reclamation Center, West Virginia University, Morgantown, WV, 254 pps.

Koryak, M., Stafford, L., and R. Reilly, 2004. Declining Intensity of Acid Mine Drainage in The Northern Appalachian Bituminous Coal Fields: Major Allegheny River Tributaries, Journal American Water Resources Association, Vol. 40, No. 3, p 677-689.

Kozar, M., and M. Mathes, 2001. Aquifer Characteristics Data for West Virginia, US Geological Survey Water Resources Investigation Report 01-4036.

Ladwig, K., Erickson, P., Kleinmann, R., and E. Posluszny, 1984. Stratification in Water Quality in Inundated Anthracite Mines. US Bureau of Mines, RI 8837.

Lamminen, M., Wood, J., Walker, H., Chin,Y., He, Y., and S. Traina, 2001. Effect of Flue Gas Desulfurization (FGD) By-Product on Water Quality At An Underground Mine, Journal Environmental Quality, Vol. 30, p 1371-1381.

Langmuir, D., and D. Whittemore, 1971. Variations in the Stability of Precipitated Ferric Oxyhydroxides, in Nonequilibrium Systems in Natural Water Chemistry, Advances in Chemistry Series 106, American Chemical Society, p 209-234.

Langmuir, D., 1997, Aqueous Environmental Chemistry. Prentice Hall, Englewood Cliffs, NJ, 600 pps.

Lappako, K., and D. Anston, 2006, Pyrite Oxidation Rates From Humidity Cell Testing Of Greenstone Rock, in Proceedings 7th International Conference on Acid Rock Drainage (ICARD), American Society of Mining and Reclamation, p 1007-1025.

Larsen, F., and D. Postma, 1997. Nickel Mobilization in a Groundwater Well Field: Release by Pyrite Oxidation and Desorption from Manganese Oxides. Environmental Science and Technology, Vol. 31, No. 9, p 2589-2595.

Leavitt, B., 1993. Discharge Potential of the Fairmont Mine-pool, Unpublished Internal Report for Consol Energy Inc, Pittsburgh, PA.

Leavitt, B., 1997, AMD in the Monongahela Basin, in Proceedings 18th West Virginia Surface Mine Drainage Task Force Symposium, West Virginia Mining and Reclamation Association.

Lessing, P., and W. Hobba, 1981. Abandoned Coal Mines in West Virginia as Sources of Water Supplies, West Virginia Geological and Economic Survey, Morgantown, WV, Circular C24, 24 pps.

Levenspiel, O., 1972. Chemcial Reaction Engineering, Advances in Chemistry Series, John Wiley & Sons Inc., New York, NY, 668 pps.

Lindberg, R., and D. Runnells, 1984. Ground Water Redox Reactions: An Analysis of Redox State Applied to Eh Measurements and Geochemical Modeling. Science, Vol. 225 p 925-927.

Liu, J., Elsworth, D., and R. Matetic, 1997. Evaluation of the Post-Mining Groundwater Regime Following Longwall Mining. Hydrological Processes, Vol. 11, p 1945-1961.

Lloyd, D., 2004. personal communication, unpublished water quality data for Lancashire 15 mine-pool and associated mines, Lloyd Environmental Services, Commodore, PA.

Lowson, R., 1982. Aqueous Oxidation of Pyrite by Molecular Oxygen, Chemical Reviews, Vol. 82, No. 5, p 461-497.

Macalady, D., Langmuir, D., Grundl, T., and A. Elzerman, 1990. Use of Model Generated Fe^{3+} Ion Activities to Compute Eh and Ferric Oxyhydroxide Solubilities in Anaerobic Systems, in Chemical Modeling in Aqueous Systems, American Chemical Society Symposium Series 416, p 350-367.

Mack, B., and J. Skousen, 2008. Acidity Decay Curves of 40 Above Drainage Mines in West Virginia, in R. I. Barnhisel (ed) Proc. American Society of Mining and Reclamation National Meeting, p 612-627.

McCarty, D., Moore, J., and A. Marcus, 1998. Mineralogy and Trace Element Association in An Acid Mine Drainage Iron Oxide Precipitate: Comparison of Selective Extractions, Applied Geochemistry, Vol. 13, p 165-176.

McCoy, K., 2002. Estimation of Vertical Infiltration into Deep Pittsburgh Coal Mines of WV-PA: A Fluid Mass Balance Approach, MS Thesis, West Virginia University, Dept of Geology and Geography, 151 pps.

McCue, J., Lucke, J. and H. Woodward, 1939. Limestones of West Virginia, West Virginia Geological Survey, Morgantown, WV, Vol. XII.

McCullogh, C., Diamond, W., Bench, B., and M. Duel, 1975. Selected Geologic Factors Affecting Mining of the Pittsburgh Coal bed, US Bureau of Mines RI 8093.

McElroy, T., 1998. Groundwater Resources of Cambria County Pennsylvania, Water Resources Report 67, Pennsylvania Dept of Conservation and Natural Resources, Bureau of Topographic and Geologic Survey, Harrisburg, PA. 49pps.

McKibben, M., and H. Barnes, 1986. Oxidation of Pyrite in Low Temperature Acidic Solutions: Rate laws and Surface Textures, Geochimica et Cosmochimica Acta, Vol. 50, No. 7, p 1509-1520.

Mehnert, E., Valocchi, A., Heidari, M., Kapoor, S. and P. Kumar, 1999. Estimating Transmissivity from the Water Level Fluctuations of a Sinusoidally Forced Well, Ground Water, Vol. 37, No. 6, p 855-860.

Michael Baker Consulting Engineers, 1978. Operation Scarlift Report SL-185, Blacklick Creek Watershed, Indiana Cambria Counties, prepared for Pennsylvania Dept of Environmental Resources, Harrisburg, PA, 152 p.

Miller, A., Sibrell, P., and T. Wildeman, 2007. Comparison of Sludge Characteristics Between Lime and Limestone/Lime Treatment of Acid Mine Drainage, in Proceedings National Meeting of the American Society of Mining and Reclamation, p 504-513.

Morin, K., Cherry, J., Dave, N., Lim, T., and A. Vivyurka, 1988. Migration of Acidic Ground Water Seepage From Uranium Tailings Impoundments, 1, Field Study and Conceptual Hydrogeochemical Model. Journal Contaminant Hydrology, Vol. 2, p 271-303.

Morse, J., Millero, F.,Cornwell, J., and D. Rickard, 1987. Chemistry of the Hydrogen Sulfide and Iron Sulfide Systems in Natural Waters, Earth Science Reviews, Vol. 24, p 1-42.

Morth, A., Smith, E., and K. Shumate, 1972. Pyrite Systems: A Mathematical Model, US EPA R2-72-002, 169 pps.

Mozley, P., 1989. Relation Between Depositional Environment and the Elemental Composition of Early Diagenetic Siderite, Geology, Vol. 17, p 704-706.

Mugunthan, P., McDonough, K., and D. Dzombak, 2004. Geochemical Approach to Estimate the Quality of Water Entering Abandoned Underground Coal Mines, Environmental Geology, Vol. 45, p 769-780.

Nicholson, R., Gillham, R., and E. Reardon, 1988. Pyrite Oxidation in Carbonate-buffered Solution: 1. Experimental Kinetics, Geochimica et Cosmochimica Acta, Vol. 52, No. 5, p 1077-1085.

Moses, C., and J. Herman, 1991. Pyrite Oxidation at Circumneutral pH, Geochimica et Cosmochimica Acta, Vol. 55, No. 2, p 471-482.

Nordstrom, D., Jenne, E., and J. Ball, 1979. Redox Equilibria in Acid Mine Waters. in Chemical Modeling in Aqueous Systems, American Chemical Society, Vol. 93, p 51-79.

Nordstrom, D., 1982a. Aqueous Pyrite Oxidation and the Consequent Formation of Secondary Iron Minerals, in Acid Sulfate Weathering, Soil Science Society of America Special Publication 10, 234 pps.

Nordstrom, D., 1982b, The Effect of Sulfate on Aluminum Concentrations in Natural Waters, Some Stability Relationships in the System Al_2O_3-SO_3-H_2O at 298 K, Geochemica et Cosmochimica Acta, Vol. 46, p 681-692.

Nordstrom, D., and F. Wilde, 1998, Oxidation Reduction Potential (Electrode Method), US Geological Survey Techniques of Water Resources Investigations, Book 9, Section 6.5.

Nordstrom, D., 2000. Aqueous Redox Chemistry and the Behavior of Iron in Acid Mine Water, in Proceedings of the Workshop on Monitoring Oxidation-Reduction Processes for Ground water Restoration. US EPA. EPA 600/R-02/002.

Nordstrom, D., 2009. Pitfalls and Limitations of Mineral Equilibrium Assumptions for Geochemical Modeling of Water-Rock Interactions at Mine Sites, in Proceedings 8th International Conference on Acid Rock Drainage, Skelleftea, Sweden.

Nuhfer, E., 1967. Efflorescent Minerals Associated With Coal. MSc Thesis, West Virginia University, Morgantown, WV, 74 pps.

Nuttall, C., and P. Younger, 2004. Hydrochemcial Stratification in Flooded Underground Mines: An Overlooked Pitfall, Journal Of Contaminant Hydrology, Vol. 69, p 101-114.

O'Neill, B., and J. Barnes, 1979. Properties and Uses of Shales and Clays, Southwestern Pennsylvania. Mineral Resources Report 77, Pennsylvania Dept. of Conservation and Natural Resources, Bureau of Topographic and Geologic Survey, Harrisburg, PA.

Palandri, J., and Y. Kharaka, 2004. A Compilation of Rate Parameters of Water Mineral Interaction Kinetics, US Geological Survey Open File Report 2004-1068.

Pantelis, G., and A. Ritchie, 1991. Macroscopic Transport Mechanisms as a Rate-limiting Factor in Dump Leaching of Pyritic Ores, Applied Mathematical Modelling, Vol. 15, No. 3, p 136-143.

Parfitt, R., and R. Smart, 1978. The Mechanism of Sulfate Adsorption on Iron Oxides. Soil Science Society of America Journal, Vol. 42, p 48–50.

Parizek, R., 1974. Prevention of Coal Mine Drainage Formation by Well Dewatering, The Pennsylvania State University, Dept of Geology and Geophysics, Special Research Report SR-52.

Parkhurst, D., and C. Appelo., 1999. User's Guide to PHREEQC (Version 2)- A Computer Program for Speciation, Batch-Reaction, One-Dimensional Transport, and Inverse Geochemical Calculations, US Geological Survey Water Resources Investigation Report 99-4259.

Peng, S., 1986. Coal Mine Ground Control, 2nd ed., John Wiley & Sons, New York, NY, 459 pps.

Perry, E., 2001. Modeling Rock–Water Interactions in Flooded Underground Coal Mines, Northern Appalachian Basin, Geochemistry: Exploration, Environment, Analysis, Vol. 1, 2001, p 61–70.

Perry, E., and H. Rauch, 2004. Long Term Water Quality Trends in a Partly Flooded Underground Mine, in R. I. Barnhisel (ed) Proc. Joint Conference of American Society of Mining and Reclamation 21st Annual National Conference and 25th West Virginia Surface Mine Drainage Task Force Symposium p 1438-1459.

Perry, E., J. Hawkins, M. Dunn, R. Evans and J. Felbinger, 2005. Water Quality Trends in a Flooded 35 Year Old Mine-pool. in R. I. Barnhisel (ed) Proc. American Society Mining and Reclamation 22st Annual National Conference, p 904-920.

Postma, D., and R. Jakobsen, 1996. Redox Zonation: Equilibrium Constraints on the $Fe(III)/SO_4$-Reduction Interface, Geochemica Cosmochemica Acta, Vol. 60, p 3169–3175.

Rasmussen, T. and L. Crawford, 1997. Identifying and Removing Barometric Pressure Effects in Confined and Unconfined Aquifers, Ground Water, Vol. 35, No. 3, p 502-511.

Renton, J., 1979. The Mineral Content of Coal. Carboniferous Coal Guidebook. Bulletin B-37-1. West Virginia Geologic and Economic Survey, Morgantown, WV.

Rhem, B., Groenwald, G,. and K. Morin, 1980. Hydraulic Properties of Coal and Related Materials, Northern Great Plains, Ground Water, Vol. 20, p 217-236.

Rimstidt, J., and D.Vaughan, 2003, Pyrite Oxidation: A State of the Art Assessment of the Reaction Mechanism, Geochemica et Cosmochimica Acta, Vol. 67, No.5, p 873-880.

Ritzi, R., Soroosh, S. and P. Hsieh, 1991. The Estimation of Fluid Flow Properties From the Response of Water Levels in Wells to Combined Atmospheric and Earth Tide Forces, Water Resources Research, Vol. 27, No. 5, p 883-893.

Robertson, J., Tremblay, G., and W. Fraser, 1997. Subaqueous Tailings Disposal: A Sound Solution for Reactive Tailings Disposal, in Proceedings of the Fourth International Conference on Acid Rock Drainage, Vol. 3, 1027–1041.

Roh, Y., Zhang, C., Vali, H., Lauf, R., Zhou, J., and T. Phelps, 2003. Biogeochemical And Environmental Factors In Fe Biominerlaization: Magnetite And Siderite Formation, Clays and Clay Minerals, Vol. 51, No. 1, p 83-95.

Rojstaczer, S., 1988. Determination of Fluid Flow Properties From the Response of Water Levels in Wells to Atmospheric Loading, Water Resources Research, Vol. 24, No. 11, p 1927-1938.

Rose, A., and C. Cravotta, 1998. Geochemistry of Coal Mine Drainage, in Coal Mine Drainage Prediction and Pollution Prevention in Pennsylvania, Pennsylvania Dept. Environmental Protection, Harrisburg, PA.

Rose, S., and W. Elliot, 2000. The Effects of pH Regulation on the Release of Sulfate From Ferric Precipitates Formed in Acid Mine Drainage, Applied Geochemistry, Vol. 15, p 27–34.

Ruppert, L., Tewalt, S. , and L. Bragg, 1997. Map Showing Areal Extent of Pittsburgh Coal Bed and Horizon and Mined areas of the Pittsburgh coal bed in Pennsylvania, Ohio, West Virginia and Maryland, digitally compiled by Tully, J., Pierce, J., Weller, A., and J. Yarnel, U.S. Geological Survey Open File Report 96-280.

Ruppert, L. , Tewalt, S. , Bragg, L. and R. Wallack. 1999. A Digital Resource Model of the Upper Pennsylvanian Pittsburgh Coal Bed, Monongahela Group, Northern Appalachian Basin Coal Region, USA. International Journal of Coal Geology, Vol. 41, p 3–24.

Sames, G., and N. Moebs, 1989. Hillseam Geology and Roof Instability near Outcrop in Eastern Kentucky Drift Mines, US Bureau of Mines RI 9267.

Sams, J., and K. Beer, 1999. Effects of Coal Mine Drainage on Stream Quality in the Allegheny and Monongahela River Basins- Sulfate Transport and Trends, US Geological Survey Water Resources Investigation Report 99-4208.

Sahu, P., 2004. Use of Time Series, Barometric and Tidal Analyses to Conceptualize and Model Flow in an Underground Mine, M.S. Thesis, Ohio University Dept. Geological Sciences, Athens, OH, 172pps.

Schmidt, R., 1985. Fracture Zone Dewatering To Control Ground Water Inflow in Underground Mines, US Bureau of Mines RI 8981.

Schnoor, J., 1990. Kinetics of Chemical Weathering: A Comparison of Laboratory and Field Weathering Rates, in Aquatic Chemical Kinetics, Reaction Rates of Processes in Natural Waters, Wiley Interscience Books, New York, NY, 557 pps.

Schoonen, M., and H. Barnes, 1991. Reactions Forming Pyrite and Marcasite From Solution II: Via FeS Precursors Below 100 C, Geochemca Cosmochemica Acta, Vol 55, p 1501–1514.

Schwertmann, U., and R. Taylor, 1977. Iron Oxides. in Minerals in Soil Environments, Soil Science Society of America, p 379-438.

Seo, H., 2001. Modeling the Influence of Changes in Barometric Pressure On Ground Water Levels in Wells, Environmental Geology, Vol. 41, p 155-166.

Sheetz, B., White, W., Shollenberger, D., and R. Hornberger, 2009. Evaluation of Particle Size and Surface Effects. in Hornberger, R., and K. Brady (eds), Development and Interpretation of the ADTI-WP2 Leaching Column Method (Kinetic Test Procedure for the Prediction of Coal Mine Drainage Quality), Final report submitted to US Office of Surface Mining, Washington D.C.

Skousen, J., McDonald, L., Mack, B., and J. Demchak, 2006. Water Quality From Above Drainage Mines Over A 35 Year Period. in Proceedings 7th International Conference on Acid Rock Drainage, American Society of Mining and Reclamation, p 2044-2054.

Smith, E., and K. Shumate, 1970. Sulfide to sulfate reaction mechanism, Water Pollution Control Res. Series 14010 US Federal Water Quality Administration.

Smith, K., 1999. Metal Sorption on Mineral Surfaces: An Overview with Examples Relating Mineral Deposits. in The Environmental Geochemistry of Mineral Deposits, Part A, Processes Methods and Health Issues, Plumlee, G., and M Logsdon (eds), Review in Economic Geology, 6A, p 161-182.

Smith, M., Brady, K., Perry, E., and J. Tarantino, 2000. Evaluation of Mining Permits Resulting in Acid Mine Drainage in Pennsylvania 1987-1996: A Post Mortem Study, in Proceedings Fifth International Conference on Acid Rock Drainage, Vol. 1, p 713-719.

Sobek, A., Schuller, W., Freeman, J. and R. Smith., 1978. Field and Laboratory Methods Applicable To Overburdens and Minesoils. U.S Environmental Protection Agency EPA600/2-78-054.

Stipp, S., 1990. Speciation in the Fe(II)-Fe(III)-SO_4-H_2O System at 25° C and Low pH: Sensitivity of an Equilibrium Model to Uncertainties, Environmental Science and Technology, Vol. 24, No. 5, p 699-706.

Stumm, W., and J. Morgan, 1981. Aquatic Chemistry, An Introduction Emphasizing Chemical Equilibria in Natural Waters, Wiley Interscience Books, New York, NY, 780 pps.

Stoertz, M., Hughes, M., Wanner, N., and M. Farley, 2001. Long-term Water Quality Trends at a Sealed, Partially Flooded Underground Mine, Environmental and Engineering Geoscience, Vol. 7, No.1, p 51-65.

Stoner, J., Williams, D., Buckwalter, T., Felbinger, J. and K. Pattison, 1987. Water Resources and the Effects of Coal Mining, Greene County, Pennsylvania. Pennsylvania Geological Survey Water Resources Report 63, Harrisburg, PA.

Tieman, G., and H. Rauch, 1987. Study of Dewatering Effects at an Underground Longwall Mine Site in the Pittsburgh Seam of Northern Appalachia, in Proceedings Eastern Coal Mine Geomechanics, Bureau of Mines Technology Seminar, US Bureau of Mines IC 9137.

To, T., Nordstrom, D., Cunningham, K., Ball, J., and R. McCleskey, 1999. New Method for the Direct Determination of Dissolved Fe(III) Concentration in Acid Mine Waters, Environmental Science and Technology, Vol. 33, No. 5, p 807-813.

United Mine Workers of America, http://www.umwa.org/ .

US Environmental Protection Agency, 1986. Quality Criteria For Water 1986. Office of Water Regulation and Standards EPA 440/5-86-001.

US Environmental Protection Agency. 1986b. Aluminum, Office of Water Regulation and Standards EPA 440/5-86-008.

US Geological Survey, National Water Information System (NWIS),
 http://waterdata.usgs.gov/nwis/qwdata .

Van Breeman, N., 1973. Dissolved Aluminum in Acid Sulfate Soils and Acid Mine Waters, Soil Science Society America Proceedings, Vol. 37, p 694-697.

Watzlaf, G., 1992. Pyrite Oxidation in Saturated and Unsaturated Coal Waste, in Proceedings of the 1992 National Meeting of the American Society for Surface Mining and Reclamation, p 191-205.

Welch, S., Kirste, D., Christy, A., Beavis, F., and F. Beavis, 2008. Jarosite Dissolution II, Reaction Kinetics, Stoichiometry and Acid Flux, Chemical Geology, Vol. 254, p 73-86.

West Virginia Geological and Economic Survey, 2002, Trace Elements in West Virginia Coals, http://www.wvgs.wvnet.edu/www/datastat/te/index.htm.

Williams, D., Felbinger, J., and P. Squilace, 1993. Water Resources and the Hydrologic Effects of Coal Mining in Washington County, Pennsylvania, US Geological Survey Open File Report 89-620.

Williamson, M., and J. Rimstidt, 1994. The Kinetics and Electrochemical Rat-Determining Step of Aqueous Pyrite Oxidation, Geochemica et Cosmochimica Acta, Vol. 58, No. 24, p 5443-5454.

Winters, W., 2000. Hydrologic and Geochemical Evolution of a Bituminous Coal Basin: Irwin Syncline, Westmoreland County, Pennsylvania, Thesis, University of Pittsburgh, Geology and Planetary Science Dept, Pittsburgh, PA.

Winters, W., and R. Capo, 2004. Ground Water Flow Parameterization of an Appalachian Coal Mine Complex, Ground Water, Vol. 5, No. 42, p 700-710.

Wood, S., Younger, P. and N. Robins, 1999. Long-term changes in the Quality of Polluted Minewater Discharges from Abandoned Underground Coal Workings in Scotland, Quarterly Journal of Engineering Geology, Vol. 32, p 69-79.

Wunderly, M., Blowes, D., Frind, D., and C. Ptacek, 1996. Sulfide Mineral Oxidation and Subsequent Reactive Transport of Oxidation Products in Mine Tailings Impoundments: A Numerical Model, Water Resources Research, Vol. 32, No. 10, p 3173-3187.

Wyrick, G., and J. Borchers, 1981. Hydrologic Effects of Stress Relief Fracturing in an Appalachian Valley, US Geological Survey Water Supply Paper 2177.

Younger, P., 1997. The Longevity of Minewater Pollution: A Basis for Decision Making, The Science of the Total Environment, Vol. 194&195, p 457-466.

Younger, P., 2000. Predicting Temporal Changes in Total Iron Concentrations in Waters Flowing From Abandoned Deep Mines: A First Approximation, Journal of Contaminant Hydrology, Vol. 44, p 47-69.

Younger, P., and P. Thorn, 2006. Predictions and Reality: Generation of Strongly Net-Acidic Mine waters Through Flooding of Underground Coal Mine Workings With Limestone Roof Strata, Blenkinsopp Colliery (Northumberland, UK), in Proceedings 7th International Conference on Acid Rock Drainage, American Society of Mining and Reclamation, p 2542-2557.

Yu, J., Heo., B, Choi, I., Pil, J., and H. Chang, 1999. Apparent Solubilities of Schwertmannite and Ferrihydrite in Natural Streams Polluted by Mine Drainage, Geochemica et Cosmochemica Acta, Vol. 63, p 3407-3416.

Zhu, C., and D. Burden, 2001. Mineralogical Compositions of Aquifer Matrix as Necessary Initial Conditions in Reactive Contaminant Transport Models. Journal of Contaminant Hydrology, Vol 51, p 145-161.

Zodrow E., and K. McCandlish, 1978. Hydrated Sulfates in the Sydney Coalfield, Cape Breton, Nova Scotia, Canadian Mineralogist, Vol. 16, p 17-22.

Zodrow E., Wiltshire, J., and K. McCandlish, 1979. Hydrated Sulfates in the Sydney Coalfield, Cape Breton, Nova Scotia.II, Pyrite and Alteration Products, Canadian Mineralogist, Vol. 17, p 63-70.

Zodrow E., 1980. Hydrated Sulfates from the Sydney Coalfield, Cape Breton Island, Nova Scotia, Canada, the Copiapite Group, American Mineralogist, Vol. 65, p 961-967.

LONG-TERM WATER QUALITY TRENDS
IN A PARTLY FLOODED UNDERGROUND COAL MINE

LONG-TERM WATER QUALITY TRENDS
IN A PARTLY FLOODED UNDERGROUND COAL MINE[1]

Eric F. Perry[2] and Henry W. Rauch

Water quality trends for an 8 year period were analyzed for two acidic springs draining from a partially flooded underground coal mine, and the composite mine-pool outflow of 10 discharges. Time series analysis was used to separate long-term data trends from short-term noise. Short-term variation usually constituted less than 30 percent of the trend concentration. Exponential functions were fitted to the trend data, and time estimates (t_{50C}) for concentration to decline 50% were generated for Total Acidity, Fe, Al, SO_4, Co, Ni, and Zn concentrations. Iron decline is similar at two springs with an estimated t_{50C} of 60 months. Sulfate t_{50C} is about 60 to 70 months at one spring and for the aggregate mine-pool. Cobalt, Ni and Zn declines are more rapid, with estimated t_{50C} of about 30 to 50 months. Aluminum decline is 2 to 3 times slower than rates for other parameters, and mine-waters are near apparent equilibrium for the mineral jurbanite, $Al(SO_4)OH*5H_2O$. Constituent fluxes are controlled mostly by flow, and decline with time. Estimated time (t_{50F}) for flux to decline 50% for the composite mine-pool outflow is about 85 months for Fe, 80 months for SO_4 and 105 months for acid flux. Fluxes are 1.5 to 3 times greater in spring than fall, and reflect seasonal distribution of precipitation and recharge to the mine. Most of the improvement in mine-pool discharge results from declining pollutant concentrations. These trends suggest a slow decline in pyrite oxidation, with significant water quality improvement occurring on the order of years to decades.

Additional Key Words: acidity, flux, jurbanite.

_____

[2]Eric Perry is a Hydrologist, Office of Surface Mining, 3 Parkway Center, Pittsburgh PA 15220. Henry Rauch is Professor of Geology, Dept of Geology and Geography, Box 6300, West Virginia University, Morgantown WV 26506-6300.

Introduction

Underground coal mining in Appalachia sometimes results in post-mining water pollution. Oxidation of iron disulfide minerals like pyrite generates strong acidity, low pH, elevated concentrations of metals and sulfate, and dissolution of carbonate and silicate minerals (Nordstrom, 1982; Rose and Cravotta, 1998). The longevity of pollutional discharges from abandoned underground mine works is a function of hydrogeologic setting, and geochemistry of the residual coal and associated rocks. This paper addresses time-dependent decline behavior, and mineralogical solubility controls on water composition from a partially flooded, closed mine that is located above the local base level drainage ("above-drainage mine"). Concentrations of Al, Fe, SO_4, and trace elements Ni, Co, Zn are declining through time, and respond to variations in flow, seasonality and reclamation activities. The time-dependent decline of dissolved constituents may represent depletion of stored acid products including metal sulfate salts, decreased availability of sulfide minerals, in situ neutralization, or less efficient leaching. Concentrations of some elements, including Al and SO_4, may be controlled by precipitation/dissolution solubility reactions of specific minerals.

Geologic Setting

The Omega mine is located about 10 km south of Morgantown, West Virginia in the Upper Freeport coal bed. This coal is stratigraphically located at the top of the Allegheny Group (Hennen and Reger, 1913). Coal thickness is commonly about 1.2 m, with a shale parting. The Bolivar fireclay, a hard siliceous mudrock, immediately underlies the coal bed. At this mine, the Uffington shale overlies the coal bed and is commonly less than 0.6 m thick. The Mahoning and Buffalo sandstones comprise most of the overburden above the Uffington shale. These rocks may reach a combined thickness exceeding 30 m, and where exposed at the mine faceup, they display prominent vertical fractures. Maximum overburden thickness at the Omega mine is about 52 m.

The West Virginia Geological and Economic Survey (2002) reports an average total sulfur content of about 2.5 % and average pyritic sulfur content of about 1.7% for the Upper Freeport coal bed. Two core samples of Upper Freeport coal retrieved from the Omega mine complex contained over 5 and 12% total sulfur, respectively (EPRI, 2001).

The Omega mine is contained within a broad ridgetop on the western flank of the Chestnut Ridge anticline, and strata dip about 11 % to the northwest. After closure, the mine partially flooded, and the general ground water flow pattern within the mine works is inferred to be in the direction of dip.

Site History

Coal was extracted by room and pillar methods from the Upper Freeport coal bed in about 69.8 ha of mine works until mine closure in 1989. Recovery ranged from 50% in first mined areas, to over 70% in areas of second mining. Average mining height was about 1.3 m. In the early 1990's, acid drainage began seeping from several locations along the coal cropline (Figure 1). Mine drainage was collected and treated after several lateral boreholes were drilled into the northern mine works to divert mine-water away from a section adjoining a stream with a public water supply. Treatment sludge was initially injected into the mine works for disposal. The West Virginia

Department of Environmental Protection (WVDEP) assumed control of the site in the mid 1990's and currently treats the drainage. WVDEP discontinued sludge injection and currently disposes of the material offsite. WVDEP also installed a series of pipelines and manholes to more easily and securely collect, sample, measure, and convey mine-water to the treatment facility. In some instances, several adjacent seeps were combined into a single monitoring point. In 1998, a cooperative state, federal and privately funded grouting project was initiated to reduce or abate acidic discharges in the "North Lobe" (Figure 1) of the mine (Gray et al., 1998; EPRI, 2001),. This area comprises about 10.5 Ha, or 15% of the mined area, but was estimated to be discharging about 55% of the acid load (EPRI, 2001). About 61,000 m^3 of grout mix containing fluidized-bed combustion ash, flyash and cement were injected in the North Lobe. Subsequent drilling and borehole camera observations confirmed that, in general, the grout mixture provided near complete filling of mine voids. Water quality remained poor after grouting; however, flow, and consequently acid load decreased (EPRI, 2001).
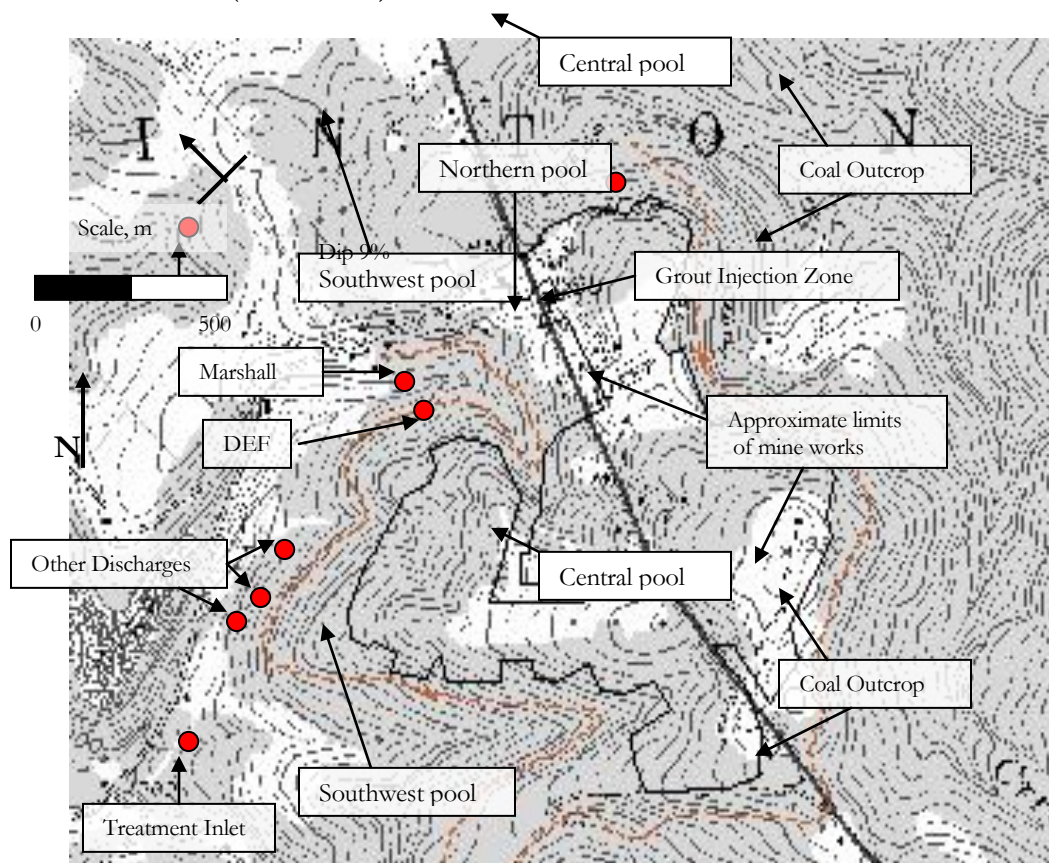
Figure 1. Extent of Omega mine works (black line), coal outcrop (dashed line) and discharge locations (red circles). (Portion of Morgantown South 7.5 min topographic quadrangle map)

Methodology

The US Department of Energy (USDOE) began monitoring water quality and flow from the principal mine discharges in 1993 on a monthly basis and continued until 1999. Data were collected for pH, Total Acidity, Fe(II), Fe(III), Al, Mn, SO_4, Ca, Mg, Na, K, Cl, NH_3, As, Ba, Be, Cd, Co, Cr, Cu, Ni, Pb, Sb, Se, Zn, and Br. The WVDEP also began sampling discharges in 1996 at monthly intervals, and in 1997, initiated daily flow and on site precipitation measurements.

WVDEP monitoring includes pH, Total Acidity, Fe, Al, Mn, SO_4, specific conductance, total dissolved solids (TDS), and Total Suspended Solids (TSS). These data sets were combined into a single chronological file providing more than 8 years of data. Water samples were collected under this study during low flow conditions in 2002 and 2003 for the same parameters as the USDOE data set, plus field measurements of pH, Eh, temperature and specific conductance. WVDEP monitoring continues as part of that organization's ongoing site management and reclamation work.

A charge balance calculation was performed on samples with all major cations and anions to assess data reliability. Total acidity was evaluated from the reported values, and acidity was also calculated based on metals concentration and pH using the following formula:

$$\text{Acidity Calc} = 50*(3*Fe/55.85 + 3*Al/26.98 + 2*Mn/54.94 + 1000*10^{-pH}) \quad (1)$$

where metal concentrations are in mg/L, and calculated acidity is in mg/L $CaCO_3$ Equivalents (Eq.). The calculated acidity values were used in subsequent calculations and analyses.

All statistical analyses were performed using Statgraphics for Windows version 4.1. Mineral saturation indices were calculated using the geochemical code PHREEQC (Parkhurst and Appelo, 1999).

Site Conditions

The Omega mine is believed to contain 3 separate mine-pools based on limited water level data, examination of mine maps, structural considerations and field observations. The pools are located in the "North Lobe", the central section of the mine, and the southwest portion of the mine (Figure 1). The maximum extent of flooding is estimated to be about 23 ha for the 3 pools combined, or about 33 % of the total mined area. Thus, at least two thirds of the mine works are not flooded, and are subjected to conditions favoring pyrite oxidation. Based on mine-pool discharge measurements and flooding extent, the equivalent of one to two mine-pool volumes per year are estimated to circulate through the mine works. It is believed that preferred flow paths exist in areas where voids remain open, and zones of minimal or slow ground water circulation may occur in collapsed areas. Leaching efficiency is likely to vary depending on localized conditions. Mine-pool discharges respond to precipitation events within a few days, suggesting rapid infiltration and flow through.

Water quality data from three monitoring points were selected for in-depth analysis. The Marshall and DEF discharges (Figure 1) are two acid springs located at and near the down dip end of the mine complex in the North Lobe mine-pool. These discharges have a continuous flow history, and represent a significant portion of the flow and acid load leaving the mine. The Marshall discharge is believed to represent water quality conditions near the end of the flow path within the North Lobe mine-pool. It is a horizontal borehole drilled into the lower end of the mine-pool. The DEF discharge is at an intermediate location on the flow path. Water quality at different flow path locations could exhibit evolutionary changes in water chemistry, as mine-water flows from unflooded to flooded portions of the mine works. The Marshall monitoring point is located near the grout injection area, and could show effects of acidic mine-pool water interacting with the

grout. The DEF discharge was thought to be located far enough upgradient to have no significant interaction with the grout. The third monitoring point, Treatment Inlet (Figure 1), represents the combined pipe flow of all discharges, and is used to assess overall conditions.

Results and Discussion

Table 1 shows median water quality data for the years 1993 at the beginning of the monitoring record, 2001 after grouting was completed, and single sample events from August, 2002 and August, 2003 for the three monitoring points.   Overall water quality was very poor, exhibiting classic characteristics of acid drainage.   The Marshall discharge exhibited the highest concentrations of acidity, metals, sulfate and trace elements, while DEF and the Treatment Inlet have similar composition and concentrations.   At each site, there was a decline in median pollutant concentrations between 1993 and 2001. During that 8 year period median acidity, Fe, Al and SO_4 declined to about half of their initial values.   Trace element concentrations of Co, Ni and Zn exhibited some variation between 1993 and 2002/2003, but declined more rapidly. Sites DEF and the Treatment Inlet shows little change in pH, while a modest improvement occurs at the Marshall site. Calcium and Mg show behavior similar to Fe, Al and SO_4.   Sodium concentration, however, increased from 1993 to 2002/2003.   Exchange of Na for other adsorbed cations, or dissolution of Na bearing minerals such as albite ($NaAlSi_3O_8$) would increase solution Na. Albite is about 8 to 10 orders of magnitude undersaturated in these waters, and Dulong et al. (2002) have shown that small amounts of albite can be present in these rocks.

Since most of the mine is not flooded, conditions are favorable for the formation of sulfate and hydroxysulfate minerals that characteristically occur in acidic environments.   Melanterite, copiapite, halotrichite, gypsum, schwertmannite, various jarosites, and others are commonly present in mine spoil and underground mine works (Nuhfer, 1967; Bigham and Nordstrom, 2000; Rose and Cravotta, 1998). The specific mineral assemblage depends on pH and Eh conditions, as well as activities of the constituent ions.   Some minerals such as melanterite are moderately soluble, and could redissolve as the mine is recharged. Mine-water outflows likely represents a combination of leaching stored sulfate minerals, and continued weathering of pyrite.

Time-Series Analysis
Concentration versus time scatter plots showed month-to-month variation.   However, an underlying long-term trend, and a shorter seasonal trend were also present.   These trends were examined with time-series analyses, including moving average, and seasonal decomposition, which breaks the data into trend, seasonal and irregular components. Log or other data transforms and nonparametric tests (Helsel and Hirsch, 1992); locally weighted scatter plot smoothing (Cleveland and Devlin, 1988); and seasonal decomposition (Cleveland and Terpenning, 1982) are suggested methods for analyzing noisy time-series data for trends and seasonal features.

Examples of raw and trend data are shown in Figures 2, 3 and 4 for Fe, Al and SO_4 concentration data at the Marshall monitoring point. The plots display similar behavior, and there was a period of declining concentration from 1993 to late 1998. Iron and SO_4 trends decrease more rapidly than Al.   In 1999, there was a rapid concentration increase for all parameters, followed by resumption in decline. The spike in concentrations closely follows the grouting conducted in mid to late 1998 in the nearby "North Lobe" of the mine.   Calcium and Mg concentrations, which had been

Table 1 Summary Water Chemistry for Marshall, DEF and Treatment Inlet Monitoring Sites [1]

Site	Year[2]	Flow	pH	Acidity Calc.	TDS	Fe	Al	Mn	SO_4	Ca	Mg	Na	Co	Ni	Zn
Marshall	1993	63	2.62	8398	8398	1613	275	6.5	5975	325	168	4.7	1.66	3.75	13.52
	2001	64	3.30	4636	4536	689	108	3.7	2955	NM	NM	NM	NM	NM	NM
	2002	23	3.48	2026	4203	564	88.7	2.9	2462	298	71	18	0.42	0.98	3.16
	2003	50	4.15	1976	3980	460	133	0.83	2200	162	59	36	0.30	1.23	3.14
DEF	1993	69	2.71	2590	4345	664	130	3.5	3141	228	120	14	1.18	2.70	9.28
	2001	29	2.60	1540	3160	314	103	2.8	1250	NM	NM	NM	NM	NM	NM
	2002	NM[3]	2.50	1542	3196	339	113	2.25	1931	135	65	23	0.44	1.04	3.07
	2003	29	2.86	1581	2820	349	115	2.43	1811	126	60	26	0.54	1.04	2.89
Treatment Inlet	1993	313	2.86	2896	5282	771	137	5.26	3915	288	147	5.3	1.20	2.62	9.12
	2001	186	2.80	1670	3406	365	104	3.6	1790	NM	NM	NM	NM	NM	NM
	2002	67	2.77	1377	3457	301	101	3.80	2004	247	77	15	0.66	1.45	4.54
	2003	172	3.11	979	2357	191	83	2.5	1404	155	52	20	0.49	1.05	3.14

(1) Flow in L/min, pH in standard units, Acidity in mg/L CaCO3 Eq., all others in mg/L.
(2) Median concentration values for 1993 and 2001, and single sample event values for 2002 and 2003.
(3) NM = Not Measured

decreasing, also increased after grouting. These data show a rapid and short-term flushing by grout injection that displaced acid weathering products already present in the mine works. This behavior suggests that leaching efficiency is low for most recharge conditions. Only extreme disturbance to the system, such as from grout injection, or very large recharge events displace major amounts of soluble weathering products.   Increasing Ca and Mg likely were derived from dissolution of the ash and cement based grout.
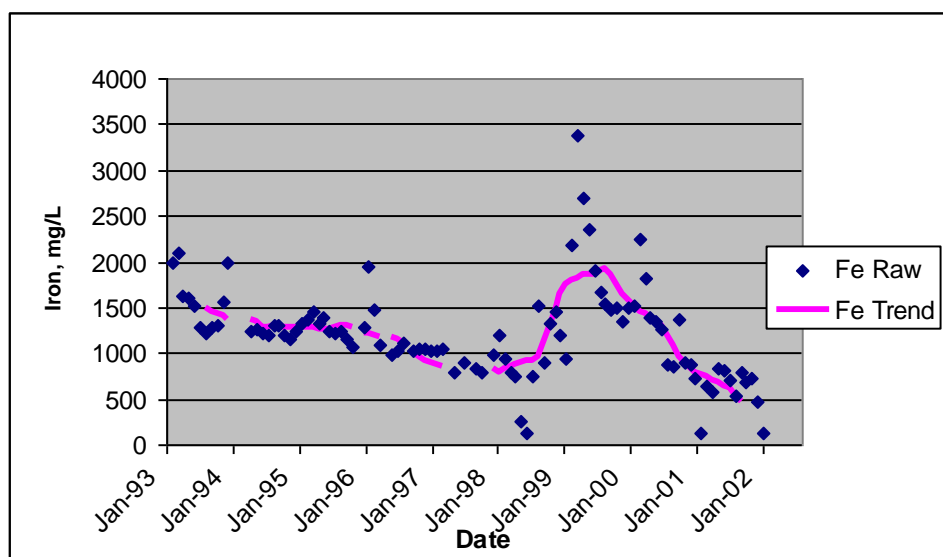
Figure 2. Iron Concentration Trend, Marshall Monitoring Point.
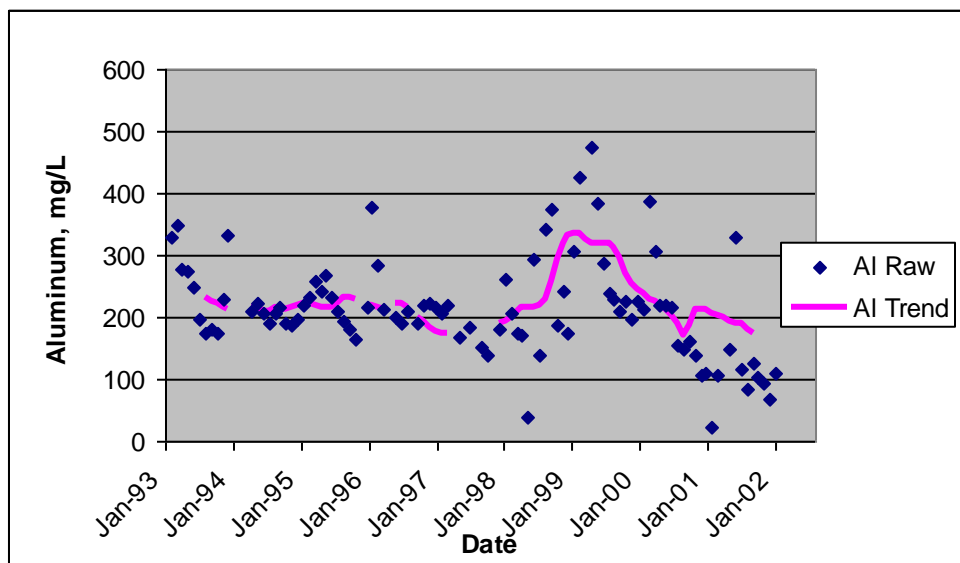
Figure 3. Aluminum Concentration Trend, Marshall Monitoring Point.
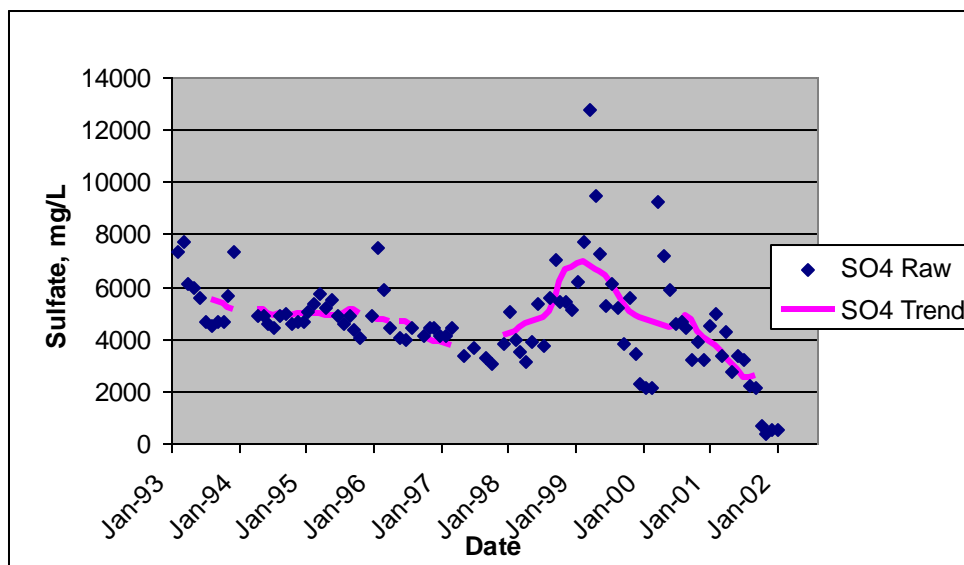
Figure 4. Sulfate Concentration Trend, Marshall Monitoring Point.

Differences between the raw unadjusted concentration and trend data represent the irregular component of the data. It may result from short-term events such as rapid recharge events, and fluctuations in mine-pool elevation or flow path.

Figure 5 is a plot of Co and Ni raw and trend data for the DEF discharge. Concentrations of both metals decreased until about 1998 (Figure 5), when grout injection occurred; then concentrations began to increase.   Based on the trend data, Ni was declining slightly faster than Co.   It was initially believed that site DEF was located far enough upgradient from the
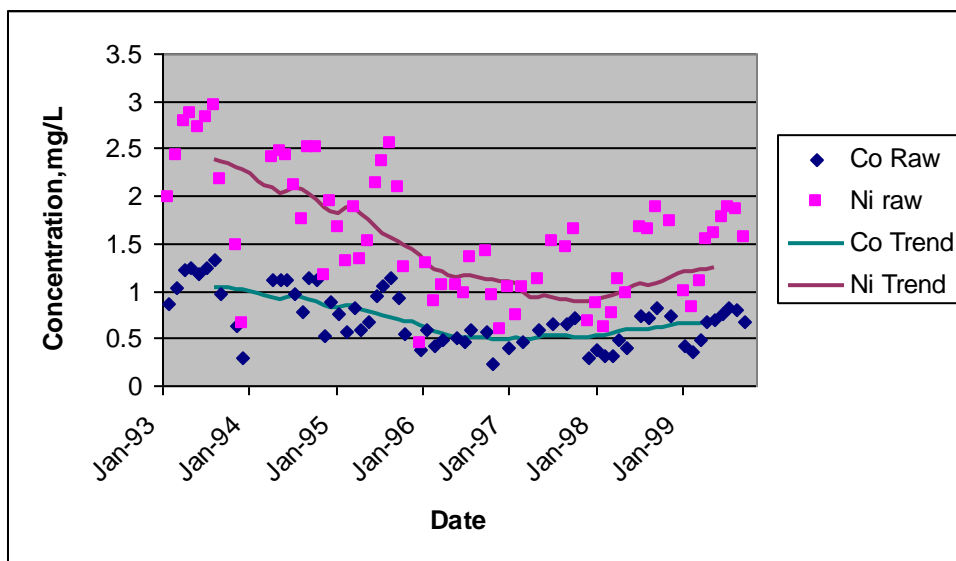
Figure 5. Cobalt and Nickel Concentrations Trends for DEF Monitoring Point.

228

mine grout zone, that its water chemistry would not be influenced by grout injection. However, behavior of these elements at site DEF suggests that its' water chemistry was affected by grout injection. Cobalt and Ni-to-SO$_4$ mole ratios (Figure 6) had a slow decline until about 1997. Both Co (r=0.97) and Ni (r=0.95) are strongly correlated to SO$_4$ concentration. Cobalt and Ni are common trace inclusions in pyrite at concentrations of less than a few percent (Rimstidt and Vaughan, 2003).
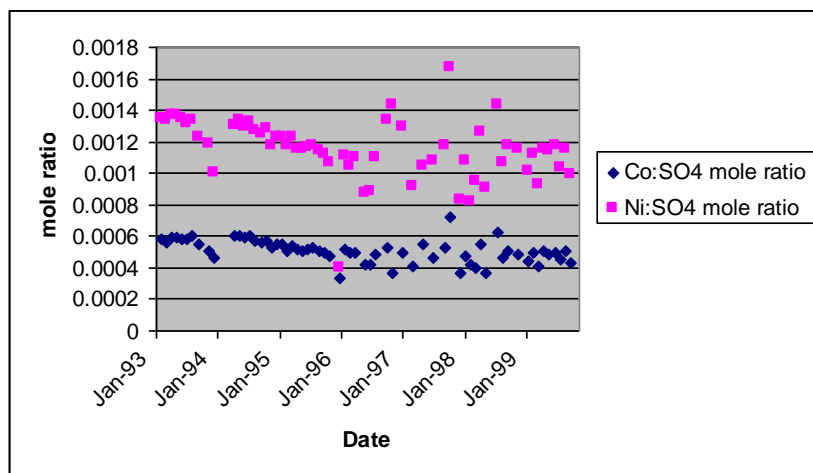
Figure 6. Cobalt and Nickel-to-Sulfate Molar Ratios, for DEF Monitoring Point.

Under the strongly acidic conditions like those at site DEF (pH<3.0), adsorption studies generally indicate little attenuation of Ni and Co (Bruemmer et al., 1988, Larsen and Postma, 1997, Geihyeon et al., 2002).   If in-situ adsorption attenuation is minimal, then declining Ni and Co to sulfate mole ratios probably reflect a decrease in pyrite oxidation. Increased scatter in the plots for 1997 and 1998 reflects disturbance from mine site modification and grouting.

Estimating Rate of Concentration Decrease
Exponential and other model functions were fitted to the pre-grouting trend data to estimate rates at which mine-water concentrations decline over time. Least squares regression was used to examine different models. Because mine grouting impacted water chemistry, no model fitting was done for data during and immediately after grouting. Examination of different models, and their associated R^2 values and residual plots, showed that the following exponential function provided a reasonable estimation of concentration change with time:

$$C_t = C_0 * \exp^{-kt} \quad (2) \text{ or}$$

$$\ln(C_t/ C_0) = -kt \quad (3)$$

229

where C_t is concentration at time t, C_0 is concentration at time zero, k is a constant in time^{-1} units and t is elapsed time. The function is identical to that used to describe radioactive decay. The constant, k, is the slope of a plot of $\ln(C_t/C_0)$ versus t. Other regression models generally did not describe the trends as well as an exponential function. The period required for a 50 % decline in concentration, designated t_{50C} in this paper, was estimated from equation 3. Estimated t_{50C} for pre-grouting data at the three monitoring points are summarized in Table 2. All Table 2 data are statistically significant at 0.05 alpha.

Time-to-half concentration ranges from about 5 to 8 years for Acidity, Fe, Ca (except at Marshall site), Mg, SO_4, and TDS. Cobalt, Ni and Zn declined more rapidly, with time to half concentration ranging from about 2.5 to 5 years. The time to half concentration estimates in Table 2 are in general agreement with direct comparisons between 1993 and 2001summary data in Table 1.

Table 2. Estimated Time to Half Concentration, t_{50C}, in Months for
Selected Water Quality Parameters, Pre-Grouting Conditions

Monitoring Point	Acidity	Al	Ca	Co	Fe	Mg	Ni	SO$_4$	TDS	Zn
Marshall	79	212	117	49	61	60	54	96	93	45
DEF	78	134	69	34	62	54	32	57	79	30
Treatment Inlet	94	146	88	51	70	57	57	72	72	47

Demchak et al. (in press) examined drainage quality from 44 above-drainage underground mines, including sites with the same stratigraphy as the Omega mine. Water quality from 1968 compared to drainage in 1999-2000 showed that acidity had decreased an average of 56% in mine drainage from the Upper Freeport coal bed. Overall, iron concentrations declined about 80 %, and sulfate declined about 50 to 75 %. Average data (Demchak et al., in press) seem to indicate a slower rate of concentration decline than data presented here for the Omega mine. However, their data show some variation among individual mines, and the rate of chemical change seems to be influenced by site specific factors.

Drainage from flooded underground coal mines in Great Britain shows about a 50 % reduction in Fe concentration for each mine-pool volume discharged (Glover, 1983), implying an exponential decay. Younger (1997) further characterized British mine-waters as consisting of two acidity sources; recently generated from ongoing sulfide oxidation, and stored acidity. Younger estimates that stored acidity is removed in the first flush of the mine-pool, usually within 40 years, while continued oxidation is projected to last for hundreds of years. Most of the long-term discharge records described by Younger (1997) exhibit an exponential decay for Fe and become asymptotic after 10 to 20 years. Long-term Fe concentrations range from 1 to 30 mg/L.

Pollutant concentration behavior in Omega mine drainage is similar to the general decay model described for British mines. Omega mine drainage has not progressed far enough through its life cycle to determine whether concentrations become asymptotic in the long term.

Mineralogical Controls

Aluminum has the longest estimated t_{50C} of the parameters in Table 2, ranging from about 12 to 18 years. The slow decline for Al is a function of mine-pool pH, which is usually between 2.6 and 3.5. Dissolution of clay minerals, such as kaolinite, and Al hydroxide minerals is favored under these conditions as reaction 4 shows:

$$Al_2Si_2O_5(OH)_4 + 6\,H^+ \rightarrow 2\,Al^{3+} + 2\,H_4SiO_4 + H_2O \tag{4}$$

So long as mine-pool pH remains below about 4.0, dissolution of clay minerals and Al hydroxides could occur; thus there is a large source for soluble Al; hence concentrations may to decline more slowly than other constituents.

Saturation indices for jurbanite, an Al-hydroxysulfate, are plotted in Figure 7 for the Marshall and DEF sites. Both waters show apparent near equilibrium conditions, where DEF (intermediate flow path location) is slightly undersaturated, and Marshall (end of flow path) is slightly oversaturated. Waters in the DEF discharge approach, but do not exceed, the equilibrium saturation index of 0, suggesting that jurbanite poses an upper limit to Al concentration at site DEF.
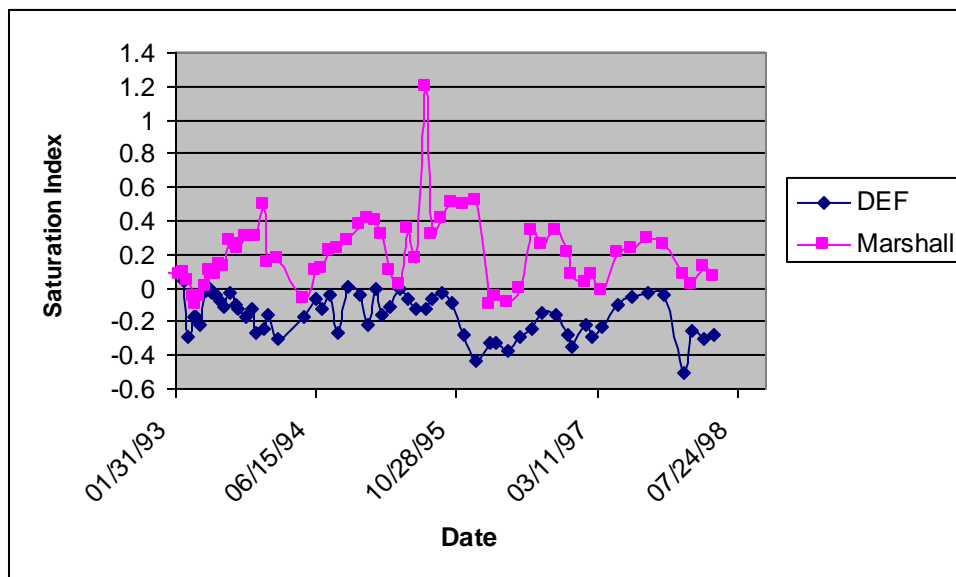
Figure 7. Jurbanite Saturation Indices at Marshall and DEF Sites.

Jurbanite is stable in acidic waters (Nordstrom, 1982b) and can persist in the pH range of zero up to 3 to 5 in sulfate rich waters. Jurbanite could form from kaolinite alteration as reaction 5 shows:
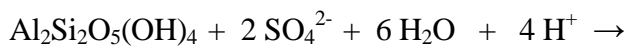
231

$$Al_2Si_2O_5(OH)_4 + 2\ SO_4^{2-} + 6\ H_2O\ +\ 4\ H^+\ \rightarrow$$

$$2\ Al(SO_4)(OH)\ *5\ H_2O+\ 2\ H_4SiO_4\quad (5)$$

Waters at the Marshall discharge are slightly oversaturated for jurbanite. Slight over saturation suggests that within the mine either a slightly more soluble poorly crystalline phase of jurbanite is forming, the jurbanite reaction rate is slow, the "dissolved" fraction on which the saturation index calculations were based, contains colloidal Al, or the jurbanite is not actually forming. Our current knowledge of the mine precludes identification of which scenario is allowing slight jurbanite super saturation at the Marshall discharge. The mine works are not accessible for sediment sampling for mineralogical analysis to confirm or deny the presence of jurbanite. However, its characteristic occurrence is in acid soils and mine-waters (Nordstrom, 1982b).

Superimposed on the overall trend in Figure 7 is a cyclic, seasonal variation in saturation index. Indices are largest in periods corresponding to low flow conditions, and smallest during high-flow periods. The inverse relation between saturation index and flow suggests mine-waters are diluted during seasonal recharge and more concentrated for drier periods of the year. Mineral saturation and precipitation should be favored during dry periods.

Goethite (FeOOH) saturation indices for the Marshall and DEF sites, computed from measured Eh in 2002 and 2003, show the mine-waters are slightly oversaturated (indices about +0.05 to +0.5). Iron could be attenuated within the mine-pool by precipitation as an oxyhydoxide, either amorphous, or crystalline form such as goethite. The metastable hydroxysulfates, schwertmannite and jarosite, if present initially, may also transform to goethite with time (Bigham and Nordstrom, 2000).

In acid oxidizing sulfate waters, formation   of the Fe bearing minerals $Fe(OH)_{3(am)}$; schwertmannite, $Fe_8O_8(OH)_6SO_4*nH_2O$; H-jarosite $HFe_3(SO_4)_2(OH)_6$; Na-jarosite $NaFe_3(SO_4)_2(OH)_6$; and K-jarosite, $KFe_3(SO_4)_2(OH)_6$ is feasible. Mine-waters are 1 to 4 orders of magnitude undersaturated for $Fe(OH)_{3(am)}$, and 2 or more orders of magnitude oversaturated for schwertmannite.   These minerals are likely not present in the Omega mine.   K-jaorosite is commonly 1-2 orders of magnitude oversaturated while H-jarosite and Na-jarosite are slightly undersaturated. K-jaorosite is reported to sometimes be super saturated without actually forming, and Na-jarosite is relatively rare (Bigham and Nordstrom, 2000). Indices decline with time, suggesting that the system is not at equilibrium with them, and they are likely not present.   The cycling of iron in the Omega mine is not clearly associated with any one mineral, with the possible exception of goethite.

Figure 8 shows gypsum saturation indices for the Marshall and DEF sites. Both sites are slightly undersaturated for gypsum and are becoming more so with time. Calcium and SO_4 solubility are not currently controlled by gypsum. However, in 1993-1994 at the beginning of monitoring, the Marshall discharge was near equilibrium for gypsum. No data are available prior to 1993 to estimate whether gypsum saturation was actually achieved shortly after mine closure. The gypsum

plot (Figure 8) shows a similar seasonal dilution/concentration effect as that for the jurbanite plot (Figure 7).
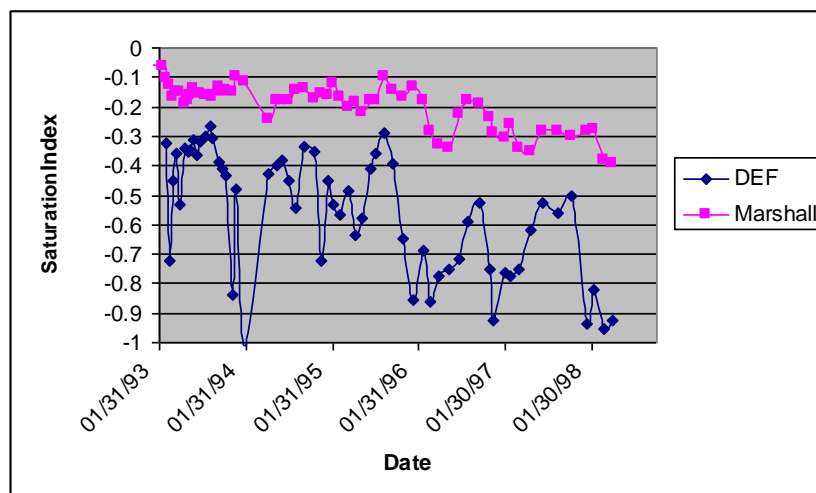
Figure 8. Gypsum Saturation Indices for Marshall and DEF Sites.

Flux(Loading)

Trends for flux data (chemical concentration x flow) versus time were poorly described by exponential or other simple mathematical functions that did not account for variable flow rates. Figure 9 is a scatter plot of sulfate flux (load) and flow rate from the Treatment Inlet for the period 1993-2002. There is a pronounced seasonal effect in flow and flux, with both constituents reaching maximums during the spring of the year and minimums in the fall. Sulfate flux is strongly correlated to flow (r=0.78), as are Acidity, Fe, Al, and TDS loadings (r= 0.77 to 0.82). An extensive study of surface mine discharges also found flow to be the dominant component of flux (Hawkins, 1994).

Within the 9 year record there is an observable trend of long-term decline in sulfate flux. Figure 9 also includes the trace of the best fit regression line from a linear model. The regression slope indicates the long term decline in flux, but clearly does not account for the seasonal cycles. Simple models cannot estimate short term flux because of variable flow rates. In turn, discharge quantity is driven by precipitation and recharge events, and changes in mine hydrology.
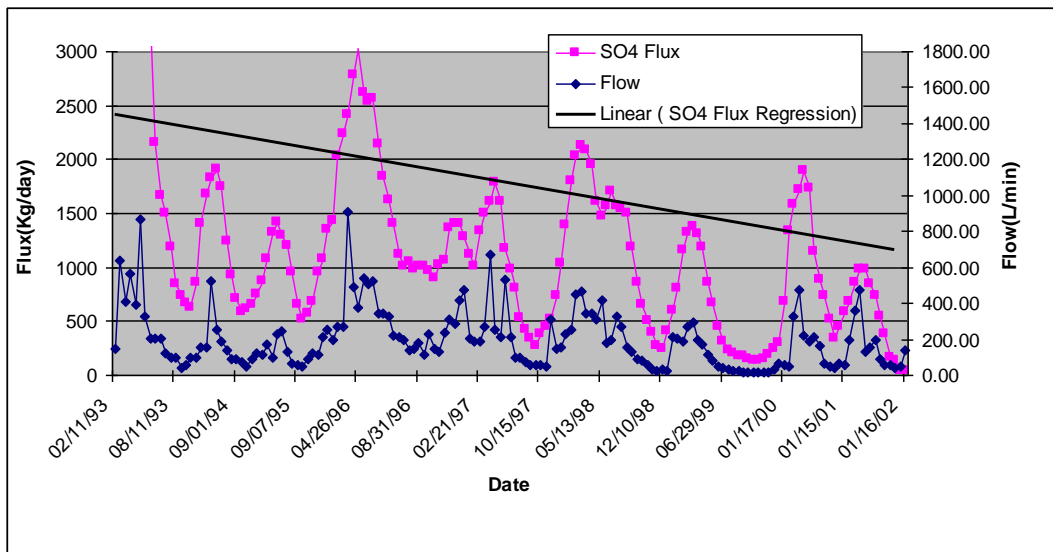
Figure 9. Sulfate Flux and Flow, 1993 to 2002, Treatment Inlet.

Table 3 summarizes estimates of time to half flux generated from best fit regression models for the Treatment Inlet. These values represent the long-term decline, and do not model the seasonal cyclical features seen in Figure 9.

Table 3. Time to Half Flux Estimates, t_{50F}, Regression Models, Treatment Inlet. [1]

Method	Acid Flux	Al Flux	Fe Flux	SO$_4$ Flux	Co Flux	Ni Flux
Regression	106	169	85	77	64	56

(1)Time in months. "Best fit" flux models are square root of time functions, except Co and Ni which show linear functions with time.

Comparing the Treatment Inlet time to half flux in Table 3, to time to half concentration (Table 2), shows that flux is declining more slowly than concentration. Thus, most of the improvement in mine-pool chemical discharge is attributable to decreasing concentrations instead of changes in flow.

Seasonality

Chemical concentration and flux both exhibit seasonal variation. Median values for each month were divided into two seasons, corresponding to periods of minimum and maximum trend values. The "spring season" for high flux data is February to July, and the "Fall Season" is August to January. Selected data from the Treatment Inlet site are shown in Figure 10, and Tables 4 and 5.

Median flux and flow for the spring season is about 2 to 3 times greater than that for the fall, and peak fluxes occur around March to April (Figure 10). About 75% of the total yearly flux is

234

discharged during the spring season. Flux is at a minimum in October to December. All median flux values and flow values for spring and fall seasons are significantly different at alpha probability =0.01, using the nonparametric Mann-Whitney test.
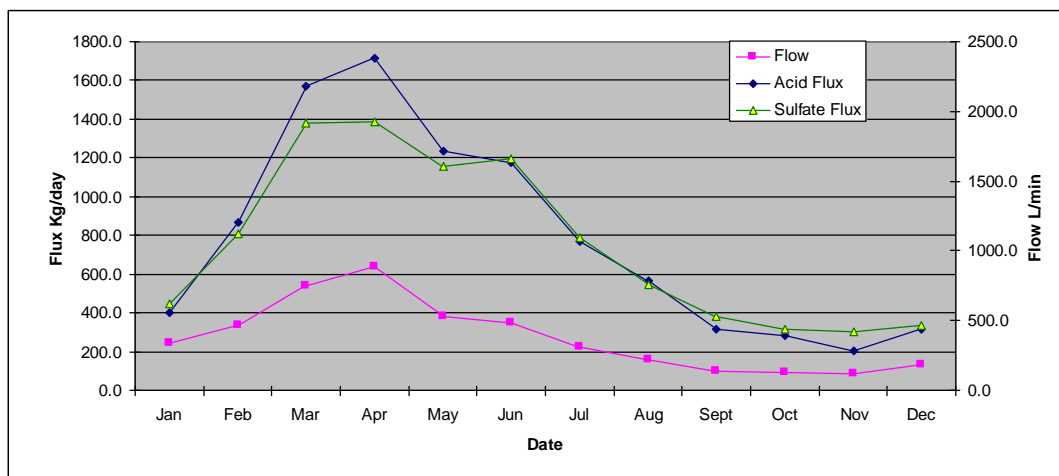
Figure 10. Median Monthly Flow, Acid Flux and Sulfate Flux at the
Treatment Inlet Site Showing Seasonality Trend.

Table 4. Median Seasonal Flux and Flow for Treatment Inlet.[1]

Season	Flow	Acidity	Al	Fe	SO$_4$
Spring	393	1219	62.6	501	1556
Fall	149	428	20.9	309	589
Significant Difference	Yes	Yes	Yes	Yes	Yes

(1) Flux in Kg/day, flow in L/min. Significant differences at p=0.01.

There is a weak inverse relationship, or slight dilution effect, between flow and concentration by season (Table 5). Median concentrations are greater in the low- flow fall season, while lower concentrations occur in the spring season. The differences are not statistically significant for Fe and Al, however.

Table 5. Median Seasonal Concentrations for Treatment Inlet.[1]

Season	Acidity	Al	Fe	SO$_4$	Co	Ni
Spring	1875	105	465	2454	0.78	1.64
Fall	2042	114	501	2870	0.95	2.04
Significant Difference	Yes	No (p=0.31)	No (p=0.10)	Yes	Yes	Yes

(1)Concentrations in mg/L. Significant differences at p=0.01.

Summary and Conclusions

The Omega mine has been discharging acidic drainage containing elevated amounts of acidity, Fe, Al, SO_4 and trace elements for about 14 years.   Pollutant concentrations declined over an 8 year period, but there was little change in pH.   The continuing concentration decline likely reflects a combination of depletion of oxidizable pyrite, continued leaching of stored acidity, in-situ neutralization, and inactivation of some pyrite surfaces by sedimentation, precipitation or other means. An exponential function described the long term concentration trends, but there are both seasonal (cyclic) and short-term irregular departures. Short-term variation represents response to transient features such as rapid recharge events.   Concentrations of Fe, SO_4, and acidity were estimated to decline by half over about 5 to 8 years for individual mine drainage springs and the composite mine-pool.

Aluminum concentrations declined 2 to 3 times slower, and mine-waters are near apparent equilibrium for the Al-hydroxysulfate mineral jurbanite. The very acid conditions which remain in the mine-pool (pH ~2.5 to 3.5) favor the dissolution of alumino-silicates and Al hydroxides. As long as pH remains below about 4.0, the reservoir of potentially mobile Al is large.

Metals and sulfate concentration declines estimated from exponential functions compared reasonably well to actual data. Concentrations estimates were usually within 15 % of actual values and most were within 30%.

Concentrations of trace elements Co, Ni, and Zn were estimated to decline by half in about 3 to 5 years. These elements occur as trace inclusions in pyrite and may be a surrogate for recently generated acidity.

Iron cycling in the Omega mine is complex. No Fe bearing hydroxysulfate mineral was identified as controlling soluble Fe.   Apparent equilibrium is indicated for goethite, based on a few measurements, and this oxyhydroxide may control soluble Fe in the long term. The presence of specific minerals cannot be confirmed because the mine works are not accessible for sediment sampling.

An apparent long-term trend for near equilibrium for jurbanite, and possibly goethite, suggests that the mine-pool chemistry is partially controlled by local equilibrium conditions. The mine-pool is however, periodically stressed by seasonal and single event recharge pulses that usually result in dilution.

Soluble acid weathering products are not uniformly leached from the mine works, due to preferential flow paths and zones of limited or slow ground water circulation. Zones with little flushing accumulate acid products, which may only be mobilized when the system is subjected to large stress. Grout injection completely filled one section of the mine works, displaced stored acidity, and caused a short-lived increase in acidity and metals concentrations.   Leachate

mobilization from the mine works is ultimately transport controlled. Aggressive reclamation strategies such as grout injection can increase pollutant discharge in the short term.

Flux or load is controlled mostly by flow, and there is a distinct seasonality to the mine-pool discharge. About 75% of the total yearly flux is discharged in the spring season. The most rapid abatement method for pollutant flux for the Omega mine-pool would be to reduce mine recharge, and grouting a portion of the mine did ultimately reduce flux from that section. However, grouting an entire underground mine complex post-closure can be technologically difficult or cost prohibitive.

It is uncertain if the Omega mine-pool will continue to follow the decline shown in its' first 10 years of activity, or if the trend will become asymptotic in the future. Most of the mine-water chemistry improvement results from declining concentrations. Current behavior shows that mine-pool drainage quality improvement occurs on the order of years to decades.

Acknowledgements

Literature Cited

Bigham, J. M. and D. K. Nordstrom, 2000, Iron and Aluminum Hydroxysulfates from Acid Sulfate Waters, in Sulfate Minerals: Crystallography, Geochemistyr and Environmental Significance, Alpers, C.N. J.L. Jambor, D.K. Nordstrom (eds), Reviews in Mineralogy and Geochemistry Vol 40, Mineralogical Society of America.

Bruemmer, G.W., J. Gerth and K.G. Tiller, 1988, Reaction Kinetics of the Adsorption and Desorption of Nickel, Zinc and Cadmium by Goethite. I, Adsorption and Diffusion of Metals. Journal of Soil Science, Vol 39, pp 37-52.

Cleveland, W.S. and I.J. Terpenning, 1982, Graphical Methods for Seasonal Adjustment, Journal of American Statistical Association, Vol 77, No 377, pp 52-62.

Cleveland, W.S. and S.J. Devlin, 1988, Locally Weighted Regression: An Approach to Regression Analysis by Local Fitting. Journal. of American Statistical Association, Vol 83, No 403, pp 596-610.

Demchek, J., J. Skousen and L.M. McDonald, (in press) Longevity of Acid Discharges from Above-Drainage Underground Mines, Journal of Environmental Quality.

Dulong, F.T, Fedorko, N., Renton, J.J., and C. B. Cecil, 2002, Chemical And Mineralogical Analyses of Coal-Bearing Strata In The Appalachian Basin, US Geological Survey Open file report 02-489.

EPRI, 2001, Omega Mine Injection Program: Monongalia County, West Virginia, report prepared by GAI Consultants for Electric Power Research Institute, Allegheny Energy Supply, and US Dept of Energy, EPRI, Palo Alto, CA.

Giehyeon, Lee, J. M. Bigham, and G. Faure, 2002, Removal of Trace Metals by Coprecipitation with Fe, Al and Mn from Natural Waters Contaminated With Acid Mine Drainage in the Ducktown Mining District, Tennessee. Applied Geochemistry, Vol 17, Issue 5, pp. 569-581.

Glover, H.G., 1983, Mine Water Pollution- An Overview of Problems and Control Strategies in the United Kingdom, Water Sci. Technology, Vol 15, pp 59-70.

Gray, T.A., T.C. Moran, D.W. Broschart, and G.A. Smith, 1998, Plan for Injection of Coal Combustion Byproducts into the Omega Mine for the Reduction of Acid Mine Drainage, in Proceedings of the Nineteenth Annual West Virginia Surface Mine Drainage Task Force Symposium. 9 p.

Hawkins, J. W., 1994, Assessment of Contaminant Load Changes Caused by Remining of Abandoned Coal Mines, in Proceedings International Land Reclamation and Mine Drainage Conference and Third International Conference on the Abatement of Acidic Drainage. Vol 1, pp20-29, US Bureau of Mines Special Publication SP 06A-94.

Helsel, D.R. and R.M. Hirsch, 1992, Statistical Methods in Water Resources, Studies in Environmental Science 49, Elesevier, 529 p.

Hennen, R.V. and D.B. Reger, 1913, West Virginia Geological Survey County Reports, Marion, Monongalia and Taylor Counties, Wheeling News Litho Co., Wheeling, WV.

Larsen, F. and D. Postma, 1997, Nickel Mobilization in a Groundwater Well Field: Release by Pyrite Oxidation and Desorption from Manganese Oxides. Environmental Science and Technology, Vol 31, No. 9, pp 2589-2595.

Nordstrom, D. K. 1982, Aqueous Pyrite Oxidation and the Consequent Formation of Secondary Iron Minerals. In J.A.Kittrick, D.S. Fanning and L.R. Hossner eds) Acid Sulfate Weathering. Soil Science Society of America Special Publication 10.

Nordstrom, D. K. 1982b, The Effect of Sulfate on Aluminum Concentrations in Natural Waters, Some Stability Relationships in the System Al_2O_3-SO_3-H_2O at 298 K, Geochemica et Cosmochimica Acta, Vol 46, pp 681-692.

Nuhfer, E , 1967. Efflorescent Minerals Associated with Coal. MS Geology Thesis, Department of Geology and Geography West Virginia University.

Parkhurst, D. L. , and C. A. J Appelo., 1999. User's Guide to PHREEQC (Version 2)- A Computer Program for Speciation, Batch-Reaction, One-Dimensional Transport, and Inverse Geochemical Calculations. US Geological Survey Water Resources Investigation Report 99-4259.

Rose, A. W. and C. A. Cravotta, 1998, Geochemistry of Coal Mine Drainage. In K. B. Brady, M. W. Smith and J. Scheuck (eds), Coal Mine Drainage Prediction and Pollution Prevention in Pennsylvania., Pennsylvania Dept. Environmental Protection.

Rimstidt, J.D., and D.J. Vaughan, 2003, Pyrite Oxidation: A State of the Art Assessment of the Reaction Mechanism, Geochemica et Cosmochimica Acta, Vol 67, No 5, pp. 873-880.

Younger, P.L.,1997, The Longevity of Minewater Pollution: A Basis for Decision Making, The Science of the Total Environment, Volume 194-195, pp. 457-466.

West Virginia Geological and Economic Survey, 2002, Trace Elements in West Virginia Coals, http://www.wvgs.wvnet.edu/www/datastat/te/index.htm.

Appendix B

Modelling rock–water interactions in flooded underground coal mines,
Northern Appalachian Basin

Modelling rock–water interactions in flooded underground coal mines, Northern Appalachian Basin

Eric F. Perry[1]

[1] West Virginia University and US Dept of Interior, Office of Surface Mining 3 Parkway Center, Pittsburgh, Pennsylvania, USA (e-mail: eperry@osmre.gov)

ABSTRACT: Inverse geochemical modelling was used to investigate rock–water interactions in flooded underground coal mines in northern Appalachia, USA. In early flooding, Pittsburgh seam mine waters are usually acidic (c. pH 3), with dissolved metals Fe and Al ranging from 10 to >100 mg l^{-1}. Within a few decades, however, waters in fully flooded mines usually have pH of about 7 S.U., and alkalinity >300 mg l^{-1} CaCO$_3$ Eq. Eh shifts from oxidizing (c. 500 to 700 mv) to reduced (-100 to -200 mv) conditions. Sodium concentrations may increase an order of magnitude; sulphate and iron concentrations may also increase. Water samples were collected from several mine-pools in West Virginia and Pennsylvania. A conceptual model was developed based on quantitative hydrology, mine-pool chemistry, mining conditions and mineralogy. The model was tested with the geochemical code PHREEQC. Simulations included mixing recharge and acid mine waters, precipitation–dissolution reactions involving carbonates, sulphates, oxy-hydroxides and sulphides, and ion adsorption and exchange. Na exchange was a dominant process in all models. Carbonates are orders of magnitude undersaturated in the juvenile mine-pool, but near saturation in the mature mine-pool, suggesting they are a primary source of acid neutralization and alkalinity. The mature mine-pool is simultaneously near equilibrium with iron sulphide, iron carbonate and iron oxy-hydroxide mineral phases. The rapid change in mine-pool water quality has substantial implications for management of these systems. Corresponding author eperry@osmre.gov

KEYWORDS: mine-pool, acid drainage, Pittsburgh seam, neutralization, inverse model, ion exchange, sulphate salts

INTRODUCTION

Bituminous coals of the northern Appalachian basin of the U.S. have been mined by underground methods for over 100 years. One of the most valuable and extensively mined coal beds is the Pittsburgh seam (Monongahela group, upper Pennsylvanian system). During active mining, underground works are de-watered by pumping. When mines are closed, however, de-watering is discontinued, and the underground mine voids flood by infiltration from overlying aquifers, stream leakage and inflow from adjacent flooded mines. In early flooding of Pittsburgh seam mines, waters are often strongly acidic (c. pH 3.0) with dissolved metals Fe and Al, ranging from 10 to >100 mg l^{-1}. Sulphate concentrations may range from 1000 to >7000 mg l^{-1}.

Mining companies and regulatory agencies have observed a change in water quality in some flooded Pittsburgh seam mines located below base level drainage, where the coal bed does not crop out. Characteristic of this is a change from acidic to circumneutral conditions within a few decades after flooding. Few of these mines have been monitored systematically, however, for long periods after closure. Donovan *et al.* (1999) describe one well documented case of water quality evolution in below-drainage Pittsburgh seam mines, where a systematic record was compiled, and mining history and geological conditions were known. They summarized 15 years of raw (untreated) water quality data from a pumping well in a Pennsylvania mine-pool. Based on reported pumping rates and analysis of detailed mine maps, the time to remove one pool volume was estimated to be about 7.4 years. Table 1 shows median values for about one year of monitoring during removal of the first pool volume (early flooding) at about 4 years of pumping, and a second subset after about 14 years of pumping (late flooding) from the data compiled by Donovan *et al.* (1999). Over about a ten year period, pH increased about two S.U. and the water changed from net acid to net alkaline. Iron, the major dissolved metal, declined to about 10% of its initial concentration, as did manganese and metal acidity. Large concentrations of sodium and sulphate were attenuated to about 30 and 20% of their initial concentrations, respectively. Donovan *et al.* (1999) also reported the acid waters to be at or near saturation for gypsum in the first two years of flooding, and approaching saturation for calcite as the water turned net alkaline and pH increased. They attribute the change in pool quality, at least in part, to carbonate neutralization and flushing of acid weathering products.

Donovan *et al.* (1999) also noted the influence of hydro-logical setting in determining post-mining water quality of

Table 1. *Early and late flooding quality from a pumped mine-pool in Pennsylvania, Pittsburgh Seam*[1]

Parameter	pH	Alkalinity	Metal acidity	Fe	Mn	Al	Ca	Mg	Na	K	Cl	SO$_4$
Early[2] ($n=50$)	4.4	N.D.	1831	931	15.8	20.6	371	200	2007	12	628	7000
Late[3] ($n=14$)	6.6	357	158	87	1.3	0.2	142	49	774	5.6	310	1445

[1]Data excerpted from Donovan *et al.* 1999. pH in S.U., metal acidity in CaCO$_3$ Eq, all others in mg/l^{-1}. [2]Median of samples from July 1984–July 1985. [3]Median of samples from February 1994–October 1995.
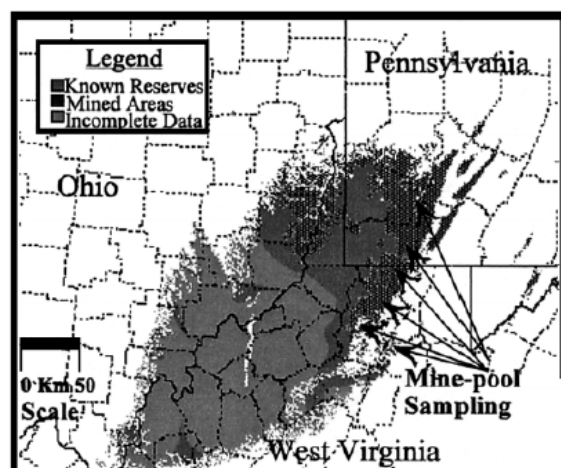
Fig. 1. Areal extent of the Pittsburgh coal and mined areas (after Ruppert *et al.* 1999), and counties with mine-pool quality sampling.

underground mines. They summarized data for six Pittsburgh seam discharges located *above* base level drainage, and compared them to water quality from *below* drainage mines. The above drainage mines are free draining and discharge strongly acidic water (pH 2–3, metal acidity about 1100 to 1800 l^{-1} CaCO$_3$ Eq) and showed little change in composition after 20 years. The flooded below drainage mines have circumneutral pH and about 10% of the metal acidity concentrations of the above drainage waters.

Flooding controls on mine water quality are usually attributed to eliminating oxidizers, either oxygen or Fe(III) for sulphide oxidation. Flooding has been advocated to limit sulphide oxidation in tailings (Robertson *et al.* 1997) and reduced pollutant loads in some Appalachian underground coal mines (Bucek & Emel 1977). This study was an initial investigation of processes controlling the observed evolution of waters from acidic to alkaline conditions in below drainage Pittsburgh seam mine-pools. The processes investigated included mixing of recharge and acid mine waters, precipitation–dissolution reactions involving carbonates, sulphates, oxy-hydroxides and sulphides; and ion adsorption and exchange. These initial investigations were not intended as site specific transport modelling efforts.

Stratigraphy and structure

The Pittsburgh coal bed is located at the base of the Monongahela group of the Upper Pennsylvanian system. This coal bed is in an elongated basin, with the main axis trending SW to NE in northen Appalachia, USA. A series of small anticlines and synclines are superimposed on the main structure. It covers parts of Pennsylvania, Maryland, West Virginia and Ohio (Fig. 1). Throughout much of the basin, the coal lies
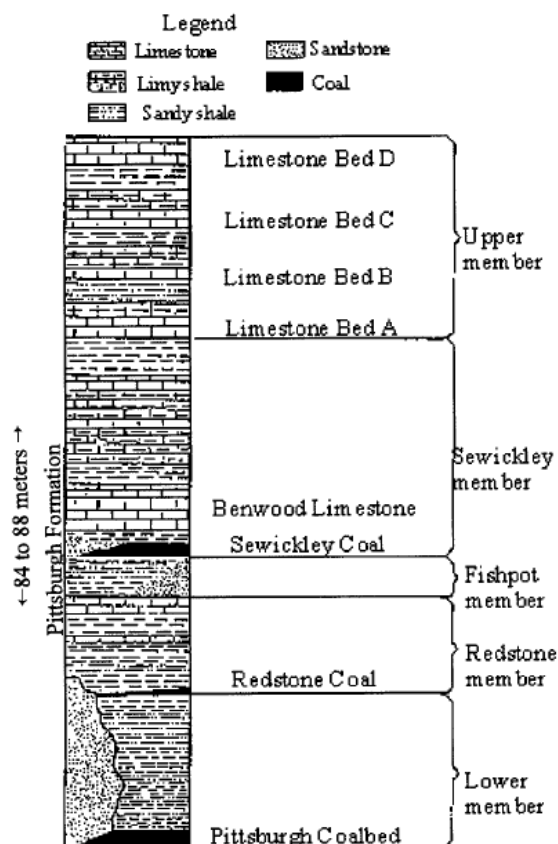
Fig. 2. Generalized stratigraphic column of the Pittsburgh coal and overburden, lower Monongahela group (after McCullogh *et al.* 1975).

below elevation of local major drainage systems, at depths ranging from 60 to >300 m, but is at or near outcrop along parts of the basin margin (McCullogh *et al.* 1975). Of the estimated 31 billion tonnes of original reserves, about 14 billion tonnes remain (Ruppert *et al.* 1999).

The Pittsburgh coal is typically 2–3 m thick, and is overlain by a sequence of interbedded calcareous shales, siltstones, limestones, coals and sandstones. A generalized stratigraphic column for the lower part of the Monongahela group is shown in Figure 2. Over much of the basin, limestones and calcareous shales overlie the coal, but rapid facies changes produced channel sandstone roofrock in some areas (McCullogh *et al.* 1975). The seatrock beneath the coal varies from limestone to shale to sandstone (Donaldson *et al.* 1979) and is usually calcareous. Kaolinite and illite are the most common clay minerals in the overburden (O'Neill & Barnes 1979) and coal (Renton 1979).

Table 2. *Representative sulphur and carbonate equivalent content of overburden above the Pittsburgh coal*

Lithology	Thickness (m)	Height above coal (m)	% S (total)	% CaCO₃ Eq.
Shale	0.79	7.70	0.82	3.9
Shale	1.18	6.52	0.49	4.2
Redstone coal	0.04	6.48	6.81	1.6
Shale	0.62	5.86	0.74	3.2
Limestone	0.94	4.92	0.88	51.3
Limestone	0.97	3.95	0.04	66.8
Limestone	0.94	3.01	0.09	54.5
Claystone	1.17	1.84	0.74	22.7
Claystone	1.16	0.68	0.73	13.8
Limestone	0.23	0.45	1.90	49.0
Shale	0.45	0	1.44	7.1
Pittsburgh coal	2.13	—	—	—
Shale	0.94	—	0.84	4.7

Table 2 shows representative total sulphur and calcium carbonate equivalent content for about 8 m of overburden directly above the Pittsburgh seam in a West Virginia mine. The analyses are unpublished data from a mine permit application, and were generated using Acid/Base Accounting (ABA). ABA was developed to assess the acid and alkalinity generating capacity of rocks on mines (Sobek *et al.* 1978), and is widely used in the Appalachian basin for mine assessments. In unweathered sedimentary rocks in Appalachia, except for coals and carbonaceous shales, total sulphur closely corresponds to pyrite content (Sobek *et al.* 1978). It is used to estimate potential acid generation from pyrite oxidation. ABA also reports a percentage CaCO₃ equivalent or acid neutralizers for the rock. This analysis does not identify the specific minerals contributing to the measurement but reports them on the basis of pure calcite equivalent. Most of the interval in Table 2 between the Pittsburgh coal and Redstone coal horizon is an impure limestone interbedded with calcareous shale. Analyses of the Redstone limestone horizon in West Virginia show a Ca:Mg molar ratio ranging from about 13:1 to as low as about 3:1 (McCue *et al.* 1939). The Pittsburgh coal itself contains about 1–3% total sulphur with higher concentrations in the top and bottom of the bed and shale partings (Donaldson *et al.* 1979).

Mining methods

Coal extraction in Pittsburgh seam mines includes room and pillar with retreat mining, and modern longwall extraction. Extraction rates typically range from about 60–80%. In longwall mines, subsidence is immediate, but more difficult to predict over room and pillar mines, where voids may stand open for decades. Before subsidence, the mine- pool aquifer consists principally of mine voids. After subsiding, the overburden rocks include a collapsed rubble zone which is estimated to extend upwards from two to eight times coal height (Peng 1986), and an overlying fractured zone estimated to extend to a height 30 to 60 times coal thickness (Tieman & Rauch 1987). The mine-pool aquifer then consists of any remaining void at coal elevation plus the collapsed zone. Thus, water quality of the mine-pool aquifer is controlled by rocks at mine level, part of the collapsed overburden, and by leakage from overlying strata.

Groundwater flow system

The mine-pool is composed of water that infiltrates from overlying strata, leakage from adjacent flooded mines, leakage
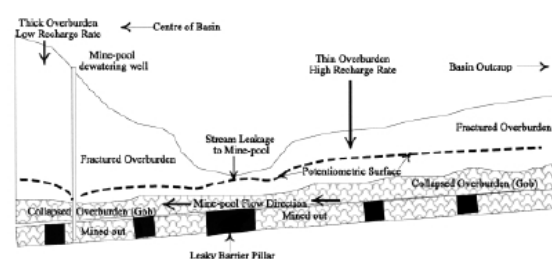
Fig. 3. Generalized cross-section of Pittsburgh Seam mine-pool flow system (no scale).

from streams, and sometimes injection of treated wastewater. The key features controlling mine-pool recharge, flow direction and storage are overburden thickness, barrier pillars, mine dewatering and structure. Figure 3 is a simplified cross-section of flow and recharge in a below drainage mine-pool. In early flooding, the down-dip mine voids fill first. As flooding progresses, hydraulic head increases until the mine either floods completely, the pool discharges to the surface or another mine, or is controlled by pumping. In a completely flooded below drainage mine, the pool acts a as leaky confined aquifer. The potentiometric surface measured in one West Virginia mine-pool ranges from about 6 to >45 m above mine level.

The overburden above the coal behaves like a leaky aquitard with vertical leakance strongly dependent on mine depth. Stoner *et al.* (1987) estimated mine recharge rates as ranging from about 2 cm a⁻¹ to 12.3 cm a⁻¹ in Pittsburgh seam mines in Pennsylvania. Highest rates were under thinner overburden. Leavitt (pers. comm. 1998) developed an exponential relationship between mine recharge rate and overburden thickness, based on records from 16 underground mines, most in the Pittsburgh seam. Mine recharge rate decreases as overburden thickness increases in Leavitt's model. Thickness effects likely relate to a decrease in fracture density and size with increasing depth (Schmidt 1985). Hobba (1984) noted that some undermined watersheds in the Pittsburgh seam contained losing streams that were leaking into (recharging) the mine-pool. Mine-pool recharge rates are therefore, not uniformly distributed, but tend to be highest under thin overburden and losing stream valleys.

The simplified mine-pool scenario shown in Figure 3 contains a barrier pillar, a zone of unmined coal left in place between mines. Barrier pillars may be as thin as 10 m, but are often 60 m or greater in modern mining, and thickness greatly influences the leakage rate between mines. In Figure 3, the down-dip barrier pillar is thin and leaky, and flow is down dip toward the centre of the basin. Leakage is accelerated by pumping from a down-dip well. If the barrier pillars are thick enough to minimize leakage, flow direction can be reversed and the mine-pool discharges at the coal outcrop. That scenario is also occurring within the basin.

METHODS

Water samples were collected along the eastern margin of the basin in counties in West Virginia and Pennsylvania (Fig. 1) and supplemented with selected literature data. Samples were collected where the mine- pool flow path was known or inferred from mine maps, water level measurements and discharge data. Samples were classed as juvenile (beginning of flowpath), intermediate or mature (end of flowpath). Water quality samples were collected after purging wells until stable temperature and specific conductance readings were obtained. Field

measurements and analytical parameters from monitoring wells, springs and mine shafts included:

(1) Field measured pH, temperature, Specific Conductance, and Eh (Pt electrode);
(2) Lab measured pH, Specific Conductance, Alkalinity, Total Acidity, Total Fe, Mn and Al, Total Dissolved Solids and Total Suspended Solids;
(3) Dissolved Ca, Mg, Na, K, Cl, SO4, Fe, Mn, Al;
(4) Trace elements As, Ba, Cd, Co, Cr, Cu, Ni, Pb, Sb, Se, Zn; and
(5) Selected samples for dissolved sulphide and ferrous iron.

Samples for dissolved constituents and trace elements were field filtered (0.45 μm pore size); total and dissolved metals were preserved with HNO_3, ferrous iron samples were preserved with HCl, and dissolved sulphide samples were preserved with Zn acetate. Samples were chilled and delivered to a commercial lab within 48 h of collection. Lab analyses were conducted following standard methods (Cherceri *et al.* 1998). Charge balance on reported analyses was typically within 2 to 3%.

Geochemical modelling simulations were run with the code PHREEQC (Parkhurst 1995; Parkhurst & Appelo 1999). Inverse modelling was conducted using three solutions, representing 'average' compositions for a juvenile mine water, a mature mine water and a recharge water. Composition of the juvenile and mine-pool waters are median values from analyses collected or reviewed in this work and were developed from about two dozen analyses of Pittsburgh seam mine waters. 'Average' composition of the recharge water is from data compiled by Hobba (1984) for groundwater analyses from 38 wells in the Monongahela Group in West Virginia. No Eh values were reported for the recharge water, so the PHREEQC default, pe equal to 4, was assigned. Initially, the three solutions were speciated using PHREEQC, and the results examined for mineral saturation indices, and partial pressures of gases. Inverse model simulations included only mixing and mineral precipitation/dissolution, followed by runs which also included ion exchange.

MINE-POOL AND RECHARGE WATER COMPOSITION

Median composition of the recharge, juvenile and mature mine-pool water used in geochemical modelling are shown in Table 2. In keeping with the objective of an initial investigation and modelling, makeup of these solutions represents a 'typical' water, not necessarily a site specific case. For each solution however, there are individual sample analyses that correspond closely to the 'average' composition. For most parameters, a range of values from which the median was taken is also shown in Table 3. Mine waters are especially variable in dissolved iron and aluminium content, yet each solution exhibits distinctive properties.

The juvenile mine water is a calcium–magnesium sulphate solution that is strongly acidic, and contains elevated concentrations of Fe, Al and sulphate, all characteristic of acid drainage in the northern Appalachian basin. Dissolved solids content is about 2800 mg l⁻¹. The mature mine water is a sodium sulphate solution and shows a pH increase of about 4 S.U., alkalinity about 500 mg l⁻¹ $CaCO_3$ equivalent, a tenfold increase in sodium content, and 50% increase in sulphate concentration compared to the juvenile mine water. Dissolved solids content is about 5700 mg l⁻¹. Redox potential declines from oxidized (Eh=+511 mv) in the juvenile mine water to reduced conditions (Eh= −170 mv) in the mature mine water. The recharge water is a calcium bicarbonate solution and is

Table 3. *Composition of solutions used in inverse modelling*[1]

Parameter	Juvenile mine water	Recharge water	Mature mine water
pH	3.3	7.4	7.3
	(2.2–4.8)	(5.8–9.0)	(6.6–8.4)
Eh, mv	511	227	−170
	(80–648)	—	(−14 to −230)
Temperature (C°)	13	13	13
Alkalinity (mg/LCaCO₃ Eq)	<1	259	510
		(5–754)	(230–1000)
Ca	340	27	305
	(280–710)	(1.1–69)	(90–448)
Mg	134	7	103
	(57–225)	(0.3–19)	(30–200)
Na	139	120	1330
	(105–823)	(9–356)	(540–1700)
K	6	—	13
	(3–10)		(5–32)
SO₄	2050	40	3185
	(600–7300)	(2–203)	(900–5450)
Cl	30	19.1	108
	(5–174)	(1–66)	(11–1300)
Fe	45	1.06	138
	(7–1655)	(0.1–16)	(3–202)
Al	30	—	0.04
	(1.5–203)		(0.02-0.2)
Si	20	15	15

[1] Elemental concentrations in mg l⁻¹. Mine water median values based on 24 analyses, recharge water based on 38 values reported by Hobba (1984). Values in parentheses are ranges.

much less mineralized than either mine water, with dissolved solids content of about 500 mg l⁻¹.

CONCEPTUAL MODEL OF MINE-POOL EVOLUTION

Pittsburgh seam mine-pools often shift from acid, oxidized conditions to reduced, alkaline, conditions within a few decades of mine closure and flooding. Mineralization increases, and solution composition evolves from calcium–magnesium sulphate to sodium sulphate with high concentrations of dissolved iron (Table 3). The observed water quality changes suggest that significant acid neutralization and generation of alkalinity occurs, and that readily soluble minerals and a sodium source are present. A conceptual model was formulated that would account for acid neutralization, soluble minerals and a sodium source, based on examination of solution compositions (Table 3), mineral saturation indices calculated in PHREEQC (Table 4), mineralogy and mine-pool flow path system. The model is focused on the behaviour of the major components Fe, Ca, Mg, Na and S, in the mine-pool system. Processes included acid neutralization, sulphate salt and carbonate dissolution, and ion exchange. Sulphate and iron oxide reduction, and carbonate and sulphide precipitation were also considered possible secondary processes. The mature mine-pool water is considered to be a product of:

(1) The initial flooding solution or juvenile mine-pool;
(2) mixing of the juvenile mine-pool with recharged (leakage) from overlying aquifers and streams, and sometimes leakage from adjacent flooded mines; and
(3) mineral precipitation/dissolution and ion exchange reactions along the flowpath.

The conceptual model is shown in Figure 4.

Mineral phase	Juvenile mine water	Recharge water	Mature mine water
Al(OH)$_3$(a)	−6.18	—	−0.80
Alunite	-2.01	—	−2.75
pCO$_2$(g)	−1.00	−1.98	−1.69
Calcite	−6.77	−0.32	0.38
Dolomite	−13.76	−1.05	0.48
Dolomite(d)	−14.36	−1.65	−0.12
Fe(OH)$_3$(a)	−2.91	2.84	−2.62
Fe$_3$(OH)$_8$	−13.25	4.89	−4.38
FeS(ppt)	−64.70	−60.47	−0.27
Goethite	2.54	8.29	2.83
Gypsum	−0.18	−2.35	−0.18
K − Jarosite	−3.96	—	−14.48
Jurbanite	−0.11	—	−2.57
Melanterite	−3.40	−6.36	−2.96
Pyrite	−96.80	−96.80	7.77
Siderite	−5.38	0.28	2.21
Siderite(d)	−5.75	−0.08	1.85

[1]Mineral saturation indices calculated in PHREEQC as log (Ion Activity Product/Equilibrium Constant).
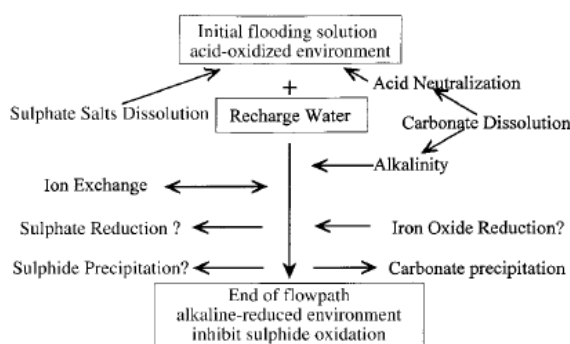
Fig. 4. Conceptual model of mine-pool water quality evolution.

Sulphate salts

During active coal removal, the mineworks are dewatered and ventilated. The humid aerated mine atmosphere provides ideal conditions for the oxidation of pyrite to produce acidity and metal oxy-hydroxide minerals as shown in the following summary equation:

$$FeS_2 + 3.75 O_2 + 3.5 H_2O \rightarrow 4 H^+ + 2 SO_4^{2-} + Fe(OH)_3 \quad (1)$$
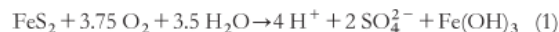
In many instances, however, sulphate minerals form as intermediate products of sulphide oxidation in coal and mine waste rock, and are often readily visible in mines as white and yellow precipitates. Some sulphate minerals that have been identified in Pittsburgh seam mines and Appalachian coal measures include gypsum, melanterite, halotrichite, pickeringite, copiapite, rozenite, and various jarosites (Nuhfer 1967; Rose & Cravotta 1998). Many of these salts are moderately soluble and can redissolve when the mine floods. Table 4 shows both the juvenile and mature mine waters to be slightly under saturated with respect to gypsum, and three or more orders of magnitude under saturated for melanterite and K–Jarosite. Similar trends for sulphate mineral saturation indices exist in about 24 individual mine water analyses compiled by the author (unpublished data). These minerals, if present, should dissolve during mine flooding, and could account for the observed increase in sulphate concentration from juvenile to mature mine water. Even though they are present in mines, some complex sulphate salts like copiapite lack consistent thermodynamic data, and are not included in PHREEQC model calculations. Except for gypsum, sulphate minerals can be a source of stored metals and acidity as shown by the net reaction for complete dissolution of copiapite, followed by oxidation and hydrolysis of iron.

$$Fe(II)Fe_4(III)(SO_4)_6(OH)_2 \cdot 20 H_2O + \tfrac{1}{4} O_2$$
$$\rightarrow 5 Fe(OH)_3 + 12 H^+ + 6 SO_4^{2-} + 7\tfrac{1}{2} H_2O \quad (2)$$
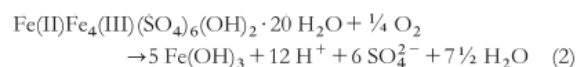
If iron hydrolysis is incomplete, the solution accumulates high concentrations of dissolved iron.

Inhibiting sulphide oxidation

Pyrite is characteristically oxidized by either Fe(III) or O$_2$ (Rose & Cravotta 1998). In fully flooded Pittsburgh seam mines, for 12 samples, the author has not found detectable levels of dissolved oxygen. In about 15 samples speciated for Fe(II)/Fe(III), ferrous iron typically is 99% or more of the dissolved fraction, and Fe(III) is often below detection. Thus, after initial flooding, dissolved oxygen and Fe(III) are present only in small concentrations and further sulphide oxidation should be inhibited.

Acid neutralization and alkalinity

Collapsed overburden or 'gob' frequently contains horizons with five to >50% carbonate (Table 2), and the seat-earth or mine floor rock is often calcareous (Donaldson *et al.* 1979). Brady (1998) reports that calcite, dolomite and siderite have been identified as the dominant carbonate minerals in the Monongahela and overlying Dunkard groups in Pennsylvania. All carbonate minerals are orders of magnitude undersaturated in the juvenile mine-pool (Table 4). The mature mine-pool, however, is slightly oversaturated for both calcite and dolomite, and about two orders of magnitude oversaturated for the iron carbonate siderite. Similar trends for carbonate mineral saturation indices exist in about 24 individual mine water analyses compiled by the author (unpublished data). Carbonate minerals are at first dissolving, neutralizing acidity and generating alkalinity in the mine-pool, and perhaps precipitating at the end of the flowpath. The recharge water is undersaturated for calcite and dolomite (Table 4), indicating both carbonates should dissolve and generate alkalinity. Acid neutralization available from the gob zone of fractured, broken carbonate rock and continuous infiltration of alkaline recharge water exceed the overall acid generating capacity (estimated from total sulphur content) of acid forming rock remaining in the mine-pool aquifer. Thus, given sufficient recharge and reaction time, acidity present initially should be neutralized, and the system should eventually turn alkaline.

Ion exchange

Sodium increases by roughly tenfold in mature mine water, and evolution from Ca/Mg dominated to Na dominated water may result from cation exchange of Ca, Mg or Fe(II) with adsorbed sodium. Donovan *et al.* (1999) also report high concentrations of sodium in Pittsburgh seam mine waters (Table 1). Chloride concentrations do not increase stoichiometrically with sodium in the mature mine water, as would be expected if brine water is entering the mine-pool. Back (1966) in a study of hydrochemical facies and groundwater flow, noted a progressive
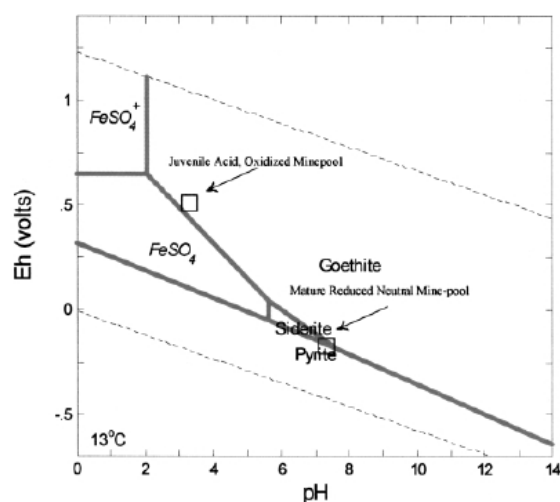
Fig. 5. Eh/pH iron stability fields for mine-pool waters with Goethite at 13°C.

change from Ca/Mg dominated water to Na dominated water along a flow path in some Atlantic Coastal Plain aquifers. The differentiation was attributed to ion exchange.

The mineral fraction of northern Appalachian coals and the seat-rock and overburden have been reported to contain kaolinite and illite (McCullogh *et al*. 1975; Renton 1979) and Johnson & Skousen (1995) reported cation exchange capacity of 10–30 cmol kg^{-1} in 25 to 33 year old waste rock from surface mine sites on the Pittsburgh seam.

Iron oxy-hydroxide minerals

Iron floc precipitating from acid mine waters commonly contains a mixture of mineral phases ranging from poorly crystalline $Fe(OH)_3$, to ferrihydrite, schwertmannite and goethite (Ferris *et al*. 1989; Bigham *et al*. 1996; Rose & Elliot 2000). The more soluble oxy-hydroxide minerals $Fe(OH)_3$(am) and ferrihydrite, are under saturated by more than two orders of magnitude in both the juvenile and mature mine-pool waters (Table 4), indicating that these minerals are not likely to precipitate. Twenty four of 28 individual mine water samples (authors unpublished data) are under saturated for $Fe(OH)_3$(am) and ferrihydrite by two or more orders of magnitude. If they are already present in the aquifer at flooding, they could dissolve, or convert to more stable oxide minerals, as suggested by Nordstrom's (1982) diagram of pyrite weathering. Goethite is over saturated by more than two orders of magnitude in both the juvenile and mature mine waters (Table 4) and 28 individual analyses, showing that precipitation of this mineral is possible.

Figure 5 is an Eh/pH plot of iron stability fields with goethite as the dominant Fe(III) mineral, and contains the juvenile and mature mine-pool waters. Iron activity in the acid juvenile water appears to be controlled by oxy-hydroxide minerals. The mature mine-pool water, however, plots near the intersection of the goethite, siderite and pyrite stability fields, suggesting that iron has several possible source/sink minerals.

Sulphate reduction

Sulphate reducing bacteria (SRB) have been detected in a present/absent test in four wells in a West Virginia mine pool.

Eh and pH conditions (Table 3) are within a range considered conducive to SRB activity (Baas Becking *et al*. 1960; Barton 1995). Individual mine-pool samples contain trace to about $0.6\,\mathrm{mg\,l^{-1}}$ dissolved sulphide, and the characteristic 'rotten egg smell' of H_2S gas has been noted in some samples.

Sulphide precipitation

Pyrite is over saturated and FeS precipitate (ppt) is approaching saturation in the mature mine-pool (Table 4). Mineral saturation indices plus the presence of dissolved sulphide and ferrous iron suggests that precipitation of an iron monosulphide is possible. Once precipitated, monosulphides gradually convert to pyrite (Schoonen & Barnes 1991).

Equilibrium Eh values were computed for several redox couples with the Nernst equation to determine how closely the mature solution approaches equilibrium for several iron sulphide and oxyhydroxide minerals. Equilibrium constants (K) from the PHREEQC databases and the standard potential E° were corrected for temperature effects. For FeS(ppt), the computed equilibrium Eh is −173 mv, which is close to the solution Eh of −170 mv. This suggests that the mature solution is near equilibrium with an iron sulphide. For pyrite, ferrihydrite and $Fe(OH)_3$ (am), the computed equilibrium Eh values were −139 mv, −45 mv and −24 mv, respectively.

PHREEQC model

The conceptual model was tested with an inverse geochemical model containing three solutions; the juvenile mine-pool, recharge water and mature mine-pool. Mixing, mineral precipitation/dissolution reactions, and ion exchange from clays and hydrous ferric oxides were simulated. The PHREEQC input file is shown in Appendix A. Modelling is based on an aquifer about 8 m thick, or four times the original coal thickness (void plus collapsed zone), and a 70% coal extraction rate. This yields an aquifer porosity, n, of about 17% and a fluid to rock mass ratio of about 1:13.

PHREEQC is a low temperature aqueous geochemical modelling system that calculates aqueous speciation and mineral saturation indices, simulates ion exchange reactions, mixing, reaction paths and transport, and solves inverse models. It is based on equilibrium chemistry concepts, and solves inverse models by simultaneous equations that maintain balance for mole fraction, charge, alkalinity, and ionic strength. For speciation and mineral saturation indices, PHREEQC estimates activities from either the extended Debye-Huckel or Davies equations. The code calculates mineral saturation indices from a user selected database of equilibrium constants.

Inverse modelling finds sets of mineral and gas mole transfers that satisfy differences in composition between waters, and is often used to account for the changes that occur along a flowpath between starting and ending waters. For further details of PHREEQC's capabilities, limitations and execution, the reader should consult Parkhurst (1995) and Parkhurst & Appelo (1999). Modelling included the following mineral phases:

(1) Carbonates; calcite, dolomite and siderite
(2) Sulphates; gypsum, melanterite, jarosite and jurbanite
(3) Sulphide FeS(ppt)
(4) Oxy-hydroxides goethite, $Fe(OH)_3$ (am), $Al(OH)3$ (am)

Siderite and goethite are about two orders of magnitude oversaturated in the mature mine-pool, and were constrained in modelling to precipitate only as potential end products. Gypsum, melanterite and K-jarosite were included as potential sources of soluble sulphate and metals, and were constrained to

Table 5. *Mixing percentages and phase transfers for 8 inverse models*[1]

	Model 1	Model 2	Model 3	Model 4	Model 5	Model 6	Model 7	Model 8
Mixing	72.3 (J)	14.6 (J)	10.1 (J)	35.9 (J)	26.7 (J)	14.6 (J)	1 (J)	1 (J)
Percent[1]	27.1 (R)	85.3 (R)	89.4 (R)	63.8 (R)	72.9 (R)	85.3 (R)	99 (R)	99 (R)
NaX	+4.719e-2	+4.767e-2	+4.772e-2	+4.750e-2	+4.758e-2	+4.767e-2	+4.779e-2	+4.779e-2
CAX2	−2.360e-2	−2.897e-3	—	—	—	−2.384e-2	−2.771e-2	−3.137e-2
MGX2	—	—	+3.263e-3	−1.801e-3	—	—	+3.809e-3	—
FeX2	—	+5.135e-3	−2.712e-3	−2.195e-3	−2.379e-3	—	—	+7.477e-3
Calcite	+2.420e-3	—	+5.790e-3	—	+2.059e-3	—	+5.180e-3	—
Dolomite	—	+3.019e-2	—	+3.658e-3	+2.357e-3	+3.019e-3	—	+3.809e-3
Melanterite	+2.011e-2	+4.055e-2	+3.224e-2	+2.724e-2	+2.902e-2	2.355e-3	+5.037e-3	—
Gypsum	—	+2.859e-2	—	—	—	—	+2.914e-2	+3.418e-2
K-Jarosite	+2.226e-4	+3.119e-4	+3.187e-4	+2.792e-4	2.932e-4	+3.119e-4	3.341e-4	+3.341e-4
FeS(ppt)	−4.278e-4	−3.089e-4	−3.028e-3	−3.448e-4	−3.299e-4	—	−2.853e-4	−2.851e-3
Siderite	−1.437e-2	—	—	—	—	—	—	−2.441e-4
Goethite	−4.092e-3	−3.411e-2	−3.068e-2	−3.599e-4	−3.522e-3	−9.394e-4	−3.289e-3	−3.288e-2

[1]Values in m kg^{-1}. '+' indicates the phase enters the solution; '−' indicates the phase leaves the solution. No entry indicates the phase is not contained in the model. [2]'J' designates mixing percentage of juvenile acid mine-pool; 'R' refers to recharge water.

dissolve only. Fe(OH)3(am) is undersaturated in both mine waters and was therefore constrained to dissolve only. $Al(OH)_3$ was included as a likely sink for Al in the mature mine-pool.

Cation exchange capacity (CEC) was fixed at 1 M, equivalent to about 100 meq/kg of aquifer, corresponding to the lower range of CEC reported by Johnson & Skousen (1995) for weathered waste rock on Pittsburgh seam surface mines. Exchange species included Na, Ca, Mg and Fe(II). Exchanger composition was determined from equilibration with the mature mine-pool solution.

A hydrous ferric oxide surface (Hfo) surface was included in modelling to examine sulphate desorption as mine pool pH increases from acid to neutral conditions. Rose & Elliot (2000) noted substantial desorption of sulphate from ferric precipitates in acid drainage, as the sediments were amended with liming agents. The aquifer matrix was assumed to contain 1% Hfo and properties were assigned following summary data and the model suggested by Dzombak & Morel (1990). The Hfo was equilibrated with both mine water solutions to estimate its starting and ending compositions.

RESULTS AND DISCUSSION

PHREEQC produced about 250 inverse models that could explain the evolution of the mature mine-pool. About 60 were examined further, because they included both the juvenile mine-pool and the recharge water as components, and had mixing fractions that summed to *c.* 100%. The remaining models were examined, then discarded from further analysis because they did not include both the juvenile mine-pool and the recharge water as components, or the mixing fractions differed significantly from 100%. The main geochemical transfers included ion exchange of adsorbed Na with Ca, Mg, or Fe(II), carbonate and sulphate dissolution, with lesser amounts of sulphide and hydroxide minerals precipitated.

Most sets of models showed the mature mine-pool to consist mainly of recharge water. Models contained from 64–99% recharge water, and 1–36% juvenile mine water. Recharge water contains over 250 mg l^{-1} alkalinity and provides initial neutralization of the juvenile mine-pool. Mixing percentages are consistent with the flow system described previously; recharge enters the mine-pool to mix, react with, and eventually displace the initial pool volume. One model set was exceptional, and showed the mature mine-pool to consist of 73% juvenile water

Table 6. *Initial composition of exchanger and maximum amounts of species transfer in models*

Species	Moles adsorbed	Exchanger composition (%)	Maximum transfer (M)	Maximum fraction exchanged (%)
NaX	2.839e-1	28.4	4.779e-2	16.8
CaX2	2.382e-1	47.7	3.137e-2	13.2
MgX2	8.701e-1	17.4	3.809e-3	4.3
FeX2	2.886e-2	5.8	7.447e-3	25.8

and 27% recharge water. However, these models allowed no Mg transfer; that is no exchange of Mg or dolomite reaction. This severely constrained scenario is considered unlikely. Models consisting of end member mixes of 99% recharge water are considered unlikely, because they require very efficient flushing of the mine-pool.

Table 5 shows calculated mineral and exchange transfers for eight inverse models, selected to represent the range of results obtained in the 60 models that passed initial screening. Sodium exchange is a dominant process in every model, transferring about 4×10^{-2} M kg^{-1} into solution from the exchanger. The exchanging cations that leave solution include Ca, Mg, or Fe(II). Initial exchanger composition, in equilibrium with the mature mine-pool, consists mostly of Ca and Na, with lesser amounts of Mg and Fe(II) (Table 6). Five of eight models in Table 5 exchange solution Ca for adsorbed Na, and this accounts for the large increase in Na concentration in the mature mine-pool. Exchange behaviour of Mg and Fe(II) was inconsistent among model sets. Adsorbed Mg enters solution by exchange with solution Ca and Fe(II) in two models, but leaves solution in one model by exchange with Na. Ferrous iron leaves solution by exchange with Na in three models, but enters solution by exchange with Ca in two other models. Ca for Na exchange is considered the most feasible exchange modelling, due to abundance of these ions in solution, the propensity of Ca to displace weakly adsorbed Na, consistent model behaviour, and identification of Ca /Na exchange in other groundwater systems (Back 1966). Smaller amounts of Mg and Fe(II) exchange are possible. For this initial modelling, however, and absent more specific exchanger characterization, no attempt was made to force all exchange species into a single model.

247

The maximum fraction of adsorbed species transferred in any model is small relative to the total adsorbed species, even with a conservative estimate of CEC. The maximum fractions transferred are about 17 and 13% for Na and Ca, respectively (Table 6). Thus, ion exchange could continue through the circulation of at least several mine-pool volumes. Removing Ca or Mg from solution by Na exchange should cause under saturation for calcite or dolomite, and induce more carbonate to dissolve.

Dissolution of calcite, dolomite, or both, occurs in all models, as a source of alkalinity and acid neutralization in the mine-pool. Given the mixed carbonate mineralogy reported for limestones and calcareous rocks of the Monongahela group (McCue *et al.* 1939; Brady 1998), model results can represent combinations of calcite, magnesian calcite and dolomite. Mineral transfers are on the order of 10^{-3} M l^{-1} (Table 5) and constitute a very small fraction of carbonate in the aquifer. For a 1:13 fluid to solid ratio used in modelling, aquifer rocks containing 5% calcite provide about 6.5 moles of carbonate per litre of solution. Siderite, which was constrained to precipitate, appears in only two of eight models (Table 5). One was considered infeasible because it did not allow Mg transfer, and the second occurs in a mix containing 99% recharge water. Siderite precipitation is therefore considered unlikely under the conditions modelled.

Sulphate salt dissolution appears in every model as sources of sulphate, Fe(II), Fe(III), Ca, or K (Table 5). Maximum melanterite dissolution is about 4×10^{-2} M l^{-1}, equivalent to about 0.08% of the aquifer. These transfers are feasible, considering that the residual coal has 1% or more total S (Donaldson *et al.* 1979) and the collapsed gob may contain >0.5% total S (Table 2). Only a fraction of the total S need be available as sulphate salts to account for the mineral transfers. Sulphate salts could persist through a number of mine-pool volumes before depletion. Melanterite dissolution provides most of the observed increase in iron and sulphate concentrations in the mature mine-pool. Gypsum dissolution appears in three models, but two of them are considered unlikely solutions containing 99% recharge water.

Iron sulphide precipitation was included in 7 of 8 models shown in Table 5. Mole transfers are equivalent to removing a total of about 10 mg l^{-1} sulphide (as S) from solution, and require that sulphate reduction take place as the mine-pool evolves. Ferrous iron is supplied by melanterite dissolution.

Goethite is included in every model as a sink for Fe(III). Poorly crystalline Fe(OH)$_3$ (am) is not in any model, even though it was included as dissolving phase in PHREEQC. K–Jarosite dissolution provides Fe(III) for goethite formation. The lack of Fe(OH)$_3$ (am) dissolution indicates that no Fe(III) reduction is taking place in any model, even though the mine-pool is progressively reduced as it matures. Fe(OH)$_3$ (am), rather than dissolve, may convert to a more stable oxy-hydroxide. Additional modelling showed, however, that dissolution of Fe(OH)$_3$ (am), could be forced into a feasible model, if the quantity of melanterite is arbitrarily limited.

Postma & Jakobsen (1996) used a partial equilibrium approach to demonstrate that simultaneous Fe (III) and sulphate reduction is possible, rather than occurring in discrete steps. They summarize several field studies where apparent simultaneous reduction has been reported, including pH and Fe(II) activity conditions similar to the mature mine-pool. Postma & Jakobsen (1996) developed a set of equations representing equal energy yield between Fe(III) reduction and sulphate reduction for several iron oxyhydroxide minerals including goethite and Fe(OH)$_3$. For a solution dominated by Fe(II) the summary reaction is:

$$9\,Fe^{2+} + SO_4^{2-} + 20\,H_2O \rightarrow 8\,Fe(OH)_3 + FeS + 16\,H^+ \quad (3)$$
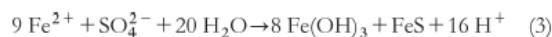
$$\log K_3 - 8 \log K_1 - \log K_7$$
$$= -16\,pH - 9 \log [Fe^{2+}] - \log [SO_4^{2-}] \quad (4)$$

where $\log K_3$ is the equilibrium constant for sulphate/sulphide couple, $\log K_1$ is the equilibrium constant for Fe(III) mineral/Fe^{2+} couple, and $\log K_7$ is the equilibrium constant for FeS precipitation. Solving equation 4 for goethite in the mature mine-pool yields a pH of 6.41 for equal energy yield. The solution pH is 7.3, therefore, with respect to goethite, sulphate reduction is favoured over Fe(III) reduction, from which FeS precipitation may follow. For Fe(OH)$_3$ (am), however, equation 4 gives an equal energy yield at pH 9.14 and Fe(III) reduction is the favoured process. This contradicts the modelling results where no Fe(OH)$_3$ (am) dissolution occurred. Since mine drainage sediments usually contain a mixture of iron oxy-hydroxide minerals (Ferris *et al.* 1989; Bigham *et al.* 1996; Rose & Elliot 2000), simultaneous reduction of sulphate and Fe(III) minerals is thermodynamically possible. Stability of the Fe(III) minerals will have a large influence on which reductive processes dominate the system.

Model results show hydrous ferric oxide (Hfo) surfaces could be sinks for Fe(II), and sources for sulphate as the mine-pool evolves from acid to alkaline conditions. About half of the sulphate originally bound to the Hfo is desorbed, while Fe(II) is removed from solution. Ninety-nine percent of 'strong' binding sites are occupied by proton acidity in the acid mine water, and by Fe(II) in the alkaline solution. 'Weak' binding sites are 53 and 47% saturated with proton acidity and sulphate, respectively, in the acid solution. In the alkaline mine-pool, 'weak' sites contain 58% Fe(II) and 26% S(6)species. Hfo surfaces can adsorb both cations and anions, with distribution and amount of adsorbed species strongly influenced by pH (Parfitt & Smart 1978; Harrison & Berkheiser 1982; Davis & Kent 1990). In general, anion adsorption dominates at low pH, and decreases with increasing pH. Overall influence of Hfo's on mine water chemistry will depend on its concentration in the aquifer, and number of binding sites.

SUMMARY AND CONCLUSIONS

A conceptual model of mine-pool evolution from acid to alkaline conditions was examined with inverse modelling. The model includes infiltration of alkaline recharge water, dissolution of carbonates and sulphate salts, and sulphide and oxy-hydroxide precipitation. These processes could account for water quality changes occurring in flooded underground coal mines of the Pittsburgh coal seam. About 60 inverse models were obtained that included both juvenile mine water and recharge water, and had mixing fractions totaling about 100%. Most of these models showed the mature mine-pool to consist mainly of recharge water, consistent with the groundwater flow system. The inverse models differ in mixing percentages and specific mineral transfers.

Neutralization of the juvenile acid mine-pool can be explained with two sources; recharge from alkaline groundwater in overlying aquifers, and reaction with broken calcareous rock collapsing from the overburden (gob) immediately above the mine. Carbonate content of the gob zone exceeds acid generating capacity from sulphide oxidation in the system. Recharge water infiltrates the mine-pool continuously and will ultimately displace most of the initial pool volume.

Ion exchange of adsorbed Na for solution Ca is a dominant process in all models, and provides a feasible explanation for the large Na increases in mature mine-pools. No other Na bearing minerals are known to occur in large concentrations in the Monongahela group that could account for the observed increases. Mine water compositions also do not reflect brine water leakage. Exchange reactions involving Mg and Fe(II) were simulated in some models, but their actual participation in mine- pool evolution is less conclusive.

Carbonates are likely the principal sources for Ca and Mg in the mine-pool aquifer, in addition to ion exchange. Carbonate composition ranges from calcite to dolomite, and one or both of these minerals dissolves in every model. They are orders of magnitude under saturated in the juvenile mine water, but near to slightly over saturation in the mature mine-pool. Calcite and dolomite provide initial acid neutralization, but could precipitate in the mature mine-pool. Siderite is near redox equilibrium with the mature mine water, but appeared in few models.

Dissolution of sulphate salts like melaneterite, K–Jarosite and gypsum can account for the sulphate rich mature mine-pool, and are in every feasible model. They may also provide soluble Fe(II), Fe(III), Ca or K. Other complex sulphates like copiapite and halotrichite are present in mine waste rock, but were not modelled, due to lack of consistent thermodynamic data. FeS precipitation was included in most models and requires sulphate reduction. Thermodynamic calculations show that sulphate reduction is possible in the mature mine-pool. Sulphate desorption from hydrous ferric oxide surfaces could occur, as the mine-pool evolves, but its significance depends on the amount of Hfo and binding sites present in the aquifer.

Iron is the most complex cycle in the mine-pool system. Iron sources included sulphate salt dissolution, ion exchange and dissolution of $Fe(OH)_3$ (am). Sinks included precipitation of FeS, goethite, siderite and binding to Hfo's in the mature mine-pool. Sulphate salt dissolution provides a feasible explanation for soluble iron. $Fe(OH)_3$ (am) dissolution was not in any model, yet thermodynamic calculations show $Fe(OH)_3$ (am) if present, could be reduced to Fe(II). The mature mine-pool is near equilibrium for FeS, siderite and goethite. All are feasible products of mine-pool evolution, and FeS and goethite consistently appear in inverse models. Exchange of Fe(II) and binding to Hfo surfaces in the mature mine water are shown in some models, but their importance in the overall system is not known.

Inverse modelling required some assumptions and approximations for these initial efforts. All mineral phases were assumed present in excess, no solid solution phases were specified, and near equilibrium conditions were assumed. Some minerals known to be present in mine waste rock, lack suitable data for modelling, and were not included.

Inverse modelling results support the major processes identified in the conceptual model. Mixing of alkaline recharge water, dissolution of carbonates and sulphate salts, and Na exchange were consistently identified as major inverse model components. These processes provide feasible explanation of the observed water quality changes in flooded underground Pittsburgh seam coal mines. Significance of some secondary processes requires further investigation, and iron cycling in the mine-pool is especially complex. Calculated mineral transfers show that these processes are able to continue through cycling of at least several pool volumes. Flushing of sulphate, iron and other constituents may therefore continue for a long period. These changes have substantial implications for treatment and management of mine-pools.

APPENDIX A

PHREEQC input file for Inverse Modelling

Title: Inverse model of mature mine-pool water from Recharge and acid Juvenile mine water.
SOLUTION 1 Acid Juvenile Water, start flowpath.
temp 13
pH 3.3
units mg l^{-1}
density 1
pe 9.0
Ca 340
Na 140
Mg 134
K 6
Fe 45
Al 30
Cl 30
S 2050
Si 20
equilibrium_phases
CO2(g) −1.0

SOLUTION 2 Median value recharge water quality (Hobba 1984 in WV).
Units mg l^{-1}
temp 13
pH 7.4
Alkalinity 259
Ca 27
Mg 7
Na 120
Cl 19.1
S 40
Fe 1.06
Si 15

SOLUTION 3 Mature mine-pool (end of flowpath).
temp 13
pH 7.3
pe −3
units mg l^{-1}
redox pe
density 1
Alkalinity 510
Ca 305
Na 1330
Mg 103
K 13
Fe 138
Al 0.05
Si 15
Cl 108
S 3185
-water 1 # kg

Exchange 1 exchanger defined, equilibrate with end flowpath water.
-equilibrate 3
× 1.0
Inverse_Modelling 1
-solutions 1 2 3
-uncertainty .05
-balances Alkalinity .2
-tolerance 1e-9
-minimal
-phases
NaX
CaX2
MgX2
FeX2
calcite
dolomite
gypsum dis
melanterite dis
FeS(ppt) ppt
jurbanite

249

halite
jarosite-k dis
siderite ppt
Al(OH)$_3$(a) ppt
Fe(OH)$_3$(a) dis
Goethite ppt

Surface 1 Iron Oxy-hydroxide surfaces
-equilibrate with solution 1
Hfo_w 0.48 600 216
Hfo_s 0.012

Surface 2 Iron Oxy-hydroxide surfaces
-equilibrate with solution 3
Hfo_w 0.48 600 216
Hfo_s 0.012

REFERENCES

BAAS BECKING, L. G., KAPLAN, R. & MOORE, D. 1960. Limits of the Natural Environment in Terms of pH and Oxidation-Reduction Potentials. *Journal of Geology*, **68**, 243–284.

BACK, W. 1966. Hydrochemical Facies and Ground-Water Flow Patterns in Northern Part of Atlantic Coastal Plain. *US Geological Survey Professional Paper 498-A.*

BARTON, L. (ed.) 1995. Sulfate-Reducing Bacteria. *Biotechnology Handbooks 8.* Plenum Publishing.

BIGHAM, J. M., SCHWERTMANN, U., TRAINA, S. J., WINLAND, R. L. & WOLF, M. 1996. Schwertmannite and the Chemical Modeling of Iron in Acid Sulfate Waters. *Geochemica Cosmochemica Acta*, **60**, 2111–2121.

BRADY, K. B. 1998. Influence of Geology on Post Mining Water Quality: Northern Appalachian Basin. *Coal Mine Drainage Prediction and Pollution Prevention in Pennsylvania.* Pennsylvania Dept. of Environmental Protection, Harrisburg, Pa.

BUCEK, M. F. & EMEL, J. L. 1977. *Long Term Effectiveness of Close Down Procedures—Eastern Underground Coal Mines.* HRB Singer Inc, for US Environmental Protection Agency, **EPA-600/7-77-083.**

CHERCERI, L. S., GREENBURG, A. E. & EATON, A. D. 1998. *Standard Methods for the Examination of Water and Waste Water*, 20th edition. American Public Health Association.

DAVIS, J. A. & KENT, D. B. 1990. Surface Complexation Modeling in Aqueous Geochemistry. *Reviews in Mineralogy*, **23**. Mineral Water Interface Geochemistry, Mineralogical Society of America.

DONALDSON, A. C., RENTON, J., KIMUTIS, R., LINGER, D. & ZAIDI, M. 1979. Distribution Pattern of Total Sulfur Content In the Pittsburgh Coal. *Carboniferous Coal Guidebook.* Bulletin B-37-3. West Virginia Geologic and Economic Survey.

DONOVAN, J. J., FLETCHER, J., STRAGER, M. & WERNER, E. 1999. Hydrogeological and Geochemical Response to Mine Flooding in the Pittsburgh Coal Basin, Southern Monongahela River Basin. West Virginia University, National Mined Land Reclamation Center Project WV-132, Final report to US Environmental Protection Agency.

DZOMBAK, D. A. & MOREL, F. M. 1990. *Surface Complexation Modeling–Hydrous Ferric Oxide.* John Wiley & Sons, New York.

FERRIS, F. G., TAZAKI, K. & FRYE, W. S. 1989. Iron Oxides in Acid Mine Drainage Environments and Their Association With Bacteria. *Chemical Geology*, **74**, 321–330.

GROWITZ, D. 1967. *Geochemistry of Mine Water, Northern Bituminous Field, West Virginia.* MSc Thesis, West Virginia University.

HARRISON, J. B. & BERKHEISER, V. E. 1982. Anion Interactions With Freshly Prepared Hydrous Iron Oxides. *Clays and Clay Minerals*, **30**, 97–102.

HOBBA. 1984. *Ground-Water Hydrology of the Monongahela River Basin.* US Geological Survey in cooperation with the West Virginia Dept of Natural Resources.

JOHNSON, C. & SKOUSEN, J. 1995. Minesoil Properties of 15 Abandoned Mine land Sites in West Virginia. *Journal of Environmental Quality*, **24**, 635–643.

McCUE, J., LUCKE, J. & WOODWARD, H. 1939. *Limestones of West Virginia.* West Virginia Geological Survey **Vol XII.**

McCULLOGH, C. M., DIAMOND, W. P., BENCH, B. M. & DUEL, M. 1975. Selected Geologic Factors Affecting Mining of the Pittsburgh Coalbed. *Report of Investigations 8093.* US Bureau of Mines.

NORDSTROM, D. K. 1982. Aqueous Pyrite Oxidation and the Consequent Formation of Secondary Iron Minerals. *Acid Sulfate Weathering.* Soil Science Society of America Special Publication 10.

NUHFER, E. 1967. *Efflorescent Minerals Associated With Coal.* MSc Thesis, West Virginia University.

O'NEILL, B. J. & BARNES, J. H. 1979. *Properties and Uses of Shales and Clays, Southwestern Pennsylvania.* Mineral Resources Report **77.**

PARFITT, R. L. & SMART, R. C. 1978. The Mechanism of Sulfate Adsorption on Iron Oxides. *Soil Science of America Journal*, **42**, 48–50.

PARKHURST, D. L. 1995. *User's Guide to PHREEQC—A Computer Program For Speciation, Reaction-Path, Advective-Transport, and Inverse Geochemical Calculations.* US Geological Survey Water Resources Investigation Report **95-4227.**

PARKHURST, D. L. & APPELO, C. A. J. 1999. *User's Guide to PHREEQC (Version 2)- A Computer Program For Speciation, Batch-Reaction, One-Dimensional Transport, and Inverse Geochemical Calculations.* US Geological Survey Water Resources Investigation Report **99-4259.**

PENG, S. 1986. *Coal Mine Ground Control*, 2nd ed. John Wiley & Sons, New York.

POSTMA, D. & JAKOBSEN, R. 1996. Redox zonation: Equilibrium Constraints on the Fe(III)/SO4-Reduction Interface. *Geochemica Cosmochemica Acta*, **60**, 3169–3175.

RENTON, J. 1979. The Mineral Content of Coal. *Carboniferous Coal Guidebook.* Bulletin B-37-1. West Virginia Geologic and Economic Survey.

ROBERTSON, J. D., TREMBLAY, G. A. & FRASER, W. W. 1997. Subaqueous Tailings Disposal: A Sound Solution for Reactive Tailings Disposal. *Proceedings of the Fourth International Conference on Acid Rock Drainage*, **3**, 1027–1041.

ROSE, A. W. & CRAVOTTA, C. A. 1998. Geochemistry of Coal Mine Drainage. *Coal Mine Drainage Prediction and Pollution Prevention in Pennsylvania.* Pennsylvania Dept. Environmental Protection.

ROSE, S. & ELLIOT, W. C. 2000. The Effects of pH Regulation on the Release of Sulfate From Ferric Precipitates Formed in Acid Mine Drainage. *Applied Geochemistry*, **15**, 27–34.

RUPPERT, L. F., TEWALT, S. J., BRAGG, L. J. & WALLACK, R. N. 1999. A Digital Resource Model of the Upper Pennsylvanian Pittsburgh Coal Bed, Monongahela Group, Northern Appalachian Basin Coal Region, USA. *International Journal of Coal Geology*, **41**, 3–24.

SCHIMDT, R. D. 1985. *Fracture Zone Dewatering To Control Ground Water Inflow in Underground Mines.* US Bureau of Mines Report of Investigations **8981.**

SCHOONEN, M. A. & BARNES, H. L. 1991. Reactions Forming Pyrite and Marcasite From Solution II: Via FeS Precursors Below 100°C. *Geochemca Cosmochemica Acta*, **55**, 1501–1514.

SOBEK, A., SCHULLER, W., FREEMAN, J. R. & Smith, R. M. 1978. *Field and Laboratory Methods Applicable To Overburdens and Minesoils.* West Virginia University. U.S Environmental Protection Agency **EPA600/2-78-054.**

STONER, J. D., WILLIAMS, D. R., BUCKWALTER, T. E., FELBINGER, J. K. & PATTISON, K. L. 1987. *Water Resources and the Effects of Coal Mining, Greene County, Pennsylvania.* Pennsylvania Geological Survey Water Resources Report **63.**

TIEMAN, G. E. & RAUCH, H. W. 1987. Study of Dewatering Effects at an Underground Longwall Mine Site in the Pittsburgh Seam of Northern Appalachia. *Proceedings Eastern Coal Mine Geomechanics, Bureau of Mines Technology Seminar, Information Circular 9137.* US Bureau of Mines.

Appendix C

GROUND-WATER FLOW AND QUALITY IN A FULLY FLOODED UNDERGROUND COMPLEX

GROUND-WATER FLOW AND QUALITY IN
A FULLY FLOODED UNDERGROUND COMPLEX[1]

Eric F. Perry [2] and Jay W. Hawkins

Abstract Water quantity and quality conditions are described for a mine-pool aquifer in a fully flooded complex of underground mines in northern West Virginia. Abandoned mines in the Pittsburgh coal bed are contiguous, and separated by coal barrier pillars ranging from as little as 9 to about 60 m thick. Barrier pillars are transmissive enough to circulate significant quantities of water between mines, yet they control head distribution and flow direction within the aquifer. The mine-pool acts as a confined aquifer, and recharge is approximately balanced by withdrawal of about 5700 L/min, leakage to adjacent mines, and unquantified outflow to unmined areas. Resulting drawdown prevents the mine-pool from discharging directly into overlying streams. A centrally located subgroup of mines within the aquifer currently acts as a ground-water sink, but water levels are slowly increasing in the sink, and in some outflow areas. Mine waters are highly reduced, with circumneutral pH, and variable Fe concentrations from 5 to over 100 mg/L. Total alkalinity is about 200 mg/L with a mixed Ca-Na-HCO_3-SO_4 composition in recharge areas. End of flow path waters contain up to 600 mg/L alkalinity, and are Na-SO_4 type waters with higher dissolved solids and metals concentrations. The shift from Ca to Na dominated waters is attributed mainly to cation exchange. Rising head in parts of the aquifer indicates withdrawal from the mine-pool may have to be increased in the future to prevent discharge. Mine-pool quality remains poor and has shown slow improvement in 6 years of monitoring.

Additional Key Words: barrier pillar, leakage, confined aquifer, cation exchange

_____

Introduction

Underground mining in the Pittsburgh coal bed of northern Appalachia has been ongoing for over 200 years. Of the original estimated reserves of about 31 billion tonnes, about 14 billion tonnes remain, and Pittsburgh seam production remains the largest in northern Appalachia (Ruppert et al., 1999). Many of the Pittsburgh seam mines are aerially extensive, covering several thousand Ha, and they frequently adjoin other mines in the same coal bed. When these mines are closed and abandoned, ground-water infiltrates from overlying aquifers, stream leakage and adjacent flooded mines. The flooding process usually occurs over a period of years to a few decades, and flooding may be complete or partial, depending on hydrological setting. Mine water quality ranges from strongly acidic to alkaline, with objectionable concentrations of Fe and SO_4. This paper reports on ground-water flow, storage, and quality characteristics of a fully flooded mine-pool near Fairmont, West Virginia, gathered from five years of monitoring effort.

Background

Geologic Setting

The Pittsburgh coal bed is present over portions of the states of PA, WV, MD and OH, extending over about 28,000 km^2 (McCullogh et al., 1975; Ruppert et al., 1999) as shown in Figure 1. The
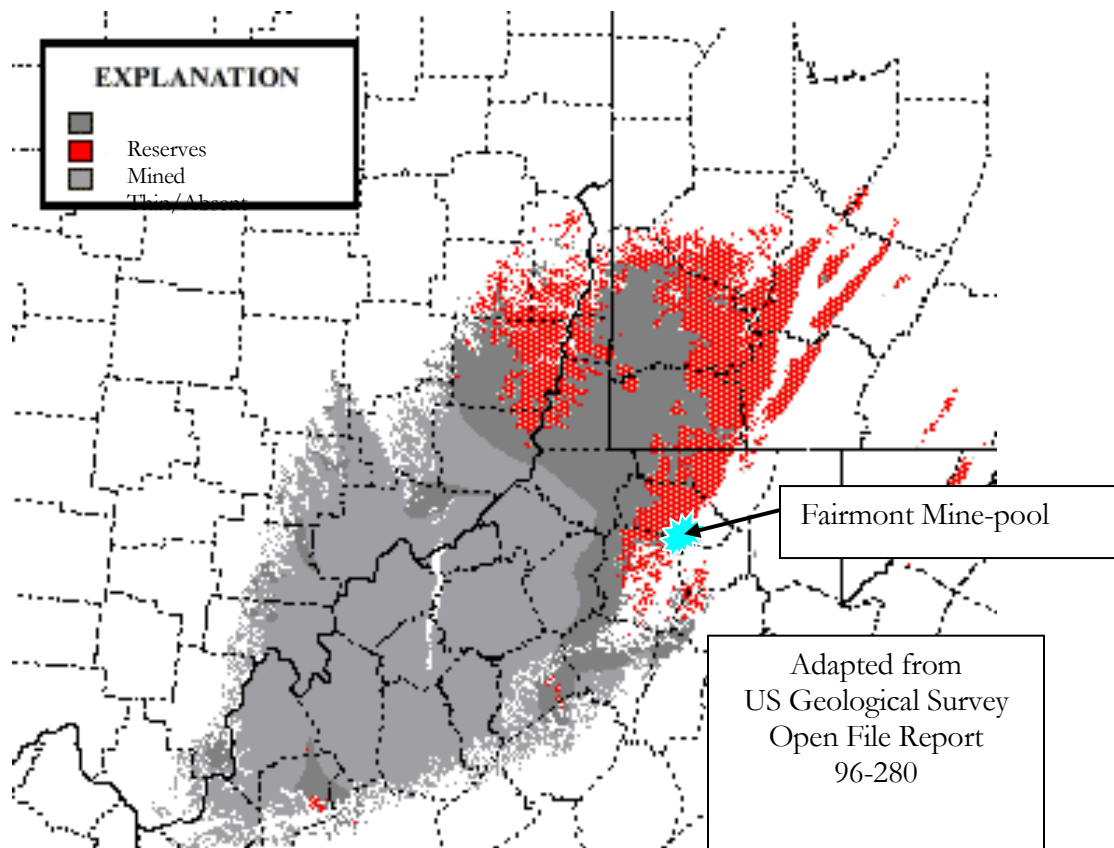
Figure 1. Extent of Pittsburgh coal bed and location of Fairmont mine-pool. (Adapted from Ruppert and Tewalt,1997).

bed is in an elongated basin with the main axis extending southwest to northeast. A series of small anticlines and synclines is superimposed on the main basin structure. Deformation including folding, and regional uplift facilitated erosion of some of the original deposit. Throughout much of the basin, the coal bed is located at depths of 60 to >300 m , but is at or near outcrop along basin margins.

Stratigraphically, the Pittsburgh is located at the base of the Monongahela Group, which ranges from about 70 to 130 meters in thickness (McCullogh et al.; 1975, Berryhill et.al.,1971; Hennen and Reger, 1913). The lower members of the Group include several limestones, calcareous shales and mudstones, interbedded with fine to medium grained sandstones.   The coal bed itself is 2 to 3 m thick and characteristically is divided into several benches (Hennen and Reger, 1913).

Project Setting
A complex of abandoned, fully flooded underground mines, termed the 'Fairmont mine-pool" in this paper, has been monitored by the Office of Surface Mining (OSM) since the mid 1990's. The Fairmont mine-pool is located on the eastern margin of the basin (figure 1) and the rocks dip at a low angle to the northwest toward the center of the basin. This structure results in the Pittsburgh coal cropping out or being present at shallow depths along the West Fork and Monongahela Rivers near Fairmont.   Thus, the rivers and tributaries are potential discharge zones for the mine-pool.

Figure 2 shows the location of principal underground mines comprising the Fairmont mine-pool and several adjacent mines that interact with it. The mine-pool extends over about 10,000 Ha and across several drainage basins. Mines closed at various dates from the 1940's to the 1980's, and were developed mostly by room and pillar methods with retreat mining in some areas. Active underground operations are located further to the northwest and southwest under thicker overburden.   Barrier pillars, ranging in thickness from about 9 to 60 m, separate individual mines. In one location, Mine 38 (figure 2), a barrier pillar is breached, allowing direct hydraulic connection between two mines.

An internal coal company report (Leavitt, 1993) predicted that hydraulic head in parts of the Fairmont mine-pool would increase to potential discharge elevation by the mid 1990's. In 1997, the mining company began withdrawing water from the Fairmont mine-pool at the Dakota mine (figure 2), to prevent a pollutional discharge to surface waters. Water is siphoned over a barrier pillar at estimated rate of about 5700 L/min into the adjacent Jordan mine complex. From there, mine water is routed to a centralized treatment facility. OSM, on behalf of the state of West Virginia, began monitoring water levels in the Fairmont mine-pool in 1997 to determine if the siphon withdrawal would maintain mine-pool head below discharge elevation.   West Virginia University and a mining company also began measuring water levels, and monitoring continues to the present.
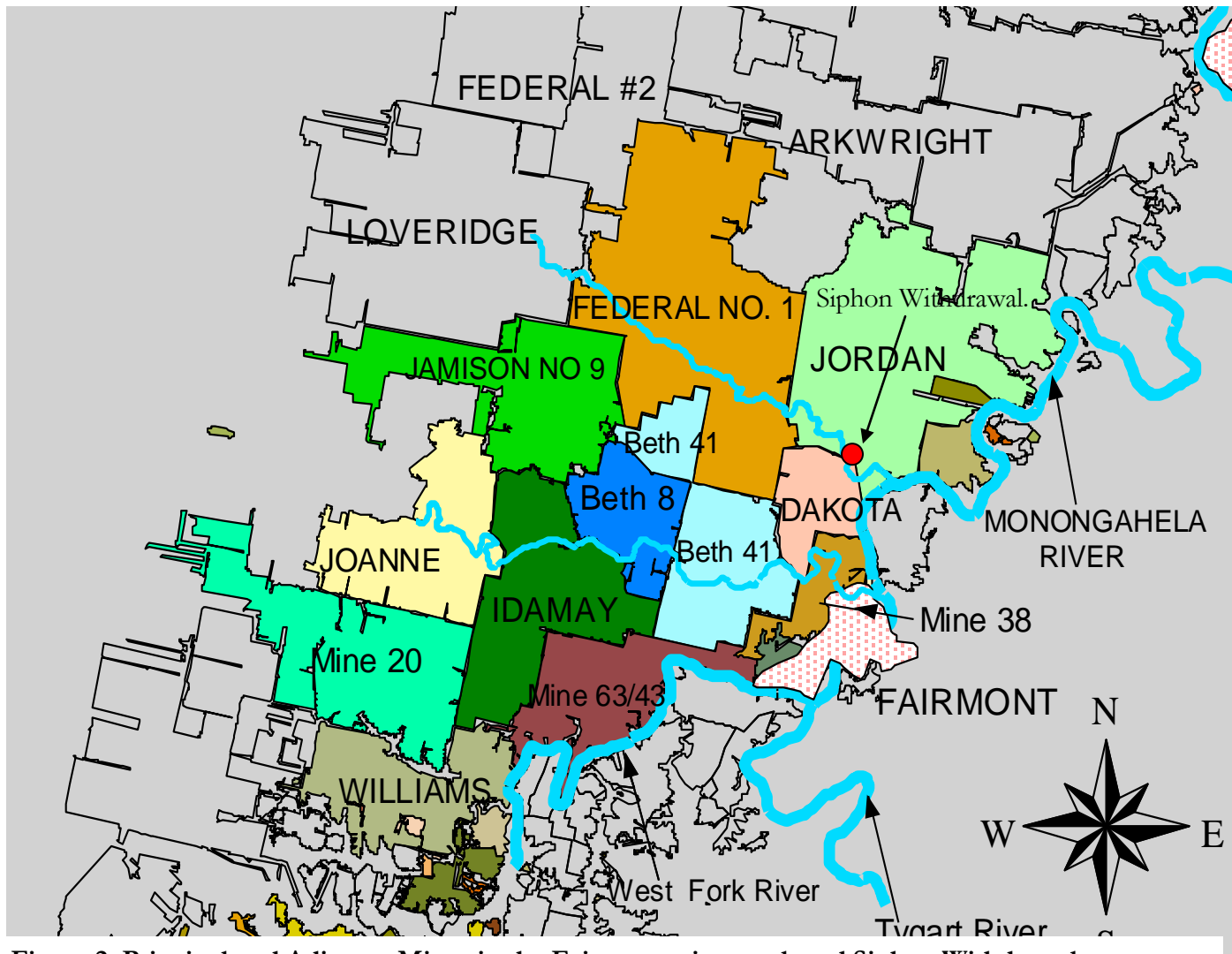
Figure 2. Principal and Adjacent Mines in the Fairmont mine-pool, and Siphon Withdrawal.

Methodology

OSM began collecting water levels on a monthly basis at six existing locations in the Fairmont mine-pool. In 1999, OSM drilled 4 additional monitoring wells to provide data from specific mines where no monitoring access had been available. Another 3 wells were drilled in 2002 to provide additional information in the western and southern parts of the mine-pool. All wells were drilled using air rotary methods, with a screened interval placed at mine elevation. Several boreholes were examined with a down-hole video camera to determine the degree of fracturing and collapse in the overburden and at mine level. Pressure transducers were installed in five OSM wells and programmed to record water level and temperature on an hourly basis. Wells without transducers are read at a monthly frequency. Weather data including hourly precipitation, air temperature, and barometric pressure were obtained for weather stations at Clarksburg and Morgantown, WV, each located within 15 to 20 km of the project area. Daily summary weather readings were also obtained for a station at Mannington, WV, located within the project area.

Water quality samples have been collected from selected mine-pool wells at semiannual to annual intervals, and more frequently at the Dakota mine siphon. Wells were purged until stable readings were obtained for pH, temperature and specific conductance. Collected samples were analyzed for Alkalinity, dissolved Fe, Al, Mn, Ca, Mg, Na, K, SO_4, Cl, As, Ba, Be, Cd, Co, Cr, Cu, Ni, Pb, Sb, Se, Zn. Field parameters include pH, Eh, temperature and specific conductance and total acidity is calculated from dissolved metals and pH. Selected samples have also been analyzed for Fe(II) and S(-II). A simple presence/absence biological reactivity test for sulfate reducing bacteria has been run on selected wells.

Geochemical calculations were performed using PHREEQC (Parkhurst and Appelo, 1999) and statistical calculations were run in Statgraphics for Windows ver 4.1.

Mine Pool Flow

The Fairmont mine-pool includes at least eight large individual mines that respond to recharge, discharge and other stresses in unison. From south to north (figure 2), they include Williams, Mine 63/43, Idamay, Beth 41, Beth 8, Mine 38, Dakota, and Federal 1. Head in other mines to the north, west, and south is less than the Fairmont mine-pool. In general, these other mines receive leakage or outflow from the Fairmont mine-pool. Head is increasing, however, in the Joanne mine to west, and this complex may become a more active participant in the Fairmont mine-pool in the future.

Inferred ground-water flow directions are shown in Figure 3, based on average head measurements compiled for the year 2002. The flow pattern is complex, and results from barrier pillars maintaining head differences between mines, and different mine closure dates and flooding records. The general direction of flow within the pool is from south to north towards the Dakota siphon. Much of the flow through the Fairmont mine-pool originates from the Williams and Idamay mines, and is apparently funneled through Mine 43/63 and Mine 38 (Figure 3) adjacent to the West Fork and Monongahela rivers. The Beth 41/8 mines in the center
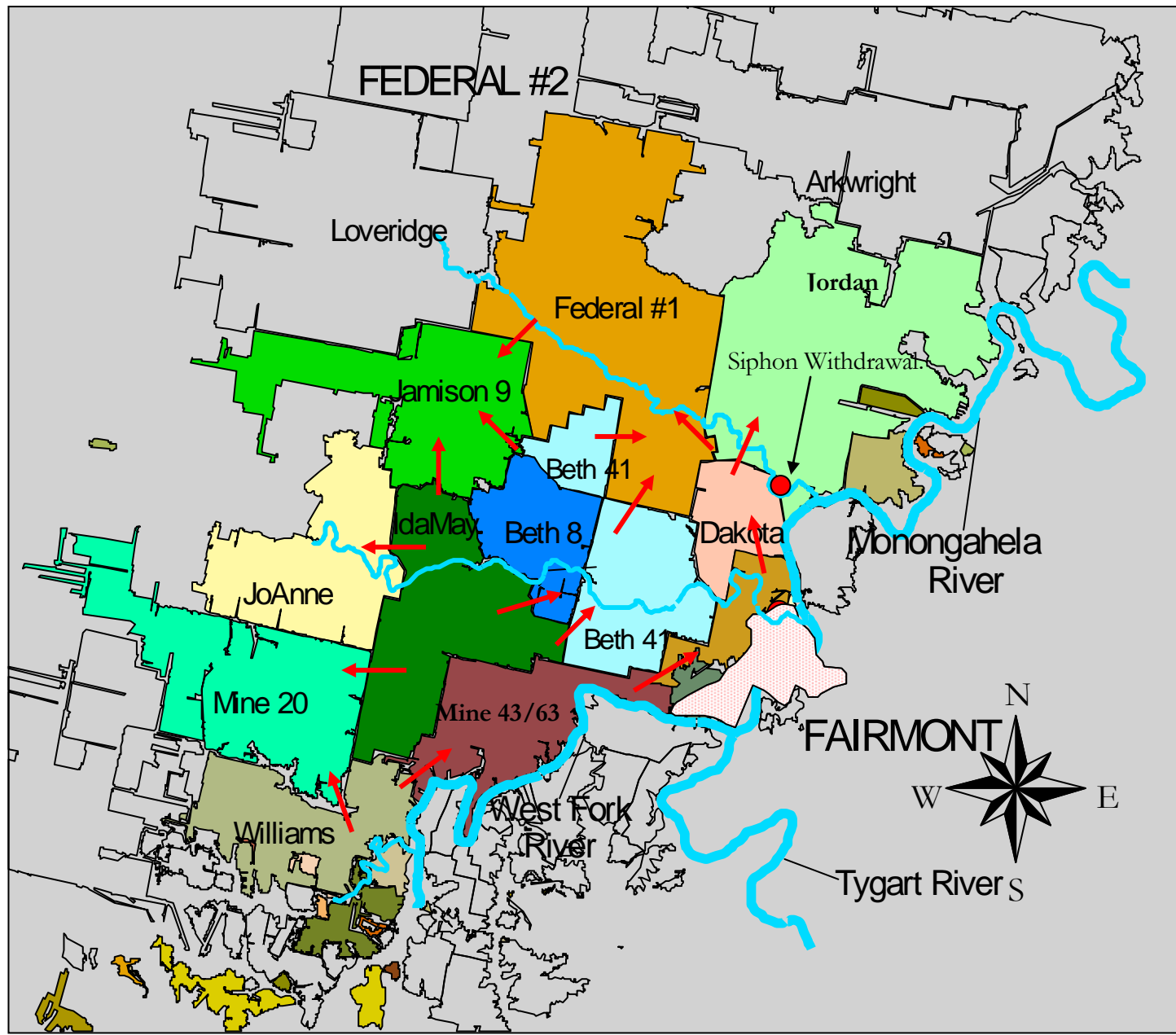
Figure 3 Generalized Ground-water Flow Pattern in the Fairmont mine-pool. Arrows indicate inferred flow direction based on head measurements and mine conditions.

of the mine-pool currently are ground-water sinks; that is water flows into it from surrounding mines on the east, south and southwest, and it does not contribute flow to the siphon. However, head is increasing and should equal or exceed the siphon within 3 to 5 years. At that time, the Beth 41/8 mines will cease to be a sink for the mine-pool and will instead contribute to outflow.

Federal #1 constitutes the northwest part of the Fairmont mine pool. Its' potentiometric head is about six to eight m lower than the north end of Beth 41/8 which adjoin it, and about 10m less than the Dakota siphon. Leakage from Beth 41/8 to Federal #1 is probably occurring. Federal #1 is a second major ground-water sink for the mine-pool. Both the Beth mines complex and Federal #1 have potentiometric head exceeding the Jamison 9 mine to the west, and are leaking into it.

Mine 20 and Jamison 9 to the southwest and northwest of the Fairmont mine-pool are pumped to protect nearby active mining. Large potentiometric head differences, on the order of 30 to 60 m or more exist across the barrier pillars separating these mines from the Fairmont mine-pool. Leakage across the barrier pillars is another outflow for the mine-pool.

Mine-pool Response to Dakota Siphon Withdrawal
The Dakota siphon began operating in April, 1997 and runs for about 10 months during the year. Figure 4 shows water levels at the siphon; mine 38 located about 2.5 km distant, and the Williams mine well, which is about 18 km from the siphon. The mine-pool was drawn down 4
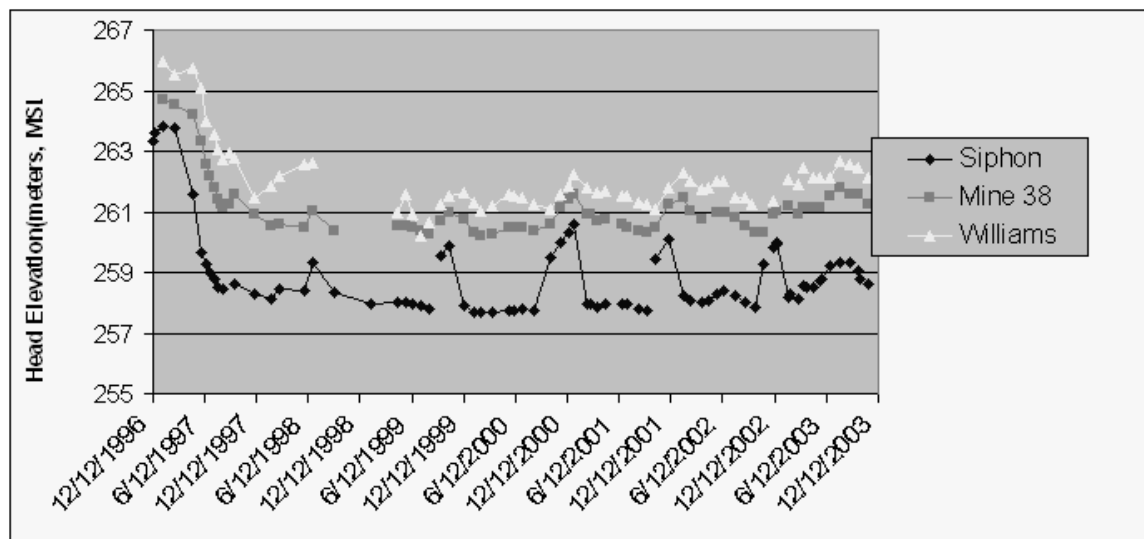
Figure 4. Water Levels at Dakota Siphon, Mine 38 and Williams Mine, 1997-2003.

to 5 meters once the siphon began operating, even at the Williams mine at the opposite end of the mine-pool. The response is indicative of a confined aquifer. The drawdown is maintaining the mine-pool below the unregulated discharge elevation, preventing a pollutional discharge to surface waters. Figure 4 also shows that when the siphon is shutoff, head begins to increase at the siphon, and that recovery is mirrored at Mine 38 and Williams. After several months, when

withdrawal resumes, the mine-pool is drawn down again. The siphon will likely have to continue operation for the foreseeable term to maintain the mine-pool below discharge elevation.

Mine-pool Conductance Properties
Water levels have been measured at three locations within the Beth 41/8 complex. Head at the three locations differs by less than two m at wells separated by several km. The very low hydraulic gradient existing within the mine complex suggests that individual mines have relatively high internal hydraulic conductivity, and head differences between mines are controlled mostly by barrier pillars. We have observed similar conditions of very low gradient between three wells of less than 1 m difference over ~ 2 km in a single mine in Pennsylvania, with simultaneous head difference of 20 m across a barrier pillar (authors unpublished data).

We estimated barrier pillar leakage for one common boundary between the Beth 41/8 complex and Federal 1 mines (figure 3) from water level data, mine map information and horizontal hydraulic conductivity (K) data of McCoy (2002). He estimated effective hydraulic conductivity from pumping records and water level data for barrier pillars in two mines on the western side of the Fairmont mine-pool. McCoy reported a range of barrier pillar hydraulic conductivity of 0.03 to 0.15 m/day, and an average of 0.091 m/day. Using McCoy's average barrier pillar K, and an average head difference of about 7 m, we estimate that about 208 L/min flows through the barrier between the Beth Mines complex to Federal 1, using a Darcy's law calculation . This barrier is just one a number of mine boundaries within the Fairmont mine-pool where flow across barriers must be taking place. The total quantity of water circulating between mines is significant from the standpoint of managing the mine-pool.

Mine-pool Storage Properties
Ground-water storage in the Fairmont mine-pool includes water in the pore space of open mine voids and collapsed and fractured overburden, as well as an elastic storage component. Figure 4 is a plot of hourly head versus barometric pressure for a well in the Beth 41/8 complex during October, 2002. The two parameters are near mirror images of each other, a behavior that is characteristic of confined aquifers. The barometric efficiency (BE) of a well can be used to estimate specific storage S_s, and porosity n, of the aquifer (Domenico and Schwartz (1990) from the relationships:

$$BE = (y_w*dh)/dP_a \qquad (1)$$

where y_w is the unit weight of water; dh is the head change; and dP_a is the change in atmospheric pressure.

$$TE = 1 - BE \qquad (2)$$

$$TE = (p_w *g*B_p)/ S_s \qquad (3)$$

where p_w is fluid density, g is the gravitational acceleration constant; and B_p is compressibility of the aquifer matrix, either measured or estimated. Finally, porosity, n is estimated from:

$$BE = (p_wgnB_w)/S_s \qquad (4)$$

where S_s, p_w and g are as previously defined, and B_w is fluid compressibility.
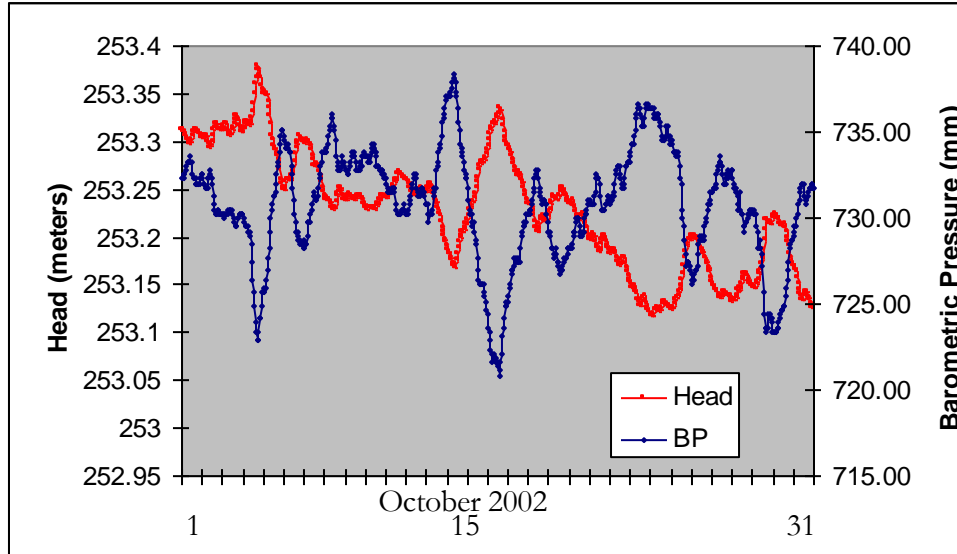
Figure 4. Hourly mine-pool head versus barometric pressure,
Beth41/8 mine complex, October, 2002.

Portions of the record were selected where a change in barometric pressure persisted for at least 18 to 24 hours, such as occurred in mid October in Figure 4. Underlying trends of rising or falling head due other factors such as seasonal variation were removed using regression methods similar to those described by Davis and Rasmussen (1993). Specific storage and porosity then were calculated using relationships 1 to 4. The process was applied to 3 to 5 different segments of the record to determine if reproducible results were obtained. For individual wells, estimated values were generally within 25% relative difference.

Specific storage, S_s was estimated to be on the order of 1.5 to 2.5 x 10^{-6}/m, and porosity estimates ranged from about 12 to 35% at three different wells. Most porosity values fell between 15 and 25%. These wells are completed in partially caved zones and crushed coal pillars, based on drilling observations. Since coal recovery typically ranged from at least 50 to upwards of 80%, these porosity data suggest the mine-pool aquifer thickness exceeds the coal thickness, perhaps by 2x to 6x. On this basis, storage coefficient, S, for the aquifer, is estimated to range from about $6x10^{-6}$ to $2x10^{-5}$. Crouch et al. (1980), working, in a mine-pool aquifer in Ohio, derived a storage coefficient of about 3 x 10^{-4} from a 29 day pump test after adjusting their hydrographs for barometric and seasonal effects. They concluded that pumped water was derived mostly from induced recharge and intercepted discharge. The apparent low storage coefficient for the Fairmont mine-pool results in relatively larger drawdown when it is pumped (siphoned).

Mine-Pool Water Quality

Mine-pool water quality shows significant spatial variability. Table 1 includes analyses from wells located in a recharge area (mine 38 well), intermediate flow-path (Mine 63) and end of flow-path for the mine-pool (Dakota siphon). A fourth sample, Beth 42 overburden, is indicative of water quality in overlying aquifers that infiltrate and recharge the mine-pool. The mine-pool has circumneutral pH at each well, in each part of the flow system. Although the initial charge of

Table 1. Representative Water Quality of Fairmont Mine-pool[1]

Site	pH (field)	Alkalinity	TDS	Eh (millivolts)	Fe	Mn	Ca	Mg	Na	Cl	SO_4
Mine 38	7.32	179.8	548	-94	3.44	0.53	60.7	14.1	105.7	34.1	207
Mine 63	7.31	589.6	3301	-130	33.9	0.64	158.4	33.1	853.4	44.2	1697
Dakota Siphon	7.20	568.7	5194	-159	134.8	1.63	250.6	89.7	1254	119.9	2812
Beth 41 Overburden	8.57	263	454	-146	0.04	0.016	21.0	5.0	138.3	52.1	47.9

(1) pH in S.U., Alkalinity in mg/L $CaCO_3$, Eh in millivolts, all others in mg/L. TDS= total dissolved Solids. Mine-pool samples collected 12/17/2002. Overburden sample collected 4/8/99.

mine water in Pittsburgh seam mines is frequently acidic, complete flooding seems to curtail pyrite oxidation and can bring about a shift of 3 to 5 S.U. in pH. Watzlaf (1992), in lab studies found acid production was curtailed in saturated pyritic mine wastes, but continued in unsaturated materials. Donavan et al. (1999) report a Pittsburgh seam mine-pool where pH shifted from about 4 to 6.5 after passage of about one pool volume. Winters (2000) describes a Pittsburgh seam mine-pool where acidic waters are present in the unsaturated up-dip end of the mine complex, shifting to circumneutral pH with titrateable   alkalinity in the down-dip flooded end. Measured Eh values in the Fairmont mine-pool indicate moderate to strongly reducing conditions prevail, even in the recharge area at Mine 38. A reduced environment is consistent with inhibiting further pyrite oxidation once the mine-pool is fully flooded.

There is about a tenfold increase in dissolved solids between recharge and discharge locations in Table 1, and about a threefold increase in alkalinity. During active mining, coal, roof and floor rock were exposed to humid oxidizing conditions, an ideal environment for pyrite oxidation and subsequent dissolution of other minerals, and formation of hydroxysulfates, oxides and other weathering products.   Nuhfer (1967) reported finding hydroxysulfate minerals such as melanterite ($FeSO_4$* 7 H_2O) and gypsum on exposed coal. Other metal sulfates including copiapite and halotrichite (Jambor et.al., 2000) have also been identified in coal mines. These minerals are moderately soluble, and can be expected to dissolve in the saturated mine-pool, yielding dissolved Fe, SO_4^{2-}, Ca^{2+}, $Mg^{2+,}$ H^+ and other constituents.

Total alkalinities approach 600 mg/L in the intermediate flowpath and discharge locations. These are among the highest values we have seen for nonsaline ground-waters circulating within 100 meters of the surface of upper Pennsylvanian rocks. The large alkalinity concentrations are likely due to a combination of carbonate dissolution and cation exchange. Limestones and calcareous rocks are abundant in the lower section of the Monongahela group (Hennen and Reger, 1913). The mine-pool aquifer consists not only of the residual coal, but also a zone of collapsed and severely fractured rock, which can range from 6x to 10x coal thickness (Kendorski, 1993). Rocks containing as little as 5 to 10 % carbonate would be a large reservoir for generating solution alkalinity. Exchange of adsorbed Na for solution Ca and Mg would favor further dissolution of carbonates and production of alkalinity. Geochemical modeling has shown that carbonate dissolution and cation exchange are possible explanations for the observed changes in mine-pool composition (Perry, 2001). Sulfate reduction could also generate alkalinity. Sulfate reducing bacteria have been detected in the mine-pool along with trace levels of dissolved sulfide, ranging up to about 0.5 mg/L.

Rocks of the Monongahela group commonly contain the clay minerals illite, chlorite and kaolinite (Berryhill et al., 1971, Dulong et al., 2001). Reported analyses show clay mineral content of mudstones and shales can easily exceed 20%. Cation exchange capacity (CEC) of kaolinite ranges from 3 to 15 meq/100g, and 10 to 40 meq/100g for illite and chlorite (Langmuir, 1997). For the clay mineral kaolinite, the lyotropic series for adsorption affinity is: Na < H < K< Ca= Mg. Calcium and Mg are more strongly adsorbed to exchange sites than Na. Exchange coefficients for Ca and Mg, with respect to Na, are about 0.40 and 0.50, following Gaines-Thompson convention (Appelo and Postma, 1993). Thus, desorption of Na and adsorption of Ca and Mg should be favored in these waters.

Even assuming a conservative CEC of 5 meq/100g of rock, a large quantity of exchange sites are theoretically available in the aquifer along a flow path covering kms to tens of km, with a residence time of years to decades.

Composition of waters also varies by location in the flow system. Recharge water at Mine 38 is a mixed Na-Ca-HCO_3–SO_4 type; Mine 63 at an intermediate flowpath position is a Na- SO_4 - HCO_3 type water, while the Dakota siphon at the end of flowpath is a Na-SO_4 water. Mine-pool composition becomes progressively enriched in Na and SO_4 as water moves from recharge to discharge. The changes are consistent with Na exchange and dissolution of sulfate minerals. The overburden aquifer is a Na-HCO_3 water. Its' composition is similar to ground-water in Monongahela group rocks summarized by Hobba (1984) and Stoner et al. 1987.

Table 2 shows mineral saturation indices for mine-pool waters calculated using PHREEQC (Parkhurst and Appelo, 1999). Recharge waters (mine 38) are under saturated for both calcite and dolomite, indicating carbonates should dissolve. Intermediate and end of flowpath waters are slightly over saturated for calcite and dolomite, suggesting that as water flows from recharge areas through the mine-pool, carbonates are dissolving. Mine waters are 3 to 5 orders under saturated for melanterite, indicating that if present initially, it is dissolving. Gypsum is also under

saturated, but approaches equilibrium at end of flow path, suggesting additional mineral dissolution in the mine-pool. Amorphous or poorly crystalline $Fe(OH)_3$ is several orders of

Table 2 Mineral Saturation Indices for mine-pool waters.[1]

Site	pCO2	Calcite	Dolomite	Gypsum	Goethite	$Fe(OH)_3$(am)	Melanterite
Mine 38	-1.82	-0.52	-1.49	-1.40	2.29	-3.17	-5.09
Mine 63	-1.61	0.30	0.10	-0.54	2.93	-2.49	-3.68
Dakota Siphon	-1.54	0.27	0.28	-0.29	2.77	-2.70	-3.01

(1)Saturation Index calculated as log (Ion Activity Product/Equilibrium constant)

magnitude under saturated, indicating that if present, it can dissolve. Goethite is, however; over saturated for all waters, suggesting that some Fe could be removed from solution by formation of FeOOH. It has not been possible to collect sediments from the mine-pool for mineralogical analyses to verify the presence of specific minerals, however, the presence of each mineral in table 2 is considered probable.

Iron is the chief pollutant of concern in the mine-pool because of deleterious effects on biota, aesthetics, and consumptive use at relatively low concentrations. Fe concentrations at the Dakota siphon are about 40x greater than the recharge area at Mine 38. Periodic sampling of these wells and others in the mine-pool have shown that Fe exhibits a high degree of spatial variability, and that variation is maintained through time. Other constituent concentrations also vary spatially, but generally to a lesser degree. Each well, however, tends to show a characteristic composition through time suggesting that a local equilibrium condition exists.

Figures 5 and 6 show Fe and SO_4 concentrations, and a moving average based trend, for the six year period of 1997 to 2003. Both parameters, especially Fe, show some scatter in raw data. Fe concentrations increased for about the first year of mine-pool withdrawal. Both parameters then began a gradual, somewhat irregular decline continuing to the present. First order decay functions were fit to the trend data for Fe and SO_4 from late 1998 to present using the following:

$$C_t = C_0 * exp^{-kt} \qquad (5)$$

where C_t is concentration at time t, C_0 is concentration at time zero, k is the decay constant in $time^{-1}$ and t is elapsed time. The decay constant was derived from a plot of $ln(C_t/ C_0)$ versus t, and estimating the slope with simple linear regression. Statistically significant results were obtained, however, the fitted relationships are weak to moderate (r=0.48 and 0.67 for Fe and SO_4, respectively) correlations, due to short term variation. Some of the observed variation seem to be seasonal. Half life estimates are about 12 years for Fe and 14 years for SO_4. For the period of record, sulfate concentrations have declined from about 4,000 to 3,000 mg/L and Fe from about 150 to around 100 mg/L. Mine-pool quality is improving, but slowly.
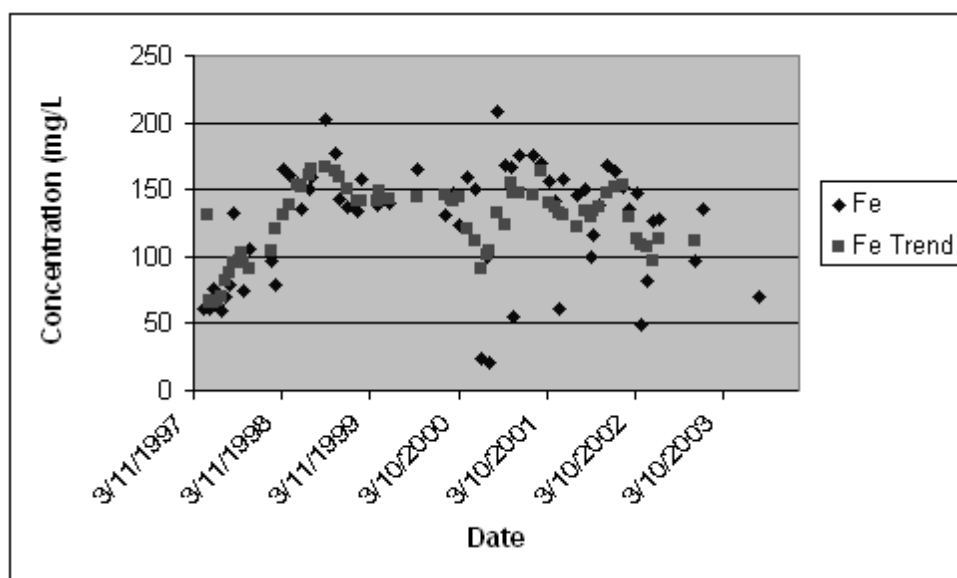
Figure 5. Raw and trend Fe concentrations, Dakota mine siphon.
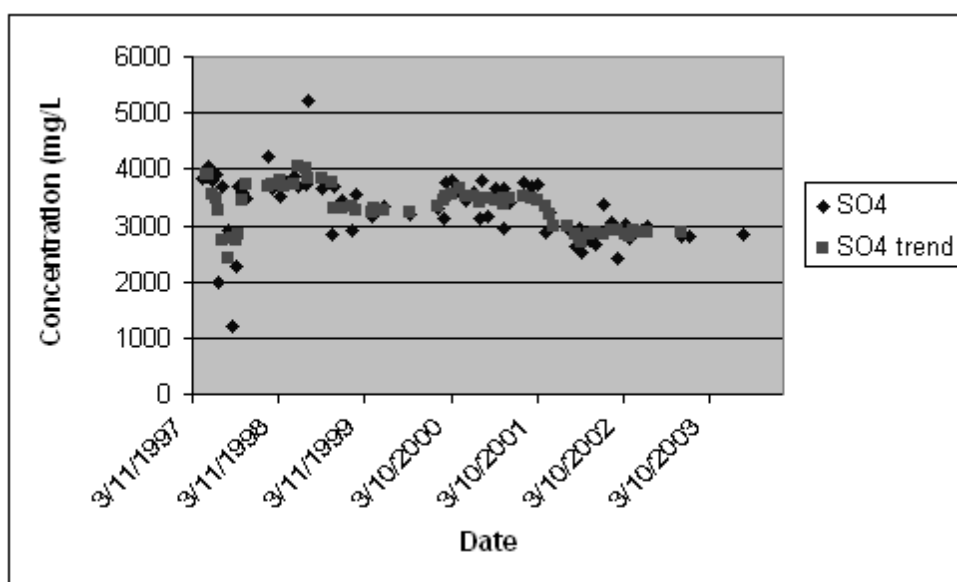
Figure 6. Raw and trend SO4 concentrations, Dakota siphon

Conclusions

The Fairmont mine-pool is a group of hydraulically connected and fully flooded abandoned underground mines. The mine-pool responds to stresses, such as pumping, as a confined aquifer. Individual mines have relatively high internal conductance, with small hydraulic gradients. Most head difference occurs across barrier pillars, and the location and orientation of barrier pillars, and flooding history result in complex flow patterns. Recharge to the mine-pool is offset by withdrawal from the Dakota siphon, leakage to adjacent mines and outflow to unmined areas.

The Dakota siphon has maintained the mine-pool below surface discharge elevation for over 6 years, and influences portions of the mine-pool located more than 15 km away. However the mine-pool has not yet reached a final steady state, as head continues to increase in some mines in and adjacent to the mine-pool. The rate of withdrawal from the siphon will likely need to be increased in the future to maintain the overall mine-pool below discharge elevation. Head levels would increase to discharge elevation within a short period, if the siphon withdrawal was stopped.

Mine-pool quality exhibits both spatial and temporal variation, especially for soluble Fe. Mineralization is least in inferred recharge areas, and increases as water moves through the flow system. Water composition evolves from mixed in recharge areas, to Na-SO_4 type waters at the end of flow path with high concentrations of alkalinity. The changes are consistent with dissolution of soluble sulfate minerals and cation exchange.

Complete flooding yields a reduced environment that seems to prevent further sulfide oxidation. The mine-pool is now undergoing a slow flushing of soluble weathering products. Discharge quality at the siphon has shown some improvement through 6 years of monitoring, but remains unacceptable without treatment.

The Fairmont mine-pool will require continuing management for the foreseeable term to prevent a pollutional discharge.

Literature Cited

Appelo, C.A.J., and D. Postma, 1993, "Geochemistry, groundwater and pollution", A.A. Balkema, Rotterdam, 536 pps.

Berryhill, H.L., Schweinfurth, S.P., and B.H. Kent, 1971, Coal-Bearing Upper Pennsylvanian and Lower Permian Rocks, Washington Area, Pennsylvania, U.S. Geological Survey Professional paper 621, 47 pps.

Crouch, T. M., Collins H.R., and J.O. Helgesen, 1980, Abandoned Subsurface Coal Mines as A Source of Water for Coal Conversion in Eastern Ohio. Report of Investigations 118, Ohio Dept of Natural Resources, Division of Geological Survey.

Davis, D.R. , and T.C. Rasmussen, 1993, A Comparison of Linear Regression With Clark's Method for Estimating Barometric Efficiency of Confined Aquifers, Water Resources Research, Vol. 29,No.6, pps1849-1854.

Domenico, P.A., and F.W. Schwartz, 1990, Physical And Chemical Hydrogeology, 824 pps.

Donovan, J. J., Fletcher, J., Strager, M. and E. Werner, 1999, Hydrogeological and Geochemical Response to Mine Flooding in the Pittsburgh Coal Basin, Southern Monongahela River Basin, West Virginia University, National Mined Land Reclamation Center Project WV-132, Final report to U.S. Environmental Protection Agency,111 pps.

Dulong, F.T, Fedorko, N., Renton, J.J., and C. B. Cecil, "Chemical And Mineralogical Analyses of Coal-Bearing Strata In The Appalachian Basin", U.S. Geological Survey Open File Report 02-489.

Hennen, R.V and D.B. Reger, 1913, West Virginia Geological Survey County Reports, Marion, Monongalia and Taylor counties, Wheeling News Litho Co., Wheeling, WV.

Hobba, W.A. 1984, Ground-Water Hydrology of the Monongahela River Basin. U.S. Geological Survey in cooperation with the West Virginia Dept. of Natural Resources.

Jambor, J.L., Nordstrom, D.K. and C.N. Alpers, 2000, Metal-sulfate salts From Sulfide Mineral Oxidation, In Sulfate Minerals Crystallography, Geochemistry and Environmental Significance, Reviews in Mineralogy and Geochemistry Vol. 40, p305-350.

Kendorski, F.S., 1993, Effect of High Extraction Mining on Surface and Ground Waters, In Proceedings 12th Conference on Ground Control in Mining, West Virginia University, Morgantown, WV.

Langmuir, D., 1997, Aqueous Environmental Geochemistry, Prentice Hall Publishers, 600 pps.

Leavitt, B.R., 1993, Discharge Potential of the Fairmont Mine-pool, Unpublished Internal Report for Consol Inc.

McCoy, K.J. 2002, Estimation of Vertical Infiltration Into Deep Pittsburgh Coal Mines of WV-PA: A Fluid Mass Balance Approach, Unpublished Thesis, West Virginia University, Dept of Geology and Geography,151 pps.

McCullogh, C. M., Diamond, W. P., Bench, B. M. and M. Duel. 1975. Selected Geologic Factors Affecting Mining of the Pittsburgh Coal Bed. Report of Investigations 8093. U.S. Bureau of Mines.

Nuhfer, E., 1967. Efflorescent Minerals Associated With Coal. Unpublished Thesis, Dept of Geology and Geography, West Virginia University.

Parkhurst, D. L., and C. A. J. Appelo, 1999. User's Guide to PHREEQC (Version 2) - A Computer Program For Speciation, Batch-Reaction, One-Dimensional Transport, and Inverse Geochemical Calculations. U.S. Geological Survey Water Resources Investigation Report 99-4259.

Perry, E. F., 2001, Modeling Rock–Water Interactions in Flooded Underground Coal Mines, Northern Appalachian Basin, Geochemistry: Exploration, Environment, Analysis, Vol. 1, 2001, pp. 61–70.

Ruppert, L. F., Tewalt, S.J. , and L. Bragg, 1997, Map Showing Areal Extent of Pittsburgh Coal Bed and Horizon and Mined areas of the Pittsburgh coal bed in Pennsylvania, Ohio, West Virginia and Maryland, digitally compiled by Tully, J., Pierce, J., Weller, A., and J. Yarnel, U.S. Geological Survey Open File Report 96-280.

Ruppert, L. F., Tewalt, S. J., Bragg, L. J. and R. N. Wallack, 1999. A Digital Resource Model of the Upper Pennsylvanian Pittsburgh Coal Bed, Monongahela Group, Northern Appalachian Basin Coal Region, USA, International Journal of Coal Geology, 41, 3–24.

Stoner, J. D., Williams, D. R., Buckwalter, T. E., Felbinger, J. K. and K. L. Pattison, 1987. Water Resources and the Effects of Coal Mining, Greene County, Pennsylvania, Pennsylvania Geological Survey Water Resources Report 63.

Watzlaf, G. R., 1992. Pyrite oxidation in saturated and unsaturated coal waste, In Proceedings of the 1992 National Meeting of the American Society for Surface Mining and Reclamation, Duluth, MN, 191-205.

Winters, W.R., 2000, Hydrologic and Geochemical Evolution of a Bituminous Coal Basin: Irwin Syncline, Westmoreland County, Pennsylvania, Thesis, University of Pittsburgh, Geology and Planetary Science Dept.

Appendix D

WATER QUALITY TRENDS IN A FLOODED 35 YEAR OLD MINE-POOL

WATER QUALITY TRENDS IN A FLOODED
35 YEAR OLD MINE-POOL[1]

Eric F. Perry[2], Jay W. Hawkins, Mike Dunn, Robert S. Evans, and John K. Felbinger

Abstract: Thirty five years of water quality data from a pumped, mostly flooded, mine-pool were examined for trends in mine drainage parameters. At the start of pumping in 1970, the Lancashire 15 mine-pool discharged acidic water with average iron (Fe) concentration exceeding 900 mg/L. Average sulfate (SO_4) concentration was about 3700 mg/L. After 14 years of pumping about 21 mine-pool volumes, Fe and SO_4 were about 20% of their initial concentrations. Alkalinity had increased from less than 50 to about 120 mg/L, and pH was about 6.0. In 1986, an overlying mine complex closed and flooded. Its' waters have low concentrations of Fe and SO_4, and are hydraulically connected to the Lancashire 15 mine-pool. The combined mine-pool waters reduced Fe by about 50% in Lancashire 15. Since 1986, Fe and SO_4 concentrations have continued a slow, irregular decline at the rate of 1 to 2 mg/L/yr for Fe and about 10 to 15 mg/L/yr for SO_4. Short term fluctuations due to seasonal and pump rate variations occur, but long term concentration trends can be described with curvilinear models.

The Lancashire 15 discharge is sodium-sulfate ($Na-SO_4$) type water. Geochemical calculations show that cation exchange of calcium (Ca) for Na is a feasible explanation for the observed water composition. Mixing calculations show that mine-pool composition can be explained by cation exchange; continuing dissolution of iron and sulfur bearing minerals, iron oxyhydroxide formation and about 80% of recharge as leakage from adjacent and overlying mines, and 20% recharge from unmined strata.

The Lancashire 15 mine-pool quality has improved significantly since closure and flooding. After leaching an estimated 55 pool volumes, Fe concentrations are about 5% of original values, and the waters are net alkaline. Continued mineral dissolution, and inefficient leaching due to dispersion and short circuiting, are likely responsible for current water quality conditions.

Additional Key Words: acid mine drainage, mineral solubility, pyrite, Eh

---

[2] Eric F. Perry, Hydrologist, Office of Surface Mining, 3 Parkway Center, Pittsburgh, PA,15220, email eperry@osmre.gov (will present paper), Jay Hawkins, Robert Evans, and John Felbinger are Hydrologists; Mike Dunn is a Geologist, all at Office of Surface Mining, Pittsburgh, PA,15220.

Introduction

Drainage from closed underground coal mines are a significant source of water pollution in northern Appalachia and elsewhere (Kleinmann et al., 2000; Younger, 1997). Mine-pool quality is controlled by geochemistry of the immediate roof and floor rock, residual coal, composition of recharge water, and extent of flooding of the mineworks. Mine-pool quality changes after closure with the poorest water quality discharged in the initial flush, followed by a gradual, (i.e. years to decades) improvement in composition. Skousen et al. (2004) reported that iron concentration had decreased an average of 80% in 44 free draining underground mine discharges over a 30 year period. Wood et al. (1999) concluded that pollution from closed underground coal mines in Scotland was most severe in the first few decades, and that iron concentrations would decline to 30 mg/L or less within 40 years. The final chemical composition of initially acidic, highly polluted mine-pools is uncertain after early flushing. In the long term, these mine-pools may also be important ground-water resources, because they are frequently transmissive enough to sustain relatively large yields when pumped (Donovan et al., 2004; Perry and Hawkins, 2004).

In this paper we describe water quality trends and geochemical processes for iron and sulfate in a 35 year old mine-pool, Lancashire 15, that is about 79% flooded (approximately 4690 Ha). The physical hydrogeology is detailed in a companion paper (Hawkins et al., 2005) and information on pool volume and storage are used to interpret observed chemical trends. The mine-pool has one principal pumped discharge that yields over 24,000 L/min and has been sampled since closure and initial flooding.

Geologic and Hydrogeologic Setting

The Lancashire 15 (L-15) mine-pool is located in Cambria County, Pennsylvania and is largely contained within an enclosed basin defined by the Barnesboro syncline, and Nolo anticline on the west and Laurel Hill anticline to the east (fig. 1). The axes of the syncline and anticlines are oriented about N 30˚ East, and form an elongated basin about 24 km long. This geologic structure influences extent of flooding and the flow direction of water in the mine-pool. The L-15 mine-pool is pumped from the Duman plant at the low point of the basin (fig. 1). The main L-15 mine-pool is in the Lower Kittanning coal bed, and is partially overlain by a second set of flooded mine works in the Lower Freeport coal bed. The vertical interval between coals is around 50 m. The two mine-pools are hydraulically connected as shown by pumping and other data (Hawkins et al., 2005). Mine works located near the crest of the two anticlines are not fully flooded, and water in these areas flows down-dip to recharge the main pool. The presence or absence of complete flooding also influences water chemistry. Unflooded or free draining areas are more likely to undergo continuing pyrite oxidation and leaching and produce acid drainage, while fully flooded mineworks may yield water with circumneutral pH and net alkaline conditions.

Figure 1. L-15 Mine-pool Flow Paths and Geologic Structure.
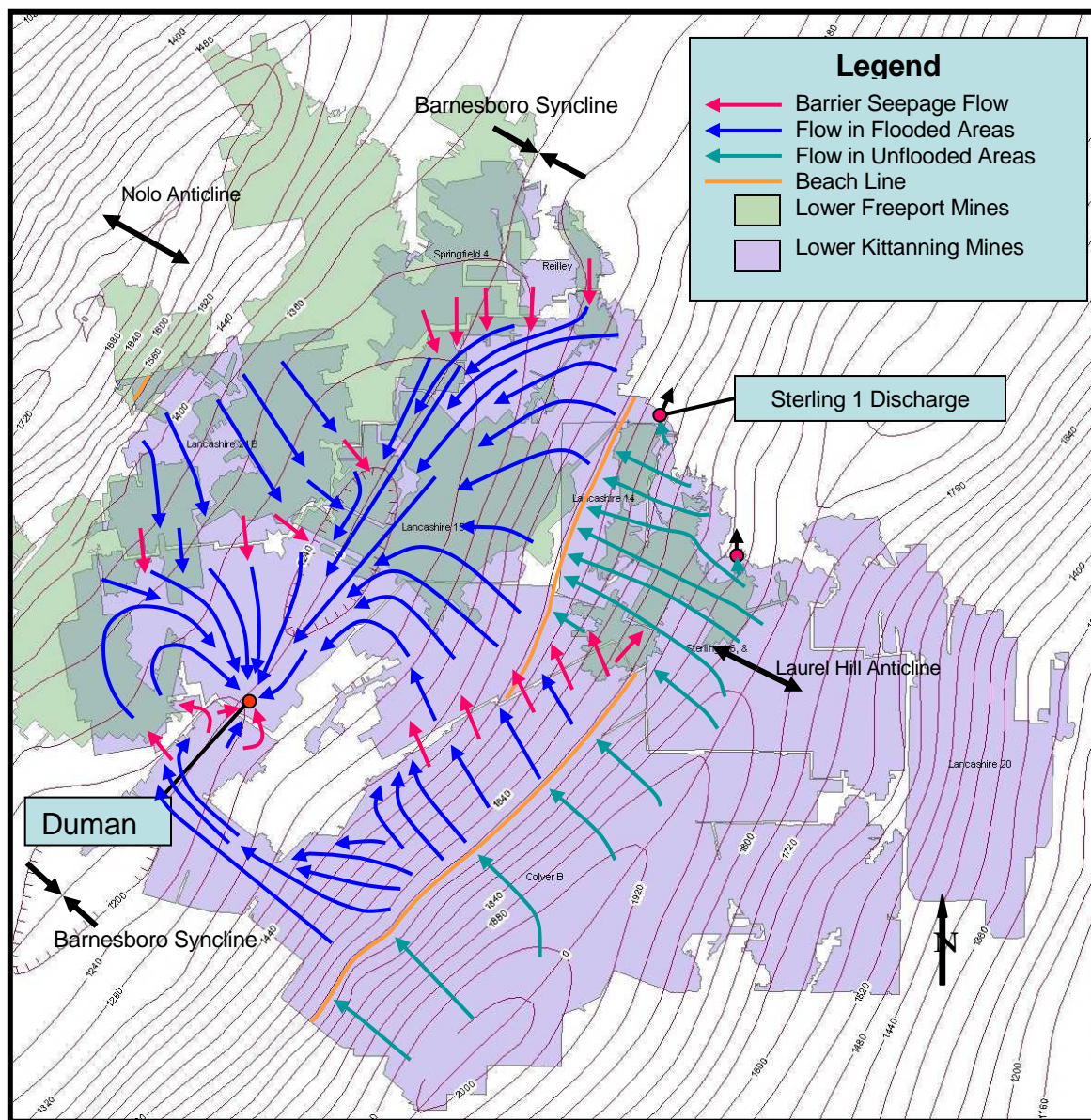
The L-15 mine-pool is also recharged by leakage through barrier pillars from adjoining flooded or partially flooded mines. About 30% of the flow at Duman is estimated to be barrier seepage from the Colver mine-pool located to the east (Hawkins et al., 2005). Some ground water also enters the mine-pool through unmined strata.

The rocks are Pennsylvanian age, Allegheny group, consisting in descending order of the Freeport, Kittanning and Clarion formations. Rock strata of this area are characterized by sandstones interbedded with shales, mineable coal beds and thin but persistent limestones near

the Lower Freeport coal bed.   Rocks in the Kittanning formation generally lack carbonates. The Lower Kittanning seam elevation varies from a high of about 610 m on the Laurel Hill anticline to a low of about 366 m near the Duman treatment plant. The Lower Kittanning seam averages about 1 m thick, and the Lower Freeport is about 1.4 m.   Area geology is described in more detail by McElroy (1998) and references cited therein.

Mine Closure and Flooding History

The L-15 mine-pool formed in adjacent and interconnected mineworks of about 15 different mines (Hawkins et al., 2005).   Coal development began in the late 1800's by room and pillar methods, and many areas had retreat mining. Later mining included longwall extraction. By the mid 1980's all significant underground mining was completed. The L-15 mine-pool began to form after the closure of several larger mineworks in the Lower Kittanning seam in 1969. At that time, dewatering was halted and the mineworks were allowed to flood. About one year later, a major blowout occurred at the north end of the mine-pool, discharging an estimated 4000 to 8000 L/min into the West Branch of the Susquehanna River. Discharge quality was extremely poor with iron and total acidity concentrations ranging from 2500 to 4000 mg/L, and about 7000 to 10,000 mg/L, respectively. A major fish kill occurred, and the Commonwealth of Pennsylvania began emergency treatment of the West Branch of the Susquehanna River. The mining company began pumping and treating at the Duman facility until water level was below breakout elevation and discharge to the West Branch of the Susquehanna River ceased.

 In 1986, mines in the overlying Lower Freeport seam and one Lower Kittanning seam mine closed and flooded. Closure of these mines increased the required pumping rate at Duman by about 60% (Hawkins et al., 2005) indicating they contribute part of the recharge to the L-15 mine-pool. The L-15 mine-pool has been pumped and treated since 1970. As shown in fig. 1, flow within the mine-pool is from northeast to southwest along the synclinal axis, and from the anticlinal axes toward the center of the basin. The northern end of the mine-pool is unflooded (about 1246 Ha). The Sterling 1 discharge (fig. 1) drains a portion of the unflooded mineworks.

Methodology

Over 1400 analyses of Duman raw water quality from offices of the Pennsylvania Dept of Environmental Resources (PADEP) (Kernic, 1999), and mine drainage reports for Blacklick Creek and West Branch of Susquehanna (Michael Baker Consulting Engineers, 1978; Gwin, Dobson and Foreman, 1972) and unpublished data (Lloyd, 2004) were used in this study. Sampling frequency ranged from daily to monthly to quarterly, and there were several years for which no data were located. However, a good record of initial water quality conditions at Duman was available, and continuous sampling of monthly frequency exists for about the last 7 years.

The compiled analyses vary in reported parameters, and were run by different laboratories which may not have used identical analytical methods. Iron, pH and acidity are the most consistently reported parameters. Values for sulfate, manganese and aluminum were reported for some but

not all samples. Acidity was calculated from reported pH and iron concentration, counting all iron as Fe(II), based on theoretical and practical considerations of iron speciation in mine waters (Kirby and Cravotta, 2004; Cravotta and Kirby, 2004). Calculated acidity was determined as:

$$\text{Acidity Calc} = 50*((Fe *2/55.85)+ 1000*(10^{-pH})) \qquad (1)$$

The available analyses show relatively small amounts of manganese present (generally less than 2 mg/L), and except in acid waters, concentrations of soluble aluminum are low. Therefore, for most samples, iron should represent most of the acidity. The calculated acidity values were used in subsequent analysis.

To supplement the historical data, four complete suite samples of the Duman raw water were collected at different seasons of the year in 2004. Samples from the unflooded works of the Sterling 1 mine (Lower Kittanning seam), and the upper mine-pool (Lower Freeport seam) and several other mine discharges were also collected. Water quality samples included field filtered, acid preserved, sub-samples for major cations (Ca, Mg, Na, K), metals (Fe, Mn, Al), trace elements(As, Ba, Be, Cd, Co, Cr, Cu, Ni, Pb, Sb, Se, Zn), raw unpreserved sub-samples for anions (SO_4,Cl) and general chemistry (pH, acidity, alkalinity, specific conductance, Total Dissolved Solids, and Total Suspended Solids).   Field measurements of pH, specific conductance, temperature, oxidation reduction potential (Eh), and dissolved oxygen were also collected. Geochemical calculations of mineral saturation indices, inverse modeling and solution mixing were performed using PHREEQC (Parkhurst and Appelo, 1999). Statistical analyses were performed using Statgraphics for Windows, version 5.1.

Results and Discussion

Temporal Trends
During the initial year of treatment at the Duman plant, overall water quality was very poor. Influent water pH varied from strongly acidic (~ 3.5) to circumneutral (~6.3); alkalinity from zero to a maximum of about 100 mg/L and acidity was usually in excess of 1000 mg/L. Iron and sulfate concentrations also showed short term fluctuation, but were typically in excess of 500 and 3000 mg/L, respectively. Table 1 summarizes median water quality conditions for initial conditions from August, 1970 to December 1971, and recent data from February, 1998 to May, 2004 at the Duman plant.

Table 1. Median Water Quality, Historical and Current Conditions, Duman Treatment Plant[1]

Date	pH	Acidity[2]	Alkalinity	Fe	SO$_4$
8/70 to 12/71	5.10	1500	0	837.50	3432
2/98 to 5/04	6.51	98.3	172.9	43.75	397

(1) pH in Standard units, acidity and alkalinity in mg/L $CaCO_3$ Eq, iron and sulfate in mg/L.
(2) Acidity is calculated from iron and pH data as described in text.

After about 35 years of leaching, L-15 mine-pool quality has improved substantially, although treatment is still required. The raw influent water is now typically net alkaline and median iron concentration has declined to about 5% of initial values. Fig. 2 shows the trend in average annual iron concentration at Duman from 1970 to present. Concentrations exceeded 900 mg/L during initial flooding and discharge, but declined rapidly afterwards, dropping to about 200 mg/L after about 8 years. This period likely represents active flushing of soluble metal sulfate salts and stored acidity. After 1986 when the overlying mine-pool flooded, iron declined further to current values of around 40 mg/L. Sulfate concentration initially declined more slowly, to about 1000 mg/L over a 10 year period, and is now about 11% of initial conditions.
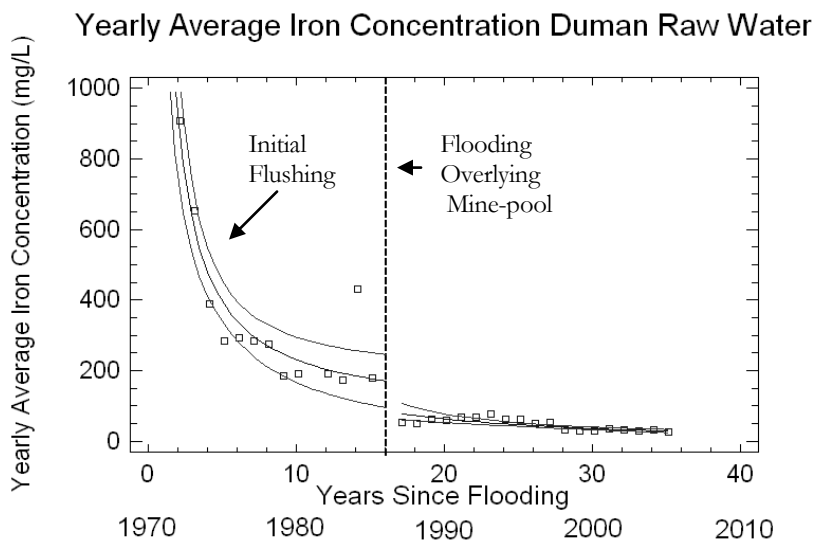
Figure 2. Plot of Average Annual Iron Concentration with Fitted Regressions, Duman Site.

The iron data in fig. 2 from 1971 to 1986 can be fitted to a reciprocal model of the form:

Fe Average (mg/L) = 82.5 + (1579.8/Years since flooding) $r = 0.92$ **(2)**

In 1986, the L-15 mine-pool was affected by closure and flooding of mines in the overlying mine-pool (Lower Freeport seam). The resultant influx of water of differing chemical composition, generally containing iron of less than 5 mg/L, changed the long term chemical behavior of the L-15 mine-pool. As seen in fig. 2, average iron concentration dropped abruptly from about 200 to 60 mg/L from dilution and mixing with the overlying mine-pool. In addition to dilution, increased precipitation of iron oxyhydroxides and/or carbonates may also have

274

occurred. Flooding of the Lower Freeport mine-pool increased average alkalinity in the L-15 mine-pool from 120 to 290 mg/L and pH increased from 6.0 to 6.7. No Eh or iron speciation measurements are available for the 1986 flooding period. However, the 2004 water samples are slightly oversaturated for both siderite and poorly crystalline iron oxyhydroxides, indicating these minerals could precipitate. The post 1986 iron data can be fitted to a model of the form:

Fe Average (mg/L) = $1/(7.59*10^{-4}*\text{Years since Flooding})$ r = 0.83   **(3)**

After 1986, iron concentration continues to decline with time, but more slowly.

 Younger (1997, 2000) and Wood et al. (1999) have reported similar discharge chemistry behavior of iron concentration in closed underground mines in the United Kingdom. Younger (1997) reports on several discharges where iron follows an exponential decay function. He attributes this behavior to depletion of "vestigal" or stored acidity, similar to the 8 year flushing period in the L-15 mine-pool. After 10 to 20 years, the curves in the British mines become asymptotic and solution iron is controlled by juvenile or ongoing acid generation. Younger (2000) concluded the main period of flushing of stored acidity is about four times as long as the flooding period, and that short-term to long term iron concentrations are about 8:1 (mg/L basis) with some site specific variation.   For the L-15 mine-pool, flushing appears to be about 8 times as long as the flooding period, and is a function of flow path length and tortuosity, residence time, and extent of flooding.   Initial iron to longer term concentrations is about 4:1 before the 1986 flooding, and about 19:1 when compared to current conditions. The 4:1 ratio suggests a slower rate of iron removal than observed by Younger, or greater ongoing acid production in L-15. The 19:1 ratio is influenced by the 1986 flooding, and shows that the quality of the recharge water can significantly affect iron behavior.

Yearly average sulfate concentration data and fitted regressions are shown in fig. 3. The pre-1986 sulfate data has a best fit model of:

SO$_4$ Average (mg/L) = $1/(2.93*10^{-4} + 6.04*10^{-5}*\text{Years since Flooding})$ r = 0.91   **(4)**

The post 1986 sulfate model is similar with a best fit regression of:

SO$_4$ Average (mg/L) = $1/(6.14*10^{-5}*\text{Years since Flooding})$ r = 0.73   **(5)**

Unlike iron, sulfate concentration shows a small response to the 1986 mine flooding. Slopes of the pre and post flooding regressions (equations 4 and 5) are nearly the same. The small response in sulfate concentration to the 1986 flooding reflects its' conservative behavior in L-15. Gypsum and other common sulfate minerals are one or more orders of magnitude under-saturated in flooded sections and do not control sulfate concentration.

The curvilinear models and post 1986 flooding behavior for both iron and sulfate suggest that the system will approach long term geochemical equilibrium slowly, on the order of decades.
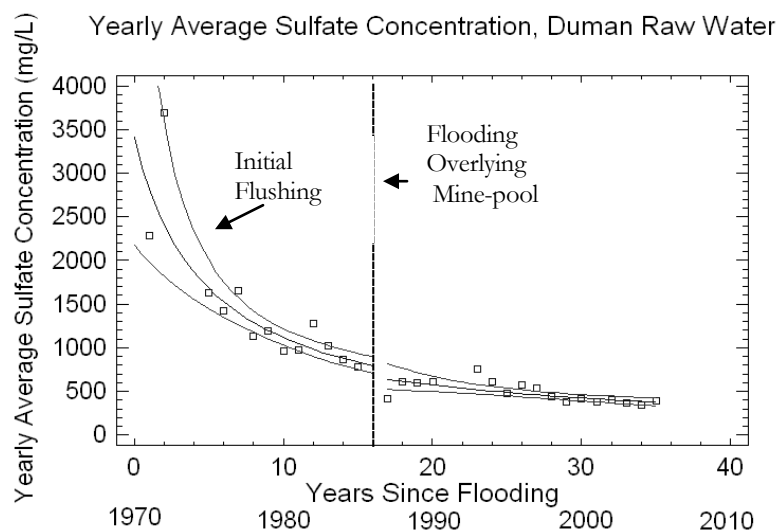
Figure 3. Plot of Average Annual Sulfate Concentration With Fitted Regressions, Duman Site.

Fig. 4 is a plot of simple moving average and raw data for iron concentration at the Duman plant for recent conditions (2000-2004). The overall trend has a current rate of decline of 1 to 2 mg/L-year but there are short term and seasonal fluctuations in concentration. Most of the raw data are within about 25% of the trend line. Sulfate exhibits similar behavior, displaying a slow irregular decline of about 10 mg/L-year in concentration over time. It is not known whether the trends will continue to decline or become asymptotic and approach equilibrium where iron is maintained at elevated concentrations indefinitely. Even if the current trends continue, it will be decades before water quality approaches some acceptable criteria. The curvilinear function derived for iron, based on post 1986 data, projects approximately 131 years from mine closure for iron to reach 10 mg/L, assuming current hydrologic and geochemical conditions are still applicable in the future. The curvilinear function for sulfate based on post 1986 data, projects approximately 65 years from mine closure for sulfate to reach 250 mg/L.

The L-15 mine-pool has been pumped at a rate equivalent to about 2 pool volumes a year based on storage calculations reported by Hawkins et al. (2005), and is approaching a total of 60 pool volumes. If the mineworks function as a simple flow through system, then soluble constituents should have been rapidly leached from the L-15 mine-pool within the first few years or pool volumes, when most flushing took place. In fact, both iron and sulfate persist in the mine-pool, suggesting that the flow system has elements of dispersion, short circuiting and no-flow zones, and that some chemical reactions are continuing.

Simple Moving Average Plot , Duman Influent Iron, 2000-2004
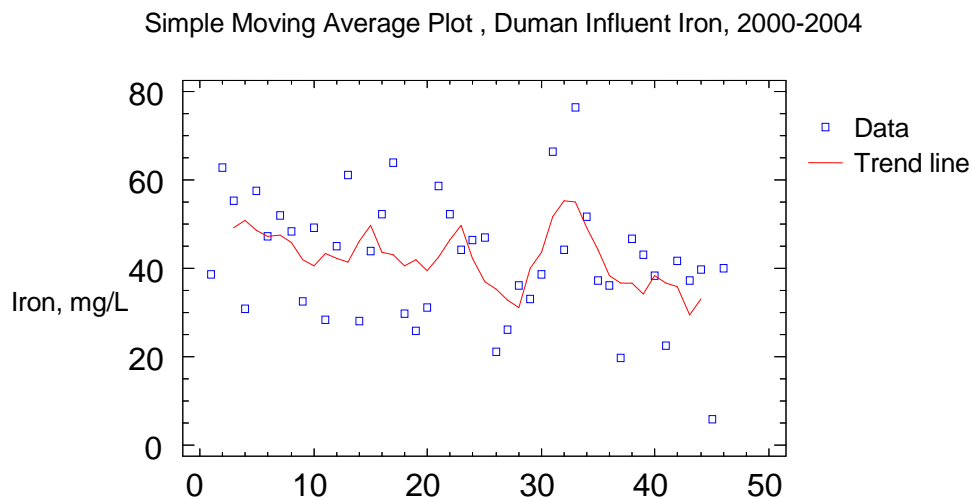
Figure 4. Plot of Simple Moving Average and Recent Iron Concentration, Duman site.

Pyrite oxidation in theory yields an Fe to SO_4 mole ratio of 0.5. Fig. 5 is a plot of Fe to SO_4
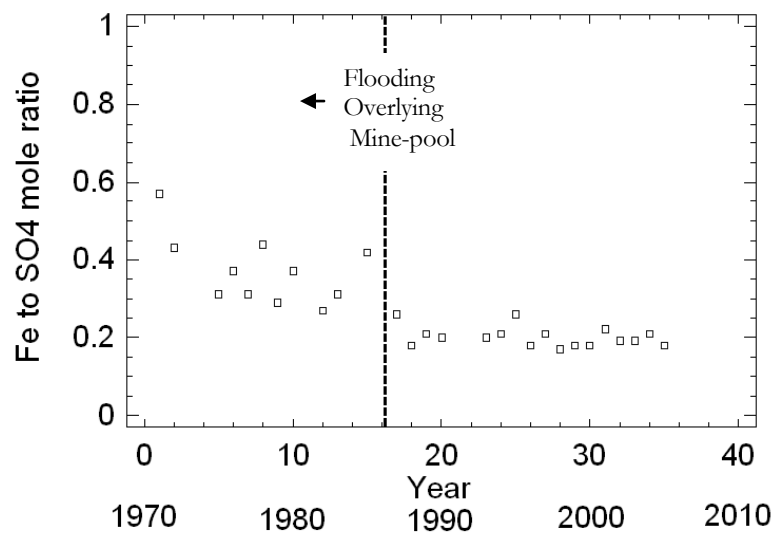
Figure 5. Plot of Average Annual Iron to Sulfate Mole Ratio, Duman Site.

mole ratio based on average annual data for the Duman site. The ratio declines over a 15 year period to around 0.2. Assuming sulfate behaves as a mostly conservative ion in the L-15 mine-pool and is derived from pyrite; about 60% of the iron is now being attenuated in the mine-pool by adsorption, precipitation or other reactions. In the first few years after flooding, less iron was retained in the mine-pool aquifer matrix.

Fig. 6 is a plot of average annual alkalinity for the Duman discharge. For at least 6 years after flooding, corresponding to the period of initial flushing, alkalinity remained at about 50 mg/L or less. After the initial flushing of the L-15 mine-pool, alkalinity continued to increase to over 100 mg/L and peaked at about 300 mg/L after flooding of the overlying Lower Freeport mines. Since that time alkalinity has remained around 200 mg/L and pH has stabilized at about 6.5.
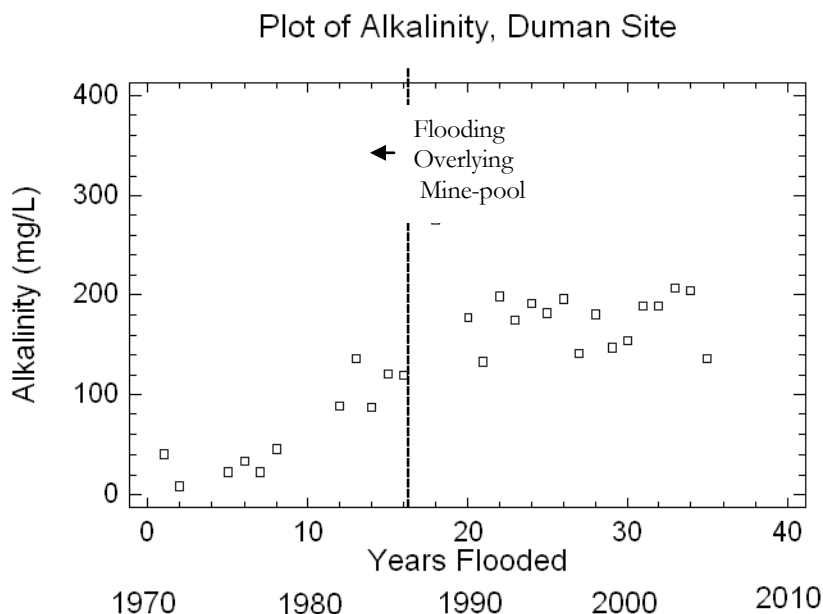
Figure 6. Plot of Average Annual Alkalinity at Duman Site

Mine-pool Chemical Composition
The Duman influent is a combination of several source waters that have mixed and reacted with the aquifer matrix as they flow toward the pump station. From the discussion of quantitative hydrogeology (Hawkins et al.,2005) and examination of water quality data, the following waters contribute to the Duman influent in varying fractions: a) leakage through a barrier pillar from the Colver mine-pool, located east of the main L-15 pool, estimated as approximately 30% of the influent, b) leakage from the overlying Lower Freeport seam mines, estimated to be about 40 to 50% of the influent, c) ground water recharge from unmined strata, and d) acidic water from unflooded areas at the northern end of the mine-pool and flanks of the two anticlines that are the eastern and western boundaries of the Lancashire 15 mine-pool. Representative analyses of each of these waters collected during 2004 are shown in table 2.

The Duman influent represents the end of the flow system for the Lancashire 15 mine-pool. It is a Na-SO$_4$ type water and is usually net alkaline. Iron and sulfate concentrations are about 40 and 400 mg/L, respectively. On several site visits, dissolved oxygen (D.O.) and/or Eh were measured on the raw influent. Fig. 7 is an Eh/pH diagram for iron in the Duman influent waters.

Table 2. Representative Full Suite Analyses of Mine-pool Waters, 2004 [1]

Source water	pH	Alkalinity	Acidity	Fe	Al	Mn	Ca	Mg	Na	K	SO₄	Cl
Duman (L. K.) [2]	6.55	137	75	40	0.19	1.0	39.9	15.1	159	1.89	390	7.0
Colver (L. K.)	6.35	63	114	62	0.05	1.17	95.7	30.2	69.8	4.63	417	8.0
Lower Freeport	6.32	124	2	0.26	0.21	0.34	75.2	19.4	11.2	2.4	157	4.0
Ground water [3]	7.0	142	1	0.32	0.14	0.03	42.9	6.2	1.7	1.64	27	6.3
Sterling 1 (Unflooded L. K.)	2.78	0	574	113	43.7	1.7	85	33.9	34.8	1.44	767	5.3

(1)pH in S.U., alkalinity and acidity in mg/L $CaCO_3$ Eq.; all others in mg/L.
(2)L. K. = Lower Kittanning coal bed.
(3)Ground water from unmined area strata. Data from McElroy,1998.

Two samples are plotted against iron oxyhydroxide, siderite and pyrite, based on field measured pH and Eh. The samples are slightly oversaturated for poorly crystalline iron oxyhydroxide, and well outside the pyrite stability field, indicating that pyrite could undergo dissolution and iron oxyhydroxide could precipitate. The dominant soluble iron species is Fe^{2+}. Speciation calculations using the geochemical code PHREEQC (Parkhurst and Appelo, 1999) show that Fe(II) species comprise almost all of the soluble iron, and Fe(III) species are present only in small concentrations.

The Colver mine water composition is similar to the Duman influent with respect to mine drainage parameters, with iron and sulfate concentrations of about 60 and 400 mg/L, respectively (table 2). It contains less sodium than the Duman discharge however, and is a Ca-Na-SO₄ type water. The Sterling 1 sample was collected from the unflooded free draining north end of the mine-pool (fig. 1). Its' composition differs sharply from waters in the flooded part of the mine-pool. It is strongly acidic with pH less than 3.0, total acidity of near 600 mg/L, and higher concentrations of iron and sulfate, with significant quantities of soluble aluminum. Both Eh and dissolved oxygen measurements (+786 millivolts and 8.1 mg/L, respectively) indicate a well aerated, oxidizing environment. Acid generation is ongoing in this portion of the mineworks.

Water from Lower Freeport seam mines can contain 100 to 200 mg/L alkalinity, with metal concentrations of about 5 mg/L or less. These waters, if mixed with the Lower Kittanning seam mine-pool, would have a net dilution effect on metals concentrations, and add alkalinity to the L-15 mine-pool. The Lower Freeport seam sample in table 2 is mixed composition Ca-Mg-SO₄-HCO₃ type water.
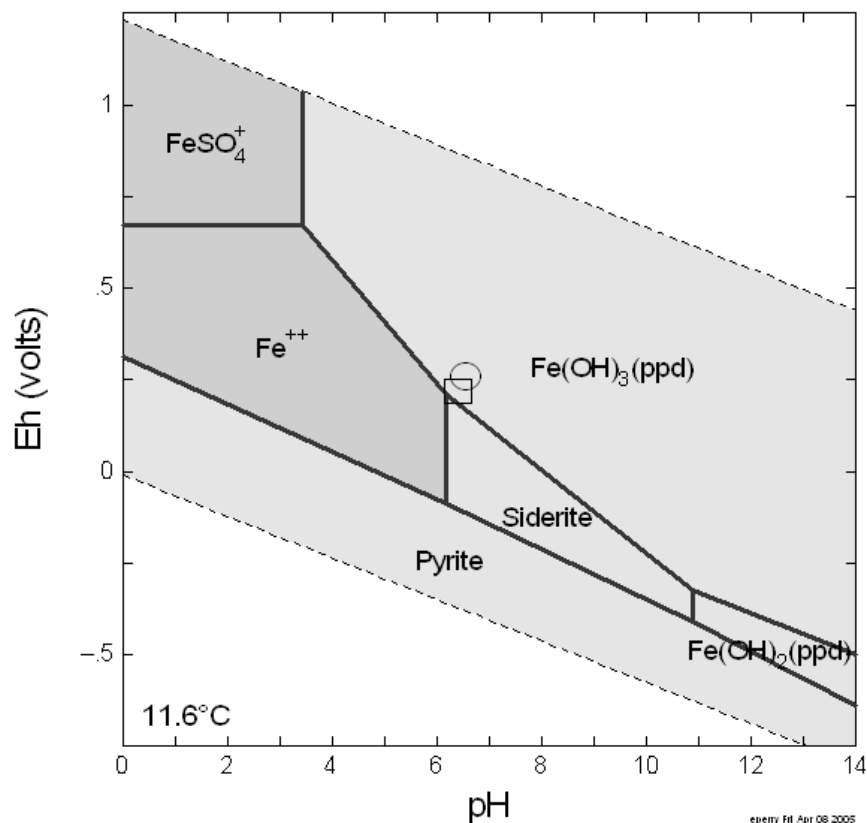
Figure 7. Eh/pH plot of Duman site mine waters for two sample events, 2004.

McElroy (1998) reported on ground water quality and quantity for Cambria County, Pennsylvania including wells in rocks above and adjacent to the L-15 mine-pool. Ground water in the Allegheny group contains about 150 to 300 mg/L dissolved solids, and the waters are mixed Ca-Mg-HCO₃ or Ca-Mg-HCO₃-SO₄ type waters. Unlike the Duman plant influent, ground waters in unmined strata contain low concentrations of sodium. Median composition data from McElroy's report was used to represent ground water from unmined areas in geochemical modeling simulations.

Geochemical Modeling of Mine-pool Water Composition
A conceptual geochemical model of mine-pool quality at the Duman plant was developed and tested with PHREEQC using inverse and forward modeling. The purpose was to determine which geochemical processes were likely to generate water of the observed composition in table 2 for the Duman site, by mixing fractions indicated by quantitative data, and using the simplest possible models. The analyses in table 2 show that most elemental transfer in mixing and reacting involves iron, calcium, magnesium, sodium and sulfate, and in acid waters, aluminum. Simulations were therefore focused on these elements.

280

The Duman influent is enriched in sodium and depleted in calcium and magnesium compared to the Colver mine-pool and Lower Freeport seam waters, which are the two principal components of the Lancashire 15 mine-pool. Cation exchange of adsorbed sodium for dissolved calcium and magnesium is a feasible explanation for the observed behavior, and has been postulated in ground water flow systems (Back, 1964; Stoner et al., 1985). To obtain the concentrations of iron and sulfate found in the Duman influent, additional sources of these elements were needed when Colver mine water, Lower Freeport seam and ground waters were mixed. Based on Eh measurements and other calculations, pyrite could still be dissolving in the mine-pool (see fig. 7) and is the likely source of additional iron and sulfate. Other geochemical processes were considered as alternatives to cation exchange and pyrite dissolution. They were abandoned as unlikely if they produced unrealistic solutions in numeric modeling or required minerals not likely to be present in these rocks.

Inverse modeling solved for all possible mathematical solutions and produced a large set of potential mixes and reactions. The results were screened for mixing fractions that were consistent with pumping records and other quantitative data, and that invoked reactions consistent with mine-pool chemistry and mineralogy. Many inverse model simulations showed that Lower Freeport seam and Colver mine waters comprise most of the source water for Duman. Acid water from the unflooded area was typically included in very small amounts of less than 1%. Scenarios with infeasible mixing fractions or very large mineral transfers were rejected.

Based on the initial screening with inverse modeling, a forward model was developed using cation exchange and adsorption, pyrite dissolution and formation of goethite, a common iron oxyhydroxide mineral. In forward modeling, a starting solution is allowed to undergo specified reactions to produce final water. Element and mineral amounts were adjusted until the final solution had a composition similar to the Duman influent. The comparison of simulated and actual water is shown in table 3. The principal constraints and conditions used in the forward model are:

Mixing Fractions – Lower Freeport seam water 50%, Colver water 30%, ground water 19%, "acid drainage" water 1%.

Mineral reactions – Dissolve pyrite 9×10^{-4} moles/liter solution; precipitate goethite if oversaturated, fix partial pressure CO_2 $10^{-1.4}$ atm.

Cation Exchange – add exchangeable cations, calcium 3×10^{-2} moles, magnesium 1.3×10^{-2} moles, sodium 1.3×10^{-2} moles, total exchange capacity 9.9×10^{-2} moles.

Table 3. Forward Modeling Simulation and Actual Composition of Duman Influent [1]

Solution	pH	Fe	Ca	Mg	Na	SO$_4$
Simulation	6.69	35.7	37.3	15.1	146	388
Actual	6.55	40.0	39.9	15.1	159	390

(1) pH in S.U., all others in mg/L

In general the simulated and actual concentrations were in close agreement. The quantities of pyrite dissolved, goethite precipitated, and cation exchange capacity were small in comparison to the aquifer matrix encountered along a flow path of several km or more in length.   The simulation showed that some of the dissolved iron was removed by exchange and adsorption. Additional iron was removed by the formation of goethite. These results were consistent with the Fe to SO_4 mole ratio plot (fig. 5) showing that about 60% of the iron dissolved from pyrite was attenuated within the mine-pool. Exchange also decreased the amount of dissolved calcium and magnesium and increased dissolved sodium. A second forward model using the calcium sulfate salt gypsum and pyrite dissolution also produced a good match between simulated and actual waters. However, solubility calculations showed that all mine waters were at least one order of magnitude or more undersaturated for gypsum. These saturation indices suggest that gypsum is not controlling sulfate concentration, and we have no mineralogical data to confirm or refute its' presence.

The initial modeling efforts showed that the Duman influent mine waters could be satisfactorily described as a product of mixing several source waters, cation exchange, pyrite dissolution and goethite formation. These modeling results were similar to work reported by Chen et al. (1999), who found that mixing, pyrite oxidation, calcite dissolution and goethite formation were the main processes controlling mine water evolution at a Scottish colliery.   There are undoubtedly additional mineral reactions and processes taking place in the L-15 mine-pool, but they seem to influence water chemistry and composition to a lesser extent.

Flooded versus Free Draining Mineworks
There are large contrasts in water chemistry between flooded mineworks at the Duman site versus unflooded mineworks at the Sterling 1 discharge. These two sites discharge water from adjoining mines in the same Lower Kittanning coal bed. The unflooded works, which have been abandoned for more than 50 years, still discharge acid water, while the Duman site began discharging circumneutral   alkaline water within 10 years after flooding. Water quality data collected in 1984, 1994 and 2004 from the Sterling 1 discharge are summarized in table 4 and compared to the Duman site for the same years. Median sulfate and pH concentrations in the unflooded mineworks are essentially unchanged for the period.   In the flooded mineworks, median pH increased about 0.6 units, and sulfate concentrations declined about 50%.   Total acidity has declined from about 700 to 500 mg/L at the Sterling discharge in 20 years, and the difference is statistically significant at p=0.01. Acidity at Duman in 2004 is 68 mg/L or about 20% of its' 1984 concentration. The unflooded Sterling 1 mine-water parameters of sulfate, iron and acidity remain 2 to 7 times greater than concentrations than at Duman, even though the Sterling mines have been abandoned for a longer time.   Flooding inhibits pyrite oxidation and increases the rate of natural remediation occurring in mine-pools.   Stortz et al. (2001) also found that mine flooding results in more rapid water quality improvement.   They noted significant increases in pH, and reductions in acid load, dissolved solids and other parameters in a mine that was mostly flooded compared to a nearby unflooded mine in the same geologic and hydrologic setting.

Table 4. Median Annual Water Quality at unflooded Sterling 1 Discharge and Flooded Duman L-15 Minepool, 1983-2004[1]

Year	Location	pH	T. Acidity	Alkalinity	Fe	SO$_4$
1983-84	Sterling 1	2.62	710	0	85	850
1994	Sterling 1	2.7	604	0	60	920
2004	Sterling 1	2.7	497	0	102	837
1984	Duman	5.98	340	121	190	775
1994	Duman	6.48	131	182	73	478
2004	Duman	6.58	68	136	38	388

(1) pH in S.U., acidity and alkalinity in mg/L CaCO$_3$, Eq, others in mg/L.

Summary and Conclusions

Water quality in the 35 year old mostly flooded L-15 mine-pool has improved significantly since closure. Changes in water quality occur in two phases, a short term initial flushing of stored relatively soluble acid products, and long term leaching of additional materials and continuing geochemical reactions. Younger (1997) characterizes this process as production of vestigial (stored) and juvenile (continuing pyrite oxidation) acidities. In the L-15 mine-pool, the main period of flushing lasted about 8 years, and iron and sulfate concentrations declined to about 20 to 25 % of their initial values. In 1986, closure and flooding of mines in the overlying Lower Freeport coal bed introduced water of different water chemistry into the L-15 mine-pool. Mixing of these waters abruptly lowered iron concentration from about 200 to 60 mg/L, while sulfate concentration was less affected. Composition of the recharge water influences mine-pool chemistry. The Fe to SO$_4$ mole ratio rapidly declined in the L-15 mine-pool to around 0.2. About 60 % of the iron dissolved from pyrite is now attenuated by precipitation, cation exchange or other reactions within the mine-pool. Iron attenuation was much less in the initial flushing phase.

The temporal declines in iron and sulfate concentration can be described using curvilinear models. Current mine-pool behavior shows a decline of about 1 to 2 mg/L-year and 10 to 15 mg/L-year for iron and sulfate, respectively. This behavior suggests that geochemical equilibrium will be approached slowly, over a period of decades.

Long term predictions of iron, sulfate or other mine drainage parameters at future dates can be generated from curvilinear models of the current data. However, long term predictions are uncertain because slope of the curvilinear function is a statistical estimate; there may be changes in the mine-pool aquifer and flow system, and mineral solubility constraints could control solution chemistry at low concentrations. The estimated slopes for functions derived for iron and sulfate have standard errors of about 13 to 16%, thus any future projected concentration values should be expressed as a range. A small change in the predictive function can change the estimated time to achieve a target concentration by years.

Mine-pools are young aquifers that are undergoing rapid physical and chemical changes. These changes can include continuing physical breakdown of rocks, collapse or subsidence of roof rock and coal pillars, and opening or closing of other mines nearby. These features may change flow paths, tortuosity, residence time and pumping and seepage rates, all of which may influence mine-pool chemistry. Predicting the exact composition of mine waters as they approach long term equilibrium requires detailed knowledge of the mineralogy and flow characteristics of the aquifer; information which may not always be available. While a local equilibrium condition seems to exist at a given sample point, overall mine-pool composition can be heterogeneous (Perry and Hawkins, 2004).

The L-15 mine-pool is actually a mixture of seepage water from the adjacent Colver mine-pool (about 30%), leakage from the overlying Lower Freeport mine-pool (about 40 to 50%), acid waters from the unflooded northern end of the mine complex, and ground water from unmined strata. Inverse modeling with PHREEQC (Parkhurst and Appelo, 1999) was used to develop and test models of the L-15 mine-pool. The goal was to approximate mixing percentages and geochemical reactions that produce the water quality of the Duman discharge. Simple mixing alone does not explain Duman's chemistry. Forward modeling showed that the continuing dissolution of small quantities of pyrite and formation of goethite provided a close match of modeled and actual water quality.

The Duman discharge is a $Na-SO_4$ type water, while the waters that contribute to it are of mixed cation composition, where Na is a secondary cation. Cation exchange of dissolved calcium and magnesium for adsorbed sodium provides a feasible explanation for the observed dominance of sodium at Duman. The presence of small amounts of exchangeable sodium along a flowpath as much as 8 km in length would be sufficient to produce a $Na-SO_4$ solution. Back (1966) in a study of water quality evolution in Coastal Plain aquifers, observed increasing dominance of sodium over calcium and magnesium the further ground water moved along its flowpath.

Comparison of mine waters from flooded and unflooded sections of the L-15 complex shows that the rate of water quality improvement is much more rapid when the mineworks are inundated. Drainage from unflooded sections remains strongly acidic 50 years after closure, while the Duman site began discharging circumneutral water within 10 years of flooding. Chemical concentrations are higher in the free draining section.

The L-15 mine-pool has been pumped at a rate equivalent to about 2 pool volumes a year and is approaching a total of 60 pool volumes. The persistence of iron and sulfate in the mine-pool after this amount of leaching suggests that dispersion, short circuiting and no-flow zones are important, and that some chemical reactions are continuing. The L-15 mine-pool is expected to continue slow improvement in water chemistry, but is likely to require treatment for an extended period.

Literature Cited

Back, W. 1966. Hydrochemical Facies and Ground-Water Flow Patterns in Northern Part of Atlantic Coastal Plain. US Geological Survey Professional Paper 498-A.

Chen, M., C. Soulsby and P Younger. 1999. Modelling the Evolution of Minewater Pollution at the Polkemmet Colliery, Almond Catchment, Scotland, p 351-362, Quarterly Journal of Engineering Geology, 32.

Cravotta, C. A. III and C. S. Kirby. 2004. Acidity and Alkalinity in Mine Drainage: Practical Considerations, p334-365, *In* R. I. Barnhisel (ed) Proc. Joint Conference of American Society of Mining and Reclamation 21st Annual National Conference and 25th West Virginia Surface Mine Drainage Task Force Symposium April 18-22, Morgantown West Virginia, , ASMR 3134 Montavesta Rd. Lexington, KY 40502.

Donovan, J and B. Leavitt. 2004. The Future of Mine-Water Discharges From Underground Coal Mines of The Pittsburgh Coal Basin, WV-PA, p518-528 *In* R. I. Barnhisel (ed) Proc. Joint Conference American Society Mining and Reclamation 21st Annual National Conference and 25th West Virginia Surface Mine Drainage Task Force Symposium, April 18-22, Morgantown WV, ASMR, 3134 Montavesta Rd, Lexington KY, 40502 .

Gwin, Dobson, & Foreman. 1972. West Branch Susquehanna River Mine Drainage Pollution Abatement Project, Operation Scarlift, prepared for Commonwealth of Pennsylvania, 181 p.

Hawkins J., E. Perry and M. Dunn. 2005. Hydrologic Characterization Of A Large Underground Mine Pool In Central Pennsylvania, *In* R. I. Barnhisel (ed) Proc. Conference American Society Mining and Reclamation 22st Annual National Conference, June 19-24, Breckinridge CO, ASMR, 3134 Montavesta Rd, Lexington KY, 40502 .

Lloyd, D. 2004. personal communication, unpublished water quality data for Lancashire 15 mine-pool and associated mines, Lloyd Environmental Services, Commodore, PA.

McElroy, T. 1998. Groundwater Resources of Cambria County Pennsylvania, 49pps, Water Resources Report 67, Pennsylvania Dept of Conservation and Natural Resources, Bureau of Topographic and Geologic Survey, Harrisburg, PA.

Kernic, J. 1999. Barnes and Tucker Company, Lancashire 15 and 20 Mines, Cambria County, Mine Pool and Discharge Report, unpublished report prepared for Pennsylvania Dept Environmental Protection, McMurray District Office, 11 pages.

Kirby, C.S. and C.A. Cravotta. 2004. Acidity and Alkalinity in Mine Drainage: Theoretical considerations, p1076-1093, *In* R. I. Barnhisel (ed) Proc. Joint Conference of American Society of Mining and Reclamation 21st Annual National Conference and 25th West Virginia Surface Mine Drainage Task Force Symposium April 18-22, Morgantown West Virginia, ASMR 3134 Montavesta Rd. Lexington, KY 40502.

Kleinmann, R.L., R. Hornberger, B. Leavitt and D. Hyman. 2000. Introduction and Recommendation, The Nature of the Problem, *In* Prediction of Water Quality at Surface Coal Mines, Acid Drainage Technology Initiative, Prediction Workgroup, National Mined Land Reclamation Center, West Virginia University, Morgantown WV.

Michael Baker Consulting Engineers. 1978. Operation Scarlift Report SL-185, Blacklick Creek Watershed, Indiana Cambria Counties, prepared for Pennsylvania Dept of Environmental Resources, 152 p.

Parkhurst, D. L., and C.A.J. Appelo. 1999. User's Guide to PHREEQC (Version 2)- A Computer Program For Speciation, Batch-Reaction, One-Dimensional Transport, and Inverse Geochemical Calculations, US Geological Survey Water Resources Investigation Report 99-4259.

Perry, E.F. and J. Hawkins. 2004. Ground-Water Flow and Quality in A Fully Flooded Underground Mine Complex, p1460-1479 *In* R. I. Barnhisel (ed) Proc. Joint Conference American Society Mining and Reclamation 21st Annual National Conference and 25th West Virginia Surface Mine Drainage Task Force Symposium, April 18-22, Morgantown WV, ASMR, 3134 Montavesta Rd, Lexington KY, 40502 .

Skousen J., L M. McDonald and J. Demchak. 2004. Longevity of Acid Discharges From Underground Mines Lying Above the Regional Water Table. p 1769, *In* R. I. Barnhisel (ed) Proc. Joint Conference American Society Mining and Reclamation 21st Annual National Conference and 25th West Virginia Surface Mine Drainage Task Force Symposium, April 18-22, Morgantown WV, ASMR, 3134 Montavesta Rd, Lexington KY, 40502 .

Stoner, J. D., D. R. Williams, T. E. Buckwalter, J. K. Felbinger and K. L. Pattison. 1987. Water Resources and the Effects of Coal Mining, Greene County, Pennsylvania, prepared by the US Geological Survey Water Resources Division, Pennsylvania Geological Survey Water Resources Report 63, Harrisburg, Pa.

Stortz, M., M Hughes, N. Wanner and M. Farley. 2001. Long Term Water Quality Trends at a Sealed Partially Flooded Underground Mine, p 51-65, Environmental and Engineering Geoscience, Vol VII, No.1.

Wood, S.C., P. Younger and N. Robins. 1999. Long-term changes in the Quality of Polluted Minewater Discharges from Abandoned Underground Coal Workings in Scotland, p 69-79, Quarterly Journal of Engineering Geology, 32.

Younger, P. 1997. The Longevity of Minewater Pollution: A Basis for Decision Making, p 457-466, The Science of the Total Environment, 194&195.

Younger, P. 2000. Predicting Temporal Changes in Total Iron Concentrations in Waters Flowing From Abandoned Deep Mines: A First Approximation, p 47-69, Journal of Contaminant Hydrology, 44(2000).

Appendix E

Omega Mine-pool Raw Chemical Data

Table E-1a, Omega Mine-pool, Treatment Inlet, Raw Chemical Data

Sampled By	Date	Location	Flow gpm	pH	Sp. Conductance umhos/cm	TDS, mg/L	Temp, C	Acid load, lbs/day CaCO3 Eq	Calc Total Acidity CaCO3 Eq
DOE	2/11/1993	Treatment Inlet	65.0	2.86		5705		2052.2	2626.7
DOE	3/3/1993	Treatment Inlet	280.0	2.79		6549		10515.1	3124.3
DOE	3/18/1993	Treatment Inlet	180.8	2.85		3525		3394.5	1562.0
DOE	4/2/1993	Treatment Inlet	248.2	2.62		5316		7473.5	2505.3
DOE	4/14/1993	Treatment Inlet	171.4	2.57		6410		6200.3	3010.1
DOE	4/29/1993	Treatment Inlet	380.3	2.68		4465		9393.1	2054.7
DOE	5/20/1993	Treatment Inlet	142.7	2.76		6179		5066.5	2953.1
DOE	6/3/1993	Treatment Inlet	91.5	2.90		4730		1991.7	1810.5
DOE	6/10/1993	Treatment Inlet	91.5	2.89		5249		2416.5	2196.6
DOE	6/23/1993	Treatment Inlet	91.5	2.81		6049		2918.5	2653.0
DOE	7/8/1993	Treatment Inlet	55.5	2.81		6147		1829.6	2740.8
DOE	7/22/1993	Treatment Inlet	42.7	2.92		6160		1343.5	2617.3
DOE	8/11/1993	Treatment Inlet	42.7	2.97		5589		1141.9	2224.6
DOE	9/10/1993	Treatment Inlet	16.3	3.03		5247		372.3	1905.8
DOE	10/7/1993	Treatment Inlet	25.4	2.89		4773		484.9	1589.6
DOE	10/25/1993	Treatment Inlet	42.7	2.89		4657		842.7	1641.8
DOE	11/10/1993	Treatment Inlet	42.7	2.80		4393		784.3	1527.9
DOE	12/7/1993	Treatment Inlet	69.9	2.96		2592		834.0	992.2
DOE	12/23/1993	Treatment Inlet	69.9	2.74		5457		2117.8	2519.5
DOE	1/28/1994	Treatment Inlet	230.8	3.01		3416		3808.9	1373.2
DOE	5/5/1994	Treatment Inlet	110.6	2.70		4937		3089.5	2323.9
DOE	6/10/1994	Treatment Inlet	82.5	2.76		4757		2084.8	2102.8
DOE	7/6/1994	Treatment Inlet	60.2	2.74		4717		1382.2	1911.3
DOE	8/3/1994	Treatment Inlet	39.6	3.02		4397		807.8	1698.0
DOE	9/1/1994	Treatment Inlet	40.7	2.65		3694		688.0	1407.9
DOE	10/7/1994	Treatment Inlet	33.7	3.03		4816		774.7	1910.9
DOE	11/16/1994	Treatment Inlet	21.2	3.16		4888		435.0	1707.5
DOE	12/14/1994	Treatment Inlet	40.4	2.97		3456		589.5	1214.1
DOE	1/10/1995	Treatment Inlet	53.4	2.74		3719		1010.0	1573.2
DOE	2/3/1995	Treatment Inlet	49.6	2.81		4283		1161.8	1950.7
DOE	3/2/1995	Treatment Inlet	77.4	2.99		3566		1358.6	1460.8
DOE	4/7/1995	Treatment Inlet	42.5	2.70		6319		1563.7	3063.8
DOE	5/10/1995	Treatment Inlet	100.5	2.91		3968		2100.6	1738.9
DOE	6/6/1995	Treatment Inlet	109.3	2.92		4414		2297.3	1748.6
DOE	7/13/1995	Treatment Inlet	57.5	2.84		5600		1814.7	2628.0

Table E-1a, Omega Mine-pool, Treatment Inlet, Raw Chemical Data

Sampled By	Date	Location	Flow gpm	pH	Sp. Conductance umhos/cm	TDS, mg/L	Temp, C	Acid load, lbs/day CaCO3 Eq	Calc Total Acidity CaCO3 Eq
DOE	8/3/1995	Treatment Inlet	28.8	2.77		4837		670.7	1936.4
DOE	9/7/1995	Treatment Inlet	26.2	2.94		4925		530.9	1686.5
DOE	10/12/1995	Treatment Inlet	20.2	2.97		4629		375.5	1543.5
DOE	11/22/1995	Treatment Inlet	40.8	3.13		3021		347.1	707.7
DOE	1/5/1996	Treatment Inlet	53.4	3.07		2741		560.1	872.4
WVDEP	1/16/1996	Treatment Inlet	50.6	2.90	7140	4342	7.8	891.5	1465.2
WVDEP	2/15/1996	Treatment Inlet	93.6	2.60	563	3183	12.2	967.7	859.9
DOE	2/21/1996	Treatment Inlet	112.2	2.63		3874		2640.7	1958.1
WVDEP	3/1/1996	Treatment Inlet	87.8	2.60	4500	3840	10	1209.9	1146.3
WVDEP	3/15/1996	Treatment Inlet	117.8	2.60	5650	4520	12.2	1925.3	1359.5
DOE	3/18/1996	Treatment Inlet	118.0	2.97		2576		1451.7	1023.5
WVDEP	3/28/1996	Treatment Inlet	398.7	2.90	4510	2765	12.2	2486.1	518.7
WVDEP	4/15/1996	Treatment Inlet	216.4	2.80	5110	3317	14.4	1840.0	707.5
DOE	4/26/1996	Treatment Inlet	166.1	2.75		3120		2894.3	1449.7
WVDEP	4/29/1996	Treatment Inlet	237.4	2.50	6150	4194	14.4	4109.6	1439.9
WVDEP	5/15/1996	Treatment Inlet	224.5	2.60	5150	2813	11.1	3833.6	1421.0
WVDEP	5/31/1996	Treatment Inlet	229.4	2.60	4510	2450	13.3	2965.9	1075.7
DOE	6/7/1996	Treatment Inlet	151.2	2.65		3785		3163.3	1740.6
WVDEP	6/14/1996	Treatment Inlet	151.4	2.60	5960	3608	15.6	3722.0	2045.0
WVDEP	6/28/1996	Treatment Inlet	144.7	2.70	6190	3642	14.4	1148.1	660.1
WVDEP	7/15/1996	Treatment Inlet	97.7	2.70	5540	3200	15.6	1111.4	946.8
DOE	7/23/1996	Treatment Inlet	94.7	2.77		2513		1082.4	950.9
WVDEP	7/30/1996	Treatment Inlet	88.3	2.70	5580	3507	14.4	1390.9	1311.1
WVDEP	8/14/1996	Treatment Inlet	59.6	2.80	6310	4202	15.6	1203.9	1681.1
DOE	8/28/1996	Treatment Inlet	63.5	2.95		4130		1216.0	1593.0
WVDEP	8/31/1996	Treatment Inlet	78.0	2.70	2370	4257	13.3	1509.8	1611.4
WVDEP	9/16/1996	Treatment Inlet	50.6	2.70	5790	3675	15	946.1	1554.9
WVDEP	9/30/1996	Treatment Inlet	101.7	2.80	5130	3096	14.4	1681.2	1375.3
WVDEP	10/14/1996	Treatment Inlet	63.6	2.70	6100	4028	15.6	1173.7	1534.8
DOE	10/16/1996	Treatment Inlet	57.5	2.84		3944		1047.2	1516.5
WVDEP	10/30/1996	Treatment Inlet	103.9	2.50	5290	3384	14.4	1632.6	1306.7
WVDEP	11/15/1996	Treatment Inlet	136.6	2.70	5950	3971	12.2	2725.9	1659.7
DOE	11/26/1996	Treatment Inlet	124.3	2.70		3195		2166.3	1449.9
DOE	12/13/1996	Treatment Inlet	182.2	2.82		3154		3198.9	1460.7
WVDEP	12/15/1996	Treatment Inlet	210.6	2.80	5710	3057	12.2	3712.7	1466.9
WVDEP	1/14/1997	Treatment Inlet	89.6	2.80	5440	3313	10	712.6	661.7
DOE	1/28/1997	Treatment Inlet	84.4	2.78		1633		741.6	731.3

Table E-1a, Omega Mine-pool, Treatment Inlet, Raw Chemical Data

Sampled By	Date	Location	Flow gpm	pH	Sp. Conductance umhos/cm	TDS, mg/L	Temp, C	Acid load, lbs/day CaCO3 Eq	Calc Total Acidity CaCO3 Eq
DOE	2/21/1997	Treatment Inlet	84.4	2.89		2450		927.6	914.6
WVDEP	3/17/1997	Treatment Inlet	119.6	2.60	3810	3098	12.2	3094.1	2151.9
DOE	3/26/1997	Treatment Inlet	295.8	2.88		2348		3905.6	1098.5
WVDEP	4/14/1997	Treatment Inlet	113.3	2.60	3600	2793	12.2	3745.9	2749.6
WVDEP	5/14/1997	Treatment Inlet	95.4	2.60	3100	2281	14.4	1706.9	1488.2
DOE	5/20/1997	Treatment Inlet	234.7	2.96		1840		2315.1	820.6
WVDEP	6/16/1997	Treatment Inlet	94.5	2.50	3420	2624	16.7	3166.8	2787.0
DOE	7/10/1997	Treatment Inlet	44.2	2.68		3570		844.1	1589.3
WVDEP	7/16/1997	Treatment Inlet	44.8	2.50	3780	3478	15.6	668.0	1240.4
WVDEP	8/17/1997	Treatment Inlet	33.6	2.70	6080	3497	23.9	957.9	2371.7
DOE	9/10/1997	Treatment Inlet	24.9	2.75		3466		425.6	1421.4
WVDEP	9/15/1997	Treatment Inlet	25.5	2.60	3780	3585	15.6	292.9	954.2
WVDEP	10/15/1997	Treatment Inlet	24.6	2.60	6150	3133		487.7	1646.5
DOE	11/5/1997	Treatment Inlet	22.5	2.83		3127		351.4	1300.3
WVDEP	11/14/1997	Treatment Inlet	135.7	2.70	3140	2232		1001.3	613.7
WVDEP	12/15/1997	Treatment Inlet	65.9	2.60	2530	2322		911.0	1150.7
DOE	1/12/1998	Treatment Inlet	70.0	2.71		2288		895.5	1064.2
WVDEP	1/16/1998	Treatment Inlet	102.6	2.70	5680	3790		1752.2	1421.0
DOE	2/9/1998	Treatment Inlet	112.2	2.71		3959		2685.9	1991.6
WVDEP	2/15/1998	Treatment Inlet	199.4	2.70	5510	4009		3530.0	1473.1
WVDEP	3/16/1998	Treatment Inlet	205.2	2.70	5860	3700		2532.4	1026.8
DOE	3/26/1998	Treatment Inlet	151.2	2.78		2906		2615.2	1438.9
WVDEP	4/15/1998	Treatment Inlet	149.6	2.60	5920	3456		3079.2	1712.0
DOE	4/29/1998	Treatment Inlet	137.3	2.92		2821		2241.3	1358.1
WVDEP	5/13/1998	Treatment Inlet	184.6	2.60	5110	3698		3876.5	1747.2
DOE	5/28/1998	Treatment Inlet	79.4	3.05		3397		1453.8	1522.5
WVDEP	6/15/1998	Treatment Inlet	85.1	2.60	6120	3544		1644.5	1607.3
DOE	6/25/1998	Treatment Inlet	144.1	3.12		4110		1937.2	1118.4
WVDEP	7/15/1998	Treatment Inlet	119.6	2.60	7130	5272		1988.4	1382.9
DOE	8/5/1998	Treatment Inlet	70.0	3.09		4580		1487.0	1767.3
WVDEP	8/13/1998	Treatment Inlet	57.8	2.70	7300	4766		1097.1	1579.4
DOE	9/3/1998	Treatment Inlet	39.0	2.98		5294		1123.7	2397.2
WVDEP	9/15/1998	Treatment Inlet	37.6	2.60	11100	5615		1177.1	2602.5
WVDEP	10/15/1998	Treatment Inlet	25.5	2.60	43700	7002		1038.9	3384.1
DOE	10/29/1998	Treatment Inlet	14.0	5.19		4089		243.1	1444.6
WVDEP	11/15/1998	Treatment Inlet	11.7	2.60	7420	4359		179.5	1282.1
DOE	12/10/1998	Treatment Inlet	15.0	9.13		3902		262.1	1453.8

Table E-1a, Omega Mine-pool, Treatment Inlet, Raw Chemical Data

Sampled By	Date	Location	Flow gpm	pH	Sp. Conductance umhos/cm	TDS, mg/L	Temp, C	Acid load, lbs/day CaCO3 Eq	Calc Total Acidity CaCO3 Eq
WVDEP	12/15/1998	Treatment Inlet	11.7	2.60	7800	4465		249.6	1782.3
WVDEP	1/17/1999	Treatment Inlet	93.6	2.90	3360	1591		690.2	613.3
WVDEP	2/14/1999	Treatment Inlet	91.4	2.70	5480	2719		1526.0	1389.1
DOE	2/18/1999	Treatment Inlet	83.0	3.20		3377		1493.6	1497.1
WVDEP	3/14/1999	Treatment Inlet	120.1	2.70	5040	2832		1846.3	1279.4
DOE	3/30/1999	Treatment Inlet	128.0	3.10		3769		2745.3	1785.0
WVDEP	4/13/1999	Treatment Inlet	86.0	2.70	6690	4492		2272.8	2198.1
DOE	4/29/1999	Treatment Inlet	74.0	2.69		4385		1984.8	2232.1
WVDEP	5/17/1999	Treatment Inlet	51.1	2.70	7460	4445		1478.0	2407.7
DOE	5/26/1999	Treatment Inlet	35.6	2.67		4417		879.7	2057.7
WVDEP	6/14/1999	Treatment Inlet	22.9	2.50	18800	5308		673.4	2452.0
DOE	6/29/1999	Treatment Inlet	16.4	4.71		4825		394.2	1999.6
WVDEP	7/13/1999	Treatment Inlet	13.0	2.60	8310	5722		404.9	2593.1
DOE	7/27/1999	Treatment Inlet	10.1	3.03		5220		282.5	2320.6
WVDEP	8/14/1999	Treatment Inlet	9.9	2.80	7990	5903		311.2	2625.7
DOE	8/26/1999	Treatment Inlet	8.0	2.93		5498		235.1	2445.1
WVDEP	9/14/1999	Treatment Inlet	8.1	2.80	9750	5722		248.3	2562.7
DOE	9/29/1999	Treatment Inlet	8.8	2.79		4551		204.3	1931.9
WVDEP	10/15/1999	Treatment Inlet	7.2	2.70	8250	4968		185.2	2148.7
DOE	10/29/1999	Treatment Inlet	7.6	2.91		4211		149.7	1631.4
WVDEP	11/15/1999	Treatment Inlet	5.8	2.80	8670	4703		138.3	1977.1
DOE	12/7/1999	Treatment Inlet	14.4	2.56		4131		305.4	1769.6
WVDEP	12/15/1999	Treatment Inlet	30.0	2.60	5870	3386		506.1	1402.5
WVDEP	1/17/2000	Treatment Inlet	24.0	2.70	7120	4323		546.4	1893.1
WVDEP	2/9/2000	Treatment Inlet	22.0	2.80	7750	4860		539.8	2041.4
WVDEP	3/14/2000	Treatment Inlet	143.0	2.70	6540	3826		3094.2	1800.2
WVDEP	4/14/2000	Treatment Inlet	209.0	2.70	5770	3371		4313.1	1717.0
WVDEP	5/15/2000	Treatment Inlet	99.0	2.80	6400	5354		860.5	723.1
WVDEP	6/15/2000	Treatment Inlet	83.0	2.60	4980	2606		1205.4	1208.0
WVDEP	7/18/2000	Treatment Inlet	92.0	2.70	6170	4018		1705.9	1542.3
WVDEP	8/15/2000	Treatment Inlet	73.0	2.70	5720	3325		1326.5	1512.2
WVDEP	9/15/2000	Treatment Inlet	29.0	2.60	5570	3934		571.8	1641.0
WVDEP	10/15/2000	Treatment Inlet	20.9	2.70	5190	3522		337.5	1342.3
WVDEP	11/15/2000	Treatment Inlet	18.0	2.80	5710	3727		340.2	1571.4
WVDEP	12/15/2000	Treatment Inlet	28.0	2.90	5870	3974		418.0	1241.9
WVDEP	1/15/2001	Treatment Inlet	24.0	2.80	4720	2589		264.2	915.4
WVDEP	2/13/2001	Treatment Inlet	88.0	2.90	6340	4309		1951.8	1845.4

Table E-1a, Omega Mine-pool, Treatment Inlet, Raw Chemical Data

Sampled By	Date	Location	Flow gpm	pH	Sp. Conductance umhos/cm	TDS, mg/L	Temp, C	Acid load, lbs/day CaCO3 Eq	Calc Total Acidity CaCO3 Eq
WVDEP	3/13/2001	Treatment Inlet	158.0	2.80	4210	2703		2219.1	1168.4
WVDEP	4/16/2001	Treatment Inlet	209.0	3.00	3930	2128		2513.6	1000.6
WVDEP	5/15/2001	Treatment Inlet	58.0	2.80	5780	3834		1216.0	1743.6
WVDEP	6/18/2001	Treatment Inlet	68.0	2.80	5290	3343		1168.7	1429.6
WVDEP	7/15/2001	Treatment Inlet	87.0	2.80	4680	3148		1299.5	1242.7
WVDEP	8/15/2001	Treatment Inlet	38.0	2.50	5610	3470		688.7	1508.1
WVDEP	9/14/2001	Treatment Inlet	24.0	2.80	5370	3584		481.9	1669.8
WVDEP	10/15/2001	Treatment Inlet	24.6	2.70	3100	3960	14.4	112.9	381.1
WVDEP	11/15/2001	Treatment Inlet	17.9	2.70	2890	4016	4	341.2	1584.1
WVDEP	12/14/2001	Treatment Inlet	22.0	2.80	2860	2948	10.5	241.9	916.7
WVDEP	1/16/2002	Treatment Inlet	59.6	3.00	1418	1892	21.6	434.8	607.1
WVDEP	2/14/2002	Treatment Inlet	83.8	3.00	1894	2264		667.1	662.4
WVDEP	3/15/2002	Treatment Inlet	55.9	3.10	2290	2852	11.1	715.8	1065.8
WVDEP	4/15/2002	Treatment Inlet	164.4	2.90	1660	1668	13.3	1389.3	702.9
WVDEP	5/15/2002	Treatment Inlet	129.5	2.90	2940	2624	13.3	1387.0	891.3
WVDEP	6/18/2002	Treatment Inlet	77.9	3.00	2120	2936	14.4	403.8	431.5
WVDEP	7/16/2002	Treatment Inlet	0.0					0.0	
WVDEP	8/12/2002	Treatment Inlet	28.9	2.80	2950	3632	15.5	432.3	1242.7
Perry	8/20/2002	Treatment Inlet	7.5	2.77	3040	3457	17.4	107.4	1191.5
WVDEP	9/16/2002	Treatment Inlet	20.0	2.80	3040	3992	15.5	202.5	843.0
WVDEP	10/15/2002	Treatment Inlet	19.3	2.80	3010	3700	15.5	208.6	900.9
WVDEP	11/15/2002	Treatment Inlet	28.9	2.80	239	2560	14.4	292.4	840.4
WVDEP	12/15/2002	Treatment Inlet	74.9	3.00	1523	71	6.1	360.6	400.7
WVDEP	1/14/2003	Treatment Inlet	107.8	2.90	2980	3604	7.8	1753.6	1353.4
WVDEP	2/24/2003	Treatment Inlet	289.5	2.90	1845	1712	6.7	2140.8	615.3
WVDEP	3/18/2003	Treatment Inlet	98.6	2.76	3310	3616	14.44	2178.0	1838.4
WVDEP	4/15/2003	Treatment Inlet	112.0	2.84	2790	2648	13.89	1259.4	935.5
WVDEP	5/20/2003	Treatment Inlet	107.5	2.64	2900	3372	15.56	1976.4	1529.3
WVDEP	6/17/2003	Treatment Inlet	192.6	2.89	1536	172	14.44	1094.2	472.5
WVDEP	8/13/2003	Treatment Inlet	58.2	2.73	2570	2880	15.56	741.3	1059.0
Perry	8/28/2003	Treatment Inlet	44.4	2.70	2450	2357	16.4	484.5	907.9
WVDEP	9/15/2003	Treatment Inlet	62.7	2.65	2360	2520	15	646.6	857.7
WVDEP	10/13/2003	Treatment Inlet	53.8	2.69	2710	3036	15.5	718.3	1111.6
WVDEP	11/18/2003	Treatment Inlet	94.1	2.88	2280	2204	12.2	403.1	356.4
WVDEP	12/19/2003	Treatment Inlet	179.2	2.66	2150	2012	13.3	1437.8	667.5
WVDEP	1/14/2004	Treatment Inlet	116.5	2.94	2810	3468	12.2	1774.1	1267.1
WVDEP	2/17/2004	Treatment Inlet	112.0	2.90	2690	3020	12.2	1437.9	1068.1

Table E-1a, Omega Mine-pool, Treatment Inlet, Raw Chemical Data

Sampled By	Date	Location	Flow gpm	pH	Sp. Conductance umhos/cm	TDS, mg/L	Temp, C	Acid load, lbs/day CaCO3 Eq	Calc Total Acidity CaCO3 Eq
WVDEP	3/23/2004	Treatment Inlet	138.9	2.80	2130	1932	10	1123.6	673.1
WVDEP	4/13/2004	Treatment Inlet	210.6	2.88	1812	1520	11.1	207.1	81.8
WVDEP	5/18/2004	Treatment Inlet	53.8	2.77	2440	2348	11.67	603.2	933.5
WVDEP	6/15/2004	Treatment Inlet	89.6	2.94	2210	2400	15.56	427.4	396.8
WVDEP	7/12/2004	Treatment Inlet	44.8	2.82	2270	2224	15.6	358.6	666.0
WVDEP	8/9/2004	Treatment Inlet	26.9	2.65	2790	3244	15.6	366.0	1132.6
WVDEP	9/14/2004	Treatment Inlet	31.4	2.66	2520	2696	15.6	309.4	820.7
WVDEP	10/18/2004	Treatment Inlet	26.9	2.82	2760	3084	10	318.1	984.4
WVDEP	11/16/2004	Treatment Inlet	58.3	2.82	1955	1704	6.1	374.8	534.5
WVDEP	12/15/2004	Treatment Inlet	71.8	2.83	2190	2304	7.22	764.1	885.3
WVDEP	1/10/2005	Treatment Inlet	179.5	2.83	1936	1696	5.56	1788.5	828.9
WVDEP	2/15/2005	Treatment Inlet	210.9	2.74	2240	2060	10	2141.5	844.6
WVDEP	3/15/2005	Treatment Inlet	152.6	2.88	2400	2652	9.4	2366.5	1290.2
Perry	3/22/2005	Treatment Inlet	75.0	2.53	3320	2904	11	1318.1	1462.1
WVDEP	4/11/2005	Treatment Inlet	125.7	2.64	2780	3420	12.2	1397.2	925.0
WVDEP	5/24/2005	Treatment Inlet	94.2	2.78	2350	2760	10.6	1108.5	978.5
WVDEP	6/14/2005	Treatment Inlet	49.4	2.89	2606	3128	15	555.5	936.1
WVDEP	7/11/2005	Treatment Inlet	31.4	2.59	3130	3984	20	572.5	1516.0
WVDEP	8/15/2005	Treatment Inlet	22.4	2.57	3090	3972	15.6	324.4	1202.7
WVDEP	9/14/2005	Treatment Inlet	18.0	2.59	3200	4092	16.7	314.3	1456.5
WVDEP	10/12/2005	Treatment Inlet	13.5	2.61	3140	4128	15.6	200.9	1241.6
WVDEP	11/15/2005	Treatment Inlet	31.4	2.68	2630	3008	15	348.4	922.7
WVDEP	12/13/2005	Treatment Inlet	49.4	2.53	2820	3632	14.4	746.8	1258.5
WVDEP	1/10/2006	Treatment Inlet	103.2	2.75	2560	3368	7.78	1697.8	1368.4
WVDEP	2/14/2006	Treatment Inlet	166.1	2.59	2880	3576	7.22	2387.5	1196.2
WVDEP	3/13/2006	Treatment Inlet	94.2	2.63	2250	2352	12.2	899.5	794.0
WVDEP	4/17/2006	Treatment Inlet	98.7	2.47	2360	2544	13.3	1135.6	956.8
WVDEP	5/15/2006	Treatment Inlet	80.8	2.67	2070	2324	15.6	697.4	718.2
Perry	5/24/2006	Treatment Inlet	139.8	2.64	2300	2572	13.2	1693.3	1007.7
WVDEP	6/12/2006	Treatment Inlet	62.8	2.36	2590	2888	13.3	912.3	1208.0
WVDEP	7/11/2006	Treatment Inlet	53.9	2.64	2490	2840	14.4	732.7	1131.9
WVDEP	8/14/2006	Treatment Inlet	49.4	2.55	3000	4176	15.6	832.8	1403.5
WVDEP	9/12/2006	Treatment Inlet	26.9	2.50	3260	3520	15.6	447.3	1382.0
WVDEP	10/17/2006	Treatment Inlet	62.7	2.80	2610	2784	14.44	610.6	810.0
WVDEP	11/13/2006	Treatment Inlet	89.6	2.73	2150	2148	14.4	792.5	735.9
WVDEP	12/13/2006	Treatment Inlet	53.8	2.79	3090	3796	12.2	877.3	1357.6
WVDEP	1/15/2007	Treatment Inlet	219.5	2.72	1826	1472	15	1384.4	524.7

Table E-1a, Omega Mine-pool, Treatment Inlet, Raw Chemical Data

Sampled By	Date	Location	Flow gpm	pH	Sp. Conductance umhos/cm	TDS, mg/L	Temp, C	Acid load, lbs/day CaCO3 Eq	Calc Total Acidity CaCO3 Eq
WVDEP	2/14/2007	Treatment Inlet	76.2	2.59	2700	2840	15	987.0	1078.2
WVDEP	3/14/2007	Treatment Inlet	179.2	2.68	2380	2572	15.6	2040.2	947.2
WVDEP	4/18/2007	Treatment Inlet	259.8	2.70	1709	1308	15.6	1670.9	535.0
WVDEP	5/16/2007	Treatment Inlet	71.7	2.63	2580	2988	17.8	649.9	754.3
Perry	5/3/2007	Treatment Inlet	86.0	2.65	2318	2508	13.7	1073.5	1038.5
WVDEP	6/14/2007	Treatment Inlet	40.3	2.51	2990	3148	13.33	544.2	1122.8
WVDEP	7/17/2007	Treatment Inlet	35.8	2.71	3070	3664	12	517.9	1202.3
Perry	8/13/2007	Treatment Inlet	22.5	2.47	3360	3062	16.6	340.0	1257.3
WVDEP	8/15/2007	Treatment Inlet	22.4	2.46	3120	3124	12	347.5	1290.8
WVDEP	9/12/2007	Treatment Inlet	22.4	2.55	2960	3316	12	289.2	1074.0
WVDEP	10/10/2007	Treatment Inlet	17.9	2.55	3130	3388	12	252.1	1170.3
WVDEP	11/26/2007	Treatment Inlet	13.4	2.78	2820	3412	10	188.7	1167.8

Table E-1b, Omega Mine-pool, Treatment Inlet, Raw Chemical Data

Sampled By	Date	Location	Fe3+, mg/L	Fe2+, mg/L	Fe Total, mg/L	Ca, mg/L	Mg, mg/L	Na, mg/L	K, mg/L	Al, mg/L	Mn, mg/L	SO4, mg/L	Cl, mg/L
DOE	2/11/93	Treatment	212	693	905	321.0	168.0	8.3	5.7	167.0	5.32	4098	10
DOE	3/3/1993	Treatment	315	783	1098	289.0	157.0	7.2	5.2	192.0	5.90	4772	7.1
DOE	3/18/1993	Treatment	303	234	537	172.0	85.9	17.6	4.7	94.5	2.70	2581	20.2
DOE	4/2/1993	Treatment	469	391	860	224.0	116.0	8.8	3.6	151.0	3.70	3925	10
DOE	4/14/1993	Treatment	487	556	1043	265.0	138.0	8.3	3.9	180.0	4.50	4744	6.6
DOE	4/29/1993	Treatment	415	291	706	222.0	102.0	7.9	4	122.0	4.70	3274	9.9
DOE	5/20/1993	Treatment	450	584	1034	281.0	145.0	7.3	5.8	181.0	5.20	4494	8.7
DOE	6/3/1993	Treatment	363	245	608	278.0	143.0	9.0	5.7	117.0	5.00	3542	8.5
DOE	6/10/1993	Treatment	342.08	409	751.08	286.1	148.1	8.7	6.93	140.1	5.20	3877	11.6
DOE	6/23/1993	Treatment	327.59	599	926.59	308.1	158.1	7.9	5.96	163.1	5.76	4446	11.8
DOE	7/8/1993	Treatment	308.05	650	958.05	318.7	159.5	7.4	7.67	168.6	6.25	4499	6.2
DOE	7/22/1993	Treatment	271.6	663	934.6	340.9	171.4	7.9	8.47	156.9	6.69	4511	7.2
DOE	8/11/1993	Treatment	269.95	522	791.95	347.5	172.0	7.8	9.15	133.4	6.54	4107	
DOE	9/10/1993	Treatment	265.77	408.2	673.97	349.4	167.1	9.1	9.86	115.4	6.47	3904	
DOE	10/7/1993	Treatment	238.77	310	548.77	328.7	156.7	10.2	9.46	95.8	5.86	3603	15
DOE	10/25/1993	Treatment	244.89	325	569.89	313.1	153.6	12.7	8.43	98.4	5.69	3465	20
DOE	11/10/1993	Treatment	265.02	260	525.02	304.9	145.9	12.5	8.99	89.7	5.68	3282	18
DOE	12/7/1993	Treatment	155.84	180	335.84	161.68	79.4	12.8	2.59	59.5	2.93	1909	22.3
DOE	12/23/1993	Treatment	353.1	517.4	870.5	264.1	137.7	7.9	4.38	155.1	4.69	3981	17.6
DOE	1/28/1994	Treatment	209.23	240.6	449.83	186.0	92.3	16.1	4.13	92.3	3.32	2535	27.7
DOE	5/5/1994	Treatment	318.36	460.5	778.86	235.3	103.9	8.5	4.46	148.1	3.80	3608	33.73
DOE	6/10/1994	Treatment	208.5	482.8	691.3	262.4	120.4	12.5	5.84	138.7	4.36	3458	51.1
DOE	7/6/1994	Treatment	249.76	381.2	630.96	289.6	130.7	13.1	6.93	122.7	4.97	3475	31.5
DOE	8/3/1994	Treatment	222.53	361.7	584.23	275.6	128.1	13.6	7.08	107.2	5.00	3223	42.5
DOE	9/1/1994	Treatment	212.55	234.2	446.75	238.6	108.4	15.4	6.47	87.9	4.30	2734	43.1
DOE	10/7/1994	Treatment	224.67	414.6	639.27	293.3	137.6	12.7	6.86	127.8	5.25	3544	38.22
DOE	11/16/1994	Treatment	149	443.52	592.52	323.2	148.9	11.6	10.07	108.2	6.18	3648	29.2
DOE	12/14/1994	Treatment	137.72	263.2	400.92	223.6	103.3	15.9	6.38	78.2	4.68	2581	34.84
DOE	1/10/1995	Treatment	171.16	343.1	514.26	222.9	109.2	14.4	1.35	99.7	4.28	2707	36.9
DOE	2/3/1995	Treatment	155.97	488.71	644.68	238.2	113.7	14.9	6.34	128.0	4.26	3088	33.92
DOE	3/2/1995	Treatment	135.34	329.73	465.07	203.3	94.1	15.3	5.7	102.3	4.96	2631	37.5
DOE	4/7/1995	Treatment	373.27	680.2	1053.47	273.32	127.9	8.21	4.54	192.14	5.79	4608	33.43
DOE	5/10/1995	Treatment	145.76	430	575.76	212.1	96.7	9.8	6.04	114.9	4.48	2917	23.3
DOE	6/6/1995	Treatment	188.95	381.1	570.05	211.0	96.3	9.5	5.7	118.9	3.98	3364	26.4
DOE	7/13/1995	Treatment	171.74	708.8	880.54	280.65	127.2	8.07	6.58	174.36	5.83	4087.54	18.3
DOE	8/3/1995	Treatment	182.01	452	634.01	309.7	134.5	9.6	8.68	126.9	6.27	3569	28.3

Table E-1b, Omega Mine-pool, Treatment Inlet, Raw Chemical Data

Sampled By	Date	Location	Fe3+, mg/L	Fe2+, mg/L	Fe Total, mg/L	Ca, mg/L	Mg, mg/L	Na, mg/L	K, mg/L	Al, mg/L	Mn, mg/L	SO4, mg/L	Cl, mg/L
DOE	9/7/1995	Treatment	66.62	494.2	560.82	345.64	150.5	10.92	10.4	110	7.75	3693.09	26.1
DOE	10/12/1995	Treatment	125.27	392	517.27	350.25	149.6	12.23	10.4	98.97	7.79	3456.69	15.85
DOE	11/22/1995	Treatment	55.04	160.4	215.44	268.8	110.0	10.4	10.26	48.3	9.33	2321	22.3
DOE	1/5/1996	Treatment	43.57	233.5	277.07	215.2	88.9	9.3	7.97	58.1	6.14	2055	18.31
WVDEP	1/16/1996	Treatment			485					93.1	9.29	3080	
WVDEP	2/15/1996	Treatment			406						4.11	2120	
DOE	2/21/1996	Treatment	286.93	323	609.93	169.9	76.6	15.0	2.79	133.8	3.20	2822	31.7
WVDEP	3/1/1996	Treatment			567						3.05	2360	
WVDEP	3/15/1996	Treatment			686						3.14	3090	
DOE	3/18/1996	Treatment	188	124.6	312.6	151.5	65.6	10.3	4.38	73.0	2.76	1927	21.09
WVDEP	3/28/1996	Treatment			252						2.56	1870	
WVDEP	4/15/1996	Treatment			347						3.87	2320	
DOE	4/26/1996	Treatment	237.52	213.2	450.72	175.7	73.6	9.4	4.31	98.5	3.62	2281	16.73
WVDEP	4/29/1996	Treatment			711						4.91	2920	
WVDEP	5/15/1996	Treatment			423					95.7	3.54	2020	
WVDEP	5/31/1996	Treatment			304					72.1	2.93	1640	
DOE	6/7/1996	Treatment	265.68	263	528.68	201.9	83.3	8.8	4.9	121.5	3.96	2811	13.28
WVDEP	6/14/1996	Treatment			620					144	5.18	2700	
WVDEP	6/28/1996	Treatment			307					0.23	5.24	2100	
WVDEP	7/15/1996	Treatment			282					59.9	5.24	1760	
DOE	7/23/1996	Treatment	195.87	80.5	276.37	184.2	70.6	12.4	4.9	65.6	3.90	1868	21.7
WVDEP	7/30/1996	Treatment			401					87.1	5.27	2570	
WVDEP	8/14/1996	Treatment			508					123	4.98	2540	
DOE	8/28/1996	Treatment	217.52	283.5	501.02	290.4	110.0	11.8	8.39	113.4	5.39	3061	19.84
WVDEP	8/31/1996	Treatment			485					114	5.53	2770	
WVDEP	9/16/1996	Treatment			465					110	6.42	2190	
WVDEP	9/30/1996	Treatment			424					95	5.1	2500	
WVDEP	10/14/1996	Treatment			472					106	0.6	2280	
DOE	10/16/1996	Treatment	207.86	266	473.86	282.5	109.2	11.6	8.1	105.5	5.32	2909	29.68
WVDEP	10/30/1996	Treatment			379					83	4.98	1450	
WVDEP	11/15/1996	Treatment			526					110	3.94	1580	
DOE	11/26/1996	Treatment	203.25	237	440.25	191.77	79.08	9.06	6.16	99.86	3.96	2342.04	16.38
DOE	12/13/1996	Treatment	238.81	213	451.81	175.28	72.1	8.44	5.19	102.47	3.77	2321.13	7.5
WVDEP	12/15/1996	Treatment			467					98	3.97	989	
WVDEP	1/14/1997	Treatment			4.56					102	4.27	1640	
DOE	1/28/1997	Treatment	96.46	108	204.46	107.62	46.08	5.83	3.05	49.99	2.5	1197.62	12.4

Table E-1b, Omega Mine-pool, Treatment Inlet, Raw Chemical Data

Sampled By	Date	Location	Fe3+, mg/L	Fe2+, mg/L	Fe Total, mg/L	Ca, mg/L	Mg, mg/L	Na, mg/L	K, mg/L	Al, mg/L	Mn, mg/L	SO4, mg/L	Cl, mg/L
WVDEP	2/21/1997	Treatment	131.04	141	272.04	189.2	72.71	11.8	4.94	64.2	3.66	1803	23.3
WVDEP	3/17/1997	Treatment			671					147	4.62	2640	
DOE	3/26/1997	Treatment	201.42	134.1	335.52	130.0	52.2	7.0	3.77	76.8	2.90	1724	11.2
WVDEP	4/14/1997	Treatment			742					232	3.66	2580	
WVDEP	5/14/1997	Treatment			457					96.7	4.01	2150	
DOE	5/20/1997	Treatment	90.59	158.1	248.69	117.0	47.6	7.2	3.71	56.9	2.56	1352	
WVDEP	6/16/1997	Treatment			831					204	4.3	1560	
DOE	7/10/1997	Treatment	258.94	213.5	472.44	225.2	87.1	9.5	6.16	113.6	4.45	2628	17.15
WVDEP	7/16/1997	Treatment			344					82.5	4.51	2450	
WVDEP	8/17/1997	Treatment			403					101	554	1420	
DOE	9/10/1997	Treatment	248.78	177.1	425.88	250.2	99.2	11.6	6.86	100.9	5.40	2514	44.75
WVDEP	9/15/1997	Treatment			458						4.8	2220	
WVDEP	10/15/1997	Treatment			500					111	5.05	1460	
DOE	11/5/1997	Treatment	190.52	205.6	396.12	233.7	93.3	12.3	6.19	91.3	5.43	2262	20.05
WVDEP	11/14/1997	Treatment			171					36.4	3.1	1080	
WVDEP	12/15/1997	Treatment			319					80.4	4.09	1850	
DOE	1/12/1998	Treatment	106.56	209.9	316.46	136.1	56.1	13.5	4.07	71.3	2.36	1660	24.2
WVDEP	1/16/1998	Treatment			428					98.8	3.34	2310	
DOE	2/9/1998	Treatment	315.56	287.3	602.86	189.2	79.3	10.35	4.21	145.5	3.5	2893	22.48
WVDEP	2/15/1998	Treatment			429					108	2.91	2410	
WVDEP	3/16/1998	Treatment			511					1.28	2.79	2420	
DOE	3/26/1998	Treatment	228.97	205.5	434.47	146.2	60.2	11.1	3.8	103.2	2.76	2138	
WVDEP	4/15/1998	Treatment			489					127	2.98	2180	
DOE	4/29/1998	Treatment	203.91	207.5	411.41	148.7	60.3	9.5	4.19	100.0	3.11	2079	
WVDEP	5/13/1998	Treatment			502					129	3.44	1900	
DOE	5/28/1998	Treatment	192.9	271.7	464.6	242.2	71.4	11.8	7.06	115.2	3.51	2454	19.72
WVDEP	6/15/1998	Treatment			435					125	4.68	2260	
WVDEP	6/25/1998	Treatment	15.6	365.8	381.4	630.0	64.9	17.5	16.24	70.7	2.79	2897	25.12
WVDEP	7/15/1998	Treatment			697					0	5.22	3410	
DOE	8/5/1998	Treatment	119.14	427.7	546.84	396.9	95.7	32.8	39.36	133.1	4.42	3282	39.99
WVDEP	8/13/1998	Treatment			461					116	5.47	2870	
DOE	9/3/1998	Treatment	226.27	517.7	743.97	333.6	117.1	25.0	26.63	180.5	5.47	3818	32.32
WVDEP	9/15/1998	Treatment			761					199	4.89	3660	
WVDEP	10/15/1998	Treatment			983					268	5.34	4160	
DOE	10/29/1998	Treatment	362.8	74.3	437.1	298.83	120.6	23.84	10.47	117.36	5.4	3021.04	44.49
DOE	11/15/1998	Treatment			348					93.6	7.49	2640	
DOE	12/10/1998	Treatment	351.17	91.73	442.9	302.4	117.6	24.4	14.19	117.0	6.21	2838	30.2

Table E-1b, Omega Mine-pool, Treatment Inlet, Raw Chemical Data

Sampled By	Date	Location	Fe3+, mg/L	Fe2+, mg/L	Fe Total, mg/L	Ca, mg/L	Mg, mg/L	Na, mg/L	K, mg/L	Al, mg/L	Mn, mg/L	SO4, mg/L	Cl, mg/L
WVDEP	12/15/1998	Treatment			526					127	5.25	2520	
WVDEP	1/17/1999	Treatment			149					50.2	2.61	867	
WVDEP	2/14/1999	Treatment			391					105	3.32	2100	
DOE	2/18/1999	Treatment	212.29	213.7	425.99	202.8	84.4	17.3	7.96	125.2	4.04	2474	27.03
WVDEP	3/14/1999	Treatment			370					92.1	3.07	1940	
DOE	3/30/1999	Treatment	234.18	285.1	519.28	209.0	83.6	19.2	8.3	145.4	4.36	2740	31.49
WVDEP	4/13/1999	Treatment			724					143	4.24	2740	
DOE	4/29/1999	Treatment	665.88	4.54	670.42	220.9	96.1	19.4	10.65	165.7	5.10	3162	25.8
WVDEP	5/17/1999	Treatment			639					208	4.6	2970	
DOE	5/26/1999	Treatment	221.36	386.3	607.66	250.0	104.4	19.4	11.11	153.5	5.56	3193	61.6
DOE	6/14/1999	Treatment			748					170	5.66	2410	
DOE	6/29/1999	Treatment	333.21	291.5	624.71	292.53	120.0	18.66	12.47	156.58	5.71	3562.43	20.91
WVDEP	7/13/1999	Treatment			833					174	5.21	2140	
DOE	7/27/1999	Treatment	322.29	394.4	716.69	318.0	132.2	20.5	14.07	176.4	6.14	3796	28.81
WVDEP	8/14/1999	Treatment			870					176	6.1	3500	
DOE	8/26/1999	Treatment	713.33	50.39	763.72	343.6	141.4	23.5	15.26	181.4	6.41	3983	28.37
WVDEP	9/14/1999	Treatment			854					170	5.55	3260	
DOE	9/29/1999	Treatment	191.61	374.7	566.31	331.8	127.9	22.5	13.29	148.2	7.55	3300	23.1
WVDEP	10/15/1999	Treatment			673					150	5.95	2840	
DOE	10/29/1999	Treatment	256.02	194.2	450.22	319.4	131.4	19.4	7	135.5	6.08	3096	35.5
WVDEP	11/15/1999	Treatment			602					146	4.95	3480	
DOE	12/7/1999	Treatment	312.2	204.7	516.9	298.0	116.3	24.5	12.16	125.3	5.80	2983	40.2
WVDEP	12/15/1999	Treatment			388					103	5.57	2180	
WVDEP	1/17/2000	Treatment			536					148	6.4	3240	
WVDEP	2/9/2000	Treatment			627					149	6.59	2980	
WVDEP	3/14/2000	Treatment			516					138	5.5	2590	
WVDEP	4/14/2000	Treatment			496					130	3.85	3080	
WVDEP	5/15/2000	Treatment			15					109	6.39	2970	
WVDEP	6/15/2000	Treatment			335					85.5	4.27	2380	
WVDEP	7/18/2000	Treatment			450					113	5.04	2490	
WVDEP	8/15/2000	Treatment			430					114	5.14	3010	
WVDEP	9/15/2000	Treatment			429					133	4.69	3630	
WVDEP	10/15/2000	Treatment			370					102	7.47	3210	
WVDEP	11/15/2000	Treatment			469					116	4.48	2790	
WVDEP	12/15/2000	Treatment			358					94.8	6.33	1300	
WVDEP	1/15/2001	Treatment			222					77.4	4.87	2210	
WVDEP	2/13/2001	Treatment			570					136	3.55	2390	

Table E-1b, Omega Mine-pool, Treatment Inlet, Raw Chemical Data

Sampled By	Date	Location	Fe3+, mg/L	Fe2+, mg/L	Fe Total, mg/L	Ca, mg/L	Mg, mg/L	Na, mg/L	K, mg/L	Al, mg/L	Mn, mg/L	SO4, mg/L	Cl, mg/L
WVDEP	3/13/2001	Treatment			331					88.4	3.02	1200	
WVDEP	4/16/2001	Treatment			298					74.2	2.69	674	
WVDEP	5/15/2001	Treatment			476					145	3.64	3340	
WVDEP	6/18/2001	Treatment			400					113	3.57	2420	
WVDEP	7/15/2001	Treatment			351					95.3	3.1	2480	
WVDEP	8/15/2001	Treatment			378					120	3.64	1480	
WVDEP	9/14/2001	Treatment			450					140	3.92	2100	
WVDEP	10/15/2001	Treatment			145					2.96	2.96	2677	
WVDEP	11/15/2001	Treatment			472.77					113.41	4.37	2715	
WVDEP	12/14/2001	Treatment			229.13					74.23	8.28	1993	
WVDEP	1/16/2002	Treatment			126.87					58.57	2.55	1279	
WVDEP	2/14/2002	Treatment			152.88					60.16	2.5	1530	
WVDEP	3/15/2002	Treatment			301.95					86.49	2.78	1928	
WVDEP	4/15/2002	Treatment			191.39					52.88	1.98	1128	
WVDEP	5/15/2002	Treatment			265.83					62.75	2.1	1774	
WVDEP	6/18/2002	Treatment			132.67					25.66	0.79	1985	
WVDEP	7/16/2002	Treatment											
WVDEP	8/12/2002	Treatment			312.42					107.79	2.92	2455	
PERRY	8/20/2002	Treatment	60.27	241.10	301.37	247.04	77.52	15.4	13.64	100.84	3.806	2116.3	12.6
WVDEP	9/16/2002	Treatment			92.9					106.35	3.71	2699	
WVDEP	10/15/2002	Treatment			214.92					77.71	2.86	2501	
WVDEP	11/15/2002	Treatment			220.75					64.99	2.74	1731	
WVDEP	12/15/2002	Treatment			87.91					34.3	1.55	48	
WVDEP	1/14/2003	Treatment			384.44					107.62	2.39	2436	
WVDEP	2/24/2003	Treatment			154.23					48.62	3.42	1157	
WVDEP	3/18/2003	Treatment			578.53					128.12	2.18	2444	
WVDEP	4/15/2003	Treatment			243.46					76.27	2.02	1790	
WVDEP	5/20/2003	Treatment			434.29					113.93	2.34	2279	
WVDEP	6/17/2003	Treatment			96.31					42.1	1	116	
WVDEP	8/13/2003	Treatment			281.15					82.57	2.09	1947	
PERRY	8/28/2003	Treatment	175.3	16	191	155	52.3	20.3	6.48	83.1	2.5	1404	5.8
WVDEP	9/15/2003	Treatment			182.29					74.79	2.16	1704	
WVDEP	10/13/2003	Treatment			285.45					89.1	1.89	2052	
WVDEP	11/18/2003	Treatment			0.23					52.21	0.03	1490	
WVDEP	12/19/2003	Treatment			160.24					48.4	1.29	1360	
WVDEP	1/14/2004	Treatment			384.26					93.25	2.03	2344	
WVDEP	2/17/2004	Treatment			338.31					71.26	1.95	2042	

Table E-1b, Omega Mine-pool, Treatment Inlet, Raw Chemical Data

Sampled By	Date	Location	Fe3+, mg/L	Fe2+, mg/L	Fe Total, mg/L	Ca, mg/L	Mg, mg/L	Na, mg/L	K, mg/L	Al, mg/L	Mn, mg/L	SO4, mg/L	Cl, mg/L
WVDEP	3/23/2004	Treatment			164.61					53.47	1.15	1306	
WVDEP	4/13/2004	Treatment			0.7					2.02	1.93	1028	
WVDEP	5/18/2004	Treatment			215.24					82.82	1.74	1587	
WVDEP	6/15/2004	Treatment			95.85					29.72	1.51	1622	
WVDEP	7/12/2004	Treatment			133.01					62.76	1.94	1503	
WVDEP	8/9/2004	Treatment			244.58					104.16	2.3	2193	
WVDEP	9/14/2004	Treatment			160.39					75.62	2.25	1822	
WVDEP	10/18/2004	Treatment			233.22					87.66	2.33	2085	
WVDEP	11/16/2004	Treatment			113.31					45.59	1.49	1152	
WVDEP	12/15/2004	Treatment			222.02					73.99	1.54	1558	
WVDEP	1/10/2005	Treatment			225.12					62.97	1.11	1146	
WVDEP	2/15/2005	Treatment			200.57					70.53	1.5	1393	
WVDEP	3/15/2005	Treatment			354.5					105.5	1.94	1793	
PERRY	3/22/2005	Treatment	267.1	105.5	372	210.75	61.03	18.1	13.28	115.91	2.54	2171.1	44
WVDEP	4/11/2005	Treatment			229.7					71.24	1.9	2312	
WVDEP	5/24/2005	Treatment			222.04					89	1.97	1866	
WVDEP	6/14/2005	Treatment			234.61					80.76	1.64	2115	
WVDEP	7/11/2005	Treatment			354.87					134.45	2.85	2693	
WVDEP	8/15/2005	Treatment			292.35					97.17	2.7	2685	
WVDEP	9/14/2005	Treatment			314.2					136.88	2.8	2766	
WVDEP	10/12/2005	Treatment			252.95					119	2.71	2791	
WVDEP	11/15/2005	Treatment			205.72					80.24	2.29	2033	
WVDEP	12/13/2005	Treatment			286.03					107.19	1.83	2455	
WVDEP	1/10/2006	Treatment			382.03					106.41	2.38	2277	
WVDEP	2/14/2006	Treatment			325.29					86.72	1.92	2417	
WVDEP	3/13/2006	Treatment			189.97					60.16	1.38	1590	
WVDEP	4/17/2006	Treatment			207.22					74.42	1.65	1720	
WVDEP	5/15/2006	Treatment			159.75					58.01	1.66	1571	
PERRY	5/24/2006	Treatment	130	123.3	253.3	144.8	45.1	15	6.6	78.52	1.89	1537.5	50
WVDEP	6/12/2006	Treatment			260.63					93.58	1.78	1952	
WVDEP	7/11/2006	Treatment			224.21					110.21	2.01	1920	
WVDEP	8/14/2006	Treatment			308.17					127.08	2.68	2823	
WVDEP	9/12/2006	Treatment			258.08					136.25	2.72	2380	
WVDEP	10/17/2006	Treatment			187.43					70.49	1.98	1882	
WVDEP	11/13/2006	Treatment			153.34					65.83	1.4	1452	
WVDEP	12/13/2006	Treatment			360.95					112.61	2.6	2566	
WVDEP	1/15/2007	Treatment			95.83					46.1	0.95	995	

Table E-1b, Omega Mine-pool, Treatment Inlet, Raw Chemical Data

Sampled By	Date	Location	Fe3+, mg/L	Fe2+, mg/L	Fe Total, mg/L	Ca, mg/L	Mg, mg/L	Na, mg/L	K, mg/L	Al, mg/L	Mn, mg/L	SO4, mg/L	Cl, mg/L
WVDEP	2/14/2007	Treatment			241.07					92.6	1.99	1920	
WVDEP	3/14/2007	Treatment			248.73					71.1	1.31	1739	
WVDEP	4/18/2007	Treatment			111.98					41.96	0.9	884	
WVDEP	5/16/2007	Treatment			185.56					54.35	1.63	2020	
PERRY	5/3/2007	Treatment	185.6	85.6	270.6	164	43.16	15.55	10.38	79.02	1.724	1679	
WVDEP	6/14/2007	Treatment			254.73					91.45	2.34	2128	
PERRY	7/17/2007	Treatment			285.24					106.18	2.34	2477	
WVDEP	8/13/2007	Treatment			259.3	181.5	61.48	34.55		111.3	2.942	2021	70
WVDEP	8/15/2007	Treatment			266.69					114.36	2.55	2112	
WVDEP	9/12/2007	Treatment			214.5					98.19	1.98	2242	
WVDEP	10/10/2007	Treatment			252.72					103.02	2.56	2290	
WVDEP	11/26/2007	Treatment			243.61					115.92	2.62	2307	

Table E-1c, Omega Mine-pool, PM-21 Spring, Raw Chemical Data

Sampled By	Date	Location	Flow gpm	pH	Sp. Conductance umhos/cm	TDS, mg/L	Temp, C	Acid load, lbs/day CaCO3 Eq	Calc Total Acidity CaCO3 Eq
DOE	11/15/1991	PM-21		2.88		4767		0.0	530.2
DOE	2/11/1993	PM-21		3.06		3288		0.0	449.2
DOE	3/3/1993	PM-21	198.6	2.98		3035		1060.7	444.3
DOE	3/18/1993	PM-21	32.6	3.09		1638		122.5	312.3
DOE	4/2/1993	PM-21	27.2	2.98		2148		153.7	470.2
DOE	4/14/1993	PM-21	39.9	2.95		2808		278.0	579.8
DOE	4/29/1993	PM-21	77.5	2.94		2243		427.4	459.0
DOE	5/20/1993	PM-21	31.6	3.00		3587		273.2	718.4
DOE	6/3/1993	PM-21	35.4	3.00		4128		334.6	787.0
DOE	6/10/1993	PM-21	24.0	2.98		3892		197.0	682.3
DOE	6/23/1993	PM-21	22.8	2.99		3972		171.4	626.4
DOE	7/8/1993	PM-21	17.2	2.97		4026		126.6	613.6
DOE	7/22/1993	PM-21	26.2	2.97		4374		211.5	671.4
DOE	8/11/1993	PM-21	18.0	2.96		4427		129.3	599.1
DOE	9/10/1993	PM-21	2.9	2.94		4405		19.4	561.0
DOE	10/7/1993	PM-21	14.8	2.99		3899		77.0	431.6
DOE	10/25/1993	PM-21	25.5	3.04		3875		131.1	427.1
DOE	11/10/1993	PM-21	25.4	2.95		3525		127.6	417.7
DOE	12/7/1993	PM-21	4.9	3.13		2107		18.8	319.3
DOE	12/23/1993	PM-21	29.5	3.08		2709		156.8	442.6
DOE	1/28/1994	PM-21	84.6	3.14		2237		416.9	410.0
DOE	5/5/1994	PM-21	14.7	3.09		2365		77.3	436.1
DOE	6/10/1994	PM-21	29.0	3.14		3399		217.2	622.9
DOE	7/6/1994	PM-21	36.5	3.12		3849		268.7	612.2
DOE	8/3/1994	PM-21	19.5	2.99		3688		130.9	558.3
DOE	9/1/1994	PM-21	21.4	2.96		3216		123.6	480.8
DOE	10/7/1994	PM-21	15.6	3.35		3689		108.5	576.9
DOE	11/16/1994	PM-21	8.5	3.05		3986		57.6	560.7
DOE	12/14/1994	PM-21	15.8	3.16		3952		100.6	530.3
DOE	1/10/1995	PM-21	19.6	3.03		3538		153.1	649.5
DOE	2/3/1995	PM-21	10.6	3.01		3161		91.4	716.9
DOE	3/2/1995	PM-21	9.9	3.33		2807		68.6	576.2
DOE	4/7/1995	PM-21	11.7	3.1		3064		79.2	561.8
DOE	5/10/1995	PM-21	25.4	3.10		2969		178.9	585.2

Table E-1c, Omega Mine-pool, PM-21 Spring, Raw Chemical Data

Sampled By	Date	Location	Flow gpm	pH	Sp. Conductance umhos/cm	TDS, mg/L	Temp, C	Acid load, lbs/day CaCO3 Eq	Calc Total Acidity CaCO3 Eq
DOE	6/6/1995	PM-21	16.0	3.09		2733		87.5	453.4
DOE	7/13/1995	PM-21	9.5	3.02		3564		62.9	549.9
DOE	8/3/1995	PM-21	11.5	2.98		4011		91.0	659.2
DOE	9/7/1995	PM-21	9.8	3.14		4391		80.7	683.6
DOE	10/12/1995	PM-21	7.3	3.3		4204		56.9	647.1
DOE	11/22/1995	PM-21	10.0	3.22		4099		65.8	546.8
DOE	1/5/1996	PM-21	13.4	3.32		3124		85.4	528.8
WVDEP	1/16/1996	PM-21	9.9	3.2	6790	4066	8.9	90.6	764.6
WVDEP	2/15/1996	PM-21	17.0	2.9	4550	2550	13.3	64.2	313.8
DOE	2/21/1996	PM-21	26.7	3.28		1797		134.6	418.7
WVDEP	3/1/1996	PM-21	20.2	3	2700	1662	8.9	49.8	205.6
WVDEP	3/15/1996	PM-21	74.8	2.9	3110	1819	11.1	200.7	223.2
DOE	3/18/1996	PM-21	85.9	3.35		1550		296.6	287.4
WVDEP	3/28/1996	PM-21	197.1				11.1	0.0	
DOE	4/26/1996	PM-21	28.8	3.02		2146		120.4	348.2
WVDEP	4/29/1996	PM-21	35.8	2.9	4650	2505	13.3	76.0	176.5
WVDEP	5/15/1996	PM-21	39.9	3	3480	1670	11.1	131.0	273.4
WVDEP	5/31/1996	PM-21	61.4	2.9	3340	1504	13.3	208.3	282.3
DOE	6/7/1996	PM-21	28.3	3.00		2363		144.4	425.3
WVDEP	6/14/1996	PM-21	26.0	2.8	5560	2539	13.3	173.7	556.3
WVDEP	6/28/1996	PM-21	25.1	2.8	6360	3550	14.4	111.2	368.7
WVDEP	7/15/1996	PM-21	22.0	2.8	6960	3926	14.4	164.0	621.6
DOE	7/23/1996	PM-21	30.1	2.96		2643		176.6	488.6
WVDEP	7/30/1996	PM-21	23.7	2.8	6390	3536	14.4	162.0	567.7
WVDEP	8/14/1996	PM-21	23.7	2.9	6360	3709	11.1	189.6	664.5
DOE	8/28/1996	PM-21	16.9	3.07		3675		133.8	658.8
WVDEP	8/31/1996	PM-21	26.0	2.9	9300	3774	12.2	177.7	569.0
WVDEP	9/16/1996	PM-21	19.7	2.8	6490	4098	12.2	165.0	696.7
WVDEP	9/30/1996	PM-21	20.6	3	6600	3718	13.3	137.1	553.2
WVDEP	10/14/1996	PM-21	22.9	2.8	6220	2949	14.4	186.5	679.1
DOE	10/16/1996	PM-21	19.0	3.00		3720		149.7	655.1
WVDEP	10/30/1996	PM-21	309.1	2.7	5400	2874	14.4	2271.3	611.3
WVDEP	11/15/1996	PM-21	37.6	2.9	5060	2342	11.1	185.9	411.0
DOE	11/26/1996	PM-21	22.0	2.97		2787		153.2	579.9
DOE	12/13/1996	PM-21	37.0	3.04		2136		190.5	428.8
WVDEP	12/15/1996	PM-21	42.6	3	4350	2255	11.1	200.5	391.9

Table E-1c, Omega Mine-pool, PM-21 Spring, Raw Chemical Data

Sampled By	Date	Location	Flow gpm	pH	Sp. Conductance umhos/cm	TDS, mg/L	Temp, C	Acid load, lbs/day CaCO3 Eq	Calc Total Acidity CaCO3 Eq
WVDEP	1/14/1997	PM-21	31.8	3.1	459	2347	10	135.7	354.9
DOE	1/28/1997	PM-21	21.1	3		1790		88.7	349.8
DOE	2/21/1997	PM-21	22.3	3.11		2200		113.1	422.1
WVDEP	3/17/1997	PM-21	36.7	3	2800	1999	12.2	157.7	357.1
DOE	3/26/1997	PM-21	85.6	3.25		1484		304.9	296.3
WVDEP	4/14/1997	PM-21	17.9	2.8	2980	2167	11.1	100.3	465.6
WVDEP	5/14/1997	PM-21	14.8	2.8	5310	2596	14.4	114.4	643.9
DOE	5/20/1997	PM-21	97.4	3.12		1657		442.1	377.8
WVDEP	6/16/1997	PM-21	13.9	2.7	3320	2676	15.6	115.2	690.0
DOE	7/10/1997	PM-21	10.6	2.97		2966		90.7	711.9
WVDEP	7/16/1997	PM-21	7.6	2.8	3920	3171	20	66.6	727.7
WVDEP	8/17/1997	PM-21	6.7	2.8	6110	3498	15.6	63.7	789.0
DOE	9/10/1997	PM-21	5.8	2.91		3392		56.9	816.0
WVDEP	9/15/1997	PM-21	6.7	2.8	4300	3543	15	39.2	485.6
WVDEP	10/15/1997	PM-21	2.7	2.9	6400	3591		29.8	921.6
DOE	11/5/1997	PM-21	4.5	2.99		3658		51.3	957.9
WVDEP	11/14/1997	PM-21	49.7	2.9	3330	2403		213.8	357.7
WVDEP	12/15/1997	PM-21	13.9	2.8	2990	2357		130.8	783.2
DOE	1/12/1998	PM-21	30.3	2.93		1770		171.5	471.5
WVDEP	1/16/1998	PM-21	179.2	2.8	4540	2372		1440.4	668.7
DOE	2/9/1998	PM-21	27.3	2.96		2500		246.9	752.6
WVDEP	2/15/1998	PM-21	15.7	2.9	3650	2436		122.5	650.2
WVDEP	3/15/1998	PM-21	33.6	2.8	4530	2128		269.2	666.5
DOE	3/26/1998	PM-21	52.2	3.00		1618		317.8	506.7
WVDEP	4/15/1998	PM-21	19.7	2.7	3050	2389		185.4	782.5
DOE	4/29/1998	PM-21	35.3	2.96		1852		253.1	597.0
WVDEP	5/14/1998	PM-21	22.4	2.8	4240	2235		184.9	686.8
DOE	5/28/1998	PM-21	20.0	3.15		2433		179.8	746.9
WVDEP	6/15/1998	PM-21	17.9	2.7	5330	3010		177.5	824.1
DOE	6/25/1998	PM-21	18.8	2.95		2308		140.8	624.3
WVDEP	7/15/1998	PM-21	17.9	2.8	5660	3394		152.5	707.8
DOE	8/5/1998	PM-21	14.3	2.95		3538		155.6	904.6
WVDEP	8/13/1998	PM-21	12.5	2.8	6480	3315		142.4	944.4
DOE	9/3/1998	PM-21	11.8	2.96		3429		124.3	875.4
WVDEP	9/15/1998	PM-21	9.9	2.8	8320	3577		106.7	900.7
WVDEP	10/15/1998	PM-21	5.8	2.8	6580	3646		56.7	810.5

Table E-1c, Omega Mine-pool, PM-21 Spring, Raw Chemical Data

Sampled By	Date	Location	Flow gpm	pH	Sp. Conductance umhos/cm	TDS, mg/L	Temp, C	Acid load, lbs/day CaCO3 Eq	Calc Total Acidity CaCO3 Eq
DOE	10/29/1998	PM-21	5.4	2.96		3979		63.4	969.3
WVDEP	11/15/1998	PM-21	3.6	2.8	7540	3752		42.0	976.2
DOE	12/10/1998	PM-21	3.7	2.96		4003		44.2	999.3
WVDEP	12/15/1998	PM-21	2.7	2.8	7330	3998		30.5	942.3
WVDEP	1/17/1999	PM-21	26.9	3	4110	1712		158.8	491.6
WVDEP	2/14/1999	PM-21	25.5	2.8	6220	3272		353.6	1151.8
DOE	2/18/1999	PM-21	25.1	3.03		3537		371.9	1234.3
WVDEP	3/14/1999	PM-21	30.9	2.9	4800	2546		320.8	863.4
DOE	3/30/1999	PM-21	28.4	3.09		2693		314.3	920.0
WVDEP	4/13/1999	PM-21	33.2	2.8	5390	3113		383.5	962.4
DOE	4/29/1999	PM-21	15.5	2.84		2835		179.6	965.2
WVDEP	5/17/1999	PM-21	18.8	2.7	6140	3254		259.4	1146.6
DOE	5/26/1999	PM-21	16.0	2.62		3142		211.4	1098.8
WVDEP	6/14/1999	PM-21	9.0	2.7	6770	3536		120.4	1117.6
DOE	6/29/1999	PM-21	5.4	2.78		3479		70.1	1085.4
WVDEP	7/14/1999	PM-21	4.0	2.8	6510	4221		50.6	1044.6
DOE	7/27/1999	PM-21	3.1	2.99		3743		41.4	1101.3
WVDEP	8/14/1999	PM-21	3.1	2.8	6630	3937		47.7	1265.0
DEO	8/26/1999	PM-21	2.7	2.90		3955		38.2	1173.9
WVDEP	9/14/1999	PM-21	1.8	2.8	8480	4411		24.2	1122.9
DOE	9/29/1999	PM-21	2.2	2.81		3906		30.3	1170.3
WVDEP	10/15/1999	PM-21	1.8	2.8	7580	4036		24.6	1142.9
DOE	10/29/1999	PM-21	1.6	1.57		6220		48.5	2559.5
WVDEP	11/15/1999	PM-21	0.9	2.8	8150	4471		14.1	1303.1
DOE	12/7/1999	PM-21	5.2	2.67		3988		81.9	1301.4
DOE	12/15/1999	PM-21	7.2	2.8	6290	3452		105.3	1221.9
WVDEP	1/17/2000	PM-21	8.0	2.8	6940	4471		157.8	1636.6
WVDEP	2/8/2000	PM-21	6.0	2.8	6990	4590		108.8	1508.9
WVDEP	3/15/2000	PM-21	30.0	2.7	5630	2958		474.8	1315.7
WVDEP	4/14/2000	PM-21	46.0	2.8	4220	2447		468.1	846.4
WVDEP	5/15/2000	PM-21	25.0	2.8	5010	2977		319.4	1063.0
WVDEP	6/15/2000	PM-21	23.0	2.7	4780	2640		297.9	1078.6
WVDEP	7/18/2000	PM-21	25.0	2.8	4990	2578		326.5	1086.5
WVDEP	8/15/2000	PM-21	19.0	2.8	5340	3453		274.1	1200.0
WVDEP	9/15/2000	PM-21	10.0	2.8	5140	3549		161.7	1346.3
WVDEP	10/15/2000	PM-21	7.0	2.8	4910	3218		111.7	1330.0

Table E-1c, Omega Mine-pool, PM-21 Spring, Raw Chemical Data

Sampled By	Date	Location	Flow gpm	pH	Sp. Conductance umhos/cm	TDS, mg/L	Temp, C	Acid load, lbs/day CaCO3 Eq	Calc Total Acidity CaCO3 Eq
WVDEP	11/15/2000	PM-21	4.0	2.8	5910	3380		94.6	1973.5
WVDEP	12/15/2000	PM-21	4.0	2.7	6040	3877		64.4	1342.4
WVDEP	1/15/2001	PM-21	7.0	2.7	5960	3750		105.7	1257.7
WVDEP	2/13/2001	PM-21	20.0	2.8	5010	2814		336.0	1399.2
WVDEP	3/13/2001	PM-21	37.0	2.8	3710	2334		418.4	940.8
WVDEP	4/16/2001	PM-21	59.0	2.9	3370	1786		560.8	790.7
WVDEP	5/15/2001	PM-21	19.0	2.8	4940	3476		313.6	1373.1
WVDEP	6/18/2001	PM-21	18.0	2.8	4640	3105		266.2	1229.4
WVDEP	7/15/2001	PM-21	19.0	2.8	4140	2687		225.1	985.4
WVDEP	8/15/2001	PM-21	12.0	2.6	5670	3590		206.6	1430.8
WVDEP	9/14/2001	PM-21	7.0	2.7	5020	3585		123.3	1468.0
WVDEP	10/15/2001	PM-21	5.8	2.6	3760	4920	10.5	100.6	1438.5
WVDEP	11/15/2001	PM-21	4.5	2.7	3110	4168	11.1	72.3	1342.3
WVDEP	12/14/2001	PM-21	4.0	2.9	3530	4052	10.5	47.2	985.0
WVDEP	1/16/2002	PM-21	15.7	3	1604	2220	23.4	141.5	750.8
WVDEP	2/14/2002	PM-21	19.0	2.9	2370	2792	11.1	195.8	859.6
WVDEP	3/14/2002	PM-21	14.8	2.9	2500	3096	14.4	13.8	77.8
WVDEP	5/15/2002	PM-21	20.6	3	2600	2436	12.2	194.5	785.3
WVDEP	6/18/2002	PM-21	20.0	3.1	1978	2332	14.4	61.4	255.6
WVDEP	7/16/2002	PM-21	0.0						
WVDEP	8/12/2002	PM-21	0.0						
PERRY	8/20/2002	PM-21	7.1	2.87	3150	3664	11.8	108.6	1279.9
WVDEP	9/16/2002	PM-21	0.0						
WVDEP	10/15/2002	PM-21	2.7	2.9	3280	4024	14.4	33.2	1028.1
WVDEP	1/14/2003	PM-21	0.0						
WVDEP	2/24/2003	PM-21	39.9	3.1	1661	1448	5.6	233.0	485.5
WVDEP	4/15/2003	PM-21	0.0						
WVDEP	4/15/2003	PM-21	0.0						
WVDEP	5/20/2003	PM-21	0.0						
WVDEP	6/17/2003	PM-21	98.6	2.96	1288	2840	15.56	372.7	314.6
WVDEP	8/13/2003	PM-21							
PERRY	8/28/2003	PM-21	11.0	2.81	3190	3021	12.6	159.0	1201.6
WVDEP	9/15/2003	PM-21	9.0	2.59	2670	3012	15	104.2	967.8
WVDEP	10/14/2003	PM-21							
WVDEP	1/14/2004	PM-21	31.4	2.81	2150	1896	7.2	274.8	729.0
WVDEP	4/13/2004	PM-21	80.6	2.88	1791	1268	12.2	75.5	77.9

Table E-1c, Omega Mine-pool, PM-21 Spring, Raw Chemical Data

Sampled By	Date	Location	Flow gpm	pH	Sp. Conductance umhos/cm	TDS, mg/L	Temp, C	Acid load, lbs/day CaCO3 Eq	Calc Total Acidity CaCO3 Eq
WVDEP	7/12/2004	PM-21	9.0	2.68	3120	3188	14.4	125.5	1165.3
WVDEP	8/9/2004	PM-21	0.0						
WVDEP	10/18/2004	PM-21	9.0	2.7	3360	3776	12.2	144.5	1341.4
PERRY	3/22/2005	PM-21	21.8	3.02	3180	5432	10.9	700.4	2671.7
PERRY	5/24/2006	PM-21	24.3	2.48	3470	4094	11.9	522.1	1787.4
PERRY	5/3/2007	PM-21	25.3	2.52	2915	3308	12	470.8	1548.2
PERRY	9/13/2007	PM-21	6.9	2.35	4630	5196	11.7	181.6	2189.5

Table E-1d, Omega Mine-pool, PM-21 Spring, Raw Chemical Data

Sampled By	Date	Location	Fe3+, mg/L	Fe2+, mg/L	Fe Total, mg/L	Ca, mg/L	Mg, mg/L	Na,mg/L	K, mg/L	Al, mg/L	Mn, mg/L	SO4, mg/L	Cl, mg/L
DOE	11/15/1991	PM-21	139.8	2.2	142	607.0	194.0	9.8		36.5	4.00	3750	23.5
DOE	2/11/1993	PM-21	91.4	3	91.4	316.0	141.0	7.7	10.5	42.2	4.14	2656	10.9
DOE	3/3/1993	PM-21	86.8	7	93.8	261.0	126.0	7.4	8.4	39.1	3.70	2482	6.5
DOE	3/18/1993	PM-21	72.5	2.7	75.2	139.0	63.5	7.5	6.1	24.1	1.70	1310	7.3
DOE	4/2/1993	PM-21	116.8	5.2	122	173.0	77.8	6.1	6.1	35.2	2.10	1713	7.3
DOE	4/14/1993	PM-21	138.7	10.3	149	214.0	98.3	6.9	6.1	45.4	2.60	2270	9.2
DOE	4/29/1993	PM-21	108.7	8.3	117	174.0	76.2	5.6	6.5	33.9	2.10	1817	5.6
DOE	5/20/1993	PM-21	156.4	42.6	199	296.0	140.0	8.4	10.4	54.6	4.80	2855	7.8
DOE	6/3/1993	PM-21	182.6	40.4	223	352.0	173.0	10.2	12.7	58.8	6.10	3274	7
DOE	6/10/1993	PM-21	160.71	23.6	184.31	322.3	160.4	8.9	10.93	52.2	5.48	3128	7.7
DOE	6/23/1993	PM-21	154.39	8.7	163.09	333.7	160.4	9.5	11.15	49.2	5.46	3222	7.8
DOE	7/8/1993	PM-21	161.31	6.2	167.51	349.2	167.4	9.3	11.68	44.7	6.49	3250	9.3
DOE	7/22/1993	PM-21	172.84	25.2	198.04	380.5	183.8	10.0	12.37	45.2	6.81	3517	9.7
DOE	8/11/1993	PM-21	152.5	12.3	164.8	394.83	192.8	9.9	13.66	42.7	6.64	3593	
DOE	9/10/1993	PM-21	140.17	9.7	149.87	401.3	191.2	9.9	15.08	40.3	6.26	3583	
DOE	10/7/1993	PM-21	106.68	5.3	111.98	348.5	166.3	9.4	12.71	30.7	5.05	3203	11.7
DOE	10/25/1993	PM-21	112.06	3.3	115.36	358.6	173.6	9.8	12.99	29.7	5.56	3157	5.9
DOE	11/10/1993	PM-21	100.48	4.3	104.78	333.7	157.3	10.4	12.09	29.6	5.15	2858	13.3
DOE	12/7/1993	PM-21	66.01	8.6	74.61	195.9	93.8	6.9	7.39	25.8	2.87	1682	12.4
DOE	12/23/1993	PM-21	88.92	3.6	92.52	242.9	119.3	7.4	8.18	41.2	3.70	2172	13.9
DOE	1/28/1994	PM-21	84.6	3.14	77.66	7.7	85.36	193.5	92.6	6.0	6.5	38.8	3.03
DOE	5/5/1994	PM-21	14.7	3.09	64.49	29.5	93.99	199.2	90.8	6.8	7.42	39.8	3.34
DOE	6/10/1994	PM-21	29.0	3.14	52.43	92.8	145.23	278.4	124.4	12.1	9.34	57.4	4.15
DOE	7/6/1994	PM-21	36.5	3.12	49.36	119	168.36	327.4	145.7	14.1	10.55	47.3	5.47
DOE	8/3/1994	PM-21	19.5	2.99	39.9	112.7	152.6	317.7	145.1	17.4	10.35	40.3	5.60
DOE	9/1/1994	PM-21	21.4	2.96	24.81	105.6	130.41	279.8	125.5	13.4	10.82	33.1	4.83
DOE	10/7/1994	PM-21	15.6	3.35	22.53	144.4	166.93	326.2	151.2	12.7	10.42	44.0	6.08
DOE	11/16/1994	PM-21	8.5	3.05	27.94	130.85	158.79	351.8	164.3	13.7	11.59	39.7	6.31
DOE	12/14/1994	PM-21	15.8	3.16	15.81	138.9	154.71	352.9	162.6	13.9	13.07	37.3	6.45
DOE	1/10/1995	PM-21	19.6	3.03	17.59	165.2	182.79	309.4	149.4	11.3	9.9	47.8	5.65
DOE	2/3/1995	PM-21	10.6	3.01	11.23	163.69	174.92	273.9	127.5	10.0	8.49	62.3	4.72
DOE	3/2/1995	PM-21	9.9	3.33	16.99	124.41	141.4	242.7	112.8	9.4	8.09	52.6	4.00
DOE	4/7/1995	PM-21	11.7	3.1	8.83	125.5	134.33	248.67	108.81	9.46	7.86	49.23	4.45
DOE	5/10/1995	PM-21	25.4	3.10	12.48	124.8	137.28	236.1	102.7	8.3	7.42	52.6	4.24
DOE	6/6/1995	PM-21	16.0	3.09	41.57	54.6	96.17	222.3	94.6	7.3	7.77	42.0	3.95

Table E-1d, Omega Mine-pool, PM-21 Spring, Raw Chemical Data

Sampled By	Date	Location	Fe3+, mg/L	Fe2+, mg/L	Fe Total, mg/L	Ca, mg/L	Mg, mg/L	Na, mg/L	K, mg/L	Al, mg/L	Mn, mg/L	SO4, mg/L	Cl, mg/L
DOE	7/13/1995	PM-21	9.5	3.02	32.51	106.8	139.31	302.5	129.77	9.22	9.54	43.59	5.82
DOE	8/3/1995	PM-21	7.55	186	193.55	370.9	149.5	10.4	11.8	44.5	7.17	3187	26.1
DOE	9/7/1995	PM-21	11.37	209.2	220.57	404.72	168.7	11.05	13.03	42.84	7.96	3491	21.2
DOE	10/12/1995	PM-21	0	216.09	216.09	396.07	168.9	10.41	12.76	39.8	7.69	3323	19.61
DOE	11/22/1995	PM-21	20.95	150	170.95	396.7	162.7	10.9	13.59	35.4	7.57	3278	15.5
DOE	1/5/1996	PM-21	2.31	142.3	144.61	299.0	120.1	9.5	9.69	42.3	5.94	2465	21.43
WVDEP	1/16/1996	PM-21			194					67	7.42	3060	
WVDEP	2/15/1996	PM-21			136						4.05	1710	
DOE	2/21/1996	PM-21	18.89	69.2	88.09	167.6	67.9	6.7	5.16	41.2	3.22	1403	8.88
WVDEP	3/1/1996	PM-21			84.1						2.74	1230	
WVDEP	3/15/1996	PM-21			86.2						3.25	1560	
DOE	3/18/1996	PM-21	22.82	35.3	58.12	141.8	58.0	5.4	5.34	28.1	2.68	1237	9.58
WVDEP	3/28/1996	PM-21											
DOE	4/26/1996	PM-21	52.09	1.5	53.59	193.7	80.6	7.1	7.52	35.7	3.46	1752	7.44
WVDEP	4/29/1996	PM-21			59.5						3.87	2050	
WVDEP	5/15/1996	PM-21			41.8					25.9	2.57	1170	
WVDEP	5/31/1996	PM-21			44.5					24.4	2.26	1090	
DOE	6/7/1996	PM-21	74.01	3.5	77.51	216.4	87.1	7.1	7.78	41.3	4.05	1903	12.16
WVDEP	6/14/1996	PM-21			103					51	5.13	2430	
WVDEP	6/28/1996	PM-21			131					8.02	5.68	2350	
WVDEP	7/15/1996	PM-21			111					59.8	6.29	2620	
DOE	7/23/1996	PM-21	94.54	8.7	103.24	258.7	98.9	7.8	8.04	43.2	4.87	2093	19
WVDEP	7/30/1996	PM-21			128					44.9	5.39	2540	
WVDEP	8/14/1996	PM-21			139					61.6	5.77	2510	
DOE	8/28/1996	PM-21	131.91	9.1	141.01	370.8	138.3	10.3	11.07	63.5	6.14	2909	14.56
WVDEP	8/31/1996	PM-21			114					51.2	9.6	2600	
WVDEP	9/16/1996	PM-21			149					60.9	6.76	2650	
WVDEP	9/30/1996	PM-21			124					48.8	5.55	2620	
WVDEP	10/14/1996	PM-21			151					57.2	6.43	2380	
DOE	10/16/1996	PM-21	121.38	27.5	148.88	368.9	141.9	10.5	10.83	58.6	7.07	2943	20.24
WVDEP	10/30/1996	PM-21			95.8					59	6.72	1930	
WVDEP	11/15/1996	PM-21			81.4					35.2	3.71	1890	
DOE	11/26/1996	PM-21	101.73	28.3	130.03	260.2	105.5	8.06	8.98	51.19	5.04	2198	11.88
DOE	12/13/1996	PM-21	75.56	21.2	96.76	201.43	80.31	6.93	7.53	36.49	3.98	1687	10.82
WVDEP	12/15/1996	PM-21			84.6					33.1	3.6	1160	
WVDEP	1/14/1997	PM-21			72.3					32.1	4.05	1350	
DOE	1/28/1997	PM-21	55.104	13.776	68.88	173.62	69.81	5.78	5.95	30.65	3.39	1417	10.1

Table E-1d, Omega Mine-pool, PM-21 Spring, Raw Chemical Data

Sampled By	Date	Location	Fe3+, mg/L	Fe2+, mg/L	Fe Total, mg/L	Ca, mg/L	Mg, mg/L	Na, mg/L	K, mg/L	Al, mg/L	Mn, mg/L	SO4, mg/L	Cl, mg/L
DOE	2/21/1997	PM-21	81.2	19.9	101.1	231.4	82.21	6.5	7.22	35.1	3.96	1715	12.7
WVDEP	3/17/1997	PM-21			81.4					28	3.18	1380	
DOE	3/26/1997	PM-21	29.26	40.7	69.96	144.6	53.8	5.4	5.41	24.8	2.76	1167	7
WVDEP	4/14/1997	PM-21			100					36	4.04	1620	
WVDEP	5/14/1997	PM-21			169					45.6	4.79	1950	
DOE	5/20/1997	PM-21	27.54	66.4	93.94	159.5	60.4	5.3	5.4	29.9	2.97	1295	
WVDEP	6/16/1997	PM-21			188					44.2	4.46	1220	
DOE	7/10/1997	PM-21	67.52	118.6	186.12	287.2	106.2	7.9	8.1	56.7	5.61	2289	11.65
WVDEP	7/16/1997	PM-21			166					61.3	5.86	2210	
WVDEP	8/17/1997	PM-21			220					54.9	5.99	1720	
DOE	9/10/1997	PM-21	80.46	149.2	229.66	342.4	130.9	8.8	8.66	59.6	6.76	2582	13.87
WVDEP	9/15/1997	PM-21			221						5.84	2250	
WVDEP	10/15/1997	PM-21			294					57.9	5.8	2100	
DOE	11/5/1997	PM-21	35.16	256.5	291.66	353.4	140.5	10.0	8.73	67.2	6.29	2757	13
WVDEP	11/14/1997	PM-21			81.1					26	2.82	1370	
WVDEP	12/15/1997	PM-21			170					70.3	4.93	2140	
DOE	1/12/1998	PM-21	60.25	37	97.25	164.1	67.5	7.2	5.57	42.0	3.00	1369	8.4
WVDEP	1/16/1998	PM-21			129					63.2	4.05	1830	
DOE	2/9/1998	PM-21	102.09	50.1	152.19	221.5	90.3	6.65	4.88	75.2	4.1	1925	11.81
WVDEP	2/15/1998	PM-21			141					59.2	3.22	1710	
WVDEP	3/15/1998	PM-21			127					63.7	3.26	1610	
DOE	3/26/1998	PM-21	73.82	28.9	102.72	145.9	57.6	5.7	3.68	48.2	2.65	1246	
WVDEP	4/15/1998	PM-21			162					69.6	3.32	1600	
DOE	4/29/1998	PM-21	68.93	55.3	124.23	161.2	64.1	5.7	4.1	56.6	2.94	1427	
WVDEP	5/14/1998	PM-21			154					58.7	3.12	1500	
DOE	5/28/1998	PM-21	63.54	103	166.54	219.1	85.6	8.0	5.08	73.1	4.04	1842	21.77
WVDEP	6/15/1998	PM-21			162					76.6	4.81	2060	
DOE	6/25/1998	PM-21	42.18	86.1	128.28	212.3	83.7	8.1	5.02	59.5	4.36	1788	10.43
WVDEP	7/15/1998	PM-21			141					65.9	5.47	2460	
DOE	8/5/1998	PM-21	139.97	25	164.97	331.4	133.7	12.0	8.05	97.3	6.92	2757	14.74
WVDEP	8/13/1998	PM-21			198					89.9	6.16	2420	
DOE	9/3/1998	PM-21	126.93	56.3	183.23	318.7	131.3	10.0	7.38	86.4	6.89	2658	16.48
WVDEP	9/15/1998	PM-21			198					81.8	6.86	2580	
WVDEP	10/15/1998	PM-21			171					74.4	6.46	2140	
DOE	10/29/1998	PM-21	115.11	109.1	224.21	379.0	156.3	13.6	7.38	89.8	7.67	3071	16.95
WVDEP	11/15/1998	PM-21			192					97.1	7.55	2300	
DOE	12/10/1998	PM-21	124.15	114.86	239.01	388.6	158.8	12.9	6.69	90.6	7.31	3073	13.2

Table E-1d, Omega Mine-pool, PM-21 Spring, Raw Chemical Data

Sampled By	Date	Location	Fe3+, mg/L	Fe2+, mg/L	Fe Total, mg/L	Ca, mg/L	Mg, mg/L	Na, mg/L	K, mg/L	Al, mg/L	Mn, mg/L	SO4, mg/L	Cl, mg/L
WVDEP	12/15/1998	PM-21			231					79	5.83	2520	
WVDEP	1/17/1999	PM-21			92.8					48.5	3.28	1190	
WVDEP	2/14/1999	PM-21			225					119	4.7	2430	
DOE	2/18/1999	PM-21	177.18	55.2	232.38	279.02	115.12	9.74	4.87	136.98	5.79	2727	14.21
WVDEP	3/14/1999	PM-21			169					88.3	4	1950	
DOE	3/30/1999	PM-21	142.91	19.84	162.75	224.0	88.0	8.1	4.64	104.4	4.52	2074	11.74
WVDEP	4/13/1999	PM-21			166					104	4.51	2070	
DOE	4/29/1999	PM-21	142.61	24.04	166.65	239.9	96.6	8.6	4.48	105.3	5.35	2183	13.35
WVDEP	5/17/1999	PM-21			260					103	4.99	2280	
DOE	5/26/1999	PM-21	150.7	49.8	200.5	258.0	106.5	8.4	4.81	109.8	5.59	2422	13.6
WVDEP	6/14/1999	PM-21			215					112	5.86	2120	
DOE	6/29/1999	PM-21	134.07	68.5	202.57	301.9	124.09	8.94	5.26	113.07	6.33	2691	12.59
WVDEP	7/14/1999	PM-21			198					108	5.96	2100	
DOE	7/27/1999	PM-21	124.19	97.78	221.97	337.7	141.6	9.9	5.07	115.3	6.62	2873	18.48
WVDEP	8/14/1999	PM-21			283					120	6.79	2800	
DEO	8/26/1999	PM-21	130.6	115.2	245.8	360.4	151.1	12.9	5.29	118.6	6.73	3025	16.18
WVDEP	9/14/1999	PM-21			248					106	5.91	2510	
DOE	9/29/1999	PM-21	115.04	138.21	253.25	367.2	151.0	11.0	4.77	112.9	6.76	2969	16.9
WVDEP	10/15/1999	PM-21			249					109	6.77	2500	
DOE	10/29/1999	PM-21	133.4	159.3	292.7	387.3	163.0	10.6	4.21	121.9	6.94	3220	2000
WVDEP	11/15/1999	PM-21			299					122	5.91	3360	
DOE	12/7/1999	PM-21	153.45	120.6	274.05	351.1	149.4	10.3	4.24	124.6	6.47	3037	16.6
DOE	12/15/1999	PM-21			248					124	5.37	2630	
WVDEP	1/17/2000	PM-21			314					177	6.5	3410	
WVDEP	2/8/2000	PM-21			296					160	5.95	3120	
WVDEP	3/15/2000	PM-21			222					146	4.06	2000	
WVDEP	4/14/2000	PM-21			131					94.8	3.29	2010	
WVDEP	5/15/2000	PM-21			166					122	4.8	2740	
WVDEP	6/15/2000	PM-21			167					121	4.18	2360	
WVDEP	7/18/2000	PM-21			183					121	4.07	2170	
WVDEP	8/15/2000	PM-21			205					134	5.11	3220	
WVDEP	9/15/2000	PM-21			240	264				149	5.25	2840	
WVDEP	10/15/2000	PM-21			249					143	5.75	2890	
WVDEP	11/15/2000	PM-21			162					287	5.35	2620	
WVDEP	12/15/2000	PM-21			261					138	4.77	2630	
WVDEP	1/15/2001	PM-21			223					135	4.75	3430	
WVDEP	2/13/2001	PM-21			237					160	3.71	2810	

Table E-1d, Omega Mine-pool, PM-21 Spring, Raw Chemical Data

Sampled By	Date	Location	Fe3+, mg/L	Fe2+, mg/L	Fe Total, mg/L	Ca, mg/L	Mg, mg/L	Na, mg/L	K, mg/L	Al, mg/L	Mn, mg/L	SO4, mg/L	Cl, mg/L
WVDEP	3/13/2001	PM-21			146					107	3.12	1860	
WVDEP	4/16/2001	PM-21			145					83.4	2.64	1500	
WVDEP	5/15/2001	PM-21			206					165	4.57	2530	
WVDEP	6/18/2001	PM-21			197					142	4.72	2610	
WVDEP	7/15/2001	PM-21			161					110	3.75	2000	
WVDEP	8/15/2001	PM-21			231					159	4.55	1820	
WVDEP	9/14/2001	PM-21			248					165	4.15	2220	
WVDEP	10/15/2001	PM-21			241					157	5.03	3326	
WVDEP	11/15/2001	PM-21			267.5					135.75	5.16	2818	
WVDEP	12/14/2001	PM-21			193.28					102.09	4.87	2739	
WVDEP	1/16/2002	PM-21			119.01					87.02	2.37	1501	
WVDEP	2/14/2002	PM-21			121.57					103.34	2.7	1887	
WVDEP	3/14/2002	PM-21			0.08					2.26	1.21	2093	
WVDEP	5/15/2002	PM-21			138.51					86.98	2.24	1647	
WVDEP	6/18/2002	PM-21			95.8					7.74	0.73	1576	
WVDEP	7/16/2002	PM-21											
WVDEP	8/12/2002	PM-21											
PERRY	8/20/2002	PM-21	45.478	181.912	227.39	214.41	87.18	9.8	3.69	143.75	3.703	2195	11.1
WVDEP	9/16/2002	PM-21											
WVDEP	10/15/2002	PM-21			189.43					111.49	3.65	2720	
WVDEP	1/14/2003	PM-21											
WVDEP	2/24/2003	PM-21			73.44					55.56	3.1	979	
WVDEP	4/15/2003	PM-21											
WVDEP	4/15/2003	PM-21											
WVDEP	5/20/2003	PM-21											
WVDEP	6/17/2003	PM-21			46.01					31.69	0.75	1920	
WVDEP	8/13/2003	PM-21											
PERRY	8/28/2003	PM-21	68.7	103.8	209	169	68.2	11.3		134	3	1792	
WVDEP	9/15/2003	PM-21			158.49					99.33	2.03	2036	
WVDEP	10/14/2003	PM-21											
WVDEP	1/14/2004	PM-21			118.41					78.62	1.54	1282	
WVDEP	4/13/2004	PM-21			1.13					1.5	0.89	857	
WVDEP	7/12/2004	PM-21			184.86					130.62	2.28	2155	
WVDEP	8/9/2004	PM-21											
WVDEP	10/18/2004	PM-21			218.24					152.22	2.87	2553	
PERRY	3/22/2005	PM-21	381.00	280.00	658.2	178.23	95.26	4.68	2.8	259.07	3.36	3858	20
PERRY	5/24/2006	PM-21	321.00	111.60	431.4	153.6	60.8	5.36	2.3	152.1	2.43	2411	6

313

Table E-1d, Omega Mine-pool, PM-21 Spring, Raw Chemical Data

Sampled By	Date	Location	Fe3+, mg/L	Fe2+, mg/L	Fe Total, mg/L	Ca, mg/L	Mg, mg/L	Na, mg/L	K, mg/L	Al, mg/L	Mn, mg/L	SO4, mg/L	Cl, mg/L
PERRY	5/3/2007	PM-21	86.00	294.00	379.27	121.1	46.6	5.07	2.72	128.58	2.07	2340	35
PERRY	9/13/2007	PM-21			432	206.5	87.23	39.36	2.108	213.2	4.02	3212	80

Table E-1e, Omega Mine-pool, Marshall Spring, Raw Chemical Data

Sampled By	Date	Location	Flow gpm	pH	Sp. Conductance umhos/cm	TDS, mg/L	Temp, C	Acid load, lbs/day CaCO3 Eq	Calc Total Acidity CaCO3 Eq
DOE	11/15/91	Marshall		3.12		6770			2631.1
DOE	02/11/93	Marshall		2.51		10961			5957.6
DOE	03/03/93	Marshall	39.6	2.54		10313		2632.5	5533.3
DOE	03/18/93	Marshall	20.5	2.49		10212		1366.8	5553.4
DOE	04/02/93	Marshall	65.3	2.37		10703		4635.3	5903.6
DOE	04/14/93	Marshall	69.2	2.31		11060		5117.6	6150.5
DOE	04/29/93	Marshall	65.3	2.37		10650		4635.3	5903.6
DOE	05/20/93	Marshall	57.7	2.52		8540		3209.6	4630.8
DOE	06/03/93	Marshall	5.0	2.62		8306		269.6	4482.2
DOE	06/10/93	Marshall	14.9	2.60		8398		812.6	4551.2
DOE	06/23/93	Marshall	31.2	2.59		8688		1743.4	4643.7
DOE	07/08/93	Marshall	27.9	2.67		8215		1498.3	4466.4
DOE	07/22/93	Marshall	10.1	2.72		7508		482.5	3972.2
DOE	08/11/93	Marshall	18.6	2.94		6680		771.1	3457.3
DOE	09/02/93	Marshall	8.8	2.95		6442		342.5	3228.0
DOE	09/10/93	Marshall	8.8	2.94		6373		340.4	3208.9
DOE	10/07/93	Marshall	5.2	3.01		6561		200.9	3216.9
DOE	10/25/93	Marshall	7.6	2.97		6855		322.7	3516.7
DOE	11/10/93	Marshall	7.6	3.01		6667		308.2	3358.8
DOE	12/07/93	Marshall	10.2	3.22		6443		388.7	3173.4
DOE	12/23/93	Marshall	10.2	2.65		9569		627.1	5119.1
DOE	01/28/94	Marshall	27.9	2.61		10216		1862.4	5551.5
DOE	05/05/94	Marshall	49.2	2.55		6781		2088.7	3528.5
DOE	06/10/94	Marshall	27.9	2.70		6874		1215.0	3621.8
DOE	07/06/94	Marshall	12.8	2.74		6519		524.8	3406.7
DOE	08/03/94	Marshall	11.5	2.88		6345		452.4	3268.0
DOE	09/01/94	Marshall	6.3	2.86		6931		269.5	3552.7
DOE	10/07/94	Marshall	8.2	2.90		7048		355.4	3625.3
DOE	11/16/94	Marshall	8.1	3.04		6500		319.9	3266.3
DOE	12/14/94	Marshall	7.6	3.09		6502		290.0	3166.4
DOE	01/10/95	Marshall	7.7	3.05		6594		312.9	3368.7
DOE	02/03/95	Marshall	10.0	2.92		7147		438.8	3666.8
DOE	03/02/95	Marshall	10.0	2.68		7447		462.2	3859.9
DOE	04/07/95	Marshall	11.3	2.55		7915		567.0	4191.3
DOE	05/10/95	Marshall	36.2	2.91		7256		1656.9	3808.8
DOE	06/06/95	Marshall	36.8	2.69		7600		1803.7	4080.6

Table E-1e, Omega Mine-pool, Marshall Spring, Raw Chemical Data

Sampled By	Date	Location	Flow gpm	pH	Sp. Conductance umhos/cm	TDS, mg/L	Temp, C	Acid load, lbs/day CaCO3 Eq	Calc Total Acidity CaCO3 Eq
DOE	07/13/95	Marshall	36.8	3.78		6855		1566.7	3537.5
DOE	08/03/95	Marshall	10.7	2.94		6470		437.5	3401.3
DOE	09/07/95	Marshall	7.5	3.07		6860		302.7	3355.5
DOE	10/12/95	Marshall	6.1	3.19		6249		225.9	3102.7
DOE	11/22/95	Marshall	5.6	3.21		5801		194.9	2872.8
DOE	01/05/96	Marshall	11.2	3.13		6915		476.9	3542.2
DOE	02/21/96	Marshall	23.4	2.29		10310		1650.3	5856.1
DOE	03/18/96	Marshall	64.3	2.44		8108		3429.1	4436.0
DOE	04/26/96	Marshall	56.4	2.51		6103		2249.0	3319.2
DOE	06/07/96	Marshall	31.0	2.62		5576		1111.0	2984.4
DOE	07/23/96	Marshall	15.1	3.00		5617		532.2	2938.0
DOE	08/28/96	Marshall	19.2	2.87		6229		744.0	3227.8
DOE	10/16/96	Marshall	17.0	3.00		5811		603.3	2944.1
DOE	11/26/96	Marshall	32.8	2.75		6121		1259.5	3194.1
DOE	12/13/96	Marshall	57.7	2.66		6087		2243.8	3235.1
DOE	01/28/97	Marshall	13.3	2.63		5755		502.8	3154.3
DOE	02/21/97	Marshall	9.5	2.69		5801		356.5	3113.3
DOE	03/26/97	Marshall	65.2	2.57		6025		2540.3	3241.7
DOE	05/20/97	Marshall	40.6	2.91		4634		1180.9	2418.6
DOE	07/10/97	Marshall	17.6	2.90		5152		570.8	2690.6
DOE	09/10/97	Marshall	9.5	3.03		4692		273.4	2404.5
DOE	11/05/97	Marshall	7.1	3.04		4375		191.0	2227.7
DOE	01/12/98	Marshall	23.4	2.75		5391		802.9	2849.3
DOE	02/09/98	Marshall	53.7	2.54		6946		2433.4	3770.5
DOE	03/26/98	Marshall	78.1	2.74		5446		2746.5	2924.1
DOE	04/29/98	Marshall	63.5	2.74		4763		1884.8	2468.2
WVDEP	05/14/98	Marshall	51.5	2.70	6900	4915		1518.5	2452.0
DOE	05/28/98	Marshall	53.2	2.91		4622		1445.2	2261.0
WVDEP	06/15/98	Marshall	26.9	2.70	17100	6002		43.7	135.4
DOE	06/25/98	Marshall	115.6	3.07		5543		1941.5	1397.4
WVDEP	07/15/98	Marshall	47.5	2.60	9500	7923		1136.8	1991.6
DOE	08/05/98	Marshall	45.6	3.43		5580		1264.1	2306.2
WVDEP	08/13/98	Marshall	25.5	3.00	8050	6641		623.4	2030.7
DOE	09/03/98	Marshall	17.1	3.15		8625		912.3	4432.4
WVDEP	09/15/98	Marshall	16.6	2.80	26300	10256		983.1	4933.1
WVDEP	10/15/98	Marshall	5.8	2.80	24700	12705		225.7	3226.3

Table E-1e, Omega Mine-pool, Marshall Spring, Raw Chemical Data

Sampled By	Date	Location	Flow gpm	pH	Sp. Conductance umhos/cm	TDS, mg/L	Temp, C	Acid load, lbs/day CaCO3 Eq	Calc Total Acidity CaCO3 Eq
DOE	10/29/98	Marshall	2.0	3.37		8772		102.9	4279.3
WVDEP	11/15/98	Marshall	2.7	3.00	16200	8281		111.8	3458.4
DOE	12/10/98	Marshall	2.5	3.23		8006		117.5	3926.3
WVDEP	12/15/98	Marshall	1.8	2.90	10900	9048		87.3	4055.2
WVDEP	01/17/99	Marshall	1.8	3.30	10600	7925		67.6	3142.8
WVDEP	02/14/99	Marshall	6.7	3.00	15400	9650		174.2	2157.2
DOE	02/18/99	Marshall	7.4	3.46		9325		416.2	4678.4
WVDEP	03/14/99	Marshall	9.0	3.10	15300	9936		539.8	5012.4
DOE	03/30/99	Marshall	9.0	3.40		13352		824.8	7663.6
WVDEP	04/13/99	Marshall	8.1	3.00	28600	19803		1024.1	10570.7
WVDEP	04/26/99	Marshall	8.1	3.20	29100	20130		937.5	9676.9
DOE	04/29/99	Marshall	7.5	3.10		16313		858.5	9496.1
WVDEP	05/17/99	Marshall	7.2	3.00	27400	15987		4.3	50.0
DOE	05/26/99	Marshall	5.8	2.96		13381		521.8	7531.7
WVDEP	06/14/99	Marshall	4.9	2.70	25500	13069		421.6	7113.8
DOE	06/29/99	Marshall	3.9	2.80		10728		276.5	5831.5
WVDEP	07/13/99	Marshall	3.6	3.00	19100	11058		235.0	5462.2
DOE	07/27/99	Marshall	3.6	3.34		8971		203.0	4675.0
WVDEP	08/14/99	Marshall	4.0	3.20	14900	9542		209.1	4315.8
DOE	08/26/99	Marshall	3.3	3.22		8581		175.2	4400.6
WVDEP	09/14/99	Marshall	3.1	2.90	18400	8831		154.6	4097.1
DOE	09/29/99	Marshall	2.7	3.10		7984		130.3	4077.8
WVDEP	10/15/99	Marshall	1.8	3.00	15900	8396		83.7	3887.9
DOE	10/29/99	Marshall	3.1	3.19		7586		141.9	3815.7
WVDEP	11/15/99	Marshall	1.8	3.10	14800	8444		86.0	3998.5
DOE	12/07/99	Marshall	5.0	2.69		7150		214.8	3597.0
WVDEP	12/15/99	Marshall	7.2	3.00	8980	6383		312.0	3620.7
WVDEP	01/18/00	Marshall	8.0	3.20	9840	7990		382.1	3989.0
WVDEP	02/08/00	Marshall	5.0	3.50	9690	7653		236.3	3916.9
WVDEP	03/15/00	Marshall	6.0	2.50	6390	3195		458.3	6354.5
WVDEP	04/14/00	Marshall	9.0	3.10	17800	9684		541.3	5003.5
WVDEP	05/15/00	Marshall	7.0	3.40	9780	7726		314.3	3740.7
WVDEP	06/16/00	Marshall	6.0	2.90	7610	6144		266.3	3692.0
WVDEP	07/18/00	Marshall	8.0	3.30	8860	6854		336.3	3489.0
WVDEP	08/15/00	Marshall	7.0	3.40	7450	5545		207.0	2463.3
WVDEP	09/15/00	Marshall	4.0	3.10	6460	5114		114.8	2392.9

Table E-1e, Omega Mine-pool, Marshall Spring, Raw Chemical Data

Sampled By	Date	Location	Flow gpm	pH	Sp. Conductance umhos/cm	TDS, mg/L	Temp, C	Acid load, lbs/day CaCO3 Eq	Calc Total Acidity CaCO3 Eq
WVDEP	10/15/00	Marshall	3.0	3.20	6000	4041		122.0	3383.9
WVDEP	11/15/00	Marshall	3.0	3.60	7310	5718		86.7	2403.9
WVDEP	12/14/00	Marshall	5.0	3.40	5445	5445		132.5	2196.6
WVDEP	01/15/01	Marshall	7.0	3.20	6180	4998		163.1	1941.8
WVDEP	02/13/01	Marshall	27.0	3.40	7290	5618		120.3	370.6
WVDEP	03/13/01	Marshall	27.0	3.50	5790	4710		571.3	1759.6
WVDEP	04/16/01	Marshall	38.0	3.40	6920	5066		2950.7	6461.7
WVDEP	05/15/01	Marshall	24.0	3.50	5910	4562		669.5	2319.7
WVDEP	06/18/01	Marshall	18.0	3.20	5620	4441		722.5	3337.4
WVDEP	07/15/01	Marshall	21.0	3.40	4930	3932		482.7	1911.3
WVDEP	08/15/01	Marshall	16.0	3.30	5870	4840		305.2	1588.0
WVDEP	09/14/01	Marshall	8.0	3.30	4920	4001		205.4	2131.1
WVDEP	10/15/01	Marshall	9.0	3.10	3840	5180	20	198.1	1839.6
WVDEP	11/15/01	Marshall	9.0	3.10	3110	4536	11.1	202.1	1876.2
WVDEP	12/14/01	Marshall	6.0	3.10	3730	4488	10.5	91.8	1281.8
WVDEP	01/16/02	Marshall	10.8	3.40	2500	4404	8.4	112.7	872.4
WVDEP	02/14/02	Marshall	24.2	3.60	3340	4804	4.4	512.6	1762.8
WVDEP	03/14/02	Marshall	16.9	3.60	3190	4632	16.7	337.5	1658.7
WVDEP	04/15/02	Marshall	44.8	3.30	3350	4860	13.8	1107.3	2056.3
WVDEP	05/15/02	Marshall	53.8	3.40	4630	5448	11.6	1283.4	1986.0
WVDEP	06/18/02	Marshall	29.6	3.60	3050	4360	15.5	145.0	408.0
WVDEP	07/18/02	Marshall	0.0					0.0	
WVDEP	08/12/02	Marshall	11.0	3.50	3320	4408	15.5	197.5	1496.5
Perry	08/20/02	Marshall	6.2	3.48	3310	4203	13.8	112.7	1525.0
WVDEP	09/16/02	Marshall	7.0	3.60	3340	4200	16.5	113.2	1347.6
WVDEP	10/15/02	Marshall	5.8	3.20	3360	4164	14.4	69.2	988.6
WVDEP	11/15/02	Marshall	7.0	3.30	3325	3808	15	110.6	1316.4
WVDEP	12/15/02	Marshall	12.0	3.30	3652	4120	13.3	180.1	1252.4
WVDEP	01/14/03	Marshall	39.9	3.50	3740	4756	8.9	783.3	1632.4
WVDEP	02/24/03	Marshall	38.0	3.50	3460	4148	11.7	370.4	812.0
WVDEP	03/18/03	Marshall	35.8	3.47	3990	4644	14.44	908.5	2108.8
WVDEP	04/15/03	Marshall	26.9	3.51	3470	4140	14.44	534.0	1652.7
WVDEP	05/20/03	Marshall	44.8	3.25	3800	4760	15.56	1165.5	2164.4
WVDEP	06/17/03	Marshall	49.3	3.53	3550	3956	15.56	745.0	1257.6
WVDEP	08/13/03	Marshall	26.9	3.38	2920	3208	15.56	414.8	1283.9
Perry	08/28/03	Marshall	12.9	3.60	3980	3092	14.7	244.5	1576.6

Table E-1e, Omega Mine-pool, Marshall Spring, Raw Chemical Data

Sampled By	Date	Location	Flow gpm	pH	Sp. Conductance umhos/cm	TDS, mg/L	Temp, C	Acid load, lbs/day CaCO3 Eq	Calc Total Acidity CaCO3 Eq
WVDEP	09/15/03	Marshall	26.9	3.38	3040	3376	15.56	346.5	1072.4
WVDEP	10/14/03	Marshall	22.4	3.26	2910	3312	14.4	292.6	1086.8
WVDEP	11/18/03	Marshall	26.9	3.27	3060	3588	9.44	227.3	703.7
WVDEP	12/19/03	Marshall	44.8	3.05	3470	3764	14.4	606.6	1126.5
WVDEP	01/14/04	Marshall	44.8	3.37	3300	3716	12.2	715.2	1328.1
WVDEP	02/17/04	Marshall	49.3	3.52	3440	4052	14.4	832.8	1405.9
WVDEP	03/23/04	Marshall	44.8	3.16	3070	3364	8.9	615.3	1142.7
WVDEP	04/13/04	Marshall	44.8	3.37	2900	3016	10	511.5	949.9
WVDEP	05/18/04	Marshall	22.4	3.66	2620	2828	12.78	268.9	998.8
WVDEP	06/14/04	Marshall	26.9	3.70	2620	2728	15	232.2	718.6
WVDEP	07/12/04	Marshall	17.9	3.34	2540	2712	15.6	191.6	889.5
WVDEP	08/09/04	Marshall	9.0	3.48	2540	2744	15	103.8	964.0
WVDEP	09/14/04	Marshall	9.0	3.34	2470	2440	15	75.5	701.4
WVDEP	10/18/04	Marshall	13.4	3.60	2520	2584	9.4	149.8	927.3
Perry	03/22/05	Marshall	36.4	3.78	2940	2788	12.8	449.6	1028.7
Perry	05/26/06	Marshall	28.8	3.54	2150	2418	13.8	256.8	741.9
Perry	05/03/07	Marshall	45.6	3.52	2565	2162	13.6	427.7	780.3
Perry	09/13/07	Marshall	10.1	3.45	2640	2152	13.4	83.5	687.8

Table E-1f, Omega Mine-pool, Marshall Spring, Raw Chemical Data

Sampled By	Date	Location	Fe3+, mg/L	Fe2+, mg/L	Fe Total, mg/L	Ca, mg/L	Mg, mg/L	Na, mg/L	K, mg/L	Al, mg/L	Mn, mg/L	SO4, mg/L	Cl, mg/L
DOE	11/15/91	Marshall	0	1091	1091	389.0	207.0	5.0		113.0	6.70	4950	8.5
DOE	02/11/93	Marshall	334	1816	2150	373.0	221.0	2.7	6.8	349.0	8.16	7815	10
DOE	03/03/93	Marshall	204	1771	1975	338.0	203.0	3.5	6.1	331.0	7.80	7425	1
DOE	03/18/93	Marshall	422	1567	1989	329.0	197.0	8.2	6.6	327.0	7.60	7319	5
DOE	04/02/93	Marshall	700	1388	2088	308.0	187.0	2.7	3.5	349.0	7.20	7725	5
DOE	04/14/93	Marshall	650	1527	2177	319.0	191.0	3.4	3.7	359.0	7.40	7967	5
DOE	04/29/93	Marshall	634	1463	2097	318.0	184.0	4.9	2.9	346.0	7.50	7657	5.69
DOE	05/20/93	Marshall	349	1281	1630	296.0	162.0	3.1	5.1	279.0	6.30	6132	5
DOE	06/03/93	Marshall	278	1305	1583	300.0	164.0	3.7	5	273.0	6.30	5941	10
DOE	06/10/93	Marshall	246.76	1366	1612.76	314.2	170.2	4.3	6.84	274.7	6.51	5974	13.1
DOE	06/23/93	Marshall	266.5	1393	1659.5	326.7	175.3	4.7	6.48	275.7	6.72	6205	6.9
DOE	07/08/93	Marshall	157.84	1443	1600.84	316.3	167.2	3.9	6.43	266.7	6.48	5824	3.1
DOE	07/22/93	Marshall	56	1394	1450	319.9	168.1	4.7	7.46	228.5	6.47	5302	2.9
DOE	08/11/93	Marshall	43.03	1243	1286.03	324.9	166.2	5.7	7.35	195.5	6.25	4672	
DOE	09/02/93	Marshall	50.07	1170	1220.07	318.5	157.5	5.2	8.48	175.8	5.85	4535	
DOE	09/10/93	Marshall	72.05	1146	1218.05	320.3	157.1	5.8	8.4	172.8	5.89	4470	
DOE	10/07/93	Marshall	77.76	1156	1233.76	341.0	163.3	6.5	10.22	170.7	6.09	4621	9.3
DOE	10/25/93	Marshall	36.14	1300	1336.14	329.0	164.2	6.1	10.08	190.8	6.07	4784	13.9
DOE	11/10/93	Marshall	93.79	1207	1300.79	336.2	161.0	7.5	12.3	174.6	6.10	4658	10.6
DOE	12/07/93	Marshall	74.88	1158	1232.88	330.1	160.2	8.1	10.84	166.6	5.90	4500	14.7
DOE	12/23/93	Marshall	276.75	1605	1881.75	350.9	190.4	3.8	7.06	292.5	7.30	6803	11.9
DOE	01/28/94	Marshall	524.43	1465	1989.43	337.3	183.7	5.1	5.6	333.6	7.38	7319	13.1
DOE	05/05/94	Marshall	360.97	876.8	1237.77	271.3	115.3	4.4	5.48	209.3	4.73	4902	15.35
DOE	06/10/94	Marshall	66.69	1202	1268.69	305.3	135.5	4.6	8.76	223.4	5.23	4896	11.5
DOE	07/06/94	Marshall	21.83	1188	1209.83	311.7	136.8	4.7	9.45	205.2	5.33	4609	13
DOE	08/03/94	Marshall	38.48	1151	1189.48	310.7	141.4	5.2	9.72	191.3	5.44	4460	17.8
DOE	09/01/94	Marshall	25.6	1273.2	1298.8	327.1	146.4	4.6	11.91	206.7	5.58	4904	11.2
DOE	10/07/94	Marshall	47.84	1266	1313.84	331.4	149.9	4.4	10.41	215.9	5.82	4992	9.38
DOE	11/16/94	Marshall	0	1200.95	1200.95	308.5	141.3	4.8	8.9	190.9	5.54	4566	59.9
DOE	12/14/94	Marshall	0	1162.56	1162.56	313.4	141.7	5.7	8.87	186.1	5.78	4664	0.85
DOE	01/10/95	Marshall	0.01	1236	1236.01	314.2	145.9	5.1	9.16	198.1	5.80	4657	9.49
DOE	02/03/95	Marshall	0	1325.89	1325.89	341.18	152.96	6.4	10.66	219.89	6.17	5053.93	15.77
DOE	03/02/95	Marshall	163.25	1202.66	1365.91	308.3	145.9	6.3	5.44	233.8	6.02	5343	17.66
DOE	04/07/95	Marshall	342.15	1109	1451.15	287.96	136.94	5.28	2.59	259.47	5.95	5736.81	14.65
DOE	05/10/95	Marshall	147.37	1187	1334.37	296.7	136.1	5.6	8.3	242.6	5.70	5198	14.5
DOE	06/06/95	Marshall	333.02	1056	1389.02	278.0	128.6	4.9	6.46	266.7	5.48	5488	19
DOE	07/13/95	Marshall	96.24	1144	1240.24	293.14	134.72	5.31	6.8	233.76	5.51	4908.41	14.1

Table E-1f, Omega Mine-pool, Marshall Spring, Raw Chemical Data

Sampled By	Date	Location	Fe3+, mg/L	Fe2+, mg/L	Fe Total, mg/L	Ca, mg/L	Mg, mg/L	Na, mg/L	K, mg/L	Al, mg/L	Mn, mg/L	SO4, mg/L	Cl, mg/L
DOE	08/03/95	Marshall	0	1215.23	1215.23	306.6	136.3	5.1	9.74	208.5	5.41	4556	14.6
DOE	09/07/95	Marshall	28.48	1215.5	1243.98	358.33	150.12	6.98	11.75	193.49	5.98	4862.04	15.2
DOE	10/12/95	Marshall	0	1151.03	1151.03	330.38	141.34	6.85	10.98	179.89	5.64	4394.77	16.9
DOE	11/22/95	Marshall	2.25	1069	1071.25	319.9	132.9	7.1	9.77	164.5	5.50	4072	8.1
DOE	01/05/96	Marshall	0	1282.65	1282.65	332.7	147.4	5.8	10.82	215.5	6.22	4887	16.04
DOE	02/21/96	Marshall	523.71	1426	1949.71	300.9	146.0	4.5	4.43	377.4	6.65	7496	5.11
DOE	03/18/96	Marshall	620.61	866	1486.61	247.7	122.2	4.0	3.17	284.9	5.68	5919	20.55
DOE	04/26/96	Marshall	362.12	735.4	1097.52	232.3	101.1	4.3	4.17	214.5	4.43	4433	1
DOE	06/07/96	Marshall	300.73	676	976.73	227.0	93.3	3.8	5.41	199.5	4.07	4055	1
DOE	07/23/96	Marshall	31.81	989.8	1021.61	285.8	110.1	5.8	8.7	189.1	4.48	3968	13.44
DOE	08/28/96	Marshall	118.2	987.5	1105.7	314.2	112.3	5.8	10.26	211.0	4.77	4442	12.24
DOE	10/16/96	Marshall	28.63	992	1020.63	305.6	114.0	5.8	9.95	190.5	4.61	4133	17.57
DOE	11/26/96	Marshall	239.96	807	1046.96	275.6	111.3	4.9	7.6	219.9	4.9	4433.5	6.31
DOE	12/13/96	Marshall	384.37	670	1054.37	253.92	102.42	4.61	5.65	221.35	4.54	4418.7	11.48
DOE	01/28/97	Marshall	98.91	925	1023.91	241.86	95.18	3.96	7.53	215.35	4.12	4145.61	7.7
DOE	02/21/97	Marshall	108.74	927	1035.74	266.7	95.5	4.1	6.81	206.8	4.32	4155	18
DOE	03/26/97	Marshall	380.6	669.5	1050.1	224.5	90.7	3.7	3.81	219.5	4.12	4412	6.5
DOE	05/20/97	Marshall	56.45	740.3	796.75	220.5	84.8	4.2	6.32	166.3	3.61	3344	
DOE	07/10/97	Marshall	61.7	836.3	898	253.4	92.1	4.7	9.29	182.3	3.99	3690	9.5
DOE	09/10/97	Marshall	39.93	800.2	840.13	262.5	98.9	5.4	9.53	152.3	4.08	3303	8.68
DOE	11/05/97	Marshall	26.37	759.2	785.57	258.3	96.3	7.3	9.16	138.3	4.05	3058	11.02
DOE	01/12/98	Marshall	63.96	909.5	973.46	255.5	96.5	5.4	8.79	181.8	4.13	3849	8.2
DOE	02/09/98	Marshall	469.44	737.7	1207.14	257.3	106.1	3.42	4.26	262.2	4.6	5047	43.44
DOE	03/26/98	Marshall	365.11	577.4	942.51	209.0	84.5	3.5	5.07	206.2	0.00	3987	
DOE	04/29/98	Marshall	266.96	520.7	787.66	205.7	81.4	3.2	4.81	172.9	3.52	3495	
WVDEP	05/14/98	Marshall			761					177	3.56	2980	
DOE	05/28/98	Marshall	102.65	620.4	723.05	322.2	69.0	10.8	11.02	161.9	3.05	3303	11.43
WVDEP	06/15/98	Marshall			9.22					2.34	3.43	3890	
DOE	06/25/98	Marshall	-16.59	530	513.41	949.7	68.8	18.8	23.87	77.6	2.52	3863	21.06
WVDEP	07/15/98	Marshall			131					292	5.14	5380	
DOE	08/05/98	Marshall	22.72	775.2	797.92	496.0	88.5	45.2	65.66	153.5	3.55	3879	42.98
WVDEP	08/13/98	Marshall			712					126	3.28	3690	
DOE	09/03/98	Marshall	0	1497.39	1497.39	466.7	138.3	38.9	60.19	307.0	5.76	6059	36.67
WVDEP	09/15/98	Marshall			1530					379	4.93	5090	
WVDEP	10/15/98	Marshall			258					481	7.23	7920	
DOE	10/29/98	Marshall	58.18	1491	1549.18	459.9	164.5	60.8	53.75	265.2	6.03	6163	33.77
WVDEP	11/15/98	Marshall			1320					186	6.52	5430	

Table E-1f, Omega Mine-pool, Marshall Spring, Raw Chemical Data

Sampled By	Date	Location	Fe3+, mg/L	Fe2+, mg/L	Fe Total, mg/L	Ca, mg/L	Mg, mg/L	Na, mg/L	K, mg/L	Al, mg/L	Mn, mg/L	SO4, mg/L	Cl, mg/L
DOE	12/10/98	Marshall	21.93	1399.78	1421.71	453.3	157.2	57.7	54.93	241.0	7.05	5574	26.5
WVDEP	12/15/98	Marshall			1480					240	5.01	5220	
WVDEP	01/17/99	Marshall			1200					173	4.5	5100	
WVDEP	02/14/99	Marshall			180					319	7.1	5910	
DOE	02/18/99	Marshall	0	1687.52	1687.52	487.4	181.9	50.7	52.08	292.4	8.53	6527	22.58
WVDEP	03/14/99	Marshall			1830					303	7.13	6120	
DOE	03/30/99	Marshall	0.84	2553	2553.84	535.6	234.7	49.4	55.22	549.1	11.51	9320	19.22
WVDEP	04/13/99	Marshall			3690					701	10.8	12800	
WVDEP	04/26/99	Marshall			3390					639	14.3	12800	
DOE	04/29/99	Marshall	534.92	2672	3206.92	505.7	267.9	44.1	52.08	663.9	14.50	11513	15.84
WVDEP	05/17/99	Marshall										9540	
DOE	05/26/99	Marshall	0	2694.41	2694.41	479.2	230.0	41.6	47.95	473.4	12.76	9377	0
WVDEP	06/14/99	Marshall			2610					418	10.4	7080	
DOE	06/29/99	Marshall	579.4045	1536.23555	2115.64	423.74	189.72	37.75	46.77	350.54	9.37	7519.73	17.13
WVDEP	07/13/99	Marshall			2080					301	8.82	4310	
DOE	07/27/99	Marshall	0	1742.22	1742.22	416.9	172.7	37.0	41.79	273.0	9.09	6236	27.07
WVDEP	08/14/99	Marshall			1680					227	8.42	6340	
DOE	08/26/99	Marshall	0	1654.74	1654.74	428.3	170.4	40.7	41.04	250.6	8.66	5947	26.49
WVDEP	09/14/99	Marshall			1560					221	7.39	4950	
DOE	09/29/99	Marshall	0	1521.04	1521.04	418.1	161.9	38.5	40.59	234.0	8.32	5526	22.2
WVDEP	10/15/99	Marshall			1490					208	8.09	2340	
DOE	10/29/99	Marshall	0	1449.87	1449.87	410.7	156.8	36.6	37.54	211.1	8.23	5239	23.49
WVDEP	11/15/99	Marshall			1500					227	6.69	5620	
DOE	12/07/99	Marshall	24.62	1304	1328.62	413.0	144.8	34.0	38.47	198.6	7.06	4946	28.1
WVDEP	12/15/99	Marshall			1380					196	6.12	1940	
WVDEP	01/18/00	Marshall			1500					227	5.91	2300	
WVDEP	02/08/00	Marshall			1510					213	7.91	2180	
WVDEP	03/15/00	Marshall			2250					388	6.83	2120	
WVDEP	04/14/00	Marshall			1820					305	5.96	9270	
WVDEP	05/15/00	Marshall			1390					220	5.48	7160	
WVDEP	06/16/00	Marshall			1340					220	4.22	5860	
WVDEP	07/18/00	Marshall			1260					216	4.44	4600	
WVDEP	08/15/00	Marshall			876					156	4.64	4640	
WVDEP	09/15/00	Marshall			851	329				148	4.04	4400	
WVDEP	10/15/00	Marshall			1370					160	5.84	3190	
WVDEP	11/15/00	Marshall			900					139	4.28	3890	
WVDEP	12/14/00	Marshall			886					105	3.89	3190	

Table E-1f, Omega Mine-pool, Marshall Spring, Raw Chemical Data

Sampled By	Date	Location	Fe3+, mg/L	Fe2+, mg/L	Fe Total, mg/L	Ca, mg/L	Mg, mg/L	Na, mg/L	K, mg/L	Al, mg/L	Mn, mg/L	SO4, mg/L	Cl, mg/L
WVDEP	01/15/01	Marshall			721					110	4.58	4490	
WVDEP	02/13/01	Marshall			127					22	0.63	4970	
WVDEP	03/13/01	Marshall			645					105	3.1	3380	
WVDEP	04/16/01	Marshall			573					973	5.75	4310	
WVDEP	05/15/01	Marshall			827					147	3.6	2720	
WVDEP	06/18/01	Marshall			821					329	4.49	3360	
WVDEP	07/15/01	Marshall			696					115	3.52	3190	
WVDEP	08/15/01	Marshall			536					84.8	74	2230	
WVDEP	09/14/01	Marshall			785					125	3.41	2130	
WVDEP	10/15/01	Marshall			682.68					102.75	3.75	3450	
WVDEP	11/15/01	Marshall			728.17					94.73	3.6	3021	
WVDEP	12/14/01	Marshall			474.68					69.35	3.86	2989	
WVDEP	01/16/02	Marshall			127.41					111.28	3.45	2933	
WVDEP	02/14/02	Marshall			640.83					107.53	3.04	3199	
WVDEP	03/14/02	Marshall			628.53					92.75	3.07	3085	
WVDEP	04/15/02	Marshall			770.83					116.84	1.1	3237	
WVDEP	05/15/02	Marshall			754.53					109.79	2.9	3628	
WVDEP	06/18/02	Marshall			218.73					0.52	0.52	2904	
WVDEP	07/18/02	Marshall											
WVDEP	08/12/02	Marshall			540.53					91.47	2.65	2936	
Perry	08/20/02	Marshall		550	564.25	298.07	71.01	18.1	25.36	88.73	2.94	2462.4	11.9
WVDEP	09/16/02	Marshall			466.25					89.13	2.83	2797	
WVDEP	10/15/02	Marshall			351.08					58.23	2.78	2773	
WVDEP	11/15/02	Marshall			513.99					65.91	2.71	2536	
WVDEP	12/15/02	Marshall			474.39					67.27	2.39	2744	
WVDEP	01/14/03	Marshall			573.94					105.1	2.82	3167	
WVDEP	02/24/03	Marshall			228.71					68.77	2.6	2763	
WVDEP	03/18/03	Marshall			770.53					127.35	2.66	3093	
WVDEP	04/15/03	Marshall			524.22					125.29	1.42	2757	
WVDEP	05/20/03	Marshall			745.92					143.29	2.63	3170	
WVDEP	06/17/03	Marshall			443.62					80.1	2	2635	
WVDEP	08/13/03	Marshall			487.12					69.72	2	2137	
Perry	08/28/03	Marshall			460	162	59.5	35.8	12.8	133	0.83	2200	
WVDEP	09/15/03	Marshall			386.9					63.96	1.97	2248	
WVDEP	10/14/03	Marshall			386.01					65.71	1.76	2206	
WVDEP	11/18/03	Marshall			199.03					57.1	1.8	2390	
WVDEP	12/19/03	Marshall			388.63					68.8	2.14	2507	

Table E-1f, Omega Mine-pool, Marshall Spring, Raw Chemical Data

Sampled By	Date	Location	Fe3+, mg/L	Fe2+, mg/L	Fe Total, mg/L	Ca, mg/L	Mg, mg/L	Na, mg/L	K, mg/L	Al, mg/L	Mn, mg/L	SO4, mg/L	Cl, mg/L
WVDEP	01/14/04	Marshall			483.23					78.89	1.81	2475	
WVDEP	02/17/04	Marshall			524.53					80.51	2.46	2699	
WVDEP	03/23/04	Marshall			393.1					72.2	1.77	2240	
WVDEP	04/13/04	Marshall			322.12					62.81	1.63	2009	
WVDEP	05/18/04	Marshall			355.37					62.75	1.66	1883	
WVDEP	06/14/04	Marshall			238.66					50.12	1.62	1817	
WVDEP	07/12/04	Marshall			313.25					54.55	1.54	1806	
WVDEP	08/09/04	Marshall			352.49					56.37	1.78	1828	
WVDEP	09/14/04	Marshall			233.96					46.07	2.05	1625	
WVDEP	10/18/04	Marshall			337.16					55.39	1.86	1721	
Perry	03/22/05	Marshall	233	155	377.49	326.26	53.04	17.92	28.54	61.36	2	1994	
Perry	05/26/06	Marshall	0.6	281	280.97	232.9	42.3	12.2		39.86	1.67	1451	
Perry	05/03/07	Marshall	3.3	284	286.84	271.7	41.9	16.04	24.85	44.8	1.55	1665	35
Perry	09/13/07	Marshall			255.1	211.6	42.08	28.07	16.22	37.73	2.07	1401	40

Table E-1g, Omega Mine-pool, DEF Spring, Raw Chemical Data

Sampled By	Date	Location	Flow gpm	pH	Sp. Conductance umhos/cm	TDS, mg/L	Temp, C	Acid load, lbs/day CaCO3 Eq	Calc Total Acidity CaCO3 Eq
DOE	11/15/1991	DEF		2.59		5204		0.0	2021.2
DOE	3/3/1993	DEF	31.8	2.83		4311		754.1	1973.5
DOE	3/18/1993	DEF	74.6	2.76		2374		971.4	1083.8
DOE	4/2/1993	DEF	68.9	2.64		4088		1632.3	1971.9
DOE	4/14/1993	DEF	53.9	2.57		4921		1564.8	2413.6
DOE	4/29/1993	DEF	58.8	2.65		3622		1254.4	1774.8
DOE	5/20/1993	DEF	36.4	2.76		4599		951.1	2173.9
DOE	6/3/1993	DEF	27.6	2.80		4719		740.9	2233.4
DOE	6/10/1993	DEF	27.3	2.74		4699		732.9	2233.3
DOE	6/23/1993	DEF	18.2	2.73		4875		496.4	2266.8
DOE	7/8/1993	DEF	8.7	2.72		4379		210.7	2026.9
DOE	7/22/1993	DEF	6.4	2.65		4704		169.3	2204.3
DOE	8/11/1993	DEF	6.2	2.70		4840		171.7	2304.5
DOE	9/2/1993	DEF	3.9	2.62		5196		113.2	2431.3
DOE	9/10/1993	DEF	4.5	2.63		4701		119.0	2175.6
DOE	10/7/1993	DEF	5.3	2.65		4074		116.5	1817.3
DOE	10/25/1993	DEF	9.5	2.73		3883		197.3	1722.7
DOE	11/10/1993	DEF	9.7	2.63		3736		191.6	1651.4
DOE	12/7/1993	DEF	42.8	2.95		1790		389.1	755.8
DOE	12/23/1993	DEF	19.4	2.68		3773		411.6	1763.8
DOE	1/28/1994	DEF	75.4	2.89		1508		625.6	689.9
DOE	5/5/1994	DEF	32.6	2.60		4221		801.5	2047.1
DOE	6/10/1994	DEF	20.7	2.71		4263		508.1	2041.4
DOE	7/6/1994	DEF	9.9	2.65		4318		247.9	2078.8
DOE	8/3/1994	DEF	8.6	2.82		3672		174.5	1697.1
DOE	9/1/1994	DEF	13.0	2.65		3150		225.3	1446.1
DOE	10/7/1994	DEF	9.9	2.75		4523		252.1	2114.1
DOE	11/16/1994	DEF	4.5	2.71		4385		111.3	2058.4
DOE	12/14/1994	DEF	17.0	2.87		2203		187.2	916.4
DOE	1/10/1995	DEF	15.4	2.84		3604		303.2	1637.3
DOE	2/3/1995	DEF	10.6	2.74		3091		180.6	1414.0
DOE	3/2/1995	DEF	19.2	2.86		2542		269.1	1163.8
DOE	4/7/1995	DEF	8.9	2.81		3433		172.2	1600.8
DOE	5/10/1995	DEF	14.4	2.89		2626		205.3	1184.1
DOE	6/6/1995	DEF	12.3	2.75		2966		204.4	1382.5
DOE	7/13/1995	DEF	7.1	2.63		4093		169.3	1975.6

Table E-1g, Omega Mine-pool, DEF Spring, Raw Chemical Data

Sampled By	Date	Location	Flow gpm	pH	Sp. Conductance umhos/cm	TDS, mg/L	Temp, C	Acid load, lbs/day CaCO3 Eq	Calc Total Acidity CaCO3 Eq
DOE	8/3/1995	DEF	6.4	2.63		4565		172.1	2241.5
DOE	9/7/1995	DEF	3.6	2.67		4996		99.4	2303.8
DOE	10/12/1995	DEF	3.1	2.65		4206		74.7	2023.1
DOE	11/22/1995	DEF	13.2	2.70		2656		190.4	1202.5
DOE	1/5/1996	DEF	24.2	2.67		2011		258.3	886.4
WVDEP	1/16/1996	DEF	14.3	2.6	5880	3122	11.1	211.4	1226.5
WVDEP	2/15/1996	DEF	17.0	2.6	4870	2832	11.1	166.7	814.7
DOE	2/21/1996	DEF	45.6	2.55		2843		794.7	1451.4
WVDEP	3/1/1996	DEF	30.0	2.7	2930	1905	11.1	179.5	497.4
WVDEP	3/15/1996	DEF	31.8	2.6	4580	2520	12.2	289.4	757.0
DOE	3/18/1996	DEF	32.6	2.72		1946		360.8	920.4
WVDEP	3/28/1996	DEF	35.8	2.6	3880	1882	0	198.5	460.7
WVDEP	4/15/1996	DEF	22.9	2.7	3670	2405	13.3	203.0	738.9
DOE	4/26/1996	DEF	18.2	2.62		2175		229.2	1047.6
WVDEP	4/29/1996	DEF	22.9	2.6	4560	2499	14.4	38.2	139.0
WVDEP	5/15/1996	DEF	31.8	2.6	3420	1453	11.1	171.3	448.1
WVDEP	5/31/1996	DEF	58.7	2.6	4140	2094	15	801.2	1135.7
DOE	6/7/1996	DEF	16.6	2.63		2483		248.7	1243.2
WVDEP	6/14/1996	DEF	13.9	2.5	5050	3032	13.9	276.3	1655.0
WVDEP	6/28/1996	DEF	21.1	2.6	5530	3232	14.4	417.4	1649.1
WVDEP	7/15/1996	DEF	9.0	2.6	5540	3668	13.3	159.6	1481.9
DOE	7/23/1996	DEF	21.6	2.72		2434		308.3	1185.3
WVDEP	7/30/1996	DEF	14.8	2.6	5090	2918	14.4	200.3	1127.2
WVDEP	8/14/1996	DEF	10.8	2.5	4420	2503	13.3	163.4	1264.5
DOE	8/28/1996	DEF	8.2	2.74		2765		129.7	1313.0
WVDEP	8/31/1996	DEF	9.0	2.6	5670	3264	13.3	128.9	1197.2
WVDEP	9/16/1996	DEF	9.0	2.6	4800	2820	14.4	162.3	1506.6
WVDEP	9/30/1996	DEF	15.7	2.7	4910	2763	13.3	202.8	1075.8
WVDEP	10/14/1996	DEF	7.6	2.6	4880	2918	14.4	125.5	1370.6
DOE	10/16/1996	DEF	6.1	2.72		3016		102.3	1394.6
WVDEP	10/30/1996	DEF	33.8	2.5	3750	1978	10	398.5	980.2
WVDEP	11/15/1996	DEF	22.0	2.6	4040	1781	11.1	185.2	702.0
DOE	11/26/1996	DEF	10.6	2.72		2167		129.4	1018.0
DOE	12/13/1996	DEF	19.1	2.8		1544		161.7	703.1
WVDEP	12/15/1996	DEF	22.0	2.8	3500	1351	12.2	149.1	565.1
WVDEP	1/14/1997	DEF	19.3	2.7	3990	2248	12.2	222.6	961.7

Table E-1g, Omega Mine-pool, DEF Spring, Raw Chemical Data

Sampled By	Date	Location	Flow gpm	pH	Sp. Conductance umhos/cm	TDS, mg/L	Temp, C	Acid load, lbs/day CaCO3 Eq	Calc Total Acidity CaCO3 Eq
DOE	1/28/1997	DEF	11.6	2.75		2114		143.8	1033.0
DOE	2/21/1997	DEF	13.2	2.76		1926		140.1	884.4
WVDEP	3/17/1997	DEF	16.1	2.6	3120	2970	14.4	349.8	1804.3
DOE	3/26/1997	DEF	21.8	2.68		2486		326.7	1249.0
WVDEP	4/14/1997	DEF	19.7	2.6	3130	3497	14.4	389.4	1643.5
WVDEP	5/14/1997	DEF	19.7	2.6	2980	2109	14.4	395.6	1669.7
DOE	5/20/1997	DEF	24.9	2.76		2878		425.3	1421.0
WVDEP	6/16/1997	DEF	17.9	2.5	3220	3003	15.6	407.0	1889.3
DOE	7/10/1997	DEF	11.6	2.75		3319		228.2	1637.5
WVDEP	7/16/1997	DEF	9.9	2.6	3480	3164	15.6	162.4	1370.5
WVDEP	8/17/1997	DEF	9.0	2.7	6310	3867	15.6	188.3	1748.5
DOE	9/10/1997	DEF	6.7	2.82		3006		116.5	1438.2
WVDEP	9/15/1997	DEF	83.8	2.7	3260	2343	15	792.0	786.5
WVDEP	10/15/1997	DEF	7.6	2.7	5460	3469		144.2	1573.9
DOE	11/5/1997	DEF	6.1	2.77		3328		119.1	1619.9
WVDEP	11/14/1997	DEF	20.6	2.6	2680	2160		278.7	1125.1
WVDEP	12/15/1997	DEF	12.5	2.6	2590	2229		169.9	1127.2
DOE	1/12/1998	DEF	32.7	2.64		1722		321.0	816.2
WVDEP	1/16/1998	DEF	20.6	2.6	3860	1918		236.1	953.2
DOE	2/9/1998	DEF	21.6	2.76		1903		234.7	903.4
WVDEP	2/15/1998	DEF	29.6	2.7	3750	1876		299.4	842.3
WVDEP	3/15/1998	DEF	25.5	2.7	3720	1716		249.9	814.0
DOE	3/26/1998	DEF	32.6	2.79		1568		297.9	759.4
WVDEP	4/15/1998	DEF	29.6	2.6	2630	2088		366.9	1032.4
DOE	4/29/1998	DEF	23.1	2.82		1631		212.2	762.4
WVDEP	5/14/1998	DEF	25.5	2.7	3570	1771		250.6	816.3
DOE	5/28/1998	DEF	11.0	2.75		2402		156.0	1182.0
WVDEP	6/15/1998	DEF	9.0	2.6	5370	2881		166.0	1541.7
DOE	6/25/1998	DEF	14.8	2.54		2104		183.9	1031.4
WVDEP	7/15/1998	DEF	12.5	2.6	5370	3199		143.8	954.2
DOE	8/5/1998	DEF	9.9	2.64		3626		218.7	1830.8
WVDEP	8/13/1998	DEF	9.9	2.7	6240	3969		224.9	1897.4
DOE	9/3/1998	DEF	9.0	2.67		3444		183.7	1703.7
WVDEP	9/15/1998	DEF	7.6	2.6	7680	3967		275.0	3002.4
WVDEP	10/15/1998	DEF	7.2	2.7	30300	7990		148.8	1726.9
DOE	10/29/1998	DEF	5.3	2.73		3983		118.6	1874.4

Table E-1g, Omega Mine-pool, DEF Spring, Raw Chemical Data

Sampled By	Date	Location	Flow gpm	pH	Sp. Conductance umhos/cm	TDS, mg/L	Temp, C	Acid load, lbs/day CaCO3 Eq	Calc Total Acidity CaCO3 Eq
WVDEP	11/15/1998	DEF	1.8	2.6	6690	3594		35.3	1639.6
DOE	12/10/1998	DEF	2.5	2.78		3673		51.5	1738.2
WVDEP	12/15/1998	DEF	1.8	2.7	6620	3875		38.4	1784.9
WVDEP	1/17/1999	DEF	39.9	2.6	3240	1037		198.0	413.2
WVDEP	2/14/1999	DEF	19.7	2.7	4110	1937		212.1	895.3
DOE	2/18/1999	DEF	15.1	2.72		2421		199.0	1094.2
WVDEP	3/14/1999	DEF	24.2	2.7	3460	1555		193.0	663.8
DOE	3/30/1999	DEF	17.8	2.80		2001		199.5	932.5
WVDEP	4/13/1999	DEF	12.1	2.7	5640	3118		198.1	1361.7
DOE	4/29/1999	DEF	11.6	2.69		2678		176.2	1260.6
WVDEP	5/17/1999	DEF	8.1	2.7	5870	3118		197.1	2034.6
DOE	5/26/1999	DEF	6.8	2.70		3319		128.3	1560.6
WVDEP	6/14/1999	DEF	4.9	2.6	6390	3622		100.7	1700.0
DOE	6/29/1999	DEF	5.4	2.63		3623		109.7	1704.9
WVDEP	7/13/1999	DEF	4.9	2.6	6480	4096		110.9	1870.6
DOE	7/27/1999	DEF	3.3	2.76		3959		75.1	1874.7
WVDEP	8/14/1999	DEF	3.1	2.6	6400	4275		78.3	2074.3
DOE	8/26/1999	DEF	2.3	2.71		4242		54.5	2004.5
WVDEP	9/14/1999	DEF	1.8	2.7	8220	4586		44.1	2049.7
DOE	9/29/1999	DEF	1.4	2.81		4038		32.4	1922.9
WVDEP	10/15/1999	DEF	1.8	2.7	6370	3807		40.9	1903.2
DOE	10/29/1999	DEF	2.8	2.68		3435		53.6	1570.1
WVDEP	11/15/1999	DEF	1.8	2.6	6680	3630		34.2	1589.4
DOE	12/7/1999	DEF	3.9	2.47		2438		52.6	1114.8
WVDEP	12/15/1999	DEF	5.8	2.6	5000	2466		43.3	619.0
WVDEP	1/17/2000	DEF	5.0	2.5	5650	3103		79.7	1320.8
WVDEP	2/8/2000	DEF	6.0	2.6	8420	3440		91.5	1268.6
WVDEP	3/15/2000	DEF	20.0	3.3	18100	11514		329.7	1373.0
WVDEP	4/14/2000	DEF	32.0	2.7	3250	1516		279.9	727.9
WVDEP	5/15/2000	DEF	13.0	2.7	5170	2553		182.3	1167.6
WVDEP	6/15/2000	DEF	12.0	2.6	4340	2126		158.8	1100.0
WVDEP	7/18/2000	DEF	15.0	2.6	4300	1814		155.3	860.8
WVDEP	8/15/2000	DEF	9.0	4.5	487	278		123.4	1140.4
WVDEP	9/15/2000	DEF	5.0	2.7	5040	3284		100.7	1668.5
WVDEP	10/15/2000	DEF	6.0	2.6	5230	3554		133.2	1846.3
WVDEP	11/15/2000	DEF	5.0	2.7	5510	4097		110.9	1838.4

Table E-1g, Omega Mine-pool, DEF Spring, Raw Chemical Data

Sampled By	Date	Location	Flow gpm	pH	Sp. Conductance umhos/cm	TDS, mg/L	Temp, C	Acid load, lbs/day CaCO3 Eq	Calc Total Acidity CaCO3 Eq
WVDEP	12/14/2000	DEF	4.0	2.6	5770	4117		77.8	1623.0
WVDEP	1/15/2001	DEF	6.0	2.6	5050	3159		97.7	1354.1
WVDEP	2/13/2001	DEF	14.0	2.6	4030	2176		159.1	943.8
WVDEP	3/13/2001	DEF	14.0	2.6	3780	2311		197.1	1169.4
WVDEP	4/16/2001	DEF	31.0	2.7	2910	1264		206.2	553.5
WVDEP	5/15/2001	DEF	7.0	2.6	4800	3185		128.8	1533.1
WVDEP	6/18/2001	DEF	9.0	2.7	4450	2841		117.1	1082.5
WVDEP	7/15/2001	DEF	17.0	2.7	5020	2059		172.0	842.8
WVDEP	8/15/2001	DEF	8.0	2.6	5080	3160		139.3	1444.5
WVDEP	9/14/2001	DEF	5.0	2.6	3310	3310		105.3	1763.1
WVDEP	10/25/2001	DEF	5.8	2.6	3270	4368	11.6	99.7	1424.5
WVDEP	11/15/2001	DEF	4.5	2.7	3000	3976	11.1	78.8	1463.4
WVDEP	12/14/2001	DEF	4.0	2.8	3300	3688	10.5	44.0	918.3
WVDEP	1/16/2002	DEF	16.9	2.7	1766	2096	11.1	141.4	695.0
WVDEP	2/14/2002	DEF	11.1	2.8	2250	2320	11.1	112.0	838.3
WVDEP	3/14/2002	DEF	8.0	2.8	2270	2278	14.4	91.0	950.1
WVDEP	4/15/2002	DEF	15.7	2.9	1980	2328	13.3	163.6	868.3
WVDEP	5/15/2002	DEF	15.7	2.8	2700	2020	12.2	134.5	713.4
WVDEP	6/18/2002	DEF	17.0	2.8	2000	2012	14.4	48.9	239.7
WVDEP	7/18/2002	DEF	0.0					0.0	
WVDEP	8/12/2002	DEF	6.9	2.7	3000		15.5	108.6	1302.0
Perry	8/20/2002	DEF		2.50	3150.00	3196.00	13.50	0.0	1396.5
WVDEP	9/16/2002	DEF	0.0						
WVDEP	10/15/2002	DEF	9.9	2.7	2800	3068	14.4	101.2	853.5
WVDEP	11/15/2002	DEF	0.0						
WVDEP	12/15/2002	DEF							
WVDEP	1/14/2003	DEF	0.0						
WVDEP	2/24/2003	DEF	59.9	2.5	3770	4084	6.1	1179.6	1638.3
WVDEP	3/18/2003	DEF	0.0						
WVDEP	4/15/2003	DEF	0.0						
WVDEP	5/20/2003	DEF							
WVDEP	6/17/2003	DEF	9.0	2.74	2030	3988	15.6	71.2	660.7
WVDEP	8/13/2003	DEF						0.0	
Perry	8/27/2003	DEF	7.7	2.86	4140.00	2820.00	13.40	123.4	1337.1
WVDEP	9/15/2003	DEF	9.0	2.68	2670	5656	15.6	107.6	998.6
WVDEP	10/14/2003	DEF							

Table E-1g, Omega Mine-pool, DEF Spring, Raw Chemical Data

Sampled By	Date	Location	Flow gpm	pH	Sp. Conductance umhos/cm	TDS, mg/L	Temp, C	Acid load, lbs/day CaCO3 Eq	Calc Total Acidity CaCO3 Eq
WVDEP	11/18/2003	DEF							
WVDEP	12/19/2003	DEF							
WVDEP	1/14/2004	DEF	4.0	2.75	2310	2284	10	40.5	844.1
WVDEP	2/17/2004	DEF							
WVDEP	3/23/2004	DEF							
WVDEP	4/13/2004	DEF	17.9	2.78	1936	1496	11.1	36.7	170.5
WVDEP	5/18/2004	DEF							
WVDEP	6/14/2004	DEF							
WVDEP	7/12/2004	DEF	9.0	2.75	2590	2596	15	117.8	1093.5
WVDEP	8/9/2004	DEF	0.0						
WVDEP	9/14/2004	DEF							
WVDEP	10/18/2004	DEF	17.9	2.76	2880	3252	12.2	273.6	1270.4
Perry	3/22/2005	DEF	16.5	2.56	2420	1614	11.2	167.9	846.5
Perry	5/24/2006	DEF	19.9	2.58	2152	1874	12.4	193.0	806.9
Perry	5/3/2007	DEF	23.4	2.57	2565	2162	12	273.0	970.6
Perry	9/13/2007	DEF	5.9	2.41	3540	2550	13.2	80.2	1131.0

Table E-1g, Omega Mine-pool, DEF Spring, Raw Chemical Data

Sampled By	Date	Location	Fe3+, mg/L	Fe2+, mg/L	Fe Total, mg/L	Ca, mg/L	Mg, mg/L	Na, mg/L	K, mg/L	Al, mg/L	Mn, mg/L	SO4, mg/L	Cl, mg/L
DOE	11/15/1991	DEF	472	168	640	313.0	165.0	9.3		133.0	4.40	3925	14
DOE	3/3/1993	DEF	229	423.5	652.5	246.5	124.0	13.7	2.6	130.5	3.50	3107	17
DOE	3/18/1993	DEF	241	106	347	121.0	58.2	23.1	2	67.1	1.60	1710	36.7
DOE	4/2/1993	DEF	397	253	650	194.0	93.0	15.4	0.7	124.0	2.60	2974	22
DOE	4/14/1993	DEF	426	378	804	232.0	114.0	12.0	1	150.0	3.40	3574	15.5
DOE	4/29/1993	DEF	304	290	594	165	85.4	14.8	1.8	107.0	2.70	2624	16.5
DOE	5/20/1993	DEF	306	431	737	237	120.0	10.4	2.7	137.0	3.50	3326	11
DOE	6/3/1993	DEF	303	459	762	228	125.0	10.0	1.8	141.0	3.60	3424	9.3
DOE	6/10/1993	DEF	282.89	474	756.89	232.51	127.0	11.6	2.31	140.5	3.64	3395.73	14.5
DOE	6/23/1993	DEF	317.14	465	782.14	248.32	137.4	12.1	2.58	137.9	3.94	3520.99	14.1
DOE	7/8/1993	DEF	266.57	409	675.57	227.1	124.5	13.3	1.12	128.8	3.65	3175.82	15.8
DOE	7/22/1993	DEF	216.42	506	722.42	247.78	133.5	13.6	1.1	142.5	3.96	3406.07	19
DOE	8/11/1993	DEF	236.07	514	750.07	256.98	141.0	12.7	0.67	153.7	4.27	3506.09	
DOE	9/2/1993	DEF	253.78	538	791.78	272.66	149.3	11.2	0.89	159.4	4.49	3790.16	
DOE	9/10/1993	DEF	231.21	471.3	702.51	252.2	137.5	15.5	0.6	142.8	4.10	3431.79	
DOE	10/7/1993	DEF	246.22	332	578.22	217.05	120.1	21.3	0.38	119.4	3.74	2977.62	36.3
DOE	10/25/1993	DEF	235.26	329	564.26	208.1	117.1	22.6	0.67	110.4	3.50	2805.24	40.5
DOE	11/10/1993	DEF	229.81	312	541.81	201.7	112.3	22.4	0.76	100.5	3.33	2708	46
DOE	12/7/1993	DEF	132.91	107.8	240.71	95.3	49.9	25.3	1.81	47.9	1.54	1290	33
DOE	12/23/1993	DEF	266.82	298.9	565.72	180.8	97.6	16.9	0.1	115.4	2.82	2754	29
DOE	1/28/1994	DEF	128.25	72.6	200.85	71.5	35.5	29.1	0.92	47.5	1.03	1057	60.6
DOE	5/5/1994	DEF	281.61	364	645.61	204.4	98.3	16.8	1.4	136.8	3.03	3019	83.22
DOE	6/10/1994	DEF	210.52	448.8	659.32	213.9	106.9	16.9	1.15	136.3	3.43	3021	91.3
DOE	7/6/1994	DEF	205.31	464.4	669.71	222.0	112.4	18.4	1.13	137.1	3.49	3052	89.2
DOE	8/3/1994	DEF	153.27	404.3	557.57	194.0	104.5	19.3	1.04	111.1	3.15	2601	69.4
DOE	9/1/1994	DEF	148.77	299.7	448.47	165.3	85.3	20.6	1.42	94.8	2.63	2239	83.4
DOE	10/7/1994	DEF	103.24	564	667.24	233.2	121.5	16.9	0.42	148.3	3.84	3261	58.75
DOE	11/16/1994	DEF	101.66	541.97	643.63	224.7	119.9	17.6	0.4	144.4	3.61	3183	36.3
DOE	12/14/1994	DEF	110.18	171.2	281.38	114.2	59.4	22.9	1.01	61.5	2.06	1595	59.83
DOE	1/10/1995	DEF	142.76	374.8	517.56	188.7	101.6	19.7	0.76	113.9	3.22	2593	55.76
DOE	2/3/1995	DEF	117.74	312.8	430.54	165.8	85.4	21.0	0.83	98.5	2.70	2229	48.86
DOE	3/2/1995	DEF	121.46	232.12	353.58	132.4	66.9	24.9	1.24	82.5	2.01	1817	55.34
DOE	4/7/1995	DEF	121.3	355.4	476.7	177.39	90.24	20.66	0.98	119.7	2.69	2483.21	51.92
DOE	5/10/1995	DEF	133.2	226.4	359.6	136.0	70.0	22.3	1.2	85.0	2.10	1891	51.9
DOE	6/6/1995	DEF	141.16	258.9	400.06	150.7	75.5	20.6	0.64	103.2	2.32	2157	48.9
DOE	7/13/1995	DEF	155.33	434.5	589.83	204.94	106.54	18.82	0.59	143.36	3.26	2967.2	47.8

Table E-1g, Omega Mine-pool, DEF Spring, Raw Chemical Data

Sampled By	Date	Location	Fe3+, mg/L	Fe2+, mg/L	Fe Total, mg/L	Ca, mg/L	Mg, mg/L	Na, mg/L	K, mg/L	Al, mg/L	Mn, mg/L	SO4, mg/L	Cl, mg/L
DOE	8/3/1995	DEF	107.69	568	675.69	225.4	119.6	16.2	0.59	163.4	3.84	3297	51.4
DOE	9/7/1995	DEF	711.68		711.68	253.11	133.03	19.88	1.38	164.67	4.34	3642.85	53.1
DOE	10/12/1995	DEF	67.77	537.4	605.17	207.69	113.95	18.12	0.5	147.79	3.67	3050.37	48.1
DOE	11/22/1995	DEF	161.62	198.5	360.12	136.1	70.3	33.7	0.57	81.7	2.29	1902	63.2
DOE	1/5/1996	DEF	102.1	139.1	241.2	106.6	51.8	32.5	0.87	62.0	1.68	1417	93.71
WVDEP	1/16/1996	DEF			341					87.1	3.6	2280	
WVDEP	2/15/1996	DEF			383						1.85	1720	
DOE	2/21/1996	DEF	203.18	206	409.18	125.2	61.1	25.1	0.95	103.4	1.89	2067	41.89
WVDEP	3/1/1996	DEF			221						1.06	1360	
WVDEP	3/15/1996	DEF			351						1.63	1840	
DOE	3/18/1996	DEF	156.72	96.5	253.22	93.1	43.8	25.9	0.79	66.5	1.33	1403	54.54
WVDEP	3/28/1996	DEF			186						1.14	1310	
WVDEP	4/15/1996	DEF			355						1.98	1560	
DOE	4/26/1996	DEF	134.3	147.3	281.6	108.0	51.9	24.2	0.49	75.7	1.49	1577	49.27
WVDEP	4/29/1996	DEF			7.46						0.04	1800	
WVDEP	5/15/1996	DEF			18.7					51.6	1.31	1000	
WVDEP	5/31/1996	DEF			318					78.7	1.95	1320	
DOE	6/7/1996	DEF	139.42	207	346.42	107.4	52.4	22.2	0.82	90.4	1.85	1815	40.75
WVDEP	6/14/1996	DEF			464					119	2.78	2140	
WVDEP	6/28/1996	DEF			454					127	2.81	1960	
WVDEP	7/15/1996	DEF			432					104	2.8	2310	
DOE	7/23/1996	DEF	160.8	190.2	351	119.6	49.7	25.5	0.42	82.5	1.74	1743	55.43
WVDEP	7/30/1996	DEF			321					76.1	2.3	1890	
WVDEP	8/14/1996	DEF			342					88.2	2.28	1680	
DOE	8/28/1996	DEF	127.51	243.6	371.11	152.6	68.1	24.3	0.05	99.8	1.90	1990	51.12
WVDEP	8/31/1996	DEF			328					86	3.66	1990	
WVDEP	9/16/1996	DEF			424					111	2.88	1880	
WVDEP	9/30/1996	DEF			299					78.6	2.25	1720	
WVDEP	10/14/1996	DEF			389					97.9	2.56	1740	
DOE	10/16/1996	DEF	102.55	300.5	403.05	169.0	75.1	23.4	0.57	103.3	2.26	2184	48.6
WVDEP	10/30/1996	DEF			257					64.6	1.71	1210	
WVDEP	11/15/1996	DEF			173					47.6	1.21	574	
DOE	11/26/1996	DEF	103.92	175.00	278.92	111.56	54.08	21.86	0.72	75.65	1.72	1574.41	43.5
DOE	12/13/1996	DEF	85.52	98.2	183.72	82.63	38.67	23.11	0.98	52.71	1.17	1121.44	36.02
WVDEP	12/15/1996	DEF			129					45.5	1.16	642	
WVDEP	1/14/1997	DEF			254					72.7	1.82	1060	

Table E-1g, Omega Mine-pool, DEF Spring, Raw Chemical Data

Sampled By	Date	Location	Fe3+, mg/L	Fe2+, mg/L	Fe Total, mg/L	Ca, mg/L	Mg, mg/L	Na, mg/L	K, mg/L	Al, mg/L	Mn, mg/L	SO4, mg/L	Cl, mg/L
DOE	1/28/1997	DEF	91.82	186	277.82	109.11	53.59	18.26	0.83	79.87	1.61	1555.48	12.9
DOE	2/21/1997	DEF	182.78	55.5	238.28	117.9	48.1	23.8	0.61	66.3	1.47	1370	55.6
WVDEP	3/17/1997	DEF			569					118	2.45	1920	
DOE	3/26/1997	DEF	133.76	216.9	350.66	107.8	51.7	21.8	0.79	92.4	1.88	1811	42.7
WVDEP	4/14/1997	DEF			451					127	2.68	3440	
WVDEP	5/14/1997	DEF			481					122	2.86	1340	
DOE	5/20/1997	DEF	139.28	271	410.28	138.0	66.3	17.2	0.25	107.1	2.50	2130	
WVDEP	6/16/1997	DEF			536					138	2.69	1530	
DOE	7/10/1997	DEF	130.52	347.9	478.42	164.1	77.6	16.8	0.88	123.7	2.70	2411	36.07
WVDEP	7/16/1997	DEF			383					100	2	2190	
WVDEP	8/17/1997	DEF			493					137	2.76	1340	
DOE	9/10/1997	DEF	96.99	322.2	419.19	156.2	78.1	20.3	1.05	109.3	2.66	2170	42.3
WVDEP	9/15/1997	DEF			381						2.54	1880	
WVDEP	10/15/1997	DEF			467					114	2.6	1500	
DOE	11/5/1997	DEF	92.52	384.7	477.22	173.7	87.0	19.1	1.14	121.6	2.93	2398	39.89
WVDEP	11/14/1997	DEF			373					59.2	1.52	840	
WVDEP	12/15/1997	DEF			299					83	2.86	1650	
DOE	1/12/1998	DEF	136.58	87.7	224.28	81.2	37.4	28.9	1.33	53.6	1.20	1247	44.5
WVDEP	1/16/1998	DEF			241					70.8	1.57	1440	
DOE	2/9/1998	DEF	118.4	109.8	228.2	102.8	46.3	33.3	1.86	73.0	1.36	1362	49.92
WVDEP	2/15/1998	DEF			220					62.4	1.09	1240	
WVDEP	3/15/1998	DEF			198					64.4	1.06	1260	
DOE	3/26/1998	DEF	118.41	73.4	191.81	78.8	36.6	34.3	1	59.9	1.04	1162	
WVDEP	4/15/1998	DEF			251					81.9	1.31	1400	
DOE	4/29/1998	DEF	104.17	89.66	193.83	86.2	40.4	29.8	1.02	60.8	1.17	1214	
WVDEP	5/14/1998	DEF			203					63.1	1.42	1160	
DOE	5/28/1998	DEF	92.84	218	310.84	120.9	58.8	24.1	1.03	96.6	0.00	1730	55.09
WVDEP	6/15/1998	DEF			401					125	2.05	2040	
DOE	6/25/1998	DEF	115.4	145	260.4	111.5	48.8	29.5	0.87	75.8	0.02	1520	53.2
WVDEP	7/15/1998	DEF			433					8.73	2.68	1960	
DOE	8/5/1998	DEF	143.2	353.6	496.8	175.1	83.6	18.8	0.8	147.9	2.72	2649	42.93
WVDEP	8/13/1998	DEF			511					158	2.75	2380	
DOE	9/3/1998	DEF	111.92	353.7	465.62	170.9	83.1	20.4	0.73	136.5	2.79	2509	47.71
WVDEP	9/15/1998	DEF			52.6					500	2.73	2500	
WVDEP	10/15/1998	DEF			480					137	3.67	2320	
DOE	10/29/1998	DEF	118.55	423.7	542.25	199.4	99.7	21.9	1.36	144.8	3.26	2916	45.18

Table E-1g, Omega Mine-pool, DEF Spring, Raw Chemical Data

Sampled By	Date	Location	Fe3+, mg/L	Fe2+, mg/L	Fe Total, mg/L	Ca, mg/L	Mg, mg/L	Na, mg/L	K, mg/L	Al, mg/L	Mn, mg/L	SO4, mg/L	Cl, mg/L
WVDEP	11/15/1998	DEF			439					130	3.24	2560	
DOE	12/10/1998	DEF	101.16	374.81	475.97	212.6	95.8	21.9	1.12	143.5	3.25	2665	46.2
WVDEP	12/15/1998	DEF			504					140	2.79	2230	
WVDEP	1/17/1999	DEF			84.6					24.3	0.65	507	
WVDEP	2/14/1999	DEF			221					71.5	1.47	1440	
DOE	2/18/1999	DEF	110.22	164.6	274.82	134.7	56.6	29.0	0.81	90.6	1.93	1747	81.29
WVDEP	3/14/1999	DEF			166					47.7	1.04	952	
DOE	3/30/1999	DEF	98.45	133	231.45	111.9	46.5	31.7	1.37	78.5	1.53	1440	54.49
WVDEP	4/13/1999	DEF			349					114	2.09	1910	
DOE	4/29/1999	DEF	116.79	204.9	321.69	144.6	62.4	23.4	0.6	104.2	2.10	1960	53.06
WVDEP	5/17/1999	DEF			644					140	2.24	1900	
DOE	5/26/1999	DEF	156.68	263	419.68	187.3	81.0	22.3	0.68	126.8	2.76	2424	47.2
WVDEP	6/14/1999	DEF			470					131	2.84	1940	
DOE	6/29/1999	DEF	123.18	326.6	449.78	199.84	88.94	16.88	0.68	139.78	3.24	2682.33	33.72
WVDEP	7/13/1999	DEF			528					143	2.92	2040	
DOE	7/27/1999	DEF	139.66	361.2	500.86	217.1	100.4	16.8	0.87	159.3	3.50	2906	45.65
WVDEP	8/14/1999	DEF			573					165	3.43	2830	
DOE	8/26/1999	DEF	125.3	420	545.3	238.7	109.8	20.9	1.48	166.3	3.77	3101	45.61
WVDEP	9/14/1999	DEF			583					162	3.38	2280	
DOE	9/29/1999	DEF	99.32	418.32	517.64	226.3	104.6	18.0	1.03	164.1	3.80	2953	40
WVDEP	10/15/1999	DEF			523					155	3.31	2640	
DOE	10/29/1999	DEF	164.2	238.6	402.8	195.0	89.9	27.3	10.5	133.0	3.08	2498	67.86
WVDEP	11/15/1999	DEF			399					134	2.76	2310	
DOE	12/7/1999	DEF	144.91	117.6	262.51	139.1	62.6	37.9	0.91	84.9	2.10	1764	79.8
WVDEP	12/15/1999	DEF			25.6					79.9	2.05	1660	
WVDEP	1/17/2000	DEF			318					106	2.5	1920	
WVDEP	2/8/2000	DEF			322					101	3.01	2650	
WVDEP	3/15/2000	DEF			369					123	2.21	7370	
WVDEP	4/14/2000	DEF			166					59.2	1.16	1340	
WVDEP	5/15/2000	DEF			278					102	1.92	2450	
WVDEP	6/15/2000	DEF			274					86.5	1.82	845	
WVDEP	7/18/2000	DEF			215					62.6	1.39	1590	
WVDEP	8/15/2000	DEF			311					104	2.34	225	
WVDEP	9/15/2000	DEF			436	146				141	2.67	2980	
WVDEP	10/15/2000	DEF			495					149	3.73	2960	
WVDEP	11/15/2000	DEF			487					155	3.11	3660	

Table E-1g, Omega Mine-pool, DEF Spring, Raw Chemical Data

Sampled By	Date	Location	Fe3+, mg/L	Fe2+, mg/L	Fe Total, mg/L	Ca, mg/L	Mg, mg/L	Na, mg/L	K, mg/L	Al, mg/L	Mn, mg/L	SO4, mg/L	Cl, mg/L
WVDEP	12/14/2000	DEF			455					122	2.79	3850	
WVDEP	1/15/2001	DEF			345					109	2.91	2210	
WVDEP	2/13/2001	DEF			224					74.5	1.83	1270	
WVDEP	3/13/2001	DEF			282					96.4	1.86	1930	
WVDEP	4/16/2001	DEF			110					45.9	0.97	1938	
WVDEP	5/15/2001	DEF			365					135	2.21	3197	
WVDEP	6/18/2001	DEF			269					89.6	1.88	2964	
WVDEP	7/15/2001	DEF			196					70.1	1.5	3343	
WVDEP	8/15/2001	DEF			362					120	2.28	3383	
WVDEP	9/14/2001	DEF			462					145	2.67	2204	
WVDEP	10/25/2001	DEF			359					117.25	2.63	2178	
WVDEP	11/15/2001	DEF			391.24					118.47	2.75	1998	
WVDEP	12/14/2001	DEF			190.28					89.08	1.94	2198	
WVDEP	1/16/2002	DEF			126.84					65.86	1.25	1176	
WVDEP	2/14/2002	DEF			179.35					78.37	1.44	1499	
WVDEP	3/14/2002	DEF			249.74					75.82	1.39	1512	
WVDEP	4/15/2002	DEF			234.34					69.06	1.17	1319	
WVDEP	5/15/2002	DEF			173.21					57.99	1.06	1798	
WVDEP	6/18/2002	DEF			77.42					3.68	0.77	1332	
WVDEP	7/18/2002	DEF											
WVDEP	8/12/2002	DEF			314.52					114.45	1.82	1998	
Perry	8/20/2002	DEF	67.742	270.968	338.71	135.1	65.4	23.0	1.12	113.0	2.25	1931	58.3
WVDEP	9/16/2002	DEF											
WVDEP	10/15/2002	DEF			204.7					69.12	1.82	1865	
WVDEP	11/15/2002	DEF											
WVDEP	12/15/2002	DEF											
WVDEP	1/14/2003	DEF											
WVDEP	2/24/2003	DEF			451.68					120.02	2.61	2511	
WVDEP	3/18/2003	DEF											
WVDEP	4/15/2003	DEF											
WVDEP	5/20/2003	DEF											
WVDEP	6/17/2003	DEF			138					57.75	0.99	1352	
WVDEP	8/13/2003	DEF											
Perry	8/27/2003	DEF			349	126.0	60.2	26.0	1.04	115.0	2.43	1811	
WVDEP	9/15/2003	DEF			248.94					80.19	1.65	1778	
WVDEP	10/14/2003	DEF											

Table E-1g, Omega Mine-pool, DEF Spring, Raw Chemical Data

Sampled By	Date	Location	Fe3+, mg/L	Fe2+, mg/L	Fe Total, mg/L	Ca, mg/L	Mg, mg/L	Na, mg/L	K, mg/L	Al, mg/L	Mn, mg/L	SO4, mg/L	Cl, mg/L
WVDEP	11/18/2003	DEF											
WVDEP	12/19/2003	DEF											
WVDEP	1/14/2004	DEF			187.45					75.11	1.25	1538	
WVDEP	2/17/2004	DEF											
WVDEP	3/23/2004	DEF											
WVDEP	4/13/2004	DEF			0.65					14.16	4.29	1289	
WVDEP	5/18/2004	DEF											
WVDEP	6/14/2004	DEF											
WVDEP	7/12/2004	DEF			254.49					98.29	1.63	1725	
WVDEP	8/9/2004	DEF											
WVDEP	9/14/2004	DEF											
WVDEP	10/18/2004	DEF			310.41					112.32	2.1	1918	
Perry	3/22/2005	DEF	104.7	63.3	168.03	102.74	42.46	37.26	1.51	72.99	1.38	1232.9	65
Perry	5/24/2006	DEF	121.7	48.3	169.79	94.2	40.4	28.96	1.33	66.4	1.37	1184	82
Perry	5/3/2007	DEF	56.7	141.4	197.75	96.23	41.7	26.66	1.06	86.3	1.41	1435	60
Perry	9/13/2007	DEF			224.9	109.3	51.24	41.14	0.77	95.4	2.1	1615	100

Appendix F

T&T Mine-pool Raw Chemical Data

Table F-1, T&T Mine-pool, Raw Chemical Data

Site	Date	Flow, gpm	pH	Acdity CaCO₃ Eq	Sp Cond. umhos/cm	TDS, mg/L	Fe, mg/L	Al, mg/L	Mn, mg/L	SO4, mg/L	Ca, mg/L
T&T	4/8/1994			1247			1024		5.1	4000	
T&T	4/25/1994			1843			700		3.6		
T&T	6/13/1994			1260			316	75.3	3.14	1860	
T&T	6/24/1994		2.8	990	3890		455	90	3.14	1910	287
T&T	7/17/1994			1400			152		2.6	3010	
T&T	7/26/1994			277			512		2.6	2650	
T&T	7/29/1994			921			241		1.4	2870	
T&T	8/11/1994			434			177		1	2900	
T&T	8/23/1994			319			10.4		0.5		
T&T	8/26/1994			20			321		0.5	2680	
T&T	8/29/1994			576			1220		5.53	2400	
T&T	9/4/1994			2194			47.4		2.07	2400	
T&T	9/20/1994			89			789		5.79	2500	
T&T	9/23/1994			1423			413		2.72	2040	
T&T	10/3/1994	100		744			600		2.98	1850	
T&T	10/25/1994			1080			311		2.67	2480	
T&T	10/31/1994	175		562			70.9		0.61	2370	
T&T	11/14/1994	150		128			220		1.42	2725	
T&T	11/28/1994	200		396			581		4.21	2340	
T&T	12/13/1994	775		1048			154		0.96	1380	
T&T	12/16/1994	550		277			265		1.94	2090	
T&T	12/27/1994	550		478			324		2.49	2360	
T&T	1/3/1995	575		585			393		3.38	2780	
T&T	1/6/1995	150		710			110		0.92	2140	
T&T	1/9/1995	550		199			269		1.91	1890	
T&T	1/12/1995			485			13.8		0.66	2650	
T&T	1/27/1995	900		26			209		1.7	2170	
T&T	2/9/1995	600		377			316		2.77	2300	
T&T	2/23/1995	600		571			225		2.32	1880	
T&T	2/28/1995			407			170		1.86	1830	
T&T	3/5/1995			308			5220		21.3	10600	
T&T	3/9/1995			9384			2500		16.5	13400	
T&T	4/10/1995	800		4506			1220		5.84	4840	
T&T	4/3/1996	928	2.6	2195	3800	2194	251		2.81	1600	
T&T	5/1/1996	888	2.6	580	4210	2058	231		2.31	1210	
T&T	5/8/1996	968	2.6	543	3560	1930	39.4		0.54	1300	
T&T	5/15/1996	1012	2.6	197	5250	2163	205		2.44	1540	
T&T	5/22/1996	1137	2.4	497	5430	2701	336		2.65	1780	
T&T	5/29/1996	1146	2.5	805	4350	2014	216		1.98	1330	
T&T	6/5/1996	1057	2.6	548	4270	2375	261		2.56	1420	
T&T	6/12/1996	703	3.6	597	4340	1897	246		2.41	1400	
T&T	6/19/1996	793	2.6	457	4040	1932	202		2.01	1250	
T&T	6/26/1996	529	2.7	491	3810	1932	229		1.88	1300	
T&T	7/3/1996	422	2.6	513	4500	2002	208		2.02	1050	
T&T	7/10/1996	422	2.7	502	3950	1954	191		2.12	1230	
T&T	7/17/1996	383	2.6	446	4130	2102	246	46	2.32	1560	
T&T	7/24/1996	721	2.6	826	4220	2030	196	32.6	1.9	1550	
T&T	7/31/1996	569	2.6	661	4120	2309	230	36.1	2.43	1450	
T&T	8/7/1996	650	2.6	742	3930	1956	216	38.3	2.48	1320	

Table F-1, T&T Mine-pool, Raw Chemical Data

Site	Date	Flow, gpm	pH	Acdity CaCO$_3$ Eq	Sp Cond. umhos/cm	TDS, mg/L	Fe, mg/L	Al, mg/L	Mn, mg/L	SO4, mg/L	Ca, mg/L
T&T	8/14/1996	569	2.6	658	3690	2014	182	36.5	2.2	1330	
T&T	8/21/1996	491	2.6	700	4160	1940	190	41.3	2.58	1320	
T&T	8/28/1996	408	2.7	796	2010	1934	265	39.1	2.35	1330	
T&T	9/3/1996	371	2.6	728	5350	2485	213	39.1	2.34	1130	
T&T	9/11/1996	335	2.7	161	4520	2141	8.17	7.98	1.51	1240	
T&T	9/17/1996	290	3.6	666	3760	2102	232	42	2.39	1260	
T&T	9/24/1996	301	2.7	661	3910	2446	181	42	2.26	1110	
T&T	10/2/1996	301	2.6	764	3820	2410	229	40.3	2.34	1230	
T&T	10/8/1996	301	2.6	798	4270	2217	232	45.4	2.58	1290	
T&T	10/15/1996	301	2.7	763	4420	2662	234	43.3	2.35	1160	
T&T	10/23/1996	435	2.7	727	4780	1986	213	43.7	1.94	1170	
T&T	10/30/1996	491	2.6	788	4440	2237	250	38	2.28	1410	
T&T	11/4/1996	516	2.6	760	4790	2222	227	40.3	2.4	1050	
T&T	11/12/1996	536	2.6	711	5440	2070	214	35.7	2.37	1170	
T&T	11/20/1996	569	2.6	811	5720	2470	246	43.2	2.71	1270	
T&T	11/27/1996	551	2.6	760	4890	2408	231	38.9	2.57	1170	
T&T	12/2/1996	569	3.2	58	864	545	13.3		1.4	265	
T&T	12/11/1996	703	2.5	808	4900	2247	232	41.2	3.13	986	
T&T	12/18/1996	618	2.6	753	4820	1940	235	36.4	2.71	1150	
T&T	12/23/1996	582	2.6	704	4450	2321	212	34.9	2.56	1350	
T&T	12/30/1996	569	2.6	700	4710	2096	214	33.7	2.35	772	
T&T	1/7/1997	618	2.6	675	4390	2068	202	33	2.36	978	
T&T	1/15/1997	614	2.6	642	4310	1921	187	32	2.16	1310	
T&T	1/22/1997	536	2.7	687	4320	1972	206	38.6	2.37	1380	
T&T	1/29/1997	533	2.6	677	4430	1729	187	38.2	2.3	1230	
T&T	3/5/1997	650	2.6	1154	2510	1642	470	33	1.89	1030	
T&T	4/2/1997	668	2.5	714	2467	1815	201	34.6	2.2	1210	
T&T	5/7/1997	521	2.5	674	2230	1716	170	37.3	2.13	1270	
T&T	6/4/1997	582	2.6	601	2630	1906	171	29.6	2.71	1130	
T&T	7/2/1997	463	2.6	580	2470	1833	147	33.9	1.75	1040	
T&T	8/5/1997	301	2.6	630	2360	2216	172	34.7	2.06	1030	
T&T	9/2/1997	288	2.7	614	2620	1938	174	35.8	1.91	980	
T&T	10/1/1997	290	2.7	606	4670	1996	186	30.6	1.67	1220	
T&T	11/5/1997	240	2.6	709	2710	296	199	40.2	2.09	953	
T&T	12/1/1997	422	2.5	732	3000	2597	189	41.6	2.55	864	
T&T	1/2/1998	358	2.6	576	4120	2161	147	33	2.26	1290	
T&T	2/5/1998	569	2.6	639	3870	1675	188	31.2	2.16	1390	
T&T	3/4/1998	569	3.2	511	762	528	166	32.1	2.34	321	
T&T	4/2/1998	551	2.7	570	2250	1771	162	31.8	2.04	1210	
T&T	5/4/1998	536	2.7	508	3530	1956	154	23.4	1.56	1150	
T&T	6/3/1998	422	2.7	492	3640	1686	139	25.2	1.7	994	
T&T	7/7/1998	491	2.6	557	3720	1820	127	35.9	2.66	1040	
T&T	8/7/1998	358	2.6	546	3880	1522	137	30.9	1.7	782	
T&T	9/2/1998	280	2.7	187	3870	1950	15.2	10.3	1.35	828	
T&T	10/7/1998	178	2.7	624	5010	2415	196	30.7	1.73	1020	
T&T	11/2/1998	133	2.7	569	3970	2154	141	38.4	1.97	1240	
T&T	12/7/1998	120	2.7	605	4350	2066	144	43.9	2.14	988	
T&T	12/7/1998	121	3	608	2361		166	46.2	2.3	1360	92
T&T	12/14/1998	102	3.1	580	2960	2222	158	45.8	1.84	1250	156
T&T	12/21/1998	102	3.2	704	2406	2253	204	54.8	1.76	1424	148
T&T	12/28/1998	91	3.1	629	2453	2244	185	45.8	1.79	1430	155

Table F-1, T&T Mine-pool, Raw Chemical Data

Site	Date	Flow, gpm	pH	730	Sp Cond. umhos/cm	TDS, mg/L	Fe, mg/L	Al, mg/L	Mn, mg/L	SO4, mg/L	Ca, mg/L
T&T	1/4/1999	91	3.4	613	4400	2293	191	44.7	1.77	1431	132
T&T	1/6/1999	91	2.8	587	3650	2114	155	40.9	1.95	1340	
T&T	1/11/1999	97	2.7	644	2970	2294	179	39.7	1.83	1510	104
T&T	1/18/1999	280	2.7	624	2576	2108	173	38.6	0.16	1510	77
T&T	1/25/1999	423	3	542	2420	1978	154	38.4	1.49	1190	66
T&T	2/1/1999	256	2.8	599	4020	2174	151	44.1	2.5	1340	
T&T	2/8/1999	280	3.2	524	2719	2198	165	34.7	2.16	1340	160
T&T	2/15/1999	318	2.7	509	2578	1821	141	27.5	2	1270	155
T&T	2/22/1999	240	2.6	559	2024	1968	146	30.2	2.12	1260	144
T&T	3/1/1999	221	2.7	514	2568	2174	131	31.7	2.04	1270	142
T&T	3/3/1999	247	2.8	586	4000	1795	172	35.1	2.33	1220	
T&T	3/8/1999	250	2.8	530	2412	1973	141	35.1	2.12	1160	109
T&T	3/15/1999	439	2.8	582	2930	2284	169	35.4	2.22	1480	127
T&T	3/22/1999	423	2.9	470	3190	2042	127	31.6	2.14	1210	126
T&T	3/29/1999	436	2.9	607	3600	2126	177	40.1	2.58	1480	105
T&T	4/5/1999	422	2.7	539	3800	2037	147	30.9	2.17	1130	
T&T	4/5/1999	423	2.9	483	3310	1962	134	31.7	2.12	1140	126
T&T	4/12/1999	378	3	449	3050	1810	131	29	2.12	1070	143
T&T	4/19/1999	396	3.2	379	2166	1701	112	25.8	1.84	1090	137
T&T	4/26/1999	302	3.3	454	3010	1750	109	41.5	1.85	1030	164
T&T	5/3/1999	302	3.3	388	3950	1752	122	25.4	1.96	1040	146
T&T	5/4/1999	301	2.7	464	3780	1691	120	26.2	1.89	1090	
T&T	5/10/1999	250	3.3	436	3040	1751	126	32.7	1.98	1050	151
T&T	5/17/1999	212	3.2	513	2400	1740	118	48.1	1.85	1090	162
T&T	5/24/1999	260	3.2	467	1410	1834	104	44.3	1.56	937	150
T&T	5/31/1999	221	3.2	497	2355	1876	111	47.4	1.71	912	150
T&T	6/2/1999	211	2.7	466	3930	1628	115	28.3	1.84	1080	
T&T	7/13/1999	192	2.7	526	3670	1675	139	31.3	1.78	1160	
T&T	7/14/1999	193	3.1	559	2192	2036	117	55.1	1.97	1140	148
T&T	7/29/1999	175	2.7	568	2345	2005	142	37.8	2.17	1230	142
T&T	7/30/1999	175	2.9	478	2345	1968	125	33.8	1.84	1210	163
T&T	8/2/1999	180	3.1	484	2347	2087	130	37.4	2.07	1180	136
T&T	8/10/1999	134	2.8	540	3790	2476	144	35.9	2.05	1300	
T&T	8/30/1999	102	3.1	444	2256	2078	121	33.2	1.85	1390	125
T&T	9/14/1999	96	2.7	554	4560	2134	142	35.4	1.93	842	
T&T	10/7/1999	80	2.8	569	4220	2319	152	38.6	2.01	1120	
T&T	10/11/1999	86	3.3	501	2402	1995	141	39.6	2.04	1190	151
T&T	11/1/1999	91	2.8	546	4590	2500	138	38.8	2.09	1150	
T&T	11/9/1999	86	3.1	458	2470	2166	127	33.8	1.98	1200	186
T&T	11/17/1999	91	3.3	458	2780	2196	132	34.7	1.97	1160	153
T&T	11/30/1999	171	3.1	533	2625	2119	155	38.2	1.79	1320	144
T&T	12/10/1999	95	2.86	599	2482	1975	166	41.2	2.29	1000	127
T&T	12/14/1999	109	2.8	523	3950	2001	139	34.4	2.07	1120	
T&T	1/11/2000	135	2.8	548	4170	2244	139	38.7	2.63	1320	
T&T	1/11/2000	135	2.8	495	2601	2282	129	32.4	2.47	1340	149
T&T	2/3/2000	151	3	594	2486	2207	169	42.7	2.43	1340	176
T&T	2/16/2000	232	2.7	541	3800	2009	116	41.1	2.69	1250	
T&T	2/28/2000	576	2.9	976	3292	2997	309	63.6	3.58	2280	159
T&T	3/8/2000	284	2.7	728	4630	2207	210	44.6	2.64	1650	
T&T	3/17/2000	232	2.79	705	2495	1961	182	52.5	3.59	1450	222
T&T	3/31/2000	291	2.59	695	2449	2004	175	44.5	3.08	1280	157
T&T	4/3/2000	297	2.7	511	4210	2113	125	33	2.36	1540	213

Table F-1, T&T Mine-pool, Raw Chemical Data

Site	Date	Flow, gpm	pH	730	Sp Cond. umhos/cm	TDS, mg/L	Fe, mg/L	Al, mg/L	Mn, mg/L	SO4, mg/L	Ca, mg/L
T&T	5/3/2000	445	2.85	518	2223	1897	130	37.9	2.02	973	147
T&T	5/10/2000	354	2.7	495	370	1828	117	32.7	2.03	1410	187
T&T	6/5/2000	290	2.8	403	3720	1607	83.6	30.7	2.04	1380	225
T&T	6/7/2000	348	2.78	501	2183	1848	114	37.7	2.68	1130	160
T&T	6/20/2000	411	2.7	634	4640	2036	180	37.4	2.34	1930	
T&T	6/28/2000	286	2.62	757	3200	3070	185	54.1	2.78	1720	222
T&T	7/10/2000	172	2.6	838	5510	3240	220	56.6	2.24	2410	481
T&T	7/18/2000	198	2.66	1594	3790	4110	384	142	4.34	2420	328
T&T	8/1/2000	196	2.6	1252	4950	3636	375	81	2.74	3200	729
T&T	8/1/2000	196	2.67	903	3870	3610	209	75	2.66	2210	393
T&T	8/25/2000	171	2.57	864	3590	3180	187	70.2	2.73	1860	502
T&T	9/6/2000	160	2.8	754	4630	3214	168	66.5	2.77	2800	397
T&T	9/12/2000	130	2.78	659	3090	3130	146	56	2.23	1780	388
T&T	9/22/2000	139	2.79	1087	3130	3020	246	101	2.35	1810	598
T&T	10/4/2000	150	2.8	566	2995	2865	117	49.3	2.11	870	324
T&T	10/12/2000	129	2.7	661	4190	2822	145	53.5	2.35	2620	390
T&T	10/20/2000	130	2.7	530	3030	2570	104	43.3	2.17	1800	363
T&T	11/3/2000	73	2.76	548	3040	2950	107	47.8	2.17	1990	319
T&T	11/6/2000	86	2.7	684	3830	3007	135	60.8	2.5	1990	365
T&T	12/1/2000	69	2.8	616	4570	2731	143	49.8	2.1	1960	393
T&T	12/1/2000	70	2.8	587	2920	3150	121	51.6	2.25	1460	343
T&T	1/2/2001	73	2.79	568	2850	2450	122	47.6	2.02	1770	322
T&T	1/2/2001	73	2.8	575	4170	2887	133	45.8	1.93	2180	346
T&T	2/1/2001	171	2.56	739	2893	2150	167	53.6	2.49	1720	367
T&T	2/5/2001	171	2.7	495	4120	2398	102	37.7	1.93	1450	288
T&T	2/28/2001	219	2.62	719	2965	2610	158	56.3	1.98	2050	232
T&T	3/7/2001	232	2.8	528	3980	2362	114	43.2	2.65	2210	372
T&T	4/2/2001	223	2.93	409	2710	2420	96	31.4	2.14	1550	336
T&T	4/9/2001	126	2.8	458	3340	2382	58.9	47.8	4.18	1410	252
T&T	5/1/2001	175	2.8	436	4190	1734	106	29.4	2.28	1480	278
T&T	5/3/2001	180	2.85	381	2582	2240	85	27.7	2.22	1640	283
T&T	6/4/2001	143	2.74	352	2416	2175	76	21.9	2.03	1470	301
T&T	6/18/2001	142	2.8	357	3500	2279	76.8	24.7	1.93	1160	389
T&T	7/2/2001	158	2.8	403	2758	2072	94	27.3	2.2	1480	342
T&T	7/10/2001	157	2.8	376	3580	1995	82.2	26.1	2.32	1850	278
T&T	8/1/2001	185	2.69	443	2960	2302	108	25.7	2.49	1470	296
T&T	8/8/2001	209	2.8	431	3730	2549	108	27.6	2.65	1220	341
T&T	8/21/2001	258	3.1	386	4520	2739	127	20.6	2.59	1410	517
T&T	8/24/2001	245	2.66	411	3270	2767	100	21.2	2.48	1800	603
T&T	8/27/2001	278	3.1	314	4150	2810	75.8	24.1	2.78	1600	467
T&T	8/27/2001	216	3.1	315	4260	2900	75.5	24.4	2.72	1570	458
T&T	8/28/2001	228	3	324	4100	2810	76.6	23.9	2.54	1470	500
T&T	9/4/2001	177	3	324	4050	2690	67.9	26.5	2.76	1590	501
T&T	9/4/2001	178	2.91	354	2940	2674	66.6	30.2	2.81	1740	439
T&T	9/24/2001	186	3.33	169	2960	3036	37	13.4	2.61	1840	685
T&T	10/1/2001	163	3.51	268	3175	3189	44.6	30.2	2.77	2080	576
T&T	10/1/2001	162	4.5	112	4210	3122	41.8	5.42	3.05	1765	1020
T&T	11/1/2001	96	2.75	371	3120	2900	112	13.4	3.73	2060	405
T&T	11/7/2001	75	3	417	2920	2948	92.91	35.13	2.83	330	360
T&T	12/3/2001	66	2.85	331	3055	2967	125	5.7	2.91	1820	437
T&T	12/4/2001	66	2.9	631	3060	3032	138.6	56.36	3.98	1759	592
T&T	1/2/2002	86	2.73	615	3060	2750	118	55.1	2.49	1680	353

Table F-1, T&T Mine-pool, Raw Chemical Data

Site	Date	Flow, gpm	pH	730	Sp Cond. umhos/cm	TDS, mg/L	Fe, mg/L	Al, mg/L	Mn, mg/L	SO4, mg/L	Ca, mg/L
T&T	1/3/2002	86	2.8	504	2780	2876	113.2	39.13	2.39	1668	293
T&T	2/4/2002	95	2.6	571	2900	2664	120.0	40.98	1.69	1545	24
T&T	3/4/2002	82	2.8	508	3320	2800	104.6	42.43	2.94	1624	210
T&T	4/1/2002	101	2.8	477	3710	2868	88.75	41.8	3.44	1663	310
T&T	4/21/2002	63	2.8	864	3170	3260	257.4	57.52	2.66	1891	309
T&T	5/1/2002	359	2.7	657	2340	2776	167.1	45.61	2.26	1610	232
T&T	6/2/2002	348	2.8	577	2330	2568	171.4	33.62	2.13	1489	280
T&T	7/1/2002	330	2.8	436	2650	2732	133.8	20.43	2	1585	249
T&T	8/4/2002	269	2.9	339	2650	2412	99.28	17.06	1.89	1399	294
T&T	9/2/2002	99	3	373	2630	2672	103.5	23.93	2.37	1550	274
T&T	9/2/2002	99	3	373	2630	2672	103.5	23.93	2.37	1550	274
T&T	10/1/2002	133	2.9	468	2600	2600	116.6	34.52	2.59	1508	239
T&T	11/2/2002	102	3	399	268	2556	86.59	34.32	2.12	1482	310
T&T	12/3/2002	141	2.9	447	244	116	153.6	19.08	1.86	67	336
T&T	1/2/2003	536	2.9	555	2700	2908	165.4	34.73	1.77	1687	382
T&T	1/7/2003	650	3	474	2470	2408	142.6	29.77	1.64	1397	330
T&T	2/4/2003	685	3	276	2570	2324	66.23	18.5	2.33	1348	324
T&T	3/16/2003	1165	2.74	659	2610	2344	182.5	43.04	1.22	1360	105
T&T	4/1/2003	735	3.12	876		2992	253.9	68.09	2.74		258
T&T	4/15/2003	977	2.5	2518	5190	7224	834.4	154.7	3.5	4190	400
T&T	4/18/2003	753	2.64	1829	4210	5152	580.3	120.4	3.51	2988	266
T&T	4/19/2003	717	2.64	1762	4420	5264	552.3	117.2	3.65	3053	268
T&T	4/20/2003	1295	2.66	1631	4080		508.1	109	3.52		262
T&T	4/21/2003	1460	2.7	1471	3800	4252	457.6	98.26	3.25	2466	256
T&T	4/22/2003	1142	2.75	1288	3650	4032	397.9	86.59	3.23	2339	239
T&T	4/23/2003	851	2.71	1464	3730	3848	446.8	101.0	2.96	2232	239
T&T	4/24/2003	551	2.65	1371	3710	3904	398.0	97.37	2.96	2264	243
T&T	4/25/2003	892	2.68	1317	3490	3756	382.7	93.97	2.96	2178	237
T&T	4/26/2003	753	2.72	1161	3280	3312	338.2	81.93	2.47	1921	226
T&T	4/26/2003	753	2.72	1161	3280	3312	338.2	81.93	2.66	1921	226
T&T	4/27/2003	596	4	1161	3400	3500	364.6	89.79	2.23	2030	217
T&T	5/5/2003	578	2.66	977	3190	3304	274.1	67.06	2.23	1916	345
T&T	6/2/2003	488	2.91	557	2640	2472	148.1	40.62	2.47	1434	145
T&T	8/4/2003	470	2.85	410	2230	1812	96.22	29.34	2.28	1051	233
T&T	9/1/2003	421	2.75	1206	2280	2520	104.8	166.6	2.18	1462	44
T&T	10/2/2003	735	2.76	422	2300	2032	79.7	34.2	1.52	1179	382
T&T	11/2/2003	475	2.63	377	2310	1848	64.39	25.44	1.92	1072	218
T&T	12/2/2003	668	2.81	81	2260	1916	0.19		1.73	1111	233
T&T	1/6/2004	918	2.81	125	1982	1576	12.75	3.95	1.64	914	84
T&T	2/15/2004	981	2.85	409	2100	1576	91.2	31.58	0.03	914	223
T&T	3/1/2004	739	2.92	349	2030	1492	73.29	28.02	1.21	865	205
T&T	4/4/2004	811	2.86	340	1960	1472	77.25	23.27	1.66	854	176
T&T	5/2/2004	793	2.8	337	1918	1420	69.68	23.14	2.51	824	152
T&T	6/1/2004	650	2.93	347	2020	1544	72.41	28.23	1.27	896	201
T&T	7/1/2004	354	2.94	286	1951	1560	61.5	20.89	1.39	905	205
T&T	8/1/2004	220	3.03	311	2050	1620	61.41	27.34	1.44	940	243
T&T	11/7/2004	372	2.81	381	2290	1972	80.37	28.24	1.43	1144	325
T&T	12/5/2004	538	2.69	334	2210	1644	60.36	21.5	2.39	954	101
T&T	1/31/2005	596	3.02	214	1985	1708	60.98	1.59	26.83	991	210
T&T	3/4/2005	551	2.83	293	2050	1504	48.92	23.15	1.39	872	207
T&T	4/4/2005	851	2.9	292	2120	1704	46.15	26.12	0.96	988	207
T&T	5/9/2005	533	2.87	276	1943	1488	44.85	22.7	1.29	863	182

Table F-1, T&T Mine-pool, Raw Chemical Data

Site	Date	Flow, gpm	pH	730	Sp Cond. umhos/cm	TDS, mg/L	Fe, mg/L	Al, mg/L	Mn, mg/L	SO4, mg/L	Ca, mg/L
T&T	6/1/2005	488	2.85	255	2010	1500	40.98	19.64	1.33	870	202
T&T	7/4/2005	246	2.9	290	1992	1727	41.98	26.87	1.43	1002	247
T&T	8/1/2005	246	2.91	274	2120	1768	39.4	25.02	1.5	1025	215
T&T	9/11/2005	143	2.86	249	2050	1708	40.51	18.87	1.49	991	220
T&T	10/2/2005	99	2.77	314	2170	1868	44.17	26.38	1.73	1083	23
T&T	11/3/2005	99	2.87	329	2140	1796	65.64	25.4	1.88	1042	253
T&T	12/1/2005	461	2.6	406	2330	1976	78.83	24.73	1.03	1146	146
T&T	1/9/2006	573	2.68	305	2460	2124	55.41	17.61	1.89	1232	323
T&T	2/12/2006	520	2.82	319	2090	1752	50.26	27.01	2.03	1016	234
T&T	3/1/2006	358	2.76	243	2000	1540	34.13	16.6	1.28	893	184
T&T	4/2/2006	305	2.83	227	1974	1604	41.2	13.73	1.42	930	359
T&T	5/6/2006	318	2.78	294	1989	1668	47.82	22.08	1.66	967	262
T&T	6/4/2006	206	2.68	338	1895	1552	48.09	25.94	1.69	900	255
T&T	7/4/2006	502	2.72	320	2040	1584	44.7	25.63	1.41	919	254
T&T	8/8/2006	309	2.79	323	2110	1768	43.68	28.93	1.62	1025	127
T&T	9/10/2006	211	2.65	332	2180	1812	40.83	25.93	1.61	1051	209
T&T	10/2/2006	152	2.87	279	2180	1728	39.15	24.93	1.45	1002	284
T&T	11/5/2006	228	2.83	295	2230	1656	40.87	26.35	1.08	960	192
T&T	12/3/2006	300	2.97	257	2250	1600	45.48	21.66	0.95	928	163
T&T	1/1/2007	349	2.94	383	2250	1684	55.87	39.91	2.22	977	32
T&T	3/13/2007	614	2.88	359	2160	1748	66.38	30.64	2.02	1014	243
T&T	9/4/2007	367	2.96	280	2220	1724	47.79	24.66	1.31	1000	262

Appendix G

Hahn Mine-pool, Raw Chemical Data

Table G-1, Hahn Mine-pool Raw Chemical Data

Site	Date	pH	Alkalinity, mg/L	Fe, mg/L	SO4, mg/L	TDS, mg/L	Ca, mg/L	Mg, mg/L	Na, mg/L	K, mg/L	Cl, mg/L
Hahn	10/7/1980	3.20				454					
Hahn	12/4/1980	4.90	5	113		119					
Hahn	2/9/1981	3.60				596					
Hahn	6/8/1982	7.90	352	2.5		424					
Hahn	10/20/1983	6.30	303	424		814					
Hahn	10/21/1983	6.30	460	422		999					
Hahn	11/3/1983	6.30	321	360		765					
Hahn	11/8/1983	6.20	310	441		84					
Hahn	11/28/1983	5.80	151	382	8400	8977					
Hahn	12/1/1983	4.90	11	478	7754	8261					
Hahn	12/6/1983	6.05	211	480	6515	7269					
Hahn	12/9/1983	6.00	89	547	7508	8177					
Hahn	12/21/1983	4.30		596		7060			6450		
Hahn	3/1/1984	4.30		656	7600	17734			9460		
Hahn	3/21/1984	3.85		739	7250	15933	385	183	6425	27.5	905
Hahn	3/28/1984	5.45	70	879	8050	12897	360	190	2490	15	800
Hahn	4/4/1984	4.75		811	5920	14144	320	118	6050	13.5	885
Hahn	4/11/1984	4.15		750	6000	14072	352	110	6000	12.7	825
Hahn	5/9/1984	5.60	90	750	9000	14082	430	192	9000	12.5	985
Hahn	5/11/1984	5.60	106	891	6900	11726	240	197	6900	12.2	860
Hahn	6/4/1984	6.15	235	762	7620	14010	862	152	7620	11.5	1125
Hahn	6/5/1984	6.10	226	719	7200	13603	840	156	7200	12	1085
Hahn	6/6/1984	6.20	186	618	7700	13897	357	195	3550	11.2	1225
Hahn	6/8/1984	5.00		757	6300	11985	385	207	3325	11.2	970
Hahn	6/11/1984	4.55		905	7620	12955	430	203	2925	9.9	834
Hahn	6/14/1984	4.90		967	7320	12602	490	204	2800	9.7	775
Hahn	6/20/1984	4.20		903	7100	11394	337	154	2136	13.2	715
Hahn	6/24/1984	4.70	4	896	8030	12371	337	153	2200	13	700
Hahn	7/2/1984	4.70		1008	6650	11199	367	210	2220	9.1	693
Hahn	7/3/1984	4.80		923	7000	11521	357	211	2240	9.1	741
Hahn	7/5/1984	5.30	47	896	6800	11450	350	211	2320	9.2	777
Hahn	7/9/1984	3.50		880	7300	11638	387	199	2040	11.7	785
Hahn	7/16/1984	4.65		907	7100	11555	366	201	2150	12.2	790
Hahn	7/30/1984	5.00	28	986	7500	12088	380	192	2160	12.5	790
Hahn	8/5/1984	4.40		784	6890	11066	385	198	2050	12.2	704
Hahn	8/7/1984	4.30		891	6650	11575	405	214	2570	12.5	809
Hahn	8/15/1984	6.20	64	840	3200	8076	393	204	2480	12	846
Hahn	8/17/1984	4.30		930	6800	11151	392	196	2048	12.2	736
Hahn	8/30/1984	5.00	25	932	6730	11371	370	191	2345	11.5	732
Hahn	9/13/1984	4.55		986	7200	11064	377	202	2100	12.2	685
Hahn	9/19/1984	3.80		914	6900	11496	364	183	2335	12.9	750
Hahn	9/24/1984	4.20		990	7300	11973	356	179	2320	12.8	787
Hahn	10/8/1984	5.60	35	699	5800	11218	415	216	3250	12.5	764
Hahn	10/17/1984	4.70		974	6850	11233	375	200	2095		678
Hahn	10/23/1984	4.40		903	7375	11667	395	199	2063	10.5	675
Hahn	10/30/1984	4.40		908	8000	12075	310	174	1932	10.4	687
Hahn	11/5/1984	4.65		1019	6970	11313	327	193	2085	10.5	657
Hahn	11/14/1984	4.20		978	7300	11428	367	175	1945	11.7	610
Hahn	11/21/1984	3.95		851		4023	370	214		10	610

Table G-1, Hahn Mine-pool Raw Chemical Data

Site	Date	pH	Alkalinity, mg/L	Fe, mg/L	SO4, mg/L	TDS, mg/L	Ca, mg/L	Mg, mg/L	Na, mg/L	K, mg/L	Cl, mg/L
Hahn	11/27/1984	4.90		968	6900	12962	365	219	2830	995	632
Hahn	12/12/1984	3.60		1079	6350	10649	365	205	1980	10	617
Hahn	12/17/1984	4.80		1030	8300	12526	345	202	1965	10.9	622
Hahn	12/28/1984	3.50		1082	7000	11276	325	260	1935	12.7	617
Hahn	1/2/1985	4.30		1059	6900	11114	337	260	1905	12.5	594
Hahn	1/8/1985	4.80		1001	7120	11373	342	252	1985	12.2	610
Hahn	1/15/1985	4.80		1008	6700	11025	352	197	2065	12.5	647
Hahn	1/22/1985	4.60		1019	6500	10770	370	204	2005		613
Hahn	1/29/1985	3.60		977	7500	11207	349	146	1570		613
Hahn	2/5/1985	4.40		945	6500	10797	345	251	2065		637
Hahn	2/12/1985	4.60		932	7200	11371	362	218			612
Hahn	2/18/1985	3.60		990	6800	11188	485	222			645
Hahn	2/26/1985	4.70		952	7400	11609	382	186			634
Hahn	3/5/1985	4.70		930	7000	11250	432	197			639
Hahn	3/12/1985	4.45		941	9400	13530	382	200	1950	12.5	605
Hahn	3/27/1985	3.20		1042	6610	10872	360	195	2005	13.2	609
Hahn	4/2/1985	3.10		1013	7170	11410	377	195	2010	13.2	599
Hahn	4/9/1985	4.80		946	7180	11362	372	197	2005	12.7	607
Hahn	4/16/1985	3.50		847	9150	13189	402	192	1950	13.2	604
Hahn	4/24/1985	4.20		845	9150	13160	382	192	1945	12.7	603
Hahn	4/30/1985	4.65		921	9100	13272	407	200	1995	13.2	606
Hahn	5/7/1985	4.30		896	8450	12541	412	202	1960	13	575
Hahn	5/14/1985	4.40		918	8400	12489	407	200	1935	13	591
Hahn	5/21/1985	3.60		873	9600	13633	397	200	1990	16.2	534
Hahn	6/4/1985	4.50		896	9600	13643	382	192	1915	16	620
Hahn	6/11/1985	3.80		878	6800	10878	385	202	1975	12.5	604
Hahn	6/18/1985	4.20		874	7400	11469	415	200	1945	12.5	601
Hahn	6/26/1985	3.95		862	5800	9877	365	200	2000	13	619
Hahn	7/2/1985	3.90		840	5800	9864	370	195	2005	12.5	624
Hahn	7/9/1985	5.00		848	5500	9638	367	192	2010	13	680
Hahn	7/16/1985	5.60	72	871	5500	9761	362	192	2070	13	650
Hahn	7/23/1985	3.90		829	7080	11324	387	202	2100	16	606
Hahn	7/30/1985	5.40	65	801	7400	11543	385	195	2025	15.2	630
Hahn	8/6/1985	5.60	59	762	7000	11166	382	162	2095	14.7	641
Hahn	8/13/1985	5.75	81	757	6500	10871	470	277	2117	12.5	620
Hahn	8/19/1985	5.10		762	6500	10654	445	180	2065	13	644
Hahn	8/27/1985	5.70	58	778	7500	11742	450	182	2095	13	638
Hahn	9/3/1985	5.40	49	739	6815	11064	412	170	2172	12.2	667
Hahn	9/10/1985	6.05	104	750	7125	11546	427	172	2240	12.5	675
Hahn	9/18/1985	4.45		727	6800	10878	307	172	2150	11.2	696
Hahn	9/24/1985	5.00		724	7150	11419	337	180	2275	11.5	708
Hahn	10/1/1985	5.80	26	727	7500	11697	337	180	2230	11.2	666
Hahn	10/8/1985	5.40		683	6900	11139	345	202	2275	13.3	682
Hahn	10/15/1985	5.40	75	728	6900	11149	340	195	2175	11.2	694
Hahn	10/22/1985	5.60	111	722	7000	11277	327	192	2187	11	688
Hahn	10/29/1985	4.20		643	6650	10684	355	177	2122	10.7	713
Hahn	11/5/1985	3.90		661	7500	11662	352	182	2200	13	740
Hahn	11/12/1985	6.00	180	668	7500	12075	375	185	2375	13.2	725
Hahn	11/19/1985	6.10	86	678	7300	11447	300	177	2165	10.7	698
Hahn	11/27/1985	5.60	29	610	7375	11560	345	172	2297	10.5	701
Hahn	12/4/1985	5.80	70	666	7375	11665	335	167	2290	10.7	723
Hahn	12/11/1985	6.20	161	706	6600	10943	382	175	2147	12	711

Table G-1, Hahn Mine-pool Raw Chemical Data

Site	Date	pH	Alkalinity, mg/L	Fe, mg/L	SO4, mg/L	TDS, mg/L	Ca, mg/L	Mg, mg/L	Na, mg/L	K, mg/L	Cl, mg/L
Hahn	12/18/1985	6.00	119	678	5999	10200	365	170	2095	11.7	723
Hahn	1/2/1986	5.95	118	650	4970	9189	357	177	2457	11.5	713
Hahn	1/9/1986	6.05	106	605	5589	9724	360	180	2140	11.2	700
Hahn	1/16/1986	5.60	25	655	6176	10344	347	190	2225	11	697
Hahn	1/23/1986	6.40	152	650	6193	10500	325	182	2240	11.5	701
Hahn	1/31/1986	5.30	26	594	6047	9998	362	177	2050	10.7	715
Hahn	2/6/1986	6.00	108	630	6194	10507	347	195	2268	11.5	720
Hahn	2/13/1986	6.40	211	633	6359	10843	352	195	2325	11.7	700
Hahn	2/20/1986	6.05	163	638	6221	10561	380	187	2207	12	704
Hahn	2/27/1986	6.28	108	648	6253	10542	417	177	2175	11.7	717
Hahn	3/10/1986	6.33	143	594	5437	9843	397	177	2302	12	738
Hahn	3/27/1986	6.15	158	627	6253	10257	365	170	1935	8.8	695
Hahn	4/3/1986	6.33	138	649	6164	10195	390	160	1955	8.8	689
Hahn	4/10/1986	6.17	190	627	6332	10407	357	157	1960	8.5	724
Hahn	4/18/1986	6.28	175	689	6159	10549	375	162	2030	9.5	900
Hahn	4/24/1986	5.99	160	638	5963	9869		157	1897	9.3	626
Hahn	5/1/1986	6.11	80	666	6039	9873	370	145	1890	9.3	646
Hahn	5/8/1986	6.34	175	627	6185	10320	415	165	2022	9.3	671
Hahn	5/15/1986	6.19	206	683	6034	10120	382	152	1936	10	661
Hahn	5/22/1986	6.20	167	661	5790	9841	392	152	1990	9.5	632
Hahn	5/29/1986	6.17	170	618	5960	10340	390	178	2360	12.3	602
Hahn	6/5/1986	6.02	173	623	6100	10347	378	167	2242	12.4	602
Hahn	6/12/1986	6.09	200	672	5965	10103	372	164	2080	13.4	582
Hahn	6/19/1986	6.24	172	666	5865	9817	365	175	1925	10.8	588
Hahn	6/26/1986	6.19	222	650	5560	9539	357	155	1950	9.4	577
Hahn	7/7/1986	6.15	165	627	5750	9906	384	159	2183	10.6	
Hahn	7/10/1986	6.22	248	644	5840	10017	385	158	2098	10.2	569
Hahn	7/17/1986	6.08	189	638	5855	9924	373	155	2074	9.5	579
Hahn	7/24/1986	6.21	229	638	5811	9801	380	147	1953	9.3	574
Hahn	7/31/1986	6.25	250	638	5770	9859	338	135	2087	9.9	568
Hahn	8/8/1986	6.08	255	644	5890	9882	372	140	1940	9.8	566
Hahn	8/14/1986	6.36	248	666	5678	9642	349	131	1934	9.5	563
Hahn	8/22/1986	6.46	246	644	5655	9666	394	132	1950	10.2	572
Hahn	8/29/1986	6.24	246	648	5665	9901	404	133	2137	10.8	594
Hahn	9/4/1986	6.18	239	571	5835	9841	401	137	1952	11.7	633
Hahn	9/12/1986	6.26	252	553	5591	9521	378	140	1978	10.7	556
Hahn	9/18/1986	6.41	249	532	5570	9455	381	139	1940	10.5	572
Hahn	10/1/1986	6.43	238	551	5372	9260	396	138	1940	10.1	554
Hahn	10/8/1986	6.28	244	544	5735	9668	366	139	2022	10.5	546
Hahn	10/15/1986	6.31	258	522	5931	9784	364	130	1938	10	567
Hahn	10/22/1986	6.43	261	508	5251	9055	363	133	1915	10.6	549
Hahn	10/29/1986	6.44	247	508	4609	8749	358	133	1949	10.3	873
Hahn	11/5/1986	6.43	255	511	5260	8984	323	127	1850	10.3	584
Hahn	11/12/1986	6.36	259	537	5240	9264	395	156	2020	10.6	580
Hahn	11/19/1986	6.24	259	498	4900	8667	355	139	1866	9.8	577
Hahn	11/26/1986	6.41	249	471	5770	9508	362	142	1868	10	575
Hahn	12/3/1986	6.50	253	452	5670	9285	355	137	1832	10.1	514
Hahn	12/10/1986	6.50	255	495	5295	8950	354	153	1740	10.6	585
Hahn	12/17/1986	6.40	259	513	5295	8930	347	151	1727	11.5	583
Hahn	12/23/1986	6.50	256	531	7375	11050	360	153	1721	10.7	580
Hahn	12/29/1986	6.20	97	528	5159	8581	369	157	1703	10.9	529
Hahn	1/8/1987	6.40	255	504	5900	9495	321	142	1765	10.4	538

Table G-1, Hahn Mine-pool Raw Chemical Data

Site	Date	pH	Alkalinity, mg/L	Fe, mg/L	SO4, mg/L	TDS, mg/L	Ca, mg/L	Mg, mg/L	Na, mg/L	K, mg/L	Cl, mg/L
Hahn	1/14/1987	6.08	200	504	5400	8976	347	144	1806	9.7	5015
Hahn	1/28/1987	6.30	262	495	5355	8776	322	127	1617	7.3	525
Hahn	2/4/1987	6.46	259	509	4789	8337	344	138	1703	12.2	518
Hahn	2/11/1987	6.36	210	487	5420	8868	334	138	1689	10.2	525
Hahn	2/20/1987	6.41	257	537	5630	9344	311	129	1612	7.7	795
Hahn	2/25/1987	6.17	309	548	5169	8661	320	128	1601	7.8	503
Hahn	3/4/1987	6.19	250	565	4659	8213	309	136	1697	9.3	526
Hahn	3/18/1987	6.12	213	615	5285	8629	312	134	1526	6.6	483
Hahn	3/25/1987	6.58	247	551	5490	8876	309	125	1565	11.2	515
Hahn	4/3/1987	6.39	200	525	4000	7224	296	126	1499	9.6	515
Hahn	4/9/1987	6.14	219	563	8537	8537	307	133	1668	8.8	508
Hahn	4/15/1987	4.78	4	536	4600	7667	300	132	1568	10.4	507
Hahn	4/23/1987	6.25	128	534	4300	7528	300	115	1599	10.4	504
Hahn	4/29/1987	6.29	197	539	4000	7252	305	128	1514	7.9	510
Hahn	5/6/1987	6.20	245	501	4900	8037	332	122	1342	6.8	527
Hahn	5/13/1987	6.30	186	549	5000	8221	312	123	1448	6.8	549
Hahn	5/19/1987	6.39	196	530	4900	8152	332	127	1478	5.1	534
Hahn	5/27/1987	6.18	154	548	4400	7862	321	135	1747	8.3	508
Hahn	6/3/1987	6.24	224	563	5000	8427	304	130	1630	8.3	512
Hahn	6/10/1987	6.29	181	563	4700	8008	302	129	1560	7.1	519
Hahn	6/16/1987	6.36	222	508	4600	8033	310	132	1656	8	541
Hahn	6/23/1987	6.35	204	537	4700	8184	313	133	1704	9.9	531
Hahn	7/2/1987	6.09	168	469	3700	6967	306	128	1612	8.6	532
Hahn	7/8/1987	6.01	75	482	4700	7881	314	131	1616	8.6	531
Hahn	7/15/1987	6.44	172	522	4750	8072	314	126	1588	8.6	547
Hahn	7/29/1987	6.35	220	486	4572	7822	303	127	1508	8.9	542
Hahn	8/6/1987	6.40	181	468	5117	8406		134	1573	8.6	562
Hahn	8/12/1987	6.50	181	463	4564	7930	315	130	1660	7.3	563
Hahn	8/18/1987	6.19	119	452	4404	8097	300	134	1924	8.6	724
Hahn	8/26/1987	6.27	171	441	4285	7590	296	124	1648	8.9	572
Hahn	9/2/1987	6.48	272	450	4360	7622	290	136	1460	7.4	581
Hahn	9/9/1987	6.24	196	441	4457	7765	306	128	1612	8.6	567
Hahn	9/16/1987	6.31	212	433	4297	7717	310	125	1696	9.2	583
Hahn	9/23/1987	6.29	139	440	4517	7970	312	124	1788	8.9	605
Hahn	10/1/1987	6.35	159	411	4244	7547	288	117	1672	7.7	608
Hahn	10/7/1987	6.43	269	411	4419	7929		116	1772	7.3	612
Hahn	10/17/1987	6.33	184	419	4480	7868		117	1716	7.3	639
Hahn	10/28/1987	6.52	235	355	4245	7740		106	1776	7.3	700
Hahn	11/5/1987	6.71	310	332	4063	7464	248	96	1660	8.2	675
Hahn	11/10/1987	6.90	157	238	3905	7277		95	1850	9	725
Hahn	11/18/1987	6.50	561	302	4301	8114	274	103	1768	8.8	669
Hahn	11/24/1987	6.83	532	319	3899	7696	251	97	1769	8.5	700
Hahn	12/1/1987	6.89	445	310	4070	7756	259	101	1766	7.4	695
Hahn	12/8/1987	7.00	366	307	4049	7727	257	99	1882	8.7	675
Hahn	12/22/1987	6.84	413	280	4496	8211	276	105	1839	7.9	700
Hahn	12/29/1987	7.10	425	275	4064	7826	277	108	1888	8.9	685
Hahn	1/6/1988	6.72	391	296	4211	7861	288	107	1756	7.5	715
Hahn	1/13/1988	7.02	360	203	4021	8072	279	103	2220	9.1	795
Hahn	1/20/1988	6.95	378	291	4357	8181	294	116	1977	9.2	674
Hahn	2/3/1988	6.95	365	303	4182	7937	289	112	1903	8.7	690
Hahn	2/10/1988	7.00	398	321	4362	8175	281	111	1921	8.3	681
Hahn	2/17/1988	6.90	365	287	4099	7863	275	108	1941	8.9	695

Table G-1, Hahn Mine-pool Raw Chemical Data

Site	Date	pH	Alkalinity, mg/L	Fe, mg/L	SO4, mg/L	TDS, mg/L	Ca, mg/L	Mg, mg/L	Na, mg/L	K, mg/L	Cl, mg/L
Hahn	2/24/1988	6.77	410	285	4023	7677	263	102	1830	7.8	663
Hahn	3/9/1988	6.70	239	279	4142	7843	267	105	1818	6.9	928
Hahn	3/16/1988	6.73	316	297	4211	7739	271	107	1823	9.1	632
Hahn	3/23/1988	6.60	388	296	4515	8217	291	116	1905	9.6	607
Hahn	3/30/1988	6.72	208	313	4126	7552	271	109	1841	9.2	625
Hahn	4/6/1988	6.34	166	302	3952	7168	258	104	1722	8.8	615
Hahn	4/15/1988	6.54	72	323	3970	7041	259	102	1667	8.2	620
Hahn	4/27/1988	6.71	296	313	3981	7445	256	106	1775	8.5	641
Hahn	5/4/1988	6.65	220	321	3980	7308		105	1736	8.4	625
Hahn	5/11/1988	6.39	334	310	4052	7576	262	108	1781	8.7	643
Hahn	5/18/1988	6.66	276	318	3955	7286	253	106	1691	8.5	614
Hahn	5/25/1988	6.22	152	340	4070	7244	269	110	1666	8.4	591
Hahn	6/2/1988	6.68	263	352	4038	7374	262	112	1688	8.5	588
Hahn	6/9/1988	6.36	107	363	3966	7089	265	111	1647	8.5	593
Hahn	6/15/1988	6.31	97	380	4049	7238	270	114	1686	8.7	607
Hahn	6/22/1988	6.57	289	366	4027	7360	266	111	1659	8.4	565
Hahn	6/29/1988	6.46	217	369	3914	7071	259	107	1580	8.2	564
Hahn	7/6/1988	6.31	190	396	4045	7293	272	112	1650	9	572
Hahn	7/14/1988	6.68	173	363	4021	7229	270	111	1649	8.4	590
Hahn	7/25/1988	6.22	62	400	3834	6741	274	104	1501	7.7	540
Hahn	8/3/1988	6.87	261	377	4165	7463	279	110	1623	8.5	577
Hahn	8/8/1988	6.65	242	372	3901	7051	267	105	1552		554
Hahn	8/23/1988	6.64	163	366	3900	7044	251	105	1609	9.1	600
Hahn	9/2/1988	6.74	140	372	3983	7091	226	107	1645	8.5	574
Hahn	9/6/1988	6.71	114	352	3826	6658	266	107	1464	8.3	490
Hahn	9/13/1988	5.75	21	358	3901	6801	262	104	1577	8.6	560
Hahn	9/20/1988	6.69	234	358	3916	7125	265	106	1629	8.4	552
Hahn	9/26/1988	6.83	347	358	3880	7240	258	104	1623	8.3	580
Hahn	10/3/1988	6.18	130	361	3971	7138	268	107	1693	8.7	566
Hahn	10/11/1988	6.78	265	363	3896	7180	263	105	1611	8.3	605
Hahn	10/18/1988	6.71	259	361	3961	7256	266	108	1661	8.6	570
Hahn	10/25/1988	6.64	182	366	3966	7173	267	108	1636	8.6	594
Hahn	11/1/1988	6.36	98	363	3913	7015	264	107	1650	8.5	585
Hahn	11/8/1988	6.59	241	366	3963	7245	269	107	1639	8.4	594
Hahn	11/15/1988	6.44	214	362	3749	6885	254	102	1574	8.5	570
Hahn	11/22/1988	6.32	164	371	3959	7087	265	104	1599	8.5	576
Hahn	12/1/1988	6.61	203	349	3847	7027	299	103	1609	8.2	600
Hahn	12/6/1988	6.74	130	355	3954	7087	268	105	1653	8.2	579
Hahn	12/14/1988	6.88	176	361	3900	7090	262	104	1653	8.1	583
Hahn	12/20/1988	6.53	107	350	3939	7022	270	107	1677	8.8	535
Hahn	12/27/1988	6.53	118	345	3945	7076	265	107	1710	8.8	547
Hahn	1/3/1989	6.71	207	413	3858	7094	259	104	1646	8.3	549
Hahn	1/10/1989	6.63	152	327	3801	6851	253	101	1611	8	560
Hahn	1/17/1989	6.35	188	336	3753	6859	252	100		7.8	
Hahn	1/24/1989	6.80	296	369	3715	7001		102	1611	7.8	571
Hahn	2/1/1989	6.63	141	355	3959	7110	267	108	1661	8.2	575
Hahn	2/7/1989	6.40	100	349	4009	7050	271	109	1634	8.3	542
Hahn	2/14/1989	6.54	210	349	3954	7209	268	108	1659	10.4	600
Hahn	2/21/1989	6.43	190	349	3839	6989	259	104	1618	8.5	575
Hahn	3/1/1989	6.98	186	338	3810	6905	260	99	1618	7.8	540
Hahn	3/8/1989	6.84	249	321	3869	7074	268	102	1628	7.9	570
Hahn	3/17/1989	6.26	137	340	3910	6944	272	104	1608	8.6	560

Table G-1, Hahn Mine-pool Raw Chemical Data

Site	Date	pH	Alkalinity, mg/L	Fe, mg/L	SO4, mg/L	TDS, mg/L	Ca, mg/L	Mg, mg/L	Na, mg/L	K, mg/L	Cl, mg/L
Hahn	3/21/1989	6.85	140	349	3807	6928	264	100	1638	8	587
Hahn	3/28/1989	6.40	138	341	3916	7034	275	104	1647	8.2	570
Hahn	4/4/1989	6.56	212	329	4057	7338	279	108	1721	8.9	572
Hahn	4/11/1989	6.72	222	352	4002	7251	282	107	1694	8.5	530
Hahn	4/18/1989	6.71	148	359	3869	6931	273		1620	8.5	509
Hahn	4/25/1989	6.61	151	352	3954	7035		107	1638	8.5	510
Hahn	5/2/1989	6.72	168	358	3856	6894	275	104	1578	8.2	505
Hahn	5/9/1989	6.61	173	361	3779	6754	268	102	1520	8.7	499
Hahn	5/16/1989	6.66	224	352	3802	6868	270	103	1556	8.4	498
Hahn	5/23/1989	6.29	150	355	3960	7017	273	106	1503	8.6	523
Hahn	5/30/1989	6.41	146	358	3866	6909	268	104	1587	8.3	535
Hahn	6/6/1989	6.86	167	349	3832	6843	264	102	1558	8.4	521
Hahn	6/13/1989	6.37	153	331	3796	6225	265	101	1532	8.2	
Hahn	6/20/1989	6.58	238	349	3836	6439	277	101	1572	8.4	
Hahn	6/27/1989	6.63	191	341	3779	6345	259	99	1522	7.7	
Hahn	7/5/1989	6.47	207	324	3777	6306	263	100	1577	8.5	
Hahn	7/11/1989	6.65	168	252	3522	5965	237	88	1649	8.2	
Hahn	7/11/1989	6.38	85	327	3610	5855	259	97	1448	8.1	
Hahn	7/18/1989	6.47	224	285	3575	6005	251	93	1515	8.5	
Hahn	7/18/1989	6.48	239	312	3600	6008	252	94	1444	8.9	
Hahn	7/25/1989	6.56	203	310	3547	5943	249	94	1483	8.1	
Hahn	7/25/1989	6.56	228	292	3612	6125	248	94	1591	8.1	
Hahn	8/1/1989	6.49	219	294	3558	6008	250	95	1532	8.2	
Hahn	8/1/1989	6.61	244	301	3514	5940	243	93	1479	8.5	
Hahn	8/8/1989	6.15	108	291	3500	5775		92	1503	8.2	
Hahn	8/8/1989	6.29	101	288	3537	5817		94	1518	7.9	
Hahn	8/15/1989	6.32	253	274	3464	5903	241	91	1513	8	
Hahn	8/22/1989	6.5	290	286	3372	5868	253	94	1497	8	
Hahn	8/29/1989	6.62	110	283	3522	5828	249	94	1532	8.5	
Hahn	9/6/1989	6.55	96	296	3487	5774	247	92	1522	8.6	
Hahn	9/12/1989	6.98	326	269	3442	5975	246	91	1517	8.4	
Hahn	9/19/1989	6.98	354	267	3489	6080	248	91	1541	8.6	
Hahn	9/26/1989	6.62	378	264	3500	6123	242	89	1555	8.6	
Hahn	10/3/1989	7.09	343	262	3457	6040	241	89	1561	8.1	
Hahn	10/10/1989	6.8	351	260	3444	6028	240	88	1554	8.1	
Hahn	10/17/1989	6.34	90	271	3449	5714	236	88	1549	8.1	
Hahn	10/24/1989	6.42	312	156	3449	6007	242	88	1579	8.1	
Hahn	11/1/1989	6.47	122	257	3616	6015	246	91	1644	8.2	
Hahn	11/7/1989	6.62	221	254	3522	6007	244	89	1616	8.1	
Hahn	12/1/1989	6.76	325	241	3519	6071	236	86	1580	8.4	
Hahn	12/5/1989	6.69	388	235	3421	6057	232	85	1599	7.9	
Hahn	12/12/1989	6.68	338	231	3336	5838	228	83	1537	7.9	
Hahn	12/19/1989	6.76	341	231	3337	5672		83	1570	8.1	
Hahn	12/29/1989	6.96	363	229	3395	5970	232	84	1576	7.9	
Hahn	1/2/1990	6.90	399	227	3350	5970	229	83	1583	8	
Hahn	1/9/1990	7.03	329	216	3302	5793	222	82	1559	7.9	
Hahn	1/16/1990	6.72	434	214	3303	5915	226	81	1550	7.9	
Hahn	1/23/1990	6.81	410	208	3202	5758	220	80	1537	7.8	
Hahn	2/2/1990	6.80	403	235	3236	5885	209	81	1621	8.3	
Hahn	2/6/1990	6.35	326	234	3207	5713	210	80	1573	8	
Hahn	2/13/1990	6.63	392	173	3126	5570	215	78	1489	7.4	
Hahn	2/20/1990	6.77	304	196	3156	5506	226	78	1488	7.3	

Table G-1, Hahn Mine-pool Raw Chemical Data

Site	Date	pH	Alkalinity, mg/L	Fe, mg/L	SO4, mg/L	TDS, mg/L	Ca, mg/L	Mg, mg/L	Na, mg/L	K, mg/L	Cl, mg/L
Hahn	3/1/1990	6.82	382	204	3221	5748	222	80	1543	7.6	
Hahn	3/6/1990	6.68	405	196	3177	5723	219	79	1547	7.3	
Hahn	3/13/1990	6.55	287	192	3069	5412	210	77	1503	7.5	
Hahn	3/27/1990	6.81	328	190	3037	5387	212	78	1464	7.4	
Hahn	4/3/1990	6.84	304	186	3001	5312	201	74	1460	7.3	
Hahn	4/10/1990	6.90	254	179	2982	5243	202	73	1487	7.2	
Hahn	4/17/1990	7.07	301	188	3035	5388	210	75	1503	7.8	
Hahn	4/24/1990	6.68	338	186	2998	5375	207	74	1490	7.7	
Hahn	5/1/1990	6.81	313	191	3109	5515	215	77	1530	7.7	
Hahn	5/8/1990	6.88	419	180	2908	5338	222	73	1434	7.3	
Hahn	5/15/1990	6.90	417	186	2979	5444	209	75	1477	7.4	
Hahn	5/22/1990	6.63	358	179	2901	5236	201	73	1436	7.4	
Hahn	5/29/1990	6.67	298	181	2893	5162	206	73	1435	7.5	
Hahn	6/5/1990	6.99	417	177	2860	5238	203	72	1407	7.3	
Hahn	6/12/1990	6.65	198	177	2798	4891	196	71	1400	7.3	
Hahn	6/19/1990	6.96	355	173	2721	4964	194	69	1365	7.2	
Hahn	6/26/1990	6.86	316	183	2918	5251	202	74	1479	7.4	
Hahn	7/3/1990	7.28	190	177	2835	4913	204	72	1384	7.3	
Hahn	7/10/1990	6.84	351	186	2910	5250	209	74	1432	7.8	
Hahn	7/17/1990	6.64	423	181	2822	5200	198	72	1401	7.3	
Hahn	7/24/1990	6.90	425	180	2796	5172	201	72	1395	7.4	
Hahn	8/1/1990	6.85	387	175	2747	4989	192	69	1324	6.9	
Hahn	8/7/1990	6.73	430	180	2742	5682	195	71	1400	7.3	560
Hahn	8/14/1990	6.84	411	184	2773	5118	201	71	1377	7.6	
Hahn	8/21/1990	6.89	368	179	2723	4993	198	70	1364	6.8	
Hahn	8/28/1990	6.94	414	180	2756	5079	198	71	1359	7.6	
Hahn	9/4/1990	6.76	298	183	2729	4936	197	72	1382	7.3	
Hahn	9/11/1990	6.78	405	161	2682	5006	188	68	1404	7	
Hahn	9/18/1990	6.65	342	171	2598	4737	188	67	1287	6.5	
Hahn	9/25/1990	6.73	221	175	2676	4709	191	69	1319	6.7	
Hahn	10/2/1990	6.88	368	171	2649	4816	188	68	1283	6.4	
Hahn	10/9/1990	7.19	353	174	2693	4905	194	69	1334	7.1	
Hahn	10/16/1990	6.92	364	165	2545	4684	185	66	1270	6.7	
Hahn	10/23/1990	6.95	379	168	2577	4776	185	57	1308	6.9	
Hahn	10/30/1990	6.65	339	166	2579	4716	185	66	1297	7	
Hahn	11/6/1990	6.91	224	172	2655	4758	196	70	1381	7.9	
Hahn	11/13/1990	6.72	332	164	2595	4734	188	67	1306	6.7	
Hahn	11/20/1990	6.46	263	167	2662	4759	195	69	1336	7	
Hahn	11/28/1990	6.41	282	164	2599	4705	187	67	1334	7	
Hahn	12/4/1990	6.60	366	163	2559	4755	187	67	1325	6.9	
Hahn	12/11/1990	6.70	428	166	2642	4969	193	69	1368	7.4	
Hahn	1/4/1991	7.16	355	149	2394	4447	177	61	1224	6.7	
Hahn	1/8/1991	7.12	360	157	2496	4621	186	63	1270	6.8	
Hahn	1/29/1991	6.53	296	174	2542	4543	196	68	1194	7	
Hahn	1/29/1991	6.45	310	158	2520	4603	188	66	1284	7.1	
Hahn	2/12/1991	6.62	282	169	2427	4391	189	66	1187	6.8	
Hahn	2/12/1991	6.76	399	143	2313	4436	169	60	1255	6.7	
Hahn	2/26/1991	6.57	323	165	2339	4391	177	69	1237	7.1	
Hahn	2/26/1991	6.58	398	144	2323	4476	167	65	1283	6.8	
Hahn	3/12/1991	7.16	202	69	2326	4086	188	67	1181	6.6	
Hahn	3/12/1991	7.41	336	48	2258	4188	166	62	1236	6.7	
Hahn	3/26/1991	6.82	301	155	2344	4331	178	67	1211	6.8	

351

Table G-1, Hahn Mine-pool Raw Chemical Data

Site	Date	pH	Alkalinity, mg/L	Fe, mg/L	SO4, mg/L	TDS, mg/L	Ca, mg/L	Mg, mg/L	Na, mg/L	K, mg/L	Cl, mg/L
Hahn	3/26/1991	6.75	339	145	2336	4400	171	65	1261	6.7	
Hahn	4/9/1991	6.74	303	148	2256	4190	172	65	1171	6.6	
Hahn	4/9/1991	6.62	333	138	2242	4272	164	63	1250	6.6	
Hahn	4/23/1991	6.71	313	139	2257	4207	169	63	1189	6.6	
Hahn	4/23/1991	6.63	401	127	2202	4267	160	60	1220	6.7	
Hahn	5/14/1991	6.68	279	128	2173	4047	164	61	1173	6.3	
Hahn	6/11/1991	6.80	383	110	2096	4092	150	57	1204	6.4	
Hahn	6/11/1991	6.86	447	126	2126	4141	160	59	1116	6.4	
Hahn	6/25/1991	6.85	339	118	2027	3846	152	56	1072	5.8	
Hahn	6/25/1991	7.01	398	104	1935	3839	138	53	1117	5.7	
Hahn	7/9/1991	6.51	303	119	2022	3778	155	56	1049	5.9	
Hahn	7/9/1991	6.65	371	102	2103	4067	149	56	1197	6.1	
Hahn	7/23/1991	7.01	455	100	1985	3989	143	54	1144	6.1	
Hahn	8/2/1991	7	442	106	2067	4085	151	57	1157	6.1	
Hahn	8/13/1991	6.95	477	103	2027	4065	148	56	1142	6.1	
Hahn	9/3/1991	6.91	466	104	2093	4097	152	56	1115	6.2	
Hahn	9/18/1991	7.15	463	101	1995	4000	146	56	1130	6.9	
Hahn	10/8/1991	6.84	338	109	2050	3945	151	57	1160	6.7	
Hahn	10/22/1991	6.77	330	87	2111	4024	157	61	1197	6.9	
Hahn	11/1/1991	7.16	352	113	2062	4003	153	59	1179	6.4	
Hahn	11/19/1991	7.07	447	117	2019	4008	153	58	1107	6.6	
Hahn	12/4/1991	7	300	107	1954	3700	151	57	1058	5.7	
Hahn	12/10/1991	6.36	365	86	2038	3895	149	57	1112	6.1	
Hahn	1/8/1992	6.73	317	111	2066	3921	156	59	1134	6.3	
Hahn	1/21/1992	6.59	387	121	2045	4000	166	61	1127	6.7	
Hahn	2/11/1992	6.66	464	117	2103	4132	161	60	1117	6	
Hahn	3/10/1992	7.32	273	64	2457	4536	226	77	1366	11.3	
Hahn	3/24/1992	6.71	253	94	2066	3792	167	61	1088	6.1	
Hahn	4/8/1992	7.48	253	33	2097	3767	173	62	1085	6.8	
Hahn	5/5/1992	6.78	400	107	2262	4278	167	62	1184	6.6	
Hahn	5/19/1992	7.05	291	147	2138	3870	179	64	979	6.7	
Hahn	6/9/1992	6.82	343	142	2109	3986	172	63	1073	5.9	
Hahn	6/23/1992	6.68	380	150	2120	4022	172	64	1043	6.6	
Hahn	7/15/1992	6.68	402	144	2099	4029	170	64	1054	6.1	
Hahn	8/11/1992	6.87	432	138	2079	4035	167	62	1054	6	
Hahn	8/26/1992	6.95	394	94	1943	3764	160	58	1020	6.1	
Hahn	9/8/1992	6.93	385	129	2044	3952	160	61	1081	6.5	
Hahn	10/6/1992	7.19	282	126	2004	3775	165	60	1068	6.3	
Hahn	10/11/1992	7.22	355	126	2043	3925	165	61	1089	6.1	
Hahn	11/17/1992	7.26	374	121	2028	3899	160	59	1067	6.5	
Hahn	12/8/1992	6.79	458	121	1974	3952	160	58	1072	5.9	
Hahn	12/15/1992	6.61	413	127	2044	4015	166	61	1105	6.1	
Hahn	1/12/1993	7.00	364	127	2085	3991	169	63	1095	6.5	
Hahn	1/19/1993	6.77	332	134	2028	3868	165	62	1066	6.6	
Hahn	2/2/1993	6.97	334	107	2053	3837	166	61	1035	6.1	
Hahn	3/2/1993	6.96	390	122	1978	3870	159		1068	6.1	
Hahn	3/16/1993	7.10	454	139	1982	3948	170	61	1034	6.1	
Hahn	4/6/1993	6.88	411	136	2159	4195	177		1153	6.1	
Hahn	4/20/1993	7.13	386	121	1982	3793	167	59	985	6.1	
Hahn	5/18/1993	7.09	404	118	1838	3651	158	57	979	6.4	
Hahn	6/15/1993	6.75	410	115	1807	3670	150	56	1034	6.1	
Hahn	7/6/1993	7.32	318	114	1911	3685	158	57	1049	6.2	

Table G-1, Hahn Mine-pool Raw Chemical Data

Site	Date	pH	Alkalinity, mg/L	Fe, mg/L	SO4, mg/L	TDS, mg/L	Ca, mg/L	Mg, mg/L	Na, mg/L	K, mg/L	Cl, mg/L
Hahn	8/3/1993	7.10	358	109	1895	3709	154	57	1050	6.1	
Hahn	9/3/1993	7.08	459	103	1871	3798	149	55	1052	6.5	
Hahn	10/5/1993	6.95	360	98	1739	3227	142	52	749	6.2	
Hahn	11/16/1993	6.91	364	96	1746	3443	150	51	949	5.9	
Hahn	12/7/1993	7.06	457	98	1711	3631	144	53	1060	6.3	
Hahn	2/8/1994	7.10	351	93	1593	3236	138	51	926	5.8	
Hahn	3/22/1994	6.93	425	95	1603	3407	138	54	992	5.8	
Hahn	4/12/1994	6.81	361	91	1608	3218	140	49	882	5.5	
Hahn	5/3/1994	6.66	439	95	1593	3322	140	51	901	5.6	
Hahn	6/22/1994	6.53	379	91	1600	3263	136	50	917	5.5	
Hahn	7/6/1994	6.55	370	86	1416	2705	129	47	569	5.4	
Hahn	9/13/1994	6.70	454	55	1250	2739	118	35	718	7.3	
Hahn	10/13/1994	6.59	354	83	1450	3015	134	48	861	5.9	
Hahn	11/23/1994	6.56	343	89	1440	2970	142	49	826	5.4	
Hahn	12/12/1994	6.66	439	92	1560	3246	149	52	850	5.9	
Hahn	1/25/1995	6.43	294	94	1500	2932	152	51	769	5.5	
Hahn	2/21/1995	6.60	395	94	1460	3047	150	61	803	5.5	
Hahn	3/7/1995	6.61	344	91	1450	2937	150	50	770	5.5	
Hahn	4/3/1995	6.63	272	85	1460	2860	150	53	774	5.6	
Hahn	5/23/1995	6.56	344	92	1520	2999	154	52	755	5.6	
Hahn	6/6/1995	6.52	386	88	1350	3196		50	770	5.8	310
Hahn	8/1/1995	6.43	338	87	1370	2842	141	49	775	5.8	
Hahn	9/6/1995	6.68	364	84	1320	2814	138	47	774	5.5	
Hahn	10/10/1995	6.44	360	83	1390	2920	142	49	811	5.6	
Hahn	12/12/1995	7.40	316	85	1200	1672					
Hahn	1/9/1996	7.40	314	81	1288	1753					
Hahn	1/20/1996	6.60	373	67	1213	1736					
Hahn	2/19/1996	6.90	310	92	1350	1821					
Hahn	3/27/1996	6.80	295	95	1600	2056					
Hahn	4/5/1996	8.20	297	68	1625	2057					
Hahn	5/6/1996	8.20	289	41	1450	1845					
Hahn	6/3/1996	6.80	313	95	1300	1779					
Hahn	7/8/1996	6.80	370	23	1275	1750					
Hahn	8/5/1996	7.60	370	70	1400	1922					
Hahn	9/9/1996	7.00	383	74	1325	1867					
Hahn	10/7/1996	7.00	400	65	1175	1729					
Hahn	11/4/1996	7.30	413	56	1500	2061					
Hahn	12/2/1996	6.90	397	62	1150	1697					
Hahn	1/20/1997	6.60	373	67	1213	1736					
Hahn	2/3/1997	6.60	361	70	1225	1737					
Hahn	3/3/1997	6.60	366	61	1063	1571					
Hahn	3/20/1997	7.04	396	182	2931	5301	202	72	1420	6.9	
Hahn	4/7/1997	6.80	309	74	1175	1627					
Hahn	5/5/1997	6.60	340	59	1138	1613					
Hahn	6/2/1997	7.30	460	60	1025	1647					
Hahn	8/11/1997	8.50	379	70	1050	1584					
Hahn	9/1/1997	6.70	378	72	1075	1609					
Hahn	10/6/1997	6.80	372	68	1213	1736					
Hahn	11/3/1997	6.90	385	72	1050	1592					
Hahn	12/8/1997	6.60	318	49	1150	1585					
Hahn	1/5/1998	7.30	392	65	1050	1594					
Hahn	1/20/1998	6.60	373	67	1231	1754					

Table G-1, Hahn Mine-pool Raw Chemical Data

Site	Date	pH	Alkalinity, mg/L	Fe, mg/L	SO4, mg/L	TDS, mg/L	Ca, mg/L	Mg, mg/L	Na, mg/L	K, mg/L	Cl, mg/L
Hahn	2/2/1998	6.70	392	64	1063	1606					
Hahn	3/2/1998	6.80	390	72	1038	1587					
Hahn	3/24/1998	6.71	312	94	2066	3864	167	61	1088	6.1	
Hahn	4/6/1998	6.90	404	62	1100	1656					
Hahn	5/4/1998	7.30	392	64	1075	1618					
Hahn	6/1/1998	8.40	379	69	1075	1607					
Hahn	7/13/1998	7.00	367	71	1050	1569					
Hahn	8/3/1998	7.00	421	52	888	1454					
Hahn	9/14/1998	7.10	435	26	975	1532					
Hahn	10/5/1998	8.30	423	61	950	1528					
Hahn	11/3/1998	6.90	433	59	963	1551					
Hahn	12/7/1998	6.90	438	46	900	1481					
Hahn	2/1/1999	7.10	413	66	950	1520					
Hahn	2/8/1999	6.76	425	46.9							
Hahn	3/2/1999	7.4	415	63.29							
Hahn	4/6/1999	7.2	390	61.61							
Hahn	5/3/1999	7.2	392	73.42							
Hahn	5/12/1999	7.23	393	56.9							
Hahn	6/8/1999	7	383	75.83							
Hahn	6/10/1999			58.7							
Hahn	7/5/1999	6.9	384	64.72							
Hahn	7/6/1999	6.49	397	55.8							
Hahn	8/9/1999	8.2	415	56.68							
Hahn	9/7/1999	7.1	508	40.95							
Hahn	10/4/1999	7.1	418	51.15							
Hahn	11/1/1999	7.4	429	51.97							
Hahn	12/6/1999	7.6	422	53.81							
Hahn	1/3/2000	7.1	477	45.72							
Hahn	2/7/2000	8.3	408	61.21							
Hahn	3/6/2000	6.9	413	65.25							
Hahn	4/3/2000	7.3	392	58.09							
Hahn	5/1/2000	6.9	403	62.73							
Hahn	6/5/2000	6.9	398	65.88							
Hahn	7/11/2000	7.3	458	65.28							
Hahn	8/8/2000	7.1	395	68.9							
Hahn	8/15/2000	6.31	405	54.7							
Hahn	9/5/2000	8.5	424	62.17							
Hahn	10/2/2000	7.3	439	51.03							
Hahn	11/6/2000	7.3	412	55.55							
Hahn	11/21/2000	6.82	444	36.4							
Hahn	12/4/2000	8.4	443	49.82							
Hahn	1/2/2001	7.3	463	42.57							
Hahn	2/5/2001	7.4	438	46.02							
Hahn	3/5/2001	7.2	433	50.96							
Hahn	4/2/2001	7.8	446	29.82							
Hahn	5/7/2001	8.2	432	49.93							
Hahn	6/4/2001	7.1	428	47.74							
Hahn	7/2/2001	8.1	423	51.24							
Hahn	8/6/2001	7	441	43.45							
Hahn	9/4/2001	7.4	459	43.29							
Hahn	10/1/2001	7.3	474	38.01							
Hahn	11/5/2001	8.2	472	40.97							

Table G-1, Hahn Mine-pool Raw Chemical Data

Site	Date	pH	Alkalinity, mg/L	Fe, mg/L	SO4, mg/L	TDS, mg/L	Ca, mg/L	Mg, mg/L	Na, mg/L	K, mg/L	Cl, mg/L
Hahn	12/3/2001	8.4	429	42.34							
Hahn	1/14/2002	6.82	473	34.5							
Hahn	5/8/2002	6.51	444	41.5							
Hahn	8/14/2002	6.46	471	43.8							
Hahn	12/4/2002	6.7	469	34.6							
Hahn	12/12/2002	6.7	469	34.6							
Hahn	2/18/2003	6.75	582	28.1							
Hahn	3/3/2003	8.2	451	40.31							
Hahn	3/5/2003	6.78	466	37.8							
Hahn	4/1/2003	7.1	450	40.01							
Hahn	5/5/2003	7.3	456	37.91							
Hahn	6/2/2003	7.2	463	38.15							
Hahn	7/1/2003	7.2	480	30.77							
Hahn	8/4/2003	7.9	417	37.06							
Hahn	9/1/2003	7.4	418	35.74							
Hahn	10/6/2003	8.88	562	25.9							
Hahn	10/6/2003	7.3	489	31.26							
Hahn	12/1/2003	7.03	475	23.86							
Hahn	1/5/2004	6.94	105	26.05							
Hahn	2/2/2004	7.02	459	21.38							
Hahn	4/5/2004	7.14	384	28.6							
Hahn	5/3/2004	7.04	364	31.42							
Hahn	6/1/2004	6.94	442	29.05							
Hahn	7/6/2004	6.8	351	29.12							
Hahn	7/7/2004	7.2	480	30.77							
Hahn	9/20/2004	6.93	511	25.4							
Hahn	9/20/2004	6.63	342	38.7							
Hahn	10/4/2004	7.2	340	34.99							

Appendix H

Barnes & Tucker Mine-pool, Raw Chemical Data

Table H -1, Barnes & Tucker Mine-pool Raw Chemical Data, Yearly Average

Site	Year	pH	Alkalinity, mg/L	Fe, mg/L	SO4, mg/L	Discharge, gpm
Barnes&Tucker	1970	5.62	40.8	751.2	2285.8	3374
Barnes&Tucker	1971	5.61	8.5	919.7	3692.6	4799
Barnes&Tucker	1972			665.8		5221
Barnes&Tucker	1973			401.7		4687
Barnes&Tucker	1974	4.51	21.5	295	1625.0	4191
Barnes&Tucker	1975	4.86	33.2	304.2	1420.4	4335
Barnes&Tucker	1976	4.79	22.6	295	1651.3	3891
Barnes&Tucker	1977	5.74	45.25	287.5	1126.8	3681
Barnes&Tucker	1978			197.5	1189.0	2543
Barnes&Tucker	1979			204.2	958.3	2497
Barnes&Tucker	1980				970.3	4851
Barnes&Tucker	1981	5.75	89.40	201.62	1273.78	5131
Barnes&Tucker	1982	5.87	136.4	185.7	1022.5	4792
Barnes&Tucker	1983	6	86.74	443.7	887.7	4236
Barnes&Tucker	1984	5.98	121	190.4	775.0	2926
Barnes&Tucker	1985	6.04	120			2473
Barnes&Tucker	1986	6.7	289.5	63.5	420.6	4432
Barnes&Tucker	1987	6.53	274.6	63.4	614.6	6629
Barnes&Tucker	1988	6.63	309.6	74.4	597.0	7088
Barnes&Tucker	1989	6.16	177.4	71.6	606.9	6517
Barnes&Tucker	1990	6.19	133	79		6843
Barnes&Tucker	1991	6.03	198.3	80		6715
Barnes&Tucker	1992	5.84	175	90	759.0	5472
Barnes&Tucker	1993	6.17	191.4	72.8	607.3	6382
Barnes&Tucker	1994	6.48	181.9	73.3	478.3	6156
Barnes&Tucker	1995	6.74	196.3	60.6	573.7	5920
Barnes&Tucker	1996	6.5	141	66	535.0	5679
Barnes&Tucker	1997	6.79	180	45.2	445.5	6639
Barnes&Tucker	1998	6.46	146.9	40.2	375.2	5680
Barnes&Tucker	1999	6.52	148.4	43.2	413.0	4967
Barnes&Tucker	2000	6.48	187.8	49.1	386.1	5284
Barnes&Tucker	2001	6.57	191.8	44.3	410.2	5028
Barnes&Tucker	2002	6.66	207.2	40.2	372.8	4406
Barnes&Tucker	2003	6.64	203.5	42.6	347.0	5253
Barnes&Tucker	2004	6.58	135.6	37.7	388.4	
Barnes&Tucker	2005	6.60	197.7	43.5	266.0	

Appendix I

Arden Mine-pool Raw Chemical Data

Table I-1, Arden Mine-pool Raw Chemical Data

Site	Date	pH	Alkalinity, mg/L	Fe, mg/L	SO4, mg/L	TDS, mg/L	Ca, mg/L	Mg, mg/L	Na, mg/L	K, mg/L	Cl, mg/L
Arden	9/8/1986	6.86	277	24	672	1369	125	38	165	4.6	0.6
Arden	10/1/1986	7.08	273	24	671	1366	124	36	171	4.5	0.6
Arden	10/8/1986	6.97	272	23	657	1359	120	36	184	4.4	1.2
Arden	10/15/1986	6.85	303	28	615	1362	122	36	184	4.5	0.9
Arden	10/22/1986	6.91	305	22	585	1362	126	38	195	4.5	17.3
Arden	10/29/1986	7.02	291	25	603	1353	132	39	184	5	8.4
Arden	11/5/1986	6.91	296	31	725	1580	148	47	228	5.4	31.4
Arden	11/12/1986	6.94	290	32	725	1594	159	51	226	5.3	38.8
Arden	11/26/1986	6.76	292	38	1020	1925	172	54	234	5.4	42
Arden	12/3/1986	6.8	283	46	1057	1976	183	57	238	5.5	41.2
Arden	12/10/1986	7	260	58	1170	2117	201	65	243	6.5	53
Arden	12/17/1986	6.76	277	68	1024	2020	211	69	247	6.5	53
Arden	12/23/1986	7	164	73	943	1838	225	73	258	6.8	55
Arden	12/29/1986	6.8	176	76	1402	2327	237	76	251	7.7	59
Arden	3/18/1987	6.75	264	38	884	1703	155	53	204	4.9	39.5
Arden	3/25/1987	6.87	260	41	825	1657	162	49	209	5.2	45
Arden	4/3/1987	6.72	273	25	800	1715	183	59	257	5.7	49
Arden	4/9/1987	6.52	265	59	1100	1995	164	56	235	4.2	51
Arden	4/15/1987	7.11	171	71	1100	1927	187	61	238	4.6	53
Arden	4/23/1987	6.89	262	78	1125	2095		61	254	5	59
Arden	5/6/1987	7.3	143	89	1100	1968	261	63	209	4.5	62
Arden	5/13/1987	6.6	219	114	1475	2506	230	72	264	5.8	74
Arden	5/19/1987	6.56	218	123	1375	2456	260	77	272	6.2	72
Arden	6/3/1987	6.52	201	114	1925	2991	243	86	300	6.4	67
Arden	6/10/1987	6.43	205	119	1510	2595	254	83	305	5.3	63
Arden	6/16/1987	6.58	231	114	1450	2593	264	88	319	5.6	65
Arden	6/23/1987	6.56	230	131	1550	2717	259	87	332	6.9	65
Arden	7/2/1987	6.59	194	116	1375	2440	248	83	308	6.6	62
Arden	7/8/1987	6.51	129	133	1600	2612	253	85	306	6.5	66
Arden	7/15/1987	6.52	171	89	1662	2713	272	85	313	6.9	71
Arden	7/22/1987	6.88	160	134	1675	2799	282	94	332	7	74
Arden	7/29/1987	6.49	174	136	1504	2495		78	256	5.7	38
Arden	8/5/1987	6.66	178	148	1554	2630		80	290	6.4	69
Arden	8/12/1987	6.49	153	136	1512	2591	271	91	317	6.5	65
Arden	8/18/1987	6.48	133	145	1574	2617	261	88	302	6.2	73
Arden	8/26/1987	6.44	152	140	1560	2618	261	87	284	6	89
Arden	9/2/1987	6.56	187	143	1536	2638	257	87	304	6.4	71
Arden	9/9/1987	6.34	130	148	1660	2699	258	87	305	6.4	70
Arden	9/16/1987	6.4	163	148	1342	2408	252	86	298	7.3	70
Arden	10/7/1987	6.59	161	151	1672	2759		84	314	7.1	79
Arden	10/13/1987	6.36	160	162	1560	2654		85	319	6.5	71
Arden	10/21/1987	6.54	96	143	1560	2565	252	85	324	6.3	72
Arden	10/28/1987	6.4	134	165	1580	2609	238	81	291	6	79
Arden	11/5/1987	6.71	149	165	1476	2495	230	79	277	5.6	75
Arden	11/10/1987	6.25	10	137	1559	2446		85	316	6.1	75
Arden	11/18/1987	6.43	192	152	1624	2726	252	84	296	6.2	72
Arden	11/24/1987	6.63	208	151	1598	2709	246	82	291	6.2	75
Arden	4/13/1988	7.46	129	91	1172	2025	196	65.8	276	5.9	57
Arden	4/20/1988	6.64	171	94	1187	2143		68.1	282	5.8	83

359

Table I-1, Arden Mine-pool Raw Chemical Data

Site	Date	pH	Alkalinity, mg/L	Fe, mg/L	SO4, mg/L	TDS, mg/L	Ca, mg/L	Mg, mg/L	Na, mg/L	K, mg/L	Cl, mg/L
Arden	4/27/1988	6.77	199	108	1254	2280	221	72.1	293	6.3	78
Arden	5/4/1988	6.72	156	113	1340	2358		77.2	311	6.5	84
Arden	5/11/1988	6.44	160	122	1461	2547	241	83.9	334	6.8	98
Arden	5/18/1988	6.74	202	134	1176	2310	243	82.7	316	6.4	100
Arden	5/25/1988	6.43	104	136	1597	2660	265	90	332	7	100
Arden	6/2/1988	6.64	168	151	1640	2819	264	91.2	350	7.1	105
Arden	6/9/1988	6.68	132	154	1687	2799	268	88.9	337	7	90
Arden	6/15/1988	6.67	127	163	1673	2812	276	91.5	351	7.2	89
Arden	6/22/1988	6.71	187	162	1714	2932	276	93.3	353	7.1	92
Arden	6/29/1988	6.62	164	137	1700	2848	274	91.9	347	7	85
Arden	7/6/1988	6.25	105	162	1711	2816	275	92.5	352	7.1	82
Arden	7/20/1988	6.38	117	151	1719	2856	275	92.8	357	7.3	105
Arden	7/25/1988	6.52	91	149	1634	2675	261	88.3	340	7	79
Arden	8/3/1988	6.79	173	154	1701	2860	269	88.6	333	6.9	90
Arden	8/24/1988	6.8	160	151	1754	2876	253	87.4	333	6.9	90
Arden	9/2/1988	6.8	106	187	1614	2712	261	86.4	332	6.9	89
Arden	9/13/1988	6.44	91	154	1625	2663	254	86.9	334	6.9	85
Arden	10/11/1988	6.69	131	137	1531	2577	243	83.3	331	6.8	80
Arden	10/18/1988	6.84	167	148	1631	2784	254	87.7	351	7.1	96
Arden	11/1/1988	6.45	75	162	1626	2665	254	87.8	350	7.1	81
Arden	11/8/1988	6.48	165	162	1611	2749	251	86.3	339	6.9	86
Arden	11/15/1988	6.49	157	165	1581	2708	252	84.5	328	6.8	94
Arden	12/1/1988	6.47	81	182	1753	2859	267	92.6	365	7.3	87
Arden	12/6/1988	6.87	129	162	1695	2838	263	95	356	7.1	96
Arden	12/14/1988	6.61	135	159	1680	2807	262	89.2	347	7	92
Arden	12/20/1988	6.4	60	148	1633	2659	258	87.6	349	7.1	97
Arden	1/3/1989	6.72	166	198	1802	3074	276	95.9	395	8	91
Arden	4/11/1989	6.66	218	106	1139	2134	197	63.7	293	6.1	60
Arden	4/25/1989	7	168	123	1296	2267	204	66.6	304	6	58
Arden	5/2/1989	7.14	185	126	1293	2309	208	68.5	312	6.2	65
Arden	5/9/1989	6.78	204	134	1373	2417	217	70.1	310	6.3	53
Arden	5/16/1989	6.58	211	137	1482	2586	234	74.3	322	6.5	68
Arden	5/23/1989	6.42	164	136	1492	2544	234	77.5	338	6.8	55
Arden	5/30/1989	6.63	180	140	1536	2764	242	79	444	6.8	91
Arden	6/13/1989	6.4	74	106	1315	2111	222	74	293	6.1	
Arden	6/20/1989	6.59	187	150	1640	2740	264	83.3	362	7.2	
Arden	6/27/1989	6.49	165	143	1732	2825	262	86.6	387	7.4	
Arden	7/5/1989	6.41	152	134	1591	2606	250	81.2	352	7.2	
Arden	7/11/1989	6.67	102	109	1314	2153	224	70.3	300	6.3	
Arden	7/25/1989	6.02	22	127	1525	2342	237	77.2	337	6.9	
Arden	8/1/1989	6.4	187	131	1547	2569	237	78.7	335	6.9	
Arden	8/8/1989	6.6	84	127	1521	2405	236	77	330	6.8	
Arden	8/22/1989	6.5	194	121	1439	2449	240	77.4	323	6.9	
Arden	8/29/1989	6.69	77	125	1433	2344	227	73.2	312	6.7	
Arden	9/6/1989	6.1	46	92	1426	2198	227	73.1	312	6.9	
Arden	9/12/1989	6.76	180	123	1413	2376	226	72.5	310	6.6	
Arden	9/19/1989	6.79	188	122	1456	2461	227	73.5	341	6.9	
Arden	9/27/1989	6.66	183	121	1409	2359	223	71.5	299	7.2	
Arden	10/10/1989	6.6	181	124	1458	2439	233	74.7	317	6.7	
Arden	10/17/1989	6.57	72	119	1411	2229	231	76	293	6.3	
Arden	10/24/1989	6.3	172	129	1523	2527	243	78.2	332	6.9	
Arden	11/1/1989	6.56	61	154	1537	2406	231	76.3	321	6.7	

Table I-1, Arden Mine-pool Raw Chemical Data

Site	Date	pH	Alkalinity, mg/L	Fe, mg/L	SO4, mg/L	TDS, mg/L	Ca, mg/L	Mg, mg/L	Na, mg/L	K, mg/L	Cl, mg/L
Arden	11/7/1989	6.43	108	88	1005	1858	234	75.9	312	6.6	
Arden	11/13/1989	6.64	75	125	1005	1862	237	76.4	315	6.8	
Arden	11/21/1989	6.38	100	136	1622	2558	244	79.7	342	7.1	
Arden	12/1/1989	6.5	155	121	1482	2417	228	74.3	311	6.7	
Arden	12/5/1989	6.79	164	126	1444	2389	226	73.2	308	6.5	
Arden	12/12/1989	6.42	156	122	1457	2393	226	73.8	312	6.5	
Arden	1/2/1990	6.47	180	130	1542	2551	240	77.9	329	6.9	
Arden	1/9/1990	6.83	148	127	1537	2502	238	77.6	330	6.9	
Arden	1/16/1990	6.49	185	133	1595	2640	247	84	343	7.2	
Arden	1/23/1990	6.53	179	128	1530	2538	242	76.1	332	6.9	
Arden	2/2/1990	6.59	189	131	1504	2510	233	75.8	324	6.7	
Arden	2/6/1990	6.16	161	134	1455	2414	213	74.3	330	6.7	
Arden	2/13/1990	6.31	163	130	1546	2530	239	77.8	327	6.6	
Arden	2/20/1990	6.5	129	129	1504	2430	241	75.2	312	6.5	
Arden	3/1/1990	6.49	159	133	1534	2519	239	77.2	330	6.9	
Arden	3/6/1990	6.37	184	133	1544	2564	239	77.5	334	6.8	
Arden	3/13/1990	6.46	141	129	1500	2450	233	76.1	328	6.8	
Arden	3/27/1990	6.71	139	131	1491	2429	231	74.7	320	6.7	
Arden	4/10/1990	6.62	173	126	1429	2382	223	71.3	311	6.3	
Arden	4/17/1990	6.84	95	137	1517	2424	232	75	335	6.7	
Arden	4/24/1990	6.44	138	131	1521	2479	232	75.6	339	6.8	
Arden	5/1/1990	6.31	66	129	1487	2346	232	74.5	331	6.9	
Arden	5/8/1990	6.72	176	127	1448	2421	226	72.3	322	6.5	
Arden	5/15/1990	6.58	176	130	1502	2501	231	74.9	337	6.7	
Arden	5/22/1990	6.46	163	128	1494	2471	229	74.3	335	6.5	
Arden	5/29/1990	6.42	92	127	1476	2360	230	73.7	330	6.6	
Arden	6/5/1990	6.68	183	129	1493	2504	237	75.2	335	6.8	
Arden	6/12/1990	5.98	6	126	1464	2262	246	74.2	333	7	
Arden	6/19/1990	6.54	140	126	1421	2348	222	70.6	326	6.6	
Arden	6/26/1990	6.44	140	131	1500	2460	227	74.5	345	6.7	
Arden	8/7/1990	6.63	187	98	1246	2250	215	73	302	6.3	78
Arden	8/14/1990	6.51	196	112	1345	2318	212	68	331	6.6	
Arden	8/21/1990	6.64	178	103	1222	2109	192	62	303	5.7	
Arden	8/28/1990	6.77	179	127	1505	2533	232	75.8	363	7.2	
Arden	9/4/1990	5.52	157	119	1392	2333	215	70	334	6.6	
Arden	9/11/1990	6.42	186	115	1354	2309	209	67.8	326	6.4	
Arden	9/18/1990	6.5	136	115	1344	2230	206	67.2	321	6.4	
Arden	9/25/1990	6.19	116	137	1650	2660	250	81.5	387	7.4	
Arden	10/2/1990	6.37	263	117	1407	2463	212	68.8	327	6.2	
Arden	10/16/1990	6.83	158	116	1387	2342	233	70	332	6.5	
Arden	10/23/1990	6.98	375	121	1414	2652	243	77	329	6.4	
Arden	10/30/1990	6.62	158	118	1404	2350	218	69.7	337	6.5	
Arden	11/6/1990	6.73	96	120	1443	2332	224	71.9	345	6.5	
Arden	11/13/1990	6.53	241	112	1372	2398	214	68	327	6.3	
Arden	11/20/1990	6.05	73	116	1425	2271	221	72	337	6.5	
Arden	11/28/1990	5.78	70	113	1372	2195	220	67.9	326	6.3	
Arden	12/4/1990	6.5	137	108	1330	2215	206	66	327	6.3	
Arden	12/11/1990	6.47	164	114	1474	2318	213	68	338	6.5	
Arden	1/15/1991	6.52	178	104	1294	2213	204	64.9	319	6.2	
Arden	1/29/1991	6.31	162	106	1294	2222	231	65.2	318	6.2	
Arden	2/12/1991	6.46	139	103	1275	2137	200	63.4	316	6.1	
Arden	2/26/1991	6.31	164	113	1285	2209	219	67.4	314	6.2	

Table I-1, Arden Mine-pool Raw Chemical Data

Site	Date	pH	Alkalinity, mg/L	Fe, mg/L	SO4, mg/L	TDS, mg/L	Ca, mg/L	Mg, mg/L	Na, mg/L	K, mg/L	Cl, mg/L
Arden	3/12/1991	6.31	67	73	1205	1935	193	63.7	309	6	
Arden	3/26/1991	6.45	126	100	1226	2063	195	65	314	6.1	
Arden	4/9/1991	6.17	100	97	1193	1992	190	64.2	316	6.2	
Arden	4/23/1991	6.28	146	95	1194	2037	190	62.6	308	6.1	
Arden	5/14/1991	6.52	137	94	1209	2051	190	64	317	6.1	
Arden	5/28/1991	6.58	117	90	1156	1945	182	61.1	304	5.8	
Arden	6/11/1991	6.45	170	94	1234	2131	206	64.6	315	6.1	
Arden	6/25/1991	6.48	141	90	1176	1991	180	61.2	303	5.7	
Arden	7/9/1991	6.57	178	90	1168	2030	184	61.2	301	5.8	
Arden	7/23/1991	6.8	191	92	1122	2022	185	63	318	6.1	
Arden	8/1/1991	6.64	169	90	1190	2047	185	62.5	304	5.8	
Arden	8/13/1991	6.64	215	101	1257	2256	231	67.8	327	6.2	
Arden	9/3/1991	6.54	199	98	1230	2184	211	66.5	326	6.1	
Arden	9/18/1991	7.02	158	97	1267	2166	201	67.4	331	6.3	
Arden	10/8/1991	6.41	122	104	1320	2207	204	70.1	350	6.6	
Arden	10/22/1991	6.08	113	102	1328	2201	206	70	347	6.6	
Arden	11/1/1991	6.76	131	101	1326	2211	202	69.5	343	6.3	
Arden	11/19/1991	6.8	181	101	1320	2272	203	69.9	347	6.4	
Arden	12/4/1991	6.5	54	102	1334	2138	205	70.3	351	6.3	
Arden	12/10/1991	5.77	70	104	1369	2217	207	72.4	369	6.6	
Arden	1/8/1992	6.48	129	106	1369	2298	214	72.7	368	6.7	
Arden	2/11/1992	6.39	200	115	1425	2482	236	74.2	377	6.6	
Arden	2/25/1992	6.7	175	108	1431	2430	215	74	378	6.6	
Arden	3/10/1992	7.06	110	109	1377	2275	213	71	361	6.4	
Arden	3/17/1992	6.75	185	110	1418	2429	221	73.1	371	6.4	
Arden	4/8/1992	6.03	46	100	1285	2068	202	66.9	348	6.3	
Arden	4/21/1992	6.64	45	106	1378	2207	208	79	371	6.5	
Arden	5/5/1992	6.34	120	108	1390	2291	215	71.3	350	6.5	
Arden	5/19/1992	6.88	168	110	1410	2381	217	72.1	356	6.6	
Arden	6/9/1992	6.71	100	106	1357	2234	205	69.9	364	6.3	
Arden	6/16/1992	6.35	150	108	1378	2337	211	71.9	375	6.6	
Arden	7/15/1992	6.41	208	104	1352	2365	204	74	367	6.5	
Arden	8/11/1992	6.54	214	94	1241	2201	190	65.1	340	6	
Arden	8/26/1992	6.77	202	98	1356	2361	202	73	375	6.6	
Arden	9/8/1992	6.6	182	103	1358	2331	200	69.4	369	6.4	
Arden	9/23/1992	6.9	155	101	1322	2249	201	68	358	6.3	
Arden	10/6/1992	6.91	44	103	1352	2172	205	69.3	379	6.6	
Arden	10/11/1992	6.85	176	99	1325	2288	199	68.3	372	6.4	
Arden	11/17/1992	7.05	197	110	1306	2297	203	66.7	361	6.4	
Arden	12/8/1992	6.67	180	98	1260	2200	194	64.7	354	6.1	
Arden	12/15/1992	6.35	192	94	1238	2181	191	64.4	350	6.1	
Arden	1/12/1993	6.71	173	98	1312	2257	195	66.8	364	6.4	
Arden	4/20/1993	7.04	171	91	1222	2121	190	62.2	338	6.1	
Arden	5/18/1993	6.86	194	89	1197	2116	181	61.3	342	6.1	
Arden	7/6/1993	6.76	116	84	1141	1936	175	59	327	5.8	
Arden	9/14/1993	6.85	85	77	1057	1790	171	56	316	6.4	
Arden	10/19/1993	6.69	181	85	1193	2102	180	67	347	6.2	
Arden	11/24/1993	6.8	154	76	1051	1853	168	55.6	306	5.5	
Arden	12/7/1993	6.67	203	82	1100	2005	171	58.3	337	5.9	
Arden	1/26/1994	7.09	110	72	1689	2430	155	49.7		9.1	
Arden	2/13/1994	7.09	158	89	1245	2149	188	63.5	361	6.4	
Arden	3/22/1994	6.64	215	89	1218	2195	184	63.9	368	6.5	

Table I-1, Arden Mine-pool Raw Chemical Data

Site	Date	pH	Alkalinity, mg/L	Fe, mg/L	SO4, mg/L	TDS, mg/L	Ca, mg/L	Mg, mg/L	Na, mg/L	K, mg/L	Cl, mg/L
Arden	4/12/1994	6.31	81	93	1228	2147	195	80	416	28.9	
Arden	5/3/1994	6.51	200	79	1096	1964	167	55.6	314	5.6	
Arden	7/6/1994	6.78	159	77	1027	1845	166	54.8	318	5.8	
Arden	9/12/1994	6.41	188	70	928	1723	157	50.2	281	5.1	
Arden	10/11/1994	6.14	113	73	1030	1770	164	53.4	304	5.6	
Arden	11/23/1994	6.16	115	74	1030	1787	167	53.6	314	5.6	
Arden	12/23/1994	6.49	207	82	1190	2118	184	60.1	340	6.4	
Arden	1/25/1995	6.04	90	77	1090	1841	174	55.9	326	5.8	
Arden	2/21/1995	6.4	193	74	1040	1888	170	53.2	307	5.6	
Arden	3/29/1995	6.27	160	77	1090	1928	171	56.7	330	5.9	
Arden	5/30/1995	6.18	144	74	1040	1826	166	53.1	310	5.4	
Arden	6/27/1995	6.18	102	72	1030	1766	166	53.6	312	5.7	
Arden	7/25/1995	6.28	130	63	907	1617	151	48.4	282	5.2	
Arden	8/1/1995	6.19	138	67	923	1674	164	49.7	294	5.4	
Arden	9/5/1995	6.25	110	76	1070	1842	172	55.5	327	5.8	
Arden	10/10/1995	6.44	181	79	1130	2015	176	57.4	344	6.1	
Arden	11/7/1995	6.2	98	54	1075	1812					
Arden	12/26/1995	7.2	115	69	887	1660					
Arden	1/2/1996	7	109	70	962	1729					
Arden	8/5/1996	7	157	58	900	1713					
Arden	9/9/1996	6.6	128	63	950	1733					
Arden	10/7/1996	6.6	111	63	875	1636					
Arden	11/4/1996	6.6	119	58	938	1705					
Arden	12/2/1996	6.3	109	64	925	1685					
Arden	1/20/1997	6.3	125	67	963	1746					
Arden	2/3/1997	6.1	106	72	950	1715					
Arden	3/3/1997	6.1	108	68	925	1689					
Arden	5/5/1997	6.3	139	59	850	1642					
Arden	6/2/1997	7.3	130	65	875	1663					
Arden	8/11/1997	6.3	125	65	838	1619					
Arden	9/1/1997	6.9	121	64	825	1601					
Arden	10/6/1997	6.6	124	58	775	1548					
Arden	11/3/1997	6.4	128	66	800	1586					
Arden	12/8/1997	6.3	141	43	863	1642					
Arden	1/5/1998	6.3	130	71	900	1693					
Arden	2/2/1998	6.4	127	75	1000	1794					
Arden	3/2/1998	6.8	137	76	913	1720					
Arden	5/4/1998	6.9	160	61	775	1594					
Arden	6/2/1998	8.2	146	67	888	1697					
Arden	7/13/1998	6.6	157	73	970	1798					
Arden	9/14/1998	6.9	159	57	838	1653					
Arden	10/5/1998	7.8	138	34	725	1491					
Arden	11/3/1998	6.5	146	78	963	1783					
Arden	1/5/1999	7.1	163	60	875	1697					
Arden	2/1/1999	6.7	164	73	788	1625					

Appendix J

PHREEQCI Files

```
TITLE Sulfate Equilibrium
PHASES
Schwertmannite
    Fe8O8(OH)4.4(SO4)1.8 + 20.4H+ = 8Fe+3 + 12.4H2O + 1.8SO4-2
    log_k     10.5
Halotrichite
    FeAl2(SO4)4:22H2O = 2Al+3 + Fe+2 + 22H2O + 4SO4-2
    log_k     -27.3




SELECTED_OUTPUT
    -file                Sulfateequilibrium.out
    -user_punch          false
    -high_precision      false
    -simulation          false
    -state               false
    -distance            false
    -time                false
    -step                false
    -ph                  true
    -pe                  true
    -reaction            false
    -temperature         false
    -alkalinity          false
    -water               false
    -charge_balance      true
    -percent_error       true
    -totals              Al  Ca  Mg  Na  K  Fe(2)  Fe(3)
                         S(6)
    -molalities          Al(OH)2+  Al(OH)3  Al(OH)4-  Al+3
                         AlHSO4+2  AlOH+2  Fe(OH)2  Fe(OH)2+
                         Fe(OH)3  Fe(OH)3-  Fe(OH)4-  Fe+2
                         Fe+3  Fe2(OH)2+4  Fe3(OH)4+5  FeHSO4+
                         FeHSO4+2  FeOH+  FeOH+2  H+
                         CaHSO4+  CaOH+  HSO4-  MgOH+
                         SO4-2  Al(SO4)2-  AlSO4+  CaSO4
                         Fe(SO4)2-  FeSO4  FeSO4+  KSO4-
                         MgSO4  MnSO4  NaSO4-
```

```
    -saturation_indices   AlumK  Basaluminite  Chlorite14A  Fe(OH)3(a)
                          Fe3(OH)8  Gibbsite  Gypsum  Halotrichite
                          Jarosite(ss)  JarositeH  Jarosite-K  Jarosite-Na
                          Jurbanite  Kaolinite  Melanterite  Schwertmannite
                          Al(OH)3(a)  Goethite
    -inverse_modeling     false

SOLUTION_SPREAD
    -pe       0
    -units    mg/l
 Description Number Temperature pH  Al   Ca  Cl   K    Mg  Mn    Na    S(6)  Si   Fe Alkalinity  pe
                                    mg/l mg/l mg/l mg/l mg/l mg/l mg/l  mg/l  mg/l
   Hahn Early  1        14       4.80 25.7 345 622  10.9 202  15.9 1965  8300  20  1082              0
    Hahn Late  2        14       7.09 0.21 158       6.4  57   1.7  979  1838  10  118    404        0
 Omega Early  3        14       2.86 167  321  5    5.7 168   5.32 8.3  4098  20  905               10.5
  Omega Late  4        14       3.03 176  318 28.8  14  132   6.14 20.5 3796  20  716.7             10.34
  Omega 2008  5        14       2.43 112  162  40   6.9 56.6  2.65 10.8 1923  43  258               10.34
  Arden 1989  6        14       6.72 .2   276  91    8  95.9  6.16 395  1802  10  198    166         0
  Arden 1996  7        14       7.0  .2   150  60   5.5  50    1.9 310   900  10   58    157         0
    T&T 1994  8        15.5     2.4  90   287  5.6  2.3 68.4   3.1 5.6  1910  20  455               10.53
    T&T 2008  9        12.1     2.7  23.4 152   6   2.4 37.5   1.17  6   840  14   45.1             10.99
   B&T 2005 10        11.5     6.01 .21   48   2   1.5 18.5   1.24 137   455   9   58.6   96        4.36
END
TITLE Equilibrate with Gypsum Hahn Early
USE solution 1
EQUILIBRIUM_PHASES 1
    Gypsum     0 10
END
TITLE Equilibrate Gypsum Hahn Late
USE solution 2
EQUILIBRIUM_PHASES 1
    Gypsum     0 10
END
TITLE Equilibrate Gypsum Omega Early
USE solution 3
EQUILIBRIUM_PHASES 1
    Gypsum     0 10
END
TITLE Equilibrate Gypsum Omega Late
USE solution 4
EQUILIBRIUM_PHASES 1
```

```
    Gypsum     0 10
END
TITLE Equilibrate Jurbanite Omega Early
USE solution 3
EQUILIBRIUM_PHASES 2
    Jurbanite 0 10
END
TITLE Equilibrate Jurbanite Omega Late
USE solution 4
EQUILIBRIUM_PHASES 2
    Jurbanite 0 10
END
TITLE Equilibrate Gypsum Omega 2008
USE solution 5
EQUILIBRIUM_PHASES 1
    Gypsum     0 10
END
TITLE Equilibrate Jurbanite Omega 2008
USE solution 5
EQUILIBRIUM_PHASES 2
 Jurbanite 0 10
END
TITLE Equilibrate with Gypsum Arden Early
USE solution 6
EQUILIBRIUM_PHASES 1
    Gypsum     0 10
END
  TITLE Equilibrate with Gypsum Arden Late
USE solution 7
EQUILIBRIUM_PHASES 1
    Gypsum     0 10
END
 TITLE Equilibrate with Gypsum T&T early
USE solution 8
EQUILIBRIUM_PHASES 1
    Gypsum     0 10
END
 TITLE Equilibrate with Gypsum T&T late
USE solution 9
EQUILIBRIUM_PHASES 1
    Gypsum     0 10
```

367

```
END
 TITLE Equilibrate with Gypsum B&T Late
USE solution 10
EQUILIBRIUM_PHASES 1
    Gypsum    0 10
END
TITLE Equilibrate with Fe(OH)3 Hahn Early
USE solution 1
EQUILIBRIUM_PHASES 1
    Fe(OH)3(a) 0 10
END
TITLE Equilibrate with Fe(OH)3 Hahn Late
USE solution 2
EQUILIBRIUM_PHASES 2
    Fe(OH)3(a) 0 10
END
TITLE Equilibrate Fe(OH)3 Omega Early
USE solution 3
EQUILIBRIUM_PHASES 3
    Fe(OH)3(a) 0 10
END
TITLE Equilibrate Fe(OH)3 Omega Late
USE solution 4
EQUILIBRIUM_PHASES 4
    Fe(OH)3(a) 0 10
END
TITLE Equilibrate Fe(OH)3  Omega 2008
USE solution 5
EQUILIBRIUM_PHASES 2
 Fe(OH)3(a) 0 10
END
TITLE Equilibrate with Fe(OH)3 Arden Early
USE solution 6
EQUILIBRIUM_PHASES 1
    Fe(OH)3(a) 0 10
END
TITLE Equilibrate with Fe(OH)3 Arden Late
USE solution 7
EQUILIBRIUM_PHASES 1
    Fe(OH)3(a) 0 10
END
```

```
TITLE Equilibrate with Fe(OH)3 T&T early
USE solution 8
EQUILIBRIUM_PHASES 1
     Fe(OH)3(a) 0 10
END
 TITLE Equilibrate with Fe(OH)3 T&T late
USE solution 9
EQUILIBRIUM_PHASES 1
    Fe(OH)3(a) 0 10
END
TITLE Equilibrate with Fe(OH)3 B&T late
USE solution 10
EQUILIBRIUM_PHASES 1
    Fe(OH)3(a) 0 10
END
TITLE Equilibrate Hahn Early with Pyrite
USE solution 1
EQUILIBRIUM_PHASES 3
    Pyrite    0 10
END
TITLE Equilibrate Hahn Late with Pyrite
USE solution 2
EQUILIBRIUM_PHASES 4
    Pyrite    0 10
END
TITLE Equilibrate Omega Early with Pyrite
USE solution 3
EQUILIBRIUM_PHASES 5
    Pyrite    0 10
END
TITLE Equilibrate Omega Late with Pyrite
USE solution 4
EQUILIBRIUM_PHASES 6
    Pyrite    0 10
END
TITLE Equilibrate Omega 2008 with Pyrite
USE solution 5
EQUILIBRIUM_PHASES 6
    Pyrite    0 10
END
```

```
TITLE Equilibrate Arden 1989 with Pyrite
USE solution 6
EQUILIBRIUM_PHASES 7
    Pyrite   0 10
END
TITLE Equilibrate Arden 1996 with Pyrite
USE solution 7
EQUILIBRIUM_PHASES 8
    Pyrite   0 10
END
TITLE Equilibrate T&T 1994 with Pyrite
USE solution 8
EQUILIBRIUM_PHASES 9
    Pyrite   0 10
END
TITLE Equilibrate T&T 2008 with Pyrite
USE solution 9
EQUILIBRIUM_PHASES 10
    Pyrite   0 10
END
TITLE Equilibrate B&T 2005 with Pyrite
USE solution 10
EQUILIBRIUM_PHASES 11
    Pyrite   0 10
END
TITLE Equilibrate Jurbanite T&T Early
USE solution 8
EQUILIBRIUM_PHASES 2
 Jurbanite 0 10
END
TITLE Equilibrate Jurbanite T&T 2008
USE solution 9
EQUILIBRIUM_PHASES 2
 Jurbanite 0 10
END
```

```
TITLE Long Term Equilibrium of Aged Acid and Net Alkaline Mine-pools
PHASES
Schwertmannite
    Fe8O8(OH)4.4(SO4)1.8 + 20.4H+ = 8Fe+3 + 12.4H2O + 1.8SO4-2
    log_k     10.5
Halotrichite
    FeAl2(SO4)4:22H2O = 2Al+3 + Fe+2 + 22H2O + 4SO4-2
    log_k     -27.3
SOLUTION 1 Long Term Acid Discharge Based on Ruthbell Drainage 5/17/05 sample, T&T Mine-pool
    temp      10.7
    pH        2.68
    pe        13.03
    redox     pe
    units     mg/l
    density   1
    Al        4.76
    Cl        5
    Fe        6.63
    K         1.15
    Mg        14.1
    Mn        0.19
    Na        1.23
    S(6)      235
    Si        6.8
    Ca        40.5
    -water    1 # kg
SOLUTION 2 Long Term Alkaline Discharge Based on Acme Mine Discharge, Fairmont Minepool 6/5/2008
    temp      13.8
    pH        6.25
    pe        1.83
    redox     pe
    units     mg/l
    density   1
    Al        0.05
    Cl        6
    Fe        5.15
    K         4.47
    Mg        39.8
    Mn        0.65
    Na        165
```

```
    S(6)       543
    Si         5
    Ca         104.3
    Alkalinity 263
    -water     1 # kg


END
USE solution 1
REACTION 1 Add CaCO3 in Increments Mixed Buffer Ruthbell Water
    Calcite    1
    5 millimoles in 100 steps
EQUILIBRIUM_PHASES 1
    Al(OH)3(a) 0 0
    CO2(g)     -1.5 10
    Fe(OH)3(a) 0 0
    Fe3(OH)8   0 0
    Jarosite-K 0 0
    Jurbanite 0 0
    Kaolinite 0 0
    O2(g)      -2 1e-006
    Schwertmannite 0 0
SELECTED_OUTPUT
    -file               LongtermEquilibrium
    -ionic_strength     true
    -percent_error      true
    -totals             Al  Alkalinity  Ca  Fe(2)  Fe(3)  K  Mg
                        Na  S(-2)  S(6)  Si
    -molalities         Al(OH)2+  Al(OH)3  Al(OH)4-  Al(SO4)2-
                        Al+3  AlHSO4+2  AlOH+2  AlSO4+
                        Fe(OH)2  Fe(OH)2+  Fe(OH)3  Fe(OH)3-
                        Fe(OH)4-  Fe(SO4)2-  Fe+2  Fe+3
                        Fe2(OH)2+4  Fe3(OH)4+5  FeCl+  FeCl+2
                        FeCl2+  FeCl3  FeCO3  FeHCO3+
                        FeOH+  FeOH+2  FeSO4  FeSO4+
    -activities         Al+3  Ca+2  CO2  Fe+2
                        Fe+3  H+  K+  Mg+2
                        Na+  O2  SO4-2  H4SiO4
                        Al(OH)2+  Al(OH)3  Al(OH)4-  Al(SO4)2-
                        AlHSO4+2  AlOH+2  AlSO4+  Fe(OH)2
                        Fe(OH)2+  Fe(OH)3  Fe(OH)3-  Fe(OH)4-
                        Fe(SO4)2-  Fe2(OH)2+4  Fe3(OH)4+5  FeCl+
```

```
                       FeCl+2  FeCl2+  FeCl3  FeCO3
                       FeOH+  FeOH+2  FeSO4  FeSO4+
    -equilibrium_phases  Al(OH)3(a)  Fe(OH)3(a)  Jarosite-K  Schwertmannite
                       Kaolinite  Jurbanite  Goethite  Fe3(OH)8
    -saturation_indices  Al(OH)3(a)  Fe(OH)3(a)  Jarosite-K  Schwertmannite
                       Kaolinite  Jurbanite  Goethite  Fe3(OH)8
    -gases             CO2(g)  O2(g)
End
USE solution 2
REACTION 1 Add Oxygen in Increments Acme Mine water, Mixed Fe Buffer
    O2(g)        1
    0.01 millimoles in 100 steps
EQUILIBRIUM_PHASES 1
    Calcite   0 0
    CO2(g)     -0.85 10
    Fe(OH)3(a)  0 0
    Fe3(OH)8   0 0
    Gypsum     0 0
    Kaolinite 0 0
    Schwertmannite 0 0
SELECTED_OUTPUT
    -file              LongtermEquilibrium2
    -ionic_strength    true
    -percent_error     true
    -totals            Al  Alkalinity  Ca  Fe(2)  Fe(3)  K  Mg
                       Na  S(-2)  S(6)  Si
    -molalities        Fe(OH)2  Fe(OH)2+  Fe(OH)3  Fe(OH)3-
                       Fe(OH)4-  Fe(SO4)2-  Fe+2  Fe+3
                       Fe2(OH)2+4  Fe3(OH)4+5  FeCl+  FeCl+2
                       FeCl2+  FeCl3  FeCO3  FeHCO3+
                       FeOH+  FeOH+2  FeSO4  FeSO4+
    -activities        Al+3  Ca+2  CO2  Fe+2
                       Fe+3  H+  K+  Mg+2
                       Na+  O2  SO4-2  H4SiO4
                       Fe(OH)2  Fe(OH)2+  Fe(OH)3  Fe(OH)3-
                       Fe(OH)4-  Fe(SO4)2-  Fe2(OH)2+4  Fe3(OH)4+5
                       FeCl+  FeCl+2  FeCl2+  FeCl3
                       FeCO3  FeOH+  FeOH+2  FeSO4
                       FeSO4+
    -equilibrium_phases  Fe(OH)3(a)  Jarosite-K  Schwertmannite  Kaolinite
                       Goethite  Fe3(OH)8
```

373

```
    -saturation_indices  Fe(OH)3(a)  Jarosite-K  Schwertmannite  Kaolinite
                         Goethite  Fe3(OH)8  Siderite
    -gases               CO2(g)  O2(g)
End
USE solution 1
REACTION 1 Add CaCO3 in Increments Kaolinite Buffer Ruth Bell Water
    Calcite    0.5
    5 millimoles in 100 steps
EQUILIBRIUM_PHASES 1
    CO2(g)     -1.5 10
    Fe(OH)3(a) 0 0
    Jarosite-K 0 0
    Kaolinite 0 0
    O2(g)      -2 1e-006
SELECTED_OUTPUT
    -file                LongtermEquilibrium3
    -ionic_strength      true
    -percent_error       true
    -totals              Al  Alkalinity  Ca  Fe(2)   Fe(3)   K   Mg
                         Na  S(-2)  S(6)  Si
    -molalities          Al(OH)2+  Al(OH)3  Al(OH)4-  Al(SO4)2-
                         Al+3  AlHSO4+2  AlOH+2  AlSO4+
                         Fe(OH)2  Fe(OH)2+  Fe(OH)3  Fe(OH)3-
                         Fe(OH)4-  Fe(SO4)2-  Fe+2  Fe+3
                         Fe2(OH)2+4  Fe3(OH)4+5  FeCl+  FeCl+2
                         FeCl2+  FeCl3  FeCO3  FeHCO3+
                         FeOH+  FeOH+2  FeSO4  FeSO4+
    -activities          Al+3  Ca+2  CO2  Fe+2
                         Fe+3  H+  K+  Mg+2
                         Na+  O2  SO4-2  H4SiO4
                         Al(OH)2+  Al(OH)3  Al(OH)4-  Al(SO4)2-
                         AlHSO4+2  AlOH+2  AlSO4+  Fe(OH)2
                         Fe(OH)2+  Fe(OH)3  Fe(OH)3-  Fe(OH)4-
                         Fe(SO4)2-  Fe2(OH)2+4  Fe3(OH)4+5  FeCl+
                         FeCl+2  FeCl2+  FeCl3  FeCO3
                         FeOH+  FeOH+2  FeSO4  FeSO4+
    -equilibrium_phases  Al(OH)3(a)  Fe(OH)3(a)  Jarosite-K  Schwertmannite
                         Kaolinite  Jurbanite  Goethite
    -saturation_indices  Al(OH)3(a)  Fe(OH)3(a)  Jarosite-K  Schwertmannite
                         Kaolinite  Jurbanite  Goethite
    -gases               CO2(g)  O2(g)
```

```
End
USE solution 1
REACTION 1 Add CaCO3 in Increments Al(OH)3 Buffer Ruthbell Water
    Calcite    0.5
    5 millimoles in 100 steps
EQUILIBRIUM_PHASES 1
    Al(OH)3(a) 0 0
    CO2(g)     -1.5 10
    Fe(OH)3(a) 0 0
    Jarosite-K 0 0
    O2(g)      -2 1e-006
SELECTED_OUTPUT
    -file               LongtermEquilibrium4
    -ionic_strength     true
    -percent_error      true
    -totals             Al  Alkalinity  Ca  Fe(2)  Fe(3)  K  Mg
                        Na  S(-2)  S(6)  Si
    -molalities         Al(OH)2+  Al(OH)3  Al(OH)4-  Al(SO4)2-
                        Al+3  AlHSO4+2  AlOH+2  AlSO4+
                        Fe(OH)2  Fe(OH)2+  Fe(OH)3  Fe(OH)3-
                        Fe(OH)4-  Fe(SO4)2-  Fe+2  Fe+3
                        Fe2(OH)2+4  Fe3(OH)4+5  FeCl+  FeCl+2
                        FeCl2+  FeCl3  FeCO3  FeHCO3+
                        FeOH+  FeOH+2  FeSO4  FeSO4+
    -activities         Al+3  Ca+2  CO2  Fe+2
                        Fe+3  H+  K+  Mg+2
                        Na+  O2  SO4-2  H4SiO4
                        Al(OH)2+  Al(OH)3  Al(OH)4-  Al(SO4)2-
                        AlHSO4+2  AlOH+2  AlSO4+  Fe(OH)2
                        Fe(OH)2+  Fe(OH)3  Fe(OH)3-  Fe(OH)4-
                        Fe(SO4)2-  Fe2(OH)2+4  Fe3(OH)4+5  FeCl+
                        FeCl+2  FeCl2+  FeCl3  FeCO3
                        FeOH+  FeOH+2  FeSO4  FeSO4+
    -equilibrium_phases Al(OH)3(a)  Fe(OH)3(a)  Jarosite-K  Schwertmannite
                        Kaolinite  Jurbanite  Goethite
    -saturation_indices Al(OH)3(a)  Fe(OH)3(a)  Jarosite-K  Schwertmannite
                        Kaolinite  Jurbanite  Goethite
    -gases              CO2(g)  O2(g)
End
USE solution 1 Jurbanite Buffer Ruthbell Water
REACTION 1 Add CaCO3 in Increments
```

```
    Calcite    0.5
    5 millimoles in 100 steps
EQUILIBRIUM_PHASES 1
    CO2(g)    -1.5 10
    Fe(OH)3(a) 0 0
    Jarosite-K 0 0
    Jurbanite 0 0
    O2(g)     -2 1e-006
SELECTED_OUTPUT
    -file              LongtermEquilibrium5
    -ionic_strength    true
    -percent_error     true
    -totals            Al  Alkalinity  Ca  Fe(2)  Fe(3)  K  Mg
                       Na  S(-2)  S(6)  Si
    -molalities        Al(OH)2+  Al(OH)3  Al(OH)4-  Al(SO4)2-
                       Al+3  AlHSO4+2  AlOH+2  AlSO4+
                       Fe(OH)2  Fe(OH)2+  Fe(OH)3  Fe(OH)3-
                       Fe(OH)4-  Fe(SO4)2-  Fe+2  Fe+3
                       Fe2(OH)2+4  Fe3(OH)4+5  FeCl+  FeCl+2
                       FeCl2+  FeCl3  FeCO3  FeHCO3+
                       FeOH+  FeOH+2  FeSO4  FeSO4+
    -activities        Al+3  Ca+2  CO2  Fe+2
                       Fe+3  H+  K+  Mg+2
                       Na+  O2  SO4-2  H4SiO4
                       Al(OH)2+  Al(OH)3  Al(OH)4-  Al(SO4)2-
                       AlHSO4+2  AlOH+2  AlSO4+  Fe(OH)2
                       Fe(OH)2+  Fe(OH)3  Fe(OH)3-  Fe(OH)4-
                       Fe(SO4)2-  Fe2(OH)2+4  Fe3(OH)4+5  FeCl+
                       FeCl+2  FeCl2+  FeCl3  FeCO3
                       FeOH+  FeOH+2  FeSO4  FeSO4+
    -equilibrium_phases  Al(OH)3(a)  Fe(OH)3(a)  Jarosite-K  Schwertmannite
                       Kaolinite  Jurbanite  Goethite
    -saturation_indices  Al(OH)3(a)  Fe(OH)3(a)  Jarosite-K  Schwertmannite
                       Kaolinite  Jurbanite  Goethite
    -gases             CO2(g)  O2(g)
End
USE solution 1
REACTION 1 Add CaCO3 in Increments No Schwertmannite Ruthbell water
    Calcite    1
    5 millimoles in 100 steps
EQUILIBRIUM_PHASES 1
```

```
     Al(OH)3(a) 0 0
     CO2(g)     -1.5 10
     Fe(OH)3(a) 0 0
     Fe3(OH)8  0 0
     Jarosite-K 0 0
     Jurbanite 0 0
     Kaolinite 0 0
     O2(g)      -2 1e-006
SELECTED_OUTPUT
     -file              LongtermEquilibrium6
     -ionic_strength    true
     -percent_error     true
     -totals            Al  Alkalinity  Ca  Fe(2)  Fe(3)  K  Mg
                        Na  S(-2)  S(6)  Si
     -molalities        Al(OH)2+  Al(OH)3  Al(OH)4-  Al(SO4)2-
                        Al+3  AlHSO4+2  AlOH+2  AlSO4+
                        Fe(OH)2  Fe(OH)2+  Fe(OH)3  Fe(OH)3-
                        Fe(OH)4-  Fe(SO4)2-  Fe+2  Fe+3
                        Fe2(OH)2+4  Fe3(OH)4+5  FeCl+  FeCl+2
                        FeCl2+  FeCl3  FeCO3  FeHCO3+
                        FeOH+  FeOH+2  FeSO4  FeSO4+
     -activities        Al+3  Ca+2  CO2  Fe+2
                        Fe+3  H+  K+  Mg+2
                        Na+  O2  SO4-2  H4SiO4
                        Al(OH)2+  Al(OH)3  Al(OH)4-  Al(SO4)2-
                        AlHSO4+2  AlOH+2  AlSO4+  Fe(OH)2
                        Fe(OH)2+  Fe(OH)3  Fe(OH)3-  Fe(OH)4-
                        Fe(SO4)2-  Fe2(OH)2+4  Fe3(OH)4+5  FeCl+
                        FeCl+2  FeCl2+  FeCl3  FeCO3
                        FeOH+  FeOH+2  FeSO4  FeSO4+
     -equilibrium_phases  Al(OH)3(a)  Fe(OH)3(a)  Jarosite-K  Schwertmannite
                        Kaolinite  Jurbanite  Goethite  Fe3(OH)8
     -saturation_indices  Al(OH)3(a)  Fe(OH)3(a)  Jarosite-K  Schwertmannite
                        Kaolinite  Jurbanite  Goethite  Fe3(OH)8
     -gases             CO2(g)  O2(g)
End
USE solution 2
REACTION 1 Add Oxygen in Increments Acme Mine water, No Schwertmannite
     O2(g)      1
     0.01 millimoles in 100 steps
EQUILIBRIUM_PHASES 1
```

377

```
     Calcite    0 0
     CO2(g)      -0.85 10
     Fe(OH)3(a)  0 0
     Fe3(OH)8   0 0
     Gypsum     0 0
     Kaolinite 0 0
SELECTED_OUTPUT
     -file              LongtermEquilibrium7
     -ionic_strength    true
     -percent_error     true
     -totals            Al  Alkalinity  Ca  Fe(2)  Fe(3)  K  Mg
                        Na  S(-2)  S(6)  Si
     -molalities        Fe(OH)2  Fe(OH)2+  Fe(OH)3  Fe(OH)3-
                        Fe(OH)4-  Fe(SO4)2-  Fe+2  Fe+3
                        Fe2(OH)2+4  Fe3(OH)4+5  FeCl+  FeCl+2
                        FeCl2+  FeCl3  FeCO3  FeHCO3+
                        FeOH+  FeOH+2  FeSO4  FeSO4+
     -activities        Al+3  Ca+2  CO2  Fe+2
                        Fe+3  H+  K+  Mg+2
                        Na+  O2  SO4-2  H4SiO4
                        Fe(OH)2  Fe(OH)2+  Fe(OH)3  Fe(OH)3-
                        Fe(OH)4-  Fe(SO4)2-  Fe2(OH)2+4  Fe3(OH)4+5
                        FeCl+  FeCl+2  FeCl2+  FeCl3
                        FeCO3  FeOH+  FeOH+2  FeSO4
                        FeSO4+
     -equilibrium_phases  Fe(OH)3(a)  Jarosite-K  Schwertmannite  Kaolinite
                        Goethite  Fe3(OH)8
     -saturation_indices  Fe(OH)3(a)  Jarosite-K  Schwertmannite  Kaolinite
                        Goethite  Fe3(OH)8  Siderite
     -gases             CO2(g)  O2(g)
End
USE solution 1
REACTION 1 Add CaCO3 and O2 in Increments Mixed Buffer Ruthbell Water
     Calcite    1
     O2(g)       0.02
     5 millimoles in 100 steps
EQUILIBRIUM_PHASES 1
     Al(OH)3(a) 0 0
     CO2(g)      -1.5 10
     Fe(OH)3(a) 0 0
     Fe3(OH)8   0 0
```

378

```
    Jarosite-K 0 0
    Jurbanite 0 0
    Kaolinite 0 0
    O2(g)      -2 1e-006
    Schwertmannite 0 0
SELECTED_OUTPUT
    -file              LongtermEquilibrium8
    -ionic_strength    true
    -percent_error     true
    -totals            Al  Alkalinity  Ca  Fe(2)  Fe(3)  K  Mg
                       Na  S(-2)  S(6)  Si
    -molalities        Al(OH)2+  Al(OH)3  Al(OH)4-  Al(SO4)2-
                       Al+3  AlHSO4+2  AlOH+2  AlSO4+
                       Fe(OH)2  Fe(OH)2+  Fe(OH)3  Fe(OH)3-
                       Fe(OH)4-  Fe(SO4)2-  Fe+2  Fe+3
                       Fe2(OH)2+4  Fe3(OH)4+5  FeCl+  FeCl+2
                       FeCl2+  FeCl3  FeCO3  FeHCO3+
                       FeOH+  FeOH+2  FeSO4  FeSO4+
    -activities        Al+3  Ca+2  CO2  Fe+2
                       Fe+3  H+  K+  Mg+2
                       Na+  O2  SO4-2  H4SiO4
                       Al(OH)2+  Al(OH)3  Al(OH)4-  Al(SO4)2-
                       AlHSO4+2  AlOH+2  AlSO4+  Fe(OH)2
                       Fe(OH)2+  Fe(OH)3  Fe(OH)3-  Fe(OH)4-
                       Fe(SO4)2-  Fe2(OH)2+4  Fe3(OH)4+5  FeCl+
                       FeCl+2  FeCl2+  FeCl3  FeCO3
                       FeOH+  FeOH+2  FeSO4  FeSO4+
    -equilibrium_phases Al(OH)3(a)  Fe(OH)3(a)  Jarosite-K  Schwertmannite
                       Kaolinite  Jurbanite  Goethite  Fe3(OH)8
    -saturation_indices Al(OH)3(a)  Fe(OH)3(a)  Jarosite-K  Schwertmannite
                       Kaolinite  Jurbanite  Goethite  Fe3(OH)8
    -gases             CO2(g)  O2(g)
End
```

CURRICULUM VITAE

Name: Eric F. Perry

Parents: William and Frances Perry

Birthplace: Fort Riley, Kansas

Date of Birth: February 3, 1954

Schools and Colleges Attended:

Sparrows Point High School, Sparrows Point, MD 1970-1972

West Virginia University, Morgantown, WV 1972-1978

Degrees Received:

Bachelor of Science in Plant and Soil Science, West Virginia University, 1976

Master of Science in Plant and Soil Science, West Virginia Ubiversity, 1978

Present Position: Hydrologist
US Dept Interior Office of Surface Mining
Pittsburgh, PA